

**The 24th International
Conference on Science and
Application of Nanotubes and
Low-Dimensional Materials**

June 23-28, 2024

Cambridge, MA U.S.A.

WELCOME

Welcome to NT24 @ MIT

We are honored to welcome you to MIT's campus, in historic Cambridge, a well-loved locality of the city of Boston in Massachusetts, U.S.A. NT returns to Boston after 22 years, and we hope to both continue the traditions of NT, as well as share the local flavors of Boston.

NT24 is centered around you, our esteemed colleagues from around the world, and we have endeavored to create a program with time and locations of events to hopefully inspire and support intellectual exchange. Following successful NT conferences over the last few years, we have structured Sunday afternoon tutorials, morning plenary sessions, parallel afternoon topical Symposia, and evening poster sessions, all supported with food and beverages. We hope you enjoy the catered welcome reception and poster sessions, the banquet Wednesday evening in the heart of Boston, and excursions of your choice on Wednesday afternoon. We all can appreciate the support of our many generous sponsors.

We look forward to greeting you, learning from you, and enjoying collegial intellectual exchanges throughout the week. We especially look forward to sharing memories of our dearly-missed Millie Dresselhaus, a huge part of early NT conferences, both through remarks from our featured morning speakers and also by sharing remembrances with all of you. Please look for us, and our broader team, identified by "NT24 Local Team" on our conference badges.

Brian L. Wardle

Jing Kong

Michael Strano

MIT campus, Cambridge, MA, June 10, 2024

LOCAL ORGANIZING COMMITTEE

Brian L. Wardle, AeroAstro and Mechanical Engineering, MIT
Luiz H. Acauan, AeroAstro Engineering, MIT
Jingyao Dai, AeroAstro Engineering, MIT
John Hart, Mechanical Engineering, MIT
Jing Kong, Electrical Engineering and Computer Science, MIT
Mingda Li, Nuclear Science and Engineering, MIT
Xi Ling, Department of Chemistry, Boston University
Desiree Plata, Civil and Environmental Engineering, MIT
Michael Strano, Chemical Engineering, MIT

STEERING COMMITTEE

Chairs

Annick Loiseau, ONERA – CNRS, France
Shigeo Maruyama, University of Tokyo, Japan

Parallel Symposia Chairs

Tobias Hertel, Univ. Würzburg, Germany
Yoshiyuki Miyamoto, AIST, Japan

Members

Tobias Hertel, University of Würzburg, Germany
Ado Jorio, University of Minas Gerais, Brazil
Esko Kauppinen, University of Aalto, Finland
Yan Li, Peking University, Peking, China
Ming Zheng, NIST, USA
Masako Yudasaka, AIST, Japan
Jing Kong, MIT, USA

Honorary member

David Tomanek, Univ. Michigan, USA

ADVISORY BOARD

Jong-Hyun Ahn (Yonsei University, Korea)
Jeffrey L. Blackburn (NREL, USA)
Adam Boies (University of Cambridge, UK)
Sofie Cambré (University of Antwerp, Belgium)
Feng Ding (National Institute of Science and Technology, Korea)
Benjamin S. Fravel (Karlsruhe Institute of Technology, Germany)
Etienne Gaufres (CNRS, Université de Bordeaux, France)
Daniel A. Heller (Sloan Kettering Institute, USA)
Kaili Jiang (Tsinghua University, China)
Ki Kang Kim (Sungkyunkwan University, Korea)
Markita Landry (UC Berkeley, USA)
Yan Li (Peking University, China)
Matteo Pasquali (Rice University, USA)
Marcos Pimenta (Federal U. Minas Gerais, Belo Horizonte, Brasil)
Riichiro Saito (Tohoku University, Japan)
Michael Strano (MIT, USA)
Brian L. Wardle (MIT, USA)
Jana Zaumseil (University of Heidelberg, Germany)

SYMPOSIA ORGANIZERS

Computation and Theory

16th Symposium on Computational Challenges in Nanotubes, 2D Materials, and Their Macroscopic Assemblies

Chair: Christophe Bichara (University of Marseille)

Co-Chair: Vincent Meunier (Penn State)

local Co-Chair: Mingda Li (MIT)

Energy & Electronics

Symposium on Nanomaterials for Energy and Electronics

Chair: Lian Mao Peng (Peking University)

Chair: Biu Liu (Tsinghua University)

local Co-Chair: Qiong Ma (Boston College)

Fundamental Properties

Symposium on Fundamental, Structural and Optical Properties of 1D and 2D Materials and their Heterostructures

Chair: Alexey Chernikov (University of Dresden)

Co-Chair: Jana Zaumseil (University of Heidelberg)

Co-Chair: Christophe Voisin (ENS Paris)

local Co-Chair: Xi Ling (Boston University)

Macromaterials

Symposium on Thin Films, Fibers, 3-D Materials and their Properties

Chair: Suguru Noda

Co-Chair: Philippe Poulin (University of Bordeaux)

Co-Chair: Esko Kauppinen (Aalto University)

local Co-Chair: Ao Geyou (University of Ohio)

SYMPOSIA ORGANIZERS

NanoBio

14th Symposium on Carbon Nanomaterials, Biology, Medicine and Toxicology

Chair: Dan Heller (Sloan Kettering Institute)

Co-Chair: Laurent Cognet (University of Bordeaux)

Co-Chair: Makita Landry (UC Berkeley)

local Co-Chair: Daniel Roxbury

Synthesis

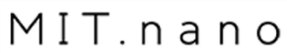
5th Symposium on Synthesis, Purification, Functionalization, and Manufacturing of Carbon Nanotubes and Low-Dimensional Materials

Chair: Yan Li (Peking University)

Co-Chair: Ming Zheng (NIST)

local Co-Chair: Piran Kidambi (Vanderbilt University)

THANKS TO OUR SPONSORS



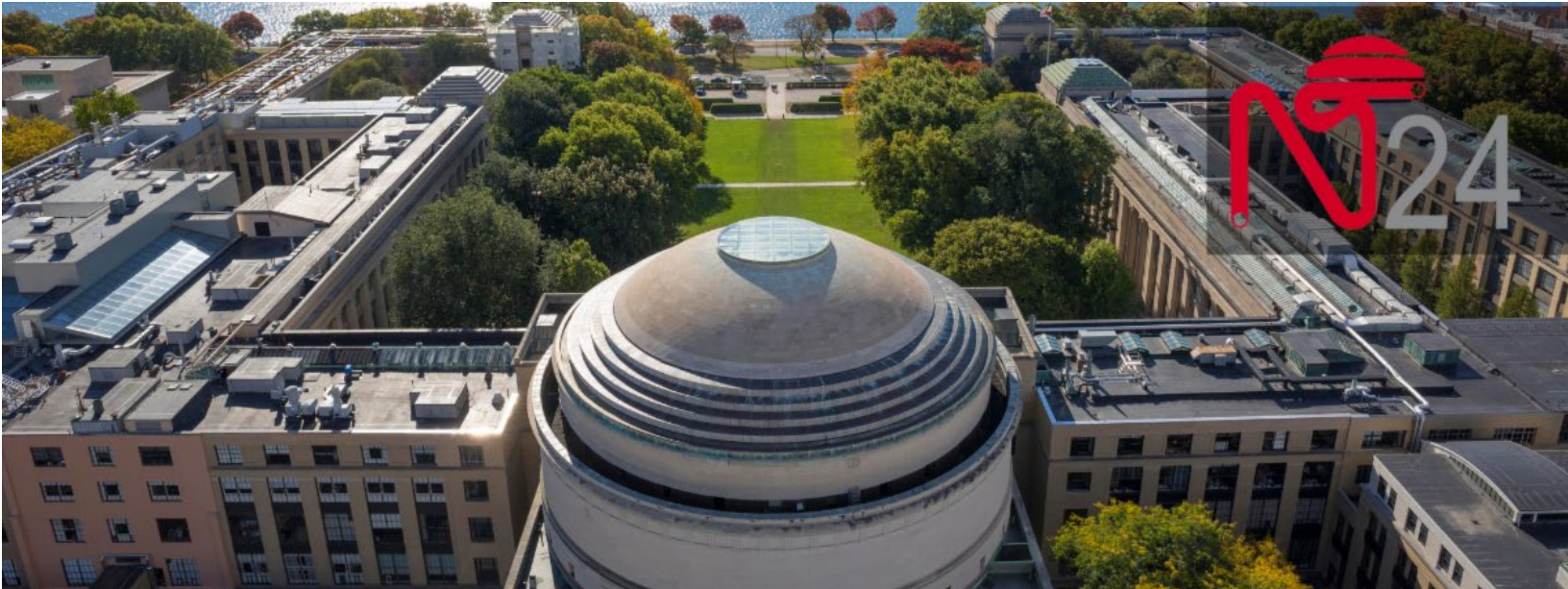


TABLE OF CONTENTS

- WIFI AT MIT**
- FIND YOUR WAY IN MIT**
- KRESGE AUDITORIUM**
- MIT CAMPUS MAP**
- WHERE AND WHEN TO GO**
- PROGRAM AT A GLANCE**
- TUTORIAL PROGRAM**
- SYMPOSIA PROGRAM**
- WEDNESDAY AFTERNOON EXCURSIONS**
- WEDNESDAY NIGHT**
- MAP OF BOSTON AREA**
- LIST OF ABSTRACTS**
- STUDENTS & STAFF CONTRIBUTION**

WIFI AT MIT

Welcome to MIT!

Just connect to **MIT GUEST** by signing in with email or text message.



MIT GUEST

I accept the Terms of Service
Terms of Service

Connect to WiFi with

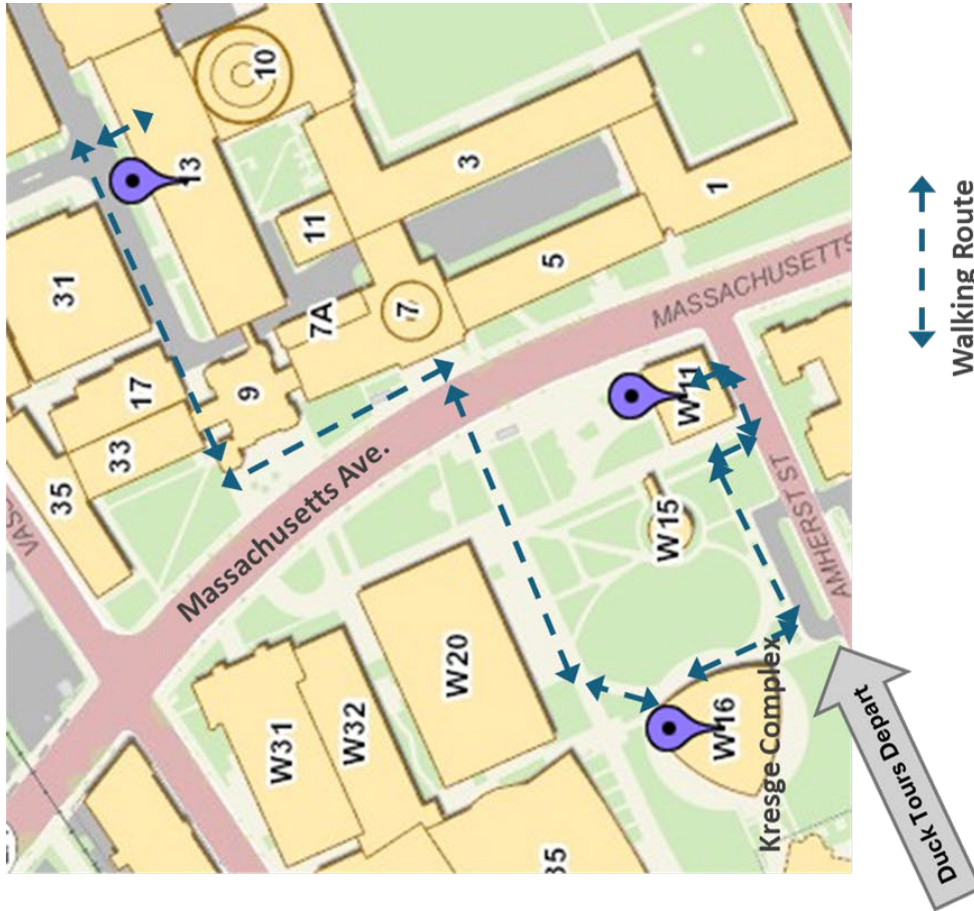
Sign in with Email

Sign in with Text Message

Request Access from Sponsor



FIND YOUR WAY AT MIT



MIT W16 Kresge Auditorium

- Tutorials: Kresge Auditorium
- Welcome Reception: Kresge Lobby
- Keynotes: Kresge Main
- Parallel Symposia:
 - Kresge Auditorium
 - Kresge Little Theater
 - Rehearsal Room A
 - Rehearsal Room B
- Coffee Breaks
- Lunch Distribution

MIT W11 (in Main Dining Room)

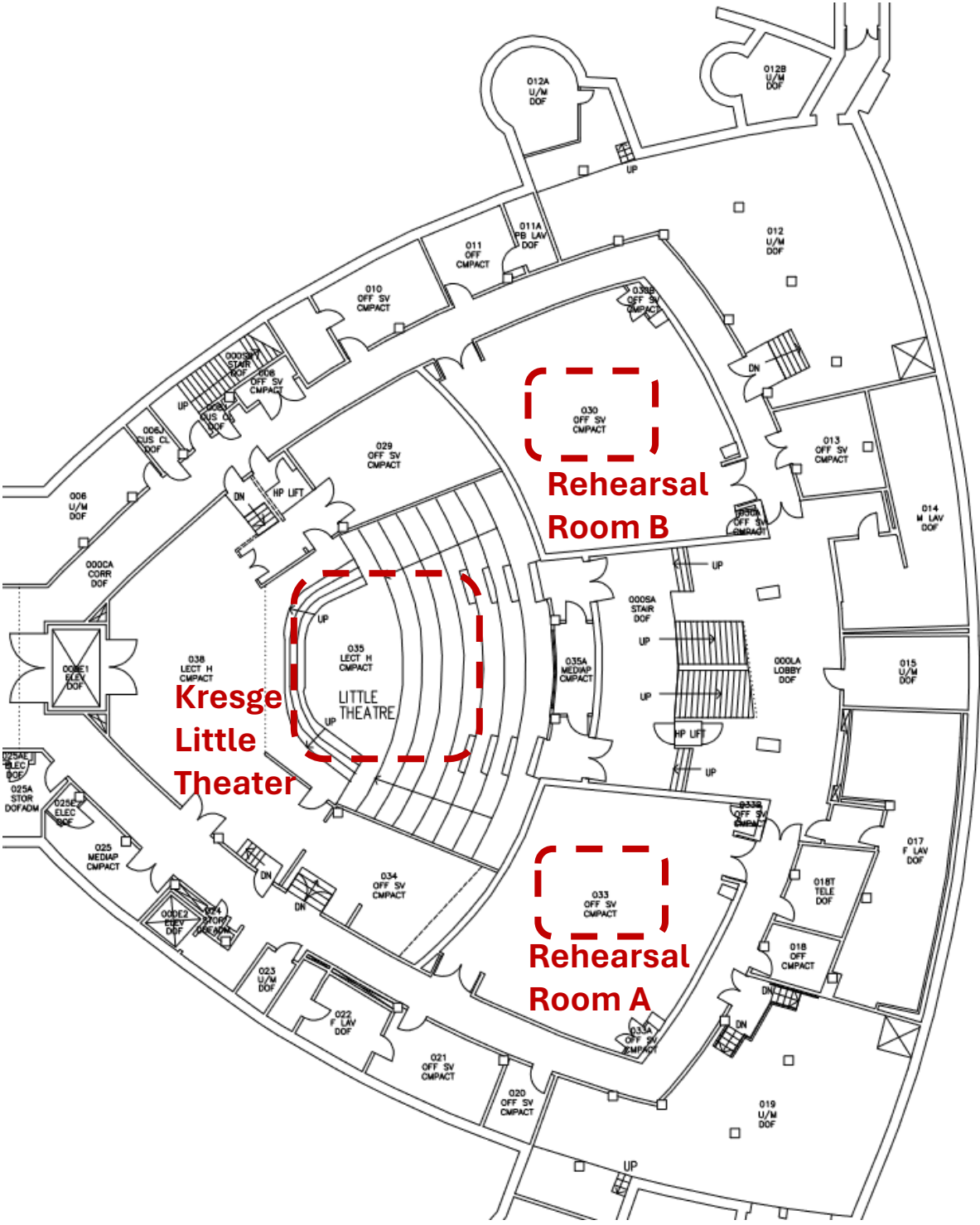
- Parallel Symposia:

MIT Building 13 (in Lobby 13)

- Poster Sessions

KRESGE AUDITORIUM

Basement of Kresge



MIT CAMPUS MAP



MIT campus
accessibility map

WHERE AND WHEN TO GO

EVENT	DAY	LOCATION
Tutorials	Sun	Kresge Main
Welcome Reception	Sun	Kresge Auditorium
Plenary Sessions	Mon-Fri	Kresge Main
Poster Sessions & Exhibition Sponsor	Mo, Tu, Th	Building 13
Symposium Synthesis	Mo, Tu, Th	Kresge Main
Symposium Energy & Electronics	Mo, Tu, Th	Kresge Little Theatre
Symposium Fundamental Properties	Mo, Tu, Th	Kresge Rehearsal A
Symposium Macromaterials	Tu, Th	Kresge Rehearsal B
	Mo	Kresge Rehearsal B
Symposium NanoBio	Th	Building W11
Symposium Computation & Theory	Mo, Tu	Building W11
		Kresge Main Level
		Lobby
		Kresge Main Level
		Kresge Basement
		Dining Room

PROGRAM AT A GLANCE

Start	Sunday June 23	Monday	Tuesday	Wednesday	Thursday	Friday
830	S. Reich 565	B. Weisman 236	U. Kaiser 505	Y. Ohno 430	P. Jarillo-Herrero 001	
915	X. Zheng 384	C. Casiraghi 383	R. Krupke 380	D. Heller 293	D. Lashmore 390	
945	D. Roxbury 325	M. Barsoum 023	M. ElAbbassi 081	X. Li 233	S. Kessler 308	
1005	Coffee Break	Coffee Break	Coffee Break	Coffee Break	Coffee Break	
1045	G. Odegard 534	H.S. Shin 262	A. Boghossian 459	C. Bichara 516	C. Giudici 094	
1115	B. Maruyama 068	B. Eller 301	P. Kidambi 376	Y.M. Tu 548	H. Richter 318	
1135	S. Cho 005	F. Fornasiero 032	Q. Zhang 278	A. Venault 585	K. Retz 103	
1155	S. Kruss 224	S. Noda 257	D. Hedman 079	D. Gailus 461	R. Misra 143	
1215	Lunch	Lunch	Lunch on Own	Lunch	Free Time	
1400	Parallel Symposia	Parallel Symposia	Excursions & Free Time	Parallel Symposia		
1700	Welcome Reception & Registration Ends 1830	Posters Ends 1930	Reception 1800 Banquet 1900	Posters Ends 1930		

TUTORIAL PROGRAM

NT24 Sunday Tutorial Session

June 23rd, 2024

Sponsored by the U.S. National Science Foundation
and U.S. Office of Naval Research

Sunday Tutorial Session – NT24 Kresge Auditorium (building W16)

1:00 – 1:05 pm	Welcome and Call to Order – Note on Tutorial Session Theme and Sponsorship	Professor Michael S. Strano, Carbon P. Dubbs Professor of Chemical Engineering
1:05 – 1:15 pm	Welcoming Remarks	Professor Vladimir Bulović MIT.nano Director Fariborz Maseeh Professor of Emerging Technologies
1:15 – 1:55 pm	Session 1: NT and the Legacy of Professor Mildred Dresselhaus	Maia Weinstock – MIT Media Office, Official M. Dresselhaus Biographer
1:55 – 2:10 pm	Coffee/Tea Break	Kresge Lobby
2:10 – 2:55 pm	Session 2: The Intersection of Nanotechnology, Nanofluidics and Sustainability	Professor Arun Majumdar, Dean, Stanford Doerr School of Sustainability, Jay Precourt Professor, Professor of Mechanical Engineering
2:55 – 3:10 pm	Coffee/Tea Break	Kresge Lobby
3:10 – 3:55pm	Session 3: Quantum Defects and Optical Color Centers in Low Dimensional Materials	Professor YuHuang Wang, Professor of Chemistry, University of Maryland
3:55 – 4:10 pm	Break	Kresge Lobby
4:10 – 4:55 pm	Session 4: Nanoscale Vibrational Electron Energy Loss Spectroscopy in Single, Isolated 1D Systems	Dr. Jordan Hatchel, Staff Scientist, Center for Nanophase Materials Sciences at Oak Ridge National Laboratory
4:55 – 5:00 pm	NT Tutorial Session - Closing Remarks and Note on Summary Report	Professor Michael S. Strano, Carbon P. Dubbs Professor of Chemical Engineering
5:00 – 6:30 pm	NT Welcome Reception	Kresge Lobby

SYMPOSIUM PROGRAM

Monday, June 24, 2024

	Synthesis	Energy & Electronics	Computation & Theory	NanoBio	Fundamental Properties
14:00	Kresge Main	Kresge Little Theatre	W11	Kresge Rehearsal B	Kresge Rehearsal A
14:20	345 Michael Arnold	483 Chongwu Zhou	Feng Ding	478 Anton Naumov	152 Kazuhiro Yanagi
14:40	388 Annick Loiseau	399 Haozhe Wang	444 Ksenia Bets	197 Lorena García hevia	25 Tobias Hertel
15:00	466 Adam Boies	35 Qiangmin Yu	381 Giacomo Sesti	93 Rachel Meidl	76 Weilu Gao
15:20	break				
16:00	160 Liu Qian	583 Xiaodong Yan	578 James Elliot	304 Nicole Iverson	418 Sébastien Roux
16:20	422 Lili Zhang	185 Shengman Li		192 Ching-Wei Lin	39 Shen Zhao
16:40	433 Song Wang	166 Irina Grigorieva	513 Natalya Sheremetyeva	Dal-Hee Min	
17:00	Gwan-Hyoung Lee	58 Rongjie Zhang	220 Eduardo Costa Girao	Mijin Kim	

SYMPOSIA PROGRAM

Tuesday, June 25, 2024

	Synthesis	Energy & Electronics	Computation & Theory	Macromaterials	Fundamental Properties
14:00	Kresge Main	Kresge Little Theatre	W11	Kresge Rehearsal B	Kresge Rehearsal A
14:20	570 Shigeo Maruyama	165 Erxiong Ding 209 Bodo Baumgartner	557 Trevor Rhone 295 Zhiping Xu	540 Adam Boies	296 Diana Qiu
14:40	107 Dawid Janas	216 Ghulam Yasin	485 Boris Yakobson	190 Yuan Chen	423 Annick Loiseau
15:00	145 Han Li	333 Yenny Hernandez		410 Jing Zhong	204 Marcos Pimenta
15:20	break				
16:00	276 Huaping Liu	497 Yutaka Ohno	538 Dmitri Kilin	139 Jingyao Dai	92 Minjung Son
16:20	367 Ki Kang Kim	502 Shivam Kajale		229 Shaan Janagi	396 Shengxi Huang
16:40	596 Rohit Karnik	240 Bon-Cheol Ku		366 S Kumar	167 Yuval Yaish
17:00	288 Sook Young Moon			281 Yoshiyuki Nonoguchi	320 Bernd Sturzda

SYMPOSIA PROGRAM

Thursday, June 27, 2024

	Synthesis	Energy & Electronics	NanoBio	Macromaterials	Fundamental Properties
	Kresge Main	Kresge Little Theatre	W11	Kresge Rehearsal B	Kresge Rehearsal A
14:00	Matteo Pasquali	322 Aaron Franklin	361 Noe Alvarez	445 Juan Jose Vilatela	393 Nikita Kavokine
14:20	Jiwoon Park		531 Tomohiro Shiraki	30 Toshihiko Fujimori	235 Jose Lado
14:40	Hiroki Ago	424 Yuxuan Cosmi Lin	313 Ryan Williams	75 Juan Fajardo	226 Jean-Baptiste Marceau
15:00	Ming Xu	476 Zhang Xu	371 Ana Champi	95 Geoff Wehmeyer	89 Pilkyung Moon
15:20	break				
16:00	312 Jinbo Bai	477 Nageh Allam	24 Aceer Nadeem	491 Virginia Davis	439 Kwabena Bediako
16:20	368 Zhiyuan Shi	592 Xinjie Zhang	56 Mervin Ang	116 Matthias Kollosche	298 Julian Klein
16:40	456 Aqeel Hussain		Nigel Reuel	348 Jandro Abot	
17:00				542 Nima Zakeri	

WEDNESDAY AFTERNOON EXCURSIONS

On Wednesday afternoon during NT24, NT24 attendees will have many options to explore Boston and Cambridge.

Boston Duck Tours

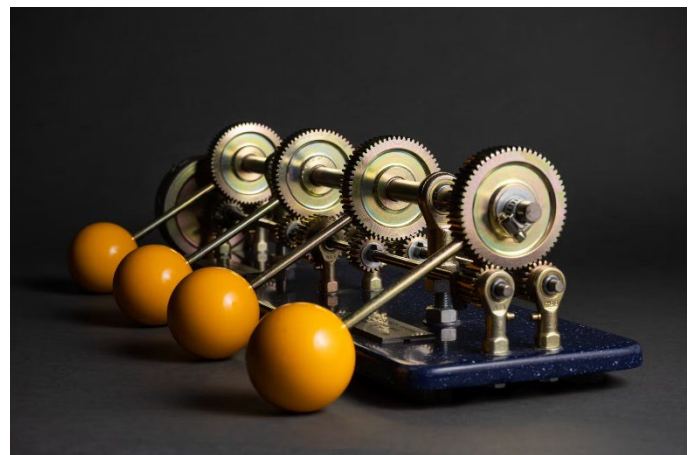
“Hop aboard Boston Duck Tours and enjoy a fully narrated and guided, historic tour of Boston in a “DUCK”, a W.W.II style amphibious landing vehicle that travels on land and water. You'll be greeted by one of our legendary ConDUCKtors, who'll be narrating your tour. You'll cruise by all the places that make Boston the birthplace of freedom. Just when you think you've seen it all, it's



time for a Big Splash as your ConDUCKtor drives the DUCK right into the Charles River for a breathtaking view of the Boston and Cambridge skylines.”

MIT Museum Guided Tour

Join a guided tour of the MIT Museum with additional time available to explore at your own pace.



MIT Walking Tour

Join a guided walking tour of the MIT Campus.

Or you can plan your own afternoon.



NT24 Event Details

WEDNESDAY NIGHT

A highlight of NT Conferences is the **conference banquet**, and we look forward to sharing this time with you at Boston's State Room on Wednesday evening during NT24.

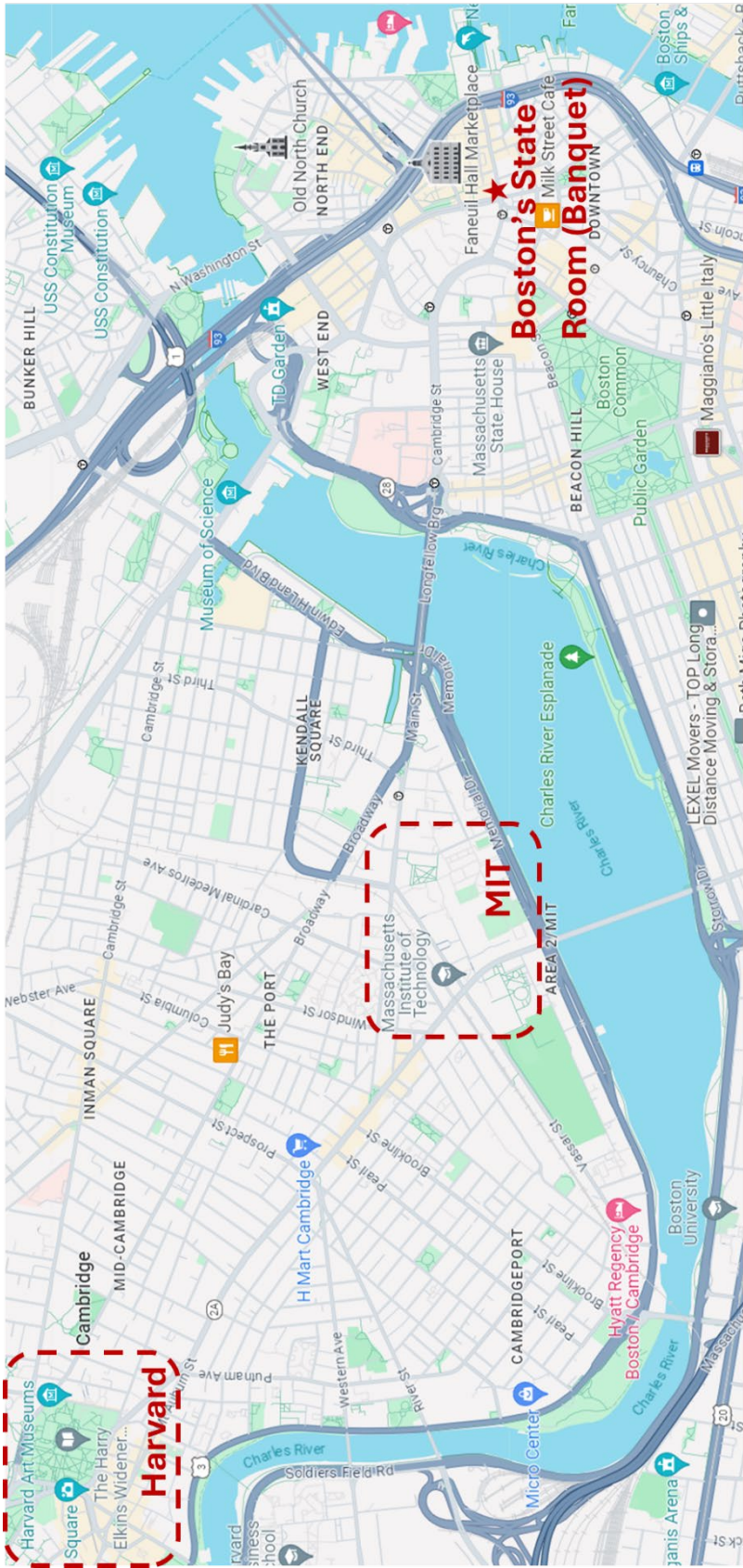


Address



Boston's State Room

MAP OF BOSTON



1000 ft

ADDITIONAL THANKS

Logo, banner, stickers and booklet

Jiangtao Wang
Xudong (Sheldon) Zheng
Tianyi Zhang

Program schedule

Jen-Hung Fang
Carina Xiaochen Li
Shweta Sharma

List of Abstracts

Tutorial

- 0854_1278_000254 **Quantum Defects in Carbon Semiconductors: An Introduction.....1**
YuHuang Wang, PhD
University of Maryland, College Park, MD, USA

Keynote (plenary)

- 0854_1278_000505 **KEYNOTE: Graphene Encapsulation and Carbon Nanotubes –
Reaction Vessels to Gain Atomic Insights into Physics and Chemistry of Matter2**
Ute Kaiser
Ulm University, Ulm, Germany

- 0854_1278_000430 **KEYNOTE: Low-frequency Noise in Flexible Carbon Nanotube
Analog Integrated Circuits for Sensor Applications3**
Yutaka Ohno, PhD
Nagoya University, Nagoya, Japan

- 0854_1278_000236 **KEYNOTE: Monitoring and Modulating the Fluorescence of
Semiconducting Single-Wall Carbon Nanotubes4**
R. Bruce Weisman
Rice University, Houston, TX, USA

- 0854_1278_000001 **KEYNOTE: Next Generation Moiré Quantum Matter5**
Pablo Jarillo-Herrero
Massachusetts Institute of Technology, CAMBRIDGE, MA, USA

- 0854_1278_000565 **KEYNOTE: Superstructures and Molecular Lattices in One and
Two Dimensions6**
Stephanie Reich
Free University of Berlin, Berlin, Germany

Invited (plenary)

- 0854_1278_000380 **Electroluminescence From Carbon Nanotubes With Quantum
Defects7**
Min-Ken Li^{1,2}, Simone Dehm¹, Manfred Kappes¹, Frank Hennrich¹, Ralph Krupke^{1,2}
*¹Karlsruhe Institute of Technology, Karlsruhe, Germany, ²Technische Universität Darmstadt,
Darmstadt, Germany*

- 0854_1278_000534 **Gamma-Ray Irradiation of CNT yarns for Improved Composite
Strength: A Molecular Dynamics Study8**
Sagar Patil, Josh Kemppainen, Trevor Wavrunek, Gregory Odegard
Michigan Technological University, Houghton, MI, USA

0854_1278_000390	Lightweight, Strong, High Conductivity, Aluminum- Carbon Nanotube Wiring	9
	David Lashmore, PhD, CEO ^{1,2} , Pavel Bystricky, PhD, CTO ¹ , Michael Matuszewski, CTO ² , Tom Kukowski, Consultant ²	
	<i>¹American Boronite Corp, Burlington, MA, USA, ²Minnesota Wire, Minneapolis, MN, USA</i>	
0854_1278_000262	Phase engineered WS2 monolayer quantum dots by rhenium doping	10
	Hyeon Suk Shin	
	<i>Ulsan National Institute of Science and Technology, Ulsan, Republic of Korea</i>	
0854_1278_000293	Quantum Well Defect Carbon Nanotubes for Biomedicine	11
	Daniel Heller, PhD	
	<i>Memorial Sloan Kettering Cancer Center, NEW YORK, NY, USA</i>	
0854_1278_000516	Structure and Dynamics of the Interface of Growing Carbon Nanotubes	12
	Christophe Bichara	
	<i>CINaM, CNRS, Marseille, France</i>	
0854_1278_000459	There's Plenty of Room at the (Nano/Bio) Boundary	13
	Ardemis Boghossian	
	<i>Ecole Polytechnique Federale de Lausanne, Lausanne, Switzerland</i>	
0854_1278_000384	Water Splitting: from Hydrogen Production to Water Disinfection	14
	Xiaolin Zheng	
	<i>Stanford University, Stanford, CA, USA</i>	
0854_1278_000383	WATER-BASED AND BIOCOMPATIBLE 2D MATERIAL INKS - FROM PRINTED ELECTRONICS TO BIOMEDICAL APPLICATIONS	15
	cinzia casiraghi	
	<i>University of Manchester, Manchester, United Kingdom</i>	

Contributed (plenary)

0854_1278_000094	A semi-detailed Kinetic Model for the production of Carbon Nanotubes and H₂ from the thermo-catalytic pyrolysis of Methane	16
	Clarissa Giudici, Mauro Bracconi, Matteo Maestri, Matteo Pelucchi	
	<i>Politecnico di Milano - Italy, Milano, Italy</i>	
0854_1278_000278	Continues Synthesis of Free-standing SWNT films for Bioelectrode Applications	17
	Qiang Zhang	
	<i>Honda Research Institute USA, Inc., San Jose, CA, USA</i>	

0854_1278_000032	Decoupling entrance and inner resistances in CNT channels.....	18
	Melinda Jue, Steven Buchsbaum, Sei Jin Park, Kathleen Moyer-Vanderburgh, Francesco Fornasiero <i>Lawrence Livermore National Laboratory, Livermore, CA, USA</i>	
0854_1278_000548	Environmental Damping and Vibrational Coupling of Confined Fluids within Isolated Carbon Nanotubes	19
	Yu-Ming Tu, Rahul Misra, Cody Ritt, Daniel Blankschtein, Michael Strano <i>Massachusetts Institute of Technology, Cambridge, MA, USA</i>	
0854_1278_000318	High Volume Manufacturing of Single-Walled Carbon Nanotubes and Their Applications	20
	Hossein Ghiassi, Darren Bischoff, Paul Brookes, Matthias Kolloche, Melissa Ricci, Henning Richter <i>Nano-C, Inc., Westwood, MA, USA</i>	
0854_1278_000376	High-Performance Hemofiltration via Molecular Sieving and Ultra-Low Friction in Carbon Nanotube Capillary Membranes	21
	Piran Kidambi, PhD <i>Vanderbilt University, Nashville, TN, USA</i>	
0854_1278_000023	Hydroxide Derived Nanomaterials and Their Properties.....	22
	Michel Barsoum, PhD <i>Drexel University, Philadelphia, PA, USA</i>	
0854_1278_000461	Impact of Purification Methods on Carbon Nanotube Material Properties.....	23
	David Gailus ¹ , Mark Banash, PhD, MBA ² , Steven Strand, PhD ¹ , Mark Hibbard ¹ <i>¹Huntsman Advanced Materials/Nanocomp Technologies, Merrimack, NH, USA, ²Neotericon LLC, Bedford, NH, USA</i>	
0854_1278_000585	Incorporation of Nanomaterials Into PVDF Porous Membranes For Improved Water Treatment	24
	Irish Maggay, PhD ¹ , Chien-Jung Wu ¹ , Chechia Hu, PhD ² , Yung Chang, PhD ¹ , Antoine Venault, PhD ¹ <i>¹Chung Yuan Christian University, Taoyuan, Taiwan, ²National Taiwan University of Science and Technology, Taipei City, Taiwan</i>	
0854_1278_000005	Integrating Fluorescent Nanosensors with Microfluidics for Label-Free Chemical Cytometry	25
	Sooyeon Cho, Ph.D <i>Sungkyunkwan University, Suwon, Republic of Korea</i>	
0854_1278_000079	Molecular Dynamics Simulations of Carbon Nanotube Growth on Solid Rhenium Catalysts	26
	Daniel Hedman, PhD <i>Institute for Basic Science, Ulsan, Republic of Korea</i>	

0854_1278_000224	Novel imaging concepts for carbon nanotube based biosensors....	27
Sebastian Kruss <i>Ruhr University Bochum, Bochum, Germany</i>		
0854_1278_000325	Optimizing Live Cell and In Vivo Sensors with Multichiral DNA-Functionalized SWCNTs	28
Daniel Roxbury, PhD, Matthew Card, Lauren Hubert, Ailill Smith <i>University of Rhode Island, Kingston, RI, USA</i>		
0854_1278_000081	Robotic assembly of high-quality nanomaterials including CNTs	29
Maria El Abbassi <i>Chiral Nano, Zurich, Switzerland</i>		
0854_1278_000257	Safe and Damage-Less Dry-Purification of Carbon Nanotubes Using Br₂ Vapor	30
Takuma Goto ¹ , Toshio Osawa ¹ , Suguru Noda, PhD ^{1,2} <i>¹Department of Applied Chemistry, Waseda University, Tokyo, Japan, ²Waseda Research Institute for Science and Engineering, Waseda University, Tokyo, Japan</i>		
0854_1278_000301	Scaling Law of Quantum Confinement in Ultrashort Carbon Nanotubes	31
Benjamin Eller, YuHuang Wang <i>University of Maryland, College Park, MD, USA</i>		
0854_1278_000308	Sensing and Ice Protection for Aerospace Applications Enabled by Macroscopic Carbon Nanotube Networks.....	32
Seth Kessler, PhD ¹ , Estelle Kalfon Cohen, PhD ¹ , Galdemir Botura ² , Yosef Stein <i>¹Metis Design Corporation, Boston, MA, USA, ²Collins Aerospace, Uniontown, OH, USA</i>		
0854_1278_000103	The Search for Multi-Functional Composite Material and Structure	34
Kevin Retz, PhD ¹ , Thomas Goislard, PhD ² <i>¹NAWA America, Dayton, OH, USA, ²NAWA Technologies, Rousset, France</i>		
0854_1278_000143	Uncovering the Role of Water Electric Fields on the Different Regimes of Diameter-Dependent Slip Flow Inside Carbon Nanotubes	35
Rahul Prasanna Misra, Shuang Luo, Daniel Blankschtein <i>Massachusetts Institute of Technology, Cambridge, MA, USA</i>		
0854_1278_000068	Using Thermodynamics & Autonomous Experimentation to understand & optimize catalyst activity for carbon nanotube yield and diameter control. .	36
Benji Maruyama, PhD ¹ , Robert Waelder, PhD ² , Rahul Rao, PhD ¹ , Chiwoo Park, PhD ³ , Jennifer Carpena-Nuñez, PhD ² , Josh Yoho, PhD ^{2,4} , Stephane Gorsse, PhD ⁵ <i>¹Air Force Research Laboratory, Materials & Manufacturing Directorate, WPAFB, OH, USA, ²UES Inc., Beavercreek, OH, USA, ³Florida State University, Tallahassee, FL, USA, ⁴UES Inc, Beavercreek, OH, USA, ⁵Institute of Condensed Matter Chemistry of Bordeaux, Centre National de la Recherche Scientifique, PESSAC, France</i>		

0854_1278_000233 **Width Controlled Growth of TMD Quantum Nanoribbons**.....37
Xufan Li, PhD, Shuang Wu, PhD, Avetik Harutyunyan, PhD
Honda Research Institute USA, Inc., San Jose, CA, USA

Overview Symposium

0854_1278_000540 **Carbon, Catalysts and Climate: Optimizing Large-Scale CNT Reactors for Sustainable Materials and Energy**38
Adam Boies
University of Cambridge, Cambridge, United Kingdom

0854_1278_000485 **Computing Nanomaterials: Insights in Equilibrium And Processes**39
Boris Yakobson¹, Ksenia Bets¹, Luqing Wang^{1,2}, Jincheng Lei^{1,3}
¹Rice University, Houston, TX, USA, ²Argonne National Laboratory, Lemont, IL, USA, ³Yale University, New Haven, CT, USA

0854_1278_000478 **Gene Delivery and Imaging by Graphene Quantum Dots**40
Anton Naumov, Ph.D.
Texas Christian University, Fort Worth, TX, USA

0854_1278_000296 **Many-body Effects on Exciton Dynamics and Nonlinear Optics in Low-Dimensional Materials**.....41
Diana Qiu
Yale University, New Haven, CT, USA

0854_1278_000345 **Self-Assembly of High Packing Density Carbon Nanotube Arrays using Microscopic Water Features**.....42
Sean Foradori, Brett Prussack, Arganthaël Berson, Michael Arnold
University of Wisconsin-Madison, Madison, WI, USA

0854_1278_000570 **Synthesis of 1D van der Waals Heterostructures Based on Single-Walled Carbon Nanotubes**43
Shigeo Maruyama^{1,2}, Yongjia Zheng^{1,2}, Wanyu Dai¹, Chunxia Yang¹, Keigo Otsuka¹, Rong Xiang^{1,2}
¹The university of Tokyo, Tokyo, Japan, ²Zhejiang University, Hangzhou, China

0854_1278_000152 **Thermoelectric performance of single-walled carbon nanotubes** .44
Kazuhiro Yanagi, PhD
Tokyo Metropolitan University, Tokyo, Japan

0854_1278_000601 **Understanding the Growth of Carbon Nanotubes: Previous Achievements, Challenges and Opportunities**.....45
Feng Ding
Shenzhen University of Advanced Technology, Shenz, China

Invited Symposium

- 0854_1278_000035 **2D transition metal disulfides: controllable preparation and green hydrogen production**46
Qiangmin Yu, PhD, Bilu Liu, PhD, Hui-Ming Cheng, PhD
Tsinghua University, Beijing, China
- 0854_1278_000145 **Advanced Surfactant-Controlled Sorting of Single-Chirality Carbon Nanotubes**47
Han Li
University of Turku, Turku, Finland
- 0854_1278_000557 **AI accelerated materials discovery of van der Waals magnets**48
Trevor David Rhone
Rensselaer Polytechnic University, Troy, NY, USA
- 0854_1278_000235 **Artificial van der Waals multiferroics with twisted two-dimensional materials**49
Jose Lado, Prof.
Aalto University, Espoo, Finland
- 0854_1278_000424 **Atomic Scale Material Engineering for Ultimately Scaled Electronics**50
Yuxuan Cosmi Lin
Texas A&M University, College Station, TX, USA
- 0854_1278_000093 **Balancing Promise and Precaution: Navigating the Environmental and Toxicological Landscape of Carbon Nanotube Materials for Informed Policy**.....51
Rachel Meidl, PhD, LPD, CHMM
Rice University's Baker Institute for Public Policy, Houston, TX, USA
- 0854_1278_000444 **Boron Nitride Phase Differentiation at The Nucleation Stage**.....52
Ksenia Bets, Ting Cheng, Boris Yakobson
Rice University, Houston, TX, USA
- 0854_1278_000190 **Carbon onions from hydrogen production for environmental and energy applications**53
Yuan Chen
The University of Sydney, Darlington, Australia
- 0854_1278_000361 **Carbon Nanomaterial based Microelectrodes for the Detection of Biomolecules and Neurotransmitters**.....54
Noe Alvarez, PhD
University of Cincinnati, Cincinnati, OH, USA

0854_1278_000322	Carbon-based Nanomaterial Inks for Print-in-place, Recyclable, and Water-based Electronics	55
Aaron Franklin, PhD <i>Duke University, Durham, NC, USA</i>		
0854_1278_000295	Cracking 2D Crystals: Patterns and Collective Behaviors	56
Zhiping Xu, PhD <i>Tsinghua University, Beijing, China</i>		
0854_1278_000596	Development of Nanoporous Atomically Thin Membranes for Challenging Chemical Separations	57
Rohit Karnik <i>MIT, Cambridge, MA, USA</i>		
0854_1278_000439	Effects of Relaxation and Strain in Moiré Superlattices	58
D. Kwabena Bediako <i>University of California, Berkeley, Berkeley, CA, USA</i>		
0854_1278_000367	Epitaxial growth of van der Waal heterostructures on wafer scale	59
Ki Kang Kim <i>Sungkyunkwan University, Suwon, Republic of Korea</i>		
0854_1278_000583	Exploring the Power of Low-Dimensional Materials for Neuromorphic Computing	60
Xiaodong Yan <i>University of Arizona, Tucson, AZ, USA</i>		
0854_1278_000030	High-Performance Nitrogen-Doped Single-Wall Carbon Nanotube Fibers	61
Toshihiko Fujimori, PhD ¹ , Zhikai Li ² , Samuel Jeong, PhD ² , Hirotaka Inoue, PhD ¹ , Keishi Akada, PhD, Takamasa Onoki, PhD, Jun-ichi Fujita, PhD <i>¹Sumitomo Electric Industries, Ltd., Osaka, Japan, ²University of Tsukuba, Tsukuba, Japan</i>		
0854_1278_000166	In-plane Staging and Limits on Lithium-ion Intercalation of Bilayer Graphene	62
Irina Grigorieva <i>University of Manchester, Manchester, United Kingdom</i>		
0854_1278_000410	Interfacial Nanoengineering of Conductive Concrete by Nanocarbon Materials	63
JING ZHONG <i>Harbin Institute of Technology, Harbin, China</i>		
0854_1278_000531	Molecular Recognition Approach for Bio-related Material Sensing Using Locally Functionalized Single-walled Carbon Nanotubes	64
TOMOHIRO SHIRAKI, PhD <i>Kyushu University, Fukuoka, Japan</i>		

0854_1278_000396	Quantum Optical Emission From Defects in 2D Materials	65
Wenjing Wu, Arka Chatterjee, Shengxi Huang <i>Rice University, Houston, TX, USA</i>		
0854_1278_000276	Recent progress on the separation of single-chirality carbon nanotubes by gel chromatography	66
Huaping Liu, PhD <i>Beijing National Laboratory for Condensed Matter Physics, Institute of Physics, Chinese Academy of Sciences, Beijing, China</i>		
0854_1278_000603	Relationship Of CNT Synthesis Conditions To Performance-Levelized Properties Of CNT Fibers	67
Matteo Pasquali, Eldar Khabushev <i>Rice University, Houston, TX, USA</i>		
0854_1278_000185	Remote doping for Carbon Nanotube Transistors	68
Shengman Li <i>Stanford University, Palo Alto, CA, USA</i>		
0854_1278_000491	Rheology, Phase Behavior, and Direct Ink Writing of MXene Dispersions	69
Virginia Davis ¹ , Francis Mekunye ¹ , Mackenzie Woods ¹ , Majid Beidaghi ² <i>¹Auburn University, Auburn, AL, USA, ²University of Arizona, Tuscon, AZ, USA</i>		
0854_1278_000107	Selective and Effective Extraction of Monochiral Single-Walled Carbon Nanotubes with Conjugated Polymers	70
Andrzej Dzienia, Dominik Just, Dawid Janas <i>Silesian University of Technology, Gliwice, Poland</i>		
0854_1278_000418	Self-trapped excitons in twisted hBN heterostructures	71
Sébastien Roux ^{1,2,3} , Christophe Arnold ² , François Ducastelle ¹ , Annick Loiseau ¹ , Julien Barjon ² <i>¹Laboratoire d'Étude des Microstructures (LEM)-UMR104, CHATILLON, France, ²Groupe d'étude de la matière condensée (GEMaC)-UMR8615, Versailles, France, ³Laboratoire de physique et chimie des nano-objets (LPCNO)-UMR5215, Toulouse, France</i>		
0854_1278_000298	Steering atoms in the quasi-1D material CrSBr	72
Julian Klein <i>Massachusetts Institute of Technology, Cambridge, MA, USA</i>		
0854_1278_000483	Stretchable Carbon Nanotube Transistors for Neuromorphic Computing	73
Chongwu Zhou, PhD <i>University of Southern California, Los Angeles, CA, USA</i>		
0854_1278_000592	SWNTs: From a Dream Material to A Material That Realizes Your Dream	74
Xinjie Zhang, Kuiyang Jiang <i>Novarials Corporation, Woburn, MA, USA</i>		

0854_1278_000578	The Effect of Amorphous Carbon on Properties of Carbon Nanotube Fibres	75
	James Elliott, Philipp Kloza <i>University of Cambridge, Cambridge, United Kingdom</i>	
0854_1278_000220	Tuning the Electronic and Transport Properties of Graphene Nanoribbons through Stone-Wales Defects	76
	Eduardo Girao ¹ , Thaina Oliveira ¹ , Paloma Silva ¹ , Vincent Meunier ² ¹ <i>Universidade Federal do Piauí, Teresina, Brazil,</i> ² <i>The Pennsylvania State University, State College, PA, USA</i>	
0854_1278_000092	Ultrafast Energy Relaxation in Carbon Nanotube Exciton-Polariton Microcavities	77
	Minjung Son <i>Boston University, Boston, MA, USA</i>	
0854_1278_000476	Ultrascaled Devices based on 2D Semiconductors for Advanced Electronic Applications	78
	Xu Zhang <i>Carnegie Mellon University, Pittsburgh, PA, USA</i>	
0854_1278_000393	Water in Carbon Nanotubes: from Giant Slippage to Hydroelectric Power	79
	Nikita Kavokine <i>Max Planck Institute for Polymer Research, Mainz, Germany</i>	

Contributed Symposium

0854_1278_000388	ADVANCES ON EPITAXIAL CVD GROWTH OF MULTI-LAYERED BN FILMS AND OPTICAL CHARACTERIZATION OF BN CRYSTALS ...	80
	Laure Tailpied ¹ , Sébastien Roux ^{1,2} , Amandine Andrieux-Ledier ³ , Christophe Arnold ² , Frédéric Fossard ¹ , Jean-Sébastien Mérot ¹ , Jean-Manuel Decams ⁴ , François Ducastelle ¹ , Julien Barjon ² , Annick Loiseau ¹ ¹ <i>LEM - ONERA - CNRS - U. Paris Saclay, Chatillon, France,</i> ² <i>GEMaC - Université Versailles Saint Quentin, Versailles, France,</i> ³ <i>DPHY - ONERA - U. Paris Saclay, Chatillon, France,</i> ⁴ <i>Annealsys, Montpellier, France</i>	
0854_1278_000333	ANISOTROPIC THERMOPOWER ON GRAPHENE THIN FILMS DEPOSITED ON FLEXIBLE SUBSTRATES	81
	Johanns Canaval, Ever Quintero, Camilo Balaguera, Daniel Olaya, Yenny Hernandez <i>Physics Department – Universidad de los Andes., Bogota, Colombia</i>	
0854_1278_000422	Atomic Origin of the Axis-Symmetrical Growth and its Breaking of a Single-Wall Carbon Nanotube	82
	Lili Zhang, PhD ¹ , Thomas Hansen ² , Jakob Wagner ² , Chang Liu ¹ , Hui-Ming Cheng ¹ <i>Institute of Metal Research, Chinese Academy of Sciences, shenyang, China,</i> ² <i>Technical University of Denmark, Lyngby, Denmark</i>	

0854_1278_000477	Boosting Selectivity Towards Formate Production Using CuAl Alloy Nanowires By Altering The CO₂ Reduction Reaction Pathway	83
Nageh Allam <i>The American University in Cairo, New Cairo, Egypt</i>		
0854_1278_000075	Carbon nanotubes-based RO membranes for desalination and low-pressure applications	84
Juan Fajardo Diaz, PhD ^{1,2} , Armando Martinez-Iniesta, PhD ¹ , Rodolfo Cruz Silva, PhD ³ , Kenji Takeuchi, PhD ¹ , Koichi Tsuzuki, PhD ¹ , Morinobu Endo, PhD ^{1,2} ¹ Global Aqua Innovation Center, Shinshu University, Nagano, Japan, ² Research Initiative for Supra-Materials, Shinshu University, Nagano, Japan, ³ Applied Chemistry Research Center, Saltillo, Coahuila, Mexico		
0854_1278_000160	Controlled Growth of Horizontally Aligned Single-Walled Carbon Nanotube Arrays	85
Liu Qian ¹ , Jin Zhang, Ying Xie, Yue Li ¹ Peking University, Beijing, China		
0854_1278_000216	Creating a Sustainable World: The Next-Generation Energy Conversion and Storage Technologies Enabled by Carbon Nanostructures	86
Ghulam Yasin, Esko Kauppinen <i>Aalto University, Espoo, Finland</i>		
0854_1278_000192	Degradations and Enantiomeric Effects of (6,5) Carbon Nanotubes In Cellulo	88
Ching-Wei Lin ¹ , Te-I Liu ¹ , Carlos Quiroz ^{1,2} , Yen-Hsuan Lin ¹ , Ai-Phuong Nguyen ^{1,3} , Marco Raabe ¹ ¹ Academia Sinica, Taipei City, Taiwan, ² Taipei Medical University, New Taipei City, Taiwan, ³ National Tsing Hua University, Hsinchu, Taiwan		
0854_1278_000204	Double-layer stacking in the commensurate CDW phase of 1T-TaS₂ observed by resonance Raman Spectroscopy	91
Marcos Pimenta <i>Universidade Federal de Minas Gerais, Belo Horizonte, Brazil</i>		
0854_1278_000320	Emissive Brightening in Molecular Graphene Nanoribbons by Twilight States	92
Bernd Sturdza ¹ , Fanmiao Kong ² , Xuelin Yao ² , Wenhui Niu ³ , Ji Ma ^{3,4} , Moritz Riede ¹ , Xinliang Feng ^{3,4} , Lapo Bogani ^{2,5} , Robin Nicholas ¹ ¹ University of Oxford, Oxford, United Kingdom, ² University of Oxford, Oxford, United Kingdom, ³ Technische Universität Dresden, Dresden, Germany, ⁴ Max Planck Institute of Microstructure Physics, Halle, Germany, ⁵ University of Florence, Sesto Fiorentino, Italy		

0854_1278_000076	Engineering Chirality in Wafer-scale Ordered Carbon Nanotube Architectures	93
	Jacques Doumani ^{1,2} , Minhan Lou ² , Oliver Dewey ¹ , Nina Hong ³ , Jichao Fan ² , Andrey Baydin ¹ , Keshav Zahn ¹ , Yohei Yomogida ⁴ , Kazuhiro Yanagi ⁴ , Matteo Pasquali ¹ , Riichiro Saito ^{4,5,6} , Junichiro Kono ¹ , Weilu Gao ²	
	<i>¹Rice University, Houston, TX, USA, ²University of Utah, Salt Lake City, UT, USA, ³J.A. Woollam Co., Inc., Lincoln, NE, USA, ⁴Tokyo Metropolitan University, Tokyo, Japan, ⁵Tohoku University, Sendai, Japan, ⁶National Taiwan Normal University, Taipei City, Taiwan</i>	
0854_1278_000281	Evaporative Self-assembly of Carbon Nanotube-polymer Superstructures	94
	Yoshitaka Tsuchie, Yoshiyuki Nonoguchi	
	<i>Faculty of Materials Science and Engineering, Kyoto Institute of Technology, Kyoto, Japan</i>	
0854_1278_000381	EXCITONIC INSTABILITY IN NARROW-GAP CARBON NANOTUBES	95
	Giacomo Sesti ^{1,2} , Daniele Varsano ² , Elisa Molinari ^{1,2} , Massimo Rontani ²	
	<i>¹Università degli Studi di Modena e Reggio Emilia, Modena, Italy, ²CNR-NANO, Modena, Italy</i>	
0854_1278_000229	Fabrication and Processing Parameters for Aligned Boron Nitride Nanotube Ceramic Matrix Nanocomposites	96
	Shaan Jagani, Jingyao Dai, Luiz Acauan, Brian Wardle	
	<i>Massachusetts Institute of Technology, Cambridge, MA, USA</i>	
0854_1278_000312	Ferrocene-Enhanced Growth of Millimeter-Long Carbon Nanotubes: Mechanism Study	97
	Delong He, Nabila Zerrouki, Jinbo Bai	
	<i>Centralesupelec, Gif sur Yvette, France</i>	
0854_1278_000502	Field-free deterministic switching of a van der Waals ferromagnet above room temperature	98
	Shivam Kajale, Thanh Nguyen, Mingda Li, Deblina Sarkar	
	<i>Massachusetts Institute of Technology, Cambridge, MA, USA</i>	
0854_1278_000497	Flexible Transmitter for Human Body Communication Based on Carbon Nanotube CMOS Electronics	99
	Dai Muto ¹ , Haruki Uchiyama, PhD ² , Hiromichi Kataura ³ , Yutaka Ohno, PhD ²	
	<i>¹Nagoya University, Nagoya, Japan, ²Nagoya University, Nagoya, Japan, ³National Institute of Advanced Industrial Science and Technology (AIST), Tsukuba, Ibaraki, Japan</i>	
0854_1278_000116	Functionalized Single-Walled Carbon Nanotube Electrodes for Dielectric Elastomer Actuators to Enhance Electro-Mechanical Durability	100
	Matthias Kollosche ^{1,2,3} , Melissa Ricci ¹ , Henning Richter ¹	
	<i>¹Nano-C, Inc., Westwood, MA, USA, ²Iowa State University, Ames, IA, USA, ³Harvard University, Boston, MA, USA</i>	

0854_1278_000371	GRAPHENE DERIVATIVES FOR BIOSENSORS APPLICATIONS	101
	Ana Champi, PhD <i>Universidade Federal do ABC, Santo André, Brazil</i>	
0854_1278_000288	High-crystallinity Single-walled Carbon Nanotube Aerogel Growth: Understanding the Real-time Catalytic Decomposition Reaction	102
	Sook Young Moon, PhD	
0854_1278_000165	High-performance Optoelectronics Enabled with Dry-transferred Transparent Carbon Nanotube Films	103
	Er-Xiong Ding, Peng Liu, Zhipei Sun, Esko I. Kauppinen, Harri Lipsanen <i>Aalto University, Espoo, Finland</i>	
0854_1278_000139	Horizontally Aligned Carbon Nanotube-Reinforced Silicon Carbide Nanocomposites with Ultrahigh Nanofiber Packing Density	104
	Jingyao Dai, Shaan Jagani, Luiz Acauan, Xiaochen Li, Palak Patel, Brian Wardle <i>Massachusetts Institute of Technology, Cambridge, MA, USA</i>	
0854_1278_000348	In-Situ Monitoring Of Mechanical, Dynamical And Thermal Responses Using Carbon Nanotube Fiber Sensors	105
	Jandro Abot, PhD <i>The Catholic University of America, washington DC, DC, USA</i>	
0854_1278_000058	Large-Scale Production and Advanced Computing of Memristor Based on Ionic Layered Minerals	106
	Rongjie Zhang <i>Tsinghua University, Beijing, China</i>	
0854_1278_000423	LUMINESCENCE OF BLACK PHOSPHORUS FILMS: EXFOLIATION-INDUCED DEFECTS AND CONFINED EXCITATIONS	107
	Etienne Carré ^{1,2} , Lorenzo Sponza ¹ , Alain Lusson ² , Ingrid Stenger ² , Sébastien Roux ^{1,2} , Frédéric Fossard ¹ , Nicolas Horezan ³ , Victor Zatzko ⁴ , Bruno Dublak ⁴ , Pierre Sénéor ⁴ , Etienne Gaufres ⁵ , Julien Barjon ² , Annick Loiseau ¹ ¹ LEM - ONERA - CNRS - U. Paris Saclay, Chatillon, France, ² GEMaC - Université Versailles Saint Quentin, Versailles, France, ³ DMAS - ONERA - U. Paris Saclay, Chatillon, France, ⁴ Laboratoire Albert Fert - CNRS - Thales - U. Paris Saclay, Palaiseau, France, ⁵ LP2N - CNRS - IOGS - Université Bordeaux, Talence, France	
0854_1278_000466	Measurements of carbon nanotube length, growth rate, and aerogel formation in a floating catalyst chemical vapour deposition reactor	108
	Adam Boies ¹ , Joe Stallard, PhD, Michael Glerum, Jack Peden, Mabel Qiao ¹ University of Cambridge, Cambridge, United Kingdom	

0854_1278_000209	MICRO-3D-AEROSOL-JET-PRINTING OF 3D ELECTRODES MADE FROM 2D SULFIDE/NANOCARBON FOR ELECTROCHEMICAL WATER SPLITTING	109
	Bodo Baumgartner, MSc ¹ , Paul Patter, MA ² , Markus Hofer, MSc ¹ , Martin Nastran, MSc ¹ , Alexander Wheeldon ² , Filippo Iervolino, PhD ³ , Dogukan Apaydin, PhD ¹ , Alexander Blümel, MSc ² , Dominik Eder, PhD ¹ , Bernhard Bayer, PhD ¹	
	¹ TU Wien, Vienna, Austria, ² JOANNEUM RESEARCH Forschungsgesellschaft mbH, Weiz, Austria, ³ Politecnico di Milano - Italy, Milano, Italy	
0854_1278_000167	Mode coupling bi-stability and spectral broadening in buckled carbon nanotube mechanical resonators	110
	Sharon Rechnitz, Tal Tabachnik, Michael Shlafman, Shlomo Shlafman, Yuval Yaish	
	<i>Technion Israel Institute of technology, Haifa, Israel</i>	
0854_1278_000095	Molecular Aspect Ratio Effect on Axial Thermal Transport in Solution-Spun Carbon Nanotube Fibers	111
	Yingru Song ¹ , Ognyan Stefanov ¹ , Michelle Duran-Chaves ¹ , Ivan Siqueira ¹ , Oliver Dewey ¹ , Natsumi Komatsu ^{1,2} , Junichiro Kono ¹ , Matteo Pasquali ¹ , Geoff Wehmeyer ¹	
	¹ Rice University, Houston, TX, USA, ² University of California, Berkeley, Berkeley, CA, USA	
0854_1278_000366	Multifunctional Performance of Topologically Tuned Auxetic Lattice Nanocomposites	112
	S Kumar, PhD ¹ , J Schneider ²	
	¹ University of Glasgow, Glasgow, United Kingdom, ² University of Glasgow, Glasgow, United Kingdom	
0854_1278_000399	Multiresponsive MXene Soft Robotics	113
	Haozhe Wang, PhD	
	<i>Duke University, Durham, NC, USA</i>	
0854_1278_000197	Multi-walled carbon nanotubes targeting the tumor microenvironment to inhibit melanoma metastasis	114
	Lorena García Hevia ^{1,2} , Rym Soltani ³ , Jesús González ^{1,2} , Olivier Chaloin ³ , Cécilia Ménard-Moyon ³ , Alberto Bianco ³ , Mónica L Fanarraga ^{1,2}	
	¹ University of Cantabria, Santander, Spain, ² IDIVAL, Santander, Spain, ³ University of Strasbourg, Strasbourg, France	
0854_1278_000089	Non-linear Landau Fan Diagram and Extraction of Landau Level Spacing by Open Orbit in Graphene Moiré Superlattices	115
	Pilkyung Moon, PhD ^{1,2,3} , Youngwook Kim, PhD ^{4,5} , Mikito Koshino, PhD ⁶ , Takashi Taniguchi, PhD ⁷ , Kenji Watanabe, PhD ⁷ , Jurgen Smet, PhD ⁵	
	¹ NYU Shanghai, Shanghai, China, ² NYU-ECNU Institute of Physics at NYU Shanghai, Shanghai, China, ³ New York University, New York, NY, USA, ⁴ DGIST, Daegu, Republic of Korea, ⁵ Max-Planck-Institut für Festkörperforschung, Stuttgart, Germany, ⁶ Osaka University, Osaka, Japan, ⁷ National Institute for Materials Science, Tsukuba, Japan	

0854_1278_000039	Observation of bright hybridized exciton in MoTe₂/MoSe₂ heterostacks	116
	Shen Zhao <i>Fakultät für Physik, Ludwig-Maximilians-Universität München, München, Germany</i>	
0854_1278_000226	Patterning dye J-aggregates by activated diffusion in bended BNNTs	117
	Jean-Baptiste MARCEAU ¹ , Duc-Minh TA ² , Alberto AGUILAR ² , Annick LOISEAU ³ , Richard MARTEL ⁴ , Pierre BON ² , Raphaël VOITURIEZ ⁵ , Gaëlle RECHER ¹ , Etienne GAUFRES ¹ <i>¹Laboratoire Photonique, Numérique et Nanosciences (LP2N)-UMR 5298, Talence, France, ²XLIM-UMR CNRS 7252, Limoges, France, ³Laboratoire d'Étude des Microstructures (LEM)-UMR104, CHATILLON, France, ⁴Département de chimie-Université de Montréal, Montréal, QC, Canada, ⁵Laboratory Jean Perrin-UMR 8237, Paris, France</i>	
0854_1278_000240	Polyaniline grafted Carbon Nanotube Composite Fibers for Flexible Fiber-Shaped Supercapacitors	118
	Dongju Lee ¹ , Junghwan Kim, PhD ¹ , Chae Won Kim ² , Seo Gyun Kim, PhD ¹ , Yuanzhe Piao, PhD ² , Bon-Cheol Ku, PhD ¹ <i>¹Korea Institute of Science and Technology, Wanju-gun, Republic of Korea, ²Seoul National University, Suwon, Republic of Korea</i>	
0854_1278_000513	Resonant Raman in Armchair Graphene Nanoribbons from First-Principles	119
	Natalya Sheremetyeva, PhD ¹ , Michael Lamparski, PhD ² , Liangbo Liang, PhD ³ , Gabriela Borin Barin, PhD ⁴ , Vincent Meunier, PhD ¹ <i>¹The Pennsylvania State University, State College, PA, USA, ²Rensselaer Polytechnic Institute, Troy, NY, USA, ³Oak Ridge National Laboratory, Oak Ridge, TN, USA, ⁴Empa, Swiss Federal Laboratories for Materials Science and Technology, Dübendorf, Switzerland</i>	
0854_1278_000025	Scaling of Coulomb Defects in Low-D Semiconductors from Variational and Modified Hueckel Calculations	120
	Klaus Eckstein, Tobias Hertel <i>Julius-Maximilians University, Wuerzburg, Germany</i>	
0854_1278_000024	Spectral Fingerprinting Coupled Machine Learning: An Optimized Tool for Cellular Phenotype Identification	122
	Aceer Nadeem ¹ , Sarah Lyons ¹ , Aidan Kindopp ¹ , Amanda Jamieson ² , Daniel Roxbury ¹ <i>¹University of Rhode Island, Kingston, RI, USA, ²Brown University, Providence, RI, USA</i>	
0854_1278_000538	Surface Functionalization for Chiral Dichroism Induction in Carbon Nanotubes	123
	Dmitri Kilin <i>North Dakota State University, Fargo, ND, USA</i>	

0854_1278_000456 **Synthesis of Iron Single-Walled Carbon Nanotube from Ferrocene as an Interlayer in Lithium–Sulfur Batteries**.....124

Aqeel Hussain, PhD

Aalto University, Espoo, Finland

0854_1278_000542 **The Structure-Function Relationship in Graphene Oxide Membranes: Beyond D-Spacing**.....125

Nima Zakeri, PhD, Marta Cerruti, PhD

McGill University, Montreal, QC, Canada

Poster

0854_1278_000469 **¹H-NMR Trajectories for Analyzing the Growth and Purification of 2D Polyaramids**.....126

Zitang Wei, PhD, Michael Strano, PhD

Massachusetts Institute of Technology, Cambridge, MA, USA

0854_1278_000070 **2D Metamaterials : Pseudo Non-Reciprocity Induced Topological Effect, Negative Stiffness Lattice**.....127

Haoran Nie, PhD, Chaoran Jiang, Lei Xu

The Chinese University of Hong Kong, Hong Kong SAR, China

0854_1278_000112 **6K UniMelt: Microwave-Based Plasma Technology for Versatile Production of Nano-Engineered Materials**.....128

Ashley Kaiser, PhD

6K Inc., North Andover, MA, USA

0854_1278_000251 **A Bond-Order-Based Machine-Learning Interatomic Potential for Carbon Allotropes**.....129

Ikuma Kohata¹, Ryo Yoshikawa¹, Kaoru Hisama², Keigo Otsuka¹, Shigeo Maruyama¹

¹*The University of Tokyo, Tokyo, Japan*, ²*Research Initiative for Supra-Materials, Shinshu University, Nagano, Japan*

0854_1278_000550 **A Machine-Learning Force Field of Cobalt–Tungsten–Carbon Systems for Growth Simulations of Single-Walled Carbon Nanotubes**130

Sida Sun, Yan Li

Peking University, Beijing, China

0854_1278_000432 **A Novel Multi-Source Static Computed Tomography Based on Carbon Nanotube X-ray Sources**131

Amar Gupta, PhD^{1,2}, Jake Hecla, PhD³, Matt Tivnan, PhD^{1,2}, Dufan Wu, PhD^{1,2}, Tim Moulton², Darash Desai, PhD², Kai Yang, PhD², Wolfgang Krull², Rajiv Gupta, MD, PhD^{1,2}

¹*Harvard Medical School, Boston, MA, USA*, ²*Massachusetts General Hospital, Boston, MA, USA*, ³*Massachusetts Institute of Technology, Cambridge, MA, USA*

0854_1278_000294	A Releasable Self-powered Chemical Sensing Platform using 2D Materials	132
	Sungyun Yang, Byungha Kang, A. Merritt Brooks, Michael Strano <i>Massachusetts Institute of Technology, Cambridge, MA, USA</i>	
0854_1278_000128	Aggregation Mechanism of High Aspect Ratio Carbon Nanotubes and Their Dispersion	134
	Zhenxing Zhu, Fei Wei <i>Tsinghua University, Department of Chemical Engineering, Beijing, China</i>	
0854_1278_000329	Aligned Boron Nitride Nanotube Transparent Epoxy Nanocomposite	135
	Luiz Acauan ¹ , Hillel Dei ¹ , Nyvia Lyles ² , Shaan Jagani ¹ , Shigeo Maruyama ³ , Rong Xiang ⁴ , Brian Wardle ¹ <i>¹Massachusetts Institute of Technology, Cambridge, MA, USA, ²Howard University, Washington, DC, USA, ³The University of Tokyo, Tokyo, Japan, ⁴Zhejiang University, Hangzhou, China</i>	
0854_1278_000232	Artificial Intelligence-Assisted Image Analysis for Fluorescence Microscope Cell Imaging	136
	Ugur Topkiran, Ali Gasimli, Anton Naumov <i>Texas Christian University, Fort Worth, TX, USA</i>	
0854_1278_000323	Atmospheric Pressure Plasma Nanoparticle Generator For Scalable CNT Production In A FCCVD Process	137
	Jui Junnarkar, Eldar Khabushev, PhD, Clay Kacica, PhD, Arthur Sloan, PhD, Glen Irvin, PhD, Matteo Pasquali, PhD <i>Rice University, Houston, TX, USA</i>	
0854_1278_000511	Atomic Insights into the Oxidation Mechanism of Ultrathin Hafnium Metal Film	138
	Zhenjing Liu, Rafael Jaramillo, Frances Ross <i>Massachusetts Institute of Technology, Cambridge, MA, USA</i>	
0854_1278_000494	Atomically Thin, Highly Packed, and Aligned Carbon Nanotube Films	139
	Jacques Doumani, Somesh Sasmal, Ting-Wei Chang, Junichiro Kono <i>Rice University, Houston, TX, USA</i>	
0854_1278_000464	ATPE sorted semiconducting, metallic and single chiral SWCNTs produced at NoPo lab	140
	Shivananad Nannuri, Eldho Kurian, Anto Godwin, Gadhadar Reddy <i>NoPo Nanotechnologies India Private Limited, Bengaluru, India</i>	
0854_1278_000086	Bandgap-coupled growth and assembly of ultrapure semiconducting carbon nanotubes	141
	Zhenxing Zhu, PhD, Fei Wei, PhD <i>Tsinghua University, Department of Chemical Engineering, Beijing, China</i>	

0854_1278_000352	Biaxial Mechanical Densification of Vertically Aligned Boron Nitride Nanotubes	142
	Armando Neto, Marianna Rogers, Luiz Acauan, Brian Wardle, Shweta Sharma <i>Massachusetts Institute of Technology, Cambridge, MA, USA</i>	
0854_1278_000395	Biosensors based on MWCNT	143
	Ovidiu Tiprişan, PhD Eng <i>Babes-Bolyai University of Cluj-Napoca, Romania, Cluj-Napoca, Romania</i>	
0854_1278_000122	Burst Nucleation of Matrix on Doped Graphene for Quantitative MALDI-ToF Mass Spectrometry with Tunable Ion Yield	144
	Sanghwan Park, PhD <i>Ulsan National Institute of Science and Technology, Ulsan, Republic of Korea</i>	
0854_1278_000299	Carbon nanotube electron blackbody and its radiation spectra .	145
	Guo Chen <i>Department of Physics, Tsinghua University, Beijing, China</i>	
0854_1278_000328	Carbon Nanotube Fiber Production for Displacement of Difficult to Decarbonize Structural Materials with Free Hydrogen Co-production	146
	Alex Dantzler ¹ , Oliver Dewey, PhD ¹ , Arthur Sloan, PhD ¹ , Robert Headrick, PhD ² , Glen Irvin, PhD ¹ , Matteo Pasquali, PhD ¹ <i>¹Rice University, Houston, TX, USA, ²Next Generation Breakthrough Research, Materials Chemistry, Shell, Houston, TX, USA</i>	
0854_1278_000372	Carbon Nanotube Platform for virus enrichment and detection	147
	Yin-Ting Yeh, Mauricio Terrones <i>The Pennsylvania State University, University Park, PA, USA</i>	
0854_1278_000344	Carbon Nanotube/Bismaleimide Nanocomposite Laminates with Ultrahigh Nanofiber Volume Fraction	148
	Carina Li, Yuying Lin, Jingyao Dai, Marianna Rogers, Brian Wardle <i>Massachusetts Institute of Technology, Cambridge, MA, USA</i>	
0854_1278_000196	Carbon Nanotube-based FET Arrays for Integrated Biosensor Platforms	149
	Leticia Alves da Silva, Sascha Hermann <i>Chemnitz University of Technology, Chemnitz, Germany</i>	
0854_1278_000136	Carbon Nanotube-based Strain-Configurable Nanodevices	150
	Simon Böttger ¹ , Martin Hartmann ¹ , Sascha Hermann ^{1,2} <i>¹Chemnitz University of Technology, Chemnitz, Germany, ²Fraunhofer Institute of Electronic Nano Systems, Chemnitz, Germany</i>	

- 0854_1278_000394 **Chalcogen Anion Type-Dependent Efficiency of Synthesizing Janus Monolayer Transition Metal Dichalcogenides by Atomic-Layer Substitution**151
Tianyi Zhang¹, Shengxi Huang², Mauricio Terrones³, Yunfan Guo⁴, Ting Cao⁵, Jing Kong¹
¹*Massachusetts Institute of Technology, Cambridge, MA, USA*, ²*Rice University, Houston, TX, USA*, ³*Penn State University, University Park, PA, USA*, ⁴*Zhejiang University, Hangzhou, China*, ⁵*University of Washington, Seattle, WA, USA*
- 0854_1278_000346 **Characterization of Carbon Nanotube / Poly(Methyl Methacrylate) Bulk Nanocomposite Laminate and Filament**.....152
Yuying Lin, Carina Li, PhD, Erick Gonzalez, Jingyao Dai, PhD, Luiz Acauan, PhD, Brian Wardle, PhD
Massachusetts Institute of Technology, Cambridge, MA, USA
- 0854_1278_000425 **Charge Transport Characteristics in Non-van der Waals 2D Transition Metal Nitrides Synthesized via Atomic Substitution Approach**153
Hongze Gao¹, Da Zhou², Zifan Wang¹, Lu Ping³, Jun Cao¹, Mauricio Terrones², Xi Ling^{1,3}
¹*Boston University, Boston, MA, USA*, ²*Penn State University, University Park, PA, USA*, ³*Boston University, Boston, MA, USA*
- 0854_1278_000362 **Chemical Bonding of Carbon Nanotubes with Metals as a Promising Path for Hybrid Materials Development**.....154
Noe Alvarez, PhD
University of Cincinnati, Cincinnati, OH, USA
- 0854_1278_000499 **Chemical substitution effect in trigonal PtBi₂ with a triply degenerate point**155
Takehito Suzuki¹, Hisashi Inoue², Ryosuke Mikawa³, Haruki Takei³, Takuro Katsufuji³
¹*Toho University, Funabashi, Japan*, ²*National Institute of Advanced Industrial Science and Technology (AIST), Tsukuba, Ibaraki, Japan*, ³*Waseda University, Tokyo, Japan*
- 0854_1278_000063 **Chemical Vapor Deposition Synthesis and Anisotropic Optical Properties of 1T₂-Phase WS₂ Atomic Layers**.....156
Mitsuhiro Okada¹, Yung-Chang Lin¹, Tarojiro Matsumura¹, Adlen Smiri¹, Wen Hsin Chang¹, Naoya Okada¹, Yasunobu Ando¹, Toshitaka Kubo¹, Kazu Suenaga^{1,2}, Takeshi Nakanishi¹, Toshifumi Irisawa¹, Takatoshi Yamada¹
¹*National Institute of Advanced Industrial and Science Technology, Tsukuba, Japan*, ²*Osaka University, Osaka, Japan*
- 0854_1278_000242 **Chiral Dependent Growth Modes of Carbon Nanotubes from Machine Learning driven Molecular Dynamics**157
Daniel Hedman, PhD¹, Christophe Bichara, PhD²
¹*Institute for Basic Science, Ulsan, Republic of Korea*, ²*Aix-Marseille Université, CNRS, CINaM, Marseille, France*

0854_1278_000080	Chirality of Double-Walled Carbon Nanotubes by TEM Electron Diffraction Pattern	158
	Zhenyu Xu, Anastasios Karakassides, Hua Jiang, Qiang Zhang, Esko Kauppinen <i>Aalto University, Espoo, Finland</i>	
0854_1278_000553	Chirality Selective Growth of Bulk Single-walled Carbon Nanotubes Using Cobalt-Sulfur Catalyst	159
	Zihan Xu ¹ , Zeyao Zhang ^{1,2} , Yan Li ¹ ¹ <i>Peking University, Beijing, China</i> , ² <i>Institute of Carbon-Based Thin Film Electronics, Peking University, Shanxi, Taiyuan, China</i>	
0854_1278_000289	Chirality-Dependent Electrical Transport Properties of Carbon Nanotubes Obtained by Experimental Measurement	160
	Huaping Liu, PhD <i>Beijing National Laboratory for Condensed Matter Physics, Institute of Physics, Chinese Academy of Sciences, Beijing, China</i>	
0854_1278_000020	Chirality-Induced Spin Selectivity in Peptide Functionalized Carbon Nanotubes	161
	Md Anik Hossain, Sandipan Pramanik, PhD <i>University of Alberta, Edmonton, AB, Canada</i>	
0854_1278_000555	Chirality-Selective Synthesis of Single-Walled Carbon Nanotubes Using Cobalt Tungstate Nanoparticles as Precursors	162
	Xinrui Zhang, Xu Liu, Sida Sun, Yan Li <i>Peking University, Beijing, China</i>	
0854_1278_000169	Collective modulation of solution-processed molybdenum disulfide for tunable electronics and optics	163
	Songwei Liu, Yingyi Wen, Jingfang Pei, Yang Liu, Guohua Hu <i>The Chinese University of Hong Kong, Hong Kong, China</i>	
0854_1278_000096	Colorimetric Paper with Inkjet-Printed Carbon Nanotube Chemiresistors for Detection of Liquid and Gas Phase Chemical Warfare Agents	164
	Seongyeop Lim, Sanghwan Park, PhD, Seongwoo Lee, Cheongha Lee, Chang Young Lee, PhD <i>Ulsan National Institute of Science and Technology, Ulsan, Republic of Korea</i>	
0854_1278_000377	Complex Refractive Index Spectra Of Single-chirality Carbon Nanotube Membranes With Birefringent Optical Response	165
	Hengkai Wu ¹ , Taishi Nishihara ¹ , Akira Takakura ¹ , Kazunari Matsuda ¹ , Takeshi Tanaka ² , Hiromichi Kataura ² , Yuhei Miyauchi ¹ ¹ <i>Kyoto University, Kyoto, Japan</i> , ² <i>National Institute of Advanced Industrial Science and Technology (AIST), Tsukuba, Ibaraki, Japan</i>	

- 0854_1278_000050 **Confinement-Induced Nonlocality and Casimir force In Transdimensional Systems**166
 Igor Bondarev, PhD¹, Michael Pugh, MS¹, Pablo Rodrigues-Lopez, PhD², Lilia Woods, PhD³, Mauro Antezza, PhD⁴
¹North Carolina Central University, Durham, NC, USA, ²Universidad Rey Juan Carlos, Madrid, Spain, ³University of South Florida - Tampa, Tampa, FL, USA, ⁴University of Montpellier, Montpellier, France
- 0854_1278_000269 **Controlled growth of semiconducting SWNT arrays through a dual-ion-implantation strategy**167
 Ying Xie, PhD, Yue Li, PhD, Liu Qian, PhD, Ziqiang Zhao, Jin Zhang
 Peking University, Beijing, China
- 0854_1278_000434 **COULD WE REPLACE DINOSAUR JUICE LUBRICANTS WITH DARK GREEN VEGAN PRODUCTS?**168
 Rafał drysiak¹, Szymon Ruczka¹, Łukasz Wojciechowski², Magdalena Skrzypek², Sławomir Boncel¹
¹Silesian University of Technology, Faculty of Chemistry, CONE, NanoCarbonGroup, Gliwice, Poland, ²Poznan University of Technology, Institute of Machines and Motor Vehicles, Poznan, Poland
- 0854_1278_000019 **Covalently Functionalized Carbon Nanotube-Based Nickel Complexes for Electrocatalytic Aryl Halide Coupling**169
 Thomas Pioch, Timothy Swager, PhD
 Massachusetts Institute of Technology, Cambridge, MA, USA
- 0854_1278_000347 **Critical roles of Fe and Co binary catalysts in ACCVD growth of SWCNTs**170
 Qingmei Hu¹, Ya Feng^{1,2}, Kunio Mori¹, Ryo Yoshikawa¹, Yongjia Zheng^{1,3}, Wanyu Dai¹, Ryotaro Kaneda¹, Aina Parera⁴, Wim Wenseleers⁴, Sofie Cambré⁴, Shohei Chiashi¹, Rong Xiang^{1,3}, Keigo Ostuka¹, Shigeo Maruyama¹
¹The university of Tokyo, Tokyo, Japan, ²Dalian University of Technology, Dalian, China, ³Zhejiang University, Hangzhou, China, ⁴University of Antwerp, Antwerp, Belgium
- 0854_1278_000414 **CROSS-LINKING OF CARBON NANOTUBES USING s-TETRAZINE DERIVATIVES**171
 Anna Blacha¹, Szymon Ruczka¹, Pierre Audebert², Artur Terzyk³, Sławomir Boncel¹
¹Silesian University of Technology, NanoCarbon Group, Gliwice, Poland, ²Université Paris-Saclay, ENS Paris-Saclay, CNRS, Paris-Saclay, France, ³Nicolaus Copernicus University in Torun, Physicochemistry of Carbon Materials Group, Torun, Poland
- 0854_1278_000468 **Decoding Adaptive Plant Signaling: Mathematical Modeling Using Single-Walled Carbon Nanotube Fluorescence Sensing Data**172
 Thomas Porter, Michael Strano, PhD
 Massachusetts Institute of Technology, Cambridge, MA, USA

0854_1278_000201	Detection Sensitivity of a Carbon Nanotube based Crack Gauge	173
	Seth Kessler, PhD ¹ , Christine Shubert Kabban, PhD ² , Yosef Stein ³ <i>¹Metis Design Corporation, Boston, MA, USA, ²Air Force Institute of Technology, Wright-Patterson AFB, OH, USA, ³Analog Devices, Inc., Norwood, MA, USA</i>	
0854_1278_000552	Diameter Control of Single-Walled Carbon Nanotubes Produced by Arc Discharge	174
	Yixi Yao ¹ , Zeyao Zhang ^{1,2} , Yan Li ¹ <i>¹Peking University, Beijing, China, ²Institute of Carbon-Based Thin Film Electronics, Peking University, Shanxi, Taiyuan, China</i>	
0854_1278_000219	Diffusion 1H-NMR (DOSY) for Analyzing 2D Polyaramid Polymers	175
	Michelle Quien, Michael Strano <i>Massachusetts Institute of Technology, Cambridge, MA, USA</i>	
0854_1278_000326	Effect of Feedback Control Systems of Catalysts in Deep-Injection Floating Catalyst Chemical Vapor Deposition (DI-FCCVD)	176
	Mingrui Gong ¹ , Ana Victoria Benavides Figueroa ¹ , Eldar Khabushev, PhD ¹ , Arthur Sloan, PhD, Glen Irvin, PhD ¹ , Matteo Pasquali, PhD ¹ <i>¹Rice University, Houston, TX, USA</i>	
0854_1278_000475	Effect of High Packing Aligned Carbon Nanotube Nanocomposites on Polysiloxane Thermal Protection Properties	177
	Palak Patel ¹ , Steven Kim ² , Norah Miller ¹ , Jingyao Dai ¹ , Jarrod Buffy ³ , Joseph Koo ² , Brian Wardle ¹ <i>¹Massachusetts Institute of Technology, Cambridge, MA, USA, ²The University of Texas at Austin, Austin, TX, USA, ³Techneglas LLC, Perrysburg, OH, USA</i>	
0854_1278_000451	Effect of oxidation on water adsorption and dissociation in transition metal chalcogenides films epitaxially grown by molecular beam epitaxy	178
	Hyuk Jin Kim, Young Jun Chang <i>University of Seoul, Seoul, Republic of Korea</i>	
0854_1278_000148	Effect of Reactor Orientation on FCCVD Synthesis of Few-Walled Carbon Nanotubes	179
	Ana Victoria Benavides Figueroa, MA, Mingrui Gong, Jui Junnarkar, Glen Irvin, PhD, Matteo Pasquali, PhD <i>Rice University, Houston, TX, USA</i>	
0854_1278_000463	Efficient green-emitting 0D Mn²⁺-doped Cs₃CdBr₅ perovskite for WLEDs and X-ray imaging	180
	Tongtong Kou, Liang Wang, William Yu <i>Shandong University, Jinan, China</i>	

0854_1278_000560	Electrical characterization of SWCNT bundles	181
Abu Khan ¹ , Nan Wei ² , Kimmo Mustonen ³ , Esko Kauppinen ¹		
¹ Aalto University, Espoo, Finland, ² Peking University, Beijing, China, ³ University of Vienna, Vienna, Austria		
0854_1278_000172	Electronic Properties of One-Dimensional Titanate Nanofilaments and their Dye-Sensitization Behavior	182
Adam Walter, Gregory Schwenk, Jacob Cope, Kaustubh Sudhakar, Michel Barsoum		
Drexel University, Philadelphia, PA, USA		
0854_1278_000306	Electronic transport properties of the carbon nanotubes with the porphyrin-like substitutional defect	183
Gunn Kim, Jinwoong Chae		
Sejong University, Seoul, Republic of Korea		
0854_1278_000077	Electrothermal free-form additive manufacturing of nanotube-loaded thermosets	184
Micah Green, PhD, Anubhav Sarmah, PhD, Ethan Harkin		
Texas A&M University, College Station, TX, USA		
0854_1278_000210	Elucidating the Prominent Role of Non-Electrostatic Barriers in the Stabilization of Individual Carbon Nanotubes in Water using Bile Salt Surfactants ...	185
Rahul Prasanna Misra ¹ , Peng Wang ² , Chiyu Zhang ² , YuHuang Wang ^{2,3} , Daniel Blankschtein ¹		
¹ Massachusetts Institute of Technology, Cambridge, MA, USA, ² University of Maryland, College Park, MD, USA, ³ Maryland NanoCenter, University of Maryland, College Park, MD, USA		
0854_1278_000097	Encapsulation of High-Frequency CNT-based FETs for RF Communication	186
Martin Hartmann, Martin Ernst, Simon Böttger, Sascha Hermann		
Chemnitz University of Technology, Chemnitz, Germany		
0854_1278_000403	Engineering Organic Color Centers along Single-Walled Carbon Nanotubes with DNA	187
Abhindek Kizhakke Veetil ¹ , Xiaojian Wu ¹ , Mijin Kim ^{1,2} , Lucy Wang ¹ , YuHuang Wang ¹		
¹ University of Maryland, College Park, MD, USA, ² Georgia Institute of Technology, Atlanta, GA, USA		
0854_1278_000416	Enhancing VRFB Performance: Horizontally Aligned CNT Nanocomposites Bipolar Plates	188
Jae-Moon Jeong ¹ , Jingyao Dai, PhD ² , Luiz Acauan, PhD ² , Kwang Il Jeong, PhD ¹ , Hyunsoo Hong ¹ , Brian Wardle, PhD ² , Seong Su Kim, PhD ¹		
¹ KAIST, Daejeon, Republic of Korea, ² Massachusetts Institute of Technology, Cambridge, MA, USA		
0854_1278_000195	Evolving the Synthesis of Horizontally Aligned Carbon Nanotube Arrays: AI-Driven Catalyst Innovation and Density Control	190
Yue Li, Shurui Wang, Zhou Lv, Ziqiang Zhao, Yaodong Yang, Liu Qian, Jin Zhang		
Peking University, Beijing, China		

0854_1278_000452	Excitonic Fano Line Shape in Scattering of Surfactant-Wrapped Carbon Nanotube Dispersion	191
	In-Seung Choi, Seongjoo Hwang, Sang-Yong Ju <i>Yonsei University, Seoul, Republic of Korea</i>	
0854_1278_000447	Excitonic-Optics Study of 2D Chalcogenides Layered Semiconductors	192
	Ching-Hwa Ho <i>National Taiwan University of Science and Technology, Taipei, Taiwan</i>	
0854_1278_000580	Experimental and Theoretical Calculations of Fluorinated Few-layer Graphene/epoxy Composite Coatings for Anticorrosion Applications	193
	Wei-Ren Liu, PhD <i>Chung Yuan Christian University, Taoyuan, Taiwan</i>	
0854_1278_000117	Exploration into Interstitial Crosslinks Capable of Strengthening Boron Nitride Nanotube Bundles	194
	Nicholas Tjahjono ¹ , Evgeni Penev ¹ , Vesselin Yamakov ² , Cheol Park ³ , Boris Yakobson ¹ ¹ Rice University, Houston, TX, USA, ² National Institute of Aerospace, Hampton, VA, USA, ³ NASA Langley Research Center, Hampton, VA, USA	
0854_1278_000101	Exploring polymer contamination cleaning and characterization approaches for aligned CNT material	195
	Marina Y. Timmermans ¹ , Carlos R. Cunha ^{1,2} , Luca Mana ¹ , Xiangyu Wu ¹ , Dennis Lin ¹ , Himanshu Sharma ¹ , Pieter-Jan Wyndaele ^{1,3} , Lijun Liu ^{1,3} , Katherine R. Jenkins ⁴ , Michael S. Arnold ⁴ , Steven Brems ¹ , Cesar J. L. de la Rosa ¹ , Gouri S. Kar ¹ , Jean-Francois de Marneffe ¹ ¹ imec, Leuven, Belgium, ² Instituto Superior Tecnico, Lisbon, Portugal, ³ KU Leuven, Leuven, Belgium, ⁴ SixLine Semiconductor, Inc., Middleton, WI, USA	
0854_1278_000290	Fabrication of SWCNT Thin Films at the Interface of Liquid-Liquid Phase Separation	196
	Seiya Nishida, Yusaku Shimada, Tsuyoshi Endo, Ryotaro Kaneda, Keigo Ostuka, Shigeo Maruyama, Shohei Chiashi <i>The University of Tokyo, Tokyo, Japan</i>	
0854_1278_000119	Facilitating Quasi-van der Waals Epitaxy of WS₂ on Sapphire through Tungsten Oxide	197
	Assael Cohen ¹ , Pranab Mohapatra, PhD ² , Simon Hettler, PhD ³ , Raul Arenal ³ , Ariel Ismach ² ¹ Technion Israel Institute of technology, Haifa, Israel, ² Tel Aviv University, Tel Aviv, Israel, ³ Instituto de Nanociencia y Materiales de Aragon (INMA), CSIC-Universidad de Zaragoza, Zaragoza, Spain	
0854_1278_000021	From Dots to Tubes – the Reverse Scenario of Bottom-Up Catalyst-free Synthesis of N-doped CNTs	198
	Slawomir Boncel, DSc, PhD, Eng, Anna Kolanowska, PhD, Eng <i>Silesian University of Technology, NanoCarbon Group, Gliwice, Poland</i>	

0854_1278_000334	Functional Materials based on wood carbon nanotubes and graphene	199
	Agnieszka Lekawa-Raus, PhD, DSc, Eng. ¹ , Damian Łukawski ² <i>¹Warsaw University of Technology, Warsaw, Poland, ²Poznan University of Technology, Poznan, Poland</i>	
0854_1278_000133	Giant Second-Harmonic Generation from Aligned Enantiomer-Enriched Carbon Nanotube Films	200
	Jacques Doumani ¹ , Rui Xu ¹ , Nina Hong ² , Fuyang Tay ¹ , Weilu Gao ³ , Riichiro Saito ^{4,5,6} , Yohei Yomogida ⁴ , Kazuhiro Yanagi ⁴ , Vasili Perebeinos ⁷ , Andrey Baydin ¹ , Junichiro Kono ¹ , Hanyu Zhu ¹ <i>¹Rice University, Houston, TX, USA, ²J.A. Woollam Co., Inc., Lincoln, NE, USA, ³University of Utah, Salt Lake City, UT, USA, ⁴Tokyo Metropolitan University, Tokyo, Japan, ⁵Tohoku University, Sendai, Japan, ⁶National Taiwan Normal University, Taipei City, Taiwan, ⁷University at Buffalo, Amherst, NY, USA</i>	
0854_1278_000488	Growth of Nanostructured Molybdenum Disulfide (MoS₂) Thin Film Using the Plasma-Enhanced Atomic Layer Deposition for the Application of Electronic Materials	201
	Ibraheem Giwa, Fabian Sanchez, Elton Mawire, Qunying Yuan, Zhigang Xiao <i>Alabama A&M University, Normal, AL, USA</i>	
0854_1278_000349	Heavy Anchoring of Silver Nanoparticles on Carbon Nanotubes	202
	Jen-Hung Fang, PhD ¹ , Luiz Acauan, PhD ¹ , Aniruddha Ghosh ¹ , Yosi Stein, PhD ² , Brian Wardle, PhD ¹ <i>¹Massachusetts Institute of Technology, Cambridge, MA, USA, ²Analog Devices, Inc., Norwood, MA, USA</i>	
0854_1278_000221	Hierarchical Mesostructures of Anatase Nanoparticles for Photodegradation of Bisphenol-A	203
	Treesa Reji, Adam Walter, Yasunori Hioki, Gregory Schwenk, PhD, Mohamed Ibrahim, Hussein Badr, PhD, Michel Barsoum, PhD	
0854_1278_000428	High Performance Dielectric Elastomer Actuators with Carbon Nanotubes	204
	Suhan Kim ¹ , YuFeng (Kevin) Chen <i>¹Massachusetts Institute of Technology, Cambridge, MA, USA</i>	
0854_1278_000066	High-Precision Sorting of Single-Walled Carbon Nanotubes Using the Aqueous Two-Phase Extraction Method	205
	Blazej Podlesny, Dawid Janas <i>Silesian University of Technology, Gliwice, Poland</i>	

0854_1278_000174	High-yield liquid phase exfoliation of graphene utilizing low boiling co-solvent solutions and ammonia	206
	Martin Nastran, MSc ¹ , Paul Peschek ¹ , Izabela Walendzik ¹ , Jakob Rath, MSc ¹ , Bernhard Fickl, MSc ¹ , Jasmin Schubert, PhD ¹ , Gabriel Szabo, MSc ² , Richard Wilhelm, PhD ² , Jochen Schmidt, PhD ³ , Dominik Eder, PhD ¹ , Bernhard Bayer, PhD ¹	
	<i>¹TU Wien, Faculty of Technical Chemistry, Vienna, Austria, ²University of Vienna, Faculty of Physics, Vienna, Austria, ³carbon-solutions Hintsteiner GmbH, Mürzhofen, Austria</i>	
0854_1278_000215	High-Yield Separation of Single-Walled Carbon Nanotubes Using Conjugated Polymer Extraction	207
	Dominik Just, Dawid Janas	
	<i>Silesian University of Technology, Gliwice, Poland</i>	
0854_1278_000261	Hysteresis in the transfer characteristics of graphene field-effect transistors elucidated by nitrogen vacancy centers in nanodiamonds	208
	Kazuki Nishibara ¹ , Seiji Akita, PhD ² , Takayuki Arie, PhD ³	
	<i>¹Osaka Metropolitan University - Osaka, Sakai, Japan, ²Osaka Metropolitan University - Osaka, Sakai, Japan, ³Osaka Metropolitan University - Osaka, Sakai, Japan</i>	
0854_1278_000072	ICEPHOBIC AND SELF-HEALING HYDROXY-NANOCARBON COMPOSITES	209
	Monika Tarnowska ¹ , Emil Korczeniewski ² , Artur Terzyk ² , Sławomir Boncel ¹	
	<i>¹Silesian University of Technology, NanoCarbon Group, Gliwice, Poland, ²Nicolaus Copernicus University in Torun, Physicochemistry of Carbon Materials Group, Torun, Poland</i>	
0854_1278_000246	Improving Energy Dissipation for Ballistic Impacts by Ion Irradiation of MWCNT Mats	210
	Ned Thomas, PhD, Kailu Xiao, PhD	
	<i>Texas A&M University, College Station, TX, USA</i>	
0854_1278_000099	In situ observation of vapor-liquid-solid growth of monolayer WS₂ in confined space of substrate-stacked microreactor for crystallinity control	211
	Hiroo Suzuki, PhD ^{1,2} , Shuhei Aso ² , Koki Tanaka ² , Senda Yutaro ² , Yasuhiko Hayashi, PhD ^{1,2}	
	<i>¹Life, Natural Science and Technology, Institute of Academic and Research, Okayama University, Okayama, Japan, ²Department of Electrical and Communication Engineering, Faculty of Engineering, Okayama University, Okayama, Japan</i>	
0854_1278_000214	In vivo and ex vivo imaging with near-infrared emitting graphene quantum dots	212
	Alina Valimukhametova, Natalia Castro Lopez, Floyd Wormley, Anton Naumov	
	<i>Texas Christian University, Fort Worth, TX, USA</i>	
0854_1278_000134	In-situ microscopy of 2-dimensional carbon nanotube liquid crystals at liquid/liquid interfaces	213
	James Unzaga, Evan Wehbe, Michael Arnold, PhD	
	<i>University of Wisconsin - Madison, Madison, WI, USA</i>	

0854_1278_000138	Intershell Locking of Double-walled Carbon Nanotubes Resulting from Enhanced Intershell Friction at High Shear Rates	215
	Hongjie Yue, Fei Wei <i>Tsinghua University, Department of Chemical Engineering, Beijing, China</i>	
0854_1278_000159	Introduction and properties of mass-producible CNT-CF-hybrid structural materials	217
	Keisuke Ishizeki, PhD, Fei Deng, PhD <i>CARBON FLY, Inc., Tokyo, Japan</i>	
0854_1278_000554	Investigating Chirality Preference of the Growth of Single-Walled Carbon Nanotubes with Machine-Learning Force Fields	218
	Sida Sun, Yan Li <i>Peking University, Beijing, China</i>	
0854_1278_000175	Iron Nanoparticles Evolution in FCCVD: Kinetic Modelling and Experimental Validation	219
	Clarissa Giudici ¹ , Miguel Vazquez-Pufleau ² , Matteo Maestri ¹ , Matteo Pelucchi ¹ , Juan Vilatela ² <i>¹Politecnico di Milano - Italy, Milano, Italy, ²IMDEA Materials Institute - Spain, Getafe, Madrid, Spain</i>	
0854_1278_000411	ISOXAZOLE-FUNCTIONALIZED CARBON NANOTUBES: SYNTHESIS AND ELECTROOPTICAL PROPERTIES	220
	Zunaira Amjad, M.Phil, Slawomir Boncel, PhD <i>Silesian University of Technology, gliwice, Poland</i>	
0854_1278_000102	Joule Heating as a High-Temperature Out-of-Oven Manufacturing Technique for Nanocarbon/Inorganic Composites	221
	Shegufta Upama ¹ , Anastasiia Mikhalchan ² , Luis Arévalo ² , Afshin Pendashteh ² , Juan Vilatela ² , Micah Green ¹ <i>¹Texas A&M University, College Station, TX, USA, ²IMDEA Materials Institute, Getafe, Madrid, Spain</i>	
0854_1278_000275	Large-Area Fabrication of Isolated Suspended Single-Walled Carbon Nanotube Arrays for Heteronanotube Growth	222
	Taiki Inoue, Makoto Shimizu, Yoshihiro Kobayashi <i>Osaka University, Osaka, Japan</i>	
0854_1278_000031	Large-area synthesis of SWCNT forests in a bulk-diffusion-dominated kinetic regime	223
	Sei Jin Park, Kathleen Moyer-Vanderburgh, Francesco Fornasiero <i>Lawrence Livermore National Laboratory, Livermore, CA, USA</i>	
0854_1278_000490	Lepidocrocite Titanium Oxide 1D Nanofilaments: A New Form of Titana for Photochemical Hydrogen Production and Electrochemical Oxygen Evolution Reaction	224
	Hussein Badr, PhD, Michel Barsoum, PhD <i>Drexel University, Philadelphia, PA, USA</i>	

0854_1278_000187	Liquid Metal Spreading on Metallic Surfaces Suppressed by Carbon Nanotubes	226
	Anar Zhexembekova, Chang Young Lee <i>Ulsan National Institute of Science and Technology, Ulsan, Republic of Korea</i>	
0854_1278_000471	Liquid processing of high aspect ratio nanowires into macrostructures	227
	David Tilve Martinez, PhD, Juan José Vilatela, PhD <i>IMDEA Materials, Getafe, Spain</i>	
0854_1278_000496	Load-Bearing Carbon Cement Supercapacitors for Structural Energy Storage Systems	228
	Damian Stefaniuk ¹ , James Weaver ² , Admir Masic ¹ , Franz-Josef Ulm ¹ <i>¹Massachusetts Institute of Technology, Cambridge, MA, USA, ²Harvard University, Boston, MA, USA</i>	
0854_1278_000225	Low Temperature Synthesis and Characterization of High Entropy Oxide Nanoparticles for Various Applications	229
	Irem Algan Simsek, PhD ¹ , Hussein Badr, PhD ² , Michel Barsoum, PhD ³ <i>¹Drexel University, Philadelphia, PA, USA, ²Drexel University, Philadelphia, PA, USA, ³Drexel University, Philadelphia, PA, USA</i>	
0854_1278_000158	Low-temperature Synthesis of Linear Carbon Chain inside Single-walled Carbon Nanotubes	230
	Bowen Zhang, PhD ¹ , Xiyang Qiu, PhD ¹ , Qingmei Hu, PhD ¹ , Ya Feng ² , Aina Parera, PhD ³ , Yongjia Zheng ⁴ , YuHuang Wang ⁵ , Yutaka Matsuo ⁶ , Shohei Chiashi ¹ , Rong Xiang ⁴ , Sofie Cambré ³ , Wim Wenseleers ³ , Slava Rotkin ⁷ , Keigo Otsuka ¹ , Shigeo Maruyama ¹ <i>¹The University of Tokyo, Tokyo, Japan, ²Dalian University of Technology, Dalian, China, ³University of Antwerp, Antwerp, Belgium, ⁴Zhejiang University, Hangzhou, China, ⁵Maryland university, College Park, MD, USA, ⁶Nagoya University, nagoya, Japan, ⁷The Pennsylvania State University, State College, PA, USA</i>	
0854_1278_000335	Lyotropic Liquid Crystalline Behavior of Boron Nitride Nanotubes in Aqueous Sodium Deoxycholate Dispersions	231
	Joe Khoury ¹ , Lyndsey Scammell ² , Cheol Park ³ , Angel Marti ¹ , Matteo Pasquali ¹ <i>¹Rice University, Houston, TX, USA, ²BNNT, LLC, Newport News, VA, USA, ³NASA Langley Research Center, Hampton, VA, USA</i>	
0854_1278_000339	Mechanical and Piezoresistive Responses of Carbon Nanotube Yarns along Axial and Transverse Directions	233
	Iriana Garcia Guerra ¹ , Jandro Abot ¹ , Ines Pereyra ² , Marcelo Carreno ² , Deissy Feria Garnica ² <i>¹The Catholic University of America, washington DC, DC, USA, ²USP – Universidade de São Paulo, São Paulo, Brazil</i>	

0854_1278_000436	Metal-lattice-heredity conversion for universal synthesis of 2D transition metal oxides	234
	Junyang Tan ¹ , Jingwei Wang, Bilu Liu ¹ , Hui-Ming Cheng ¹ <i>¹Tsinghua University, Shenzhen, China</i>	
0854_1278_000129	Micro-scale Metal Plating on Carbon Nanotubes	235
	Yuanqi Wei, PhD ¹ , Dalue Tang, PhD ² , Kaili Jiang, PhD ¹ <i>¹Tsinghua University, Beijing, China, ²McMaster University, Hamilton,, ON, Canada</i>	
0854_1278_000417	Microstructure, Mechanical Properties and Tribological Behavior of Cu-nano TiO₂-MWCNT Composite Sintered Materials	236
	Adam Marek ^{1,2} , Slawomir Boncel ^{1,2} , Adam Piasecki ³ <i>¹Silesian University of Technology, Gliwice, Poland, ²Silesian University of Technology, NanoCarbon Group, Gliwice, Poland, ³Poznan University of Technology, Poznan, Poland</i>	
0854_1278_000307	Mixed-Scale Fabrication of a Carbon Nanotube based Corrosivity Gauge	237
	Seth Kessler, PhD ¹ , Estelle Kalfon Cohen, PhD ¹ , Luiz Acauan, PhD ² , Brian Wardle, PhD ² , Yosef Stein ³ <i>¹Metis Design Corporation, Boston, MA, USA, ²Massachusetts Institute of Technology, Cambridge, MA, USA, ³Analog Devices, Inc., Norwood, MA, USA</i>	
0854_1278_000211	Modular Chemical Patterning of Graphene by Direct Laser Writing Using »3-iodanes	238
	Kevin Gerein <i>Friedrich-Alexander-Universität Erlangen-Nürnberg, Erlangen, Germany</i>	
0854_1278_000473	Molecular Impermeability of Irreversibly Bonded Two-Dimensional Polyaramid (2DPA-1) Nanofilms	239
	Cody Ritt, PhD ¹ , Michael Strano <i>¹Massachusetts Institue of Technology, Cambridge, MA, USA</i>	
0854_1278_000026	Molecule Super-transport Through Macroscopic Length of Individual Carbon Nanotube	240
	Fei WEI, PhD, Jingwei WU, PhD student <i>Tsinghua University, Beijing, China</i>	
0854_1278_000453	Morphology Changes and Stoichiometry Based MoS₂ Growth by Chemical Vapor Deposition using Kinetic Monte Carlo (KMC) Simulation	241
	Yoonbeen Kang, Sang-Yong Ju <i>Yonsei University, Seoul, Republic of Korea</i>	
0854_1278_000029	Multifunctional Carbon Nanotube-based Composite Carbon Fibers for Enhanced Mechanical Properties	242
	Junghwan Kim, PhD, So Jeong Heo, PhD, Seo Gyun Kim, PhD, Bon-Cheol Ku, Ph.D. <i>Korea Institute of Science and Technology, Wanju-gun, Republic of Korea</i>	

0854_1278_000438	MXENE / METAL NANOMATERIALS FOR ENERGY CONVERSION APPLICATION	243
	Sergii Sergiienko, PhD <i>University of Chemistry and Technology, Prague, Czech Republic</i>	
0854_1278_000401	Near-Infrared Fluorescent Carbon Nanotube Sensors for the Plant Hormone Family Gibberellins	244
	Mervin Ang ¹ , Jianqiao Cui ² , Nam-Hai Chua ^{1,3} , Daisuke Urano ^{1,3} , Michael Strano ^{1,2} <i>¹Disruptive & Sustainable Technologies for Agricultural Precision, Singapore-MIT Alliance for Research and Technology, Singapore, Singapore, ²Massachusetts Institute of Technology, Cambridge, MA, USA, ³Temasek Life Sciences Laboratory Limited, Singapore, Singapore</i>	
0854_1278_000341	New Architectures for Heat Sink Less Carbon Nanotube Film Thermoelectric (TE) Devices Inspired by Kirigami	245
	Chongyang Zeng, Emiliano Bilotti <i>Imperial College London, London, UK, United Kingdom</i>	
0854_1278_000543	Nonadiabatic Dynamics for Assessing Yield of Emission of sp³ defect carbon nanotubes	246
	Dmitri Kilin <i>North Dakota State University, Fargo, ND, USA</i>	
0854_1278_000218	Non-covalently Functionalized Cobalt-Phtalocyanine Transition Metal Dichalcogenide Nanosheet Networks	247
	Elena Mack ¹ , Alejandro Cadranel ² , Kevin Synnatschke ³ , Leandro Lourenço ⁴ , Dirk Guldi ⁵ <i>¹Friedrich-Alexander-Universität Erlangen-Nürnberg, Erlangen, Germany, ²Friedrich- Alexander-Universität Erlangen-Nürnberg, Erlangen, Germany, ³Technische Universität Dresden, Dresden, Germany, ⁴University of Aveiro, Aveiro, Portugal, ⁵Friedrich-Alexander- Universität Erlangen-Nürnberg, Erlangen, Germany</i>	
0854_1278_000541	OBTAINING BAMBOO STRUCTURE USING MWCNT	248
	OVIDIU TIPRIGAN, PhD.Eng <i>Babes-Bolyai University of Cluj-Napoca, Romania, Cluj-Napoca, Romania</i>	
0854_1278_000243	One-Dimensional, Titania-Based Lepidocrocite Nanofilaments: Large Scale Production, Characterization, Properties and Potential Applications	249
	Hussein Badr, PhD, Michel Barsoum, PhD <i>Drexel University, Philadelphia, PA, USA</i>	
0854_1278_000060	One-step hydrothermal Synthesis of 3D Garland BiOI, Spherical ZnO, and CNFs for advancing Supercapacitor Performance with Enhanced Electrochemical Properties	251
	Jyothi Nallapureddy, PhD, Ramesh Reddy Nallapureddy, PhD, Mohan Reddy Pallavolu, PhD, Sang Joo, PhD <i>Yeungnam University, GYEONGSAN, Republic of Korea</i>	

0854_1278_000263	One-Zone Chalcogenization for Fabrication of Few-Layer Transition Metal Dichalcogenide Films	252
	Michaela Sojkova, PhD. ¹ , Jana Hrdá ¹ , Lenka Pribusová Slušná, PhD. ¹ , Karol Vegso, PhD. ² , Martin Hulman, PhD. ¹	
	<i>¹Institute of Electrical Engineering, Slovak Academy of Sciences, Bratislava, Slovakia, ²Institute of Physics, Slovak Academy of Sciences, Bratislava, Slovakia</i>	
0854_1278_000132	Optimized Purification of Efficiently-synthesized Carbon Nanotubes for Fiber Spinning	253
	Michelle Duran Chaves, MA, Oliver Dewey, PhD, Ana Victoria Benavides Figueroa, MA, Mingrui Gong, Kathryn Dale, Alex Dantzler, Matteo Pasquali, PhD	
	<i>Rice University, Houston, TX, USA</i>	
0854_1278_000314	Oxygen-Rich Amorphous Carbon as a Functional Interphase in Industrial Carbon Nanotube Yarn Networks	254
	Michael Durso, Anastasios Hart	
	<i>Massachusetts Institute of Technology, Cambridge, MA, USA</i>	
0854_1278_000321	Pristine SWCNT-based composite materials for Lithium battery applications	255
	Oleg Kuznetsov ¹ , Avetik Harutyunyan ²	
	<i>¹Honda Research Institute USA, Inc., San Jose, CA, USA, ²Honda Research Institute USA, Inc., San Jose, CA, USA</i>	
0854_1278_000078	Proper Electrolytes and Reaction Conditions for Prelithiation of SiO-Carbon Nanotube Sponge Anode for Lithium-Ion Batteries	256
	Ben HUANG, Tomotaro MAE, Suguru NODA	
	<i>Waseda University, Tokyo, Japan</i>	
0854_1278_000223	Quantum Defects in Carbon Nanotubes for Functionalization and Sensing	257
	Sebastian Kruss	
	<i>Ruhr University Bochum, Bochum, Germany</i>	
0854_1278_000258	Rapid Degradation of Single-Wall Carbon Nanotubes via Sodium Hypochlorite and UV-Light Irradiation	258
	Minfang Zhang, Mei Yang, Yoko Iizumi, Toshiya Okazaki, Don Futaba	
	<i>Nano Carbon Device Research Center/AIST, Tsukuba, Japan</i>	
0854_1278_000255	Recent Advances in 2D Nanomaterials-Based Triboelectric Nanogenerators: Structure, Properties, Performance, and Device Applications	259
	Prasanjit Dey	
	<i>Indian Institute of Technology Bombay, Mumbai, India</i>	
0854_1278_000108	Reconfigurable Chiro-optical Response in Twist Stacks of Aligned Carbon Nanotubes and Phase Change Material Heterostructure	260
	Jichao Fan, Ph.D. Candidate	
	<i>University of Utah, Salt Lake City, UT, USA</i>	

0854_1278_000379	RECONFIGURABLE NONLINEAR LOSSES OF NANOMATERIAL COVERED WAVEGUIDES	261
	Ayvaz Davletkhanov ^{1,2} , Aram Mkrtchyan ² , Alexey Bunkov ² , Albert Nasibulin ² , Yuriy Gladush ² <i>¹Institute of Quantum Materials and Technologies, Karlsruhe Institute of Technology, Eggenstein-Leopoldshafen, Germany, ²Skolkovo Institute of Science and Technology, Moscow, Russian Federation</i>	
0854_1278_000205	Remote-contact catalysis for high-purity semiconducting carbon nanotube array	262
	Jiangtao Wang ¹ , Xudong Zheng ¹ , Gregory Pitner ² , Jing Kong ¹ <i>¹Massachusetts Institute of Technology, Cambridge, MA, USA, ²Taiwan Semiconductor Manufacturing Company, Corporate Research, San Jose, CA, USA</i>	
0854_1278_000049	Resonance Fluorescence Anisotropy of a Dipole Emitter Near an Ultrathin Aligned Carbon Nanotube Film	263
	Igor Bondarev, PhD, Michael Pugh, MS, Firoz Seikh, PhD <i>North Carolina Central University, Durham, NC, USA</i>	
0854_1278_000064	Revealing the mechanism of carbon nanotubes in Si-based anodes	264
	Ziying He, PhD, Fei Wei, Prof <i>Tsinghua University, Beijing, China</i>	
0854_1278_000104	Role of Spin-orbit coupling on Chiral-induced Spin Selectivity in Carbon Nanotube Networks	265
	SEYEDAMIN FIROUZEH, PhD, Sandipan Pramanik, PhD <i>University of Alberta, Edmonton, AB, Canada</i>	
0854_1278_000272	Room-temperature spin field effect transistor based on carbon nanotube array	266
	zhisheng Peng, ying Xie, liu Qian, jin zhang <i>Peking University, Beijing, China</i>	
0854_1278_000274	Selective Formation of Analyte-Matrix Cocrystals on the Surface of Carbon Nanomaterials for MALDI Mass Spectrometry of Neuropeptides	267
	Cheongha Lee, Sanghwan Park, PhD, Chang Young Lee, PhD <i>Ulsan National Institute of Science and Technology, Ulsan, Republic of Korea</i>	
0854_1278_000431	Self-assembling Semiconducting Conjugated Polymers for SWCNT Separation	268
	Ben McLean ¹ , Luke Salter ² , Molly Stevens ^{2,3} , Irene Yarovsky ¹ <i>¹RMIT University, Melbourne, Australia, ²Imperial College London, London, UK, United Kingdom, ³University of Oxford, Oxford, United Kingdom</i>	
0854_1278_000135	SEM imaging of insulating specimen through a transparent conducting veil of carbon nanotube	269
	Yuchen Ju <i>Tsinghua University, Beijing, China</i>	

0854_1278_000245 **SIMULATION OF THE SULFUR EFFECT ON THE CATALYTIC GROWTH OF SWCNTS BY REACTIVE MOLECULAR DYNAMICS ..270**

Morinobu Endo¹, Rodolfo Cruz-Silva², Aaron Morelos-Gomez³, Juan Fajardo-Diaz⁴, Jono Ryota⁵, Syogo Tejima⁶

¹Shinshu University, Nagano, Japan, ²Center for Applied Research in Chemistry CIQA, Saltillo, Mexico, ³Shinshu University, Nagano, Japan, ⁴Shinshu University, Nagano, Japan, ⁵Research Organization for Information Science and Technology, Tokyo, Japan, ⁶Research Organization for Information Science and Technology, Tokyo, Japan

0854_1278_000489 **Single-Chirality Nanotube Synthesis by Guided Evolutionary Selection271**

Ksenia Bets, Ting Cheng, Boris Yakobson
Rice University, Houston, TX, USA

0854_1278_000551 **Single-walled Carbon Nanotubes Synthesized by Laser Ablation from Coal274**

Shaochuang Chen¹, Zeyao Zhang^{1,2}, Yan Li¹

¹Peking University, Beijing, China, ²Institute of Carbon-Based Thin Film Electronics, Peking University, Shanxi, Taiyuan, China

0854_1278_000591 **Small-load rGO as partial replacement for the large amount of zinc dust in PU zinc-rich composites applied in heavy-duty anticorrosion coatings275**

Yun-Xiang Lan, PhD¹, Yu-Ting Tseng^{2,3}, juiming yeh, PhD⁴

¹Chung Yuan Christian University, Tao-Yuan, Taiwan, ²Chung Yuan Christian University, Tao-Yuan, Taiwan, ³Chung Yuan Christian University, Tao-Yuan, Taiwan, ⁴Chung Yuan Christian University, Tao-Yuan, Taiwan

0854_1278_000521 **Solvent Isotope Effects on the Formation of Fluorescent Quantum Defects in Carbon Nanotubes via Aryl Diazonium Chemistry276**

Brandon Heppe¹, Nina Dzombic¹, Joseph Keil, PhD², Xue-Long Sun, PhD^{1,2}, Geyou Ao, PhD¹

¹Washkewicz College of Engineering, Cleveland State University, Cleveland, OH, USA, ²Center for Gene Regulation in Health and Disease (GRHD), Cleveland State University, Cleveland, OH, USA

0854_1278_000052 **STABLE DISPERSIONS OF CARBON NANOMATERIALS IN IONIC AND NON-IONIC LIQUIDS277**

Szymon Ruczka, MD, Rafał drysiak, Sławomir Boncel
Silesian University of Technology, NanoCarbon Group, Gliwice, Poland

0854_1278_000343 **Stacked 2D Materials For Temporal Gating of Ion Transport Through Nanopores278**

Matthew Schiel, Ethan Cao, Aaron Barajas-Aguilar, Javier Sanchez-Yamagishi, Zuzanna Siwy
University of California Irvine, Irvine, CA, USA

0854_1278_000556	Strong Artificial Muscle Fibers by Carbon Nanotube@Double Network Liquid Crystal Elastomer	279
	Guang Yang, Mr <i>Suzhou Institute of Nano-Tech and Nano-Bionics, Chinese Academy of Sciences, Suzhou, China</i>	
0854_1278_000460	Structure and Charge Transfer in Fibers of Carbon Nanotube Intercalation Compounds	280
	Ana de Isidro-Gómez ^{1,2} ¹ <i>IMDEA Materials, Getafe, Spain, </i> ² <i>Universidad Autónoma de Madrid (UAM), Madrid, Spain</i>	
0854_1278_000252	Study of thermal resistance at the metal-CNT interface through thermal structure function measurements	281
	Kosuke Hayashi, Takayuki Nakano, Yoku Inoue <i>Shizuoka University, Hamamatsu City, Shizuoka Prefecture, Japan</i>	
0854_1278_000111	SUPERHYDROPHOBIC HYDROGENATED NANOCARBONS	282
	Magdalena Małecka ¹ , Adam Marek ¹ , Emil Korczeniewski ² , Artur Terzyk ² , Sławomir Boncel ¹ ¹ <i>Silesian University of Technology, NanoCarbon Group, Gliwice, Poland, </i> ² <i>Nicolaus Copernicus University in Torun, Physicochemistry of Carbon Materials Group, Toruń, Poland</i>	
0854_1278_000426	Surface Engineering of MXene and its Applications in Light-Driven Actuation	283
	Dhamelyz Silva-Quinones, PhD, Haozhe Wang, PhD <i>Duke University, Durham, NC, USA</i>	
0854_1278_000400	Surface-Enhanced Raman Spectroscopy of Twisted Bilayer hBN	284
	Xinyue Li, Cong Su <i>Yale University, New Haven, CT, USA</i>	
0854_1278_000487	Synthesis and Cycloadditions of Cyclooligo(3,3"-para-terphenylene ethynylene)s: Precursors of Armchair Carbon Nanobelts	285
	Thomas Hughes, Ph.D., Karalyn Murray, Lukas Sodergren <i>Siena College, Loudonville, NY, USA</i>	
0854_1278_000198	Synthesis and optical characterization of NbS₂ based van der Waals heterostructures	286
	Wanyu Dai ¹ , Yongjia Zheng ^{1,2} , Akihito Kumamoto ¹ , Mina Maruyama ³ , Susumu Okada ³ , Slava Rotkin ⁴ , Esko Kauppinen ⁵ , Keigo Otsuka ¹ , Yuichi Ikuhara ¹ , Rong Xiang ^{1,2} , Shigeo Maruyama ¹ ¹ <i>The University of Tokyo, Tokyo, Japan, </i> ² <i>Zhejiang University, Hangzhou, China, </i> ³ <i>University of Tsukuba, Tsukuba, Japan, </i> ⁴ <i>The Pennsylvania State University, State College, PA, USA, </i> ⁵ <i>Aalto University, Espoo, Finland</i>	

0854_1278_000100	Synthesis of carbon nanotubes using higher alkanes as a carbon source	287
	Lukasz Nowicki, M. Eng, Sandra Lepak-Kuc, PhD, Eng., Agnieszka Lekawa-Raus, PhD, DSc, Eng. <i>Warsaw University of Technology, Warsaw, Poland</i>	
0854_1278_000061	Telecom-band Light-emitting Diodes based on Chirality-sorted (10, 5) Carbon Nanotube Films	288
	Bing Han <i>Peking University, Beijing, China</i>	
0854_1278_000267	THE EFFECT OF DOPANT ORDERING IN CHARGE TRANSFER TO GRAPHITIC INTERCALATION COMPOUNDS – A CASE OF STUDY	289
	Cristina Madrona ¹ , Juan J. Vilatela ² , José M. Guevara-Vela ³ ¹ ICMol - Universidad de Valencia, Paterna, Valencia, Spain, ² IMDEA Materials Institute, Getafe, Madrid, Spain, ³ Universidad Autónoma de Madrid (UAM), Madrid, Spain	
0854_1278_000193	The Impact of Oxidized Ferrocene (Ferrocenium) Catalyst on Chiral Distribution of SWCNT TCFs in FCCVD Synthesis	290
	Anastasios Karakasidis ¹ , Hirotaka Inoue ^{1,2} , Hua Jiang ¹ , Ghulam Yasin ¹ , Esko Kauppinen ¹ ¹ Aalto University, Espoo, Finland, ² Sumitomo Electric Industries, Ltd., Osaka, Japan	
0854_1278_000121	The Important Role of Ethylene in Floating Catalyst Chemical Vapor Deposition for Tuning of Carbon Nanotube Chirality Distribution	291
	Hirotaka Inoue ^{1,2} , Anastasios Karakassides ² , Ghulam Yasin ² , Hua Jiang ² , Takamasa Onoki ¹ , Toshihiko Fujimori ^{1,3} , Akira Takakura ¹ , Soichiro Okubo ¹ , Daisuke Tanioka ¹ , Esko Kauppinen ² ¹ Sumitomo Electric Industries, Ltd., Osaka, Japan, ² Aalto University, Espoo, Finland, ³ University of Tsukuba, Tsukuba, Japan	
0854_1278_000154	The Role of Many-Body Polarization Interactions in the Interfacial Behavior of Hexagonal Boron Nitride	292
	Shuang Luo, PhD, Rahul Misra, PhD, Daniel Blankschtein, PhD <i>Massachusetts Institute of Technology, Cambridge, MA, USA</i>	
0854_1278_000046	The underappreciated importance of polymer characteristics in extractive purification of single-walled carbon nanotubes	293
	Andrzej Dzienia, PhD, Dominik Just, Tomasz Wasiak, Dawid Janas, PhD, DSc <i>Silesian University of Technology, Gliwice, Poland</i>	
0854_1278_000253	Thermal conductivity of twisted CNT yarns and continuous ultra-long CNT	294
	Haruto Kurono ¹ , Takayuki Nakano ¹ , Hisashi Sugime ² , Hiroya Ikeda ¹ , Yoku Inoue ¹ ¹ Shizuoka University, Hamamatsu, Japan, ² Kindai University, Higashiosaka, Japan	
0854_1278_000332	Thermoelectric devices with carbon nanomaterials	295
	Frederik van Veen <i>Empa, Swiss Federal Laboratory for Materials Science and Technology, Dübendorf, Switzerland</i>	

0854_1278_000206	Transforming Dairy Waste into High-Value Carbon Dots for Biomedical Applications	296
	MONICA FANARRAGA ¹ , RAFAEL VALIENTE ² , JESUS GONZALEZ ² , MARINA CANDELA ² , LORENA GARCIA HEVIA ²	
	¹ <i>The Nanomedicine Group, IDIVAL- Universidad de Cantabria (Spain), SANTANDEWR, Spain,</i> ² <i>The Nanomedicine Group, IDIVAL- Universidad de Cantabria (Spain), SANTANDER, Spain</i>	
0854_1278_000115	Twisted 2D materials for polarization optics	297
	Kaveh Khaliji, PhD ¹ , Luis Martin-Moreno ² , Phaedon Avouris ¹ , Sang-Hyun Oh ¹ , Tony Low ¹	
	¹ <i>University of Minnesota, Minneapolis, MN, USA,</i> ² <i>Instituto de Nanociencia y Materiales de Aragon (INMA), CSIC-Universidad de Zaragoza, Zaragoza, Spain</i>	
0854_1278_000265	Ultra-Clean and High-Semiconducting-Purity Carbon Nanotube Arrays for High-Performance Electronics	298
	Lan Bai, PhD ^{1,2}	
	¹ <i>Peking University, Beijing, China,</i> ² <i>Shanxi Institute of Carbon-Based Thin Film Electronics, Peking University (SICTFE-PKU), Taiyuan, China</i>	
0854_1278_000124	Ultra-dense CNT forests by adding ferrocene and aluminum isopropoxide to the growth process	299
	Sota Goto ¹ , Takayuki Nakano ¹ , Hisashi Sugime ² , Yoku Inoue ¹	
	¹ <i>Shizuoka University, Hamamatsu, Japan,</i> ² <i>Kindai University, Higashiosaka, Japan</i>	
0854_1278_000407	Ultrafast and CMOS-compatible transfer of carbon nanotube horizontal arrays and other van der Waals materials	300
	Xudong Zheng, Jiangtao Wang, Jing Kong	
	<i>Massachusetts Institute of Technology, Cambridge, MA, USA</i>	
0854_1278_000034	Ultra-thick Carbon Nanotube Fiber and Copper Hybrid wires with a High Electrical Properties	301
	Gwansik Kim, PhD ¹ , Chaeyoon Kim ² , Kyong Hwa Song ¹ , Seokmin Lee ¹ , Eunsoo Shim ² , Deok Woo Yun ¹ , Jae-Hong Lim ²	
	¹ <i>Hyundai Motor Company, Uiwang-si, Republic of Korea,</i> ² <i>Gachon University, Seongnam-si, Republic of Korea</i>	
0854_1278_000462	Unlocking the Potential of Phenanthroimidazole-based Bipolar Derivatives for High-performance Blue-Emitting OLEDs	303
	Anna Pidluzhna, PhD, Aivars Vembris, PhD ¹ , Raitis Grzibovskis, PhD ¹	
	¹ <i>Institute of Solid State Physics, University of Latvia, Riga, Latvia</i>	
0854_1278_000207	Unlocking the Role of Sulfur in Carbon Nanotube Synthesis	304
	Ghulam Yasin ¹ , Hirotaka Inoue ^{1,2} , Anastasios Karakassides ¹ , Hua Jiang ¹ , Esko Kauppinen ¹	
	¹ <i>Aalto University, Espoo, Finland,</i> ² <i>Sumitomo Electric Industries, Ltd., Osaka, Japan</i>	

0854_1278_000398	Variable-amplitude fatigue testing of aerospace-grade composites reinforced with aligned carbon nanotube interlayers	305
	Vishnu Saseendran, PhD ¹ , Carina Li ² , Charles Bakis, PhD ¹ , Namiko Yamamoto, PhD ¹ , Brian Wardle, PhD ²	
	<i>¹The Pennsylvania State University, University Park, PA, USA, ²Massachusetts Institute of Technology, Cambridge, MA, USA</i>	
0854_1278_000340	Vertically Aligned Carbon Nanotubes as Toughening Interleaves for Advanced Composite Manufacturing	306
	Thomas GOISLARD DE MONSABERT, PhD ¹ , Aurélien BOISSET, PhD ¹ , Blagoj KARAKASHOV, PhD ¹ , Kevin RETZ, PhD ² , Lingchuan LI, PhD ³ , Paul KLADITIS, PhD ³	
	<i>¹NAWA Technologies, Rousset, France, ²NAWA America, Dayton, OH, USA, ³University of Dayton Research Institute UDRI - Dayton (OH), Dayton, OH, USA</i>	
0854_1278_000587	Visualizing Living Cells and Nanoparticles via Total Internal Reflection Scattering Device	307
	Cheng-An Lin, Ph.D, Tzu-Yin Hou, You-Wei Li, Pin-Jun Liao, Yu-Wen Xu	
	<i>Chung Yuan Christian University, Taoyuan, Taiwan</i>	
0854_1278_000091	Wafer-Scale Fabrication of Wearable All-Carbon Nanotube Photodetector Arrays.....	308
	Peng Liu, Erxiong Ding, Qiang Zhang, Zhipei Sun, Esko Kauppinen	
	<i>Aalto University, Espoo, Finland</i>	
0854_1278_000120	X-ray filter based on SACNT film.....	309
	ZI YUAN	
	<i>Department of Physics, Tsinghua University, Beijing, China</i>	

Quantum Defects in Carbon Semiconductors: An Introduction

YuHuang Wang¹

¹ *Department of Chemistry and Biochemistry, University of Maryland, College Park, MD 20742 (United States);*

E-mail: yhw@umd.edu

Not all defects are a setback. In low-dimensional materials like semiconducting single-wall carbon nanotubes, covalently attaching organic functional groups to the sp^2 carbon lattice leads to the creation of molecularly tunable quantum defects, also known as “organic color centers.” These chemical defects are remarkable for their bright fluorescence in the shortwave infrared, emitting pure single photons at room temperature. Unlike native defects, which often compromise material integrity, quantum defects introduce exciting new functionalities that unlock new possibilities in fields ranging from chemistry and physics to materials science, biomedical engineering, and quantum technologies. This tutorial introduces the vibrant field of quantum defects and optical color centers in low-dimensional materials, focusing on the chemistry and physics behind these atomic-scale modifications. We will also explore how these defects can be used to probe the confined spaces within nanotube nanopores and enable new optoelectronic functionalities of materials. Additionally, we will highlight some of the pressing questions and challenges this rapidly evolving field faces, aiming to provide a solid understanding of the current landscape and future directions.

References

- [1] Brozena, A.; Kim, M.J.; Powell, L. R.; Wang, Y. H. *Nature Reviews Chemistry* **2019**, 3, 375–392.
- [2] Gifford, B. J.; Kilina, S.; Htoon, H.; Doorn, S. K.; Tretiak, S. *Accounts of Chemical Research* **2020**, 53, 1791-1801.
- [3] Shiraki, T.; Miyauchi, Y.; Matsuda, K.; Nakashima, N. *Accounts of Chemical Research* **2020**, 53, 1846-1859.
- [4] Wang, Y. H. *Science* **2022**, 377, 473-474.
- [5] Aluru, *et al.* *Chemical Reviews* **2023**, 123, 2737-2831.
- [6] Faucher, *et al.* *Journal of Physical Chemistry C* **2019**, 123, 21309-21326.

KEYNOTE: Graphene Encapsulation and Carbon Nanotubes – Reaction Vessels to Gain Atomic Insights into Physics and Chemistry of Matter

Ute Kaiser¹

¹University of Ulm (Germany)

In honor of the Queen of Carbon, Millie Dresselhaus, whose pioneering work revolutionized our understanding of carbon-based materials and paved the way for advancements in carbon nanotubes and graphene [1,2], we present our research on these tiny materials when utilization single-walled carbon nanotubes [3] and graphene [4] encapsulation as reaction vessels—the thinnest possible. These experiments were conducted using our recently developed, state-of-the-art spherical and chromatic aberration-corrected high-resolution transmission electron microscope, which operates in the voltage range between 80kV and 20kV [5,6]. Despite fascinating technical developments that have increased the power of electron microscopy in the low-voltage range, there are often compromises that must be made to answer real-world questions. Here, we employ the reaction vessels also in conjunction with a MEMS-based heating holder to protect the material under study from destructive electron-beam-induced inelastic interactions with the specimen and from the vacuum environment in the TEM.

We begin by establishing a basic understanding of the interactions of 80keV and 20keV electrons with matter, which can serve as stimuli and initiators for reactions or can destroy the material during imaging. We elucidate the electron energy-dependent formation of defects, using monolayer MoS₂ as an example. Our results indicate that knock-on damage and electronic excitations exist in combination, and this way, we understand that the knock-on damage threshold of the material can be significantly lowered [7,8]. This insight helps us understand the protective behavior of the reaction vessels employed in this study.

Building upon this foundation, I will discuss in my presentation our recent studies conducted in the reaction vessels, which provide insights—on the scale of a single atom—into dynamics of bonding [9,10,11], nucleation and growth [12,13], and solid-solid phase transitions [14,15,16].

References

- [1] M.S. Dresselhaus & G. Dresselhaus, *Advances in Physics* **51**(1), 1-186, (2002).
- [2] M.S. Dresselhaus & G. Dresselhaus, *Carbon Nanotubes* Springer Science & Business Media. (2002).
- [3] S. Iijima, *Nature*, **354** (6348), 56-58, (1991)
- [4] AK Geim, KS Novoselov, *Nature Materials*, **6**: 183-91. PMID 17330084 DOI: 10.1038/Nmat1849 (2007)
- [5] U. Kaiser et al., *Ultramicroscopy*, **111**, 8, 1239-1246, (2011)
- [6] M. Linck, et al. *PRL* **117**, 076101, (2016).
- [7] S. Kretschmer, T. Lehnert, et al. *Nano Lett.*, **20**, 2865-2870, (2020).
- [8] T. Lehnert, et al. *ACS Appl. Nano Mater.*, **2** 3262-3270 (2019).
- [9] I. Cardillo-Zallo, et al. *ACS Nano*, **18** 2958–2971, (2024).
- [10] K. Cao, et al., *Science Advances*, **6** eaay5849 (2020).
- [11] J. Biskupek et al., *ACS Nano* **14**, 9, 11178-11189 (2020).
- [12] K. Cao, et al., *Nature Chemistry*, **12**, 10, 921-928(2020).
- [13] M. Kühne, F. Börrnert et al., *Nature*, 564 234-239 (2018).
- [14] V. O. Khaustov et al, *ACS Applied Nano Materials*, doi.org/10.1021/acsnm.3c01314 (2023)
- [15] J. Köster et al., *Nanotechnology* **35** 1453015bb (2024).
- [16] A. Storm et al., *ACS Nano* **17** 4250-4260 (2023).

KEYNOTE: LOW-FREQUENCY NOISE IN FLEXIBLE CARBON NANOTUBE ANALOG INTEGRATED CIRCUITS FOR SENSOR APPLICATIONS

Yutaka Ohno

Nagoya University (Japan)

Since flexible devices can come into close contact with the human body, they are suitable for wearable sensor applications for long-term and non-invasive monitoring of biological and physiological signals in various fields such as medical/health care and sports. In order to achieve a fully flexible sensor system, various electronic circuits need to be integrated on a flexible film, including the analog front-end (AFE) and radio-frequency (RF) front-end, as well as the sensors. Recently, we have demonstrated low-voltage CNT-based analog/digital mixed-signal circuits with excellent stability and robustness against variability, including the AFE. [1] One of remaining issues with carbon nanotube-based analog circuits is low-frequency noise, which directly impacts the sensitivity of the sensor system within the frequency range of physiological signals such as electrocardiogram (ECG) and electroencephalogram (EEG).

Here, we study the low-frequency noise of flexible carbon nanotube thin-film transistors and their influence on analog circuits. Bottom-gate CNT TFTs were fabricated on a polyethylene naphthalate (PEN) substrate using a self-align process. Al₂O₃ (40 nm) was deposited as the gate insulator by the low-temperature atomic layer deposition technique. A dense and uniform CNT film was deposited by the immersion deposition method. The TFT has a channel length and channel width of 100 μm. The noise power density (S_I) of the drain current (I_D) was measured using a vector signal analyzer.

Clear $1/f$ noise was observed in the fabricated flexible CNT TFTs. By applying Hooge's empirical formula $S_I / I_D^2 = \alpha_H / fN$ (f : frequency, N : number of carriers, α_H : Hooge's constant), $\alpha_H = 0.6$ was obtained. This is about two orders of magnitude higher than that of back-gate CNT TFTs on Si/SiO₂ substrates [2]. The challenge lies in reducing traps in the gate dielectrics deposited at low temperatures on flexible substrates. Inserting an interface layer between the CNT channel layer and gate insulator layer reduced Hooge's parameter. The results indicate that maintaining a distance from the channel to traps in the gate oxide is important for reducing low-frequency noise.

References

- [1] T. Kashima *et al.*, *Research Square* (2020). DOI:10.21203/rs.3.rs-68702/v1.
- [2] T. Tanaka and E. Sano, *Jpn. J. Appl. Phys.* **53**, 090302 (2014).

KEYNOTE: Monitoring and Modulating the Fluorescence of Semiconducting Single-Wall Carbon Nanotubes

R. Bruce Weisman¹

¹Rice University (USA)

Fluorescence spectroscopy of semiconducting single-wall carbon nanotubes (SWCNTs) is a powerful method to monitor their band gaps through direct optical transitions. These transition energies depend on π -electron quantum confinement transverse to the nanotube axis and are specific to the SWCNT (n,m) structural species. Three spectroscopic topics of current interest will be discussed. These involve the detailed characterization of SWCNT samples and the alteration of SWCNT band gaps by chemical or mechanical perturbations.

The method of Variance Spectroscopy statistically analyzes fluorescence spectra measured from many (ca. 1000) small regions of a uniformly dispersed SWCNT sample. When the probed volumes are small enough, their spectra differ slightly because of random differences in the numbers of specific SWCNT species present within them. For each wavelength in the set of measured fluorescence spectra, we compute values of the mean and variance (squared standard deviation). The squared mean intensity divided by variance then gives the number of particles emitting at that wavelength. This provides the calibration needed to convert raw fluorescence intensities into species-specific SWCNT concentrations. Correlations in the variance data can also be analyzed through co-variance spectra, which isolate the spectral components arising from one species in a mixed SWCNT sample and reveal subtle levels of nanotube aggregation.

Another topic is the controlled tailoring of SWCNT band gaps through guanine functionalization. Here, SWCNTs coated by ssDNA are exposed to singlet oxygen, which induces a covalent reaction linking guanine bases in the ssDNA to the nanotube sidewall. The reacted hybrids show optical transitions that are red-shifted and broadened compared to unreacted SWCNTs. In contrast to SWCNTs with sparse, deep exciton traps formed by methods such as oxygen doping or diazonium reactions, the guanine-functionalized nanotubes have dense and shallow traps that globally reduce the band gap of the entire nanotube. This causes red-shifts in the absorption as well as emission spectra. In addition, the depth and spatial pattern of band gap modulation can be controlled by choosing the fraction of guanine bases and the separations between them in the ssDNA sequence.

The final topic is band gap modulation of pristine SWCNTs through mechanical strain. E_{11} and E_{22} transitions are linearly shifted (in opposite directions) by axial stretching or compression. We have applied this effect to devise a new method, called S^4 , for industrial strain measurement. Here, semiconducting SWCNTs dilutely embedded in a polymer are applied as a thin film to specimen surfaces of interest. Subsequent strains in the specimen are transmitted by load transfer through the film to the nanotubes. The resulting spectral shifts are quantified by using a laser to optically excite the specimen surface and spectrally analyzing the fluorescence to deduce strain values at the probed locations. Direct comparisons to digital image correlation (the competing method for non-contact strain mapping) show that S^4 is superior in mapping small strains, in detecting accumulated strains without constant observation, and in giving operator-independent results. Using a custom-built hyperspectral imager, we can measure small spectral peak shifts at hundreds of thousands of pixels to obtain strain maps with 50 microstrain noise levels and 0.2 mm spatial resolution within ~ 100 seconds. A successful recent prototype demonstration of S^4 at a major aerospace testing facility suggests that this technology may grow into a valuable industrial application of carbon nanomaterials.

KEYNOTE: Next Generation Moiré Quantum Matter

P. Jarillo-Herrero¹

¹*Massachusetts Institute of Technology (U.S.A.)*

The understanding of strongly-interacting quantum matter has challenged physicists for decades. The discovery five years ago of correlated phases and superconductivity in magic angle twisted bilayer graphene has led to the emergence of a new materials platform to investigate strongly interacting physics, namely moiré quantum matter. In this talk I will review recent experiments on next generation moiré quantum matter, both twisted multilayer graphene systems as well as dual (or asymmetric) moiré systems. In particular, first I will briefly discuss our experiments on magic-angle twisted multilayer graphene as a family of robust moiré superconductors. Second, I will discuss the engineering of moiré quasicrystals and a new type of unconventional ferroelectricity and electron ratchet in asymmetric moiré systems.

KEYNOTE: Superstructures and Molecular Lattices in One and Two Dimensions

Stephanie Reich¹

¹*Free University of Berlin (Germany)*

Two-dimensional monolayers and one-dimensional nanotubes may act as templates and containers for molecules and nanomaterials. In this talk, we will explore this opportunity into two directions: First, we will examine the formation of well-controlled molecular lattices inside nanotubes and on atomically flat two-dimensional substrates. We will show how in such lattices the optical molecular excitations couple into collective, delocalized excitons and vibrations. The coupling changes the energetics and dynamics of the collective states giving rise to effects such as superradiance and a strongly enhanced collective Raman response. We will examine how the interaction with the one- and two-dimensional hosts and substrates induces hybridized states with a particular emphasis on changes in the molecule-related response. Second, we will discuss double-walled carbon nanotubes as the realization of a one-dimensional moiré structure. Depending on the exact combination of inner and outer nanotube, this platform can yield excitonic moiré structures with weak and strong coupling. We will show how the interwall coupling affects the optical and vibrational states in double-walled nanotubes and discuss the potential for interwall excitons and the formation of flat bands.

Mildred Dresselhaus contributed greatly to our understanding of optical excitations and vibrations in nanotubes and two-dimensional materials. I will highlight how many of her ideas continue to be re-examined and how she inspired the development of this field.

Electroluminescence From Carbon Nanotubes With Quantum Defects

Min-Ken Li^{1,2}, Simone Dehm³, Manfred M. Kappes^{1,2,4}, Frank Hennrich¹, Ralph Krupke^{1,2,3}

¹*Institute of Quantum Materials and Technologies, Karlsruhe Institute of Technology, 76131 Karlsruhe (Germany),*

²*Institute of Materials Science, Technische Universität Darmstadt, 64287 Darmstadt (Germany),* ³*Institute of Nanotechnology, Karlsruhe Institute of Technology, 76131 Karlsruhe (Germany),* ⁴*Institute of Physical Chemistry, Karlsruhe Institute of Technology, 76131 Karlsruhe (Germany)*

Individual single-walled carbon nanotubes with covalent sidewall defects have emerged as a new class of photon sources whose photoluminescence spectra can be tailored by the carbon nanotube chirality and the attached functional group/molecule. Here we present electroluminescence spectroscopy data from single-tube devices based on (7, 5) carbon nanotubes, functionalized with dichlorobenzene molecules, and wired to graphene electrodes [1]. We observe electrically generated, defect-induced emissions that are controllable by electrostatic gating and strongly red-shifted compared to emissions from pristine nanotubes [2]. The defect-induced emissions are assigned to excitonic and trionic recombination processes by correlating electroluminescence excitation maps with electrical transport and photoluminescence data. At cryogenic conditions, additional, gate-dependent emission lines are assigned to phonon-assisted hot-exciton electroluminescence from quasi-levels. We will report on single-photon defect-state emission observed in second-order correlation function measurements from a Hanbury Brown and Twiss experiment, and discuss the dependence of the intensity correlation measurement on electrical power and emission wavelength, and the challenges of performing such measurements [3]. If time allows, we will also report on the integration of electroluminescent semiconducting carbon nanotubes into hybrid 2D-3D photonic circuits [4].

References

- [1] M-K. Li *et al.*, *ACS nano*, **16**, 11742–11754 (2022).
- [2] M. Gaulke *et al.*, *ACS nano*, **14**, 2709–2717 (2020).
- [3] M-K. Li *et al.*, *under review*.
- [4] A. Ovvyan *et al.*, *Nat. Commun.*, **14**, 3933 (2023).

Gamma-Ray Irradiation of CNT yarns for Improved Composite Strength: A Molecular Dynamics Study

S.U. Patil¹, J. Kemppainen¹, T. Wavrunek¹, G.M. Odegard¹

¹Michigan Technological University (USA)

CNT yarns are used in ultra-high strength composites for use in manned deep-space vehicles [1]. It has been previously demonstrated through experiments that gamma-ray irradiation substantially improves the mechanical performance of these composites [2, 3]. It is unclear how the irradiation affects the mechanical response of the CNT yarn/polymer interface that ultimately leads to these panel-level performance improvements. Physical insight into this process could enable further improvements in the CNT yarn/polymer interface design in the future. The objective of this research is to use molecular dynamics simulation to provide physical insight into the effect of gamma-ray irradiation on the mechanical behavior of the CNT yarn/polymer interface for a range of high-performance polymer systems, including Bismaleimide (BMI), epoxy, polybenzoxazine (PBZ), and cyanate ester. Simulations were performed to predict the interaction energy, mechanical shearing response, and mechanical tension response at the CNT yarn/polymer interface.

The results of the simulations indicate that gamma-ray irradiation of CNT yarns results in a significant increase in interfacial shear properties for all the polymer systems. In tension, gamma-ray irradiation only improves the toughness in the BMI and cyanate ester systems. The interaction energy is mostly unaffected by gamma-ray irradiation. Taken together, it is clear that gamma-ray irradiation does improve the overall mechanical performance the CNT yarn/polymer interface, which likely contributes to the increases in composite panel-level performance observed experimentally [2]. The results of the study also demonstrate the power of computational modeling to provide physical insight into bulk-scale observations of high-performance composites. The computational tools developed herein could be applied to other nanocomposite systems for a wide range of engineering applications.

References

1. Odegard, G.M., Z. Liang, E.J. Siochi, and J.A. Warren, *A successful strategy for MGI-inspired research*. MRS Bulletin, 2023. **48**: p. 434-438.
2. Park, J.G., C. Evers, C. Jolowsky, B. Vondrasek, K. Thagard, M. Czabaj, B. Ku, Y. Wang, T. Dumitrică, G.M. Odegard, and Z. Liang, *Gamma-ray irradiation to achieve high tensile performance of unidirectional CNT yarn laminates*. Carbon, 2024. **216**: p. 118530.
3. Kataria, A., Z. Liang, and T. Dumitrică, *Computational Investigation of Interacting Nanohole Defects for Carbon Nanotube Cross-Linking and Functionalization with Bismaleimide: Implications for Ultrastrong, Lightweight Nanocomposites*. ACS Applied Nano Materials, 2023. **6**(8): p. 6474-6479.

Lightweight, Strong, High Conductivity, Aluminum- Carbon Nanotube Wiring

David Lashmore PhD, CEO, Pavel Bystricky PhD, CTO at Boronite, and Michael Matuszewski, CTO and Tom Kukowski, consultant at Minnesota Wire

American Boronite Corp, 11B Cypress Drive, Burlington, MA 01805
Minnesota Wire, 1835 Energy Park Drive, Minneapolis, MN 55108

ABSTRACT

We propose a new wiring class for new power lines. A lighter weight cable, for example, would provide an increase in carrying capacity, lighter weight support structures, longer lengths between supports, and improved EMI resistance. Highly conductive carbon nanotube (CNT) based composite cables can be produced by wrapping a high-quality CNT wire around: (1) pure aluminum wire, (2) a copper-zirconium wire, (3) coated pure silver coated copper wire, followed all followed by thermal treatment. The zirconium alloy composition is formulated to just wet the surface of the CNTs^[j] (US Patent Application US 2020/0399748 A1 Dec. 24, 2020, and US 16/468,363: December 29, 2017). The specific conductivity may be dramatically improved by using pure aluminum alloys. We have determined specific conductivity of aluminum wires exceeding 8000 Sm²/kg and expect they we may attain conductivities of near 14,000 Sm²/Kg, this aluminum composites would be strengthened tremendously by continuous CNT avoiding the need of steel reinforcement and saving significant weight. For power lines this weight translates into weight saved throughout the infrastructure, the stiffer cable will not vibrate as much in the wind so longer lengths of cable can be set and a lower cost copper can be used thereby saving money.

[j] P. Bystricky, D. Lashmore, and I. Kalus-Bystricky, *Metal Matrix Composite Comprising Nanotubes and Method of Producing Same*, Patent Pending PCT/US16/468,363 (2017)

Phase engineered WS₂ monolayer quantum dots by rhenium doping

Hyeon Suk Shin

Department of Chemistry, Ulsan National Institute of Science and Technology (UNIST) (Republic of Korea)

Transition metal dichalcogenides (TMDs) occur in the thermodynamically stable trigonal prismatic (2H) or the metastable octahedral (1T) phase. Phase engineering of TMDs has proven to be a powerful tool for applications in energy storage devices as well as in electrocatalysis. However, the mechanism of the phase transition in TMDs and the synthesis of phase-controlled TMDs remain challenging. Here we report the synthesis of Re-doped WS₂ monolayer quantum dots (MQDs) using simple colloidal chemical process. We find that the incorporation of small amount of electron-rich Re atoms in WS₂ changes the metal–metal distance in the 2H phase initially, which introduces strain in the structure (strained 2H (S2H) phase). Increasing the concentration of Re atoms sequentially transforms the S2H phase to the 1T and 1T' phases to release the strain. In addition, we performed controlled experiments by doping Re in MoS₂ to distinguish between Re and Mo atoms in scanning transmission electron microscopy images, and quantified the concentration range of Re atoms in each phase of MoS₂ indicating that the phase engineering of WS₂ or MoS₂ is possible by doping different amounts of Re atoms. We demonstrate that the 1T' WS₂ MQDs with 49 at. % Re show superior catalytic performance (low Tafel slopes of 44 mV/dec, low overpotentials of 158 mV at a current density of 10 mA/cm², and long-term durability up to 5000 cycles) for the hydrogen evolution reaction. Our findings provide understanding and control of phase transitions in TMDs, which will allow efficient manufacture and translation of phase engineered TMDs.

Quantum Well Defect Carbon Nanotubes for Biomedicine

D.A. Heller¹

¹ *Memorial Sloan Kettering Cancer Center, New York, NY, USA,*

Improved measurements of biomarkers, drugs, and metabolites in live cells and organisms would allow for improvements in disease detection, drug development, and biomedical research. Quantum well-modified carbon nanotubes (QWNTs) have exciting optical properties for applications as sensors for use in live cells and in vivo, including the potential to increase quantum yield over pristine SWCNTs, and to improve control over photoluminescence modulation in response to the local environment. To develop QWNTs into sensors, we devised new methods to encapsulate them for biocompatibility, as well as new instrumentation for measurements. We also investigated mechanisms of QWNT photoluminescence environmental responsivity, including the dependence of electrostatic charge on spectral red-shifting. We found that this mechanism can amplify measurements of biomarkers, enhancing the development of sensors.

Structure and Dynamics of the Interface of Growing Carbon Nanotubes

Christophe Bichara¹

¹*Affiliated Institution1 (Country)*, ³ *CINaM, Aix-Marseille University and CNRS, Marseille (France)*.

Thirty years of relentless research suggest that understanding the interaction, structure and dynamics of the few tens of carbon atoms forming the tube edge and their catalytic counterpart is essential to control carbon nanotube growth. Since experiments on such a small scale are extremely difficult, modeling and computer simulations at different levels of complexity are highly desirable.

While previous attempts focused on the carbon–catalyst interactions, we change our point of view and investigate how the very small size of the tube edge influences the nanotube crystal growth. The small number of metal-carbon bonds formed at the tube/catalyst interface and the large number of possibilities for growing tube edges with different chiralities reinforce the relative weight of the edge's configurational entropy, which has consequently proved to be the driving force behind the stability of so-called "chiral" tubes [1]. Recent measurements of the growth kinetics of individual carbon nanotubes, that have revealed abrupt changes in the growth rate of nanotubes retaining the same crystalline structure [2] have been interpreted within the same framework. A simple model supported by kinetic Monte Carlo [3] suggests that these changes are caused by tilts of the growing nanotube edge between two main orientations, near armchair or near zigzag, which induce different growth mechanisms.

These very simple lattice models lead to extremely fast KMC simulations, but need to be backed up by more realistic atomistic simulations. Using a machine-learning force field developed for Fe-C interactions, D. Hedman et al [3] show that tube edges fluctuate strongly during growth. Interestingly, tubes do not always grow with their "natural" interface, cut perpendicular to the tube axis. For example, an armchair tube may grow with a majority of zigzag edge atoms. Moreover, the observed edge fluctuations seem to depend on the tube's chirality.

In addition to providing new insights into nanotube growth, these results point to ways of controlling the dynamics of nanotube edges, with the ultimate goal of obtaining a coherent picture of carbon nanotube growth mechanisms, in close connection with experiments.

References

- [1] Magnin Y., *et al.* Entropy-driven stability of chiral single-walled carbon nanotubes. *Science*, 362(6411), 212–215 (2018).
- [2] Pimonov V. *et al.* Dynamic Instability of Individual Carbon Nanotube Growth Revealed by In Situ Homodyne Polarization Microscopy. *Nano Letters*, 21(19), 8495–8502 (2021).
- [3] Förster G. D., *et al.* Swinging Crystal Edge of Growing Carbon Nanotubes. *ACS Nano*, 17(8), 7135–7144 (2023).
- [4] Hedman D. *et al.* Dynamics of growing carbon nanotube interfaces probed by machine learning-enabled molecular simulations, submitted to Nature Communications.

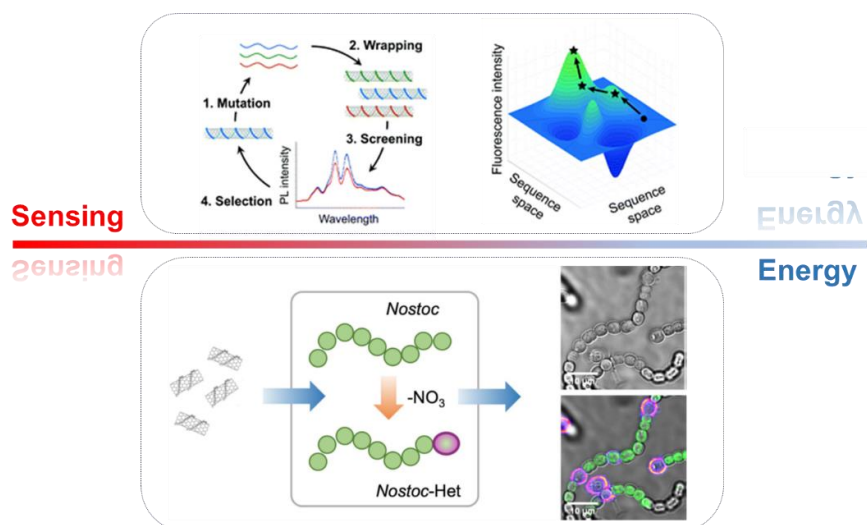
INVITED: There's Plenty of Room at the (Nano/Bio) Boundary

A. A. Boghossian¹

¹Ecole Polytechnique Fédérale de Lausanne (Switzerland)

The vast expansion of available synthetic biology tools has led to explosive developments in materials science. The increased accessibility of these tools has pushed the frontier of materials science into the field of engineering biological and even living materials. By coupling the tunable and robust optoelectronic properties of synthetic nanomaterials with the specificity and adaptability of biomaterials, one can re-purpose biology to fulfil needs that are otherwise intractable using traditional engineering approaches.

This presentation highlights applications in sensing and energy technologies that exploit the synergistic coupling of nanobio-hybrid materials at the boundary. This talk will discuss the development of bio-conjugated single-walled carbon nanotubes (SWCNTs) for near-infrared fluorescence sensing. We discuss recent advancements in applying synthetic biology approaches, such as directed evolution[1-3], xeno nucleic acid engineering[4-5], and protein mutagenesis[6], to control the optical properties of these synthetic nanoparticle sensors for a range of applications. This presentation will also discuss complementary efforts in re-purposing biological materials for electronic applications. This talk will focus on developing living electronics, such as fuel cells[7] and photovoltaics[8-9], through concomitant genetic re-programming and nanomaterial engineering. These demonstrations exemplify but a few examples of nanomaterial bottlenecks that we can overcome through anti-disciplinary approaches.



Nanotube Applications in Sensing (TOP) and Energy (BOTTOM) Enabled Through Bioengineering:

(TOP, left) Steps for the directed evolution of DNA sequences for wrapping nanotubes. (TOP, right) Each iterative modification of the wrapping DNA sequence improves sensor performance in a guided manner. Figure adapted from ref. [1]. (BOTTOM) Functionalized nanotubes (left) are incubated with living cells (middle) to create nanobionic cells (right) for energy applications. Figure adapted from ref. [9].

References

- [1] B. Lambert *et al.*, *Chem. Commun.* **55**, 3239–3242 (2019).
- [2] B. P. Lambert *et al.*, *bioRxiv*, DOI: 10.1101/2023.06.13.544576 (2023).
- [3] Y. Rabbani *et al.*, *bioRxiv*, DOI: 10.1101/2023.09.07.556334 (2023).
- [4] A. J. Gillen *et al.*, *J. Phys. Chem. Lett.* **9**, 15, 4336–4343 (2018).
- [5] A. J. Gillen *et al.*, *bioRxiv*, DOI: 10.1101/2021.02.20.428669 (2021).
- [6] V. Zubkova *et al.*, *Nanoscale Adv.* **4**, 2420–2427 (2022).
- [7] M. Mouhib *et al.*, *Joule* **7**, 2092–2106 (2023).
- [8] A. Antonucci, *et al.*, *Nat. Nanotechnol.* **17**, 1111–1119 (2022).
- [9] A. Antonucci, *et al.*, *Photochem. Photobiol. Sci.* **22**, 103–113 (2023).

Electrochemical Production of Hydrogen and Hydrogen Peroxide

Xiaolin Zheng

Mechanical Engineering, Energy Science & Engineering, Stanford University

ABSTRACT Hydrogen is indispensable for achieving deep decarbonization of the global economy. Green hydrogen production from renewable electricity, *i.e.*, electrolysis, is expected to play an important role, and yet it is not economical. The green hydrogen cost can be lowered by using less amount of noble metals and/or producing other valuable chemicals simultaneously. In this talk, I will present three examples of improving the rate-limiting oxygen evolution reaction (OER) through material innovation and electrolyte optimization. First, I will discuss the use of metal oxide stabilized Ir sites as an acid-stable catalyst for OER. Then, I will discuss a new class of material, high entropy oxide, as an active and stable catalyst for OER. Finally, I will discuss the production of an alternative chemical H_2O_2 , instead of O_2 , through catalyst and electrolyze innovation.

INVITED: WATER-BASED AND BIOCOMPATIBLE 2D MATERIAL INKS - FROM PRINTED ELECTRONICS TO BIOMEDICAL APPLICATIONS

C. Casiraghi

Department of Chemistry, University of Manchester, UK

Solution processing of 2D materials allows simple and low-cost techniques, such as ink-jet printing, to be used for fabrication of heterostructure-based devices of arbitrary complexity [1]. Our group has developed a supramolecular-based approach able to provide highly concentrated, defect-free, printable and water-based 2D crystal inks [2-3], which have been used to fabricate photosensors on papers [2], programmable logic memory devices [2], capacitors [4], transistors [4-5], memristors [6], as well as humidity sensors that can be used to monitor the full breathing cycle [7]. Furthermore, inkjet printing can be easily combined with 2D materials produced by chemical vapour deposition, allowing simple and quick fabrication of complex circuits on paper [8-9].

Finally, our supramolecular approach allows to easily tune the surface charge of graphene, enabling production of amphoteric, cationic and anionic graphene [10-11]. Cytotoxicity tests confirm biocompatibility of the graphene inks, with cationic graphene showing exceptional intracellular uptake profile as well as stability in the biological medium, making it very attractive for various applications in drug delivery and imaging [12].

References

- [1] Conti *et al*, Nature Rev Mat, 2023, <https://doi.org/10.1038/s41578-023-00585-7>
- [2] McManus *et al*, Nature Nano, 12, 343 (2017)
- [3] Tringides *et al*, Nature Nano, 16, 1019 (2021)
- [4] Worsley *et al*, ACS Nano, 2018, DOI: 10.1021/acsnano.8b06464
- [5] Lu *et al*, ACS Nano, 13, 11263 (2019)
- [6] Peng *et al*, Mat. Horizons, just accepted
- [7] Chen *et al*, Adv. Materials, just accepted
- [8] Conti *et al*, Nature comms, 11 (1), 1-9 (2020)
- [9] Brunetti *et al*, npj 2D Materials and Applications 5 (1), 85 (2021)
- [10] Shin *et al*, Faraday Discussion, 2019, <https://doi.org/10.1039/C9FD00114J>
- [11] Shin *et al*, Nanoscale, 2020, DOI: 10.1039/D0NR02689A
- [12] Chen *et al*, Nanoscale, 5 (21), 9348-9364 (2023)

A semi-detailed Kinetic Model for the production of Carbon Nanotubes and H_2 from the thermo-catalytic pyrolysis of Methane

C. Giudici¹, M. Bracconi¹, M. Maestri¹, M. Pelucchi¹

¹Politecnico di Milano – Milano (Italy)

Floating Catalyst Chemical Vapor Deposition (FCCVD) is a promising method for the continuous industrial scale production of hydrogen and carbon nanotubes (CNTs). Thanks to the remarkable properties of CNTs, the large-scale implementation of such technology would allow the production of hydrogen, a carbon neutral energy vector, at a price that is comparable to the largely diffused steam reforming processes. However, the design of a suitable industrial reactor is still a challenge due to the complex interplay between the multiple chemical and physical phenomena involved. Starting from the chemistry side, a well-directed CNT kinetic model can be a game-changing tool to support reactor design and accelerate scale-up efforts.

This work proposes a CNT model describing the main chemical steps involved in FCCVD reactors. A discrete-section approach is applied to address the extreme complexity related to the different chemical routes of carbon formation, aggregation, and CNT growth (Figure 1). The surface kinetic model is combined with a validated gas-phase pyrolysis mechanism also accounting for the competitive soot formation process, and then the model is used in a one-dimensional numerical simulation of the FCCVD reactor.

To the best of our knowledge, this is the first semi-detailed chemical kinetic framework, hierarchical and modular in nature, able to describe the relationships between catalyst, reaction conditions and CNT yields in the thermo-catalytic pyrolysis of methane. Although a thorough validation of the model requires further quantitative data, especially in terms of methane conversion, gas-phase species formation and nanotube yield. Results show very good agreement with the limited number of experimental observations and provide key guidelines on the optimal reactor conditions to minimize competitive amorphous carbon formation.

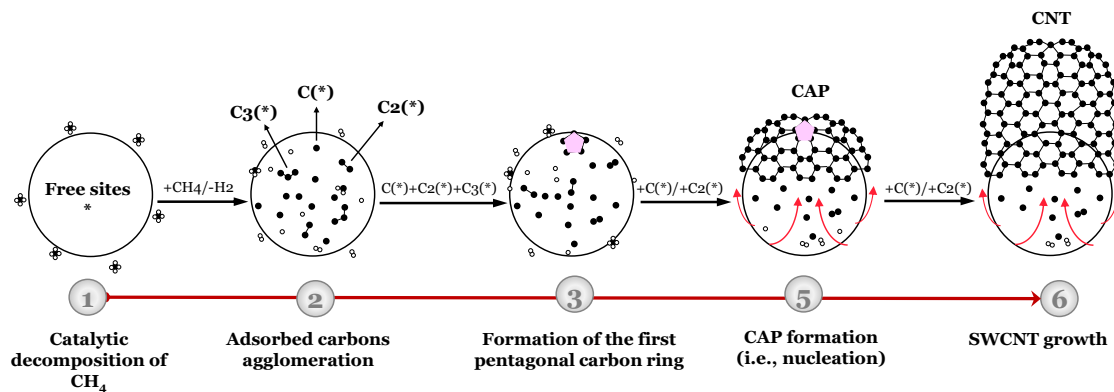


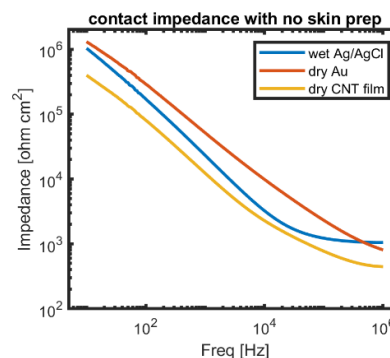
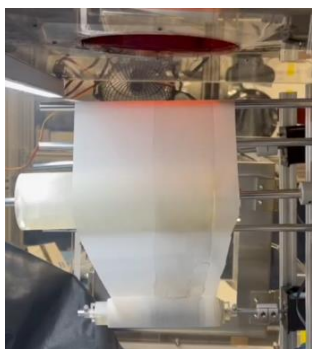
Figure 1: Schematic representation of the main steps involved in CNT growth.

Continues Synthesis of Free-standing SWNT films for Bioelectrode Applications

Qiang Zhang, David Fox, Yuhan Wen, Avetik Harutyunyan

Honda Research Institute USA, Inc. (USA)

Thin single wall carbon nanotube (SWNT) films have attracted attention for their high optical transmittance, electrical conductivity, and mechanical flexibility. High volume applications on energy devices and electronics have been demonstrated based on carbon nanotube films as platform materials. In this work, we developed an advanced floating catalyst chemical vapor deposition (FCCVD) method for the direct production of freestanding SWNT aerosols and roll-to-roll collection. This FCCVD method can provide over 10 m²/h free standing continues SWNT films with the typical thickness less than 10 nm that opens the path for broad range applications. By the optimization of synthesis conditions, we achieve the sheet resistance of SWNT thin film about 80 ohm/sq @ 90% optical transmittance, which can be used directly as a transparent electrode in a variety of applications. In addition, we applied these thin carbon nanotube films as dry bioelectrodes for biophysiological monitoring. The ultra-thin and conformal SWNT film is transferred directly to the human skin as a tattoo-style electrode. We found that dry electrodes mased on our SWNT films have a better electrode/skin interface with lower contact impedance, compared to other traditional electrodes, such as dry gold electrodes and wet Ag/AgCl electrodes considered the gold standard and benchmark in literature. Meanwhile, the dry CNT electrodes also have advantages in terms of cost, flexibility, stability and biocompatibility.



Roll-to-roll collection of CNT film (left); Photograph of dry CNT electrodes on skin (middle); Contact impedance results for the three types of electrodes (right).

Decoupling entrance and inner resistances in CNT channels

M. L. Jue¹, S. F. Buchsbaum¹, S. J. Park¹, K. E. Moyer-Vanderburgh¹, F. Fornasiero¹

¹ *Lawrence Livermore National Laboratory (USA)*

Due to their high transport rates, a great deal of attention has been recently given to 2D materials and slippery 1-D nanochannels as promising building blocks for next generation membranes. While in 2-D materials high flux is expected because of the classical inverse scaling of the flow rate with the pore thickness, in smooth channels such as carbon nanotubes (CNT), orders of magnitude rate enhancements with respect to classical theories are attribute to a vanishing friction at the pore wall. Irrespectively of the high flux origin, in both atomically thin and thicker but slippery nanopores, the flow rates are largely dictated by the entrance/exit hydrodynamic resistance.

For CNT channels, experimental quantification of the magnitude of end and inner resistances is still lacking despite its importance for both practical applications and fundamental understanding. This has led to inaccuracy and disagreement in the calculation of slip lengths and flow rate enhancements from experimentally measured permeation rates, since often entrance/exit resistances are neglected altogether, or an arbitrary magnitude is assumed. Here, we quantified these resistances for both gases and liquids in CNT channels by fabricating membranes with controlled CNT length and known number of open pores. We found that the end resistance dominates the total resistance. For liquid water, measured viscous energy dissipation at the nanotube ends is quantitatively described by Sampson equation. For 2.4 nm wide single-walled CNTs, measured slip lengths approach several microns. A prevailing contribution of the end resistance was also found in pressure-driven gas transport, and recorded flow rate enhancements with respect to Knudsen theory appear to be independent of the gas type. These findings further advance the community understanding of the peculiar and often unusual CNT fluidic properties and may help reconciling “conflicting” literature reports on the subject.

This work was performed under the auspices of the U.S. Department of Energy by Lawrence Livermore National Laboratory under Contract DE-AC52-07NA27344.

Symposia topics: Fundamental Properties

Title: Environmental Damping and Vibrational Coupling of Confined Fluids within Isolated Carbon Nanotubes

Authors and Affiliations:

Yu-Ming Tu¹, Matthias Kuehne^{1,2}, Rahul Prasanna Misra¹, Cody L. Ritt¹, Samuel Faucher¹, Daniel Blankschtein¹, and Michael S. Strano^{1*}

¹Department of Chemical Engineering, Massachusetts Institute of Technology, Cambridge, MA 02139, USA

²Department of Physics, Brown University, Providence, RI 02912, USA

Abstract:

Recent interest in the unique thermodynamic properties of fluids under nano-confinement is confounded by the enormous surface areas of nanotube systems, imparting exquisite mechanical coupling to their environment. Herein, we demonstrate extreme examples as temperature-dependent Radial Breathing Mode (RBM) frequencies in free-standing, electron-diffraction-assigned Double-Walled Carbon Nanotubes (DWNTs) that show large hyperbolic downshifts of 10 to 15%, for systems otherwise completely isolated in vacuum. Alternatively, when such systems are opened and filled using saturated water vapor, the RBMs trace Langmuir isobars and exhibit elliptical trajectories, allowing measurement of the enthalpy of phase change. We assign the former behavior using a harmonic oscillator model, describing the distinctive frequency cusp and hyperbolic trajectory to a reversible increase in damping from external graphitic domains. The resulting quantitative theory allows the isolation of confined fluid contributions to nanotube vibrations, providing new insights into nanomechanical coupling, and the basis for new devices and nanofluidic conduits.

High Volume Manufacturing of Single-Walled Carbon Nanotubes and Their Applications

Nano-C has developed an industrial scale process for manufacturing nanocarbon materials, both fullerenes and single-walled carbon nanotubes (SWCNT) in high volume. The increased scale and reliable supply, combined with the associated economics, enables device developers to commercialize highly differentiated products using these materials.

Nano-C was formed after a proof-of-concept in the Chemical Engineering Department of MIT. The patent-protected exothermic and easy-to-scale manufacturing approach for producing single-walled carbon nanotubes (SWCNT) has evolved from R&D reactors that can supply a few kilograms a year, to now having designs which are capable of > 500 kg annually per unit.

This process is based on the premixed oxidation of a hydrocarbon while introducing simultaneously a catalyst precursor such as iron pentacarbonyl. SWCNT are formed selectively under suitable non-sooting but fuel-rich conditions while supplying the catalyst-precursor at a concentration resulting in the formation of catalyst particles in a size optimized for the initiation of the SWCNT-growth process. All process parameters (and as a result the characteristics of the material formed) are well-defined and therefore highly reproducible. The growth of SWCNT in Nano-C's reactor is, at least as first approximation, a uni-dimensional process, i.e., the residence time in the reactor depends on the height above the burner and the velocity of the incoming gas mixture. The *in-situ* formation of water and hydrogen avoids the deactivation of the catalyst during the growth process. While the initial work at MIT was done using acetylene as hydrocarbon source, Nano-C's current operation is based on natural gas (methane) as fuel taking advantage of its very small tendency to form soot even at high fuel-to-oxygen ratios and therefore allowing to synthesize SWCNT selectively at high yield without the formation of other carbonaceous materials.



Fig.1 Nano-C's SWCNT reactor.

Nano-C has demonstrated the efficient formation of SWCNT using alternative carbon sources such as ethylene and ethanol. In an effort to enable net-zero carbon operations of SWCNT-manufacturing, Nano-C is targeting the use of renewable carbon sources, particularly, biogas and/or carbon-neutral alcohol. Also, the exhaust gas contains significant (up to nearly 50%) quantities of hydrogen (H_2) which can be either recovered or used for energy generation, together with this heat generated by the SWCNT manufacturing process.

One of the key aspects of Nano-C's approach is the continuous nature of its operations. The material produced by the reactor is collected in a baghouse filter allowing for 24x7 operation. Process conditions can be optimized for the control of the SWCNT characteristics (e.g., length) to fit the technical needs of a specific end use. The opportunity for higher output reactors is central to Nano-C's development pipeline. As an example, larger or multiple burners can be used to increase output and yield further driving down the cost curve.

Equally important as the synthesis of the nanocarbon materials themselves, Nano-C has developed technology and processes for the efficient purification of SWCNT followed by their dispersion in a range of solvents targeting the improvement of electric and/or mechanical properties in applications such as batteries, transparent or opaque films used, e.g., as electrodes for photovoltaic devices or actuators.

High-Performance Hemofiltration via Molecular Sieving and Ultra-Low Friction in Carbon Nanotube Capillary Membranes

Piran Kidambi, PhD

No Abstract

Hydroxide Derived Nanomaterials and Their Properties

Michel W. Barsoum

Department of Materials Science and Engineering, Drexel University, Philadelphia, PA 19104 USA

The aim of this talk is to describe what happens when a number of Ti-, Mn-, Si-, and Fe-based precursor powders are placed in high pH environments at temperatures < 100 °C under ambient pressures for tens of hours. In the Ti-case, we converted more than a dozen different precursors (TiC, TiB₂ etc.) into lepidocrocite titania-based sub-nano filaments, (1DLs), $\approx 5 \times 9$ Å² or 2x6 Ti atoms (Fig. 1) in cross-section that are remarkably water stable.^{1,2} Depending on how they are washed, the 1DLs self-assemble into quasi-2D flakes, mesoscopic particles, nanofilaments or totally inorganic titania gels, the latter a first.^{3,4} The photochemical production of H₂ – for over 6 months - and dye degradation using these 1DLs will be discussed.⁵ How common dyes sensitize the 1DLs allowing them to absorb light in the visible spectrum will be touched upon.⁶ In the Mn-case, five water-insoluble Mn-bearing precursors, were converted to birnessite 2D MnO₂ flakes, that are quite crystalline and perform well for OER. In the Si-case we end up with a silica with a band gap energy of > 5 eV. In the Fe-case we end up with ferrimagnetic 20-30 nm spherical NPs. Two years after discovery, we routinely make 100 g 1DL batches, in a lab setting, with nothing more sophisticated than plastic bottles and hot plates. In most cases, conversions are 100% precluding the need for centrifuges, filters, etc. I will argue that our processes' surprising simplicity, universality and scalability in making nanomaterials of all shapes and sizes, in general, and 1DLs, in particular, is paradigm shifting and constitutes a veritable leap forward in the manufacturing of nanomaterials.

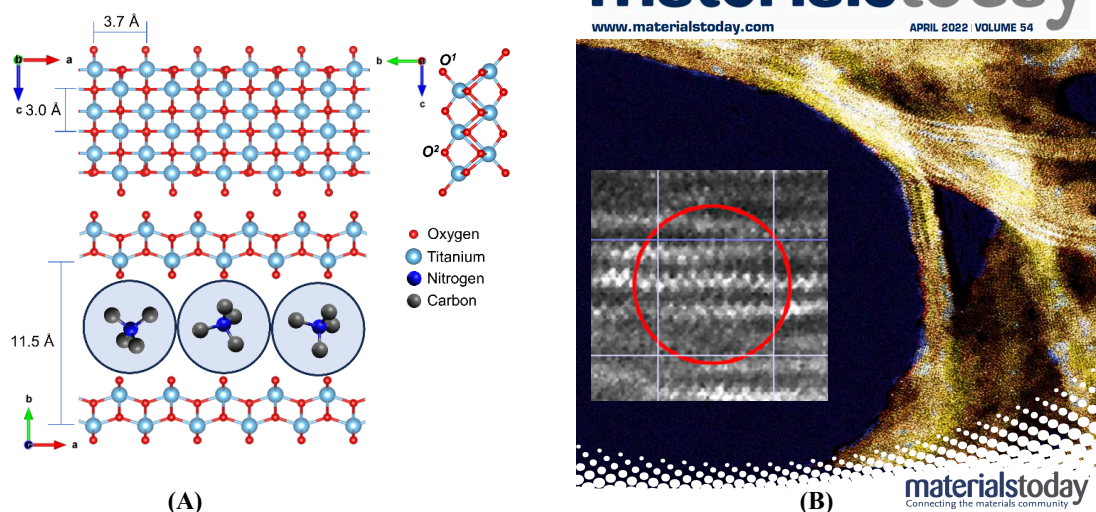


Figure 1: (A) Three views of DFT generated structure that fits the diffraction results. a-b plane shows hydrated TMA cations between the 1DLs. (B) Colorized HRTEM micrograph of 1DLs. Inset shows two Ti atom motive (bottom left in A) characteristic of 1DLs. Micrograph taken by Dr. P. Persson, Linkoping University, Sweden. and colorized and aesthetically enhanced by P. Lyons of Moorestown, NJ.

References

- [1] Badr, H. *et al.* Bottom-up, Scalable Synthesis of Anatase Nanofilament-based Two-dimensional Titanium Carbo-oxide Flakes. *Mater. Today* **54**, 8-17 (2022).
- [2] Badr, H. O. *et al.* On the Structure of One-Dimensional TiO₂ Lepidocrocite. *Matter* **6**, 128–141 (2023).
- [3] Badr, H. O. *et al.* Self-assembly of 1D Lepidocrocite Titania into 2D Sheets and Mesoporous Particles. *Matter* **6**, 1-17 (2023).
- [4] Sudhakar, K. *et al.* One-dimensional, Titania-based Lepidocrocite Nanofilaments and their Self-assembly. *Matter* **6**, 2834-2852 (2023).
- [5] Badr, H. *et al.* Ultra-stable, 1D TiO₂ Lepidocrocite for Photocatalytic Hydrogen Production in Water-Methanol Mixtures. *Matter* **6**, 2853–2869, (2023).
- [6] Walter, A. D. *et al.* Adsorption and Self-Sensitized Photodegradation of Rhodamine 6G and Crystal Violet by One-Dimensional Titanium Dioxide-based Lepidocrocite Under Visible Light. *Matter* (2023).

Impact of Purification Methods on Carbon Nanotube Material Properties

D.W.Gailus¹, M.A. Banash², S.R.Strand, D.Varshney¹, M.S.Hibbard¹

¹*Nanocomp/Huntsman Advanced Materials (USA)*, ²*Neotericon, LLC (USA)*

Floating catalyst chemical vapor deposition (FC-CVD) offers several advantages over alternative CNT growth methods but also carries with it some unique challenges. In FC-CVD the metal nanoparticles that are needed to initiate CNT growth are borne by a carrier gas rather than supported on a fixed substrate as in forest growth or on a moving ceramic particle in a fluidized bed process. Since there is no support for the metal nanoparticle catalyst, FC-CVD can operate at high temperatures without the issue of metal diffusing into the substrate or other negative substrate interactions. The higher temperatures allow for rapid growth of high aspect ratios CNTs with cycle times typically measured in seconds. A downside however is the metal catalyst, both the nanoparticles that successfully initiate CNT growth and any excess, are retained in or on the CNT product. These particles are typically encapsulated in a graphitic shell making them chemically benign and acceptable for most applications, but for some uses removing this residual metal is desirable. The carbon passivation layer that makes these residual particles relatively unreactive also makes them difficult to remove by chemical means. Removing the graphitic shell is possible, but the process conditions needed can damage or remove some of the CNTs impacting the product properties or yield. This work describes the effectiveness various iron removal methods and their impact on the CNT material properties.

Incorporation of Nanomaterials Into PVDF Porous Membranes For Improved Water Treatment

I. Maggay¹, C.-J. Wu¹, C.C. Hu², Y. Chang¹, A. Venault^{1*}

¹*Department of Chemical Engineering and R&D Center for Membrane Technology, Chung Yuan Christian University, Chungli (Taiwan),* ²*Department of Chemical Engineering and R&D Center for Membrane Technology, National Taiwan University of Science and Technology, Taipei (Taiwan)*

The performance of porous poly(vinylidene fluoride) (PVDF) membranes, commonly used in water treatment, can be significantly enhanced by incorporating nanomaterials into the matrix. In this context, we discuss two specific cases involving the use of graphene oxide (GO) and MIL-53(Fe) to improve the separation of emulsions and the removal of antibiotics from water, respectively.

In the first case, the GO was blended to PVDF and membranes formed by vapor-induced phase separation. Due to its amphiphilic nature, GO neither hydrophilized nor hydrophobized the surface in air. However, it improved oil repellence under water. Subsequent gravity-driven filtration tests, performed after pre-wetting the membranes with the dispersing phase, revealed that the inclusion of GO accelerated the separation process by a factor of 8-10 for both oil-in-water (O/W) and water-in-oil (W/O) emulsions. Furthermore, GO enhanced interactions with the wetting liquid, effectively eliminating air pockets. This prevented the dispersed phase in complex emulsions (such as those involving diesel or soybean oil) from permeating through the pores, and so, enhanced the separation efficiency.

Moreover, MIL-53(Fe) was incorporated into PVDF membranes formed by the liquid-induced phase separation, and utilized for the removal of tetracycline (TC) from water. The incorporation of MIL-53(Fe) into the casting solution led to a rise in viscosity, effectively mitigating the formation of macrovoids along the polymer matrix's cross-section. As a result, the bulk pore size was reduced. Additionally, this process augmented the bulk tortuosity by inhibiting macrovoid formation, thereby improving the depth-filtration mechanism within the modified membranes. Notably, the optimized membrane achieved a 87% rejection rate against TC. Subsequently, the nanoparticles facilitated the degradation of 93% of the unrejected TC. With less than 1% TC remaining undegraded, the photocatalytic membrane demonstrated highly competitive effectiveness, presenting a viable approach to addressing the challenges posed by pharmaceutical products in wastewater.

Integrating Fluorescent Nanosensors with Microfluidics for Label-Free Chemical Cytometry

Sooyeon Cho^{1,*}

¹ School of Chemical Engineering, Sungkyunkwan University (Republic of Korea)

*Email: sooyeonc@skku.edu

Label-free profiling and quantification of multivariate single cell properties including both biophysical and molecular attributes can lead to the most fundamental technological innovation for future medicine such as cell therapy and realization of precision medicine.

In this talk, we will introduce a new label free single cell analytics: nanosensor chemical cytometry (NCC). An array of fluorescent nanosensors is integrated with microfluidics in which a population of flowing cells will be guided, using specific integration technique of particulate form of the nanosensors. One can utilize the flowing cell itself as highly informative Gaussian lenses projecting near infrared (nIR) emission profiles and extract rich information on a per cell basis in real time and a label free manner. With a deep learning-based software that our team designed, this unique biophotonic waveguide allows users to quantify the cross correlation of the real time biomolecular efflux profile such as reactive oxygen species (ROS) or reactive nitrogen species (RNS) with biophysical properties of single cells such as cell size, shape (e.g. eccentricity), and refractive index (RI). We show that it operates as a label free chemical cytometer for the measurement of cellular heterogeneity of versatile cell line and patient cells with unprecedented precision for various types of cells and their target analytes.

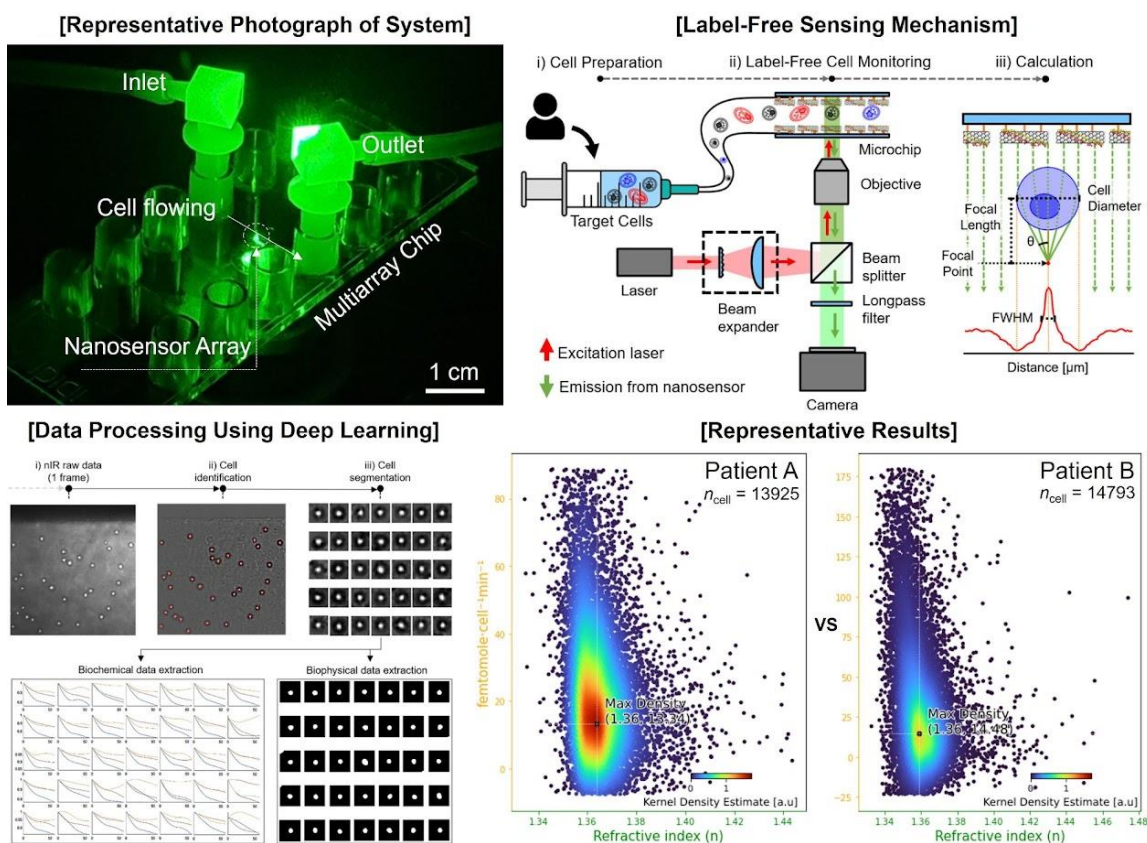


Figure: Systematic design and representative single cell data of NCC.

References

- [1] Youngho Song, Soo-Yeon Cho*, et al. *ACS Meas. Sci. Au* **3**, 393-403 (2023).
- [2] Seunghye Han, Soo-Yeon Cho*, et al. *ACS Sens.* **8**, 1676–1683 (2023).
- [3] Soo-Yeon Cho, Michael S. Strano*, et al. *Nat. Commun.* **12**, 3079 (2021).
- [4] Soo-Yeon Cho, Michael S. Strano*, et al. *ACS Nano* **15**, 13683-13691 (2021).

Molecular dynamics simulations of carbon nanotube growth on solid rhenium catalysts

Daniel Hedman¹

¹Center for Multidimensional Carbon Materials (CMCM), Institute for Basic Science (IBS) (Republic of Korea)

Carbon nanotubes (CNTs) are typically grown via catalytic chemical vapor deposition using catalysts such as iron, cobalt or nickel in the form of nanometer-sized clusters. At the temperatures used for growth, these small clusters are typically liquid resulting in limited control over the CNT structure, leading to a broad chirality distribution. Using catalysts with a high melting temperature such as CoW, has in contrast shown to result in a significantly narrower chirality distribution[1]. In-situ transmission electron microscopy further confirms that these catalysts remain solid during growth[2]. Recent molecular dynamics (MD) simulations have revealed the mechanisms of CNT growth on liquid Fe catalysts[3], reproducing the experimentally observed broad chirality distribution. However, MD simulations of CNT growth on solid catalysts are lacking and thus the mechanisms of growth on such catalysts are mostly unexplored.

Here I present MD simulations of CNT growth using rhenium catalysts, which have a high melting temperature and are experimentally known to grow CNTs[4]. The simulations are driven by a Neuroevolution potential (NEP) machine learning force field, trained on dispersion-corrected density functional theory calculations. NEP's efficiency enables growth simulations exceeding 150 ns/day while maintaining high accuracy with an RMSE of 13.6 meV per atom in energy and 387 meV/Å in force. Preliminary results, shown in Figure 1, reveal that the Re₁₄₄ cluster remains solid during growth at 1300 K with distinct facets and a hexagonal close-packed structure. The low solubility of carbon in rhenium prevents diffusion into the bulk, leading to carbon only on the catalyst surface in the form of dimers and short chains. During growth, the CNT-cap is formed on top of a facet at its edge. Likewise, continuous growth occurs on top of a facet where parts of the growing tube overhang the edge of the facet. These MD simulations advance our understanding of the mechanisms of CNT growth on solid catalysts and provide valuable insight into controlled synthesis.

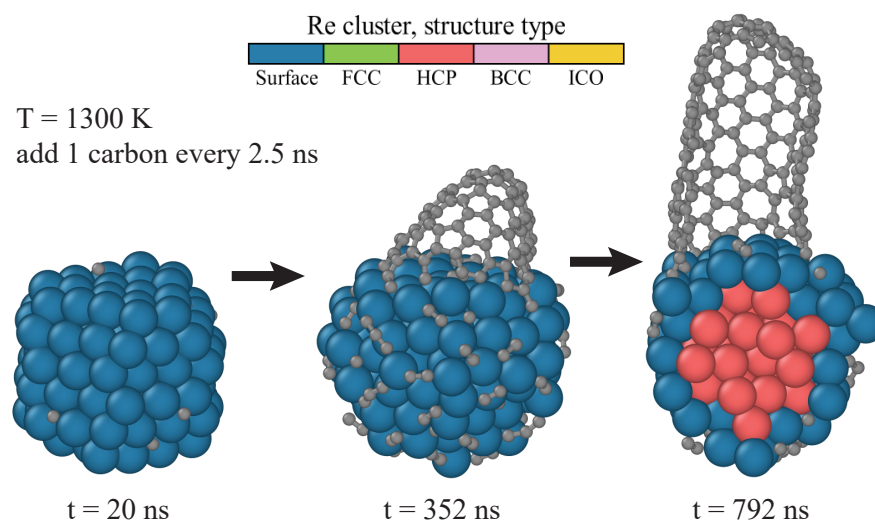


Figure 1: Snapshots from MD simulations of CNT growth on a solid Re₁₄₄ cluster.

References

1. F. Yang *et al.*, *Nature*. **510**, 522-524 (2014).
2. F. Yang *et al.*, *Science Advances*. **8**, eabq0794 (2022).
3. D. Hedman *et al.*, *arXiv*. (2023).
4. X. Zhang *et al.*, *Science Advances*. **6**(2020).

Novel imaging concepts for carbon nanotube based biosensors

S. Kruss¹

¹*Ruhr Universität Bochum, Germany*

Single wall carbon nanotubes (SWCNTs) are versatile building blocks for biosensors. Their near infrared (NIR) fluorescence enables detection of biomolecules in the optical tissue transparency window. By changing their surface chemistry they are tailored to selectively interact with analytes, which typically changes the fluorescence intensity. However, such signals are affected by external factors such as sample movement or fluctuations in excitation light. Here, we show concepts to improve imaging of SWCNT-based biosensors. First, we demonstrate fluorescence lifetime imaging microscopy (FLIM) of SWCNT-based sensors in the NIR as absolute and calibration-free method. For this purpose, we use a tailored laser scanning confocal microscope (LSCM) optimized for NIR signals (>800 nm) and time correlated single photon counting (TCSPC). (GT)₁₀-DNA modified SWCNTs change their fluorescence lifetime in response to the neurotransmitter dopamine. These lifetime sensors are used as paint to cover cells and report extracellular dopamine in 3D [1]. Additionally, we demonstrate ratiometric imaging by using non-responsive NIR fluorescent nanosheets as reference signal. Another implementation uses quantum defects as internal reference for the sensor. Both approaches increase the signal to noise ratio and improve sensitivity. In summary, we show that fluorescence lifetime and ratiometric imaging concepts advance SWCNT-based biosensors.

References (if desired)

[1] Sistemich et al. *Angew. Chem.* 2023

Assessing the Stability and Aggregation Behavior of DNA-functionalized SWCNTs in Various Biofluids

M. Card, L. Hubert, A. Smith, D. Roxbury

University of Rhode Island
Department of Chemical Engineering

Abstract

A challenge of particular interest in the fields of *in vivo* biosensing and bioimaging is the acquisition of real-time readouts of localized bioanalyte concentration through live tissue in a minimally-invasive fashion. The intrinsic fluorescence of single-walled carbon nanotubes (SWCNTs), which exhibits exceptional photostability, near-infrared (NIR) tissue-penetrating emission, and microenvironmental sensitivity, makes them ideal candidates for a variety of biomedical imaging and sensing applications. By functionalizing SWCNTs with appropriate biopolymers, we can simultaneously impart biocompatibility and sensitivity for certain biomolecules of interest. Using novel spectroscopy and microscopy approaches, this talk features our recent advances in the characterization of such engineered nanomaterials in various fluids of physiological relevance. In particular, we probe the solution-phase stability of DNA-functionalized SWCNTs in biofluids and report significantly different aggregation behavior (i.e. size, shape, kinetics). We further address the mechanisms of the various types of aggregation behaviors that were observed. Our data will guide the rational design of SWCNT-based sensors for future *in vivo* use.

Robotic assembly of high-quality nanomaterials including CNTs

M. El Abbassi¹, F. van Veen², A. Butzerin¹, L. Ornago¹, M. Nikolic¹, M. Perrin²,
S. Jung¹, N. Lanz¹

¹Chiral Nano AG (Switzerland), ²EMPA laboratory 405 (Dübendorf, Switzerland)

Nanomaterials, and in particular nanowires and TMDs, have attracted an increasing interest from the major semiconductor players due to their unique properties and potential [1,2].

In particular, Carbon NanoTubes (CNTs) have been demonstrated to be promising candidates for sensing applications with very high selectivity if functionalized. Several studies have demonstrated the potential of arrays of CNTs as high-performance FETs and processors [3]. Furthermore, several recent studies have also demonstrated the unique properties of CNTs as host materials in quantum computing with a very high potential for scalability [4,5].

However, to enable any robust industrial application of these materials, one needs to gain a better understanding and control of their properties. In the case of CNTs, reproducible and robust chirality control during growth as well as large scale integration has not been demonstrated yet. Developments of wafer scale methods for integration and characterization are crucial to bridge this milestone.

Chiral Nano, a spin-off of ETH Zurich, combines high precision robotics, machine vision and advanced data analysis to develop high speed and high precision robots that can assemble high quality nanomaterials on a 4-inch wafer with more than 100 transfers per hour. In this talk, I will present our workflow for the growth and integration of high quality SWCNT into a FET geometry. Several robotic and machine learning techniques have been combined to reach a 4inch wafer efficient for all the steps including the growth, characterization, and transfer. We also developed different recipes for the cleaning of the electrodes and the selection of the tubes prior to transfer that lead to a very high yield of clean devices [6,7]. The cleanliness of the devices is confirmed by large statistics of transport data at low temperatures.

[1] O'Brien, K.P., Naylor, C.H., Dorow, C. et al. Process integration and future outlook of 2D transistors. *Nat Commun* 14, 6400 (2023).

[2] Montblanch, A.R.P., Barbone, M., Aharonovich, I. et al. Layered materials as a platform for quantum technologies. *Nat. Nanotechnol.* 18, 555–571 (2023).

[3] Hills, G., Lau, C., Wright, A. et al. Modern microprocessor built from complementary carbon nanotube transistors. *Nature* **572**, 595–602 (2019).

[4] Chen, J.S., Trerayapiwat, K.J., Sun, L. et al. Long-lived electronic spin qubits in single-walled carbon nanotubes. *Nat Commun* 14, 848 (2023).

[5] Cubaynes, T., Delbecq, M.R., Dartailh, M.C. et al. Highly coherent spin states in carbon nanotubes coupled to cavity photons. *npj Quantum Inf* 5, 47 (2019).

[6] Zhang, J., Perrin, M.L., Barba, L. et al. High-speed identification of suspended carbon nanotubes using Raman spectroscopy and deep learning. *Microsyst Nanoeng* 8, 19 (2022).

[7] Seoho Jung, et al., Understanding and improving carbon nanotube-electrode contact in bottom-contacted nanotube gas sensors, *Sensors and Actuators B: Chemical*, Volume 331, 2021, 129406.

Safe and damage-less dry-purification of carbon nanotubes using Br₂ vapor

Takuma Goto¹, Toshio Osawa¹, ◯Suguru Noda^{1,2,*}

¹Department of Applied Chemistry, Waseda University (Japan)

²Waseda Research Institute for Science and Engineering, Waseda University (Japan)

Various purification methods have been developed to remove catalyst metals from carbon nanotubes (CNTs). Cl₂-gas treatment at high temperatures ~1000 °C enables catalyst removal without damaging or agglomerating CNTs [1,2], however it has safety concerns of possible corrosion by and leakage of highly toxic Cl₂ gas. We have previously proposed and developed the FeCl₃-vapor treatment and demonstrated efficient removal of various catalysts (Fe, Ni, Y, Mg, and Al) from single-wall CNTs (SWCNTs by arc-discharge and Tuball-CNTs) and multi-wall CNTs (MWCNTs by chemical vapor deposition) [3,4]. Careful temperature adjustment was shown effective in preserving the structure of small diameter SWCNTs [5]. However, when applied to CNTs that contain little Fe, the FeCl₃-vapor treatment caused Fe contamination of ~0.3 mass% [4].

Here we propose Br₂ as an alternative etching gas [6]. Although it is toxic and has a vapor pressure of 22 kPa at 20 °C, it is liquid at ambient condition and thus has lower risk upon leakage than Cl₂ gas. Various CNT samples were purified by 10 vol% Br₂/Ar gas at 100 Torr for 30 min at 1000 °C. Fig. 1 shows that catalyst particles of Fe, Co, Ni, Y were removed from the CNTs, leaving empty carbon shells with reduced metal contents. Especially when applied to JENOTUBE 10B MWCNTs with high purity, Co impurity was reduced from 9300 to 50 ppmw. Raman scattering spectroscopy showed no degradation in CNT structures and TG-DTA showed the reduced ash content with increased combustion temperature. The purification results using Br₂ will be compared with those using Cl₂ and FeCl₃.

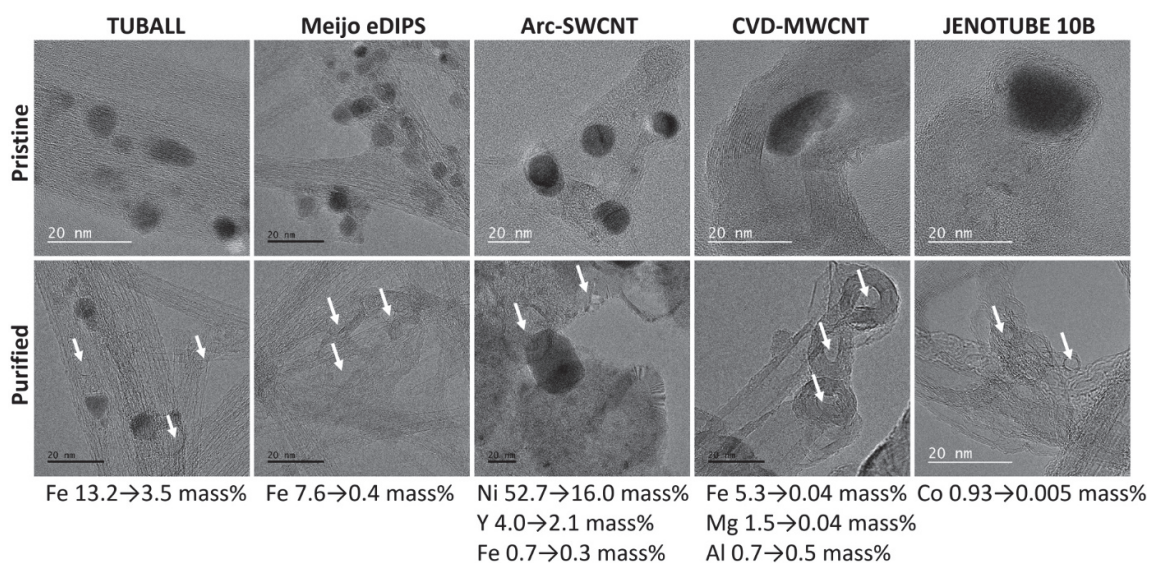


Fig. 1. TEM images with ICP-OES results of various CNTs before/after the Br₂ vapor treatment.

References

- [1] Y. Takimoto, et al., Patent (2008). WO2008/126534.
- [2] G. Mercier, et al., New J. Chem. 37 (2013) 790.
- [3] S. Noda, et al., Patent (2023). JP7278539.
- [4] H. Tanaka, et al., Carbon 212 (2023) 118171.
- [5] Y. Kuwahara, et al., Carbon 213, (2023) 118207.
- [6] S. Noda and K. Hamada, Patent (2022). JP7044372.

Scaling Law of Quantum Confinement in Ultrashort Carbon Nanotubes

Benjamin R. Eller¹, YuHuang Wang^{1,2}

¹Chemical Physics Program, University of Maryland, College Park, MD 20742 (USA), ²Department of Chemistry & Biochemistry, University of Maryland, College Park, MD 20742 (USA)

Quantum confinement significantly influences the properties of sub-10 nm carbon nanotubes (CNTs), crucial for advancements in transistor technology [1-4] and the development of novel optoelectronic materials such as fluorescent ultrashort nanotubes (FUNs) [5,6]. However, the specifics of this effect in ultrashort CNTs are not yet fully understood. Here, we conducted excited state calculations using time-dependent density functional theory on geometry-optimized models of these nanomaterials. Our results reveal a notable spectral shift of the dominant low-energy transition, $E_{conf}(L)$, which follows a length-dependent scaling law. This scaling law can be understood through a geometric, dimensional argument. This scaling is consistently observed in FUNs, suggesting its universality. Intriguingly, the defect-induced peak (E_{sp^3}), which is redshifted from E_{conf} , remains largely independent of the nanotube length even in these ultrashort lengths. We attribute this anomaly to orbitals localized around the quantum defect installed near the nanotube edge. Our results illuminate the complex interplay of defects and quantum confinement effects in ultrashort CNTs and provide a foundation for further explorations of these nanoscale phenomena.

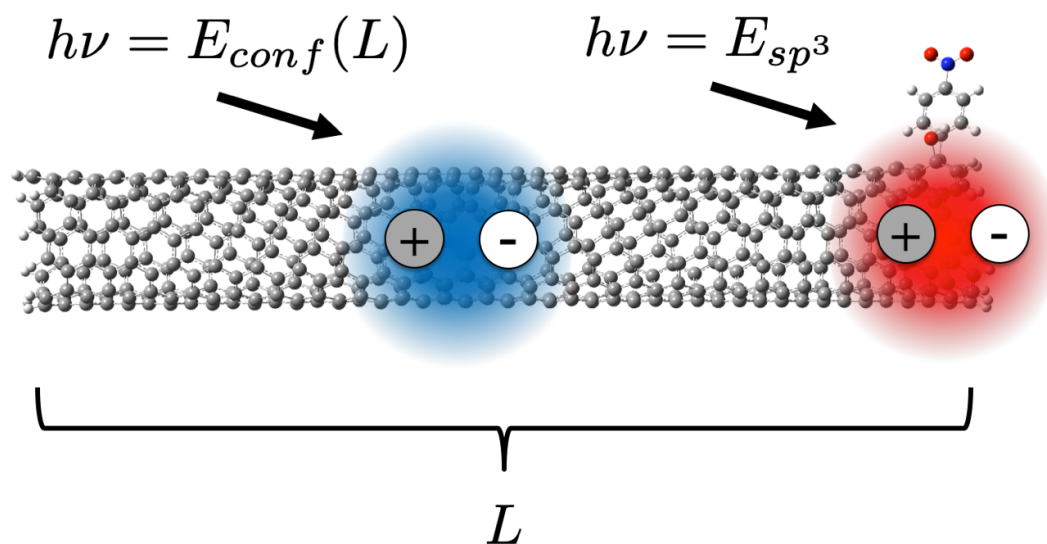


Figure 1. Model of a FUN, consisting of a finite (6,5) single-walled CNT of length L and an sp^3 -defect (nitrobenzene with an OH pairing group) defined near the edge of the nanotube. The defect introduces an absorption peak (E_{sp^3}) redshifted from the pristine transition (E_{conf}). The defect-induced peak is weakly dependent on L , whereas the CNT peak blueshifts as L decreases.

References

- [1] A. D. Franklin *et al.*, *Nature Nanotech.* **5**, 858-862 (2010).
- [2] A. D. Franklin *et al.*, *Nano Lett.* **12**, 758-762 (2012).
- [3] C. Qiu *et al.*, *Science* **355**, 271-276 (2017).
- [4] Q. Cao *et al.*, *Science* **356**, 1369-1372 (2017).
- [5] N. Danné *et al.*, *ACS Nano* **12**, 6059-6065 (2018).
- [6] Y. Li *et al.*, *Chem. Mater.* **31**, 4536-4544 (2019).

Sensing and Ice Protection for Aerospace Applications Enabled by Macroscopic Carbon Nanotube Networks

S. Kessler¹, E. Kalfon Cohen¹, G. Botura², and Y. Stein³

¹Metis Design Corporation (USA), ²Raytheon Technologies (USA), ³Analog Devices Inc.(USA)

While CNT are nanoscopic by definition in stature, they can accomplish significant feats when assembled into macroscopic networks. Specifically for aerospace applications where size, weight and power (SWaP) are at a premium, CNT-enabled functionality can be extremely valuable. Two examples of CNT-enabled technologies that have been matured from proof-of-concept laboratory experiments all the way through successful flight testing are sensors for fatigue crack monitoring, and heaters for aerosurface ice protection.

A crack gauge sensor was formed by blending CNT in “powder” format with an epoxy binder to form a polymer nanocomposite (PNC), which is then sealed between flexible thermoplastic sheets along with silk-screened metallic electrodes. CNT are advantages for this application due to their resilience to corrosion, creep and fatigue, and offering a greater resistivity than metal traces resulting in higher precision measurements with common electronics. An in-situ compensation strategy was implemented, and proved effective in counteracting all studied external factors. A simple fatigue experiment was conducted on 60 aluminum bars with EDM notches to define the initiation point, and a PNC crack gauge was bonded to each bar. One hundred data points were collected during each experiment as the crack grew up toward 2mm in length, and a probability of detection (PoD) curve was established using a hit/miss statistical model. The resulting $a_{90|95}$ value (smallest crack found with 90% probability and 95% confidence) was 0.32mm. Based on these PoD results, the PNC crack gauge participated in a high-g flight-test campaign on an F-15 through the U.S. Air Force.

A novel approach to electrothermal heating has been developed by using CNT in “sheet” format that generates joule heat by running a current across this resistive layer. CNT offers resilience to corrosion and fatigue, and has the potential to provide a very stable and uniform sheet resistance when properly implemented. The largest benefit to using CNT heaters is a substantial weight reduction for the same heated area, simply because copper has ~5x higher density over carbon. A continuous CNT heater has the potential for total power saving by taking much less time to uniformly heat a given area. Finally, CNT-based heaters are better matched with increasingly popular carbon fiber airfoils in terms of coefficient of thermal expansion, making them less prone to causing delamination due to residual or induced thermal stress. We have thoroughly characterized the performance of CNT deicing heaters, including their thermal profile, durability through electrical and mechanical fatigue testing, and operation through more than 500 hours of wind-icing tunnel testing. Finally, a flight test campaign was conducted for a CNT heater applied to an Embraer Phenom 300 operating in both dry and icing conditions.

References

- [1] Lee J., Stein I.Y., Devoe M.E., Lewis D.J., Lachman N., Kessler S.S., Buschhorn S.T. and B.L. Wardle “Impact of carbon nanotube length on electron transport in aligned carbon nanotube networks.” *Applied Physics Letters* 106, 053110 (2015)
- [2] Kessler, S.S., Raghavan A. and B.L. Wardle (2017). Multifunctional CNT-Engineered Structures (U.S. Patent No. 9,839,073). U.S. Patent and Trademark Office.
- [3] Stein Y., Kessler, S.S. and H. Primo (2023). Self-Calibrating Polymer Nano Composite (PNC) Sensing Element. (U.S. Patent No. 11,656,193). U.S. Patent and Trademark Office.
- [4] Kessler S.S., Thomas, G.A., Dunn C.T., Borgen M. and B.L. Wardle (2023). Multifunctional Assemblies (U.S. Patent No. 11,706,848). U.S. Patent and Trademark Office.
- [5] de Villoria R.G., Kessler S.S., Wicks S., Miravete A. and B.L. Wardle “Multi-physics nano-engineered structural damage detection and de-icing.” *Proceedings of the 18th International Conference on Composite Materials, Jeju Korea (2011).*

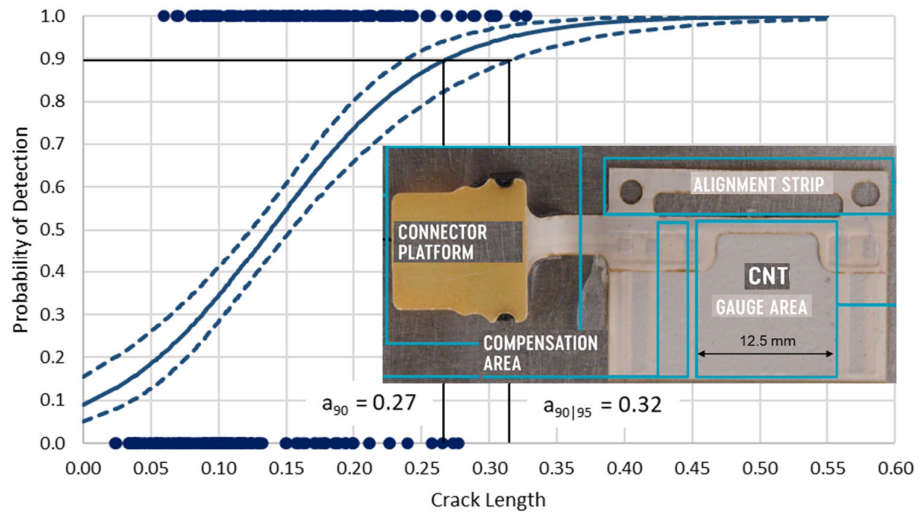


Figure 1: Probability of Detection (PoD) for a carbon nanotube crack gauge as a function of crack length.

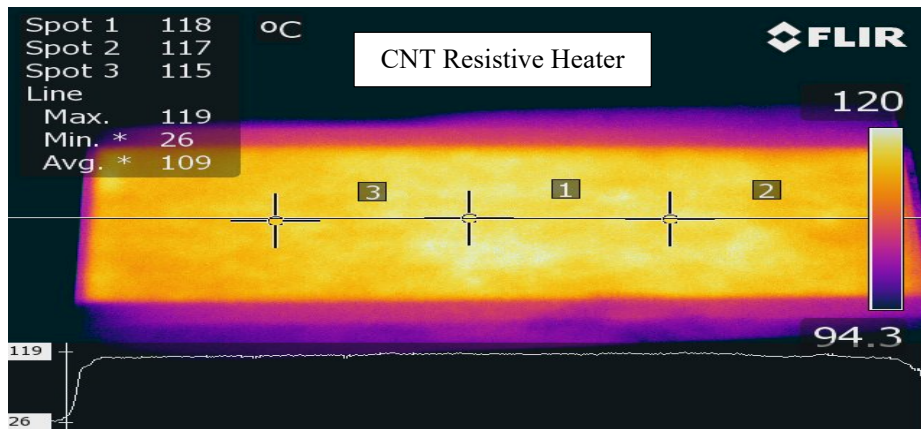


Figure 2: Infrared thermograph illustrating the thermal profile of a carbon nanotube (CNT) deicing heater.

The Search for Multi-Functional Composite Material and Structure

Kevin Retz Ph.D, Thomas Goislard Ph.D²,

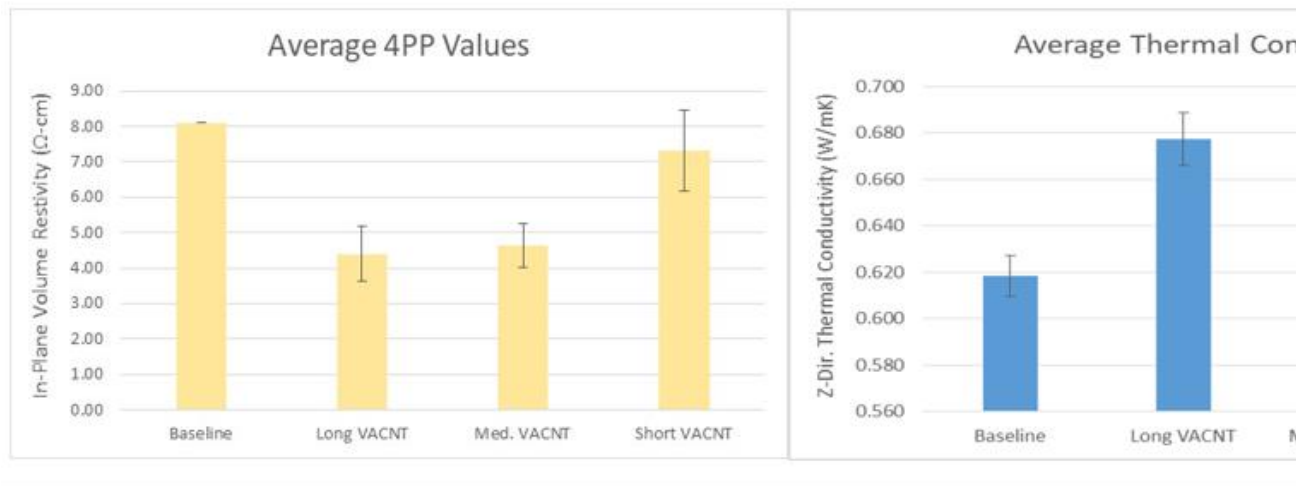
¹NAWA America (U.S.A), ²NAWA (France), ...

The utilization of composite materials is growing rapidly. The sporting goods industry, automotive, energy, infrastructure and the growing E-VTOL market are all increasing the utilization of composite materials. In today's competitive market engineering teams must develop multifunctional integrated designs that are lighter, cost effective, easy to manufacture and yet meet very tough structural requirements.

This presentation will explore the benefits of adding NAWASTitch to a composite material to develop a material that can deliver multifunctionality to composite structures. NAWASTitch is a new composite innovation where a vertically aligned carbon nanotube (VACNT) forest is located between plies of a laminate composite resulting in improved mechanical properties as well as other multifunctional properties such as thermal and electrical conductivity. With the addition of NAWASTitch the engineer can change the behavior of the composite material to deliver a true multifunctional structure. NAWASTitch changes the composite structures properties in the Z direction or through plane direction and increases the ply to ply and intra-ply properties of the composite.

A key area that the team has explored in addition to multifunctional structures is the benefits that the addition of NAWASTitch can have to materials used in composite repairs. NAWA has demonstrated that the addition of NAWASTitch to a prepreg can enable vacuum bag composite repairs without the use of autoclaves or heating blankets. The NAWA team has also demonstrated that the utilization of NAWASTitch can greatly improve the damage tolerance of a composite structure.

This paper explores the path that NAWA has taken to define and validate the multi functionality that the addition of VACNT's can give the composite design engineer. Besides the typical mechanical testing the team has completed extensive testing to understand the Z direction property enhancements that the addition of VACNT's to the resin layer interface can provide. The following images demonstrate this capability: the addition of VACNT's increases both the electrical and thermal properties of the composite material in the Z direction.



Properties in the Z direction: Electrical and Thermal properties in the Z direction with different lengths of Vertically Aligned Carbon Nanotubes (VACNT).

References (if desired)

- [1] M. S. Dresselhaus *et al.*, *Phys. Rep.* **409**, 47–99 (2005).
- [2] A. K. Geim, *Science* **324**, 1530–1534 (2009).
- [3]

Uncovering the Role of Water Electric Fields on the Different Regimes of Diameter-Dependent Slip Flow Inside Carbon Nanotubes

Rahul Prasanna Misra¹, Shuang Luo¹ and Daniel Blankschtein¹

¹*Department of Chemical Engineering, Massachusetts Institute of Technology, Cambridge, Massachusetts 02139, United States*

The enormous promise of carbon nanotubes (CNTs) for applications at the water-energy nexus, including seawater desalination, energy storage, and as chemical and flow sensors, has in turn triggered tremendous interest to develop a deeper fundamental understanding of the water/CNT interface. Previous experimental studies have found that the CNT wall acts like a low friction surface resulting in a large slippage of water in 30-100 nm diameter CNTs [1] and inside sub-1 nm diameter CNT porins which exhibit enhanced water permeabilities compared to biological channels [2]. Because water is a polar molecule and CNTs are highly polarizable nanomaterials, the electric fields exerted by the water molecules can strongly polarize the charge distribution in the CNTs, yet the role of the ensuing water-carbon polarization interactions on the different regimes of diameter-dependent slip flow remains unknown. In this work, we utilize a recently introduced theoretical framework which can accurately model the many-body polarization interactions at graphitic surfaces [3,4] to investigate the diameter-dependent friction coefficients and slip lengths of water inside CNTs. To this end, we first demonstrate that our model can self-consistently describe the water-CNT polarization interactions in both metallic and semiconducting CNTs, and then utilize this model to uncover two different water transport regimes. Specifically, for narrow CNTs with diameters in the range of 0.8 to 1.5 nm, we show that the water-CNT polarization interactions have a pronounced effect on the water friction coefficients through an enhancement in the water density. On the other hand, in the case of larger diameter CNTs with a distinct bulk-like region in the center and an interfacial region near the CNT wall, the water-CNT polarization interactions contribute to a significant diameter dependence of the water friction coefficients through an alteration of the orientation of the interfacial water molecules. Overall, our findings underscore the crucial role of the water electric fields and the ensuing water-nanopore polarization interactions on water transport, which is vital for the rational design of CNTs and other 1-dimensional nanomaterials in membrane-based applications.

References

- [1] Secchi, E., Marbach, S., Niguès, A., Stein, D., Siria, A. & Bocquet, L. Massive radius-dependent flow slippage in carbon nanotubes. *Nature* **537**, 210 (2016).
- [2] Tunuguntla, R., Henley, R., Yao, Y.-C., Pham, T. A., Wanunu, M. & Noy, A. Enhanced water permeability and tunable ion selectivity in sub-nanometer carbon nanotube porins. *Science* **357**, 792–796 (2017).
- [3] Misra, R. P. & Blankschtein, D. Insights on the Role of Many-Body Polarization Effects in the Wetting of Graphitic Surfaces by Water. *The Journal of Physical Chemistry C* **121**, 28166-28179 (2017).
- [4] Li, Z., Misra, R. P., Li, Y., Yao, Y.-C., Zhao, S., Zhang, Y., Chen, Y., Blankschtein, D. & Noy, A. Breakdown of the Nernst–Einstein relation in carbon nanotube porins. *Nature Nanotechnology* **18**, 177-183 (2023).

Using thermodynamics & Autonomous Experimentation to understand & optimize catalyst activity for carbon nanotube yield and diameter control

B. Maruyama¹, R. Waelder², R. Rao¹, A. Sloan³, C. Park⁴, J. Carpena², J. Yoho², S. Gorsse⁵

¹ US Air Force Research Laboratory, Materials & Manufacturing Directorate (USA),

²UES Inc. (USA), ³ National Research Council (USA), ⁴ Florida State University (USA), ⁵ ICMCB-CNRS (France)

...

Carbon nanotube synthesis is highly inefficient largely due to poor catalyst usage efficiency. This makes CNT production expensive and poorly controlled. Catalyst reduction and resistance to size and number evolution are critical to improving efficiency. We confirmed our hypothesis that growth in conditions near the catalyst oxidation/reduction phase transformation would maximize the catalyst activity by minimizing Ostwald ripening and associated catalyst deactivation, and found optimal conditions for CNT yield and diameter control.

We achieved this using our Hypothesis-Driven ARES Autonomous Experimentation System to search over a vast growth space encompassing 500° C and 10 orders of magnitude ratio of catalyst reduction gases to oxidizing gases. We used a novel Jump Regression planning algorithm to experimentally search for the discontinuous phase transformation from oxidized to reduced catalyst, thereby reducing the number of needed experiments by orders of magnitude.

Our results bring a powerful new understanding of catalyst activity because it enables us to optimize growth conditions to the catalyst, as well as the optimize the catalyst for the needed growth conditions.

Figure

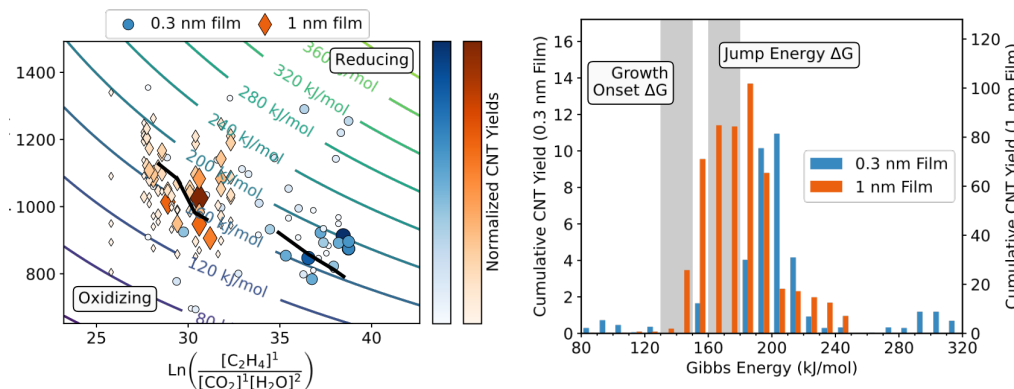


Figure Caption: (LHS) CNT yield as a function of temperature and the ratios of reducing gas (ethylene) to oxidants (water and CO₂). Contours represent the Gibbs energy at each point. The jump regression discontinuities (black splines) agree with the direction of the Gibbs energy contours, suggesting their physical origin is thermodynamic. The jump regions of best growth for each catalyst thickness separate entirely in thermodynamic space, accompanied by precipitous decline in CNT yield away from the jump region. (RHS) Cumulative G band area for both catalyst thicknesses binned by Gibbs energy. Onset of CNT growth in both campaigns occurs at roughly ~140 kJ/mol. The additional 140 kJ/mol required for CNT growth in this formalism is consistent with the energy required to reduce a mixed iron/aluminum oxide.

Width Controlled Growth of TMD Quantum Nanoribbons

Xufan Li, Shuang Wu Avetik R. Harutyunyan

Honda Research Institute USA, Inc., San Jose, CA, 95134, USA.

Controllable downscaling the dimensionality of atomically thin transition metal dichalcogenides (TMDs) provides a unique potential for realizing new quantum devices. However, realization of this additional spatial confinement typically relies on post-synthesis processes that interfere with their intrinsic properties. Here we report a new method for directly growing single and double atomic layer of MeX_2 nanoribbons (Me=Mo, W; X=S, Se) with width down to sub-10 nm. The nanoribbon growth is sensitive to substrates and occurs via precipitation from pre-deposited seed nanoparticles with properly selected constituents in a chalcogen vapor atmosphere. The width of nanoribbon is determined by the seed nanoparticle's diameter. The grown nanoribbons demonstrate remarkable elastic robustness with strain up to ~14%. Width-dependent Coulomb blockade oscillations are observed in the transfer characteristics of MoS_2 nanoribbons with width <20 nm at temperatures up to 80 K, attributed to single electron transfer¹. Moreover, by applying external strains, TMD nanoribbons generate high performance quantum emission of up to ~90% single photon purity, which is indicative of strain-induced localized electronic states. Our new synthesis method provides a general route for width-controllable growth of families of atomic layer quantum nanoribbons, paving a pathway to the synthesis of novel quantum materials.

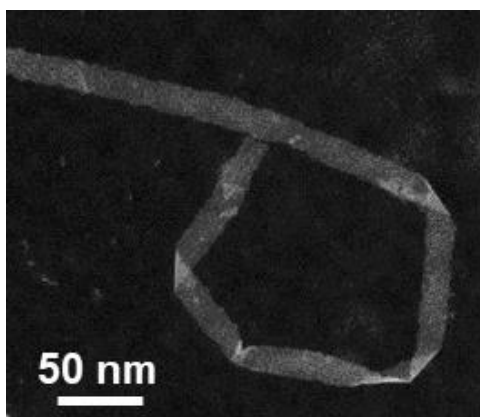


Figure. STEM image of a single layer MoS_2 nanoribbon.

References

1. X. Li., et al. *Sci. Adv.* 7 (50), eabk1892 (2021).
2. X. Li., et al. *ACS Nano* **14**, 6570 (2020).

Carbon, Catalysts and Climate: Optimizing Large-Scale CNT Reactors for Sustainable Materials and Energy

Adam M. Boies¹

¹*Department of Engineering, University of Cambridge, Trumpington St. CB2 1PZ, UK.*

The functional properties of nano-carbons are well known, but only in the last five years have large-scale materials composed of nano-carbons demonstrated strength, thermal and electrical properties that meet or exceed steel, aluminum and carbon fiber. Macroscopic materials composed of carbon nanotubes (CNTs) form networks of bundles which serve as the functional unit that spans the extent of the aerogel material. When CNTs are produced from methane, the effluent streams contain H₂ as well as CNT bulk aerogels. This has provided the enticing possibility that large-scale CNT production could meet both critical low-CO₂ energy and climate needs. However, the current CNT reactors must be optimized for high-density synthesis, energy efficiency and high quality if successful scaled production is to be achieved at the kiloton to megaton scale.

This presentation will give an overview of CNT reactor development spanning macroscopic characteristics of fluidized bed, substrate growth and floating catalyst chemical vapor deposition (CVD) reactors. The work will highlight how these systems have been operated in relatively dilute streams of hydrocarbons, thus making them large and energy inefficient. Higher carbon concentrations with better utilization of reactor volumes must be achieved with high quality CNT production without soot production and vapor grown carbon fibers. Our review has found that fluidized beds produce CNTs at higher reactor densities and at lower temperatures than floating catalyst CVD (FC-CVD), but CNT length and crystallinity are typically better for FC-CVD.

Advances in FC-CVD CNT production show promise in scaled production with high crystallinity, but critical metrics must be controlled from the nanometer to meter scale, including molecular C₂ species formation, catalyst size, CNT nucleation and growth and downstream processing to harvest the CNTs and H₂. An international group of researchers tied to various initiatives are leading efforts to advance these technologies with significant promise. Critically, if new reactors can be designed to achieve control of catalyst and C₂ species interaction to improve catalyst efficiencies from 0.1% to ~10% there is a possibility of two orders of magnitude greater production. To achieve these advancements, optically accessible reactors must be coupled to new in-situ techniques from complimentary fields must be incorporated to achieve rapid optimization, including on-line laser induced incandescence, Coherent anti-Stokes Raman spectroscopy and scattering. The presentation will give a perspective on how such coupling can be achieved.

Ultimately, the CNT materials must have properties sufficient in to warrant large-scale use and thus the processes must control micron to meter scale properties of CNT assembly and fiber density. The talk will discuss two new methods of CNT alignment for the enhancement of CNT fiber strength, electrical conductivity and thermal conductivity. Alternating electrical fields enable CNTs to stiffen, align and bundle during CNT self-assembly. Post processing with aerogels via wet acid stretching increases the tensile strength of CNT fibers beyond the strength, conductivity and toughness of steel with holistic properties that are superior to any high-performance fiber. Larger questions remain regarding whether bulk materials can be produced at sufficient density for wide-scale applications. New techniques for measuring the rates of catalyst formation and kinetics of CNT growth will provide a means for studying the ultimate limitations of reaction density and reactor throughput. These techniques are being applied to study new CO₂e net-sequestering carbon materials when produced from new sources of methane, such as gasified biomass and landfill gas. These processes include the use of recycled products, thus for the first time demonstrating a net production of hydrogen in addition to CNTs.

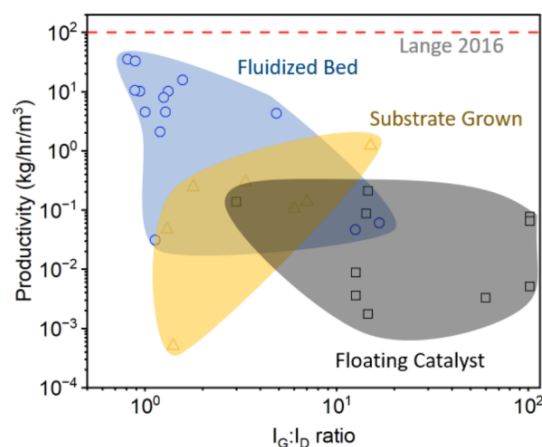


Figure 1: Reactor productivity for floating catalyst, substrate growth and fluidized bed for these process by intensity of Raman G band to D band.

Computing nanomaterials: insights in equilibrium and processes

Boris I. Yakobson, Ksenia V. Bets, Luqing Wang, Jincheng Lei

Rice University (USA)

The computational materials research encounters compelling problems in both *thermodynamic equilibrium* and, even more so, in *nonequilibrium synthesis*. We will discuss two recent “problem solved” examples of both kinds.

The equilibrium shape of crystals is a fundamental property of both aesthetic appeal and practical importance: the shape and its facets control the catalytic, light-emitting, sensing, magnetic, and plasmonic behaviors. It is also a visible macro-manifestation of the underlying atomic-scale forces and chemical makeup, most conspicuous in two-dimensional (2D) materials of keen current interest. If the crystal surface/edge energy (γ) is known for different directions (angles θ), its shape can be obtained by the geometric Wulff construction, a tenet of crystal physics. However, if symmetry is lacking, the crystal edge (or surface) energy cannot be even defined, never mind computed, and so its shape becomes elusive, presenting an insurmountable problem for the theory. We show, however, how to add auxiliary edge energies towards a constructive prediction, through well-planned computations, of a unique crystal shape [1,2]. The method is successful in shape prediction for challenging actual materials such as SnSe, which is of C_{2v} symmetry, and even $AgNO_2$ of C_1 , which has no symmetry at all!

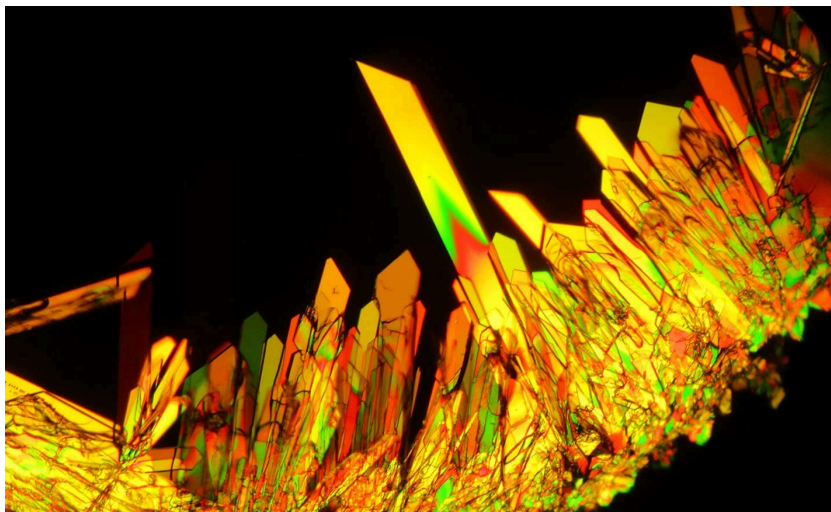


Figure 1: Potassium dichromate $K_2Cr_2O_7$ in cross-polarized light, a low symmetry crystal shape.

In the kinetics of synthesis, one key question is of the *immediate growth precursor*, whose accretion to the growing crystal is the last step, through many intermediates. The complexity of the synthesis setup, the use of various feedstock in different states of matter (gas, liquid, solid), the catalysts, and other assisting substances make the determination of these fundamental building blocks challenging, yet necessary for evaluating the growth rate, anisotropy, and product morphology. For MoS_2 , as an archetypal TMD example, we demonstrate how complex gas phase reactions lead to the formation of the precursor and then how the chemistry of this process can be modified to accelerate the synthesis of the TMD [3,4]. Combining ab initio molecular dynamics (AIMD) and first-principles calculations allowed us to determine the dramatic change in precursor chemistry in conventional and *salt-assisted* processes and further rank the halogens by efficiency, exemplifying the abilities of the computational approach.

References

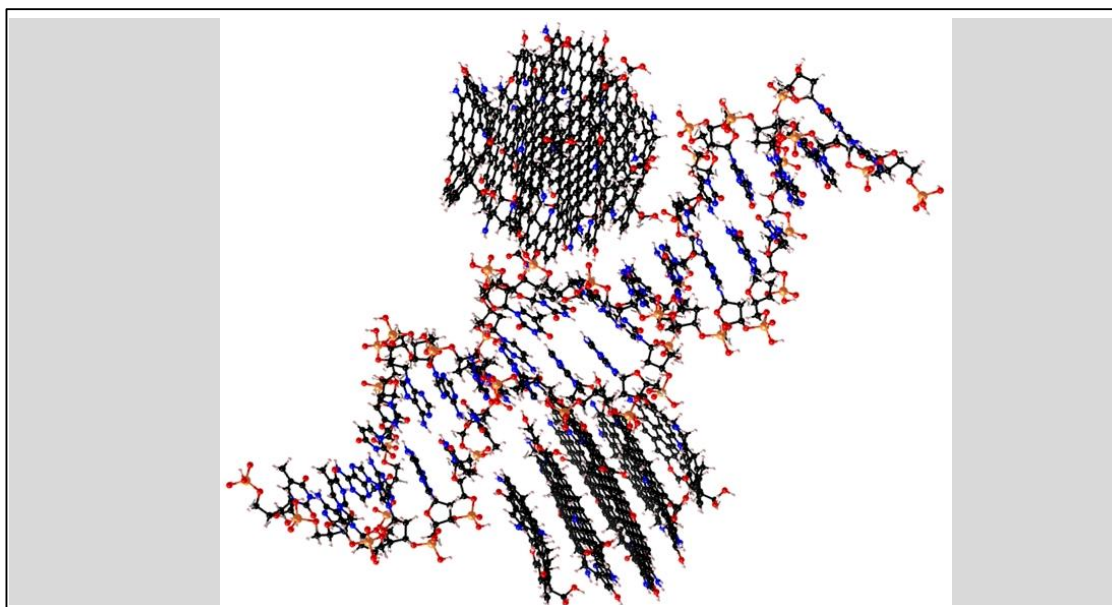
- [1] L. Wang, S. N. Shirodkar, Z. Zhang, and B. I. Yakobson, *Defining Shapes of Two-Dimensional Crystals with Undefinable Edge Energies*, Nat. Comput. Sci. **2**, 11 (2022).
- [2] *Predicting the Shape of Crystals with ‘Unknowable’ Surface Energies*, Nat. Comput. Sci. **2**, 11 (2022).
- [3] J. Lei, Y. Xie, and B. I. Yakobson, *Gas-Phase “Prehistory” and Molecular Precursors in Monolayer Metal Dichalcogenides Synthesis: The Case of MoS_2* , ACS Nano **15**, 10525 (2021).
- [4] J. Lei, Y. Xie, A. Kutana, K. V. Bets, and B. I. Yakobson, *Salt-Assisted MoS_2 Growth: Molecular Mechanisms from the First Principles*, J. Am. Chem. Soc. **144**, 7497 (2022).

Gene Delivery and Imaging by Graphene Quantum Dots

A. V. Naumov¹

¹Texas Christian University (USA)

Gene therapeutic strategies including RNA interference and CRISPR-Cas9 allow for silencing or direct removal of aberrant genes responsible for specific diseases. The power of gene therapeutics is their ability to treat only select target genes without detrimental effects to the healthy tissue. Their clinical translation, however, is hampered by limited cell transfection capabilities, potential degradation in blood, and the lack of delivery tracking capabilities. In our recent work graphene quantum dots (GQDs) have emerged as a novel biocompatible platform allowing targeted drug delivery and fluorescence imaging in the visible and near-infrared. These capabilities can aid in overcoming primary obstacles to gene therapeutics. In this work we have for the first time utilized biocompatible nitrogen and neodymium-doped graphene quantum dots for the delivery of Kirsten rat sarcoma virus (KRAS) and epidermal growth factor receptor (EGFR) siRNA effective against a variety of cancer types. The therapeutic efficacy of the GQDs/siRNA complex is verified by successful protein knockdown in HeLa cells at nanomolar siEGFR and siKRAS concentrations. A range of GQDs/siRNA loading ratios and payloads is tested to ultimately provide substantial inhibition of protein expression down to 31-45% comparable with conventional Lipofectamine-mediated delivery. CRISPR-Cas9 therapeutic delivery was accomplished by cationic GQDs enabling strong complexation with CRISPR Ribonucleic Protein (RNP) containing negatively-charged sgRNA. GQD/RNP complex produced successful double-stranded breaks of the TP53 414delC frameshift mutation locus overexpressed in approximately 50% of cancer cases and tested in our work in PC-3 prostate cancer cells. Activating this “suicide” gene can promote cellular repair pathways and lead to cancer cell apoptosis. Its restoration to the healthy form was performed by simultaneous GQD delivery of the CRISPR RNP and a single-stranded oligonucleotide (ssODN) repair template aimed to cut out and fix the mutation in the TP53 gene. This treatment led to a successful therapeutic outcome: 40% apoptotic cancer cell death, while having no effect on non-cancerous HeK293 cells. Both siRNA and CRISPR-Cas9 therapeutic delivery was successfully imaged in vitro via intrinsic GQD visible and near-infrared fluorescence also enabling in vivo imaging of the select gene targets. This work demonstrates the promising potential of GQDs for non-toxic gene delivery, complemented by multiwavelength image-tracking.



Many-body Effects on Exciton Dynamics and Nonlinear Optics in Low-Dimensional Materials

Diana Y. Qiu¹

¹*Yale University (USA)*

In low-dimensional and nanostructured materials, the optical response is dominated by correlated electron-hole pairs---or excitons---bound together by the Coulomb interaction. Understanding the energetics and dynamics of these excitons is essential for diverse applications across optoelectronics, quantum information and sensing, as well as energy harvesting and conversion. By now, it is well-established that these large excitonic effects in low dimensional materials are a combined consequence of quantum confinement and inhomogeneous screening. However, many challenges remain in understanding their dynamical processes, especially when it comes to correlating complex experimental signatures with underlying physical phenomena through the use of quantitatively predictive theories. In this talk, I will discuss three different frontiers related to the first principles understanding of exciton dynamics. Firstly, we will explore the relationship between exciton dispersion and exciton-phonon interactions. Secondly, we will look at how the electron-hole exchange interaction drives dynamical excitons processes for both bound and resonant exciton states in halide perovskites, transition metal dichalcogenides (TMDs), and topological insulators. Finally, we will look at many-body effects in nonlinear optical response going beyond the perturbative regime. We reveal many-body effects on the enhancement of transverse high harmonic generation (HHG) in monolayer TMDs.

References (if desired)

- [1] M. S. Dresselhaus *et al.*, *Phys. Rep.* **409**, 47–99 (2005).
- [2] A. K. Geim, *Science* **324**, 1530–1534 (2009).
- [3]

Self-Assembly of High Packing Density Carbon Nanotube Arrays using Microscopic Water Features

A. Sean M. Foradori¹, Brett Prussack¹, Arganthaël Berson¹, Michael S. Arnold¹

¹*University of Wisconsin-Madison (U.S.A.)*

Dense arrays of aligned semiconducting carbon nanotubes (CNTs) are needed for high-performance microelectronics. Recent research has demonstrated that the collection of CNTs at a water-organic solvent interface can induce nanotube self-alignment and array formation. In past work, the confining interface has been a macroscopic, large-area feature. Here, we report on CNT assembly on microscopic water features. Microdroplets of water are formed on hydrophilic stripes (10-100 μm wide) lithographically patterned on a target substrate. The water microdroplets are surrounded by organic solvent containing polymer wrapped CNTs. The CNTs accumulate at the microdroplet-solvent interface, align, and deposit onto the substrate at the microdroplet-solvent-substrate contact-line. In contrast to macroscopic approaches during which the contact-line translates unreliably across the substrate as it is pulled out of the liquids, the hydrophilic patterns and microdroplets allow pinning of the contact-line. As CNTs deposit, the contact-line self-translates allowing for dense CNT packing. We realize monolayer CNTs (average diameter 1.5 nm) arrays aligned within $\pm 3.9^\circ$ at density of $250 \mu\text{m}^{-1}$ and field-effect transistors with high current density of $1.9 \text{ mA } \mu\text{m}^{-1}$ and transconductance of $1.2 \text{ mS } \mu\text{m}^{-1}$ at -0.6 V drain bias and 60 nm channel length.

References

[1] S. M. Foradori *et al.*, *In Review* (2024).

Synthesis of 1D van der Waals Heterostructures Based on Single-Walled Carbon Nanotubes

Shigeo Maruyama^{1,2}, Yongjia Zheng^{2,1}, Wanyu Dai¹, Chunxia Yang¹, Keigo Otsuka¹, Rong Xiang^{2,1}

¹ Department of Mechanical Engineering, The University of Tokyo (Japan),

² School of Mechanical Engineering, Zhejiang University (China)

Single-walled carbon nanotubes (SWCNTs) with diverse optical and electronic properties (metallic or semiconducting) depending on chiral indices (n, m) have been the critical nanomaterials in advanced applications [1,2]. Even though a mixture of metallic and semiconducting SWCNT can be used for bulk and film-form applications such as batteries and solar cells [3], the controlled growth of (n, m) or the sorting of (n, m) is essential for electronics applications such as field effect transistors (FET) [4]. On the other hand, the controlled modulation of properties can also be possible either by employing the inner space of the SWCNTs to encapsulate various materials or by externally wrapping the SWCNT template with additional atomic layers [5]. Here, we mainly discuss the latter case as a one-dimensional (1D) van der Waals (vdW) heterostructure based on SWCNT [6]. We have demonstrated the atomically precise one-dimensional (1D) van der Waals (vdW) heterostructure -- SWCNTs, boron nitride nanotubes (BNNTs), and molybdenum disulfide (MoS₂) sequentially wrapped in radial direction -- by chemical vapor deposition in 2020 [6]. One of the obvious extensions of this work is the use of BNNT-SWCNT [7], which have superior semiconductor properties such as field effect transistors [8,9]. We have developed various characterization techniques for BNNT-SWCNT for the growth optimization and quality control of BNNT in several types of SWCNTs [10-12].

Yet another extension is the various kinds of transition metal dichalcogenides (TMD) nanotubes. We have optimized CVD conditions for various metal dichalcogenides such as tungsten disulfide (WS₂), niobium disulfide (NbS₂), and molybdenum diselenide (MoSe₂) so far in addition to the original MoS₂. Here, we further broaden the concept of 1D vdW heterostructure by combining 2 transition metal species. By setting WS₂ growth right after the MoS₂ growth, we can observe the axial junction of the outermost tube, MoS₂ - WS₂. The junction is atomically smooth within a few nanometers. On the other hand, by setting the 2 transition metal species at the same CVD time, we can observe {W_xMo_(1-x)}S₂ alloy nanotube. Both axial junction and alloy nanotubes are preferentially monolayers. Various Yanus TMD nanotubes, such as MoSSe, are also composed by employing the hydrogen plasma technique. They can be preferentially monolayer or bilayer tubes. At this stage, sulfur at the center side is preferred.

Part of this work was supported by JSPS KAKENHI Grant Numbers JP23H00174, JP23H05443 and by JST, CREST Grant Number JPMJCR20B5, Japan.

References

- [1] Y. Li, S. Maruyama, *Single-Walled Carbon Nanotubes*, Springer (2019).
- [2] S. Maruyama, M. S. Arnold, R. Krupke, L.-M. Peng, *J. Appl. Phys.* **131**, 080401 (2022).
- [3] J.-M. Choi, J. Han, J. Yoon, S. Kim, I. Jeon, S. Maruyama, *Adv. Funct. Mater.* **32**, 2204594 (2022).
- [4] D.-M. Tang, O. Cretu, S. Ishihara, Y. Zheng, K. Otsuka, R. Xiang, S. Maruyama, H.-M. Cheng, C. Liu, D. Golberg, *Nat. Rev. Electr. Eng.*, [DOI:10.1038/s44287-023-00011-8] (2024).
- [5] S. Cambre, M. Liu, D. Levshov, K. Otsuka, S. Maruyama, R. Xiang, *Small* **17**, 2102585 (2021).
- [6] R. Xiang, et al., *Science* **367**, 537 (2020).
- [7] Y. Zheng, et al., *P. Natl. Acad. Sci.* **118**, e2107295118 (2021).
- [8] S. Matsushita, et al., *ACS Appl. Mater. Inter.* **15**, 10965 (2023).
- [9] K. Otsuka, et al., *Nano Res.* **16**, 12840 (2023).
- [10] M. Liu, et al., *ACS Nano* **15**, 8418 (2021).
- [11] R. Zhang, et al., *Carbon* **199**, 407 (2022).
- [12] S. Wang, et al., *ACS Nano*, (2024) in press.

Thermoelectric performance of single walled carbon nanotubes

K. Yanagi

Tokyo Metropolitan University (Japan)

Lowering the dimensionality of materials can enhance their thermoelectric performance, and one-dimensional (1D) materials are expected to have potential to achieve the highest thermoelectric performance among various materials [1]. However, the realization of gigantic ZT values, which theoretical calculations have estimated in 1D systems, has not been achieved yet, and thus experimental studies on how 1D electronic structures can enhance thermoelectric performance has been one of important subjects in thermoelectric science. To understand the relationships among 1D electronic structures, location of Fermi-level and thermoelectric performances, we have investigated the thermoelectric properties of single walled carbon nanotubes (SWCNTs) [2-6]. Here I will discuss three unique thermoelectric characteristics in SWCNTs, which reflect 1D electronic structures. First, we can observe the violation of thermoelectric trade-off relation in metallic SWCNT. In contrast to the trade-off characteristics, i.e. increase of electrical conductivity σ as the decrease of Seebeck coefficient S , in conventional metals, we can observe simultaneous enhancement of σ and S around 1st van Hove singularity (vHS) in metallic SWCNT [3]. Second, we can observe unique behavior in thermoelectric conductivity around the vHS of semiconducting band-edge [4]. Third, although σ exhibits an-isotropic characteristics reflecting their structural aspect ratio, S exhibits isotropic characteristics [5]. Based on these characteristics, power factor (PF) in SWCNTs can be enhanced through the control of morphology and high-doping. As a result, a very large PF, $14 \text{ mWm}^{-1}\text{K}^{-2}$, is observed in the aligned CNT fiber at room temperature [6], which is the largest among flexible nanomaterials without supporting substrates (Fig. 1). Figure 1 shows a summary of the relationships between PF and σ in various flexible materials at room temperature [7]. The graph suggests that the performance of the (6,5) SWCNTs can be improved along the dotted red line by improving σ through the control of morphology, which can cross the thermoelectric performance of Bi_2Te_3 , suggesting that aligned (6,5) SWCNTs will have a potential to exhibit similar ZT value to that of Bi_2Te_3 . Recently, we have investigated how the thermal conductivity is influenced by the carrier injections [8] and estimated the ZT value of aligned SWCNTs. In addition, the presence of interfacial Seebeck coefficient at CNT-CNT-junction is also recently identified [9], and thus how to design the interfacial Seebeck coefficient will also be an important topic for thermoelectrics using flexible materials with van der Waals interfaces.

References (if desired)

- [1] Hicks & Dresselhaus, Phys. Rev. B 47, 16631 (1993) [2] Yanagi et al., Nano Lett. 14, 6437 (2014) [3] Ichinose et al., Nano Lett. 19, 7370 (2019) [4] Ichinose et al., Phys. Rev. Mater. 5, 025404 (2021). [5] Fukuhara et al., Appl. Phys. Lett. 113, 243105 (2018). [6] Komatsu et al., Nat. Commun. 12, 4931 (2021). [7] Yanagi, JSAP review 230424, (2023) [8] Ueji et al., ACS Nano Mater. 5, 6100 (2022) [9] Hamasaki et al, ACS Nano (accepted in 2023).

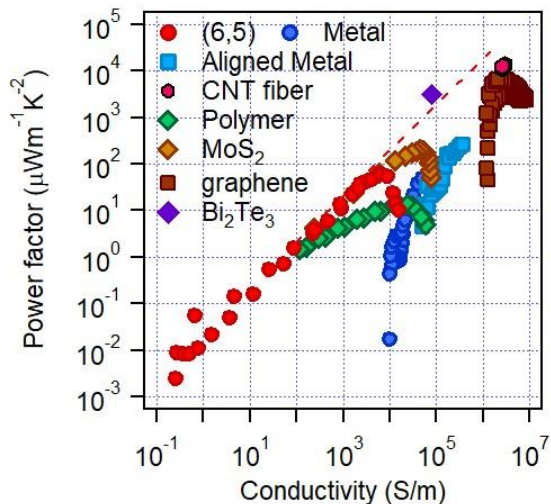


FIG1: PF vs electrical conductivity σ in various flexible materials

Understanding the Growth of Carbon Nanotubes: Previous Achievements, Challenges and Opportunities

Feng Ding

Shenzhen Institute of Advanced Technology (China)

Since the discovery of single-walled carbon nanotubes (SWCNTs) 30 years ago, great efforts have been dedicated to the controllable synthesis of SWCNTs and many industrial applications have been established. Yet, great challenges remain for the industrial applications of SWCNTs, such as the large-scale synthesis of SWCNTs at a low price and the structure specific synthesis of SWCNTs. To overcome these challenges, understanding the mechanisms of SWCNTs' synthesis is essential. In this talk, I will firstly review our previous efforts on understanding the mechanism of SWCNTs' growth, including *(i)* the efforts for simulating the catalytic growth of SWCNTs by molecular dynamics, *(ii)* the kinetics of SWCNT nucleation and growth, *(iii)* solid catalyst for selective SWCNT growth and the synthesis of $(2n, n)$ SWCNTs, *(vi)* the advantages of using alloy catalysts in SWCNT growth. Then I will present our recent progresses on understanding the mechanisms of SWCNTs' growth enabled by "AI for Science" technology, including the *(v)* simulating perfect SWCNTs' growth by machine learning force fields (MLFFs) and *(vi)* the role of sulfur in SWCNTs synthesis revealed by MLFF. Finally, I will briefly present the opportunity of deeply understanding the mechanism of SWCNTs' growth at the era of "**AI for Science**" and the possible route towards true controllable synthesis of SWCNTs.

2D Transition Metal Sulfides: Controllable Preparation and Green Hydrogen Production

Qiangmin Yu¹, Hui-Ming Cheng^{1,2}, and Bilu Liu¹

¹*Shenzhen Geim Graphene Center (SGC), Tsinghua-Berkeley Shenzhen Institute (TBSI) & Tsinghua Shenzhen International Graduate School (SIGS), Tsinghua University (China)*

²*Faculty of Materials Science and Engineering / Institute of Technology for Carbon Neutrality, Shenzhen Institute of Advanced Technology, Chinese Academy of Science (China)*

Hydrogen (H₂) is a clean energy carrier with zero-carbon emission and can be produced by water electrolysis driven by renewable energy, which is beneficial for future global carbon neutrality.^{1,2} Water electrolysis technique is highly efficient and allows for high hydrogen production rates with current densities up to 2,000 mA cm⁻², but suffers from problems of poor stability, high cost and low efficiency.³⁻⁵ The challenge in producing a high performance electrode is how to achieve a high-efficiency and long-durability hydrogen production under large current densities. In this talk, we will mainly focus on high performance hydrogen evolution catalysts based on 2D transition metal sulfides (TMDs). The contents of this talk include the large scale preparation of 2D TMDs, the mechanism of hydrogen evolution, and the applications of hydrogen production at large current density.⁶⁻⁸ Specifically, first, we invented an intermediate-assisted grinding exfoliation method to achieve the large-scale preparation of 2D materials. Second, we elucidated the mechanism by which the interface effects regulate the hydrogen evolution activity of 2D TMDs. Finally, we realized the high-performance hydrogen production application of 2D TMDs at large current density, and applied them in water electrolyzer.

Dr. Qiangmin Yu is an associate professor of Shenzhen International Graduate School (SIGS), Tsinghua University. He received his PhD from University of Chinese Academy of Science in 2017. Then, he conducted his postdoctoral research in Tsinghua-Berkeley Shenzhen Institute in collaboration with Profs. Bilu Liu and Hui-Ming Cheng from 2017 to 2019. Dr. Yu main research interest concentrates on the growth of low dimensional materials and their energy conversion applications, including water electrolysis, fuel cells, and metal-air battery. He has published over 40 papers in peer reviewed journals such as Nature Communications, Advanced Materials, InfoMat, ACS Nano, and Materials Today.

References (if desired)

- [1] Mallapaty, S. How China could be carbon neutral by mid-century. *Nature* 586, 482-483 (2020).
- [2] Dresselhaus, MS., et al., Alternative energy technologies. *Nature* 414, 332-337 (2001).
- [3] Yu, Q., et al., Engineering two-dimensional materials and their heterostructures as high-performance electrocatalysts. *Electrochem. Energ. Rev.* 2, 373-394 (2019).
- [4] Holladay, JD., et al., An overview of hydrogen production technologies. *Catal. Today* 139, 244-260 (2009).
- [5] Hu, SQ, et al., Low-dimensional electrocatalysts for acidic oxygen evolution: intrinsic activity, high current density operation, and long-term stability. *Adv. Funct. Mater.* 32, 2201726 (2022)
- [6] Zhang, C., et al., Mass production of 2D materials by intermediate-assisted grinding exfoliation. *Natl. Sci. Rev.* 7, 324-332 (2020)
- [7] Zhang, C., et al., High-throughput production of cheap mineral-based two-dimensional electrocatalysts for high-current-density hydrogen evolution. *Nat. Commun.* 11, 3724 (2020)
- [8] Yu, Q., et al., A Ta-TaS₂ monolith catalyst with robust and metallic interface for superior hydrogen evolution. *Nat. Commun.* 12, 6051 (2021)

Advanced Surfactant-Controlled Sorting of Single-Chirality Carbon Nanotubes

H. Li^{1,2}

¹Department of Mechanical and Materials Engineering, University of Turku (Finland)

²Turku Collegium for Science, Medicine and Technology, University of Turku (Finland)

Surfactant-assisted aqueous two-phase extraction (ATPE) is a highly efficient and scalable approach for the sorting of single-walled carbon nanotubes (SWCNTs) [1]. The co-surfactant is used to modulate the partitioning of various (n,m) SWCNT species within the ATPE system. While the fluorescence-based titration method offers insights into partition coefficient change conditions (PCCCs) without the need for physical ATPE separation [2], the complexity of co-surfactant interactions, environmental influences, and the overlapping partition coefficients for certain SWCNT species still present challenges to the accurate determination of the separation conditions. To address these challenges, this study utilizes pre-sorted and enriched SWCNTs as starting materials. Through systematic ATPE across various (n,m)s and measurement of PCCCs under different co-surfactant conditions, we obtain precise partition data, particularly for metallic SWCNT species, which are typically undetectable via fluorescence. Our findings not only facilitate the refinement of sorting conditions but also contribute to a deeper understanding of the sorting mechanisms, laying the groundwork for the standardization of the SWCNT sorting process.

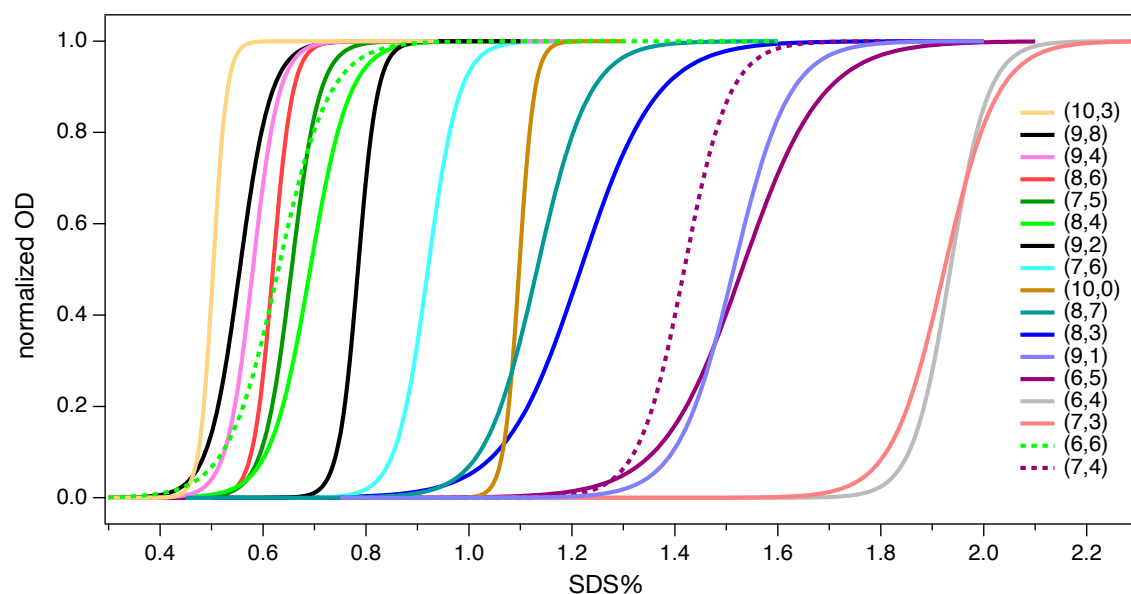


Figure 1: SDS concentration profiles for partitioning various (n,m) species of SWCNTs at 0.05% DOC concentration within the ATPE system. SWCNT concentrations on the top phase are measured by absorption spectroscopy and normalized for better comparison. Sigmoid equation is used to fit the data. Solid lines represent the partition of semiconducting species, while dashed lines demonstrate that of metallic tubes.

References

- [1] J. A. Fagan, *Nanoscale Advances* **1**(9), 3307–3324 (2019).
- [2] C. M. Sims *et al.*, *Carbon*. **165**, 196–203 (2020).

AI accelerated materials discovery of van der Waals magnets

Trevor David Rhone

Department of Physics, Applied Physics and Astronomy, Rensselaer Polytechnic Institute

The discovery of van der Waals (vdW) materials with intrinsic magnetic order in 2017 has given rise to new avenues for the study of emergent phenomena in two dimensions. In particular, monolayer CrI₃ was found to be ferromagnet. Other vdW transition metal halides were later found to have different magnetic properties. How many vdW magnetic materials exist in nature? What are their properties? How do these properties change with the number of layers? A conservative estimate for the number of candidate vdW materials (including monolayers, bilayers and trilayers) exceeds $\sim 10^6$. A recent study showed that artificial intelligence (AI) can be harnessed to discover new vdW Heisenberg ferromagnets based on Cr₂Ge₂Te₆ [1], [2] and vdW magnetic insulators based on MnBi₂Te₄ [3]. In this talk, we will harness AI to efficiently explore the large chemical space of vdW transition metal halides and to guide the discovery of magnetic vdW materials with desirable spin properties. That is, we investigate crystal structures based on monolayer Cr₂I₆ of the form A₂X₆, which are studied using density functional theory (DFT) calculations and AI. Magnetic properties, such as the magnetic moment are determined. The formation energy is also calculated and used as a proxy for the chemical stability. We show that AI, combined with DFT, can provide a computationally efficient means to predict the thermodynamic and magnetic properties of vdW materials [4]. This study paves the way for the rapid discovery of chemically stable magnetic vdW materials with applications in spintronics, magnetic memory and novel quantum computing architectures.

- [1] T. D. Rhone *et al.*, “Data-driven studies of magnetic two-dimensional materials,” *Sci. Rep.*, vol. 10, no. 1, p. 15795, 2020.
- [2] Y. Xie, G. Tritsarlis, O. Granas, and T. Rhone, “Data-Driven Studies of the Magnetic Anisotropy of Two-Dimensional Magnetic Materials,” *J. Phys. Chem. Lett.*, vol. 12, no. 50, pp. 12048–12054.
- [3] R. Bhattarai, P. Minch, and T. D. Rhone, “Investigating magnetic van der Waals materials using data-driven approaches,” *J. Mater. Chem. C*, vol. 11, p. 5601, 2023.
- [4] T. D. Rhone *et al.*, “Artificial Intelligence Guided Studies of van der Waals Magnets,” *Adv. Theory Simulations*, vol. 6, no. 6, p. 2300019, 2023.

This research was primarily supported by the NSF CAREER, under award number DMR-2044842.

Artificial van der Waals multiferroics with twisted two-dimensional materials

Jose Lado

Department of Applied Physics, Aalto University, Finland

Twisted van der Waals materials have risen as a powerful platform to engineer artificial quantum matter. Artificial moire heterostructures, in general, display two length scales: the original lattice constant and the emergent moire length. Here we reveal a microscopic mechanism to engineer van der Waals multiferroics from the interplay of non-collinear magnetism and spin-orbit coupling, both in van der Waals monolayers [1,2] and twisted multilayers [3]. First, focusing on the recently isolated NiI₂ multiferroic monolayer [1], we reveal the origin of the helimagnetic order and the critical role of halide spin-orbit coupling in driving a ferroelectric distortion. We demonstrate that the electronic reconstruction accounting for the ferroelectric order emerges from the interplay of such a non-collinear magnetism and spin-orbit coupling, and we demonstrate how the ferroelectric distortion can be probed experimentally with scanning tunneling spectroscopy [2]. Second, we show the emergence of multiferroic order in twisted chromium trihalide bilayers, an order fully driven by the moiré pattern and absent in aligned multilayers. We show that a spin texture is generated in the moiré supercell of the twisted system as a consequence of the competition between stacking-dependent interlayer magnetic exchange and magnetic anisotropy [3]. An electric polarization arises associated with such a non-collinear magnetic state due to the spin-orbit coupling, leading to the emergence of a local ferroelectric order following the moiré. Among the stoichiometric trihalides, our results show that twisted CrBr₃ bilayers give rise to the strongest multiferroic order. We further show the emergence of a strong magnetoelectric coupling, which allows the electric generation and control of magnetic skyrmions. Our results put forward van der Waals materials as a powerful platform to engineer artificial multiferroic order and electrically control exotic magnetic textures.

[1] Adolfo O Fumega and Jose L Lado 2022 2D Materials. 9 025010 (2022)

[2] Mohammad Amini, Adolfo O. Fumega, Héctor González-Herrero, Viliam Vaňo, Shawulienу Kezilebieke, Jose L. Lado, Peter Liljeroth, arXiv:2309.11217 (2023)

[3] Adolfo O. Fumega, Jose L. Lado, 2D Matererials 10 025026 (2023)

Atomic Scale Material Engineering for Ultimately Scaled Electronics

Yuxuan Cosmi Lin¹

¹*Department of Materials Science and Engineering, Texas A&M University (USA)*

At the atomic scale, new forms of physical phenomena emerge that can provide remarkable opportunities for next-generation tools with unprecedented functionality and energy efficiency. Further down-scaling of electronic devices for the emerging computing systems requires the capability of engineering material properties at the limit of the atomic scale. While scaling of silicon technologies is running out of steam, low-dimensional materials, such as 2D transition-metal dichalcogenides (TMDs) and 1D carbon nanotubes (CNT) or graphene nanoribbons (GNRs) have been envisioned as promising materials for the ultimately scaled transistors and non-classical computing devices. This talk will discuss some of the key challenges and possible solutions on the material level for low-dimensional material electronics. First, I will talk about two recent works that addresses the material challenges for forming an energy-barrier-free electrical contacts to 2D semiconductors, including the semimetal contact strategy that eliminates the metal-induced gap states, and the oxygen-incorporated chemical vapor deposition approach that effectively passivates the natural chalcogen vacancies in monolayer TMDs and reduces the defect-induced gap states. Record-high 2D transistor performance is achieved, with the contact resistance on par with silicon technologies, and approaching the quantum limit. Second, I will introduce our material-level and device-level co-optimization efforts on the bottom-up synthesized GNRs towards the ultimately scaled transistor applications.

Balancing Promise and Precaution: Navigating the Environmental and Toxicological Landscape of Carbon Nanotube Materials for Informed Policy

Carbon nanotubes are a large family of carbon-based hollow cylindrical structures with unique physicochemical properties that have motivated research for diverse applications; some have reached commercialization. Due to their superior physical and chemical properties, including high tensile strength, thermal conductivity, and tunable semiconductivity, they are researched for a wide array of applications ranging from batteries, to high-strength concrete, to photovoltaic cells. Industrial applications of carbon nanotubes are rapidly expanding, with annual global production of carbon nanotubes surpassing 5000 tonnes and increasing. However, emerging evidence paints a nuanced picture of the toxicological risks of carbon nanotubes, and policymakers must consider a context-dependent approach to ensure that risks are minimized to industry workers and the public while also minimizing the regulatory burden on industry and research if carbon nanotubes are to commercialize and scale. Despite recent progress demonstrating methods of production and processing that minimize occupational and consumer risk, as well as methods of degrading and eliminating carbon nanotubes that enter the environment, negative perceptions persist. Recent actions in the European Union that propose to ban this entire class of materials highlight an unmet need to precisely define carbon nanotubes, to better understand their toxicological risks for human health and the environment throughout their life cycle (from cradle-to-grave), and to communicate science-based policy-driving information regarding their taxonomy, safe sourcing, processing, production, manufacturing, handling, use, transportation, and disposal. Current information and knowledge gaps regarding these issues are needed to provide R&D and regulatory clarity regarding the material properties of different carbon nanotube materials. As applications of carbon nanotubes expand, safety, environmental, societal, economic, and other potential impacts and externalities should be assessed across all stages of the life cycle of carbon nanotubes and carbon nanotube composite materials. This presentation will cover the benefits and risks of the use of carbon nanotubes in advanced materials and offer policy recommendations to minimize risks to workers and the public, while facilitating the materials transition to a more sustainable future.

Boron nitride phase differentiation at the nucleation stage

Ksenia V. Bets, Ting Cheng, Boris I. Yakobson

Rice University (USA)

The realization of scalable monocrystalline growth remains an obstacle for industrial applications for many materials, both two- (2D) and three-dimensional (3D). Boron nitride holds became a prominent material in 3D (cubic, cBN) and 2D (hexagonal, hBN) forms. The existence of several stable forms complicates the synthesis process with the necessity to achieve phase selectivity. The cubic BN is most commonly grown on the diamond substrate due to a very close epitaxial match, yet even in these conditions, the inclusions of hBN, as well as amorphous domains (aBN), are hard to avoid. The detailed first-principle investigation of the nucleation process through the nanoreactor approach [1] allowed us to demonstrate the nucleation and growth mechanism of cBN on the diamond surface. Even more importantly, we have determined that the presence and concentration of hydrogen (within the BN-precursor and as H₂ gas) during the nucleation process dictate the phase of the forming BN [2]. Hydrogen-poor conditions promoted strong and less selective binding of BN units to the surface of diamond, developing amorphous domains. The limited presence of H atoms allowed for slower BN incorporation, leading to crystalline growth of cBN. Finally, high levels of hydrogen promoted the development of the sp² network and hBN formation.

Interestingly, on more catalytically active metals, the BN precursor undergoes rapid dehydrogenation [3], yet strong lateral interaction with the substrate strongly favors the formation of 2D hexagonal BN [4]. This process, however, is subject to the formation of another type of disorder - the antiparallel domains. Counterintuitively, the presence of defects on the surface of the substrate (e.g., steps, kinks, and corners) can prevent antiparallel domain formation by providing convenient nucleation sites. The higher energy surface defects, such as corners, provide stronger bonding and stabilization in the initial nucleation stage, giving rise to the preferential orientation of hBN domains [5].

Understanding the selective nucleation mechanism for cBN formation on diamond surface, as well as preferential nucleation of hBN of defects of metal substrates, provides valuable insight and guidance to experimental exploration.

References

- [1] V. I. Artyukhov, Y. Liu, and B. I. Yakobson, Equilibrium at the Edge and Atomistic Mechanisms of Graphene Growth, *Proc. Natl. Acad. Sci.* **109**, 15136 (2012).
- [2] T. Cheng, K. V. Bets, and B. I. Yakobson, Hydrogen-Driven Boron Nitride Phase Differentiation during the Epitaxial Nucleation on Diamond (001) Surface, *submitted* (2024).
- [3] T. Cheng, K. V. Bets, and B. I. Yakobson, Synthesis Landscapes for Ammonia Borane CVD of H-BN and BNNT: Unraveling Reactions and Intermediates from First Principles, *submitted* (2024).
- [4] K. V. Bets, N. Gupta, and B. I. Yakobson, How the Complementarity at Vicinal Steps Enables Growth of 2D Monocrystals, *Nano Lett.* **19**, 2027 (2019).
- [5] K. V. Bets and B. I. Yakobson, Entropic Origin of the hBN Monocrystallinity on Cu (111) Surface, *submitted* (2024).

Carbon onions from hydrogen production for environmental and energy applications

Yuanyuan Yao¹, Yuqi Pan¹, Yuan Chen¹

¹School of Chemical and Biomolecular Engineering (Australia)

Methane pyrolysis ($\text{CH}_4 \rightarrow 2\text{H}_2 + \text{C}$) is a promising H_2 production process with low CO_2 emissions. Utilizing its solid carbon co-products is critical for its economic competitiveness.[1] We show that catalytic CH_4 pyrolysis using low-cost Fe ore catalysts yields carbon onions encapsulated with magnetic Fe cores (Fe@C). Un-purified Fe@C can serve as efficient and recyclable Fenton catalysts for pollutant degradation, outperforming commonly used Fenton's reagent ($\text{FeSO}_4/\text{H}_2\text{O}_2$). Fe@C can be quickly recovered from an aqueous solution and reused due to the encapsulated magnetic Fe particles. Over three reused cycles, Fe@C/ H_2O_2 yields 1/8 of Fe sludges compared to $\text{FeSO}_4/\text{H}_2\text{O}_2$, significantly reducing Fe sludge treatment costs.[2] Further, Fe@CNO shows a high adsorption capacity and fast pseudo-second-order adsorption kinetics for antibiotics in wastewater. Surface oxidized Fe@CNO also presents a high catalytic activity for *in situ* electrochemical H_2O_2 production. Based on these properties, an integrated Fe@CNO-enabled wastewater treatment process is demonstrated.[3]

Fe@C can be purified by standard high-temperature thermal treatment or an alternative new electrochemical method to reach the purity of 99.82 and 99.59 wt.%, respectively. The purified carbon onions show a high electrical conductivity of up to 98 S cm^{-1} when incorporated in MnO_2 cathodes and a suitable electrolyte absorption capability. Primary zinc/carbon batteries assembled using purified carbon onions show advantages in superior conductivity, specific capacity, rate performance, internal resistance, and long-term stability compared with commercial carbon conductive additives.[4] Purified carbon onions can also work as cathodes and anodes to enable high-rate-performance dual-carbon batteries, outperforming commercial natural and synthetic graphite. Purified carbon onions have smaller crystalline sizes and larger surface areas, allowing faster surface redox reactions and better structural stability upon electrolyte ion intercalation.[5] These findings open new application opportunities for carbon co-products from the low-emission H_2 production process.

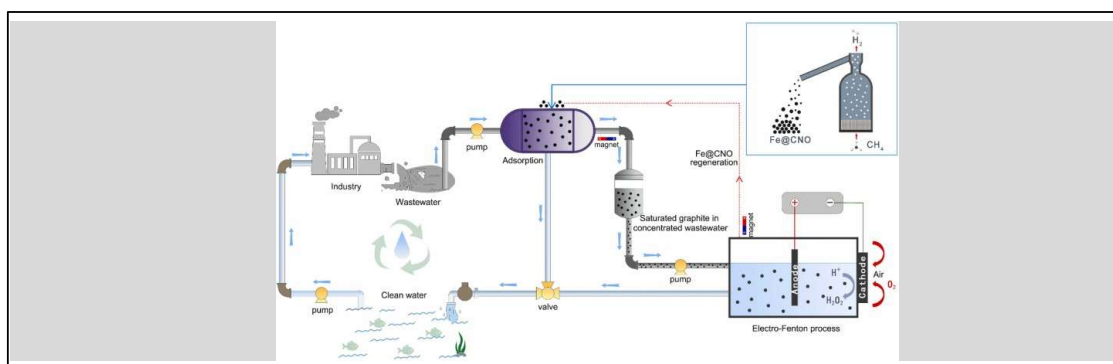


Figure: Schematic illustration of Fe@CNO-enabled wastewater treatment process.

References

- [1] J. Prabowo *et al.*, *Carbon* **216**, 118507 (2024).
- [2] Y. Yao *et al.*, *J. Hazard. Mater.*, **437**, 129328 (2022).
- [3] Y. Yao *et al.*, *Appl. Catal., B*, **342**, 123380 (2024).
- [4] Y. Pan *et al.*, *Carbon* **192**, 84 (2022).
- [5] Y. Pan *et al.*, *Adv. Energy Mater.* **13**, 2300495 (2023)

Carbon Nanomaterial based Microelectrodes for the Detection of Biomolecules and Neurotransmitters

Noe T. Alvarez, Pankaj Gupta and Chethani Ruhunage

Departments of Chemistry, University of Cincinnati, Cincinnati, OH 45221, United States

alvarene@ucmail.uc.edu

Abstract

Electrode miniaturization offers an alternative approach to developing highly sensitive electrochemical sensors. Microelectrodes, characterized by low charging currents, enhanced mass transport and compatibility with resistive mediums, have become appealing for biomolecule detection. Carbon nanotubes (CNTs), distinguished by high electrical conductivity and mechanical strength, present a unique nanomaterial option. Their chemical stability and ability to form nano and microelectrodes make them an attractive alternative compared to traditional metals. This presentation will discuss the fabrication of an electrochemical set featuring CNT microelectrode assemblies as working, reference, and counter electrode components.[1] The set has undergone testing for detecting heavy metals (Pb^{2+}), neurotransmitters (dopamine), and other biomolecules (nicotinamide adenine dinucleotide (NADH), furosemide). The talk will provide assembly and fabrication characteristics that are responsible for achieving impressive limits of detection of 0.5 nM for dopamine, 18 nM for NADH, 2 nM for Furosemide, and 0.4 ppb for Pb^{2+} in drinking water. The engineering design, focusing on maintaining vertically standing CNTs structures with open ends, will be highlighted as key factor in achieving these performance levels.[2]

Various voltametric techniques were employed during the study, including cyclic voltammetry (CV), square wave voltammetry (SWV), amperometry, and square wave anodic stripping voltammetry (SWASV). Additionally, the presentation explores the broader impact of this simple fabrication method for the development of microelectrode arrays that can be employed as working electrodes for multiple applications.[3,4]

References

1. Gupta, P. et al.. Carbon Nanotube Microelectrode Set: Detection of Biomolecules to Heavy Metals. *Anal Chem* **2021**, *93*, 7439-7448, doi:10.1021/acs.analchem.1c00360.
2. Gupta, P. et al. Electrochemistry of Controlled Diameter Carbon Nanotube Fibers at the Cross Section and Sidewall. *ACS Applied Energy Materials* **2019**, *2*, 8757-8766, doi:10.1021/acsaem.9b01723.
3. Gupta, P. et al. Parts per trillion detection of heavy metals in as-is tap water using carbon nanotube microelectrodes. *Anal Chim Acta* **2021**, *1155*, 338353, 1-11, doi:10.1016/j.aca.2021.338353.
4. Ruhunage, C.K. et al. Hydrophilic Micro- and Macroelectrodes with Antibiofouling Properties for Biomedical Applications. *ACS Biomater Sci Eng* **2022**, *8*, 2920-2931, doi:10.1021/acsbmaterials.2c00173.

Carbon-based Nanomaterial Inks for Print-in-place, Recyclable, and Water-based Electronics

A. D. Franklin¹

¹Duke University (USA)

For decades we've been hearing about the promise of printing electronics directly onto any surface. However, despite significant progress in the development of inks and print processes, reports on fully, direct-write printed electronics continue to rely on excessive thermal treatments and/or fabrication procedures that are external from the printer. In this talk, recent progress towards print-in-place electronics will be discussed; print-in-place involves loading a substrate into a printer, printing all needed layers, then removing the substrate with electronic devices immediately ready to test [1]. A key component of these print-in-place transistors is the use of inks from various nanomaterials, including 2D graphene and 1D carbon nanotubes. Using an aerosol jet printer, these mixed-dimensional inks are printed into functional 1D-2D thin-film transistors (TFTs) without ever removing the substrate from the printer and using a maximum process temperature of 80 °C with most processing occurring at room temperature [2]. Using a similar print-in-place process, completely recyclable printed transistors will be discussed, fabricated entirely using nanocarbon-based inks [3]. These recyclable devices employ a printed crystalline nanocellulose (CNC) ionic dielectric, which provides low-voltage operation that is reasonably robust to high voltage sweep rate [4]. Finally, the same set of nanomaterials will be demonstrated for use in all-aqueous (completely water-based) printed CNT-TFTs, eliminating dependence on processing with hazardous chemicals [5]. These advances give evidence for the potential of an electronic future involving devices with fabrication and/or function that goes beyond what is possible with traditional semiconductor technologies [6].

In case you are wondering why anyone would want to print thin-film electronics (e.g., TFTs), you must consider the expansive utilization of transistors beyond their employment in high-performance digital computing. Potential application areas include distributed sensing devices for the internet-of-things, flexible/wearable electronics, and display backplanes. All three of these areas are rapidly growing, with no signs of slowing down. Using nanomaterials for printed TFTs yields devices with highly competitive performance, nearing that of low-temperature polysilicon (LTPS) and metal-oxide semiconductor (LTPO) TFTs, yet the nanomaterials open the way for making these technologies recyclable or biodegradable. The incumbent TFT technologies have a highly deleterious environmental impact due to heavy vacuum-based processing and toxic gas dependence [7]. In fact, the US Environmental Protection Agency (EPA) recently identified the greenhouse gas emissions from display manufacturing to be one of the foremost challenges for climate change [8]. Ongoing progress in the low-cost, versatile printing of nanomaterial-based TFTs has the potential to disrupt our escalating dependence on electronics manufactured with high environmental cost.

References

- [1] J. A. Cardenas *et al.*, *ACS Appl. Nano Mater.*, vol. 1, pp. 1863 (2018). <https://doi.org/10.1109/LED.2021.3055787>
- [2] S. Lu *et al.*, *ACS Nano*, vol. 13, pp. 11263 (2019). <https://doi.org/10.1021/acsnano.9b04337>
- [3] N. X. Williams *et al.*, *Nature Electronics*, vol. 4, pp. 261 (2021). <https://doi.org/10.1038/s41928-021-00574-0>
- [4] B. N. Smith *et al.*, *Nanoscale*, vol. 14, pp. 16845 (2022). <https://doi.org/10.1039/D2NR04206A>
- [5] S. Lu, B. N. Smith, H. Meikle, M. J. Therien, and A. D. Franklin, *Nano Lett.*, (*in press*, 2023). <https://doi.org/10.1021/acs.nanolett.2c04196>
- [6] A. D. Franklin, M. S. Hersam, and H.-S. P. Wong, *Science*, vol. 378, pp. 726 (2022). <https://doi.org/10.1126/science.abp8278>
- [7] Flat Panel Display Manufacturing; Souk, J.; Morozumi, S.; Luo, F.-C.; Bitá, I., Eds.; John Wiley & Sons, Ltd: Hoboken, NJ, 2018.
- [8] Sector Spotlight: Electronics <https://www.epa.gov/climateleadership/sector-spotlight-electronics>

Cracking 2D Crystals: Patterns and Collective Behaviors

Zhiping Xu, PhD

No Abstract

Development of Nanoporous Atomically Thin Membranes for Challenging Chemical Separations

Rohit Karnik

*Tata Professor, Department of Mechanical Engineering
Associate Director, Abdul Latif Jameel Water and Food Systems Lab
Massachusetts Institute of Technology, 77 Massachusetts Avenue, Cambridge MA 02139, USA*

Abstract: Nanoporous atomically thin membranes, wherein nanopores in a single layer of two-dimensional material such as graphene provide pathways for rapid and selective fluidic transport, constitute the thinnest possible membrane and have potential for improving the efficiency, selectivity, productivity, versatility, and chemical resistance for a variety of membrane separations. Through controlled nucleation of defects via ion bombardment and oxidative etching, sub-nanometer pores are created in a single layer of graphene placed on a porous support. We discuss strategies for the design of membranes that are tolerant of defects in the graphene layer, and show that appropriate choice of the porous support is critical for exploiting the selectivity of nanoporous graphene. We further demonstrate that the impermeability of graphene can be exploited to selectively seal defects to tighten the pore size distribution and functionalize the pores to improve its selectivity. Through these developments, we realize centimeter-scale graphene membranes for nanofiltration and dialysis, demonstrating ultrahigh permeance and Angstrom-scale molecular geometry-based selectivity in organic liquids, high-temperature hydrogen/hydrocarbon separations, and separation of metal ions such as lithium and rare earths. These studies illustrate the interplay between material structure and transport in nanoporous graphene and demonstrate its potential to realize versatile, tunable, and chemically-stable next-generation membranes for chemical separations, resource recovery and recycling, and water purification to unlock industrial materials circularity and energy efficiency for a sustainable future.

Bio: Rohit Karnik is Tata Professor in Mechanical Engineering and Associate Director of the Abdul Latif Jameel Water and Food Systems Lab at the Massachusetts Institute of Technology, where he leads the Microfluidics and Nanofluidics Research Group. His research focuses on the physics of micro- and nanofluidic flows and the design of micro- and nanofluidic systems for applications in water, healthcare, energy, and environment. He obtained his B. Tech. degree from the Indian Institute of Technology at Bombay in 2002, and his PhD from the University of California at Berkeley in 2006. After postdoctoral work at MIT, he joined the Department of Mechanical Engineering at MIT in 2007. Among other honors, he is a recipient of the Institute Silver Medal (IIT Bombay, 2002), NSF Career Award (2010), Keenan Award for Innovation in Undergraduate Education (2011), DOE Early Career Award (2012), IIT Bombay Young Alumnus Achiever Award (2014), and the Ruth and Joel Spira Award for Distinguished Teaching (2018).



EFFECTS OF RELAXATION AND STRAIN IN MOIRE SUPERLATTICES

D. Kwabena Bediako¹

¹ *University of California, Berkeley (USA)*

Atomically thin or two-dimensional (2D) materials can be assembled into bespoke heterostructures to produce some extraordinary physical phenomena. Likewise, these highly tunable materials are useful platforms for exploring fundamental questions of interfacial chemical/electrochemical reactivity. One exciting and relatively recent example is the formation of moiré superlattices from azimuthally misoriented (twisted) layers. These moiré superlattices result in flat bands that lead to an array of correlated electronic phases. However, in these systems, complex strain relaxation can also strongly influence the fragile electronic states of the material. Precise characterization of these materials and their properties is therefore critical to the understanding of the behavior of these novel moiré materials (and 2D heterostructures in general). In this talk, I will discuss how spontaneous mechanical deformations (atomic reconstruction) and resultant intralayer strain fields at moiré superlattices of twisted bilayer graphene, twisted trilayer graphene, and twisted transition metal dichalcogenides have been quantitatively imaged using 4D-STEM Bragg interferometry. I will also discuss the impact of these mechanical deformations to the electronic band structure, correlated electronic phases, and interfacial ferroelectricity in these materials.

Epitaxial growth of van der Waal heterostructures on wafer scale

Ki Kang Kim¹

¹*Department of Energy Science, Sungkyunkwan University, Suwon 16419 (Republic of Korea)*

Van der Waals layered materials are renowned for their distinctive physical and chemical properties, including strong spin-orbit coupling, substantial Coulomb interaction, and gigantic magnetoresistance. When these materials are stacked, they exhibit new and unusual properties. These exotic properties pave the way for fabricating innovative functional devices in fields such as twistronics and spintronics. However, the development of a robust growth platform for vertical heterostructures remains a challenge. In this presentation, I introduce a heteroepitaxial and homoepitaxial growth platform for vertical heterostructures, including combinations such as MoS₂/WS₂, MoSe₂/WSe₂, and MoS₂/MoS₂/WS₂, using chemical vapor deposition []. The epitaxial growth of the overlayer on the bottom layer was confirmed via transmission electron microscopy. The resulting vertical heterostructures exhibit stacking orders of AA', AA, and AB. I will also discuss some applications of these heterostructures, demonstrating their potential in advancing current technology.

References (if desired)

[1] J. Kim, S. J. Yun, S. H. Choi, and K. K. Kim et al., in preparation (2024).

INVITED (SYMPOSIUM): Exploring the Power of Low-Dimensional Materials for Neuromorphic Computing

Xiaodong Yan^{1,2}

¹Department of Materials Science and Engineering, University of Arizona (USA), ²Department of Electrical and Computer Engineering, University of Arizona (USA)

Neuromorphic computing is an emerging technology that aims to overcome the limitations of the von Neumann bottleneck by taking inspiration from our human brain. Nevertheless, designing neuromorphic computing devices and hardware that can tackle vast quantities of information and offer sustainable, power-efficient computational methods possesses several challenges. To address these challenges, low-dimensional materials have emerged as an important family of materials due to their superlative physical properties and mixed-dimensional integration capability. Novel low-D materials-based neuromorphic devices offers rich opportunities to push the boundary of neuromorphic hardware.

In this presentation, I will discuss state-of-the-art opportunities offered by low-dimensional materials for neuromorphic computing and discuss our efforts in exploring an interdisciplinary path that connects the study of low-dimensional materials, devices, circuits and algorithms together. First, I will introduce our recent work on the room-temperature hexagonal boron nitride/bilayer graphene moiré synaptic transistors¹ and elucidate our efforts to interpret and harness the unique quantum electronic states in the material system, which lead to novel computing functionalities. The moiré synaptic transistor provides diverse bio-realistic neuromorphic functionalities and efficient compute-in-memory designs for low-power artificial intelligence and machine learning hardware accelerators. Second, I will introduce an unprecedented mixed-kernel transistors based on MoS₂/carbon nanotubes (CNTs) heterostructures². The reconfigurable nature of mixed-kernel heterojunction transistors also allows for personalized digital healthcare applications using Bayesian optimization. A single mixed-kernel heterojunction device can generate the equivalent transfer function of a complementary metal–oxide–semiconductor circuit comprising dozens of transistors and thus provides a low-power approach for support vector machine classification applications. Finally, the potential of building eco-friendly neuromorphic computing hardware³⁻⁵ by scaling our efforts from building single devices towards circuit-level integration will be discussed.

References (if desired)

- [1] X. Yan *et al.*, *Nature* **624**, 551–556 (2023).
- [2] X. Yan *et al.*, *Nat. Electronics* **6**, 862–869 (2023).
- [3] X. Sui *et al.*, *Adv. Mater. Technol.* **8**, 22, 2301288 (2023).
- [4] Z. Zhang *et al.*, *Nat. Sustain.*, in press (2024).
- [5] L. Kuo *et al.*, *Adv. Mater.* **34**, 2203772 (2022).

HIGH-PERFORMANCE NITROGEN-DOPED SINGLE-WALL CARBON NANOTUBE FIBERS

T. Fujimori^{1,2}, Z. Li², S. Jeong², H. Inoue^{1,3}, K. Akada², T. Onoki¹, J. Fujita²

¹Sumitomo Electric Industries, Ltd. (Japan), ²University of Tsukuba (Japan), ³Aalto University (Finland)

Substitutional doping of heteroatoms has offered a rich potential for tuning the electronic properties of carbon nanotubes (CNTs). Despite extensive research on nitrogen (N)-doped multi-wall CNTs (N-MWCNTs), a challenge is to synthesize N-doped single-wall CNTs (N-SWCNTs) with precise control of the C-N bonding states. We have shown the synthesis of high-crystallinity N-SWCNTs using a floating-catalyst chemical deposition under a high hydrogen flow rate (6 L min⁻¹) as the carrier gas [1]. X-ray photoelectron spectroscopy reveals that a relative ratio of the so-called graphitic-N configuration in the *sp*²-hybridized CNTs lattice increases with increasing synthesis temperature. An n-type doping behavior of the N-SWCNTs is confirmed by Raman spectroscopy. A particular interest of the N-SWCNTs can be found in their macroscopic assembly as a fiber, which provides a promising application for the next-generation light-weight electric wires. Here we show a way to produce N-SWCNT fibers using a superacid-based wet-spinning method. Interestingly, N-SWCNTs can be dispersed in chlorosulfonic acid (CSA) with an extremely high concentration (> 8 wt%). In this talk, we demonstrate that density and surface orientation of the N-SWCNT fibers can be improved by increasing the concentration of N-SWCNTs/CSA solution (~8 wt%), resulting in increasing the electric conductivity (3.9 MS m⁻¹, after annealing at 1000°C under hydrogen gas flow) and the tensile strength (3.2 GPa) of the N-SWCNT fiber. To better understand electronic transport properties of the N-SWCNT fibers, temperature dependence of electric resistance measured under cryogenic temperature will be discussed. Our finding will open the way to further developing high-performance CNT-based fibers for the future application.

References

[1] Z. Li *et al.*, *Appl. Phys. Express* **16**, 095001 (2023).

IN-PLANE STAGING AND LIMITS ON LITHIUM-ION INTERCALATION OF BILAYER GRAPHENE

I. V. Grigorieva^{1,2}

¹ *Department of Physics and Astronomy, University of Manchester (UK)*, ² *National Graphene Institute, University of Manchester (UK)*

The ongoing efforts to optimize rechargeable Li-ion batteries have led to the emergence of interest in intercalation of nanoscale derivatives of bulk layered compounds such as, e.g., bilayer graphene (BLG). Lithium intercalation of BLG has been demonstrated previously [1,2] but factors underpinning its ion storage capacity and limiting mechanisms remain poorly understood. We have used magneto-transport measurements to study in-operando intercalation dynamics of Li ions in BLG devices. Unexpectedly, intercalation of BLG is found to exhibit up to four distinct stages corresponding to well-defined Li-ion configurations and in-plane densities n_{Li} . Transitions between the stages occur rapidly (within 1 sec) over the entire device area. We refer to these as in-plane stages (I to IV), not to confuse the effect with the well-known staging in bulk graphite, where Li ions fill interlayer spaces to the full capacity in one step and different stages correspond to different sequences of out-of-plane domains. We found that in-plane stage IV in BLG provides a stoichiometric compound $\text{C}_{14}\text{LiC}_{14}$ and maximum $n_{\text{Li}} \approx 2.7 \cdot 10^{14} \text{ cm}^{-2}$, notably lower than n_{Li} for fully intercalated graphite. Combining the experimental findings and DFT calculations, we show that $\text{C}_{14}\text{LiC}_{14}$ corresponds to the thermodynamic equilibrium for intercalated AA-stacked bilayers. Another observed stage ($\text{C}_{18}\text{LiC}_{18}$) is close to this equilibrium configuration, whereas stages I and II at much lower n_{Li} are attributed to metastable states within the original AB stacking of the bilayer. The transition between the two types of stacking occurs at a threshold density of $\sim 0.9 \cdot 10^{14} \text{ cm}^{-2}$, resulting in an increase by $>250\%$ in Li ion density. This implies that AB to AA stacking transition represents a crucial step for achieving highest Li storage in BLG. In turn, this transition is seen to be facilitated by formation of AB/BA boundaries during intercalation-deintercalation cycles. Our findings not only reveal the mechanism and limits for electrochemical intercalation of BLG but also hint at possible avenues for increasing the Li storage capacity.

References

- [1] Kühne, M. et al. *Nature Nanotech.* **12**, 895–900 (2017).
- [2] Zhao, S. Y. F. et al. *Nano Lett.* **18**, 460–466 (2018).

Interfacial Nanoengineering of Conductive Concrete by Nanocarbon Materials

Jing Zhong

School of Civil Engineering, Harbin Institute of Technology, Harbin, 150090, PR China

Key Lab of Structures Dynamic Behavior and Control of the Ministry of Education (Harbin Institute of Technology), Harbin, 150090, PR China

Traditionally, conductive fillers are mixed directly with cement matrix before binding with aggregates to develop piezoresistive cement-based sensors. This results in the most vulnerable region, interfacial transition zone (ITZ), from which microcracks are initiated, merely located at the periphery of the conductive network and thus limits the sensitivity of the smart sensor. Recently, we propose a strategy to construct a three-dimensional (3D) conductive network in the mortar with ITZ directly embedded in it, thus greatly increasing both the conductivity and piezoresistivity without significantly sacrificing mechanical property. Highly conductive graphene-coated fine aggregates (termed conductive G@FAg particles) are prepared by adsorption of graphene oxide (GO) onto the fine aggregates (FAg) surface, followed by simple annealing and microwave treatment. The combined usage of conductive G@FAg particles and results in an outstanding electrical conductivity and an excellent fractional change in resistivity under cyclic compressive loading, with a negligible compressive strength loss. The much-improved conductivity and FCR value with such a low weight percentage of conductive carbon materials are attributed to the unique 3D network of conductive channels. Such general strategy of nano-interface engineering with graphene derivatives can also be readily extended to the promotion of other physical properties (strength, EMI, damping, mass transportation, et al), thus opens a new window to optimize properties of cementitious materials.

Molecular Recognition Approach for Bio-related Material Sensing Using Locally Functionalized Single-walled Carbon Nanotubes

T. Shiraki¹

¹Department of Applied Chemistry, Kyushu University, Fukuoka 819-0395 (Japan), ²WPI-I2CNER, Kyushu University, Fukuoka 819-0395 (Japan)

Photoluminescence (PL) of single-walled carbon nanotubes (SWCNTs) in the near infrared (NIR) region is applicable to advanced optical applications such as bio-imaging and sensing. Local chemical functionalization (slight amount of chemical modification) of SWCNTs has been developed to introduce sp^3 carbon defects in the sp^2 carbon network of the tube walls for the luminescent defect formation [1-3], producing locally functionalized SWCNTs (lf-SWCNTs). lf-SWCNTs show defect PL with red-shifted wavelengths and increased quantum yields compared to original E_{11} PL of pristine SWCNTs. For lf-SWCNTs, molecularly designed modifier molecules have enabled the defect PL wavelength modulation[4] and the sensing function creation.[5,6]

We have reported the unique microenvironment responsiveness of defect PL of lf-SWCNTs; that is, the greater wavelength shifts of defect PL than E_{11} PL by dielectric effects[7] and the PL shifting behavior modulation based on the chemical structure difference of the functionalized sites and the exciton localized states[8] are observed. Recently we apply the microenvironment responsiveness of the defect PL of lf-SWCNTs to the biological sensing application development.

To investigate protein detection/recognition functions of lf-SWCNTs, we introduced an avidin-biotin interaction with a selective and strong binding fashion at the defect sites of lf-SWCNTs. The lf-SWCNTs tethering biotin groups (lf-SWCNTs-b) were synthesized through diazonium chemistry, followed by its subsequent-modification of the biotin group[9]. When neutravidin was mixed with a lf-SWCNTs-b solution, the defect PL peak was red-shifted, indicating the higher polarity environment formation by the neutravidin adsorption on lf-SWCNTs-b. When avidin or streptavidin was used, wavelength shifting behaviors of the defect PL of lf-SWCNTs-b were clearly changed depending on the used avidin derivatives. The results indicate the different polarity environment formation deriving from structural differences of each avidin derivative. Moreover, the detection signal enhancement was observed in a film device using lf-SWCNTs-b.

As another example, we produced serum albumin (SA) detection system using lf-SWCNTs with a long-chain fatty acid group for SA recognition (Figure 1) [10]. The red-shifts of the defect PL occurred by formation of a high dielectric environment based on the specific binding between SA and the fatty acid groups on the defect sites. The lf-SWCNTs detected SA-spiked serum and albuminuria of diabetic mouse in body fluids.

Therefore, the molecular design-based defect engineering of lf-SWCNTs have a high potential for development of advanced protein detection/recognition systems using NIR PL.

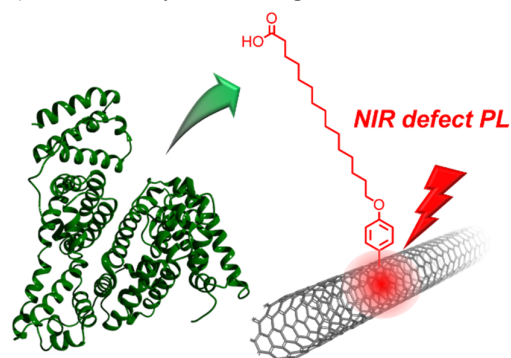


Figure 1: SA detection using defect PL of lf-SWCNTs.

References

- [1] T. Shiraki *et al.* *Acc. Chem. Res.* **53**, 1846 (2020).
- [2] B. J. Gifford *et al.*, *Acc. Chem. Res.* **53**, 1791(2020).
- [3] A. H. Brozena *et al.*, *Nat. Rev. Chem.* **3**, 375 (2019).
- [4] B. Yu *et al.*, *ACS Nano*, **16**, 21452 (2022).
- [5] T. Shiraki *et al.*, *Chem. Commun.* **52**, 12972 (2016).
- [6] S. Kruss *et al.*, *Angew. Chem. Int. Ed.* **59**, 17732 (2020).
- [7] T. Shiraki *et al.*, *Chem. Commun.* **55**, 3662 (2019).
- [8] Y. Niidome *et al.*, *J. Phys. Chem. C* **125**, 12758 (2021).
- [9] Y. Niidome *et al.*, *Nanoscale* **14**, 13090 (2022).
- [10] Y. Niidome *et al.*, *Carbon*, **216**, 118533 (2024).

Quantum Optical Emission From Defects in 2D Materials

Wenjing Wu¹, Arka Chatterjee¹, Shengxi Huang¹

¹*Rice University (USA)*

Defect engineering of 2D materials offers enormous opportunities to tune material properties. Isolated, optically-active defects could lead to single photon emission in 2D materials. However, single photon emission from 2D materials typically suffers from low purity and lack of controllability, due to the sensitivity of 2D monolayers to external dielectric environments, surface defects and adsorbents, and strains and wrinkles introduced during material processing. This talk introduces our recent efforts to improve the single photon purity and controllability in 2D materials. We propose novel defect structures that can overcome several current issues, and explore their electronic structure and tunability in optical emission. Through a combination of engineering approaches, including heterostacking, control of excitation and emission, optimization of material handling and transfer, we were able to achieve high purity (> 90%) for single photons emitted from 2D transition metal dichalcogenides (TMDs) and hBN in cryogenic temperature and room temperature, respectively. This work paves way towards the application of 2D materials for quantum optical applications. The materials engineering approaches developed here can be applied to the optimization of other optical and quantum materials.

Recent progress on the separation of single-chirality carbon nanotubes by gel chromatography

Huaping Liu^{1,2,*}

¹Beijing National Laboratory for Condensed Matter Physics, Institute of Physics, Chinese Academy of Sciences, Beijing 100190, China, ²University of Chinese Academy of Sciences, Beijing 100049, China

Corresponding author(s): liuhuaping@iphy.ac.cn

Single-wall carbon nanotubes (SWCNTs) are considered as ideal materials for the fabrication of high-performance electronic devices in the post-molar era due to their extremely high-carrier mobility, tunable band gap and nanoscale size. However, even slight difference in the structures of different SWCNTs induces huge difference in their optical and electrical properties [1-3]. The mixture structure of the as-grown SWCNTs hinder their applications in device applications. Therefore, mass production of single-chirality SWCNTs have long been the goal in SWCNT area. However, the large-scale preparation of single-chirality SWCNTs, both growth and separation, still faces great challenges.

Most recently, we found a simple, yet effective, method to increase the yield of gel chromatography separation of single-chirality SWCNTs by enabling significantly higher concentrations of raw nanotubes solution. With this technique, milligram-scale separation of multiple single-chirality SWCNTs have been achieved. To increase the concentration of SWCNTs, we developed a strategy for dispersing a highly concentrated individualized SWCNT solution by redispersion, in which the SWCNT solution was first ultrasonically dispersed, followed by ultracentrifugation and re-ultrasonic dispersion. With this technique, the dispersible initial concentration of SWCNTs increased from 1 to 8 mg/mL, and the corresponding concentration of the resulting individualized SWCNT solution increased from 0.19 to ~1.02 mg/mL [4]. In combination with the binary surfactant system [5], the separation yields of multiple single-chirality species, including (6, 4), (6, 5), (11, 1), (7, 5), (7, 6), (8, 3), (8, 4) and (9, 1), were increased by approximately six times to the milligram scale in one separation run with gel chromatography, reaching milligram scale.

References:

- [1] W. Su et al., *Nat Commun*, **14**, 1672 (2023).
- [2] F. T. Wang et al., *Adv. Funct. Mater.* **32**, 2107489 (2022).
- [3] S. L. Li et al., *Nano Res* **16**,1820 (2023).
- [4] D. H. Yang et al., *Nat Commun* **14**, 2491 (2023).
- [5] D. H. Yang et al., *Sci Adv* **7**, eabe0084 (2021).

RELATIONSHIP OF CNT SYNTHESIS CONDITIONS TO PERFORMANCE-LEVELIZED PROPERTIES OF CNT FIBERS

M. Pasquali and E. Khabushev

Department of Chemical and Biomolecular Engineering, Rice University (USA), Department of Chemistry, Rice University (USA), Department of Materials Science and NanoEngineering, Rice University (USA), The Carbon Hub, Rice University (USA), The Smalley-Curl Institute, Rice University (USA)

Based on property overlap, Carbon Nanotube (CNT) macroscopic materials could displace CO₂-intensive materials such as steel, aluminum, and copper. Moreover, CNTs can be made from natural gas and other light hydrocarbons and can be converted into macroscopic shapes via scalable room-temperature solution processing. Because hydrogen is a byproduct of CNT synthesis, displacing metals with CNT materials at the scale of hundreds of MT/yr would provide a comparable amount of hydrogen that would be, essentially, free. For this to happen, significant challenges must be overcome in synthesis and processing efficiency. In this talk, we will explain the fluid mechanics and transport phenomena that control one of the most efficient methods for making high-quality, fiber-grade CNTs—the deep injection method by S. M. Kim (KIST). We also clarify the role of oxygen in the CNT purification process necessary for dissolution in acids. We estimate the plant-scale efficiency of the current reactor and liquid crystal fiber spinning process and assess the projected performance of CNT fibers against incumbent fibers and cables of conventional materials (metals and carbon fibers). We introduce the concept of property levelization and show that, even with the currently low process efficiency, levelized properties are competitive against incumbent materials.

Remote doping for Carbon Nanotube Transistors

Shengman Li

Stanford University, Stanford, CA, USA; sml2020@stanford.edu

Carbon nanotubes (CNTs) are promising candidates as channel material for high-performance and energy-efficient field-effect transistors (FETs) at advanced technology nodes. Doping in CNT MOSFETs is crucial to reduce the parasitic resistance of the device, including both the contact resistance and the extension resistance. However, controlled, localized, and stable doping remains a significant long-term challenge. Although substitutional doping is well-established for silicon FETs, it is not sufficient in CNT FETs due to the strong doping-induced scattering and due to the difficult fabrication, resulting from the low-dimensionality of CNTs. This talk will concentrate on remote doping techniques for CNT FETs. We will explore both the fundamental mechanisms and the device-level technology targets. The presentation will cover effective strategies for the implementation and advancement of remote doping in CNT FETs, including:

1. Achieving controllable n-type doping with a contact resistance of sub-10 k Ω per CNT at $L_C = 20$ nm, utilizing Pd metal for both n- and p-type contacts. [1]
2. Developing a self-aligned doping integration flow for CNT MOSFET extensions, enabling a high drain current (I_D) exceeding 1.2 mA/ μm and a subthreshold swing (SS) of 170 mV/dec at 0.75 V of V_{DS} . [2]
3. A new doping technique based on a barrier booster, leveraging extensive Design-Technology Co-Optimization and applicable to other low-dimensional materials [3]. Such technique is crucial to enable up to 7 \times EDP CNT FETs benefits vs. Si FETs at 2nm technology node.

The talk will provide a comprehensive overview of remote doping strategies for CNFETs and propose guidelines for future research in this field.

We are grateful for support and collaboration from TSMC Corporate Research, DoD, Stanford SystemX Alliance, Stanford Nanofabrication Facility, Stanford Nano Shared Facility, and University of California at San Diego.

References:

- [1] N. Safron, et al, "Low N-Type Contact Resistance to Carbon Nanotubes in Highly Scaled Contacts through Dielectric Doping," 2023 IEEE International Electron Devices Meeting (IEDM), 10-5, Dec. 2023.
- [2] S. Li, et al, "High-performance and low-parasitic-capacitance CNT MOSFET with 1.2 mA/ μm at V_{DS} of 0.75 V enabled by self-aligned doping in sub-20 nm spacer," 2023 IEEE International Electron Devices Meeting (IEDM), 10-6, Dec. 2023.
- [3] C. Gilardi, et al, "Barrier Booster for Remote Extension Doping and its DTCO for 1D & 2D FETs," 2023 IEEE International Electron Devices Meeting (IEDM), 3-1, Dec. 2023.

Rheology, Phase Behavior, and Direct Ink Writing of Aqueous MXene Dispersions

Virginia A. Davis¹, Francis Mekunye¹, Mackenzie B. Woods², Majid Beidaghi^{1,2}

¹*Auburn University (USA)*, ²*University of Arizona (USA)*

The self-assembly of anisotropic nanomaterials provides unique opportunities to manufacture 2D and 3D materials with controlled microstructures. This talk describes the rheology and phase behavior of MXene dispersions as a function of size distribution. It also elucidates how these dispersion properties affect the manufacture and properties of 3D materials produced by direct ink writing (DIW). Specifically, we explored aqueous dispersions containing large ($\langle L \rangle = 3 \mu\text{m}$) and small ($\langle L \rangle = 0.3 \mu\text{m}$) $\text{Ti}_3\text{C}_2\text{T}_x$ produced by the minimally intensive layer delamination (MILD) process. Dispersions of large sheets exhibited lyotropic liquid crystalline phase behavior with long-range ordering, but they also exhibited aggregation with increasing concentration. With increasing concentration, dispersions of small sheets exhibited birefringence in the absence of large aggregates, but they did not possess long-range ordering. In contrast, mixtures of large and small sheets exhibited long-range liquid crystalline ordering with little to no aggregation. These intentionally polydisperse dispersions were selected for additional study using a combination of optical microscopy, small amplitude oscillatory shear rheology (SAOS), three interval thixotropy testing (3ITT), and large amplitude oscillatory rheology (LAOS). These studies provided additional understanding of the effects of size distribution on quiescent dispersion microstructure as well as deformation and recovery dynamics. The dispersion characteristics were then compared to qualitative and quantitative measures of printability, print quality, and the electrochemical performance of printed microsupercapacitors. Together, these results provide an increased understanding of structure-process-property relationships for microdevices printed from anisotropic nanomaterial inks.

Selective and Effective Extraction of Monochiral Single-Walled Carbon Nanotubes with Conjugated Polymers

A. Dzienia¹, D. Just¹, D. Janas¹

¹*Silesian University of Technology, Gliwice (Poland)*

Semiconducting single-walled carbon nanotubes (SWCNTs) are highly valuable in a broad spectrum of application fields spanning from photonics via nanomedicine to microelectronics. Currently, the implementation of many promising concepts based on SWCNTs is hindered by the scarcity of chirality-defined fractions with a particular set of desired properties. Various sorting methods have been developed to approach this issue in recent years [1].

Conjugated Polymer Extraction is particularly useful, as it offers high selectivity, and the isolated SWCNTs are already suspended in volatile organic solvents, which are highly convenient for making devices. Unfortunately, the mechanism of the sorting process is not fully understood, so only (6,5) and (7,5) SWCNTs are routinely extracted using such polymers.

This contribution will disclose how we extract specific SWCNTs from their complex mixtures using self-made conjugated polymers and various organic solvents [2-4]. Thoughtful selection of separation conditions and tailoring of the polymer characteristics enabled us to generate monochiral suspensions of (7,3) SWCNTs [3]. Concomitantly, we tackled a common problem with the purification of nanomaterials: the product's separation yield and purity are typically mutually exclusive. By employing mixed-solvent engineering involving toluene and tetralin, we created a medium wherein both high yield and exceptional purity were attained simultaneously.

Moreover, we also substantially improved the yield of the isolation of (6,5) SWCNTs extracted using the conjugated polymer most widely employed by the community, i.e., PFO-BPy [4]. The introduction of low molecular weight compounds into the extraction system increased the concentration of the obtained monochiral SWCNTs by order of magnitude without negatively affecting the purity of the fractions. A comprehensive analysis of the system, supported by modeling, revealed that the newly added compounds acted as polymer chaperones and promoted the appropriate folding of polymers around SWCNTs, thereby boosting both the selectivity and the yield of differentiation.

The authors would like to thank the National Science Centre, Poland (under the SONATA program, Grant agreement UMO-2020/39/D/ST5/00285).

References

- [1] D. Janas, Towards monochiral carbon nanotubes: a review of progress in the sorting of single-walled carbon nanotubes, *Materials Chemistry Frontiers* **2** (2018) 36-63.
- [2] A. Dzienia, D. Just, D. Janas, Nanoscale, Solvatochromism in SWCNTs suspended by conjugated polymers in organic solvents, *Nanoscale* **15** (2023) 9510-9524.
- [3] A. Dzienia, D. Just, P. Taborowska, A. Mielanzyk, K.Z. Milowska, S. Yorozya, S. Naka, T. Shiraki, D. Janas, Mixed-Solvent Engineering as a Way around the Trade-Off between Yield and Purity of (7,3) Single-Walled Carbon Nanotubes Obtained Using Conjugated Polymer Extraction, *Small* **19** (2023) 2304211.
- [4] D. Just, A. Dzienia, K.Z. Milowska, A. Mielanzyk, D. Janas, High-yield and chirality-selective isolation of single-walled carbon nanotubes using conjugated polymers and small molecular chaperones, *Materials Horizons* (in press).

Self-trapped excitons in twisted hBN heterostructures

S. Roux^{1,2,3*}, C. Arnold¹, E. Carré^{1,2}, L. Ren³, C. Robert³, X. Marie³, F. Ducastelle², A. Loiseau² and J. Barjon¹

¹Université Paris-Saclay, UVSQ -CNRS, GEMaC, (France), ²Université Paris-Saclay, ONERA-CNRS, LEM, (France), ³Université de Toulouse, INSA-CNRS-UPS, LPCNO, (France)

A new luminescence line has recently been discovered in cathodoluminescence (CL) on twisted hBN-hBN structures. It is characterized by a large linewidth (~ 2 eV) and a maximum arising at 4 eV, i.e. 2 eV below the hBN gap [1,2], as shown in the figure below. The origin of this band and of the 2-eV shift is debated. First, a giant exciton Moiré trapping at the interface has been proposed [2,3]. However, this is not consistent with theoretical studies, which estimate the interface trapping potential to be only a few hundreds of meV [4,5]. Therefore, a recent work has discarded its excitonic nature and rather attributed this emission to deep defects near the interface [4].

In this talk, we present a deterministic approach to elucidate the interplay between twist angles, defects and excitons. For this purpose, we have fabricated 30 twisted hBN-hBN heterostructures from mechanically exfoliated crystals. Based on the diffusion length of free excitons in hBN crystals [6], we have optimized the flakes thicknesses in order to favor an efficient diffusion of free excitons towards the twisted interface. The exciton-interface interaction is studied by temperature-dependent time-resolved CL experiments. From the analysis of our sample set, we propose that the 4-eV emission originates from an intrinsic self-trapping mechanism of the exciton at the twisted interface, which consists in a local distortion of the lattice around the site on which the exciton has trapped itself.

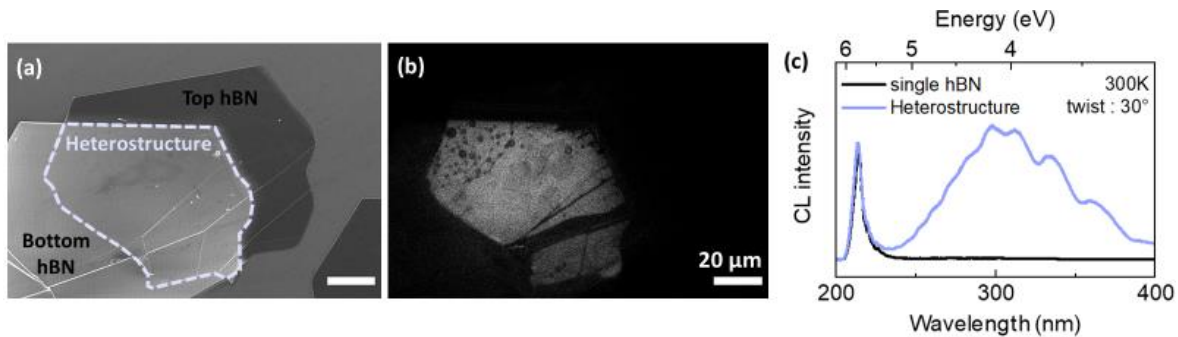


Figure (a) SEM image of a hBN-hBN structure composed of two hBN crystals twisted by 11° . (b) Image of the cathodoluminescence signal at 4 eV. The luminescence only comes from the hBN-hBN stack. (c) Cathodoluminescence spectra from a single hBN and from a 30° twisted hBN-hBN structure. The free exciton luminescence occurs at 6 eV in hBN crystals, while the new luminescence appears between 3 and 5 eV in the twisted hBN-hBN structure.

- [1] A. Plaud, *PhD manuscript* (2020).
- [2] H. Y. Lee *et al.*, *Nano Letters* **21**, 7, 2832–2839 (2021).
- [3] Y. Li *et al.*, *Optics Express* **30**, 7, 10596-10604 (2022)
- [4] C. Su *et al.*, *Nature Materials* **21**, 896-902 (2022)
- [5] S. Latil *et al.*, *SciPost Physics* **14**, 053 (2023)
- [6] S. Roux *et al.*, in review to *Physical review B* (2024)

Steering atoms in the quasi-1D material CrSBr

J. Klein¹

¹ *Department of Materials Science and Engineering, Massachusetts Institute of Technology, Cambridge, MA 02139, USA*

The ability to program optical, electronic, and magnetic, properties at the atomic scale into materials is attractive for designing quantum phenomena. The aberration corrected scanning transmission electron microscope serves as a unique tool for atomic manipulation with a focused electron probe size of tens of picometer. However, unfavorable defect energetics and surface effects in commonly studied van der Waals (vdW) materials (e.g. MoS₂, graphene, hBN) in addition to the absence of intelligent beam strategies prevent precise and repeated structural control. In my talk I will address these current obstacles and showcase the development of innovative electron probe control strategies, applying them to the structurally amenable vdW magnetic semiconductor CrSBr.

In the first part of my talk, I will highlight the extraordinary electronic, optical, and magnetic properties of CrSBr. This includes that bulk CrSBr is a quasi-1D material manifested in its highly anisotropic electronic band structure, quasi-1D excitons and defect states, the observation of a Peierls-type structural instability, strong exciton-phonon, and electron-phonon interactions. [1, 2]

In the second part of my talk, I will demonstrate the deliberate and repeated manipulation of Cr atoms, which is connected to the reduced electronic dimensionality and peculiar crystal structure of CrSBr. Exposing an area of multilayer CrSBr with electrons drives a structural phase transformation with Cr atoms becoming mobile moving into interstitial sites in the van der Waals gap. [3] Leveraging this mechanism, we developed a fast and picometer precise beam targeting approach, termed “atomic lock-on” [4], which in combination with machine intelligence enables the repeated and deliberate steering of Cr atoms. [5] This realization represents a significant step towards creating artificial atomic quantum systems, constructing physics at the atomic level in materials.

References

- [1] J. Klein *et al.*, *ACS Nano* **17**, 5316–5328 (2023).
- [2] J. Klein *et al.*, *ACS Nano* **17**, 288–299 (2023).
- [3] J. Klein *et al.*, *Nat. Comms.* **13**, 5420 (2022).
- [4] J. Klein, K. M. Roccapriore *et al.*, *patent pending & manuscript in preparation.*
- [5] J. Klein, K. M. Roccapriore *et al.*, *manuscript in preparation.*

Stretchable Carbon Nanotube Transistors for Neuromorphic Computing

Chongwu Zhou¹

¹*Dept. of Electrical and Computer Engineering, University of Southern California, Los Angeles, CA 90089 (USA)*

Carbon nanotubes (CNTs) have found extensive applications in stretchable electronics owing to their unique electrical and mechanical properties. The network structure enables CNTs with exceptional stretchability, while their one-dimensional nature makes them highly sensitive to ambient charge, facilitating effective modulation of channel conduction. Various fabrication techniques, such as inkjet printing, stencil masks, and other lithography-free methods, have been employed to produce intrinsic stretchable CNT transistors. However, these processes often involve using of numerous polymers, leading to potential drawbacks such as device degradation, low current density, poor scalability, and large device dimensions. Consequently, these challenges impede the practical implementation of stretchable CNT transistors.

Here we reported a low-temperature methodology for direct fabrication of CNT synaptic transistors on elastic substrate without the need of transfer process. This approach affords advantages of cost-effectiveness, high throughput, uniformity, and stable device performance, thereby enabling large-scale production of stretchable CNT devices. First, a polydimethylsiloxane (PDMS) elastomer is spin coated onto rigid substrate with polymethyl methacrylate (PMMA) serving as sacrificial layer. Subsequently, an ultra-thin polyethylene terephthalate (PET) film is attached to the PDMS. Serpentine-shaped transistors, comprising a CNT channel, SU-8 dielectric, and palladium (Pd) contacts, are directly fabricated on the PET film. Finally, oxygen plasma is employed to selectively etch the PET film into a serpentine shape, and the dissolution of PMMA renders the device stretchable. Our transistors exhibit remarkable performance within stretchable devices, demonstrating an on-current density of $1.0 \mu\text{A}/\mu\text{m}$, an on/off ratio of 106, and a mobility around $100 \text{ cm}^2/(\text{V}\cdot\text{s})$. These devices show a minimal degradation of less than 8% under strains up to 30%. The synaptic behavior in these transistors is attributed to charge-trapping effects, a phenomenon commonly observed in carbon-based nanoelectronics. Specific, charge trapping in the SU-8 dielectric layer of top-gated CNT transistors enables the gradual analog programmability of the CNT channel conductance. The stability of the hysteresis property over months is also ensured by the top-gate structure. We then demonstrate adaptive online learning schemes by the implementation of pattern recognition using a spike-timing-dependent-plasticity scheme. The nonlinearity of long-term potentiation (LTP) and long-term depression (LTD) can be as low as 1.01 and more than 50 conductance states is achieved, leading to a superior 90% accuracy in pattern recognition using the MNIST dataset.

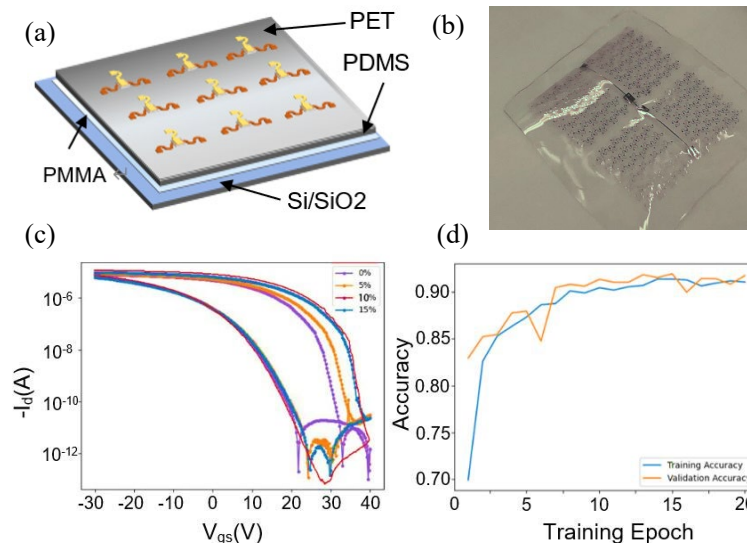


Figure (a) Schematic of the device fabrication method. (b) Photograph of as-fabricated stretchable CNT transistors. (c) Transfer characteristics of a representative device under strain from 0 to 15%. (d) Pattern recognition simulation using the stretchable CNT transistors.

Abstract

SWNTs: From a Dream Material to a Material That Realizes Your Dream

Single-walled carbon nanotubes (SWCNTs) have emerged as a fascinating material with a plethora of promising applications, spanning from electronics to medicine. Initially hailed as a "dream material" due to their exceptional properties such as high electrical conductivity, mechanical strength, and thermal stability, SWCNTs have captivated the imagination of scientists and engineers worldwide. However, realizing the full potential of SWCNTs in practical applications has been a formidable challenge, hindered by issues related to scalability, purity, and cost-effectiveness of production methods.

This talk delves into the journey of SWCNTs from the realm of scientific fascination to the realm of practical realization, highlighting the remarkable progress made in recent years. Through advancements in synthesis techniques, purification methods, and functionalization strategies, researchers have overcome many of the hurdles impeding the widespread adoption of SWCNTs. Consequently, SWCNT-based technologies are now poised to revolutionize various industries, offering solutions to pressing challenges in fields such as electronics, energy storage, sensing, and biomedicine.

Furthermore, the versatility of SWCNTs as building blocks for innovative materials and devices continues to inspire novel concepts and applications, fueling further research and development efforts. Despite the tremendous strides made, ongoing research aims to address remaining challenges and unlock the full potential of SWCNTs, ensuring their seamless integration into real-world technologies. As SWCNTs transition from a dream material to a material that realizes your dream, they stand poised to shape the future of technology and catalyze transformative advancements across diverse domains.

By Xinjie (Jeff) Zhang

President of Novarials Corporation

www.novarials.com

INVITED (COMPUTATION & THEORY): THE EFFECT OF AMORPHOUS CARBON ON PROPERTIES OF CARBON NANOTUBE FIBRES

J. A. Elliott¹ & P. A. Kloza¹

¹ *Department of Materials Science & Metallurgy, University of Cambridge, UK*

For CNT fibres produced by the floating catalyst chemical vapor deposition (FC-CVD) method, it is common to find small amounts of amorphous carbon (typically between 4 to 20 wt%) present in the final material. This can have a significant, and sometimes beneficial, effect on its mechanical properties [1, 2] although it is usually deleterious to the electrical and thermal properties. To date, there have been no studies which attempt to model the effect of amorphous carbon (aC) at the level of the CNT network, particularly the way in which they modulate interactions between CNT bundles. Here, we apply a coarse-grained (CG) model of CNTs developed for aerogel formation [3] to generate CNT networks from 100 nm to 1 micron in size containing between 10-30 wt% aC. The aC is modelled as soft spherical particles using a CG potential derived from a potential-of-mean-force for interaction with CNTs. We find that for shorter CNTs (aspect ratio < 100), the lower the fraction of aC, the more disconnected the network, and that for higher fractions, aC is primarily located at CNT junctions, stabilizing them, and thus preventing collapse of the network. For longer CNTs (aspect ratio > 200), the effects are less significant, but for both cases we present comparisons between the elastic modulus and viscosity of networks as a function of aC content and strain rate.

References

- [1] Bulmer, J. S., Kaniyoor, A., Gspann, T., Mizen, J., Ryley, J., Kiley, P., Ratering, G., Sparreboom, W., Bauhuis, G., Stehr, T., Oudejans, D., Sparkes, M., O'Neill, W. and Elliott J. A., Forecasting continuous carbon nanotube production in the floating catalyst environment. *Chemical Engineering Journal* 2020, **390**, 124497.
- [2] Bulmer, J. S., Kaniyoor, A. and Elliott, J. A., A Meta-Analysis of Conductive and Strong Carbon Nanotube Materials. *Advanced Materials*, 2021, **33**, 2008432.
- [3] Kateris, N., Kloza, P., Qiao, R., Elliott, J. A. and Boies A. M., From Collisions to Bundles: An Adaptive Coarse-Grained Model for the Aggregation of High-Aspect-Ratio Carbon Nanotubes. *Journal of Physical Chemistry C*, 2020, **124** 8359-8370.

TUNING THE ELECTRONIC AND TRANSPORT PROPERTIES OF GRAPHENE NANORIBBONS THROUGH STONE-WALES DEFECTS

E. C. Girão¹, T. A. Oliveira¹, P. V. Silva¹, V. Meunier²

¹Universidade Federal do Piauí (Brazil), ²The Pennsylvania State University (USA)

The precise synthesis of graphene nanoribbons (GNRs) using surface-assisted reactions has achieved substantial success in the last few years [1]. This scenario provides opportunities to direct experiment-simulations comparisons and to expand the set of systems investigated through theory while maintaining the focus on potentially feasible systems. This work was particularly motivated by the synthesis of a quantum-dot similar to a graphitic structure containing a Stone-Wales (SW) defect, consisting of a pair of pentagon-heptagon units [2]. We propose a series of carbon nanoribbons based on such a molecular block (57-GNRs) and study their electronic and transport properties with density functional theory and tight-binding based methods [3]. We demonstrate that 57-GNRs preserve the semiconducting character of their pristine counterparts, but the hierarchical dependence of the band gap with the systems widths is drastically modified. This is due to the introduction of characteristic conduction bands associated with the interaction involving successive defects. The changes in the electronic structure of the 57-GNRs further affect carrier mobilities of both electrons and holes. We also investigate the electronic transport properties of graphene-like nanojunctions with a localized distribution of SW-defects, indicating that the electronic transmission can be strategically controlled by the position and concentration of SW-defects.

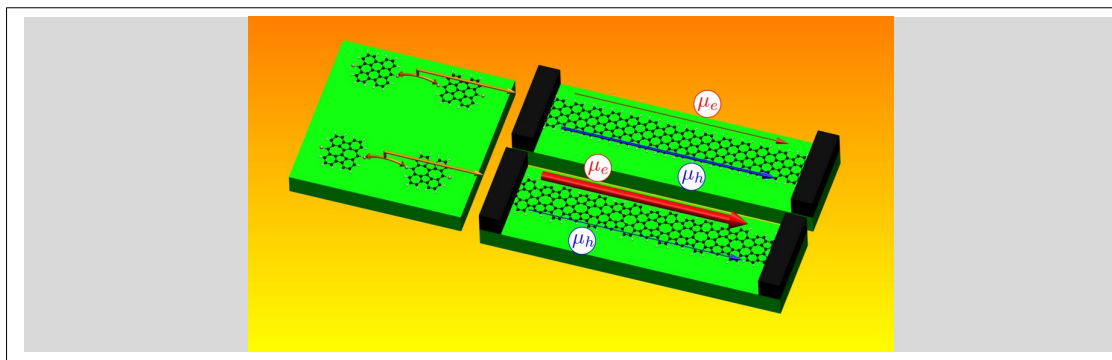


Figure caption: Illustration of the different carrier mobility values of pristine and defective carbon nanoribbons.

References

- [1] R. S. K. Houtsma et al., *Chem. Soc. Rev.* **50**, 6541–6568 (2021).
- [2] A. Konishi et al., *J. Am. Chem. Soc.* **141**, 10165–10170 (2019).
- [3] T. A. Oliveira et al., *Carbon* **201**, 222-233 (2023).

ULTRAFAST ENERGY RELAXATION IN CARBON NANOTUBE EXCITON-POLARITON MICROCAVITIES

M. Son¹

¹*Department of Chemistry, Boston University (USA)*

Coupling between light and matter in an optical cavity creates hybrid states known as polaritons with properties that are not observed in purely molecular systems. We fabricate and investigate polariton microcavities and devices containing semiconducting single-walled carbon nanotubes, which are an ideal class of molecules to create polaritons with due to their strong and narrow absorption in the visible and the near-infrared. Applying ultrafast 2D white-light spectroscopy in a donor-acceptor carbon nanotube polariton, we find that the interplay between light-matter coupling and molecular parameters, such as interchromophore coupling and disorder in the carbon nanotubes, enables a long-range energy transport process across several hundreds of nanometers. Furthermore, we find that long-range energy transport persists even in the presence of weak light-matter coupling, highlighting the active role of polariton light-matter interaction in controlling the dynamics and function of molecular materials.

Ultrascaled Devices based on 2D Semiconductors for Advanced Electronic Applications

Xu Zhang

Department of Electrical and Computer Engineering,

Carnegie Mellon University

xuzh@cmu.edu

The atomically thin body thickness of two-dimensional (2D) semiconductors, especially 2D transition metal dichalcogenides (TMDCs), makes them ideal for ultimate scaling while maintaining a tight gate electrostatic control over channel [1], [2]. Unlike silicon, the dangling-bond-free nature of 2D semiconductors makes their carriers' mobility largely immune to thickness scaling [3], [4]. It holds great prospects in enabling scaling electronic devices, for both computing and memory applications, down to a territory that would be fundamentally challenging for conventional 3D semiconductors, such as silicon and germanium. In this talk, we will share recent advances on the scalable fabrication of MoS₂ electronics devices with sub-10-nm channel length. A combined experimental and theoretical investigation was done to systematically study their short channel effects and performance limits.

References

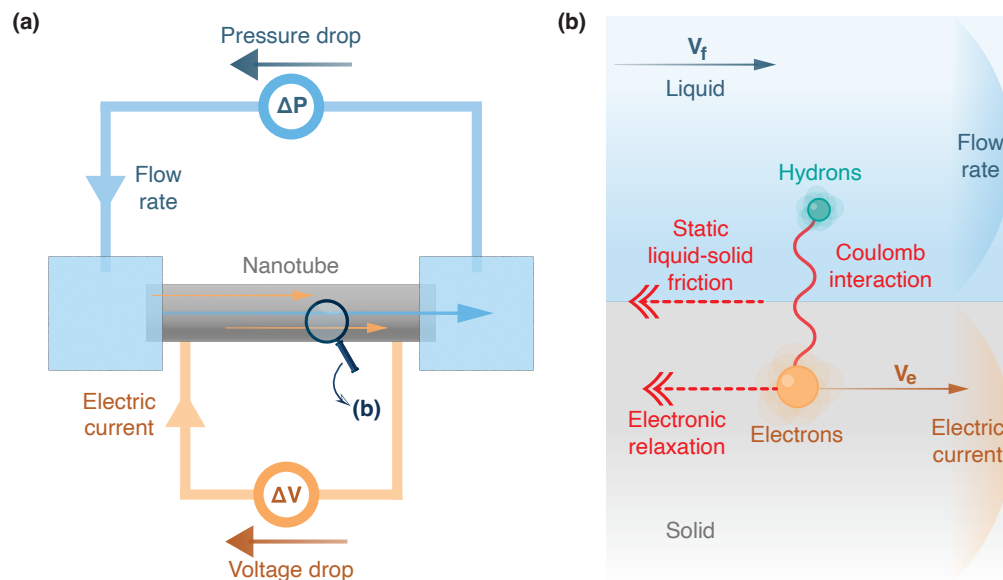
- [1] Y. Liu, X. Duan, H.-J. Shin, S. Park, Y. Huang, and X. Duan, "Promises and prospects of two-dimensional transistors," *Nature*, vol. 591, no. 7848, Art. no. 7848, Mar. 2021, doi: 10.1038/s41586-021-03339-z.
- [2] S. M. Sze and K. K. Ng, *Physics of Semiconductor Devices*, 3rd edition. Hoboken, N.J: Wiley-Interscience, 2006.
- [3] M. Chhowalla, D. Jena, and H. Zhang, "Two-dimensional semiconductors for transistors," *Nat Rev Mater*, vol. 1, no. 11, Art. no. 11, Aug. 2016, doi: 10.1038/natrevmats.2016.52.
- [4] D. Akinwande et al., "Graphene and two-dimensional materials for silicon technology," *Nature*, vol. 573, no. 7775, Art. no. 7775, Sep. 2019, doi: 10.1038/s41586-019-1573-9.

Water in carbon nanotubes: from giant slippage to hydroelectric power

Nikita Kavokine^{1,2}

¹Max Planck Institute for Polymer Research, Mainz (Germany), ²Flatiron Institute, New York (USA)

Liquids are usually described within classical physics, whereas solids require the tools of quantum mechanics. We have shown that in nanoscale channels, such as carbon nanotubes, this distinction no longer holds [1]. At these scales, the liquid flows become intertwined with electron dynamics in the channel walls, resulting in a wealth of phenomena beyond the reach classical fluid mechanics. I will discuss, in particular, our recent results on the coupling of liquid flows with electric currents in the channel walls [2], and implications for hydroelectric energy conversion at the nanoscale.



Principle of nanoscale hydroelectric energy conversion through the hydrodynamic Coulomb drag effect.

References

- [1] N. Kavokine, M.-L. Bocquet and L. Bocquet, *Nature* **602**, 84–90 (2022).
- [2] B. Coquinot, L. Bocquet and N. Kavokine, *Phys. Rev. X* **13**, 011019 (2023).

ADVANCES ON EPITAXIAL CVD GROWTH OF MULTI-LAYERED BN FILMS AND OPTICAL CHARACTERIZATION OF BN CRYSTALS

L. Tailpied¹, S. Roux^{1,2}, A. Andrieux-Ledier³, C. Arnold², F. Fossard¹, J.-S. Mérot¹, J.-M. Decams⁴, F. Ducastelle¹, J. Barjon², A. Loiseau¹

¹Université Paris Saclay, ONERA-CNRS, LEM, (Chatillon, France), ² Université Paris Saclay, UVSQ-CNRS, GEMaC (Versailles, France), ³Université Paris Saclay, ³ONERA, DPHY (Chatillon, France), ⁴Annealsys, 139 rue des Walkyries, (Montpellier, France)

Due to its unique properties, sp² hybridized boron nitride (BN) has been identified as a key towards integration of 2D materials into devices. Indeed, this capability has been demonstrated using mechanically exfoliated BN from low defective and highly crystalline single crystals. Yet, this process strongly limits the size of the devices. In order to develop devices at a wafer scale, it is therefore critical to master the synthesis of BN layers at low cost, large scale and desired quality. This implies a double effort on the synthesis and on the characterization.

Our synthesis effort aims at full filling these requirements. In a first step we demonstrated that heteroepitaxial growth of a few nanometer-thick BN film of well-stacked and flat layers could be achieved by CVD on Ni (111) surface of polycrystalline substrate [1]. On this basis we have developed a process on a dedicated Rapid Thermal CVD reactor using borazine as B and N sources and wafer-scale single crystalline Ni (111) pseudo substrates. We will show that thanks to an appropriate preparation of the substrate, continuous layers with a single crystalline orientation can be grown at a wafer scale and transferred for being integrated in appropriate devices [2].

Our characterization effort has focused on the development of a multiscale methodology able to qualify the nature and the structural quality of BN films and crystals from the atomic scale to the macroscopic scale. This is done by combining a set of spectroscopic (Raman, EELS, luminescence) and imaging (SEM, AFM, TEM-STEM) techniques which provide information at different scales. Concerning the films, we will show that the key issue is to perform characterizations in a statistical way for being able to crosslink and correlate the nature and the density of structural and chemical defects at the different scales [3]. Concerning hBN crystals, we will present the new method we have developed for ranking quantitatively their quality by measuring the decay time of free excitons responsible for the intense luminescence of this material [4].

References

- [1] H. Prevost et al. 2D Materials, 7 045018 (2020)
- [2] L. Tailpied et al, submitted (2024)
- [3] L. Tailpied, PhD thesis, Sorbonne University (2023)
- [4] S. Roux et al, Phys. Rev.B 104, L161203 (2021)

ANISOTROPIC THERMOPOWER ON GRAPHENE THIN FILMS DEPOSITED ON FLEXIBLE SUBSTRATES

J. Canaval¹, E. Quintero¹, C. Balaguera¹, D. Olaya¹, Y. Hernandez¹

¹*Physics Department – Universidad de los Andes. 111711 Bogota, Colombia.*

Liquid phase exfoliation of graphene has proven successful in producing unfunctionalized samples at a near kg-a-day level [1, 2]. However, applications that truly harvest the quantum properties of graphene are yet to be implemented [3]. The work of Dresselhaus and Hicks demonstrated that low-dimensional materials display an enhanced thermopower [4]. Graphene has been used as a filler material in traditional thermoelectric nanostructured composites [5], nevertheless, it has been overlooked on its own due to its extremely high thermal and electrical conductivity in-plane. In this talk, the mild oxidation of electrochemically exfoliated graphene [6] as well as its large area results in a measurable thermopower in the out-of-plane direction will be discussed. The processing of the dispersions for film formation results in wrinkles [7] and moiré patterns that lead to van Hove singularities in the density of states and therefore an increased thermopower [8].

[1] Y. Hernandez, et al, Nature Nanotechnology, **3**, 563–568 (2008)

[2] A. Amiri, et al, FlatChem, **8**, 40-71, (2018)

[3] *Nat. Phys.* **20**, 1 (2024).

[4] M. S. Dresselhaus, et al. Phys. Solid State, **41**, 679–682 (1999)

[5] N. A. Khoso, et al, RSC Adv., **11**, 16675-16687 (2021)

[6] J Rico, et al, J. Phys.: Condens. Matter **34** 105701 (2022)

[7] Khaled Parvez, et al, ACS Nano **2013**, **7**, **4**, 3598–3606 (2013)

[8] J. Canaval, E. Quintero, C. Balaguera, D. Olaya, Y. Hernandez, in preparation (2024)

Atomic Origin of the Axis-Symmetrical Growth and its Breaking of a Single-Wall Carbon Nanotube

Lili Zhang^{1,*}, Thomas W. Hansen², Jakob B. Wagner^{2,*}, Chang Liu^{1,*}, Hui-Ming Cheng^{1,3}

¹ Shenyang National Laboratory for Materials Science, Institute of Metal Research, Chinese Academy of Sciences, 72 Wenhua Road, Shenyang 110016, China,

² National Centre for Nano Fabrication and Characterization, Technical University of Denmark, 2800, Kgs. Lyngby, Denmark,

³ Institute of Technology for Carbon Neutrality, Shenzhen Institute of Advanced Technology, Chinese Academy of Sciences, 1068 Xueyuan Road, Shenzhen 518055, China

Corresponding author(s): zhangll@imr.ac.cn, jabw@dtu.dk, cliu@imr.ac.cn

The chirality of a single-wall carbon nanotube (SWCNT) is usually considered to be closely related to the atomic configuration of catalyst seed nanoparticles. Hence, a change in the local atomic structure of the catalyst may generate a local defect on the tube and then break the symmetry in the tube chirality. However, the axis symmetry and its variation during the early stage of SWCNT growth remains unexplored and its origins at the atomic scale are elusive. Here, we report the direct atomic-scale visualization of both the axis-symmetrical growth and its alteration processes of a SWCNT by using *in situ* environmental transmission electron microscopy [1-3]. Our results reveal that in contrast to the continuous growth of a straight tube, the formation of topological defects on the sidewall of a SWCNT acts as a buffer for stress release, inherently breaking its axis-symmetrical growth (Figure 1). Atomic-level details reveal the importance of the tube/catalyst interface and how the atom rearrangement of the solid-state platinum catalyst around the interface influences the final tubular structure. Theoretical simulations confirm that the active sites responsible for trapping carbon dimers and providing enough driving force for carbon incorporation and asymmetric growth are the low-coordination step edges.

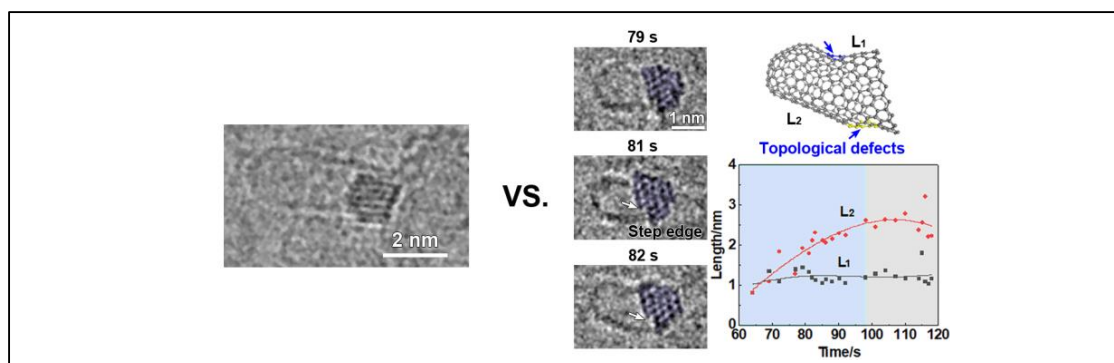


Figure 1: The symmetrical growth and the transition from symmetrical to asymmetrical growth of a SWCNT from a Pt nanoparticle.

References

- [1] L. Zhang, *et al. Adv. Sci.* 2304905 (2023).
- [2] R. Ma, *et al. ACS Nano* **16**, 16574-16583 (2022).
- [3] Y. Wang, *et al. Sci Adv* **8**, eabo5686 (2022).

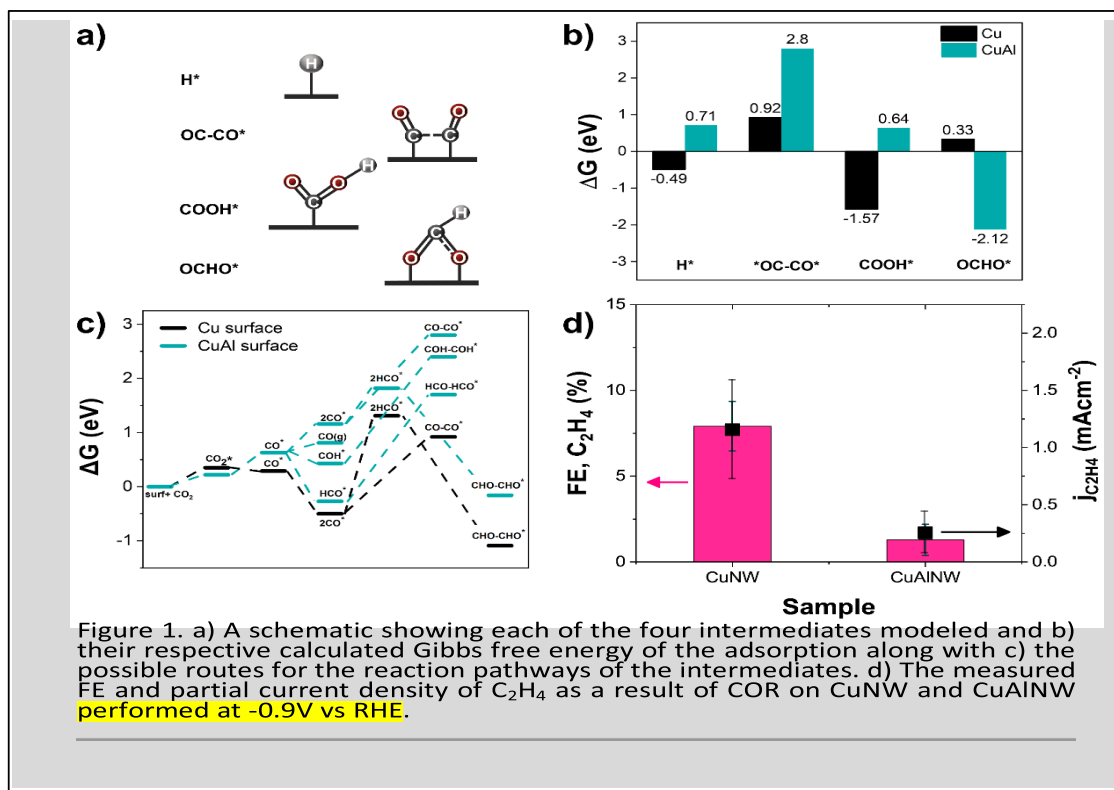
BOOSTING SELECTIVITY TOWARDS FORMATE PRODUCTION USING CuAl ALLOY NANOWIRES BY ALTERING THE CO₂ REDUCTION REACTION PATHWAY

Nageh K. Allam¹

¹The American University in Cairo, Egypt

Abstract

Understanding the fundamentals behind an electrocatalyst's selectivity enables the ability to steer product formation. Herein, we study Cu nanowires doped with a small amount of Al (12%) for CO₂R, which enhances formate production by 16.9% over pure Cu nanowires. Density functional theory calculations and COR were employed to posit the preference of the formate formation pathway as a result of the Al doping.



Controlled Growth of Horizontally Aligned Single-Walled Carbon Nanotube Arrays

Liu Qian*¹, Ying Xie¹, Yue Li¹, Mingzhi Zou², Jin Zhang*^{1,2}

¹*School of Materials Science and Engineering, Peking University (China)*, ²*College of Chemistry and Molecular Engineering, Peking University (China)*

Single-walled carbon nanotubes (SWNTs) are ideal for constructing field effect transistors and logic circuits because of their high mobility, high carrying current, and high stability. However, to achieve high device performance, horizontal arrays of carbon nanotubes are required to have both high density (> 125 tubes/ μm) and high semiconducting purity (> 99.9999%). Although significant breakthroughs have been made in research on the density and structure-controlled preparation of SWNTs in arrays,^[1] current array materials are still a long way from practical production and application. This report is based on the chemical vapor deposition preparation method of carbon nanotube horizontal arrays, which starts from several key factors, including substrate, catalyst, airflow and external field, to regulate the density of the arrays and the structure of the carbon nanotubes.

Through the introduction of ion implantation technology and spray chemical vapor deposition system, the direct preparation of wafer-scale uniform and high-density SWNT horizontal arrays has been realized, and the polarized optics-based high throughput characterization technique has been developed for wafer-scale samples. Based on the floating solid catalyst method,^[2] a spatially confined growth strategy was developed to realize the enriched growth of semiconducting tubes based on the improvement of the deposition efficiency of titanium-based solid-state catalysts.^[3] In addition, based on the intrinsic difference of energy band structures of semiconducting and metallic carbon nanotubes, a light-induced charge transfer method was developed to realize the advantageous growth of semiconducting carbon nanotubes, and the selective growth law of semiconductor tubes related to the energy band structure was also developed. Furthermore, based on the plasma-enhanced chemical vapor deposition system, an electric field-assisted method was developed for the growth of horizontal arrays of semiconducting carbon nanotubes. From fine structure tuning to array density control, we provide new ideas for the preparation of high-density, structure-specific SWNTs, aiming to realize the direct preparation of wafer-scale, high-density, structurally controllable horizontal arrays of SWNTs, and to promote the advancement of the carbon-nanotube-based chip industry.

References

- [1] Zhang, S.; Kang, L.; Wang, X.; Tong, L.; Yang, L.; Wang, Z.; Qi, K.; Deng, S.; Li, Q.; Bai, X.; Ding, F.; Zhang, J. * *Nature* 2017, **543**: 234.
- [2] Qian, L.; Xie, Y.; Yu, Y.; Wang, S.; Zhang, S.; Zhang, J. * *Angew. Chem. Int. Ed.* 2020, **59** (27):100884.
- [3] Qian, L.; Shao, Q.; Yu, Y.; Liu, W.; Wang, S.; Gao, E.; Zhang, J. * *Adv. Funct. Mater.* 2022, **32**: 2106643.

Creating a Sustainable World: The Next-Generation Energy Conversion and Storage Technologies Enabled by Carbon Nanostructures

Ghulam Yasin, Esko I. Kauppinen

Aalto University (Finland)

Green energy conversion and storage technologies have paid significant consideration owing to the continuously rising energy demand for sustainable social and economic development [1]. To comprehend the sustainable use of energy, particularly from renewable sources, next-generation systematized energy conversion and storage technologies are greatly desired, which can be enabled by carbon nanostructures. For this purpose, the construction of new materials with excellent practical permanency and extraordinary activity for electrochemical energy generation is deemed a very competitive and active avenue in energy applications. With the rapidly expanding research areas and emerging uses of nanoscience and nanotechnology, advanced carbon nanomaterials with several unique morphologies are proposed to fabricate promising electrocatalysts and/or energy storage materials [2,3].

Batteries are the promising energy storage technologies among all available storage systems. Recently, lithium-ion batteries (LIBs), have successfully powered electronic gadgets, stationary storage devices, and electric vehicles [4]. However, so far, the desires for new energy storage materials with higher energy and power densities are still continuously increasing, to enable large-scale energy storage for the power grid. The adaptability of carbon nanostructures nanomaterials could originate the proficient power sources for various technologies, such as portable, foldable, flexible electronic appliances, electric transport, and grid-scale energy storage. In this talk, we will briefly discuss the design and development of carbon nanostructures and nanomaterials for high-performance next-generation electrochemical energy conversion and storage devices.

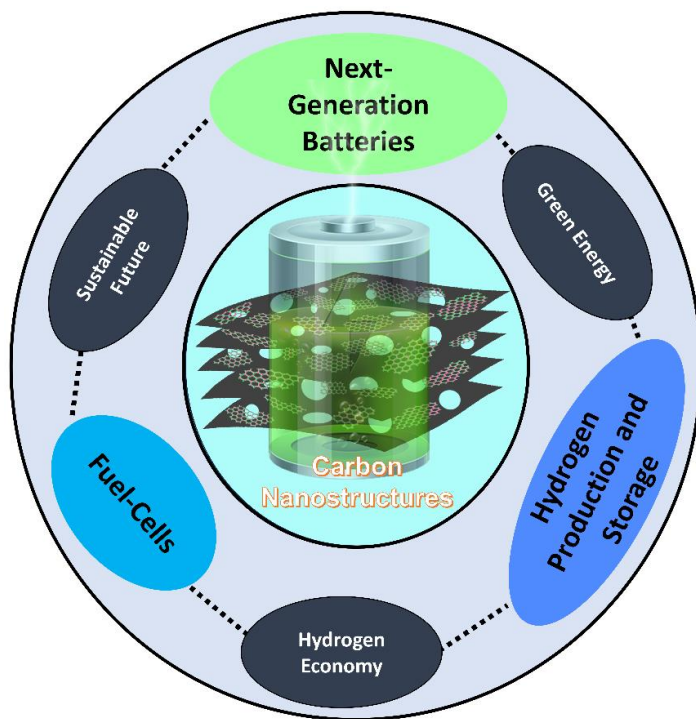


Figure 1: Carbon nanostructures for electrochemical energy conversion and storage technologies.

References

- [1] F. Bonaccorso *et al.*, *Science* **347**, 1246501 (2015).
- [2] G. Yasin *et al.*, *ACS Catal.* **13**, 2313-2325 (2023).
- [3] G. Yasin *et al.*, *Inorg. Chem. Front.* **9** 1058-1069 (2022).
- [4] G. Yasin *et al.*, *Energy Storage Mater.* **25**, 644-678 (2020).

Decoding Early Stress Signaling Waves in Living Plants using Nanosensor Multiplexing

M.C.Y. Ang¹, J.M. Saju², T.K. Porter³, S. Mohaideen¹, S. Sreelatha², D.T. Khong¹, S. Wang¹, J. Cui³, S.I. Loh¹, G.P. Singh¹, M.S. Strano³, S. Rajani²

¹*Disruptive & Sustainable Technologies for Agricultural Precision IRG, Singapore-MIT Alliance for Research and Technology (Singapore)*, ²*Temasek Life Sciences Laboratory Limited (Singapore)*, ³*Department of Chemical Engineering, Massachusetts Institute of Technology (United States of America)*

Environmental stresses have a substantially negative impact on plant growth and productivity, further amplified by global climate change. In response to stress, plants activate a signaling cascade, involving multiple molecules ultimately leading to resistance or stress adaptation. However, the temporal ordering and composition of the resulting cascade, and the specific stress it encodes for, remain largely unknown. Reactive oxygen species, such as H₂O₂, act as key early stress signaling molecules and are known to subsequently interact with different plant hormones like salicylic acid (SA) to mediate specific and distinct stress responses. It remains a puzzle as to how or if the early ROS wave carries the information encoding the specific type of stress stimulus. In this work, we utilize a newly developed and validated SA nanosensor, multiplexed with one for H₂O₂ for simultaneous monitoring of stress-induced H₂O₂ and SA signals when *Brassica rapa subsp. Chinensis* (Pak choi) plants were subjected to distinct stress treatments, namely light stress, heat stress, pathogen stress and mechanical wounding. The nanosensors are developed using the corona phase molecular recognition (CoPhMoRe) platform with single-walled carbon nanotubes (SWNTs) that are fluorescent in the near-infrared (NIR) region [1,2]. The nanosensors reported distinct dynamics and temporal wave characteristics of H₂O₂ and SA generation in tandem for each type of stress stimuli. For all stress treatments, the H₂O₂ wave was observed within minutes of stress followed by recovery within the 1st hour (h). The subsequent SA production occurs at distinct later time points within 2 h, specific to the type of stress, with the exception of mechanical wounding, which exhibits no SA production. This sensor multiplexing and temporal insight enables the formulation of a biochemical kinetic model that describes the mechanism by which stress specificity is captured by the distinct H₂O₂ waveform for each stress generated shortly after stress perception by the plant. These results demonstrate that sensor multiplexing can reveal stress signalling mechanisms in plants towards acclimation aiding in future development of climate-smart crops, and for potential pre-symptomatic diagnoses of stress in fields.

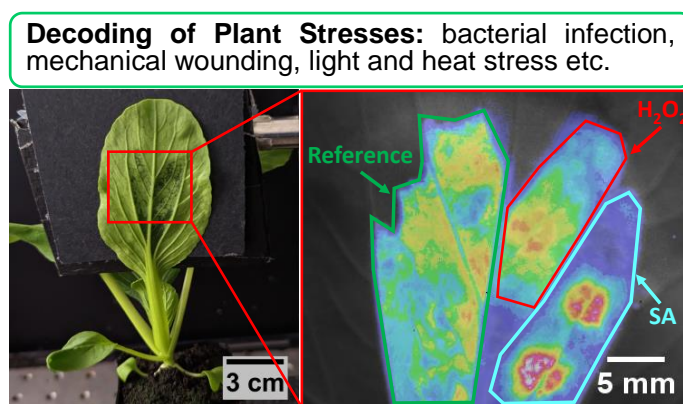


Figure caption (if desired): Photograph (left) and false-color zoomed in image of SWNT nanosensor NIR fluorescence (right) of a leaf infiltrated with multiplexed sensors (SA and H₂O₂) for the early decoding of different plant stresses (bacterial infection, mechanical wounding, light and heat stresses) using an *in planta* SA nanosensor (blue) paired with H₂O₂ nanosensor (red) and a reference sensor (green).

References (if desired)

- [1] T.T.S. Lew *et al.*, *Nature Plants* **6(4)**, 404-415 (2020).
- [2] M.C.Y. Ang *et al.*, *ACS Sensors* **6(8)**, 3032-3046 (2021).

Degradations and Enantiomeric Effects of (6,5) carbon nanotubes *in cellulo*

Ching-Wei Lin¹, Te-I Liu², Carlos J. Quiroz^{1,2}, Yen-Hsuan Lin¹, Ai-Phuong Nguyen^{1,3}, Marco Raabe¹

¹*Institute of Atomic and Molecular Sciences, Academia Sinica (Taiwan)*, ²*International PhD Program in Biomedical Engineering, Taipei Medical University (Taiwan)*, ³*Department of Chemistry, National Tsing Hua University (Taiwan)*

The unique emission wavelength of semiconducting single-wall carbon nanotubes (SWCNTs) in the short-wave infrared window provides the capability for high-resolution *in vivo* imaging at considerable depths. Numerous studies have showcased the utility of SWCNTs in applications such as angiography, optical sensing, and image-guided surgery. However, the deployment of these SWCNTs in *in vivo* systems necessitates a thorough examination of their toxicity and physiological effects. In addition, previous investigations did not focus on high-purity, individualized SWCNTs. Furthermore, recent chemical modifications in SWCNT structures, such as fluorescent quantum defects and guanine covalent functionalization, have significantly altered the surface properties of SWCNTs, warranting new studies to explore these novel materials.

In this context, I will present our recent studies on the chemical and biological degradation of individualized (6,5)-SWCNTs. We subjected pristine and defect-containing (6,5)-SWCNTs to oxidation using hydrogen peroxide and sodium hypochlorite. Our results revealed distinct degradation outcomes based on the oxidants used and the nanotube structures involved. Additionally, we observed intriguing and unexpected Raman and fluorescence spectra. In cellular systems, a reciprocal relationship was noted between SWCNTs and macrophages; specifically, SWCNTs activated macrophages, while macrophages concurrently degraded SWCNTs.

Secondly, the enantiomeric effects of SWCNTs in biological systems have not been systematically studied to date. Previous research has indicated varying interactions with biomolecules between enantiomers. In this presentation, I will share our findings on the enantiomeric effects in macrophages, revealing nuanced differences in cellular responses under specific conditions.

Delivery and Detection of Intracellular Single Walled Carbon Nanotube Sensors for Quantification of Subcellular Reactive Species

P. Plange¹ and N.M. Iverson¹

¹*University of Nebraska Lincoln (USA)*

For a long time it was believed that the concentration of nitric oxide (NO) within a cell could change, but was not spatially different throughout the cell. In 2014, through the use of NO-sensing single walled carbon nanotubes (SWNT), we demonstrated that melanoma skin cells exposed to an NO initiator had increases/decreases of NO at various points throughout the cell [1]. This exciting discovery was put aside in favor of other interesting advances in the SWNT-sensing field, but the Iverson lab has once again started looking at the concentration gradients that occur within cells. We have shown that NO-sensing SWNT, when internalized by cells, do not themselves cause alterations in the health of MDA-MB-231 breast cancer cells. We have also been able to co-localize SWNT with intracellular organelles, specifically lysosomes and mitochondria, allowing for quantification of NO concentration associated with specific organelles during various cellular processes. We have also demonstrated that biotinylated SWNT sensors, which can be used to deliver drugs/analytes intracellularly, can be co-localized with intracellular organelles without altering SWNT localization within cells. These are just the first steps into use of SWNT sensors to better understand subcellular analyte dynamics. With the continued use of SWNT sensors in additional cell types we will continue to expand basic knowledge into cellular function.

References

[1] Z.W. Ulissi *et al.*, *Nano letters* **14**, 4887–94 (2014).

Design of Multiplexed Fluorescent SWCNT Sensors for Rapid Cytokine Detection and Inflammatory Disease Surveillance

R.M. Williams¹, P. Gaikwad¹, A. Ryan¹, A. Israel¹, H. Yafai¹, Z. Cohen¹, and S. Rahman¹

¹The City College of New York, Biomedical Engineering (United States of America)

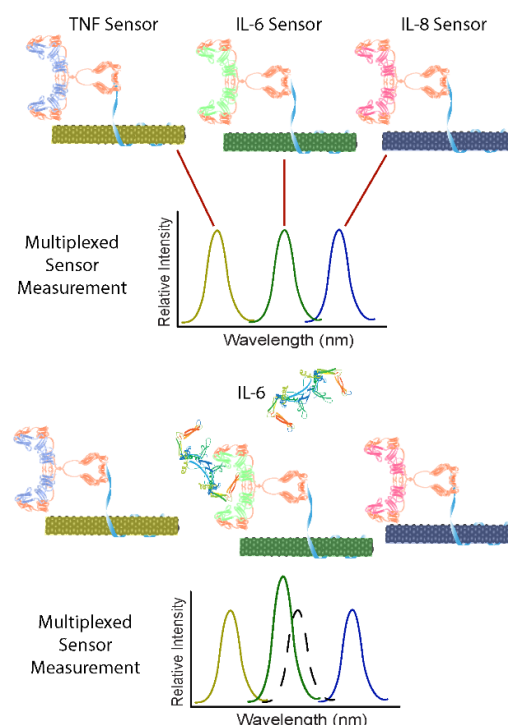
Single-walled carbon nanotubes (SWCNT) are uniquely able to serve as sensor transducers for multiple analytes at once. This is in part due to their highly sensitive detection and functionality in complex biological environments, including in cells, serum, and animals. In our work, we are using the near-infrared fluorescent properties of SWCNT to engineer multiplexed sensors against inflammatory cytokines, which play an important role in chronic diseases such as neurodegenerative and cardiovascular diseases, as well as acute infection.

In this work, we developed nanosensors that selectively and sensitively detect several inflammatory cytokines, including interleukin-6 (IL-6), IL-8, IL-1 β , and tumor necrosis factor α (TNF α). To engineer multiplexed sensors, individual chirality SWCNT were obtained through aqueous two-phase extraction (ATPE) using amine-functionalized ssDNA. Separately, SWCNT were constructed for each target using cytokine-specific antibodies and aptamers decorating the SWCNT surface through various supramolecular chemical strategies. Each sensor construct was evaluated for functionality across a broad range of target protein concentrations in buffer and in bovine serum to mimic complex biological environments. Further, cytokine nanosensors were tested using an in vitro model of acute infection, as well as in human serum containing elevated cytokine levels. Finally, ongoing work in the lab is using an injectable methylcellulose hydrogel-based sensor immobilization platform for non-invasive detection in animal models of disease.

Our studies have demonstrated the ability to detect four inflammatory cytokines using an integrated nanosensor platform based on molecularly-specific SWCNT optical transducers. For each sensor, quantifiable and robust changes in fluorescent emission intensity and/or wavelength occurred in response to increasing amounts of the cognate cytokine of interest. Several surface passivation strategies were employed to overcome effects of serum interference, allowing functionality in complex biological environments. We also demonstrated the ability to quantify individual cytokines in both bacterial-infected macrophage cell models in vitro as well as in human serum. Finally, we have validated a platform for non-invasive in situ gelation of SWCNT-hydrogel hybrids while we continue its application to chronic rodent disease models.

We anticipate that long-term translation of this fluorescent SWCNT-based cytokine sensor array will provide early-stage diagnostics for the development and progression of acute infection and chronic inflammatory diseases in patients. We are working toward such translation through an integrative chip-based sensor array for ex vivo diagnostics and as well as non-invasive disease surveillance from implantable devices in patients. This information would allow physicians more timely information related to neurodegenerative and cardiovascular disease progression and response to treatment, ultimately allowing for better treatment regimens and improved patient outcomes.

Figure 1: Schematic of multiplexed sensor detection for individual inflammatory cytokines.



Double-layer stacking in the commensurate CDW phase of 1T-TaS₂ observed by resonance Raman Spectroscopy

M. A. Pimenta¹, S. L. L. M. Ramos¹, B. R. Carvalho², R. L. M. Lobato³, J. Ribeiro-Soares³, C. Fantini¹, L. Molino⁴, R. Plumadore⁴, A. Luican-Mayer⁴.

¹Departamento de Física, Universidade Federal de Minas Gerais, Belo Horizonte, 30123-970 (Brazil),

²Departamento de Física, Universidade Federal do Rio Grande do Norte, Natal, 59078-970 (Brazil),

³Departamento de Física, Universidade Federal de Lavras, Lavras, 37200-000 (Brazil), ⁴Department of Physics, University of Ottawa, Ontario K1N6N5 (Canada)

The layered transition-metal dichalcogenide material 1T-TaS₂ possesses successive phase transitions upon cooling, resulting in the formation of charge density waves (CDWs) and a commensurate CDW structure below 160 K. Recently, a double-layer stacking configuration was shown to form a Peierls-like instability in the electronic structure of the commensurate phase. In this work, we employ a multiple excitation and polarized Raman spectroscopy to resolve the behavior of phonons and electron-phonon interactions in the commensurate CDW phase of 1T-TaS₂ [1]. We observe a distinct behavior from what is predicted for a single layer, and a richer number of phonon modes that are compatible with the formation of double-layer units. The multiple-excitation results show a selective coupling of each Raman-active phonon with specific electronic transitions hidden in the optical spectra of 1T-TaS₂, suggesting that selectivity in the electron-phonon coupling must also play a role in the CDW order of 1T-TaS₂ [1].

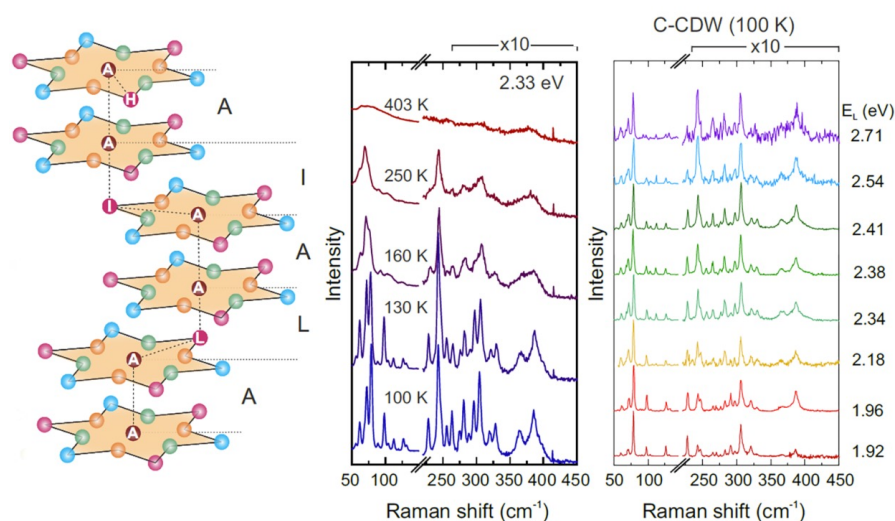


Figure caption: Schematic of the double-layer stacking order showing the A, L, A, I, and A stacking sequence, from the bottom to the top. Raman spectra at different temperatures for bulk 1T-TaS₂ collected with an excitation energy of 2.33 eV. Unpolarized resonant Raman spectra of the same 1T-TaS₂ flake collected at 100 K (C-CDW) with different laser excitation energies.

References

Sergio L. L. M. Ramos et al, *ACS Nano*, 17, 15883-15892 (2023)

Emissive Brightening in Molecular Graphene Nanoribbons by Twilight States

Bernd K Sturdza,[†] Fanmiao Kong,[‡] Xuelin Yao,[‡] Wenhui Niu,^{§,¶} Ji Ma,^{§,¶}
Moritz K Riede,[†] Xinliang Feng,^{§,¶} Lapo Bogani,^{‡, #,*} Robin J Nicholas^{†,*}

[†] *Department of Physics, University of Oxford, Parks Road, OX1 3PU, Oxford, UK.*

[‡] *Department of Materials, University of Oxford, 16 Parks Road, OX1 3PH, Oxford, UK.*

[§] *Center for Advancing Electronics Dresden (CFAED), Faculty of Chemistry and Food Chemistry, Technische Universität Dresden, Mommsenstraße 4, 01062, Dresden, Germany.*

[¶] *Max Planck Institute of Microstructure Physics, Weinberg 2, 06120, Halle, Germany.*

[#] *Departments of Chemistry and Physics, University of Florence, V. della Lastruccia , 50019,Sesto Fiorentino, Italy*

Carbon nanomaterials are expected to be bright and efficient emitters, but structural polydispersity, intermolecular interactions and the intrinsic presence of dark states suppress their photoluminescence. Here, we study synthetically-made graphene nanoribbons with reduced polydispersity and which are designed to suppress intermolecular interactions to demonstrate strong photoluminescence in both solutions and thin films. The resulting high spectral resolution reveals strong vibron-electron coupling from the radial-breathing-like mode of the ribbons. In addition, their cove-edge structure produces inter-valley mixing, which brightens conventionally-dark states to generate hitherto-unrecognized twilight states as predicted by theory.

The coupling of these new states to the nanoribbon phonon modes unexpectedly affects absorption and emission differently, suggesting a complex interaction with both Herzberg–Teller and Franck–Condon coupling present.

We present photoluminescence, absorbance, Raman, and time-resolved PL data as well as computational results to support our findings.

Detailed understanding of the fundamental electronic processes governing the optical response opens the path to the tailored chemical design of nanocarbon optical devices, via gap tuning and side-chain functionalization.

Engineering Chirality in Wafer-scale Ordered Carbon Nanotube Architectures

Jacques Doumani^{1,2,3}, Minhan Lou³, Oliver Dewey^{4,5}, Nina Hong⁶, Jichao Fan³, Andrey Baydin^{1,7}, Keshav Zahn¹, Yohei Yomogida⁸, Kazuhiro Yanagi⁸, Matteo Pasquali^{4,5,7,9,10}, Riichiro Saito^{8,11,12}, Junichiro Kono^{1,4,7,10,13} & Weilu Gao^{3,4,*}

¹Department of Electrical and Computer Engineering, Rice University, Houston, TX, USA.

²Applied Physics Graduate Program, Smalley–Curl Institute, Rice University, Houston, TX, USA.

³Department of Electrical and Computer Engineering, The University of Utah, Salt Lake City, UT, USA.

⁴Carbon Hub, Rice University, Houston, TX, USA.

⁵Department of Chemical and Biomolecular Engineering, Rice University, Houston, TX, USA.

⁶J.A. Woollam Co., Inc., Lincoln, NE, USA.

⁷Smalley–Curl Institute, Rice University, Houston, TX, USA.

⁸Department of Physics, Tokyo Metropolitan University, Tokyo, Japan.

⁹Department of Chemistry, Rice University, Houston, TX, USA.

¹⁰Department of Materials Science and NanoEngineering, Rice University, Houston, TX, USA.

¹¹Department of Physics, Tohoku University, Sendai, Japan.

¹²Department of Physics, National Taiwan Normal University, Taipei, Taiwan.

¹³Department of Physics and Astronomy, Rice University, Houston, TX, USA

*Email: weilu.gao@utah.edu

The interaction of chiral matter and structures with circularly polarized light has profound implications in quantum photonic applications. The key enabler of these applications is a versatile macroscopic chiral photonic matter platform with strong, controllable, and quantum-confinement-induced chiro-optical properties. Here, we present two simple and scalable approaches based on controlled vacuum filtration - twist stacking and mechanical rotation - for fabricating wafer-scale chiral architectures of ordered carbon nanotubes (CNTs) with tunable and large circular dichroism (CD) [1]; see Fig. 1. By controlling the stacking angle and handedness in the twist-stacking approach, we maximize the CD response and achieve a high deep-ultraviolet ellipticity of 40 mdeg/nm. Our theoretical simulations using the transfer matrix method reproduce the experimentally observed CD spectra and further predict that an optimized film of twist-stacked CNTs can exhibit an ellipticity as high as 150 mdeg/nm, corresponding to a g factor of 0.22. Furthermore, the mechanical rotation method not only accelerates the fabrication of twisted structures but also produces both chiralities simultaneously in a single sample, in a single run, and in a controllable manner. The created wafer-scale objects represent an alternative type of synthetic chiral matter consisting of ordered quantum wires whose macroscopic properties are governed by nanoscopic electronic signatures and can be used to explore chiral phenomena and develop chiral photonic and optoelectronic devices.

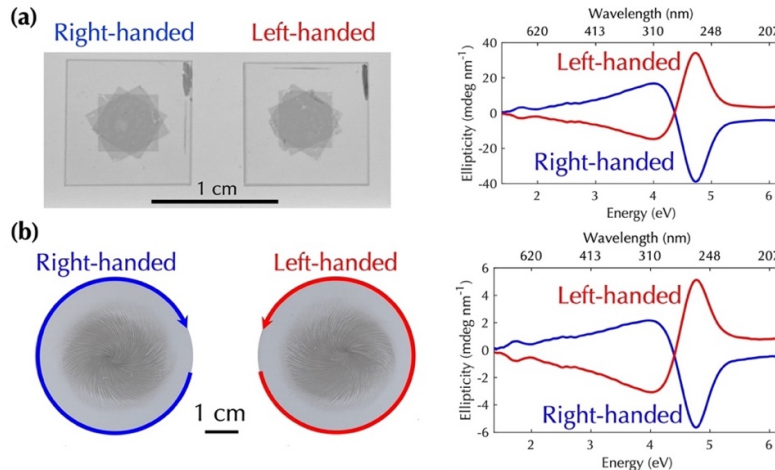


Figure 1: Photos and CD spectra of samples manufactured through (a) twist stacking (b) mechanical rotation.

References

[1] J. Doumani *et al.* *Nat Commun* **14**, 7380 (2023).

Evaporative self-assembly of carbon nanotube-polymer superstructures

Yoshitaka Tsuchie, Yoshiyuki Nonoguchi

Faculty of Materials Science and Engineering, Kyoto Institute of Technology, Kyoto 606-8585, Japan

The application of colloidal nanomaterials to create self-assembled superstructures is recognized as a method for exploiting novel functionalities; however, the assembly of high aspect ratio nanofibers is still challenging. Carbon nanotubes (CNTs) are a kind of nanofiber with exceptional mechanical, electrical, and thermal properties. There are methods for CNTs self-assembly which make use of the driving forces such as liquid crystalline dispersant,¹ and droplet capillary effect.² Herein we find liquid crystal-like self-alignment phenomena with non-liquid crystalline surfactant polymers, which leads to create carbon nanotube-polymer superstructures simply by drop-casting colloidal dispersions.

Our procedure developed here started with the poly(vinyl butyral) (PVB)-assisted dispersion of CNTs in organic solvents, representatively benzyl alcohol.³ This dispersion shows liquid crystal-like optical anisotropy through polarized microscopy (Fig.1b). By drop-casting and evaporating the dispersion on aluminum foils (Fig.1a), we prepared a polymer composite film impregnating highly aligned CNTs (Fig.1c). By etching the substrate, this composite film could be isolated while preserving their organized structures (Fig.1d, e). The alignment evaluation by polarized Raman scattering spectroscopy provided the extinction ratio of 2.6 times. It seems that most carbon nanotubes (CNTs) are isolated in the polymer matrix and that the CNTs do not entangle with others, based on the anisotropic periodic structure (*ca.* 4.7 nm) seen by SAXS and the non-conductive properties of the composite film. We will further discuss the microstructures of CNTs' surface to drive the self-assembly.

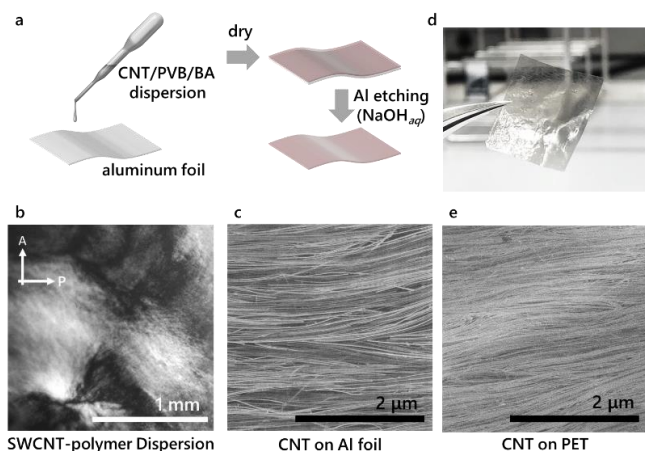


Figure caption (if desired): a, A procedure of aligned CNTs film preparation via drop casting and Al etching. b, A polarized microscopy image of CNTs dispersion. c, e, SEM images of an Al foil, drop-casted CNTs films on an Al foil (c) and transferred onto a PET sheet (e). d, A photograph of a self-standing aligned CNTs film after Al etching.

References (if desired)

- [1] MD. Lynch *et al.* *Nano Lett.* **2**, 1197–1201 (2002).
- [2] Y. Joo *et al.* *Langmuir* **30**, 3460–3466 (2014).
- [3] Nonoguchi, Y. *et al.* *Adv. Mater. Interfaces* **9**, 2101723 (2022).

EXCITONIC INSTABILITY IN NARROW-GAP CARBON NANOTUBES

G.Sesti^{1,2}, E Molinari¹, D. Varsano², M. Rontani²

¹ FIM, Università degli Studi di Modena e Reggio Emilia, Via Campi 213a, 41125 Modena, Italy

² CNR-NANO, Via Campi 213a, 41125 Modena, Italy

Ultraclean suspended carbon nanotubes, which are predicted to be metallic by band theory, always exhibit a many-body transport gap at low temperature [1,2]. Whereas the correlated ground state was early interpreted as a Mott insulator [1], we recently predicted that, in gapless (armchair) tubes, the gap is enforced by the permanent condensation of excitons [3]. Here we investigate thoroughly the screening of nanotubes [4], developing a model fit to samples of any size and chirality (Figure 1), which is validated by state-of-the-art first principles calculations. Our key result is that the long range of Colomb interaction, which remains largely unscreened even in the presence of Fermi points, stabilizes the excitonic insulator phase in all narrow-gap nanotubes. Furthermore, we show that the EI phase is better suited than the Mott insulator to explain available experiments [1,2], which focus on the closure of the many-body gap with the magnetic field.

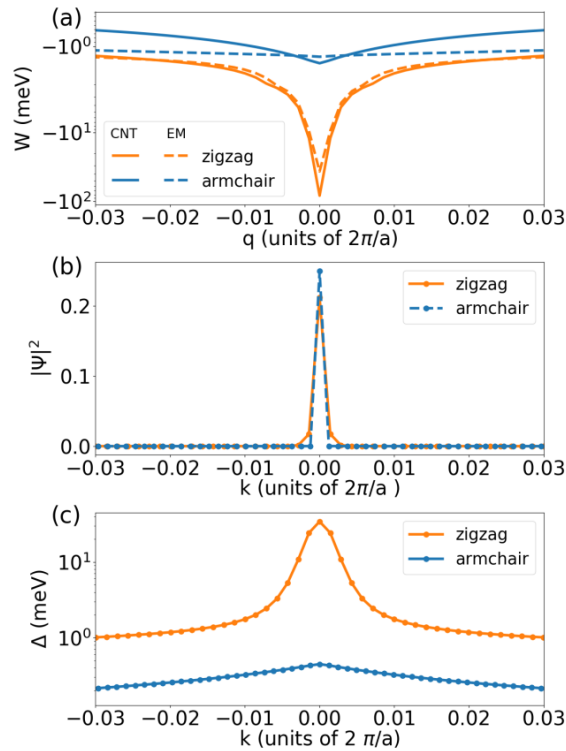


Figure 1: Plot of the screened Coulomb potential $W(q)$ (a), the excitonic wavefunction (b), and the excitonic order-parameter (c) in the (18,0) zigzag nanotube and the (10,10) armchair nanotube. In plot (a), we compare $W(q)$ using our model (CNT) with the standard effective-mass (EM) derivation. (a) and (c) figures are in semilogarithmic scale.

References

- [1] V. V. Deshpande, B. Chandra, R. Caldwell, D. S. Novikov, J. Hone and M. Bockrath, *Science* 323, 107 (2009).
- [2] J. O. Island, M. Ostermann, L. Aspirtarte, E. D. Minot, D. Varsano, E. Molinari, M. Rontani, and G. A. Steele, *Phys. Rev. Lett.* **121**, 127704 (2018).
- [3] D. Varsano, S. Sorella, D. Sangalli, M. Barborini, S. Corni, E. Molinari and M. Rontani, *Nat. Comm.* 8, 1461 (2017).
- [4] G. Sesti, D. Varsano, E. Molinari, and M. Rontani *Phys. Rev. B.* 105 195404 (2022)

Fabrication and Processing Parameters for Aligned Boron Nitride Nanotube Ceramic Matrix Nanocomposites

Shaan Jagani¹, Luiz H. Acauan¹, Jingyao Dai¹, and Brian L. Wardle¹

¹Massachusetts Institute of Technology (USA)

The exceptional thermal, electrical, and mechanical properties of boron nitride nanotubes (BNNTs) make them promising candidates for the reinforcement of ultra-high temperature technical ceramics. In this study, we have developed preliminary processing parameters for the manufacture of dense ceramic matrix nanocomposites with horizontally-aligned BNNT reinforcement via polymer infiltration and pyrolysis (PIP) of preceramic resins. As-grown BNNTs were fabricated using a scaffolded chemical vapor deposition (CVD) process [1] and horizontally aligned and densified using a bulk nanocomposite laminating (BNL) process [2]. Polycarbosilane and polysiloxane resin systems were used. Microstructural characterization of single-ply unidirectional laminates via scanning electron microscopy and polarized Raman spectroscopy indicated anisotropic nanotube alignment in samples before pyrolysis. Resin behavior was investigated using Fourier transform infrared spectroscopy and thermogravimetric analysis, indicating no negative effects of nanotube volume fraction of ceramic yield. This work provides a basis for further investigation into the mechanical properties of ceramic matrix composites with nanofiber reinforcement as well as subsequent examination of multifunctional capabilities, such as piezoelectric response.

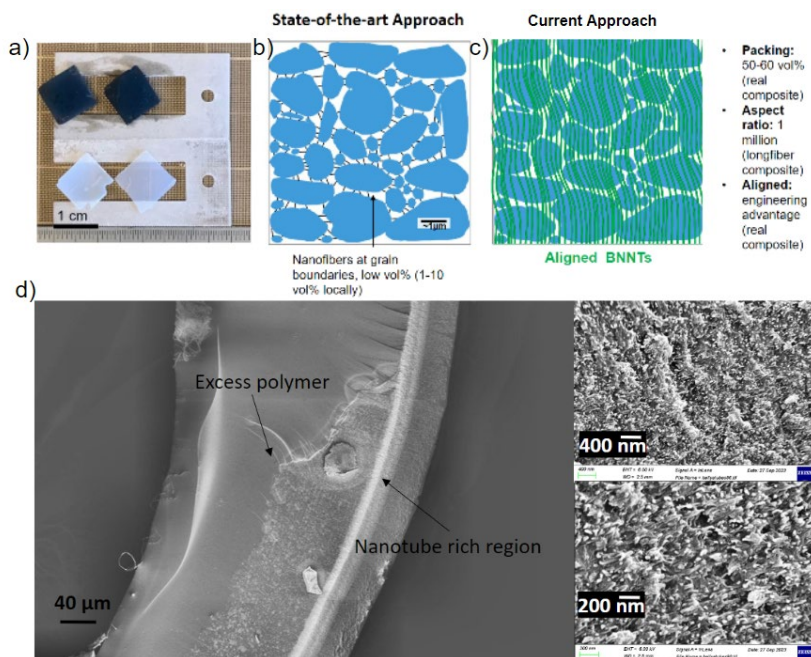


Figure: (a) BN-coated carbon nanotubes and BNNTs; (b) Representation of nanofiber reinforced CMCs in literature. Nanofibers agglomerate at grain boundaries resulting in minimal reinforcement; (c) Representation of material in this study. Technical ceramics are reinforced across grains with aligned nanofibers; (d) SEM images fracture of polymer matrix BNNT composite fracture surface. Higher magnification images (right) indicate fiber pullout behavior.

References:

- [1] Acauan, L. H. *et al.*, *ACS Nano*, 16(11), 18178–18186. (2022)
[1] Dai, J. *et al.*, *AIAA SciTech 2023 Forum*. (2023)

Ferrocene-Enhanced Growth of Millimeter-Long Carbon Nanotubes: Mechanism Study

Delong HE, Nabila ZERROUKI, Jinbo BAI

Delong.he@centralesupelec.fr, jinbo.bai@centralesupelec.fr

Laboratoire de Mécanique Paris-Saclay (LMPS), CNRS UMR 9026, Centralesupelec, ENS Paris-Saclay, Université Paris-Saclay, 3-8 Joliot Curie, 91190 Gif/Yvette, France

Ferrocene-Enhanced Growth of Millimeter-Long Carbon Nanotubes: Mechanism Study

Keywords : Carbon nanotube, CVD, Ferrocene, Mechanism

Abstract

Carbon nanotubes (CNTs) have exhibited outstanding mechanical and functional properties both theoretically and experimentally since their discovery. However, despite their immense potential, their applications remain somewhat limited in certain domains even after three decades of development. This limitation is attributed to various factors, with the small size of CNTs making them challenging to manipulate and explore fully for their intrinsic properties. Growing longer CNTs has thus become a key objective in the field, and while some promising results have been reported in recent years [1-2], challenges persist.

The synthesis of millimeter and centimeter-long carbon nanotubes using the Chemical Vapor Deposition (CVD) method has shown promise. However, the quantities obtained are often insufficient, and the growth rates are too slow for practical industrial production. Identifying the factors limiting growth and proposing innovative solutions to enhance CNT growth rates and extend the lifespan of catalyst nanoparticles are crucial objectives.

In this study, we present recent findings on the role of ferrocene in boosting CVD CNT growth. A conventional CVD reactor was employed, with iron nanoparticles and acetylene serving as catalyst and carbon sources, respectively. Ferrocene was introduced into the reactor through a side-line carrying gas, with its quantity controlled by the gas flow rate and temperature. Remarkably, introducing a small quantity of ferrocene led to a nearly tenfold improvement in the CNT growth rate. This enhancement is attributed to the increased catalytic activity of iron nanoparticles under CVD conditions.

A significant effort was dedicated to evaluating the evolution of catalyst nanoparticles during carbon nanotube growth and their interaction with introduced ferrocene. In-situ gas-atmospheric analyses, along with microscopic studies of CNTs, nanoparticles, and substrates, shed light on the importance of ferrocene under the studied conditions. These findings offer valuable insights for designing more efficient CVD reactors and developing cost-effective procedures that enable the growth of longer CNTs. This research represents a crucial step forward in unlocking the full potential of carbon nanotubes for various industrial applications.

References:

[1] R. Zhang et al., Growth of Half-Meter Long Carbon Nanotubes Based on Schulz-Flory Distribution, *ACS Nano* 2013, 7, 7, 6156–6161, Doi: 10.1021/nn401995z

[2] H. Sugime et al., Ultra-long carbon nanotube forest via in situ supplements of iron and aluminum vapor sources, *Carbon* 2021, 172, 772-780, Doi: 10.1016/j.carbon.2020.10.066

Field-free deterministic switching of a van der Waals ferromagnet above room temperature

S. N. Kajale¹, T. Nguyen², M. Li², D. Sarkar¹

¹MIT Media Lab, Massachusetts Institute of Technology (USA), ²Department of Nuclear Science and Engineering, Massachusetts Institute of Technology (USA)

Spintronic devices are key to enabling energy-efficient and high-performance non-volatile memories, as well as driving new paradigms of computing like neuromorphic stochastic and in-memory computing. However, only a few bulk material systems, like CoFeB/MgO, have been identified to be optimally suited for commercial applications. Such bulk systems pose challenges in device performance and device-to-device variability upon scaling to advanced technology nodes [1]. The discovery of emergent magnetism in two-dimensional (2D) van der Waals (vdW) magnets has broadened the space for materials exploration, while offering an unprecedented combination of scalability and reliability, to overcome the limitations of bulk magnetic materials [2]. In this regard, recent advances in the discovery of near-room temperature vdW magnets with perpendicular magnetic anisotropy (PMA) [3], [4], as well as current or voltage-based control of vdW magnets at cryogenic temperatures are promising [5], [6]. Yet, the technologically crucial goal of achieving room temperature, field-free, electrical switching of vdW magnets has remained elusive.

Here, we present an all-vdW solution to this issue using a spin-orbit torque (SOT) switching system comprising of a newly discovered vdW ferromagnet, Fe₃GaTe₂ and the low-symmetry vdW semimetal, Td-WTe₂. Fe₃GaTe₂ exhibits above room temperature ferromagnetism (T_C ~ 350 K) with a strong perpendicular magnetic anisotropy making it a potent vdW candidate for spintronic applications. Through a series of systematic experiments, involving spin-orbit coupling materials like Pt and WTe₂, we establish that the PMA magnetism in Fe₃GaTe₂ can be switched above room temperature using current densities as low as ~ 2 × 10⁶ A/cm². While Pt, owing to its high symmetries, requires an in-plane magnetic field to enable the deterministic switching of Fe₃GaTe₂ magnetization, the use of WTe₂ overcomes this requirement too. We show that by driving current along the low-symmetry in-plane axis of WTe₂, we can generate an “unconventional” out-of-plane anti-damping-like SOT, which is strong enough to induce field-free deterministic switching of the PMA magnetization in Fe₃GaTe₂. Thus, this work provides a scalable, all-vdW solution for the room temperature, electrical switching of vdW ferromagnets and opens a path to integrating 2D magnetic materials in the next generation of scalable and energy-efficient spintronic devices.

References

- [1] H. Yang *et al.*, “Two-dimensional materials prospects for non-volatile spintronic memories,” *Nature*, vol. 606, no. 7915, pp. 663–673, 2022.
- [2] S. N. Kajale, J. Hanna, K. Jang, and D. Sarkar, “Two-dimensional magnetic materials for spintronic applications,” *Nano Res*, 2024.
- [3] G. Zhang *et al.*, “Above-room-temperature strong intrinsic ferromagnetism in 2D van der Waals Fe₃GaTe₂ with large perpendicular magnetic anisotropy,” *Nat Commun*, vol. 13, no. 1, pp. 1–8, 2022.
- [4] J. Seo *et al.*, “Nearly room temperature ferromagnetism in a magnetic metal-rich van der Waals metal,” *Sci Adv*, vol. 6, no. 3, p. eaay8912, Jun. 2020.
- [5] I. H. Kao *et al.*, “Deterministic switching of a perpendicularly polarized magnet using unconventional spin-orbit torques in WTe₂,” *Nat Mater*, vol. 21, no. 9, pp. 1029–1034, 2022.
- [6] S. Liang *et al.*, “Small-voltage multiferroic control of two-dimensional magnetic insulators,” *Nat Electron*, vol. 6, no. 3, pp. 199–205, 2023.

Flexible Transmitter for Human Body Communication Based on Carbon Nanotube CMOS Electronics

D. Muto¹, H. Uchiyama¹, H. Kataura², and Y. Ohno¹

¹Nagoya University (Japan), ²National Institute of Advanced Industrial Science and Technology (Japan)

Human body communication (HBC) is a method for communication that utilizes the human body, and it has the potential to enable communication between wearable sensor devices with low power consumption. HBC utilizes the low-loss MHz band, but conventionally, oscillation signals are generated using rigid components such as a crystal oscillator or inductor [1]. Consequently, there have been issues regarding communication stability and comfort. In this study, we utilized carbon nanotubes (CNTs), which possess excellent electrical properties and mechanical flexibility, to develop a flexible CMOS-based oscillator and transmitter that operates in the MHz band. We also demonstrated communication through a biological phantom.

We fabricated a transmitter IC constructed using a ring oscillator (RO) to generate MHz-band oscillation signals as shown in Fig. 1(a). Polyethylene naphthalate (PEN) substrate was used along with a semiconducting CNT thin film for the channel, Al₂O₃ (45 nm) as the gate insulator, and Ti/Au (0.06/100 nm) as the source and drain electrodes. The channel length (L) and channel width (W) are 3 and 100 μm , respectively. We employed a self-align process to reduce the overlap capacitance between the gate and source/drain electrodes. The output stage of the transmitter IC comprises a CMOS inverter ($W = 1 \text{ mm}$) and a transistor ($W = 10 \text{ mm}$).

The fabricated RO in the transmitter IC was observed to oscillate at 2.3 MHz at V_{DD} of 10 V, thereby confirming its MHz band operation. The maximum output power of the transmitter IC was evaluated to be 5.5mW at a load impedance of 220 Ω . Subsequently, a flexible transmitter for HBC was fabricated by placing the CNT transmitter IC and coin cells ($V_{\text{DD}} = 8.3 \text{ V}$) onto a PDMS film as shown in Fig. 1(b) and 1(c). To form a transmitter antenna, a CNT conductive film was affixed to the backside. We used this device to demonstrate communication through a biological phantom as shown in Fig. 1(d). By utilizing aluminum foil as the receiving antenna, we observed a square wave signal that corresponded to the RO oscillation signal with an oscilloscope. This result demonstrates the feasibility of HBC using flexible CNT CMOS ICs, which maintain a high level of compatibility with the human body.

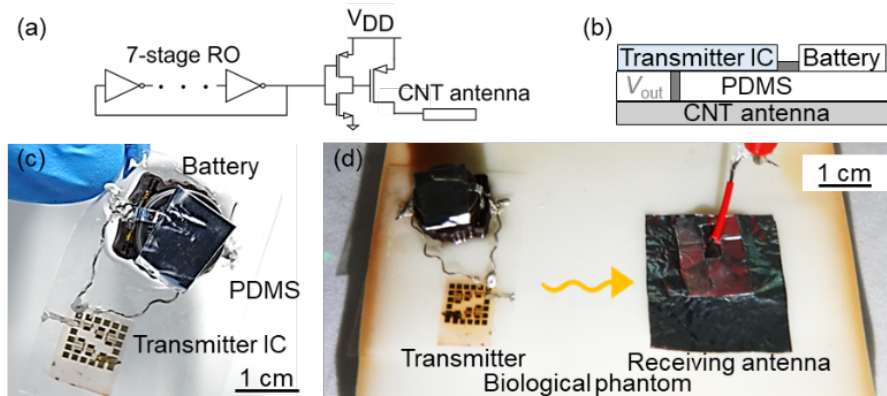


Figure 1: CNT-based flexible transmitter. (a) Circuit diagram, (b) schematic structure, (c) photograph, (d) setup for human-body communication with human body phantom.

Reference

[1] J. Bae et al., *IEEE Trans. Microw. Theory Tech.* **60**, 582 (2012).

Functionalized Single-Walled Carbon Nanotube Electrodes for Dielectric Elastomer Actuators to Enhance Electro-Mechanical Durability

M. Kolloosche^{1,2,3}, M. Ricci¹, H. Richter¹

¹ Nano-C, Inc., 33 SW Park, Westwood, MA 02090

² Iowa State University, Ames, IA, USA

³ Harvard University, Cambridge, MA, USA

Soft robotics, soft optics and soft sensors represent an emerging class of all-soft and compliant technology that aims to operate in direct proximity to humans. So-called artificial muscles or Dielectric Elastomer Actuators (DEAs) are active building blocks of this soft technological development and aim to have comparable properties as their natural counterparts. DEAs are soft, stretchable capacitors that rely on stretchable, conductive and compliant electrodes, e.g., single-wall carbon nanotubes (SWNTs). These soft and active elements have shown a significant potential to provide voltage-controlled geometric changes of several 100% strains using high voltage but also enable scalable additive manufacturing and tailored modifications of the elastomer host material to embed desired functionalities.

One of the limiting factors is the unexplored interplay of conductive stretchable electrodes, especially those using SWNTs and soft stretchable dielectrics under high static and dynamic electric fields and consequent large geometric changes. The challenge to explore that interplay is the complexity of mechanical and electric contributions and joined effects such as voltage-induced electromechanics instabilities [1]. To enable an exhaustive optical and electric evaluation of the SWCNT-elastomer interphase under high voltage and large deformation, an optomechanical design [2] is used to determine the impact of SWCNT purity and characteristics resulting of a novel chemical treatment.

This talk illustrates processing strategies to treat SWCNT, remove agglomerates and contaminations chemically and how to process these SWCNT into sprayable binder-free inks. We show that the successful minimization of defects in the SWCNT results in a significant lifetime enhancement of the optomechanical DEA and shifts the electric breakdown field of a soft silicone up to a predicted intrinsic breakdown limit [3]. Our expertise on functionalization of SWCNTs, their purification and ink-making capabilities are expected to enable more durable and scalable DEAs and transducer applications in general.

[1] M. Kolloosche *et al.*, *JMPS*. **76**, 47–64 (2015).

[2] S. Shian *et al.*, *Opt. Lett.* **41**, 1289-1292 (2016).

[3] M. Kolloosche *et al.*, *Appl. Phys. Lett.* **96**, 071904 (2010).

GRAPHENE DERIVATIVES FOR BIOSENSORS APPLICATIONS

Ana Champi

*Laboratory of New Carbon Materials: Graphene. Center of Natural and Human Sciences,
Federal University of ABC, Santo André, SP 09210-580, Brazil.*

Nanomaterials such as nanoparticles metallic, magnetic, carbon nanotubes, carbon dots, TiO₂ nanotubes, graphene and its derivatives, has shown an easy functionalization with biological molecules such as DNA, enzymes, antibodies, RNA, c-DNA, viruses and bacteria among other biological systems generating a wide range of applications in order to develop new disease biosensing devices due to the low cost and speed to obtain results compared to conventional techniques. In this study we report a novel electrochemical portable biosensor for viruses' detection and quantification based on reduced graphene oxide films. The working electrode was built following the synthesis of lysozyme-reduced graphene oxide (rGO) films proposed by Graphene oxide is synthesized using modified Hummer's method and chemically reduced using hydrazine and lysozyme [1]. Thin-films were produced by dip-coating deposition using rGO solution onto a gold substrate pre-treated with cysteine. We report the successfully application for RNA virus detection using cDNA functionalization on the working electrode surface and quantification of RNA concentration with a linearly dependency of chronoamperometric current. Also, it shows selectivity against an RNA different from the one used for electrode functionalization. The novel biosensor was applied for RABV and Sars Cov-2 in-situ detection in nasopharyngeal swab samples of bat and humans showing a difference in response of positive samples from negative samples. Experiments using a portable detector were performed using nasopharyngeal swab samples and clustered in three groups according to electrochemical response using PBS solution and surface characterization after PBS response. These three groups were named GO-1, GO-2 and rGO due to characterization and surface analysis [2]. This novel biosensor showed to be an innovative electrochemical method for in-situ diagnosis of rabies disease in bats with a fast response.

References (if desired)

1. J.Zuñiga, T.Pinheiro, M.Rivera, L.Barreto, K.F.Albertin and **A. Champi**, Synthesis of lysozyme-reduced graphene oxide films for biosensor applications, **Diamond & Related Materials**, 126, 109093, 2022.
2. Ronaldo Challhua, Larissa Akashi, Jose Zuñiga, Helena Beatriz de Carvalho Ruthner Batista, Ricardo Moratelli and **A. Champi**, Portable reduced graphene oxide biosensor for detection of rabies virus in bats using nasopharyngeal swab samples, **Biosensors & Bioelectronics**, 2023.

[1]

High-crystallinity Single-walled Carbon Nanotube Aerogel Growth: Understanding the Real-time Catalytic Decomposition Reaction

S.Y. Moon

Korea Institute of Science and Technology (KIST)

Carbon nanotubes (CNTs) have been considered for many applications because of their extraordinary physical, chemical, and mechanical properties. Despite their many desirable properties, the short aspect ratio of CNTs hinders their commercial utilization. The synthesis of carbon nanotube's bulk scale structures is major challenges toward future applications. Recent research in the organization of carbon nanotubes into fibers and sheets are mainly reviewed, including methods based on spinning from forests, and direct spinning from the gas phase during synthesis.

Floating Catalyst Chemical Vapor Deposition (FC-CVD) is an optimum method for bulk production of carbon nanotube fibers and sheets. These continuous and scalable one-step production became possible by adding sulfur (S) [1]. In this process, the organometallic precursor as a catalyst, and carbon precursor simultaneously pyrolyzed with carrier gases and the residence time in reactor during process is very short which approximately a few seconds. Thus each component, such as catalyst, carbon source, temperature, and carrier gases, strongly affected to final macroscale structures. In this study, high-purity single-walled carbon nanotubes (SWCNTs) are synthesized with additional carrier gas through floating catalyst chemical vapor deposition. The presence of Ar during the SWCNT aerogel formation affects to the precursor decomposition and to the formation of different reactive hydrocarbons. Furthermore, the concentration of produced various carbon species is sensitive to the carrier gas compositions. The in-situ sampling methods prove the thermodynamic pathway for the hydrocarbon cracking during carbon nanotube (CNT) aerogel formation process. The addition of Ar promoted the formation of reactive hydrocarbon species, such as CH_3 , CH_4 , and $\text{C}_2\text{H}_4/\text{CO}$, to improve CNT morphology and graphitization. Ar has improved purity of CNTs compared to when only H_2 is used. The synthesized CNTs were narrow in size, and the diameter decreased from 1.8 to 1.2 nm with the carrier gas composition (R_x) according to Ar addition. The I_G/I_D ratio of the CNTs changed from 78 to 3 at $R_{0.1}$ and $R_{0.57}$, respectively. Furthermore, the purity also increased to approximately 10% from 78% to 91% depending on R.

High-performance Optoelectronics Enabled with Dry-transferred Transparent Carbon Nanotube Films

E.-X. Ding^{1,*}, P. Liu², Z. Sun¹, E.I. Kauppinen², H. Lipsanen^{1,*}

¹Department of Electronics and Nanoengineering, ²Department of Applied Physics, Aalto University, Espoo, FI-00076, Finland

Due to their outstanding optical, electronic, and mechanical properties, one-dimensional (1D) carbon nanotubes (CNTs) are considered the most promising candidate for the flexible/stretchable transparent conducting component in electronics and optoelectronics. Here, we introduce our facile electrode fabrication process which is free of lithography, lift-off, and reactive ion etching by directly press-transferring CNT films for optoelectronics. High-performance 2D semiconductor-based photodetectors and photovoltaics were fabricated with press-transferred single-walled CNT (SWCNT) films as the transparent electrode to increase light absorption in the photoactive materials. Specifically, we found that, compared with a lateral device configuration, MoS₂ flake vertically stacked with an SWCNT electrode can exhibit excellent photodetection performance with a responsivity of 2.01×10^3 A/W and a detectivity of 3.2×10^{12} Jones [1]. The photovoltaics based on MoS₂/WSe₂ heterostructure show a high open circuit voltage of 0.36 V, a power conversion efficiency of 2.1% with a 532 nm laser shining at 100 nW [2]. In addition, we realized wafer-scale manufacturing of wearable all-CNT photodetectors by laser-assisted patterning and dry deposition techniques. As-synthesized double-walled CNTs and highly enriched semiconducting SWCNTs are employed as the device electrode and photosensitive channel, respectively. The all-CNT photodetector showcases high-performance broadband photodetection, exhibiting an excellent responsivity of 2 A/W and a detectivity of 1.6×10^{10} Jones at telecommunication wavelength (1550 nm) [3].

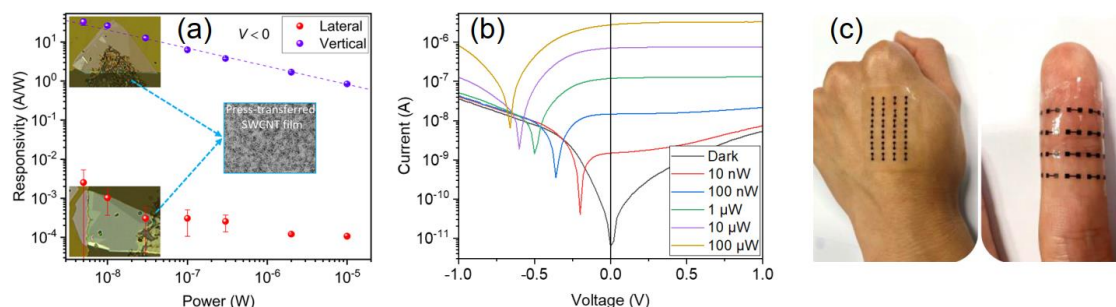


Figure 1: (a) Responsivities of MoS₂-based photodetectors with SWCNT film as the transparent top electrode. (b) Current-voltage curves of MoS₂/WSe₂-based photovoltaics with SWCNT film as the top electrode. (c) Photograph of wearable all-CNT photodetectors.

References

- [1] E.-X. Ding *et al.*, *ACS Appl. Mater. Interfaces*. **15**, 4216-4225 (2023).
- [2] E.-X. Ding *et al.*, in preparation, 2024.
- [3] P. Liu, E.-X. Ding* *et al.*, submitted to *ACS Nano*, 2024.

Horizontally Aligned Carbon Nanotube-Reinforced Silicon Carbide Nanocomposites with Ultrahigh Nanofiber Packing Density

J. Dai¹, S. Jagani¹, L. Acauan¹, X. Li¹, P. Patel¹, B.L. Wardle¹

¹*Massachusetts Institute of Technology (the United States)*

Nanofibers such as carbon nanotubes (CNTs) and boron nitride nanotubes (BNNTs) offer excellent mechanical, thermal, and electrical properties, making them ideal reinforcements for ceramic matrix composites (CMCs) to enable enhanced mechanical and multi-functional properties. However, common approaches to introduce nanofibers into ceramic matrices usually involve direct mixing that can cause damage, random alignment, agglomeration, and low packing density of the introduced nanofibers. To overcome these issues, we developed the bulk nanocomposite laminating process for ceramic matrix composite (BNL4CMC) process. During the BNL4CMC process, horizontally aligned nanofibers were first prepared using as-synthesized vertically aligned nanofibers via a mechanical orientation technique. Ceramics' polymer precursor can then be infused into the horizontally aligned nanofiber dry plies to form a nanofiber-polymer nanocomposite. After curing, the nanocomposite can be pyrolyzed to convert the pre-ceramic polymer to ceramics, followed by additional heat treatment to transform the amorphous ceramic matrix into a polycrystalline one. Using the BNL4CMC process, we have fabricated 8-ply horizontally aligned CNT (HACNT) reinforced silicon carbide (HACNT/SiC) nanocomposite laminates using commercially available polycarbosilane (PCS) resin as the SiC precursor. The fabricated HACNT/SiC nanocomposites exhibited microstructures free of micro or macro-voids. The retainment of CNT alignment for the fabricated samples was confirmed using polarized Raman spectroscopy. From microstructure inspection, the laminates contained well-aligned and uniformly distributed CNTs of ultra-high (up to ~40-50 vol%) packing density. Detailed characterizations of the mechanical and multifunctional properties are being performed to investigate the effect of CNT packing density on the fabricated HACNT/SiC nanocomposites.

IN-SITU MONITORING OF MECHANICAL, DYNAMICAL AND THERMAL RESPONSES USING CARBON NANOTUBE FIBER SENSORS

J.L. Abot¹

¹The Catholic University of America (USA)

Carbon nanotube yarns (CNTY) are microscale fiber-like hierarchical structures composed of thousands of carbon nanotubes in their cross-section that could be made meters-long and integrated in materials without significantly altering their microstructure[1]. The change in the electrical resistance of CNTYs when subjected to either strain, known as piezoresistivity, or to a temperature change, known as thermoresistivity, are the main mechanisms that could be tapped for sensing using CNTYs. The piezoresistive response of the CNTY in the direction of the yarn (axial direction) and its transverse direction, under both tension and compression, and for the freestanding yarn or the yarn embedded in a polymeric material (monofilament composite) are available and continuously being investigated for a variety of loading and material parameters [2-4]. The sensitivity or gauge factor of the CNTY sensors under mechanical/dynamic loading as well as the sensitivity or thermal coefficient of resistance under thermal loading are available and enable the monitoring of material/structural responses relying on the electrical resistance measurements of the CNTY [1-4]. Integrated and distributed CNTY sensors could be used to monitor the deformation of materials including polymers and composites subjected to quasi-static and dynamic loadings. The same CNTY sensors could be used to monitor the temperature of these materials when subjected to a variety of thermal programs. Experimental results show that the mechanical or dynamical, or thermal cyclic responses of material samples being tested are shown to be exactly in-sync with the electrical responses of the CNTY sensors. The progress in developing CNTY integrated sensors to measure strain, temperature or detect damage, chemicals concentrations may lead to new smart materials for a variety of applications.

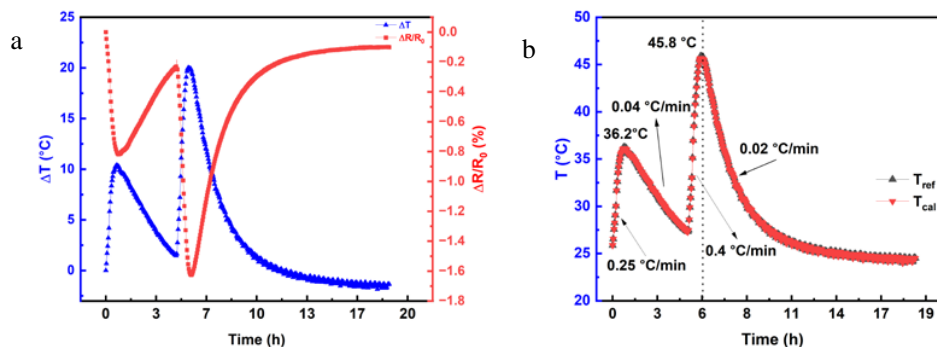


Figure 1: (a) Fractional change in electrical resistance of CNTY/Vinylester monofilament composite and temperature change versus time during an incremental-cyclic temperature program, and (b) comparison of temperature history calculated from resistance measurements for CNTY/Vinylester monofilament composite and that from a reference thermocouple.

References

- [1] J. C. Anike, J. L. Abot, Sensors Based on CNT Yarns, Carbon Nanotube Fibres and Yarns - Production, Properties and Applications In Smart Textiles, Elsevier (2019).
- [2] J. C. Anike, K. Belay, J. L. Abot, *Carbon* **142**: 491–503 (2019).
- [3] T. Tayyarian, O. Rodríguez-Uicab, J. L. Abot, *J. Carbon Res.* **7**: 60 (2021).
- [4] I. Garcia Guerra, T. Tayyarian, O. Rodríguez-Uicab, J. L. Abot, *J. Carbon Res.*, **9**: 89 (2023).

Large-Scale Production and Advanced Computing of Memristor Based on Ionic Layered Minerals

Rongjie Zhang¹, Yujie Sun¹, Keyou Wu¹, Bilu Liu¹

¹ Shenzhen Geim Graphene Center, Tsinghua-Berkeley Shenzhen Institute and Institute of Materials Research, Shenzhen International Graduate School, Tsinghua University, Shenzhen 518055, China

Abstract.

The semiconductor industry has encountered inherent limitations defined by Moore's Law and the Von Neumann bottleneck. Recent discoveries in two-dimensional (2D) materials and their associated memristors offer promising avenues for overcoming these challenges. However, the production of large-scale 2D material-based memristor devices with high stability remains a formidable challenge, primarily due to undesirable operating mechanisms, including defects, vacancies, and grain boundaries. This study centers on the intrinsic memristor behaviors found in natural minerals, driven by inner ion transport mechanisms. We validate this ion transport mechanism through in-situ EDS mapping, SIMS analysis, and dynamic *I-V* transfer characteristics. Leveraging scalable liquid exfoliation and thin-film assembly techniques, we successfully demonstrate large-scale production with remarkable performance attributes. These attributes encompass extended stability (storage time of up to 10^8 seconds), year-long air stability, operational viability across temperatures ranging from room temperature to 550 °C, high repeatability (over 500 sweep cycles with minimal device-to-device variations), rapid switching speed (on the order of tens of nanoseconds), and a flawless 100% yield in device production on a 2-inch wafer. Furthermore, we showcase applications in synaptic and neuromorphic computing, along with fully self-powered, real-time, long-range deformation monitoring functions. Within the context of inner ion transport processes, we achieve non-Markov chain behavior and reversible n⁺/p⁺ doping—a feat challenging to attain with traditional electron-based structures. These findings emphasize the substantial potential of ionic minerals for future applications in emerging electronic technologies, positioning them as promising candidates for next-generation memory and computing solutions.

Keywords: Memristors; Two-dimensional materials; Ion transport; Large-scale production;

References

- [1] Sun Y, Zhang R, Teng C, *et al.*, *Materials Today*, 6(66), 9-16 (2023).
- [2] Zhang R, Sun Y, Chen W, *et al.*, *Advanced Functional Materials*, 2213809 (2023).

LUMINESCENCE OF BLACK PHOSPHORUS FILMS: EXFOLIATION-INDUCED DEFECTS AND CONFINED EXCITATIONS

E. Carré^{1,2}, L. Sponza¹, A. Lusson², I. Stenger², S. Roux^{1,2}, F. Fossard¹, N. Horezan³, V. Zatko⁴, B. Dublak⁴, P. Sénéor⁴, E. Gaufrès⁵, J. Barjon², A. Loiseau¹

¹Université Paris Saclay, ONERA-CNRS, LEM, (Chatillon, France), ² Université Paris Saclay, UVSQ-CNRS, GEMaC (Versailles, France), ³Université Paris Saclay, ³ONERA, DMAS (Chatillon, France), ⁴Laboratoire Albert Fert, Université Paris Saclay, CNRS-Thales (Palaiseau, France), ⁵LP2N, CNRS-IOGS-U. Bordeaux (Bordeaux, France)

Black phosphorus (BP) stands out from other 2D materials by the wide amplitude of the band gap energy that sweeps an optical window from Visible (VIS) to Infrared (IR) wavelengths, depending on the layer thickness. This singularity made optical and excitonic properties of BP difficult to map.

In this work [1], we report a comprehensive study of the intrinsic (i.e. measured at 4K) optical properties of 79 passivated BP flakes obtained by mechanical exfoliation of thickness ranging from 4 to 700nm. By following single and multi-stamp exfoliation protocols and by combining micro-Raman and photoluminescence experiments, we demonstrate that the exfoliation step induces line defects which open new radiative recombination paths that compete and then replace those of the crystalline bulk.

We also show that the evolution of the photoluminescence energy *versus* thickness follows an inverse square law. We discuss how this behavior can be related to a quantum well model and be justified in an intermediate thickness range. Finally, we report that the emission energy of BP slabs placed in different heterostructures is not significantly modulated by the dielectric environment.

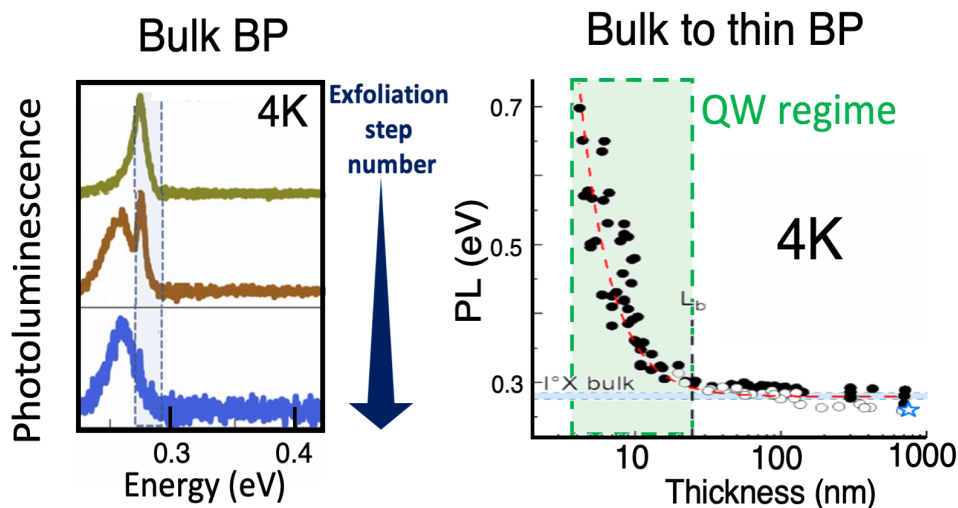


Figure caption: Left: Photoluminescence spectra recorded at 4K from a thick BP chip after a single-stamping exfoliation step (top) and from a 700 nm thick flake obtained after multiple-stamping exfoliation steps (bottom). Right: Evolution of the photoluminescence peak energy as a function of the thickness (black bullets and circles) and its fit based on a quantum well (QW) model (red dashed line). The thickness range where the QW regime applies is indicated by the green rectangle. The bound exciton energy of the BP crystal is marked as a horizontal blue line.

References

[1] E. Carré et al, Phys. Rev. B 109, 035424 (2024)

Measurements of carbon nanotube length, growth rate, and aerogel formation in a floating catalyst chemical vapour deposition reactor

Shahzad Hussain¹, Joe C. Stallard¹, Michael J. Glerum¹, Jack Peden¹, Mabel R. Qiao¹, and Adam M. Boies¹

¹Department of Engineering, University of Cambridge, Trumpington St. CB2 1PZ, UK.

Carbon nanotubes synthesized via floating catalyst chemical vapor deposition (FCCVD) often agglomerate into an aerogel structure with sufficient strength to be drawn continuously. This aerogelation of CNTs within the FCCVD synthesis is unique to gas-phase techniques and produces a continuous CNT product of theoretically infinite length. A survey of the reported experimental parameters used to manufacture spinnable aerogels [A] reveals that all provide residence times in the range 5 s to 240 s, operate at temperatures between 1100°C and 1500°C. Gellation of the growing nanotubes within the reactor occurs upon their collision during random Brownian motion; their propensity to collide increases with their increasing length and number density within the gas [P]. The mechanism by which an aerogel forms and is preserved continuously in the reactor is also unclear: whether the 3D network structure forms from CNT growth from the surface of existing CNTs, or by the collision-induced aggregation of increasingly large CNT aggregates. Regardless of the formation mechanism, a key factor in the aerogel formation and ultimate bulk material properties is the length of CNTs grown within the finite reactor residence time. Thus, CNT growth rates are critical to both understand and enhance for high performing materials, greater CNT reactor density and efficient synthesis from catalysts.

This study seeks to make the first on-line measures of CNT growth within an aerosol in conditions consistent with aerogel producing reactors. Operating conditions are used so that an aerogel does not form within the reactor, but precursors are the same as common aerogel production, significantly including the addition of sulphur as a growth promotor. This facilitates the extraction of gases containing an aerosol of individual and agglomerated carbon nanotubes at a series of locations along its length. The particles extracted from the reactor are collected upon a grid and studied with a transmission electron microscope to determine the length of the nanotubes within them. The number density and mass distribution of particles within the reactor is measured with a centrifugal particle mass analyser; experiments are performed to verify its operation in deducing the particle mass distribution. The residence time available for growth is deduced from the distance over which the density of product within the reactor increases in a zone of increasing temperature. A lower bound for growth rate is defined as the average mass-weighted tube length, measured to be 17 μm divided by this residence time, which is $\sim 280 \mu\text{m/s}$. This growth rate is the highest reported growth rate in the literature and is discussed in the context of a reactor temperature that is much above that typically used in substrate-based growth rate measurements. The agglomerated morphology of particles extracted from the reactor is identified and studied using statistics. A further trend is revealed that the nanotubes are increasingly bundled with increasing distance along the reactor axis giving indications as to the early stages of aerogel formation.

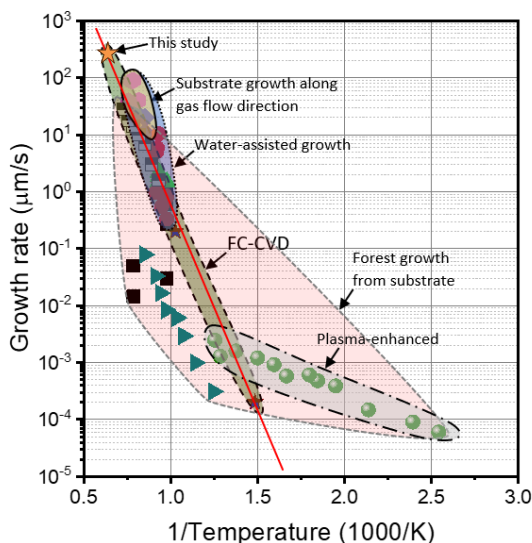


Fig. 1: Growth rate of CNTs versus the inverse temperature of the synthesis.

MICRO-3D-AEROSOL-JET-PRINTING OF 3D ELECTRODES MADE FROM 2D SULFIDE/NANOCARBON FOR ELECTROCHEMICAL WATER SPLITTING

B. Baumgartner^{1*}, P. Patter², M. Hofer¹, M. Nastran¹, A. Wheeldon², F. Iervolino³, D. Apaydin¹, A. Blümel², D. Eder¹, B. C. Bayer¹

¹*Institute of Materials Chemistry, Technische Universität Wien (Austria)*

²*MATERIALS - Institute for Surface Technologies and Photonics, JOANNEUM RESEARCH (Austria)*

³*+Lab, Politecnico Milano (Italy)*

Two-dimensional (2D) sulfides such as 2D MoS₂ are promising non-noble catalysts for sustainable hydrogen production by electrochemical water splitting. Here we present the development of a functional ink for novel micro-3D aerosol jet printing (AJP) of 3D electrodes made from 2D sulfide/nanocarbon electrocatalysts. Our study investigates variations in AJP conditions (planar versus 3D-printing) as well as variations in the functional 2D ink composition and their respective impact on the electrochemical water splitting performance of the resulting catalyst electrodes. We demonstrate, that with our ink it was possible to print functional electrodes using micro-3D AJP, which could directly be used for electrocatalysis without any postprocessing.

Mode coupling bi-stability and spectral broadening in buckled carbon nanotube mechanical resonators

S. Rechnitz¹, T. Tabachnik¹, M. Shlafman¹, S. Shlafman¹, Y. E. Yaish¹

¹Andrew and Erna Viterbi Faculty of Electrical and Computer Engineering, Technion, Haifa, Israel

Bi-stable mechanical resonators play a significant role in various applications, such as sensors, memory elements, quantum computing and mechanical parametric amplification. While carbon nanotube-based resonators have been widely investigated as promising NEMS devices, a bi-stable carbon nanotube resonator has never been demonstrated. Here, we report a class of carbon nanotube resonators in which the nanotube is buckled upward^{1,2}. We show that a small upward buckling yields record electrical frequency tunability, whereas larger buckling can achieve Euler-Bernoulli bi-stability, the smallest mechanical resonator with two stable configurations to date. We believe that these recently-discovered carbon nanotube devices will open new avenues for realizing nano-sensors, mechanical memory elements and mechanical parametric amplifiers. Furthermore, we present a three-dimensional theoretical analysis revealing significant nonlinear coupling between the in-plane and out-of-plane static and dynamic modes of motion, and a unique three-dimensional Euler-Bernoulli snap-through transition³. We utilize this coupling to provide a conclusive explanation for the low-quality factor in carbon nanotube resonators at room temperature, key in understanding dissipation mechanisms at the nano scale.

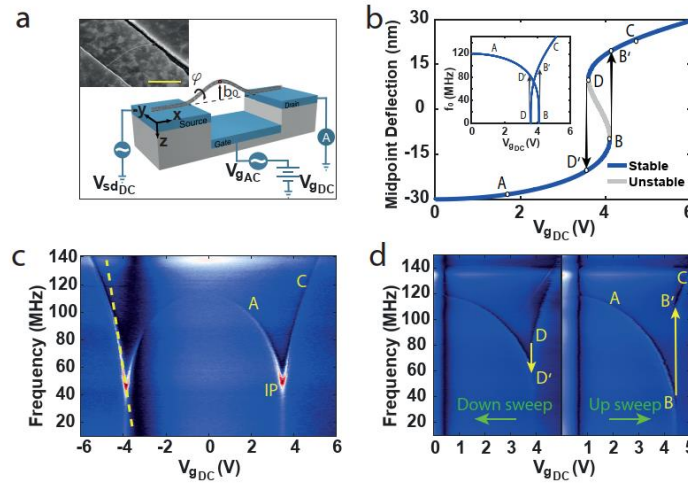


Figure caption: Suspended CNT based bi-stable NEMS device. (a) Schematic layout of the device, coordinates system and experimental setup for the resonance frequency measurement. Note that our coordinates system is such that the positive z direction points downward. Inset: SEM image of a typical device, displaying initial upward buckling. Scale bar - $1\ \mu\text{m}$. (b) Theoretical 2D model for the midpoint static deflection (red dot in a) as a function of the DC gate voltage. Our coordinates were chosen such that negative/positive values represent upward/downward curvature (respectively). The blue line represents a stable solution while the gray is unstable. Inset is the corresponding theoretical resonance frequency dependence on the DC gate voltage. (c) Resonance frequency measurement of device I, displaying continuous transition via an inflection point (IP), exhibiting $df_0/dV_G \sim 100\ \text{MHz/V}$ (dashed yellow line). (d) Upward (right) and downward (left) sweeps measurement of device II, exhibiting the snap-through and release phenomena, resulting in a "jump" of nearly 80 MHz in the resonance frequency.

References

- [1] S. Rechnitz, T. Tabachnik, M. Shlafman, S. Shlafman, and Y. E. Yaish, *Nat. Commun.* **13**, 5900 (2022).
- [2] S. Rechnitz, T. Tabachnik, M. Shlafman, S. Shlafman, and Y. E. Yaish, *Nano Lett.* **22**, 7304 (2022).
- [3] S. Rechnitz, Y. Tovi, S. Shlafman, T. Tabachnik, M. Shlafman, and Y. E. Yaish, *Nonlinear Dyn.* **111**, 11791 (2023).

MOLECULAR ASPECT RATIO EFFECT ON AXIAL THERMAL TRANSPORT IN SOLUTION-SPUN CARBON NANOTUBE FIBERS

Y. Song¹, O. Stefanov¹, M. Durán-Chaves¹, I.R. Siqueira¹, O. Dewey¹, N. Komatsu^{1,2}, J. Kono¹, M. Pasquali¹, G. Wehmeyer¹

¹Rice University (USA), ²University of California Berkeley (USA)

Neat, densely packed, and highly aligned carbon nanotube fibers (CNTF) have appealing room-temperature axial thermal conductivity (k) and thermal diffusivity (α) for applications in lightweight axial heat spreading or flexible thermal connections [1,2]. Although increasing the molecular aspect ratio L/d (i.e., ratio of nanotube length L to nanotube diameter D) of the constituent single-wall and few-wall carbon nanotubes (CNTs) is known to improve the electrical and mechanical properties of the CNTF [3], no prior work has quantified the molecular aspect ratio effect on thermal transport for solution-spun CNTF. Here, we perform self-heated steady-state and three-omega thermal measurements at room temperature on suspended CNTF in vacuum. The CNT viscosity-averaged molecular aspect ratios range from 960 to 5610, as quantified by rheological measurements of liquid crystalline CNT solutions [4]. The thermal measurement results show that k increases from 150 W/m. K to 350 W/m. K with increasing L/d . The axial electrical conductivity σ also increases from 3 MS/m to 9 MS/m with increasing L/d , and the Wiedemann–Franz law predicts the electronic contribution to k is near 50 W/m. K for the highest σ sample. CNTF made with varying volume fraction ϕ of constituent high- L/d and low- L/d CNTs generally fall within typical macroscopic rule-of-mixtures bounds for $k(\phi)$ and $\sigma(\phi)$. The thermal diffusivity α scales with k , leading to a sample-averaged volumetric heat capacity of 1.5 ± 0.3 MJ/m³K. Thus, this work shows that increasing the molecular aspect ratio enhances k and α of solution-spun CNTF, motivating further investigation into thermal transport mechanisms and applications of carbon nanotube fibers.

References

- [1] Behabtu et al., *Science*, **339**, 182-186 (2013).
- [2] Taylor et al., *Carbon*, **171**, 689-694 (2021).
- [3] Tsentlovich et al., *ACS applied materials & interfaces*, **9**(41), 36189-36198 (2017).
- [4] Tsentlovich et al., *Macromolecules* **49**(2), 681–689 (2016).

MULTIFUNCTIONAL PERFORMANCE OF TOPOLOGICALLY TUNED AUXETIC LATTICE NANOCOMPOSITES

J. Schneider¹, S. Kumar¹

¹James Watt School of Engineering, University of Glasgow (United Kingdom)

This study delves into the intricate exploration of topologically tuned nanocomposite lattices, emphasizing their multifunctional capabilities and piezoresistive properties tailored for adjustable strain and damage sensing. The central focus of this investigation lies in the development of architected cellular structures in both 2D and 3D formats, fabricated through additive manufacturing techniques like fused filament fabrication, utilizing nanoengineered polymers such as polyetheretherketone (PEEK) as filament feedstock. These methods are pivotal in achieving the complex geometries necessary for the desired mechanical and functional attributes.

The research primarily concentrates on the piezoresistive features of these lattices under diverse loading conditions. By incorporating carbon-based nanomaterials such as carbon nanotubes (CNTs) and graphene nanoplatelets (GNPs), the lattices exhibit enhanced piezoresistive properties, enabling precise and tuneable strain sensing as well as damage detection. This is particularly crucial for applications demanding real-time monitoring of structural integrity and health. A significant facet of the study underscores the exceptional weight-specific mechanical characteristics of these lattice structures. Through topological tuning, involving adjustments in geometric parameters like unit cell configuration and dimensions, the lattices achieve a delicate balance of high stiffness and strength while maintaining material efficiency. Some structures even demonstrate an auxetic nature, characterised by a negative Poisson's ratio, contributing to their distinctive mechanical behaviour, rendering them suitable for various engineering applications, including structural sensors.

While the study primarily focuses on mechanical and piezoresistive aspects, it also explores the potential for biocompatibility, especially when utilising nanomodified PEEK, as seen in bone tissue engineering. This suggests employing these materials in biomedical applications, complementing their mechanical and sensing functionalities. Finite element analyses corroborate the experimental observations, furnishing precise mechanical and piezoresistive outcomes. Additionally, the incorporation of physics-informed machine learning, particularly Gaussian Process Regression, extends the design exploration beyond the confines of experimental assessment. In conclusion, this research sheds light on the design and application of topologically tuned auxetic nanocomposite lattices, highlighting their multifunctional nature. The synergy of advanced additive manufacturing, meticulous geometric design, and the integration of nanomaterials results in materials that are not only mechanically superior but also adept at sophisticated strain and damage sensing, with a notable mention of potential biocompatibility through the use of nanomodified PEEK.

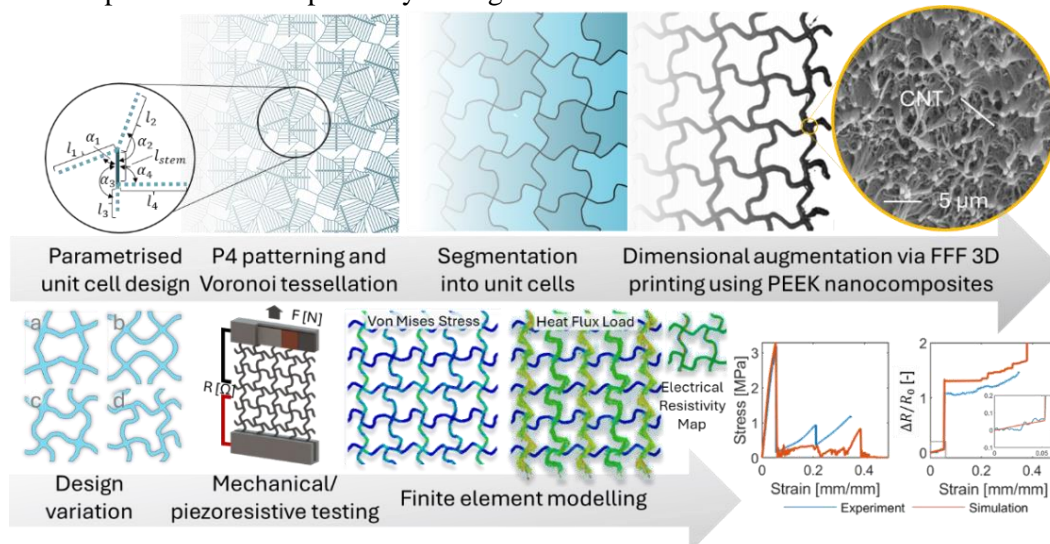


Figure: Mechanical and piezoresistive behaviours of nanoengineered lattices: Geometric modelling of topologically tuned architectures, 3D printing, multiscale characterization, FE modelling and data-driven prediction.

Multiresponsive MXene Soft Robotics

H. Wang¹

¹ *Electrical and Computer Engineering Department, Duke University, Durham, NC 27708, USA*

MXenes, a class of two-dimensional materials including transition metal carbides, nitrides, and carbonitrides, have garnered widespread interest for their exceptional characteristics. This presentation will cover the development of MXene-based actuators, highlighting their responses to thermal, optical, and moisture stimuli. We will showcase origami-inspired soft robotics utilizing MXene actuators and delve into our innovative fabrication of Ti₂C₃T_x/cellulose soft robots. By examining nanocrystal, nanofiber, and microfiber cellulose phases, we aim to enhance actuation performance. Our findings reveal that the Ti₂C₃T_x/cellulose actuators exhibit robust reactions to light, heat, and humidity, making them ideal for soft robotics and sensing technologies. Additionally, we will explore the underlying mechanisms of these multi-responsive actuators.

Multi-walled carbon nanotubes targeting the tumor microenvironment to inhibit melanoma metastasis

Lorena García-Hevia¹, Rym Soltani², Jesús González¹, Olivier Chaloin², Cécilia Ménard-Moyon², Alberto Bianco² and Mónica L. Fanarraga¹

¹ The Nanomedicine Group, Universidad de Cantabria-IDIVAL, University of Cantabria, Avda Herrera Oria s/n, 39011, Santander, (Spain)

² CNRS, Immunology, Immunopathology and Therapeutic Chemistry, UPR 3572, University of Strasbourg, ISIS, 67000 Strasbourg, (France)

Metastasis, the intricate process through which cancer cells disseminate from their primary origin to form secondary tumors in distant parts of the body, poses a formidable challenge in cancer management, substantially contributing to the severity and mortality associated with the disease. Multi-walled carbon nanotubes (MWCNTs) present a biomimetic interference with cytoskeletal nanofilaments upon penetration into tissues and cells, exhibiting intrinsic antitumoral effects akin to microtubule-binding chemotherapies like Taxol® [1–5].

This investigation delves into the potential of oxidized MWCNTs to selectively target vascular endothelial growth factor receptors (VEGFR), aiming to evaluate their effectiveness in impeding metastatic growth by inducing anti-proliferative, anti-migratory, and cytotoxic effects on both cancer cells and the tumor microenvironment. Our findings unveiled a noteworthy reduction of over 80% in malignant melanoma lung metastases following the intravenous administration of the targeted biodegradable MWCNTs. Furthermore, the synergistic combination of these nanomaterials with the conventional chemotherapy agent Taxol® resulted in a remarkable 90% increase in the antimetastatic effect [6].

This integrated therapeutic approach exhibits promising potential in the battle against metastatic disease, as underscored by these compelling findings. Considering the nearly 60,000 annual deaths attributed to metastasis, the significance of these results becomes even more profound, offering a glimpse into a potential breakthrough in metastatic cancer treatment.

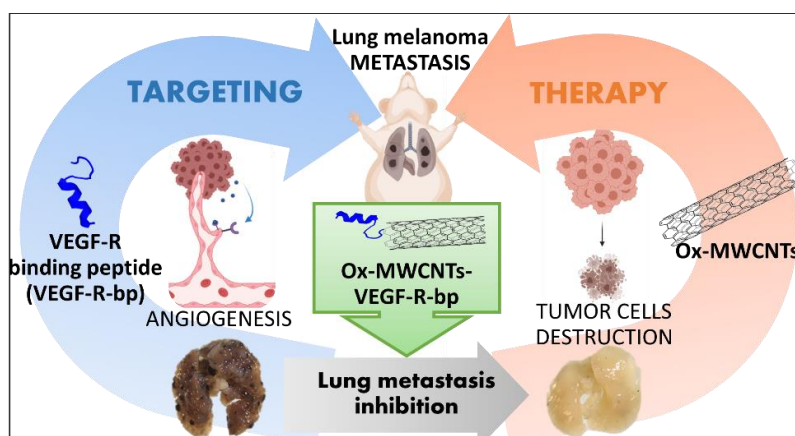


Figure: Biodegradable Multi-walled Carbon Nanotubes (MWCNTs), guided to lung metastases with a neovasculature-binding peptide, demonstrated a 90% reduction in metastases after only three doses. These CNT-conjugates synergistically enhanced Taxol® efficacy in preclinical metastatic melanoma models, showcasing their potential for combating metastatic disease.

References

- [1] L. Rodríguez-Fernández, *et al. ACS Nano*. **6** (2012) 6614–6625.
- [2] L. García-Hevia, *et al. Nanomedicine*. **9** (2014) 1581–1588.
- [3] L. García-Hevia, *et al. Curr Pharm Des*. **21** (2015) 1920–1929.
- [4] L. García-Hevia, R. *et al. Curr Pharm Des*. **21** (2015).
- [5] L. García-Hevia, M.L. Fanarraga, *J Nanobiotechnology*. **18** (2020) 1–11.
- [6] L. García-Hevia, *et al. Bioactive Materials* **34** (2024) 237-247.

Non-linear Landau Fan Diagram and Extraction of Landau Level Spacing by Open Orbit in Graphene Moiré Superlattices

Pilkyung Moon¹⁻³, Youngwook Kim^{4,5}, Mikito Koshino⁶,
Takashi Taniguchi⁷, Kenji Watanabe⁷, Jurgen H. Smet⁴

¹NYU Shanghai (China), ²NYU-ECNU Institute of Physics at NYU Shanghai (China),

³New York University (USA), ⁴Max-Planck-Institut für Festkörperforschung (Germany), ⁵DGIST (Korea),

⁶Osaka University (Japan), ⁷National Institute for Materials Science (Japan)

Due to Landau quantization, the conductance of two-dimensional electrons exposed to a perpendicular magnetic field exhibits oscillations that generate a fan of linear trajectories when plotted in the parameter space spanned by density and magnetic field. This fan looks identical regardless of the details of the electron dispersion that determines the field dependence of the Landau level energy. This is not surprising since the location of the conductance minima depends only on the level degeneracy which is linear in flux. The fractal energy spectrum that emerges within each Landau band when electrons are exposed to a two-dimensional superlattice potential produces a number of additional oscillations, but they also create just linear fans for the same reason. Thus, such a regular Landau fan cannot give any information about the spectral gap of Landau levels.

In this talk, we report conductance oscillations in graphene electrons exposed to moiré potentials that deviate from the general law of magnetic flux linearity (Fig. 1a) [1]. Then, we explain that such anomalous behavior is due to the coexistence of multiple orbits, resulting from the simultaneous occupation of multiple minibands and magnetic breakdown (Fig. 1b). Finally, we propose a novel method to extract the spectral gaps, without measuring activation energy or carrying out tunneling spectroscopy, by using the density of states of open orbits as a measure (Fig. 1c). This method is quite general, so it can be applicable to any systems with multiple bands.

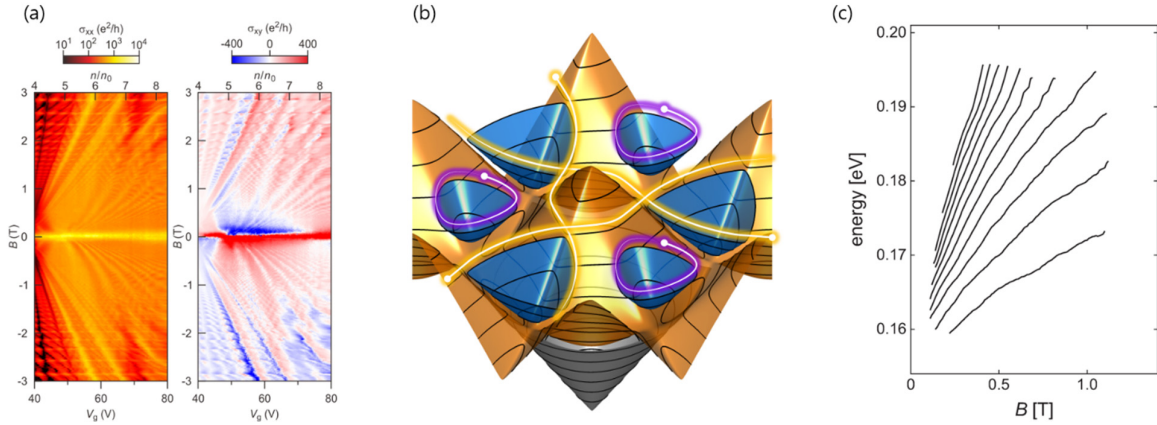


Figure 1: (a) Longitudinal (σ_{xx} , left) and Hall (σ_{xy} , right) conductivities of a graphene/hBN moiré superlattice measured as a function of magnetic field strength B and back-gate voltage V_g (and normalized electron density n/n_0). Both plots show the anomalous, non-linear trajectories of conductance oscillations which converge to $n/n_0 \sim 5.5$. (b) Conduction band structures calculated with an effective continuum model [2]. The gray, orange, and blue surfaces show the first, second, and third bands, respectively. The purple and yellow lines indicate the closed and open orbits that give rise to the non-linear Landau fan diagram in (a). (c) Energy spectrum of the Landau levels which emerge from the closed orbits in (b), decoded from the peaks of σ_{xx} measured in experiment.

References

- [1] P. Moon, Y. Kim, M. Koshino, T. Taniguchi, K. Watanabe, J. H. Smet (Nano Lett. (in print), doi:10.1021/acs.nanolett.3c04444)
- [2] P. Moon and M. Koshino, *Phys. Rev. B* **90**, 155406 (2014).

Observation of bright hybridized exciton in MoTe₂/MoSe₂ heterostacks

S. Zhao¹, X. Huang¹, R. Gillen², A. Baimuratov¹, A. Högele¹

¹Fakultät für Physik, Ludwig-Maximilians-Universität München, Geschwister-Scholl-Platz 1, 80539 München, Germany

²Friedrich-Alexander Universität Erlangen-Nürnberg, Staudtstraße 7, 91058 Erlangen, Germany

Heterostacks of atomically thin transition metal dichalcogenide (TMDC) with strong exciton transitions provide the unique opportunity to rationally tailor the optical properties of solids. Recently, theory [1] and experiment [2] show that in a TMDC heterobilayer when the conduction band edges of the two constituent layers are near-degeneracy, the electrons could delocalize over both layers, producing new resonant hybridized excitonic states that inherit the spectral properties of both intra- and interlayer excitons. Here, we report on the cryogenic optical spectroscopy results on MoTe₂/MoSe₂ bilayers, which are predicted to be a suitable candidate for studying the hybridization effect. We observe a strong interlayer exciton transition with high oscillator strength in aligned MoTe₂/MoSe₂ samples. Moreover, the hybridization effect makes aligned MoTe₂/MoSe₂ bilayer have much brighter interlayer exciton emission than the other non-resonant TMDC bilayers that have larger band offsets. In addition, g-factors and optical selection rules of these hybridized excitonic states in MoTe₂/MoSe₂ bilayers are discussed as well as doping and twist angle dependence of the degree of hybridization. Our findings pave the way for understanding and engineering the rich exciton physics in TMDC heterostacks and the attractive emission energy (1.1 eV) of the interlayer exciton in MoTe₂/MoSe₂ bilayers provides possibilities for integration with silicon photonics.

References

[1] D. A. Ruiz-Tijerina and V. I. Fal'ko, Phys. Rev. B **95**, 125424 (2019).

[2] E. M. Alexeev *et al.*, Nature **567**, 81-86 (2019).

Patterning dye J-aggregates by activated diffusion in bended BNNTs

J.-B. Marceau¹, D.-M. Ta², A. Aguilar², A. Loiseau³, R. Martel⁴, P. Bon², R. Voituriez⁵, G. Recher¹, and E. Gaufres^{1*}

¹ Laboratoire Photonique Numérique et Nanosciences, Institut d'Optique, CNRS UMR5298, Université de Bordeaux, F-33400 Talence, France

² XLIM UMR CNRS 7252, Limoges, France

³ Laboratoire d'Étude des Microstructures, ONERA-CNRS, UMR104, Université Paris-Saclay, Châtillon, France

⁴ Département de chimie, Université de Montréal, Montréal, Québec H3C 3J7, Canada

⁵ Laboratoire Jean Perrin et Laboratoire de Physique Théorique de la Matière Condensée
CNRS Sorbonne Université, 4 place Jussieu, 75005 Paris, France

*Correspondance etienne.gaufres@cnrs.fr

Single walled carbon nanotubes (SWCNTs) have been used as a 1D template for assembling various organic and inorganic compounds thanks to their hollow, crystalline and cylindrical architectures. In the context of fluorescent molecules assembly, it was unfortunately demonstrated that the overlap of the emission bands of the adsorbed dyes with the absorption bands of semiconducting nanotubes in the visible range (2-3 eV) leads to effective energy transfers that both readily quench the dyes fluorescence and sensitize the nanotube host.^{1,2} As an alternative, boron nitride nanotubes (BNNTs) have been identified as a promising dielectric host template for fluorescent molecules because of their wide-gap semiconductors of ~5.5 eV, opening the way for the design of fluorescent nano-hybrids.³

In this presentation, we will first present an activated and guided diffusion mechanism of luminescent dyes molecules initially confined inside boron nitride nanotubes.^{4,5} This mechanism leads to the formation of periodic luminescent chains of aligned molecules with chain lengths ranging from 500 nm to 2 microns.⁵ Correlative measurements between BNNT bending and the position of molecules along the BNNT axis reveal an efficient and long-range migration of molecules from the curved to the straight parts of a BNNT. We combined a phenomenological model of the molecular transport in 1D with the description of the bending properties of BNNTs to decipher this mechanism and to predict the position and morphologies of a cluster as a function BNNT length. This mechanism leads to the formation of bright J-aggregates with periodic spacing and defined lengths.

In the second part, we will present preliminary results of the encapsulation of two different molecules (sexithiophene and anthracene) inside individual BNNT. These results shows than depending of the distance between two single emitters (6T) the lifetime and the emissivity of the molecules are changing at room temperature which lead to possible superradiance regime in the nanohybrid⁶.

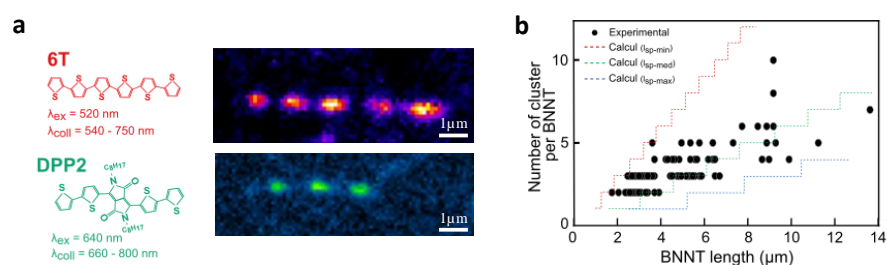


Figure 1-(a) Confocal imaging after deconvolution of typical 6T@BNNTs and DPP2@BNNT found in PMMA after stretching at 150°C (b) Calculated and experimental measurement of the number of clusters per 6T@BNNT as a function of the BNNTs length.

References

- [1] S Van Bezouw, *ACS Nano* (2018)
- [2] E. Gaufres *ACS Nano* (2016)
- [3] C. Allard et al, *Advanced Materials* (2020)
- [4] A. Badon & J.-B Marceau et al, *Materials Horizons* (2023)
- [5] J.-B. Marceau et al, submitted (2024)
- [6] J.-B. Marceau et al, *in prep.*

Polyaniline grafted Carbon Nanotube Composite Fibers for Flexible Fiber-Shaped Supercapacitors

Dongju Lee^{1,2}, Junghwan Kim¹, Chae Won Kim², Seo Gyun Kim¹,
Yuanzhe Piao^{2*}, Bon-Cheol Ku^{1*}

¹Korea Institute of Science and Technology (KIST), ²Seoul National University,

Republic of Korea

*E-mail; parkat9@snu.ac.kr and cnt@kist.re.kr

CNT fibers have attracted considerable attention as an outstanding framework for fiber-shaped supercapacitors, owing to their notable electrical conductivity and strength as current collectors [1]. Simultaneously, polyaniline (PANI), characterized by its remarkable redox activity, has been employed in the composition of supercapacitor electrode materials [2]. Furthermore, the nanostructured PANI actively facilitates redox reactions and promotes the diffusion of electrolyte ions [3]. In our previous work, we introduced an effective methodology for manufacturing CNT-g-PANI composite fibers with specific electrical conductivity and tensile strength [4]. Despite the intrinsic high capacitance of PANI, the utilization of simply wet-spun CNT-g-PANI composite fibers for supercapacitors resulted in a conspicuously low capacitance, attributed to the restricted chemical resistance of pristine PANI within the composite fibers.

To address this issues, we present an innovative approach— CNT-g-PANI composite fibers covalently bonded with PANI on CNTs. The strong bond formed between PANI and CNTs facilitates the production of composite fibers with increased PANI content, effectively overcoming the challenge of limited PANI content. Consequently, the enhancement of PANI content improved pseudocapacitor characteristics, leading to a significant increase in the specific capacitance of the composite fibers. This innovative methodology demonstrates significant potential in overcoming challenges associated with the solvent susceptibility and chemical resistance of PANI. Moreover, this method represents a significant breakthrough in the utilization of composite materials for advanced applications.

References

- [1] D. Lee *et al.*, *Funct. Compos. Struct.* **5**, 045007 (2023).
- [2] A. Eftekhari *et al.*, *J. Power Sources* **347**, 86–107 (2017).
- [3] J.-G. Kim *et al.*, *ACS Appl. Energy Mater.* **4**, 1130–1142 (2021).
- [4] D. Lee *et al.*, *Carbon* **213**, 118308 (2023).

Resonant Raman in Armchair Graphene Nanoribbons from First-Principles

N. Sheremetyeva¹, M. Lamparski², L. Liang³, G. Borin Barin⁴, and V. Meunier^{1,2}

¹*The Pennsylvania State University (USA)*, ²*Rensselaer Polytechnic Institute (USA)*, ³*Oak Ridge National Laboratory (USA)*, ⁴*Empa, Swiss Federal Laboratories for Materials Science and Technology (Switzerland)*

This contribution will discuss resonant Raman spectra of armchair graphene nanoribbons (AGNRs) computed using Density Functional Theory (DFT) and third-order perturbation theory. Low-dimensional materials continue to be widely studied as promising building blocks for novel electronic devices. These materials' electronic properties are highly sensitive to structural changes like *e.g.* the width of AGNRs. Careful structural characterization is thus a key requirement for exercising exact control over the structural properties of these materials and as a result being able to effectively tune their electronic properties. To this end, Raman spectroscopy has become an increasingly practical tool due to its nondestructive nature and high sensitivity to structural features of the samples. I will also present a numerical analysis carried out to provide a justification for the resonant modeling method based on the use of the frequency-dependent dielectric tensor in the Placzek approximation that has been previously used in the literature. Additional predictions and references for wide AGNRs that have not been broadly investigated with Raman scattering experiments to date will also be provided.

Scaling of Coulomb Defects in Low-D Semiconductors from Variational and Modified Hückel Calculations

K.H. Eckstein¹ and T. Hertel¹

¹*Institute of Physical and Theoretical Chemistry, Julius-Maximilians University Wuerzburg (Germany)*

Understanding doping and its underlying microscopic mechanisms is critical to advancing nanoscale technologies. Here we discuss the case of semiconducting single-wall carbon nanotubes (s-SWNTs), where doping levels can be controlled by adsorbed counterions. However, modeling counterion-induced 'Coulomb defects' at low doping levels presents a challenge due to the need for the simulation of very large unit cells. Here, modified Hückel calculations on 120 nm long s-SWNTs with adsorbed Cl⁻ ions are used to address the scaling properties of shallow Coulomb defect states at the valence band edge and quantum well (QW) states in the conduction band. Interestingly, the QW states may underlie some of the observed exciton band shifts in inhomogeneously doped semiconductors. Using a variational approach, the binding energies of Coulomb defects are found to scale with counterion distance, effective band mass, relative permittivity, and counterion charge as $d^{\alpha-2} m^{\alpha-1} \epsilon_r^{-\alpha} z_j^\alpha$, where α is an empirical parameter. This deepens our understanding of doping in low-dimensional semiconductors with delocalized band states, such as those found in s-SWNTs.

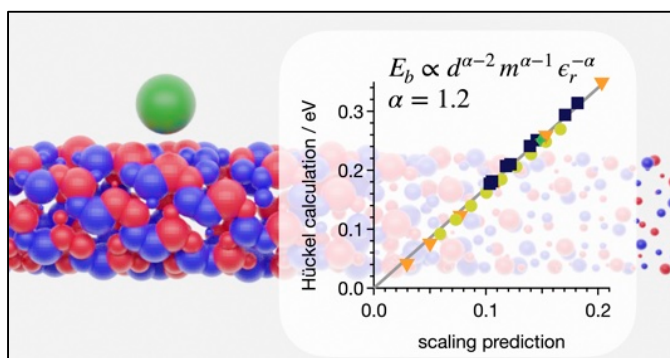


Figure caption: Comparison of variational predictions of the scaling of binding energies with modified Hückel calculations on (6,5) nanotubes and other nanotube types with varying diameter, counterion-surface distance, counterion charge and environmental permittivity.

References

1. K.H. Eckstein and T. Hertel, J. Phys. Chem. C (doi.org/10.1021/acs.jpcc.3c06007).

Single Crystal 2D Covalent Organic Frameworks for Plant Biotechnology

Song Wang¹, Rajani Sarojam², Michael S. Strano^{1,3}...

¹ Disruptive & Sustainable Technologies for Agricultural Precision IRG, Singapore-MIT Alliance for Research and Technology, (Singapore), ² Temasek Life Sciences Laboratory Limited, (Singapore), ³ Department of Chemical Engineering, Massachusetts Institute of Technology, (United States)

Abstract text [1]: Molecules chemically synthesized as periodic two-dimensional (2D) frameworks via covalent bonds can form some of the highest surface area and charge density particles possible. There is significant potential for applications such as nanocarriers in the life sciences if biocompatibility can be achieved, however, significant synthetic challenges remain in avoiding kinetic traps from disordered linking during 2D polymerization of compatible monomers, resulting in isotropic polycrystals without long-range order. Here, we establish thermodynamic control over dynamic control on the 2D polymerization process of biocompatible imine monomers by minimizing the surface energy of nuclei. As a result, polycrystal, mesocrystal and single crystal 2D covalent organic frameworks (COFs) are obtained. We achieve COF single crystals by exfoliation and minification methods forming high surface area nanoflakes that can be dispersed in aqueous medium with biocompatible cationic polymers. We find that these 2D COF nanoflakes with high surface area are excellent plant cell nanocarriers that can load bioactive cargos, such as the plant hormone abscisic acid (ABA) via electrostatic attraction, and deliver them into the cytoplasm of intact living plants, traversing through the cell wall and cell membrane due to their 2D geometry. This synthetic route to high surface area COF nanoflakes has promise for life science applications including plant biotechnology.

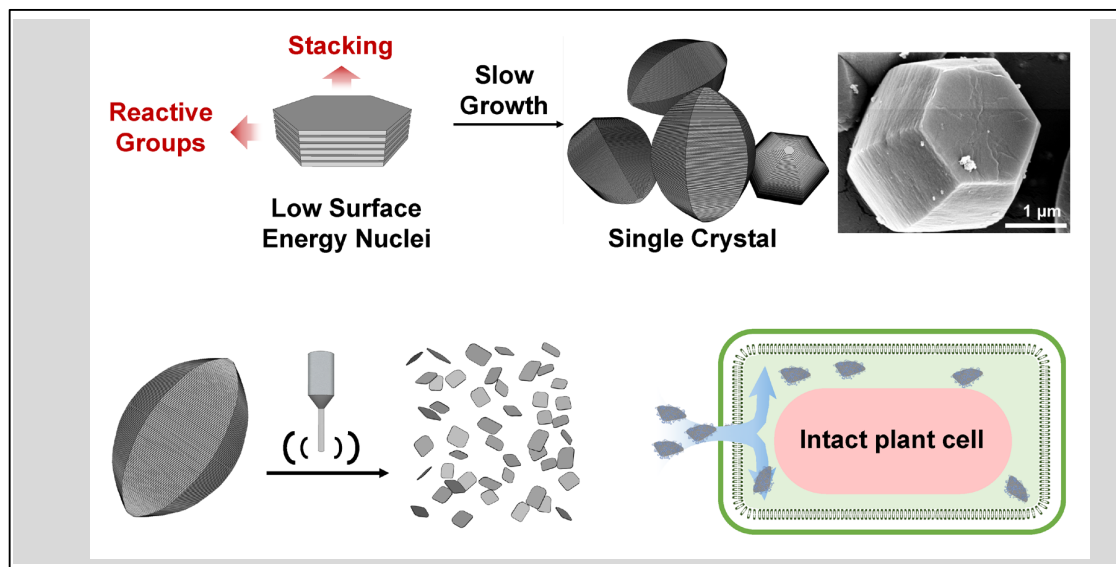


Figure caption: Controlled 2D polymerization by slow nucleation and growth, and their application as intact plant nanocarrier.

References

[1] S. Wang *et al.*, *J. Am. Chem. Soc.* **145**, 12155–12163 (2023).

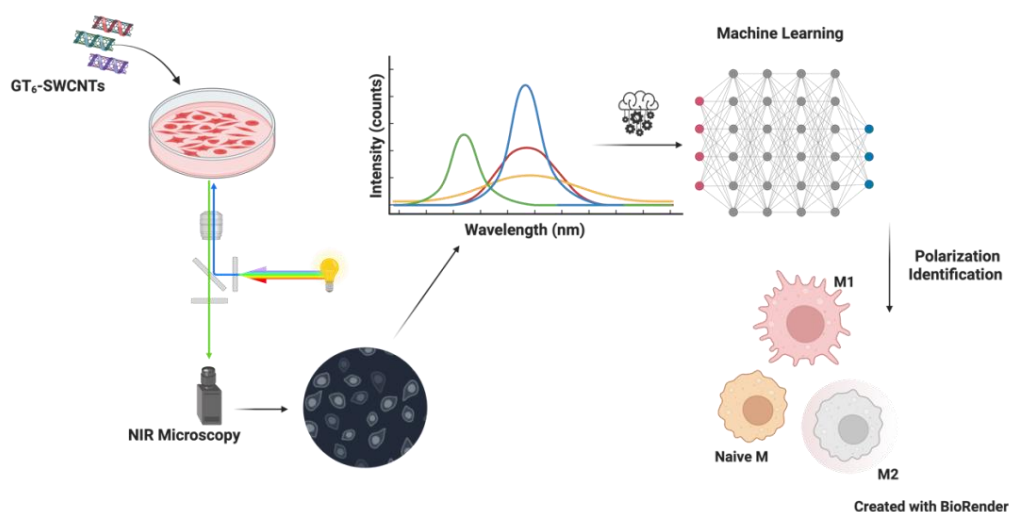
Spectral Fingerprinting Coupled Machine Learning: An Optimized Tool for Cellular Phenotype Identification

A. Nadeem¹, S. Lyons¹, A. Kindopp¹, A. Jamieson², D. Roxbury¹

¹Department of Chemical Engineering, University of Rhode Island, Kingston, Rhode Island 02881 (United States),

²Department of Molecular Microbiology and Immunology, Brown University, Providence, Rhode Island 02912 (United States),

Spectral fingerprinting has emerged as a powerful tool for identifying chemical compounds in addition to unraveling intricate interactions between the intracellular environment and engineered nanomaterials. Additionally, machine learning has revolutionized essentially all scientific disciplines, from biomedicine to nanotechnology. Here, we leverage spectral fingerprinting and machine learning to deepen our comprehension of the interplay between macrophages and DNA-functionalized single-walled carbon nanotubes (DNA-SWCNTs), utilizing their near-infrared (NIR) fluorescence to discern cellular characteristics. We found that M1 macrophages have a significantly higher uptake as compared to both M2-type and naïve macrophages. NIR fluorescence data also indicated that distinctive intra-endosomal environments of these cell types gave rise to significant differences in many NIR features such as emission peak intensities and center wavelengths. Such features served as distinctive markers for identifying different macrophage phenotypes. We further used a support vector machine learning model trained on SWCNT fluorescence data to accurately identify M1 and M2 type macrophages, achieving an impressive accuracy of > 95%. Finally, we observed that DNA-SWCNT complex stability pertaining to DNA sequence length is an important factor that needs to be considered for applications like cell phenotyping or intra-endosomal microenvironment mapping using machine learning approaches. Our findings suggest that shorter DNA-sequences like GT₆ give rise to more improved model accuracy due to increased active interactions of SWCNTs with biomolecules in the endosomal microenvironment. This innovative approach holds great promise in advancing our understanding of dynamic cellular processes, disease states, disease progression, and response to stimuli in-vivo.



Spectral fingerprinting schematic. A summarized process flow diagram for identifying unknown cell phenotypes using near infrared features of GT₆-SWCNTs and an optimized machine learning model.

Surface Functionalization for Chiral Dichroism Induction in Carbon Nanotubes

Amara Arshad¹, Brendan J. Gifford², Aaron Forde³, Wenjie Xia,^{1,4} Sergei Tretiak,^{2,3} Svetlana Kilina,⁵ and Dmitri Kilin⁵

¹Department of Civil, Construction and Environmental Engineering, North Dakota State University, Fargo, North Dakota 58108, USA; ²Center for Nonlinear Studies, Theoretical Division, and Center for Integrated Nanotechnologies, Materials Physics and Applications Division, Los Alamos National Laboratory, Los Alamos, New Mexico 87545, USA; ³Center for Nonlinear Studies, Los Alamos National Laboratory, Los Alamos, New Mexico 87545, USA; ⁴Department of Aerospace Engineering, Iowa State University, Ames, Iowa 50011, USA; ⁵Department of Chemistry and Biochemistry, North Dakota State University, Fargo, North Dakota 58108, USA

Chiroptical properties of confined nanostructures are of interest in applications to polarized photoluminescence, polarized nanosensors, polarized photodetectors. Adsorption of chiral molecules as ligands for nanostructures holds promise to induce and enhance overall chirality of nanomaterials. First principles modeling by time-dependent density functional theory (TD-DFT) allows to explore chirality performance in SWCNTs with hydrogen capped edges and different chirality indices. Computed chiroptical signatures of SWCNTs covalently functionalized with phenylalanine enantiomers (D, L) at ortho binding configurations demonstrate enhancement in comparison to the unbound species. The observed chirality enhancement is hypothetically explained via coupling between the chiral ligands to the transition dipole moment of the nanotubes. The computed CD spectra and thus the chirality induction depends on a specific binding configuration. With site- specific phenylalanine bound to SWCNTs at different positions, anisotropy factors are found to deviate based on different sites, providing mechanistic insight toward improving chiroptical functionality in confined nanomaterials.¹

The work is supported by DE-SC0021287 for exploring IR-emission of carbon nanotubes.

1) Forde, A., Ghosh, D., Kilin, D., Evans, A. C., Tretiak, S., & Neukirch, A. J. (2022). Induced Chirality in Halide Perovskite Clusters through Surface Chemistry. *J. Phys. Chem. Lett.*, **13**(2), 686-693.

Synthesis of Iron Single-Walled Carbon Nanotube from Ferrocene as an Interlayer in Lithium–Sulfur Batteries

A. Hussain^{1,2}, K. Murashko¹, A. Lahde¹

¹*Department of Environmental and Biological Sciences, University of Eastern Finland, Kuopio Finland,*

²*Department of Chemistry and Materials Science, Aalto University, P.O. Box 16100, FI-00076, Espoo, Finland*

Floating catalyst chemical vapor deposition (FCCVD) is a continuous and scalable method for manufacturing conductive single-walled carbon nanotube (SWCNT) thin films. Hydrocarbons or hydrocarbon derivatives have been conventionally used as carbon sources and ferrocene as a Fe nanoparticle (NP) precursor in FCCVD for the fabrication of SWCNT thin films. However, carbon, released from ferrocene decomposition, has not been well investigated for the fabrication of SWCNT thin films. Here, we have developed an FCCVD process for the fabrication of SWCNT thin films using ferrocene as a single source for the generation of catalyst NPs and carbon. Moreover, the absence of hydrocarbons and their derivatives makes the process safe, cost-effective, and environmentally friendly. We fabricated freestanding Fe-SWCNT thin films composed of small diameter nanotubes (1.2 nm) and Fe NPs, synthesized at a high yield of 0.46 mg per 30 min. Fe-SWCNT thin films exhibited good conductivity with a sheet resistance of 800 ohm/sq for 80% transmission at 550 nm. Conductive SWCNTs significantly improved sulfur utilization, with an obvious 27% increase in the capacity of lithium–sulfur batteries (LiSBs). A HNO₃-treated Fe-SWCNT separator significantly improved the cyclic stability of LiSBs with 18% capacity loss of initial capacity compared to 32% capacity loss for polypropylene separator after 100 cycles.[1]

References (if desired)

[1] A. Hussain et al. *The Journal of Physical Chemistry C*, 127, 23577-23585 (2023).

The Structure-Function Relationship in Graphene Oxide Membranes: Beyond D-Spacing

Nima Zakeri, Marta Cerruti

Department of Mining and Materials Engineering, McGill University (Canada)

With their nanochannel-based microstructure, graphene oxide (GO) membranes can act as reliable molecular sieves for fast water transport and ion rejection. The permeation through GO membranes is commonly believed to be primarily determined by the size of the nanochannels (d-spacing). Reported d-spacing values for pristine GO membranes range between 7.4 Å and 9.5 Å [1]. This variability hinders result reproducibility between different studies [2] and prevents a thorough understanding of the structure-function relationship in GO membranes. The variations in d-spacing stem from intrinsic differences in the GO material and in membrane fabrication parameters. In this study, we aim to unravel these effects by studying how membrane fabrication method, thickness, and size influence their microstructure and vapor permeation through them.

Using either vacuum-filtration (VF) or air drying (AD), we fabricated GO membranes across two distinct surface area (0.0314 to 0.1256 cm² and 0.785 to 12.56 cm²) and thickness (500 to 750 nm and 4 to 7.6 μm) ranges. We characterized the membrane d-spacing and crystallite size using X-ray diffraction and Raman spectroscopy, surface morphology and roughness using scanning electron microscopy (SEM) and profilometry and assessed vapor permeation through the membranes using ethanol and water vapor diffusion tests.

Contrary to common beliefs [1], our results revealed that AD does not necessarily result in higher d-spacing, as we found no significant differences between VF and AD membranes. This highlights that the fabrication method does not independently affect d-spacing. We also showed that d-spacing decreases with increasing thickness (Fig. 1a). We attribute this to the longer persistence of water applying capillary forces on the GO sheets before evaporation in thicker membranes, thus resulting in a denser assembly. SEM images and surface profilometry showed that thinner membranes, regardless of the fabrication method, tend to closely mimic the substrate's morphology and roughness. However, with increasing thickness, the surface roughness differs significantly between VF and AD membranes: AD membranes are rougher and show large blunt surface features (Fig. 1b). Despite the similar d-spacing, permeation tests showed significant differences in ethanol diffusion between AD and VF membranes. This may be related to the presence of a larger fraction of defective amorphous domains in AD membranes, not captured in the d-spacing measurement, which may facilitate ethanol transport (Fig. 1c). This result emphasizes the importance of considering parameters beyond d-spacing to characterize GO membrane structure and understand their permeation properties.

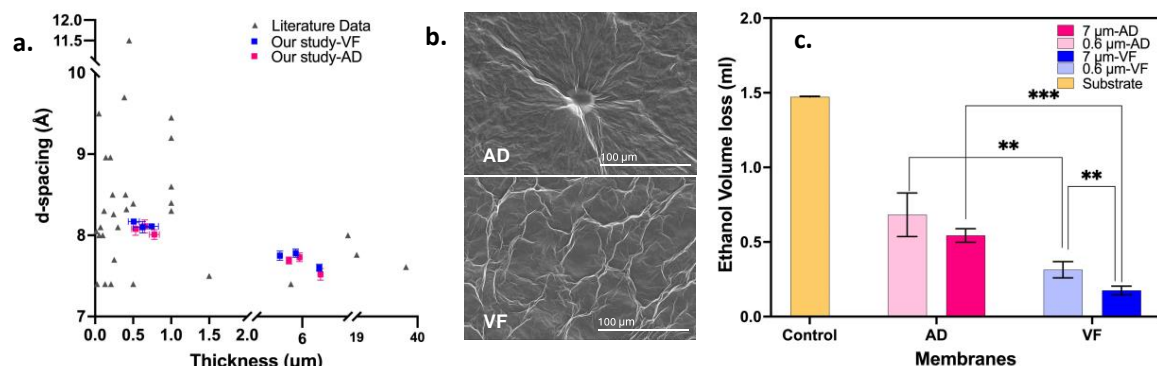


Figure 1. (a) d-spacing of GO membranes as a function of membrane thickness, (b) SEM images of GO membrane surfaces (c) ethanol volume loss through GO membranes with variable thicknesses. Volume loss was measured after 96 hours and with an initial volume of 2 ml.

References

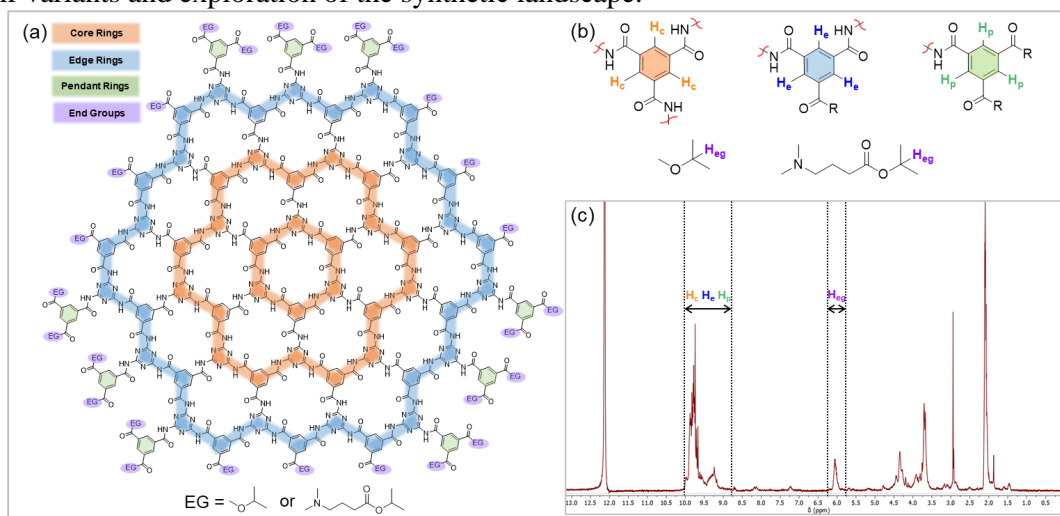
- [1] Tsou, Chi-Hui, et al., *Journal of Membrane Science* **477**, 93-100 (2015).
- [2] Zheng, Bingzhu, et al., *Chemical Reviews* **122.6**, 5519-5603 (2022).

¹H-NMR Trajectories for Analyzing the Growth and Purification of 2D Polyaramids

Zitang Wei¹ and Michael Strano¹

¹Department of Chemical Engineering, Massachusetts Institute of Technology, Cambridge, MA, USA

The recent synthesis of two dimensional (2D) polyaramid (PA) polymers has shown that they exhibit remarkable mechanical and gas barrier properties. Herein, we use ¹H-NMR peak analysis of the aromatic and proton end group regions to characterize 2DPA growth from monomeric precursors, and purification using a two-stage filtration and washing step. The ratio of aromatic-to-end group protons provides a metric for molecular weight and discoidal size, while the skewness of the aromatic region provides a relative weighting between dendritic, small polycyclic intermediates from reaction filtrate after purification (2DPA-1f) and larger polycyclic domains from retentate (2DPA-1r). These two metrics are shown to chart a two-dimensional trajectory that has utility in analyzing the results of differing synthetic and processing conditions. Theoretical analysis of ideal dendrimer and polycyclic limits as a function of repeat unit size are derived as an aid in trajectory analysis. These results provide an analytical framework for evaluating 2DPA and their variants and exploration of the synthetic landscape.



(a) Chemical structure of 3x3 hexagon 2DPA-1. (b) Protons on different components of 2DPA-1. Protons on core rings are labeled in orange (H_c); protons on edge rings are labeled in blue (H_e); protons on pendant rings are labeled in green (H_p); protons on the α-carbon of the end groups are labeled in purple (H_{eg}). (c) ¹H NMR spectra of 2DPA-1r in deuterated trifluoroacetic acid. Regions that correspond to different protons are highlighted between dotted lines.

Non-Reciprocity Induced Valley Hall Effect and Negative Stiffness Lattice in 2D Metamaterials

Haoran Nie¹, Chaoran Jiang¹, Lei Xu¹

¹*The Department of Physics, The Chinese University of Hong Kong, Shatin, Hong Kong, China*

Topological insulators (TPI) are very attractive materials with robust edge modes protected by global topology rather than local environment. Besides the original electron system, TPI has aroused wide attention in various other low-dimensional physical systems since its first discovery, i.e. in electro-dynamic, acoustic, and elastic metamaterials. Here we introduced a mechanical nonreciprocity-like interaction induced 2D Valley Hall insulator (VHI) in elastic system, which utilizes mechanical nonreciprocity in lattice dynamic matrix (Hamilton matrix) D . Unlike previous elastic VHI induced by breaking mass distribution symmetry, the mechanical nonreciprocity only impacts on diagonal terms of D . We experimentally verify this VHI system, showing the effectiveness of the topological edge mode. Besides, we proposed a negative-stiffness elastic VHI based on this mechanical nonreciprocity effect. The negative stiffness system's band gap and topological edge modes can be manipulated near zero frequency oscillation area, enabling significant apply of mechanical VHI in low frequency wave guidance, such as shock absorption in high precision systems. Our method builds a new connection between mechanical nonreciprocity and topology and expands the application prospect of VHI in low-dimensional materials.

6K UniMelt: Microwave-Based Plasma Technology for Versatile Production of Nano-Engineered Materials

A. Kaiser¹

¹6K, Inc. (USA)

Headquartered in North Andover, Massachusetts, 6K is accelerating the industrial transformation of advanced material production and redefining sustainable manufacturing through the world's first industrial microwave plasma platform, the UniMelt system (see Figure 1) [1]. 6K's UniMelt technology enables the development of advanced materials across many markets, such as additive manufacturing and energy storage. It is positioned to replace today's traditional manufacturing with significantly lower cost and a much cleaner, more sustainable process.

For additive manufacturing, the UniMelt process precisely spheroidizes metal powders while controlling the chemistry and porosity of the final product. For battery material, the same process is used to synthesize chemical elements and control particle size and microstructure to produce advanced battery materials at a fraction of the time and cost as conventional processes. The UniMelt capabilities extend to a variety of other materials, including carbon and nano-engineered materials for application areas including batteries, optical materials, advanced abrasives, pigments, and nanomagnets, transparent ceramics, coatings, thermal barriers, and engineered powders.

6K's UniMelt process is a small footprint, low energy consumption, high throughput, and continuous flow operation. Material processing can occur in as short as 2 seconds, with minimal ramp time into a process zone that can operate >6000C. A combination of high heat, highly reactive ions, and designed chemistries create tunable process environments. Variable feedstock materials can be used, and the microwave plasma provides a uniform thermal production zone. Other systems that utilize electrode-based plasma can introduce a source of contamination. 6K's electrode-less system eliminates this problem and assures the highest purity of processed materials. With these capabilities, 6K's system dramatically reduces cost and improves throughput and yield, while increasing control over particle size, purity, and morphology, enabling new material development.



Figure 1: Schematic of the 6K UniMelt[®] plasma reactor showing the stages of material processing (left), images of the UniMelt[®] including the plasma glowing at 6000K and the full production system (top right), and exemplary material process capabilities including tailoring crystallinity, density, morphology, and size (bottom right) for a variety of microscale and nanoscale engineered materials.

References

[1] 6K UniMelt[®] Plasma Technology. 6K Inc. (2024). <https://www.6kinc.com/>.

A Bond-Order-Based Machine-Learning Interatomic Potential for Carbon Allotropes

Ikuma Kohata¹, Ryo Yoshikawa¹, Kaoru Hisama², Keigo Otsuka¹,
and Shigeo Maruyama¹

¹*Department of Mechanical engineering, the University of Tokyo, Tokyo 113-8656, Japan*

²*Center for Research Initiative for Supra-Materials, Shinshu University, Nagano 380-8553, Japan*

Classical molecular dynamics simulations based on bond-order potentials such as the Tersoff potential [1] have been effectively used for the computational studies of carbon materials. However, these interatomic potentials have difficulty in accurately predicting the physical properties of various morphologies of carbon with one set of parameters, due to the limited number of parameters. Recently, the application of machine learning methods to interatomic potentials has been actively studied, and such interatomic potentials are called machine-learning interatomic potentials. The machine-learning interatomic potentials achieve highly accurate interpolative prediction. However, they are not interpretable because of a weak physical foundation, and suffer from a high computational cost due to a large number of potential parameters.

In this study, we proposed a machine-learning interatomic potential model to improve the interpretability and to reduce the number of potential parameters by combining the multilayer perceptron and the formula of bond-order potential. Based on this model, we developed an interatomic potential optimized for the dataset of carbon allotropes including highly disordered structures (Fig.1a), and the developed potential nicely reproduces the ab initio energies of the testing dataset (Fig.1b). Our potential acquired a better test performance in terms of mean absolute error (MAE) of energies and forces than SchNet [2], while the number of parameters of our model is reduced to almost 1/100, suggesting the advantage of a physics-based constraint of bond-order potential (Table 1). The excellent accuracy of this interatomic potential for various bonding states can provide a powerful tool for the study of carbon allotropes.

Table 1: Model comparison between the SchNet and the developed interatomic potential.

	Energy MAE [meV/atom]	Force MAE [eV/Å]	Number of parameters
SchNet	18.3	0.501	150785
This work	15.5	0.317	1765

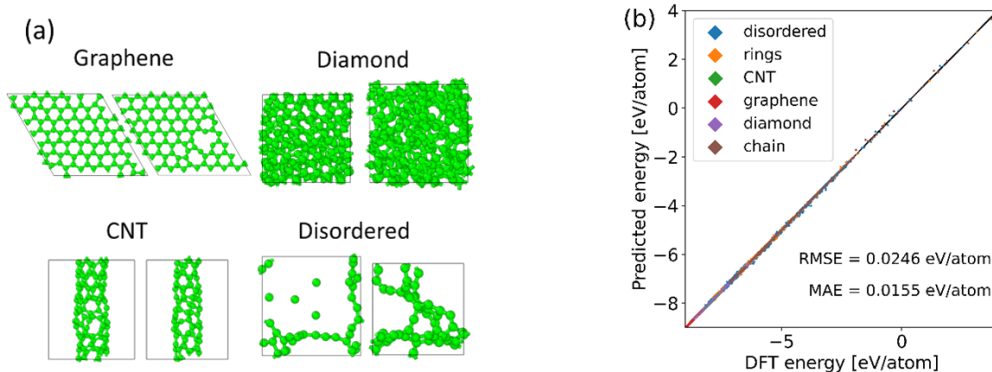


Fig. 1 (a) Examples of the training dataset structures of carbon allotropes. (b) Comparison of energies for the testing dataset between density functional theory (DFT) calculation and the developed interatomic potential.

[1] Tersoff, Phys. Rev. B, 37 (1988) 6991–7000. [2] Schütt, J. Chem. Phys. 148 (2018) 241722.

A MACHINE-LEARNING FORCE FIELD OF COBALT–TUNGSTEN–CARBON SYSTEMS FOR GROWTH SIMULATIONS OF SINGLE-WALLED CARBON NANOTUBES

S. Sun¹, Y. Li^{1,*}

¹College of Chemistry and Molecular Engineering, Peking University (China)

Since 2014, our group has achieved chirality-specific growth of single-walled carbon nanotubes (SWCNTs) with three different chiralities, namely (12,6), (16,0), and (14,4), using Co₇W₆ nanocrystal as the catalyst [1-4]. Theoretical studies on the catalyzed growth process are highly needed to further understand the mechanism of its chiral selectivity. Multiple thermodynamical models have been developed based on density functional theory (DFT), but they largely conflict over the possible routes of action. In recent years, the rapid development of machine-learning force fields (MLFFs) enables the direct growth simulation of defect-free SWCNTs by molecular dynamics (MD) at DFT accuracy. However, current works are limited to liquid monometallic cluster catalysts and shed little light on the mechanism of chiral selectivity [5,6].

Utilizing our group's in situ environmental transmission electron microscopy results [7-9], we developed an MLFF of cobalt-tungsten-carbon systems for subsequent SWCNT growth simulations on Co₇W₆ (001) surfaces based on the DeepPot-SE architecture and a home-made active learning workflow. 11-fold cross-validation over the whole training set provided the energy and force RMSE of 9.4 meV/atom and 0.37 eV/Å, respectively, demonstrating the high accuracy of the MLFF. Using this MLFF, we performed microsecond-scale MD simulations and obtained multiple chirality-defined SWCNTs with diameters ~1.3 nm under 1300 K, observing the formation of defect-free tube walls in the process.

References

- [1] F. Yang *et al.*, *Nature* **510**, 522–524 (2014).
- [2] F. Yang *et al.*, *J. Am. Chem. Soc.* **137**, 8688–8691 (2015).
- [3] F. Yang *et al.*, *ACS Nano* **11**, 186–193 (2017).
- [4] F. Yang *et al.*, *Acc. Chem. Res.* **49**, 606–615 (2016).
- [5] I. Kohata *et al.*, arXiv:2302.09264.
- [6] D. Hedman *et al.*, arXiv:2302.09542.
- [7] F. Yang *et al.*, *J. Am. Chem. Soc.* **141**, 5871–5879 (2019).
- [8] F. Yang *et al.*, *Sci. Adv.* **8**, eabq0794 (2022).
- [9] X. Zhao *et al.*, *Acc. Chem. Res.* **55**, 3334–3344 (2022).

A NOVEL MULTI-SOURCE STATIC COMPUTED TOMOGRAPHY BASED ON CARBON NANOTUBE X-RAY SOURCES

A.P. Gupta^{1,2}, J. Hecla³, M. Tivnan^{1,2}, D. Wu^{1,2}, T. Moulton³, D. Desai³, K. Yang³, W. Krull³, and
R. Gupta^{1,2*}

¹Harvard Medical School (USA), ²Massachusetts General Hospital, (USA),

³Massachusetts Institute of Technology (USA)

*rajgupta1@mgh.harvard.edu

X-ray computed tomography (CT) is a technique that reconstructs a three-dimensional image from multiple X-ray images taken at different angles, serving as a primary method for diagnosing various medical conditions. Modern CT scanners consist of rotating gantry with one or two X-ray sources. As the gantry revolves around the patient, X-ray projections are collected from different angles and processed to create a 3D image [1]. However, the rotating gantry adds bulk, size, and power requirements, limiting its use in resource-constrained environments. Recently, research groups worldwide have shown interest in developing a non-rotating and gantry-less CT system based on multi-X-ray sources [2].

In this context, Carbon Nanotubes (CNTs) emerge as a promising material for compact vacuum-sealed X-ray sources due to their exceptional electric conductivity, high aspect ratio, and chemical stability. Compared to alternative nanomaterials such as Si nanorods and nano-crystalline diamonds, CNTs exhibit superior field electron emission performance with higher current and longer lifetime stability [3]. Furthermore, the CNT-based X-ray source offers several advantages, including lower power consumption, digital switching, and a smaller footprint compared to thermionic counterparts. This study discusses the development of a multi-X-ray source-based CT system using Photocathodes, Si emitters, and CNT field emitters. X-ray images of a plasticized pig's lung phantom were acquired using a Varex flat panel detector at approximately 35 kV, and subsequently, the images were reconstructed using the Filtered Back Projection (FBP) algorithm to generate 3D volumetric images. This research contributes to the understanding of multi-X-ray source-based static CT systems, providing insights into their development and comparing their advantages and disadvantages against conventional CT approaches.

References

- [1] W. A. Kalender *et al.*, *Physics in Medicine and Biology*. **51**, pp. 29–43 (2006)
- [2] V. B. Neculaes *et al.*, *IEEE Access*, **2** 1568–1585, (2014)
- [3] R.J. Parmee *et al.*, *Nano Convergence* **2**, 1-5 (2015)

A Releasable Self-powered Chemical Sensing Platform using 2D Materials

Sungyun Yang¹, A. Merritt Brooks¹, Byungha Kang¹, and Michael S. Strano^{1*}

¹ *Department of Chemical Engineering, Massachusetts Institute of Technology, Cambridge, MA (USA)*

The recent interest in microscopic autonomous systems, including micron-sized robots and smart dust, necessitates the development of miniaturized electronic components to enhance their functional capabilities. To achieve full autonomy in these systems, a microscale energy storage and harvesting system is necessary for untethered operation. Herein, we demonstrated the integration of microbattery-powered colloidal particles with an onboard chemical sensor based on two-dimensional (2D) materials. Zinc-air battery chemistry was adopted for its superior energy density in a microbattery system at the picoliter scale. These devices were mass-fabricated using photolithography, achieving dimensions of approximately 100 μm in lateral size and 10 μm in thickness. A monolayer molybdenum disulfide (MoS_2) was integrated with the microbattery system to function as a chemical sensor. The presence of triethylamine as an analyte led to an accelerated discharge rate of the microbattery, validating the effectiveness of MoS_2 as a chemiresistor at the microscale. Our work contributes to the advancement of self-powered releasable sensor systems at the microscale, offering significant potential for applications in autonomous colloidal robots, smart chemical reactor tracers and microscale robotic systems for targeted drug delivery.

ADVANCEMENTS IN NO GAS SENSING: HEAT-INDUCED ALIGNMENT OF SINGLE-WALLED CARBON NANOTUBE

O. Sadak¹, U. Kilic¹, M. Schubert¹, Nicole Iverson¹

¹ University of Nebraska- Lincoln (United States)

Nitrogen oxides (NO_x), particularly nitric oxide (NO), pose significant threats to human health and the environment, necessitating accurate and rapid detection methods to prevent harmful levels of accumulation. Current NO gas sensors employ spectroscopic or electrochemical techniques, with spectroscopic methods limited by complex instrumentation and potential for permanent adduct formation hindering real-time monitoring. While electrochemical sensors offer advantages like low cost and fast response, they face challenges such as interference from redox active species and restrictions in temperature range, durability, shelf life, and power consumption. A highly selective, sensitive, reliability and stable NO gas sensor is still emerging [1].

Single-walled carbon nanotubes (SWNT) exhibit optical sensing capabilities in the near-infrared (nIR) region when excited, and when wrapped with single-stranded DNA, (AT)₁₅, they can be utilized as NO optical sensors [2], [3]. The fluorescence intensity of the (AT)₁₅-wrapped SWNT remains constant until it is exposed to NO; once exposed to NO, the fluorescence intensity decreases. Despite advancements in SWNT-based sensor characteristics, such as length sorting and chiral enrichment, challenges in SWNT sensor immobilization on substrates, including random distribution and high fiber entanglement, resulting in unreliable and low fluorescence yield and limit their wider potential [4], [5], [6]. There are few numbers of studies investigating alignment of SWNT sensors on substrates and low packing density, narrow range suspension pH or ionic strength limits their potential to use as a universal sensing approach for SWNT-based sensors. Here, we report a heat-induced SWNT alignment on a glass substrate for use as a NO gas sensor. The alignment requires no pre-treatment of the glass substrate, takes less than 10 minutes, and may be used on a variety of substrates including Si wafer, ITO coated glass slide, and Cu foil, etc. When the (AT)₁₅-wrapped SWNT sensor was exposed to NO gas, the aligned SWNT sensor quenched and recovered much faster than the non-aligned SWNT sensor. Hence, experimentally acquired Mueller matrix spectra were analyzed with an effective medium approach based on the Bruggeman formalism and successfully extracted anisotropic complex dielectric function of aligned and nonaligned SWNT platforms within the spectral range from near infrared (0.72eV) to vacuum ultraviolet (6.5eV). With the integration of the extracted dielectric function into our finite element modeling framework, we also present and discuss the near- and far- electric field distributions, accordingly. These findings contribute to a deeper understanding of the physical mechanisms underlying the extraordinary sensing capability of SWNT. We envision that this research will pave the way for the development of a high degree of SWNT alignment for a new generation of SWNT-based electronics and optical biosensors.

References

- [1] R. Li *et al.*, *Nat Commun* **11**, 3207 (2020)
- [2] J. Zhang *et al.*, *J. Am. Chem. Soc.*, **133**, 567-581 (2011).
- [3] J. P. Giraldo *et al.*, *Small*, **11**, 3973-3984 (2015)
- [4] Z. W. Lin *et al.*, *ACS Nano*, **16**, 4705-4713 (2022)
- [5] F. Wang *et al.*, *J. Am. Chem. Soc.*, **132**, 10876-10881 (2010)
- [6] A. S. R. Bati *et al.*, *Nanoscale*, **10**, 22087-22139 (2018)

Aggregation mechanism of high aspect ratio carbon nanotubes and their dispersion

Zhenxing Zhu¹, Fei Wei¹

¹ Beijing Key Laboratory of Green Chemical Reaction Engineering and Technology, Department of Chemical Engineering, Tsinghua University, Beijing 100084, China

Carbon nanomaterials are unique with excellent functionality and diverse structures. However, agglomerated structures are commonly formed because of nanoscale limitations and surface effects. Their hierarchical assembly into micro particles enables carbon nanomaterials to break the boundaries of classical Geldart particle classification before stable fluidization under gas-solid interactions. Currently, there are few systematic reports regarding the structural evolution and fluidization mechanism of carbon nano agglomerations. Based on recent research on carbon nanomaterials, we will introduce the fluidized structure control and fluidization principles of prototypical carbon nanotubes (CNTs) as well as their nanocomposites. The controlled agglomerate fluidization technology leads to successful mass production of agglomerated and aligned single walled CNTs. In addition, the self-similar agglomeration of individual ultralong CNTs and nanocomposites with silicon as model systems further exemplify the important role of surface structure and particle-fluid interactions. These emerging nano agglomerations have endowed the classical fluidization technology with more innovations in the advanced applications like energy storage, biomedical and electronics. We aim to provide insights about the connections between fluidization and carbon nanomaterials by highlighting their hierarchical structural evolution and the principle of agglomerated fluidization, expecting to showcase the vitality and connotation of fluidization science and technology in the new era.

References

- [1] Zhu *et al.*, *Sci. Adv.* **2**, e1601572 (2016).
- [2] Zhu *et al.*, *ACS Nano* **15**, 5129 (2021).
- [3] Zhu *et al.*, *Nat. Commun.* **10**, 4467 (2019).
- [4] Zhu *et al.*, *Adv. Funct. Mater.* 2109401 (2021).
- [5] Zhu *et al.*, *Adv. Sci.* 2205025 (2022).
- [6] Zhu *et al.*, *Adv. Sci.* 2003078 (2021).

Aligned Boron Nitride Nanotube Transparent Epoxy Nanocomposite

Luiz H. Acauan¹, Hillel Dei¹, Nyvia Lyles^{1,2}, Shaan Anand Jagani¹, Shigeo Maruyama³, Rong Xiang⁴ and Brian L. Wardle¹

¹Massachusetts Institute of Technology (USA), ²Howard University (USA), ³The University of Tokyo (Japan), ⁴Zhejiang University (China)

Controlled-morphology nanocomposites of aligned boron nitride nanotubes (A-BNNTs) [1] could lead the next generation of multifunctional materials due to the mechanical, optical, and thermal properties of BNNTs, among others. Here we present the properties of an A-BNNT nanocomposite in an optically transparent EPON 862 matrix. The capillary pressure from the nanoporous network of the A-BNNTs [2] allow full infusion of the polymer matrix. The A-BNNT reinforcement provides an anisotropically enhanced modulus, with an increase of 12.8% in the transverse direction and 21.8% in the axial direction. UV-VIS testing indicates the BNNTs do not significantly alter the absorbance of the optical polymers, but do increase scattering, which is angle dependent due to the BNNT alignment. This work provides a platform for further investigation including other multifunctional properties (such as piezoelectricity) and BNNT process-structure relations at higher BNNT loading towards a broad range of applications.

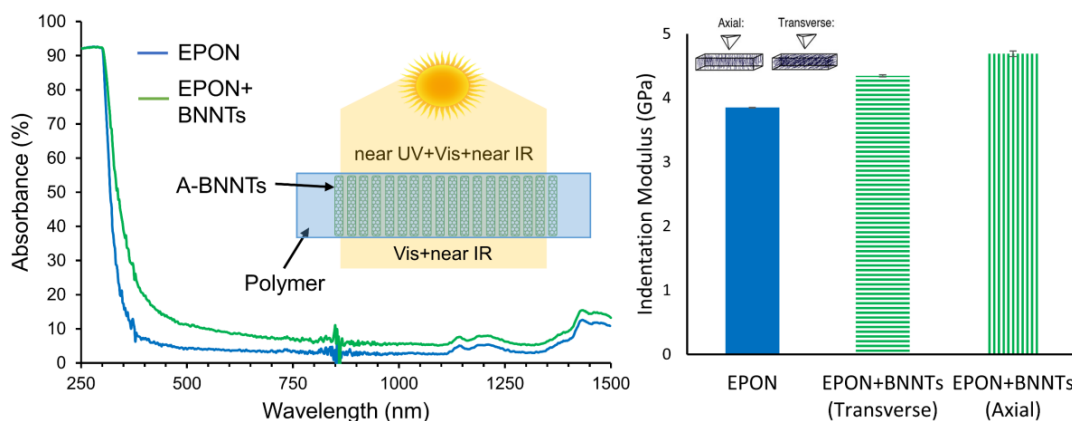


Figure 1: (Left side) Absorbance of the EPON with and without BNNTs and (right side) indentation modulus of pure EPON and of EPON with BNNTs in the axial and transverse direction.

References (if desired)

- [1] L. H. Acauan *et al.*, *ACS Nano* **16**, 18178 (2022).
- [2] J. Lee *et al.*, *Adv. Mater. Interfaces* **7**, 1901427 (2020).

Artificial Intelligence-Assisted Image Analysis for Fluorescence Microscope Cell Imaging

Fluorescence microscopy remains an important analytical tool since 1913. In our work it is used to confirm internalization of nanomaterials in biological cells and tissues. However, performing statistical analysis over a large ensemble of cells to evaluate nanoparticle internalization is time-consuming as well as biased on researcher's ability to identify live versus dead cells. To address these issues, we herein provide an artificial intelligence (AI)-assisted image analysis software for fluorescence cell imaging. We employed a large database of biological cells including HeLa, HEK293 and MCF7 treated with Graphene Quantum Dot (GQD) acquired in our prior work to train the AI. GQDs are a forerunner amongst nanocarbon materials owing to their delivery and imaging capabilities. They exhibit high (> 1 mg/mL) biocompatibilities and emit fluorescence in the visible and near-infrared allowing for AI training for fluorescence analysis in various spectral ranges. In this process instance segmentation was used to localize each cell due to their property of identification, classification, and separation. Initially, artificial intelligence would differentiate between dead and alive cells and finally attain a corrected total cell fluorescence (CTCF) over a range of cell images. The end product is aimed to produce results with a single command. The development of such AI-assisted image analysis is a significant step toward fully automating fluorescence microscopy and minimizing the work effort of the user.

ATMOSPHERIC PRESSURE PLASMA NANOPARTICLE GENERATOR FOR SCALABLE CNT PRODUCTION IN A FCCVD PROCESS

Jui Junnarkar^{1,2,3}, Clay Kacica^{1,2,3}, Eldar Khabushev^{1,2,3}, Arthur Sloan^{1,2,3}, Glen Irvin^{1,2,3}, Matteo Pasquali^{1,2,3}

¹Department of Chemical and Biomolecular Engineering, Rice University (U.S.A), ²Smalley-Curl Institute (U.S.A), ³Carbon Hub (U.S.A)

Carbon nanotubes (CNTs) have emerged as promising candidates for next-generation material applications due to their unique electrical, mechanical, and thermal properties. However, large-scale adoption of CNTs has been hindered by the lack of cost-effective, scalable production methods of the required high aspect ratio, highly crystalline few-walled CNTs (FWCNTs). Continuous production techniques, such as the floating-catalyst chemical vapor deposition (FCCVD) process, often suffer from limited process efficiency, poor reactor utilization, and difficulty in controlling catalyst particle size and distribution, leading to prohibitively high production costs.

One critical challenge in FCCVD is the generation of a catalyst aerosol flow with narrow size distribution and appropriate diameter [1]. Most FCCVD processes rely on the thermal decomposition of organometallic precursors *in-situ* to generate catalyst nanoparticles. However, this process occurs concurrently with hydrocarbon feedstock activation and decomposition, making it difficult to precisely control particle size and size distribution [2]. Moreover, there is an apparent trade-off between high throughput particle synthesis and particle size, having direct consequences on the high yield of FWCNTs with well-defined diameters. The high energy density of plasma makes it ideal for the formation of catalyst particles, as it can utilize metallic catalyst sources, such as an iron wire, as well as an organometallic precursor (ferrocene). In addition, it is well known that nanoparticles created in plasma are primarily negatively charged. This slows particle agglomeration, enabling narrow size distributions [3].

In this work, we present a novel catalyst generation system using an atmospheric pressure radio frequency plasma in an argon-hydrogen mixture. We systematically investigate the effects of process parameters such as geometry, plasma power, post-plasma dilution, and process additives (e.g., sulfur compounds) on catalyst particle size distribution and concentration using scanning mobility particle sizer measurements. We further complement our experimental findings with plasma and fluid dynamics modeling. We then coupled this system to a FCCVD process and demonstrate the synthesis of high quality, few-walled CNTs with high aspect ratios. Although some challenges remain (e.g., substitution of Argon with Nitrogen as carrier gas), we expect this work to serve as a starting point for improving the control and scalability of catalyst particle delivery for FCCVD reactors.

References

- [1] M. B. M. P. A. B. Christian Hoecker *et al.*, *Carbon* **96**, 116–124, (2016).
- [2] M. D. V. W. Y. T. J. B. W. W. S. R. N. S. X. Xiao Zhang *et al.*, *Science* **6**, (2020).
- [3] J. Goree, *Plasma Sources Science and Technology* **3**, (1994).

Atomic Insights into the Oxidation Mechanism of Ultrathin Hafnium Metal Film

Z. Liu¹, R. Jaramillo¹, F.M. Ross¹

¹*Department of Materials Science and Engineering, Massachusetts Institute of Technology, Cambridge, Massachusetts 02139, United States*

Hafnium oxides with rich crystal phases are important family of electronic materials considering their high dielectric constants, ferroelectricity and potential application in resistive switching random access memory. Understanding the oxidation of ultrathin hafnium (Hf) film at atomic level will offer opportunities to realize the integration of high-quality dielectric layers with two-dimensional (2D) materials. Here, starting with the epitaxial deposition of Hf on graphene at ultrahigh vacuum, we demonstrate that native oxidation results in the formation of amorphous oxides, metastable hexagonal oxides (h-HfO_x) and monoclinic HfO₂ (m-HfO₂). m-HfO₂, the thermodynamically stable phase at ambient environmental, exhibits three equivalent orientations due to its low structure symmetry, while h-HfO_x is first observed and proposed to be an intermediate between hcp Hf and m-HfO₂. Further thermal oxidation leads to the conversions from both amorphous oxides and h-HfO_x to m-HfO₂, along with the crystallization of amorphous phase into h-HfO_x. Based on the crystallographic orientation relation observed, it is found that a stacking sequence of Hf layers from AB stacking to ABC stacking is required for the phase transformation from hcp Hf to m-HfO₂. It inevitably leads to the appearance of a hexagonal phase, consistent with our observations. We proposed that h-HfO_x consists of both AB stacking and ABC stacking Hf layers in the out-of-plane direction. This work reveals the atomic oxidation mechanism of ultrathin Hf film, providing fundamental insights into the phase control of hafnium oxides. It also demonstrates the great potential of scalable formation of conformal dielectric 2D materials by combining the epitaxy between metals and 2D materials with controllable oxidation process.

Atomically Thin, Highly Packed, and Aligned Carbon Nanotube Films

J. Doumani¹, S. Sasmal¹, T.W. Chang¹, and J. Kono^{1,*}

¹Rice University (USA)

Atomically thin, aligned carbon nanotube (CNT) films are pivotal for various applications ranging from electronics to quantum emission. While dimensional-limited self-assembly methods offer atomically thin films useful for electronics [1], achieving an ultrahigh CNT packing density remains elusive. The controlled vacuum filtration technique has demonstrated superior advantages in that respect [2], aligning CNTs with nematic order parameter S approaching unity and creating a crystalline structure with 1×10^6 CNTs/ μm^2 packing densities. However, achievable film thicknesses in controlled vacuum filtration are limited to 10 to a few 10s of nanometers to preserve alignment during fabrication. In this work, we introduce a thinning methodology for controlled-vacuum-filtration-produced CNT films using a chemical etch protocol similar to that of multilayer graphene [3], enabling the production of aligned CNT films at monolayer thicknesses. This results in a 2D sheet of aligned CNTs with 1D character, maintaining the high packing density across wafer scales, with etch precision down to 1 nm/etch cycle. This approach marks a significant stride towards controlling light-matter interaction, opening avenues for advanced optoelectronic applications similar to 2D bilayers with a twist.

References

- [1] L. Liu *et al.*, *Science* **368**, 850-856 (2020).
- [2] X. He *et al.*, *Nat. Nanotechnol.* **11**, 633-638 (2016).
- [3] A. Dimiev *et al.*, *Science* **331**, 13495-13507 (2011).

Industrial scale separation of single chiral SWCNTs via ATPE approach

S.H. Nannuri¹, E. Kurian², A. Godwin¹, G. Reddy¹

¹NoPo Nanotechnologies India Private Limited (India)

The mass production of high-purity semiconducting and single-chiral single-wall carbon nanotubes (SWCNTs) is indispensable for their seamless integration into electronic and optoelectronic devices. Aqueous two-phase extraction (ATPE) has emerged as a formidable method, demonstrating its capacity to achieve semiconducting purities surpassing 99.5% and single-chiral enrichment purities exceeding 85%, highlighting its scalability potential. The ATPE method exhibits robust chirality selectivity and offers comprehensive diameter separation coverage, positioning it as a promising solution for future commercial applications.

In our approach, we have explored the adjustment of surfactant ratios as a means to potentially mass-separate various diameter single-chirality SWCNTs using the ATPE method¹⁻³. Through this endeavor, we have successfully isolated high-purity semiconducting, metallic SWCNTs and single chiralities including (6,5), (8,6), (7,5) and (7,6), which are polymer free and dispersed in a 1 wt% DOC solution, along with the production of bucky paper on a milligram scale. The characterization of these SWCNT populations involves meticulous analyses through absorbance spectroscopy, Raman spectroscopy, and photoluminescence mapping techniques.

Our research outcomes establish a fundamental framework for the industrial-scale separation of multiple single-chirality SWCNTs, encompassing a broad distribution of diameters. This progress, coupled with the strategic adjustment of surfactant ratios within the ATPE method, holds significant promise for advancing the field and addressing the challenges associated with mass-producing high-purity SWCNTs for diverse applications in electronic and optoelectronic realms.



Figure: ATPE sorted semiconducting, metallic and single chiral SWCNTs produced at NoPo lab

References (if desired)

- (1) Fagan, J. A. Aqueous Two-Polymer Phase Extraction of Single-Wall Carbon Nanotubes Using Surfactants. *Nanoscale Adv.* **2019**, *1* (9), 3307–3324. <https://doi.org/10.1039/C9NA00280D>.
- (2) Avramenko, M.; Defiliet, J.; Carrillo, M. Á. L.; Martinati, M.; Wenseleers, W.; Cambre, S. Variations in Bile Salt Surfactant Structure Allow Tuning of the Sorting of Single-Wall Carbon Nanotubes by Aqueous Two-Phase Extraction. *Nanoscale* **2022**, *14* (41), 15484–15497. <https://doi.org/10.1039/D2NR03883H>.
- (3) Cao, L.; Li, Y.; Liu, Y.; Zhao, J.; Nan, Z.; Xiao, W.; Qiu, S.; Kang, L.; Jin, H.; Li, Q. Iterative Strategy for Sorting Single-Chirality Single-Walled Carbon Nanotubes from Aqueous to Organic Systems. *ACS Nano* **2024**, *18* (4), 3783–3790. <https://doi.org/10.1021/acsnano.3c11921>.

Bandgap-coupled growth and assembly of ultrapure semiconducting carbon nanotubes

Zhenxing Zhu¹, Fei Wei¹

¹ Beijing Key Laboratory of Green Chemical Reaction Engineering and Technology, Department of Chemical Engineering, Tsinghua University, Beijing 100084, China

Carbon nanotubes (CNTs) are the promising candidates for the novel integrated electronics. Whereas, it's a challenge to mediate their bandgap or chiral structures from a vapor-liquid-solid growth process. Here, we demonstrate the molecular evolution of ultralong semiconducting CNT (s-CNT) arrays based on an interlocking between the atomic assembly rate and bandgap of CNTs. Rate analysis verified the different evolutionary rates of metallic (m-) and s-CNTs as length increased. Quantitatively, a nearly ten-fold faster decay rate of m-CNTs, led to a spontaneous purification of 99.9999% s-CNTs at a length of 154 mm and wafer-scale ultralong CNTs with the maximum length up to 650 mm were achieved within a precisely designed micro reactor. Transistors fabricated on them delivered a high current of 1.4 mA/ μm with an on/off ratio around 10^8 and mobility over $4000 \text{ cm}^2/\text{V}\cdot\text{s}$.

Furthermore, ordered chirality-consistent CNT tangles and coils were synthesized by entangling an individual monochromatic ultralong CNT under the effect of “acoustic-induced vortices”. Each as-synthesized high-density CNT tangle was made of one self-entangled CNT with the length over 100 mm, tandem with a $(1\sim 10)\times 10^4 \mu\text{m}^2$ area range controlled by a minimum consumed energy model. Devices fabricated with the large-area CNT tangles exhibited unique photoelectronic properties with an on/off ratio up to $10^3\sim 10^6$ at 4 mA on-state current, which is also the highest output current record so far among single-CNT-based transistors. Our self-purification strategy based on molecular evolution offers more freedom to *in-situ* control the CNT purity and provides a robust method to synthesize perfectly entangled condensate over a wide length scale.

References

- [1] Zhu *et al.*, *Sci. Adv.* **2**, e1601572 (2016).
- [2] Zhu *et al.*, *ACS Nano* **15**, 5129 (2021).
- [3] Zhu *et al.*, *Nat. Commun.* **10**, 4467 (2019).
- [4] Zhu *et al.*, *Adv. Funct. Mater.* 2109401 (2021).
- [5] Zhu *et al.*, *Adv. Sci.* 2205025 (2022).
- [6] Zhu *et al.*, *Adv. Sci.* 2003078 (2021).

Biaxial Mechanical Densification of Vertically Aligned Boron Nitride Nanotubes

Armando R.C. Neto¹, Marianna Rogers¹, Luiz Acauan¹, Shweta Sharma¹, and Brian L. Wardle¹

¹Massachusetts Institute of Technology (United States of America)

With applications ranging from structural reinforcement to energy storage, boron nitride nanotubes (BNNTs) have recently gathered a lot of attention in the field of nanomaterials [1]. Hence, the intrinsic BNNT properties can be further enhanced by exploring the anisotropic aspect of nanotubes through the alignment of these 2D materials. Although the synthesis of vertically aligned BNNTs is possible [2], the volume fraction is around ~1%, which can limit, for example, their use as piezoelectric sensor/actuators [3]. Herein we demonstrate the technique of biaxial densification, previously used on vertically aligned carbon nanotubes (VA-CNTs) [4], increasing 4 times the volume fraction of VA-BNNTs.

Based on a process that coats VA-CNTs with hexagonal-boron nitride (VA-CNT/BN) and then removes the CNT scaffold by thermal oxidation [2], this study explores and compares three different routes for densifying VA-BNNTs: (1) biaxially densifying the VA-BNNTs directly; (2) biaxially densifying the VA-CNT/BN and posteriorly removing the VA-CNT scaffold or; (3) coating the pre-densified VA-CNTs with BN and posteriorly removing the VA-CNT scaffold.

In this work we demonstrated that method (3) results in a poor coating of CNTs with BN while method (1) creates a nonuniformly densified VA-BNNT structure that breaks easily upon release of the densifying forces. Method (2), contrarily, achieves a homogeneously densified VA-BNNT structure after removal of the VA-CNT scaffold. These results indicate that further densification is achievable through the same methodology, enabling applications where high-volume fraction is needed.



Biaxial Mechanical Densification: Schematic of the biaxial mechanical densification process (left side), VA-CNT/BN compressed (middle) and final compressed VA-BNNT after CNT removal (right side).

References

- [1] J.H. Kim *et al.*, *Nano Convergence* **5**, 17 (2018).
- [2] L. H. Acauan *et al.*, *ACS Nano* **16**, 18178 (2022).
- [3] J. H. Kang *et al.*, *ACS Nano* **12**, 11942 (2015).
- [4] B.L. Wardle *et al.*, *Adv. Mater.* **20**, 2707 (2008).

Biosensors based on MWCNT

O.Tiprișan, O. Liliana

Faculty of Physics, Babes-Bolyai University of Cluj-Napoca, Romania
National Institute for R&D in Isotopic and Molecular Technologies, Cluj-Napoca, Romania

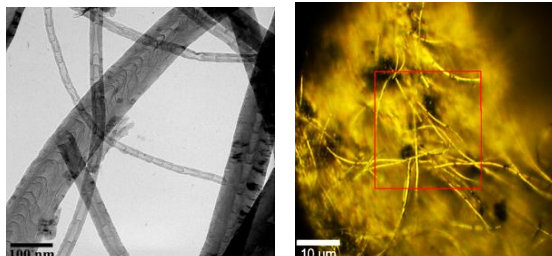
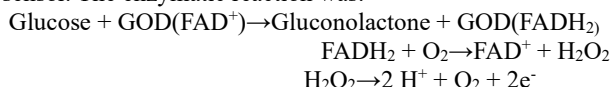
INTRODUCTION

In this paper we described the investigation of the absorption properties of carbon nanotubes with respect to absorbates of biological origin (amino acids :alanine, aspartic acid glutamic acid and enzyme :glucose oxidase).

EXPERIMENTAL

Carbon nanotubes (CNT) were prepared by CVD method, using spray pyrolysis method. The CNT were purified in 40% H₂SO₄. The enzyme activity of immobilized GOD was determined by amperometric method[1].

The enzyme immobilized on CNT was used as an amperometric sensor. The enzymatic reaction was:



The glucose oxidase(GOD) concentration was determined by Bradford method.

RESULTS AND DISCUSSIONS

We have reported that glucose oxidase adsorbs preferentially to edge-plane sites on nanotubes. It has been established that such sites contain a significant amount of oxygenated functionalities. The hydrophilicity and ionic character of the nanotubes are responsible for the 'nesting' of the protein on the nanotube film. This may well increase the permeability of the void space between the tubes to increased quantities of electrolyte ions which will result in a change in the interfacial potential distribution.[2-6]

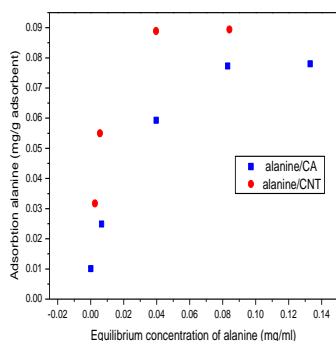


Fig.1

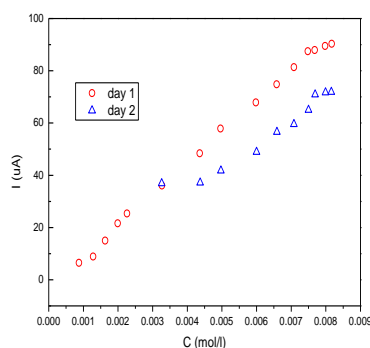


Fig.2

The adsorption isotherms of alanine and aspartic acid on CNT and CA (Fig.1)

That attachment of GOx to high surface area of MWCNTs facilitates a higher rate of direct electron transfer between the active sites of immobilized GOx, which, can increase the peak current at when the sample was injected. First the calibration curve was recorded until the electrical signal reached saturation (the glucose concentration was about 0.008 M. (Fig.2) [7-14]

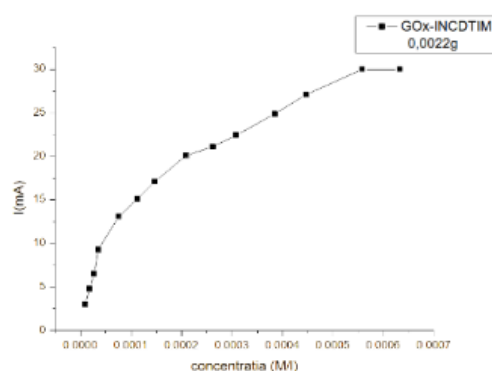
CONCLUSIONS

The adsorption of amino acids on CNT increase due to the molecular weight and the acid-base groups of amino acid molecule. The morphology structure of CNT is responsible for the greater stability of immobilized enzyme than the enzyme used in solution. The similarity in length scales between nanotubes and redox enzymes suggest the presence of interactions that may be favourable for biosensor electrode applications. [15-21]

Enzyme activity and biosensor response

REFERENCES

- [1]G.A.Kovalenko, E.V.Kuznetova, Yu.I.Mogilnykh, I.S.Andreeva, D.G.Kuvshinov, N.A.Rudina, Carbon 39 (2001) 1033-1043.
- [2]Practical Guide, Cambridge University, Department of Biochemistry,2003
- [3]H.H.P.Bhowmik, B.Zhao, M.A.Hamon, M.E.Itkis, R.C.Haddon, Chem.Phys.Lett. 345(2001) 25-28 [4]...[21].



Burst Nucleation of Matrix on Doped Graphene for Quantitative MALDI-ToF Mass Spectrometry with Tunable Ion Yield

Sanghwan Park¹, Chang Young Lee^{1,2}

*¹School of Energy and Chemical Engineering, ²Graduate School of Carbon Neutrality
Ulsan National Institute of Science and Technology (UNIST), Ulsan 44919, Republic of Korea*

Matrix-assisted laser desorption/ionization time-of-flight mass spectrometry (MALDI-ToF MS) is an effective and widely used mass spectrometric approach that provides multiple information of biomolecules such as structural characterization and label-free identification. Quantitation using MALDI MS, however, has been limited mainly due to uncontrollable ion yield in MALDI MS resulting from heterogeneous cocrystallization of analyte and matrix. In this work, we observed the highly uniform formation of matrix crystals on graphene surface via preferential nucleation of the matrix on the graphene surface. The uniformly distributed analyte-matrix cocrystal films formed on graphene substrate allow highly reproducible mass spectra with improved mass resolution and mass accuracy. Based on the area of MALDI MS laser irradiation, the amount of analyzed peptide at a defined area can be estimated, allowing the direct measurement of ion yield of MALDI MS. In addition, we demonstrate that ion yield of MALDI MS can be tuned by controlling the electron and hole doping of the graphene substrates, thus enabling selective suppression of spectral interference or enhancing the ion yields of the analyte signal. Finally, with a constant ion yield, we demonstrate that the total ion count of analyte ion is linearly corresponding to amount of analyte, thus enabling absolute quantitation of analyte in MALDI MS.

Carbon nanotube electron blackbody and its radiation spectra

Ke Zhang¹, Guo Chen², Kaili Jiang^{2,3}

¹*Fert Beijing Research Institute, School of Microelectronics & Beijing Advanced Innovation Centre for Big Data and Brain Computing (BDBC), Beihang University, Beijing 100191, China*

²*State Key Laboratory of Low-Dimensional Quantum Physics, Department of Physics, Tsinghua University, Beijing 100084, China*

³*Collaborative Innovation Center of Quantum Matter, Beijing 100084, China*

Optical blackbody is an ideal absorber for all incident radiations, and theoretical study of its radiation spectra opens the door to quantum mechanics (Planck's law). Meanwhile, blackbody materials continues to evolve, from black paint to NiP alloy, and recently carbon nanotubes, of which the standard radiation spectra have played crucial roles in IR calibration. Here we proposed the concept of electron blackbody, which is a perfect electron absorber, as well as an emitter of electrons with standard energy spectra at different temperatures. It is found that vertically aligned carbon nanotube array (VACNTA) is such an electron black body. The unique structure of VACNTA and the small secondary electron emission coefficient of carbon atom make it an ideal electron trap with the corresponding electron absorption coefficient of around 0.95 for incident electrons' energy ranging from 1 keV to 20 keV. At high temperatures, it shows electron emission spectra which fits well with the free electron gas model, holding the promise to be a calibration standard in the field of electron spectroscopy. Such a concept might also be generalized to blackbodies for neutrons, protons, and other fundamental particles.

Carbon Nanotube Fiber Production for Displacement of Difficult to Decarbonize Structural Materials with Free Hydrogen Co-production

A. Dantzer^{1,2,3}, O. Dewey^{1,2,3,4}, A. Sloan^{1,2,3,5,6}, R. Headrick⁷, G. C. Irvin Jr.^{1,2,3}, M. Pasquali^{1,2,3}

¹Chemical and Biomolecular Engineering Dept., Rice University (USA), ²Smalley Curl Institute (USA), ³Carbon Hub (USA), ⁴Dexmat (USA), ⁵Materials and Manufacturing Directorate, AFRL (USA), ⁶National Research Council (USA), ⁷Next Generation Breakthrough Research, Materials Chemistry, Shell (USA)

Manufacturing structural materials is responsible for an enormous amount of CO₂ emissions, with steel alone constituting ~7% of global CO₂ annually [1]. Structural materials like metals and cement are required in large volumes for infrastructure, and the manufacturing processes are CO₂ intensive and considered difficult to decarbonize because of stoichiometric emissions from high-temperature reduction steps. Lower CO₂ intensity alternatives with similar or better engineering properties are needed.

High-performance materials like carbon fiber seek to address these issues by requiring less material to meet the same strength requirements due to high strengths and low densities; however, the many-step process to produce carbon fiber is low efficiency, and ~50% of original feedstock mass is lost during a high-temperature carbonization step. Despite decades of commercial development, carbon fiber has yet to meet the cost demands for large-scale structural applications.

Carbon nanotube fibers (CNTF) and their macrostructures (e.g., yarns, woven mats) have much higher predicted strength and electrical/thermal conductivity than carbon fiber, similar density, and a simpler manufacturing process, and thus a lower floor for production cost and environmental footprint. Research on CNTF to date has largely focused on property improvement, but with the reported tensile strength of CNT fibers already an order of magnitude higher than steel (on mass basis) and demonstrated doubling of fiber properties every three years [2], the question of scalability becomes important [3].

Here, we introduce a life cycle analysis (LCA) model for the scale-up of CNT production with H₂ co-production via methane pyrolysis and CNTF spinning. The model supposes plant-scale unit operations but uses current lab-scale conditions such as reaction conversion, selectivity, temperature, and spinning concentration. The model outputs environmental footprint as measured by CNTF CO₂ intensity and embodied energy. With current experimental CNT reactor and spinning conditions, CNTF is estimated to have a better environmental footprint than steel and carbon fiber, and approaching that of copper and aluminum, when considering the specific tensile strength, specific thermal conductivity, and specific electrical conductivity per environmental footprint. The LCA model highlights key parameters needed to drive down environmental footprints and production cost, which is strongly a function of embodied energy. This tractable model, confirmed by process simulation (Aspen Plus), points to areas for focused research and investment to push CNTF along its learning curve and towards a new carbon materials economy.

References

- [1] IEA (2020), Iron and Steel Technology Roadmap, <https://www.iea.org/reports/iron-and-steel-technology-roadmap>
- [2] Taylor *et al.*, *Carbon* **171**, 689-694 (2021).
- [3] Pasquali, Mesters, *PNAS* **118** 31 (2021).

Carbon Nanotube Platform for Virus Enrichment and Detection

Yin-Ting Yeh^{1,3}, Morinobu Endo², Elodie Ghedin¹, and Mauricio Terrones³

¹National Institute of Health, Bethesda, MD USA

²Shinshu University, Nagano, Japan

³The Pennsylvania State University, University Park, PA USA

Emerging and re-emerging viruses are responsible for a number of recent epidemic outbreaks. A crucial step in predicting and controlling outbreaks is the timely and accurate characterization of emerging virus strains. However, surveillance efforts by sequence-specific identification or capture are limited by the high evolvability of viruses. We present a portable platform, composed of aligned multiwall carbon nanotubes and embedded gold nanoparticles, for the rapid enrichment and optical identification of viruses. Different emerging strains (or unknown viruses) can be enriched and identified in real time, through a multi-virus capture component in conjunction with surface-enhanced Raman spectroscopy. More importantly, after rapid viral capture and detection on-a-chip, viruses remain viable and can be purified in a microdevice that permits subsequent in-depth characterizations by various conventional methods, i.e., polymerase chain reaction and next generation sequencing. We validated this platform using different subtypes of avian influenza A viruses and human samples with respiratory infections. This platform successfully enriched rhinovirus, influenza virus, and parainfluenza viruses, and maintained the stoichiometric viral proportions when the samples contained more than one type of virus, thus emulating coinfection. Viral capture and detection took only a few minutes with two orders of magnitude decrease in host contaminants and detection could be achieved with as little as 10^2 EID₅₀/mL, with a virus specificity of 90%. After enrichment using the device, we demonstrated by sequencing that the abundance of viral-specific reads significantly increased from 4.1% to 31.8% for parainfluenza and from 0.08% to 0.44% for influenza virus. This enrichment method coupled to Raman virus identification constitutes an innovative system that could be used to quickly track and monitor viral outbreaks in real-time.

Carbon Nanotube/Bismaleimide Nanocomposite Laminates with Ultrahigh Nanofiber Volume Fraction

Carina Xiaochen Li¹, Yuying Lin¹, Jingyao Dai¹, Marianna Rogers², Erick Gonzalez¹, Chloe Curtis-Smith¹, Luiz H. Acauan¹, Ashley L. Kaiser¹, Jeonyoon Lee¹, and Brian L. Wardle^{1,2}

¹*Department of Aeronautics and Astronautics, Massachusetts Institute of Technology (United States)*

²*Department of Mechanical Engineering, Massachusetts Institute of Technology (United States)*

Aligned carbon nanotubes (CNTs), known for their advantageous mass-specific mechanical properties such as elastic modulus and strength, along with high electrical conductivity and unique property, are excellent candidates for reinforcing polymer nanocomposites (PNCs) for structural and multifunctional applications. Achieving enhanced PNC properties necessitates a uniform and densely packed distribution of aligned CNTs. However, past methods for creating CNT-reinforced PNCs often led to challenges like low CNT density (< 10 vol%), agglomeration, and uneven fiber distribution, hindering optimal property enhancement. In this study, we introduce a novel bulk nanocomposite laminating (BNL) process, facilitating scalable production of CNT-reinforced nanocomposite plies and laminates with horizontally-aligned CNT distribution and a nanofiber density exceeding 50 vol%. We successfully fabricated centimeter-scale CNT/Bismaleimide (BMI) polymer nanocomposite laminates with CNT volumes fraction of ranging from 37 to 52 vol%, and explored their process-structure-property relationships through various analytical techniques, including tensile testing, scanning electron microscopy, X-ray micro-computed tomography, thermogravimetric analysis, electrical conductivity test, and polarized Raman. This research offers insights into the impact of high CNT densities (> 50 vol%) on the properties of aerospace-grade bismaleimide thermoset resins, aiding in the development of next-generation high volume fraction PNCs with enhanced mechanical and multifunctional characteristics.

Carbon Nanotube-based FET Arrays for Integrated Biosensor Platforms

L. Alves da Silva^{1,2}, S. Hermann^{1,2}

1 Center for Materials, Architectures and Integration of Nanomembranes (MAIN) - TU Chemnitz, Chemnitz, 09126, Germany

2 Center for Advancing Electronics Dresden (cfaed), - TU Chemnitz, Chemnitz, 09126, Germany

Biosensors target the detection of biological moieties such as biomarkers for diseases and biomolecules in general. (1) Field-effect transistors (FET) have been exploited as electrochemical transducers where the output signal is monitored in real-time, allowing a label-free detection and device miniaturization favoring emerging point-of-care platforms. (2, 3) Carbon nanotube field-effect transistors (CNT-FETs) is an ideal sensor basis. (3) Their one-dimensional structure promotes highly sensitive biosensors (BioFET) (2) when combined with biological receptors. Therefore, such devices can reach detection levels in the pico- and nanomolar range, opening doors for applications like early detection of diseases or low-concentration targets, while avoiding exhaustive sample preparation steps used in common detection methods. In this work, CNT-based BioFETs were fabricated under Fab-compatible conditions on a 200 mm wafer level. The FETs were gated in a saline buffer and their reliability and reproducibility could be ensured, where the transistor parameters such as $I_{on}/I_{off} > 10^4$ and low gate current were monitored for over 2 hours, with negligible drift on the drain current. For biosensor investigations, we applied a controlled microfluidic environment enabling automatized parallel studies of many FETs with channel lengths of 5 and 10 μm . The sensing area was functionalized with 5 μM capture ssDNA (cDNA) and FETs were electrolyte-gated over Pt gates close of the FETs. We show systematic studies on the sensitivity and dynamics of the interaction with fully complementary target DNAs (tDNA) in a concentration range from 0.1 to 10 nM. Selectivity was confirmed by respective non-complementary target DNA. In addition, studies were conducted to understand the binding dynamics, especially for very low concentrations on the detection of the 0.1 nM tDNA. Finally, we illuminate the reproducibility of sensor properties based on parallel readout of many devices per experiment and comparisons between different studies.

References

- [1] Li, T. X. *et al.*, *Analytical Chemistry*, **93** N. 46 15501–15507 (2021).
- [2] Shkodra, B. *et al.*, *Applied Physics Reviews*, **8**, N. 4 41325 (2021).
- [3] Saikia, O. *et al.*, *Materials Today: Proceedings*, 2214-7853 (2023).

Carbon Nanotube-based Strain-Configurable Nanodevices

S. Böttger^{1,2}, M. Hartmann^{1,2}, S. Hermann^{1,2,3}

¹Center for Microtechnologies, Chemnitz University of Technology, 09116 Chemnitz (Germany),

²Center for Materials, Architectures and Integration of Nanomembranes, 09126 Chemnitz (Germany)

³Fraunhofer Institute for Electronic Nano Systems, 09126 Chemnitz (Germany)

The incorporation of mechanical strain in integrated nanomaterials such as carbon nanotubes (CNTs) is a necessary and ambitious task to fully enfold their diverse properties for a wide range of applications. On the material side, external strain allows to broadband tune the nanomaterial properties such as the bandgap. For CNT-based device, tensile strain holds the potential to mitigate issues related to inhomogeneous assembly structures and reduce parasitic slack effects as has been observed in *e.g.* CNT nanoresonators. Notably, inadequate strain conditions like slack and hang-trough of suspended CNTs can lead to a short-term degradation of the resonance frequency by 60 % [1, 2], accompanied by undesired multi-mode oscillation [3]. Consequently, the local variation of strain in suspended nanomaterials promises technological advances as well as manifold exploitation in *e.g.* tunable optical emitters/absorbers, nanoresonator-based sensors, or even in quantum devices [4, 5].

On the example of suspended CNT-based nanodevices, we show a comprehensive strain technology which allows to control incorporated strain by device design and fabrication process conditions. These nanodevices are fabricated using a sacrificial layer approach with residual stressed membranes for strain relaxation as shown in figure 1. By means of dimension-limited self-assembly, semiconducting CNTs were assembled perpendicular to pre-structured trenches, so that the membrane stress is transferred into longitudinal CNT strain. Manufactured as CNT-based field-effect transistors, these nanodevices are organized in arrays with configurable strain states. The strain states are determined by means of Raman spectroscopy of the strain-dependent G^+ mode [6, 7]. We finally emphasize the manifold exploitation possibilities of this approach on the example of a piezoresistive CNT transducer with 40 % improvement of the detection limit.

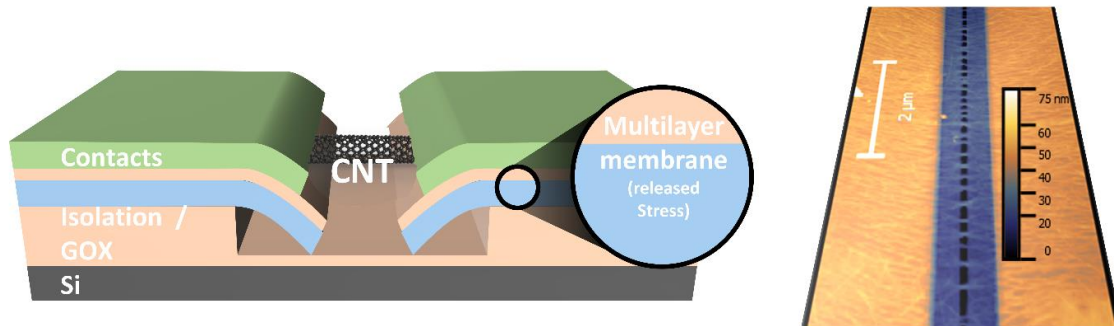


Figure 1: Schematic of the CNT-based nanodevices (left) and atomic force microscopy image at intermediate manufacturing state with self-assembled CNTs over a pre-structured trench.

References

- [1] M. Vollmann, *et al.*, in *2023 IEEE 36th International Conference on Micro Electro Mechanical Systems Conference (MEMS)*, 925, (2023)
- [2] L. Kumar *et al.*, *Journal of Applied Physics* **126**, 184302, (2019)
- [3] Z. Ning *et al.*, *Nanoscale* **8**, 8658, (2016)
- [4] J.-S. Chen *et al.*, *Nature communications* **14**, 848, (2023)
- [5] A. Baydin *et al.*, *Materials* **15**, (2022)
- [6] S. Böttger *et al.*, in *2022 Smart Systems Integration (SSI)*, 1, (2022)
- [7] Z. Liu *et al.*, *Chemical communications*, 6902, (2009)

Chalcogen Anion Type-Dependent Efficiency of Synthesizing Janus Monolayer Transition Metal Dichalcogenides by Atomic-Layer Substitution

T. Zhang¹, K. Xie², Z. Yu³, J.H. Park¹, A.Y. Lu¹, K. Zhang⁴, W. Wu⁴, S. Huang⁴, M. Terrones³, Y. Guo⁵, T. Cao², J. Kong¹

¹*Department of Electrical Engineering and Computer Science, Massachusetts Institute of Technology (USA),*
²*Department of Materials Science and Engineering, University of Washington (USA),* ³*Department of Materials Science and Engineering, The Pennsylvania State University (USA),* ⁴*Department of Electrical Engineering, Rice University (USA),* ⁵*Key Laboratory of Excited-State Materials of Zhejiang Province, Department of Chemistry, State Key Laboratory of Silicon and Advanced Semiconductor Materials, Zhejiang University (China).*

Janus monolayer transition metal dichalcogenides (TMDs) are a unique category of two-dimensional (2D) materials with intriguing properties arising from their out-of-plane asymmetry and inherent electric dipole. Room-temperature (RT) synthesis and patterning of Janus TMDs have recently been realized through an atomic-layer substitution (ALS) approach that steers the reaction pathway in a diverse energy landscape compared to the high-temperature process [1]. In principle, the RT-ALS synthesis of MSSe-type Janus TMDs (M = Mo, W, etc.) can start from either MS₂ or MSe₂, but the associated energy landscapes of these pathways may vary, influencing the reaction efficiency. Herein, we investigate the conversion of Janus MSSe monolayers from MS₂ and MSe₂ prepared by different methods, and our experimental results indicate that the RT-ALS process is more efficient and has a broader reaction window for converting MSe₂ to MSeS than starting the conversion from MS₂. Density functional theory calculations reveal that the reaction energy barrier and overall reaction energy are considerably lower when MSe₂ is employed as the starting material, agreeing with experimental findings. These results improve our understanding of the RT-ALS process, and provide useful guidance for the future design of optimum reaction pathways for various Janus materials with high yield, enhanced uniformity, and controlled dipole orientations.

Reference

[1] Y. Guo *et al.*, *Proc. Natl. Acad. Sci. U.S.A.* **118**, e2106124118 (2021).

Characterization of Carbon Nanotube / Poly(Methyl Methacrylate) Bulk Nanocomposite Laminate and Filament

Yuying Lin¹, Carina X. Li¹, Erick Gonzalez¹, Jingyao Dai¹, Luiz H. Acauan¹, Brian L. Wardle^{1,2}

¹*Department of Aeronautics and Astronautics, Massachusetts Institute of Technology (USA)*, ²*Department of Mechanical Engineering, Massachusetts Institute of Technology (USA)*

Aligned carbon nanotubes (CNTs) have numerous high mass-specific physical properties, including strength, elastic modulus, thermal conductivity, and electrical conductivity, making them excellent reinforcements for polymer nanocomposites (PNCs) with potential applications in both structural reinforcement and multifunctionality. These advantageous properties of CNTs are best realized when the fibers are aligned and densely packed within the polymer matrix. However, in conventional fabrication methods for CNT-reinforced PNCs, nanofibers are randomly dispersed in the matrix, which results in low packing density and agglomeration of fibers. These characteristics make it challenging to fully exploit the benefits of reinforcing PNCs with CNTs. In previous work, the fabrication of high volume fraction PNCs using the bulk nanocomposite laminate (BNL) process was demonstrated for the aerospace-grade thermoset polymer bismaleimide (BMI). PNC laminates containing uniform, horizontally-aligned and highly-dense CNTs at volume fractions of > 50 vol% were achieved. Recently, there has been an increased interest in thermoplastic polymer matrix composites due to their recyclability and simple processing; they have also been used extensively in aerospace and civil structures due to their high ductility, recyclability, and repairability. The BNL process was adapted to fabricate a CNT-reinforced PNC with a thermoplastic matrix, poly(methyl methacrylate) (PMMA). Characterization of the CNT/PMMA composites showed CNT content > 45 vol% with a void-free morphology. The T_g of the PMMA matrix is unaffected by the presence of CNTs. Further characterization of the laminates through IR spectroscopy shows that the BNL process does not chemically alter CNTs and PMMA. Polarized Raman measurements demonstrate that the alignment of CNTs is maintained throughout the fabrication process. In addition, a 790mm \times 1.75mm filament-width sample was fabricated; preliminary results give minimum radius of curvature \sim 2mm. Combining the high mass-specific properties and multifunctionality of aligned CNTs with the rapid processability of thermoplastics, the thermoplastic BNL is a scalable candidate for applications in additive manufacturing and electronics.

Charge transport characteristics in non-van der Waals 2D transition metal nitrides synthesized via atomic substitution approach

Hongze Gao¹, Da Zhou², Zifan Wang¹, Lu Ping³, Jun Cao¹, Mauricio Terrones², Xi Ling^{1,3}

¹*Boston University, Department of Chemistry (U.S.A.),* ²*Department of Physics, Penn State University (U.S.A.)* ³*Division of Materials Science and Engineering, Boston University (U.S.A.)*

Abstract

Two-dimensional (2D) materials have been extensively explored in the past decade to advance the development of nanoelectronic devices by virtue of their exciting properties emerging at the reduced dimension. Numerous 2D crystals have been synthesized and studied, including graphene, transition metal dichalcogenides (TMDs), and h-BN, which are van der Waals (vdW) layered materials with vdW gaps between two adjacent atomic layers. Such vdW gaps result in an anisotropic bonding in the crystal and hence a weak interlayer interaction, which facilitates the separation of ultra-thin layers of these crystals. In contrast, such gaps are absent in non-vdW crystals, imposing technical difficulties in the downscaling of these materials into 2D forms. Moreover, majority of experimentally known compounds possess non-vdW structures [1], which raises the demand for alternative synthesis approaches to obtain non-vdW 2D crystals in order to access unprecedented properties at the 2D limit. Targeting on this challenge, our group developed an atomic substitution approach to prepare ultra-thin non-vdW 2D crystals, where vdW 2D crystals (e.g., MoS₂ and WSe₂) are used as precursors and converted into non-vdW materials through a chemical reaction [2-5]. Non-vdW 2D metal nitrides (MN_x) (e.g., Mo₅N₆ and W₅N₆) with high crystallinity, smooth surface, and well controlled thicknesses have been successfully synthesized. Hereby, we further investigated the charge transport characteristics in these 2D MN_x prepared through the atomic substitution approach. Four probe electrical measurements show that MoN_x and WN_x exhibit relatively high electrical conductivity with δ-MoN being the most conductive ($\sigma = 3126$ S/cm), comparable to widely studied Ti₃C₂T_x. Hall measurements show high 2D carrier concentrations of the MN_x in the order of $10^{16}\sim 10^{17}$ /cm², which is comparable to that of Au thin film with similar thicknesses. . Temperature-dependent resistance (R-T) measurements further revealed the thermal excitation mechanisms and weak localization effect in the charge transport behaviors of the 2D MN_x.

Reference

- [1] N. Mounet *et al.*, *Nat. Nanotechnol.*, **13**(3), 246–252 (2018).
- [2] J. Cao *et al.*, *Sci. Adv.*, **6**(2), eaax8784 (2020).
- [3] H. Gao *et al.*, *Chem. Mater.*, **34**(1), 351-357 (2022).
- [4] T. Li *et al.*, *ACS Appl. Mater Interfaces*, **14**(51), 57144-57152 (2022).
- [5] J. Cao *et al.*, *J. Electron. Mater.*, **52**(11), 7554-7565 (2023).

Chemical Bonding of Carbon Nanotubes with Metals as a Promising Path for Hybrid Materials Development

Noe T. Alvarez^{†*}, Chaminda P. Nawarathne[†], Jorge Seminario[‡] and Diego G. Aranda[‡]

[†]Department of Chemistry, University of Cincinnati, Cincinnati, OH 45221, USA

[‡]Department of Chemical Eng., Texas A&M University, College Station, TX, 77843, USA

*E-mail: alvarene@ucmail.uc.edu

This talk will report fundamental calculations and experimental results for chemical bond formation of open-ended vertically oriented carbon nanotubes (CNTs) to copper metal surfaces.¹ Chemical bonds, preferentially covalent, between metal atoms and functional groups (linkers) at the open ends of CNTs is highly desired in order to create a robust connection and anchoring the CNTs to macroscopic metal surfaces.²⁻³ In addition, a chemical connection between metals and CNTs is critical for wiring two metals through a single CNT.⁴⁻⁵ Unlike traditional methods that rely on synthesis, where good quality CNTs are grown directly on metal substrates at temperatures above 600 °C this method reports covalent bond formation at temperatures as low as 120 °C.^{1, 6-7} The reported theoretical calculations demonstrate that C atoms on aminophenyl can form a bridge like covalent bonds with two adjacent Cu atoms on (100), (110), and linear bond on (111) Cu crystal lattice substrates. The strength of the bonding was experimentally evaluated by placing the hybrid (CNT/Cu) material in solution and exposing to bath sonication. To our surprise, the CNTs remained attached to the substrate even after 30 min sonication. In addition, adhesive tape was applied to remove the bonded CNT array from the metal surface. The area from where CNT arrays were removed revealed that some CNTs still remained attached to the copper surface, supporting the strong bonding to the metal. XPS, FT-IR, Raman analysis and scanning electron microscopy images support the formation of direct connections between the vertically aligned CNTs and the metal substrates.⁷ The reported covalent bond formation is expected to facilitate the application of CNTs in multiple fields such as biomaterials, electrocatalysis, sensor development and electronics.

1. Nawarathne, C. P.; Aranda, D. G.; Hoque, A.; Dangel, G. R.; Seminario, J. M.; Alvarez, N. T., *Nanoscale Adv* **2024**, 6 (2), 428-442.
2. Kaur, S.; Raravikar, N.; Helms, B. A.; Prasher, R.; Ogletree, D. F., *Nature Comm.* **2014**, 5, 3082, 1-8.
3. Daneshvar, F.; Chen, H.; Noh, K.; Sue, H.-J., *Nanoscale Advances* **2021**, 3 (4), 942-962.
4. Fediai, A.; Ryndyk, D. A.; Cuniberti, G., *Physical Review B* **2015**, 91 (16).
5. Gao, F.; Qu, J.; Yao, M., *Journal of Electronic Packaging* **2011**, 133, 020908 (2), 1-4.
6. Nawarathne, C. P.; Hoque, A.; Ruhunage, C. K.; Rahm, C. E.; Alvarez, N. T., *Applied Sciences-Basel* **2021**, 11 (20).
7. Nawarathne, C. P.; Hoque, A.; Dangel, G. R.; Alvarez, N. T., *ACS Applied Nano Materials* **2023**, 6 (23), 22001-22014.

Chemical substitution effect in trigonal PtBi₂ with a triply degenerate point

T. Suzuki¹, Y. Oda¹, H. Inoue², R. Mikawa³, H. Takei³, and T. Katsufuji^{3,4}

¹Dept. of Phys., Toho Univ. (Japan), ²National Institute of Advanced Science and Technology (Japan), ³Dept. of Phys., Waseda University (Japan), ⁴Kagami Memorial Research Institute for Materials Science and Technology, Waseda University (Japan)

A crossing of linearly dispersing electronic bands is responsible for various unusual material properties [1]. A graphene has a four-fold degenerate crossing point of doubly degenerate linear dispersing band, called Dirac point, at K and K' points in the Brillouin zone and exhibits quantum Hall effect [2]. Furthermore, a doubly degenerate point from non-degenerate linear band crossing is found in many three-dimensional materials without combined symmetry of time-reversal and inversion. This crossing point (Weyl point) with characteristic chirality behaves as a sink or a source of Berry curvature and gives rise to topologically nontrivial properties including the presence of Fermi arc surface state and negative longitudinal magnetoresistance [1, 3]. In addition, recent classification of electronic band structure based on lattice symmetry reveals that the additional type of crossing beyond the fundamental Dirac and Weyl points are stabilized by crystallographic symmetry [4]. While such an advanced crossing has a potential to exhibit exotic properties due to their character as unconventional quasiparticles, they have been yet observed experimentally.

Trigonal PtBi₂ has a layered crystal structure without inversion symmetry and is theoretically proposed to possess topologically nontrivial triply degenerate crossing point of non-degenerate and doubly degenerate bands protected by crystallographic symmetry at ~ 0.3 eV above the Fermi level [5,6]. In addition, superconductivity is reported in the pristine PtBi₂ with thin flake form, the bulk PtBi₂ under pressure, as well as the hole-doped bulk compound [7–9]. In this presentation, we discuss the detailed chemical substitution effect on the thermodynamic and transport properties of the bulk trigonal PtBi₂.

References

- [1] N. P. Armitage *et al.*, *Rev. Mod. Phys.* **90**, 015001 (2018).
- [2] Y. Zhang *et al.*, *Nature* **438**, 201–204 (2005).
- [3] B. Yan and C. Felser, *Annu. Rev. Condens. Matter Phys.* **8**, 337–354 (2017).
- [4] B. Bradlyn *et al.*, *Science* **353**, aaf5037 (2016).
- [5] Z. Zhu *et al.*, *Phys. Rev. X* **6**, 031003 (2016).
- [6] W. Gao *et al.*, *Nature Commun.* **9**, 3249 (2018).
- [7] A. Veyrat *et al.*, *Nano Lett.* **23**, 1229–1235 (2023).
- [8] J. Wang *et al.*, *Phys. Rev. B* **103**, 014507 (2021).
- [9] G. Shipunov *et al.*, *Phys. Rev. Mater.* **4**, 124202 (2020).

CHEMICAL VAPOR DEPOSITION SYNTHESIS AND ANISOTROPIC OPTICAL PROPERTIES OF 1T'-PHASE WS₂ ATOMIC LAYERS

M. Okada¹, Y.-C. Lin¹, T. Matsumura¹, A. Smiri, W. H. Chang¹, N. Okada¹, Y. Ando¹,
T. Kubo¹, K. Suenaga^{1,2}, T. Nakanishi, T. Irisawa¹, T. Yamada¹

¹AIST (Japan), ²Osaka Univ. (Japan)

WS₂ possesses a metastable, monoclinic structure known as 1T'-phase (Fig. 1a). The 1T'-phase WS₂ is semimetallic and is anticipated to function as a topological superconductor and a catalyst for hydrogen evolution [1]. However, synthesizing 1T'-phase WS₂ is challenging due to the large phase transition barrier and energy difference from the most stable 2H-phase [2]. In this study, we report the synthesis of 1T'-phase WS₂ using chemical vapor deposition (CVD) synthesis [3] and detail the determination of its crystallographic orientation via polarized Raman spectroscopy. Our research contributes to the expansion of the field of 2D materials through phase engineering.

1T'-phase WS₂ was synthesized via the CVD method, employing H₂S and WF₆ as precursors and NaCl as a growth promoter. Figure 1b displays typical optical images of WS₂ grown under various conditions. As observed, adjusting the concentration of H₂S and/or NaCl alters the contrast of the crystals (Fig. 1b). Raman spectra (Fig. 1c) reveal that the WS₂ crystals (Fig. 1b center) with brighter regions are in the 2H-phase, while darker areas indicate the 1T'-phase. These results demonstrate that varying the concentration of H₂S and/or NaCl enables the synthesis of WS₂ with different crystal phases, including pure 2H-phase (Fig. 1b left), pure 1T'-phase (Fig. 1b right), and a mixture of these two phases (Fig. 1b center).

Owing to the zigzag W-W chain structure of 1T'-phase WS₂ (Fig. 1a), the material exhibits in-plane anisotropic properties. Therefore, determining the crystallographic orientation of 1T'-phase WS₂ is essential. We utilized polarized Raman spectroscopy to correlate structure with optical response. Figure 1d illustrates the evolution of peak intensity, which is angle-dependent, for the Raman peak around 410 cm⁻¹ (identified as A_g² peak from group theory and density functional theory calculations) under a parallel-polarization configuration. The orientation of the zigzag W-W chain was set at 0° parallel. As shown in Fig. 1d, the peak intensity reaches its maximum when the zigzag W-W chain aligns parallel to the polarization of the excitation laser. Hence, the crystallographic orientation of 1T'-phase WS₂ can be determined by polarized Raman spectroscopy.

In conclusion, we have successfully synthesized 1T'-phase WS₂ and investigated its anisotropic optical properties, thereby determining its crystallographic orientation. The synthesis and characterization of metastable WS₂ herald a new research avenue in the field of layered materials.

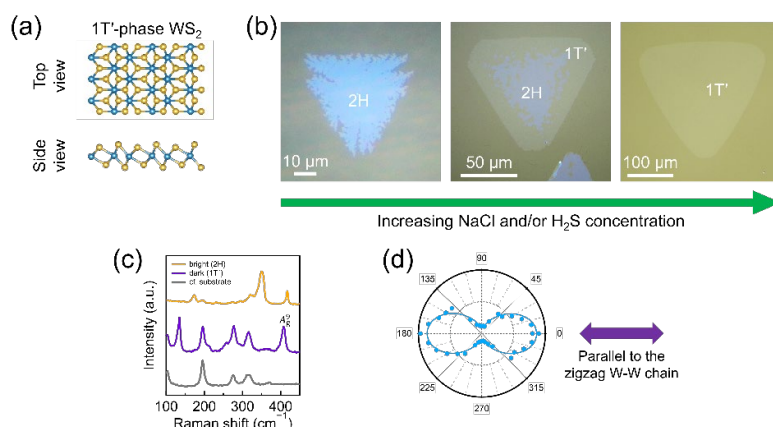


Figure caption: (a) schematics of 1T'-phase WS₂ structure. (b) optical images of WS₂ grown under various growth condition. (c) Raman spectra of obtained WS₂. (d) Polar plot of A_g² peak intensity under parallel-polarized configuration. (a-c): Reprinted with permission from Ref. 3. Copyright 2022 American Chemical Society.

References

- [1] H. H. Huang *et al.*, *Nanoscale* **12**, 1247–1268 (2020).
- [2] U. Patil *et al.*, *Phys. Rev. B* **100**, 075424 (2019).
- [3] M. Okada *et al.*, *ACS Nano* **16**, 13069–13081 (2022).

Chiral dependent growth modes of carbon nanotubes from machine learning driven molecular dynamics

Daniel Hedman¹, Christophe Bichara²

¹Center for Multidimensional Carbon Materials (CMCM), Institute for Basic Science (IBS) (Republic of Korea),

²Aix-Marseille Université, CNRS, CINaM (France)

A widely accepted mechanism to describe the growth of carbon nanotubes (CNTs) is dislocation growth or spiral growth[1]. However, this mechanism overlooks the role of the configurational entropy of the growing CNT-edge[2]. Which propose that the number of armchair pairs and zigzag atoms can fluctuate and is therefore not necessarily the same as the edge of a perpendicularly cut tube. Configurational entropy of growing CNT-edges was recently demonstrated via machine learning force field (MLFF) driven molecular dynamics (MD) simulations[3].

Here, we delve deeper into the configuration of the CNT-edge during growth. Using an updated version of our DeepCNT-22 MLFF, we perform microsecond MD simulations of CNTs with different chiralities attached to an Fe₁₄₇ cluster. Our preliminary results shown in Figure 1 reveal that CNTs with a chiral angle larger than $\sim 8^\circ$ have no dominant edge configurations during growth, indicating a high configurational entropy. Conversely, tubes with lower chiral angles show dominant edge configurations, with specific cases such as the (13,1) and (14,0) CNTs having only a single predominant edge configuration. Our results thus show a significant shift in the growth modes of CNTs as a function of their chiral angle, transition from high to low configurational entropy at the edge. This suggests that the growth mechanisms of CNTs are more complex than previously presumed and warrants further investigation into the mechanism of CNT growth at the atomic scale.

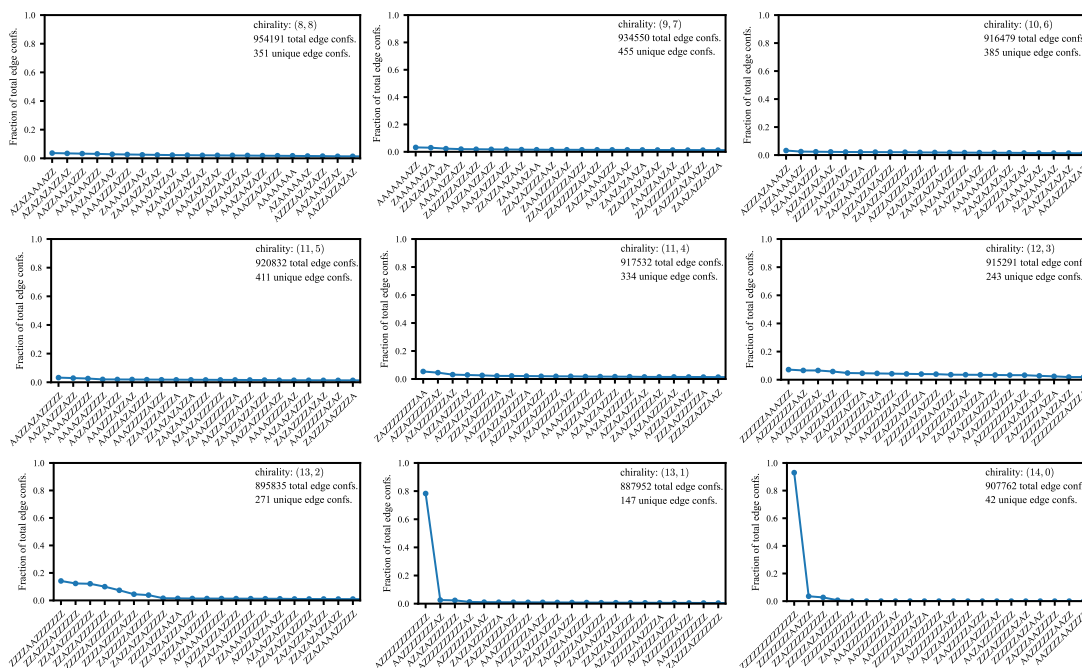


Figure 1: The 21 most frequent edge configurations for each chirality. The x-labels indicate the unique edge configuration and the y-axis is the fraction of all observed edges of that particular configuration.

References

1. F. Ding, A. R. Harutyunyan, B. I. Yakobson, *Pnas.* **106**, 2506-2509 (2009).
2. Y. Magnin, H. Amara, F. Ducastelle, A. Loiseau, C. Bichara, *Science.* **362**, 212-215 (2018).
3. D. Hedman *et al.*, *arXiv.* (2023).

Chirality of Double-Walled Carbon Nanotubes by TEM Electron Diffraction Pattern

Zhenyu Xu¹, Anastasios Karakassides¹, Hua Jiang¹, Qiang Zhang¹, Esko I. Kauppinen¹,

¹*Department of Applied Physics, School of Science, Aalto University (Finland)*

Double-walled carbon nanotubes (DWCNTs) consist of two coaxially aligned single-walled carbon nanotubes (SWCNTs) that held together with weak van der Waals forces. Due to their unique structure, they exhibit exceptional electrical conductivity, as well as mechanical and chemical stability. However, their structural identification is quite challenging due to the strong wall coupling, which depends on the wall spacing, Moiré interference, and relative chiral angle.

Transmission electron microscopy (TEM) is a powerful tool to get intel on the CNT structure, especially through electron diffraction (ED) patterns that can be utilized to analyze the chirality of CNTs. By combining the analysis method of SWCNTs chirality with the analysis method of the CNT bundle's chiral angle, the chiral index of DWCNTs could be accurately identified.^[1, 2]

In this work, high-quality DWCNTs were synthesized in a floating catalyst chemical vapor deposition (FC-CVD) system.^[3] CH₄, ferrocene, and elemental sulfur were used as the carbon source, catalyst precursor and growth promoter, respectively. The furnace temperature was set to 1100 °C, and the total gas flow to 458 standard cubic centimeters per minute (sccm), consisting of H₂ and N₂ as reducing agent and carrier gas.

High-resolution TEM was used to obtain the morphological information of the nanotubes, while ED patterns were acquired and systematically analyzed for 60 DWCNTs. The results revealed that about 60% of the outer wall diameters are between 3 - 4 nm, while the mean wall spacing about 0.367 ± 0.038 nm. The chirality distribution was found to be random and widely distributed, comprising 35.1% metallic tubes (M) and 64.9% semiconducting tubes (S). The DWCNTs exhibited a diverse structure, with 44% featuring a semiconducting outer wall and semiconducting inner wall (S@S), and 14% displaying a metallic outer wall and metallic inner wall (M@M). The chiral angles of both the inner and outer walls were concentrated in the range of 15° - 25°, with no significant trend in the angle difference between the inner and outer tubes. Only 5% of DWCNTs exhibited the same chiral angle for both walls. Our comprehensive analysis, combining Bessel function based SWCNT chirality analysis and CNT bundle chiral angle analysis, facilitated accurate identification of the chiral index of DWCNTs.

References

- [1] H. Jiang, et al., Phys. Rev. B **74**, 035427 (2006).
- [2] H. Jiang, et al., Appl. Phys. Lett. **93**, 141903 (2008).
- [3] Q. Zhang, et al., Adv. Funct. Mater. **32**, 2103397 (2021).

Chirality Selective Growth of Bulk Single-walled Carbon Nanotubes Using Cobalt-Sulfur Catalyst

Zihan Xu¹, Zeyao Zhang^{1,2,*}, Yan Li^{1,*}

¹Peking University, ²Institute of Carbon-Based Thin Film Electronics, Peking University, Shanxi (China)

zeyaozhang@pku.edu.cn; yanli@pku.edu.cn

Single-walled carbon nanotubes (SWCNTs) have excellent mechanical and electrical properties, together with flexibility. Thus, they have a wide range of potential applications in the field of flexible semiconductor devices. Carbon-based field-effect transistors and integrated circuits with better performance than silicon-based devices require SWCNTs whose semiconductor purity is greater than 99.9999% after separation and whose tube diameters range from 1.0 to 1.5 nm. Chirality controlled growth of SWCNTs is the basis for efficiently obtaining samples with narrow diameter distribution and high semiconductor purity, and the separation of semiconducting SWCNTs requires bulk SWCNTs. It is generally recognized that the growth of SWCNTs with near-armchair chiralities has dynamic advantage. By controlling catalyst diameter and growth condition, it is possible to selectively grow SWCNTs of specific (n, n-1) chirality.

Yuan Chen *et al* used CoSO₄ as catalyst precursor and SiO₂ as carrier. The diameter of Co catalyst could be controlled by forming Co₉S₈ intermediate, then selective growth of SWCNTs of (9, 8) could be realized [1]. In this work, Co precursor together with sulfate additive were loaded on MgO by co-precipitation combining impregnation. Using CO as carbon source, under optimal growth condition, samples enriched with SWCNTs of (6, 5) and (9, 8) could be obtained. Both growth condition and carbon source impacted the chiral distribution of SWCNTs.

After being removed of carrier, the samples grew under optimal growth condition were dispersed into aqueous sodium deoxycholate solution. Based on UV-visible absorption spectroscopy, through further analysis including curve-fitting and peak area calculation, (6, 5) and (9, 8) accounted for 39.5% and 28.0% of the total, respectively. Due to the significant difference in tube diameters between SWCNTs of (6, 5) and (9, 8), these two chiralities can be easily separated from each other, so that to get pure SWCNTs of (6, 5) and (9, 8), respectively. The diameter of SWCNTs of (9, 8) are about 1.2 nm, suitable for applications in semiconductor devices.

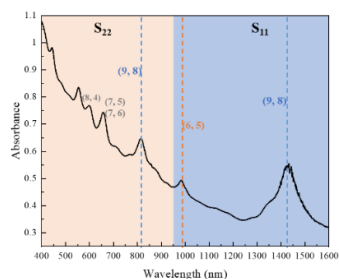


Fig. 1 UV-vis absorption spectroscopy of dispersion of SWCNTs grew under optimized condition with Co-S precursor system loaded on SiO₂

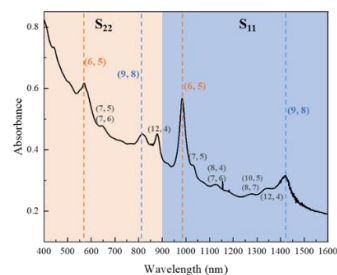


Fig. 2 UV-vis absorption spectroscopy of dispersion of SWCNTs grew under optimized condition with Co-S precursor system loaded on MgO

[1] Wang, H., Wei, L., Ren, F. *et al.* ACS Nano **7** (1), 614 (2013).

Chirality-Dependent Electrical Transport Properties of Carbon Nanotubes Obtained by Experimental Measurement

Huaping Liu^{1,2,*}

¹Beijing National Laboratory for Condensed Matter Physics, Institute of Physics, Chinese Academy of Sciences, Beijing 100190, China, ²University of Chinese Academy of Sciences, Beijing 100049, China

Corresponding author(s): liuhuaping@iphy.ac.cn

Establishing the relationship between the electrical transport properties of single-wall carbon nanotubes (SWCNTs) and their structures is critical for the design of high-performance SWCNT-based electronic and optoelectronic devices. Here, we systematically investigated the effect of the chiral structures of SWCNTs on their electrical transport properties by measuring the performance of thin-film transistors constructed by eleven distinct (n, m) single-chirality SWCNT films [1-2]. The results show that, even for SWCNTs with the same diameters but different chiral angles, the difference in the on-state current or carrier mobility could reach an order of magnitude. Further analysis indicates that the electrical transport properties of SWCNTs have strong type and family dependence. With increasing chiral angle for the same-family SWCNTs, Type I SWCNTs exhibit increasing on-state current and mobility, while Type II SWCNTs show the reverse trend. The differences in the electrical properties of the same-family SWCNTs with different chiralities can be attributed to their different electronic band structures, which determine the contact barrier between electrodes and SWCNTs, intrinsic resistance and intertube contact resistance. Our present findings provide an important physical basis for performance optimization and application expansion of SWCNT-based devices.[3]

References

- [1] D.H. Yang *et al.*, *Nat Commun*, **14**, 2491 (2023)
- [2] D.H. Yang *et al.*, *Sci Adv* **7**, eabe008 (2021)
- [3] W. Su *et al.*, *Nat Commun* **14**, 1672 (2023).

Chirality-Induced Spin Selectivity in Peptide Functionalized Carbon Nanotubes

Md Anik Hossain¹, Sandipan Pramanik¹

¹University of Alberta (Canada)

Spin-based electronics (spintronics), where electron spin is utilized instead of the charge for information processing, has triggered significant research interest in recent years. One necessary requirement of spintronics is generating spin-polarized carriers in an efficient manner. Chirality-induced spin selectivity (CISS) is a recently discovered phenomenon in which a chiral medium can act as a spin filter. In this effect, an unpolarized spin population gets spin-polarized after transmission through a chiral medium. The polarized spin is either parallel or antiparallel to the direction of velocity, depending on the chirality of the medium, as shown schematically in Figure 1(a) [1]. The CISS effect holds immense relevance in spintronics because it potentially allows magnet-free spintronic devices as well as molecular-scale generation of spin-polarized beams. Several theoretical, and experimental studies have been conducted to explore this effect using different organic molecules such as single-stranded DNA (ssDNA), double-stranded DNA (dsDNA), oligopeptides, inorganic chiral crystals etc [1]. Carbon nanotubes (CNTs) functionalized with chiral molecules is also a promising candidate in this regard [2], [3], [4].

In this work, we demonstrated the presence of the CISS effect in peptide-functionalized (FMOC FF, where FMOC: Fluorenylmethyloxycarbonyl; FF: L/D diphenylalanine) CNTs [5]. Spin polarization has been detected by a Ni spin detector (Figure 1(b)). For a given Ni magnetization, device conductance has been found to be chirality-dependent, indicating the presence of the CISS effect (Figure 1(c)) [5]. Using peptide-functionalized CNTs as candidate systems we have addressed some of the open questions in CISS [5]. Our findings reveal (a) the presence of chirality-dependent spin components that are transverse to carrier velocity, (b) the validity of Onsager's reciprocity relation in a two-terminal CISS device with one magnetic contact, and (c) the persistence of the CISS signal even in the absence of electric magnetochiral effects, suggesting an alternative physical origin of CISS.

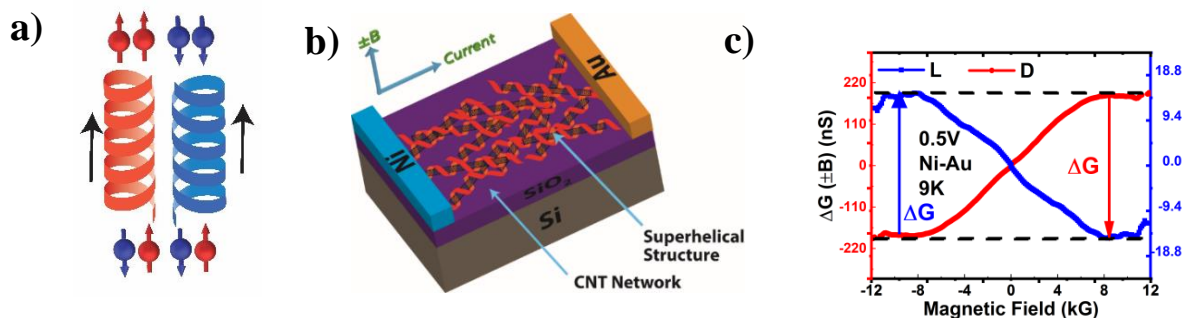


Figure 1: (a) Schematic illustration of the CISS phenomenon. (b) Schematic representation of a typical CISS device with peptide-functionalized CNTs [5] (c) Typical magnetoconductance measurements for L and D chirality showing opposite behavior for opposite chiralities [5].

References

- [1] D. H. Waldeck, R. Naaman, and Y. Paltiel, "The spin selectivity effect in chiral materials," *APL Mater.*, vol. 9, no. 4, p. 040902, Apr. 2021, doi: 10.1063/5.0049150.
- [2] Md. W. Rahman *et al.*, "Chirality-Induced Spin Selectivity in Heterochiral Short-Peptide–Carbon-Nanotube Hybrid Networks: Role of Supramolecular Chirality," *ACS Nano*, vol. 16, no. 10, pp. 16941–16953, Oct. 2022, doi: 10.1021/acsnano.2c07040.
- [3] M. W. Rahman, S. Firouzeh, and S. Pramanik, "Carrier localization and magnetoresistance in DNA-functionalized carbon nanotubes," *Nanotechnology*, vol. 32, no. 45, p. 455001, Nov. 2021, doi: 10.1088/1361-6528/ac18d9.
- [4] M. W. Rahman, S. Firouzeh, and S. Pramanik, "Carrier localization and magnetoresistance in DNA-functionalized carbon nanotubes," *Nanotechnology*, vol. 32, no. 45, p. 455001, Nov. 2021, doi: 10.1088/1361-6528/ac18d9.
- [5] M. A. Hossain, S. Illescas-Lopez, R. Nair, J. M. Cuerva, L. Álvarez De Cienfuegos, and S. Pramanik, "Transverse magnetoconductance in two-terminal chiral spin-selective devices," *Nanoscale Horiz.*, vol. 8, no. 3, pp. 320–330, 2023, doi: 10.1039/D2NH00502F.

CHIRALITY-SELECTIVE SYNTHESIS OF SINGLE-WALLED CARBON NANOTUBES USING COBALT TUNGSTATE NANOPARTICLES AS PRECURSORS

X. Zhang¹, X. Liu¹, S. Sun¹, Y. Li^{1,*}

¹College of Chemistry and Molecular Engineering, Peking University (China)

The physical and chemical properties of single-walled carbon nanotubes (SWCNTs) are closely related to their structure. In order to realizing important applications of SWCNTs, chiral-controlled synthesis of them is an essential step. Our previous work has shown that tungsten-cobalt bimetallic alloy solid catalysts have the potential to grow chirality-selective SWCNTs [1-4]. In this work, we propose a new strategy for the preparation of tungsten-cobalt bimetallic alloy catalysts and the selective growth of SWCNTs. We used “water-in-oil” type microemulsion system constructing from several different surfactants, and generated cobalt tungstate nanoparticle precursors in the aqueous micro-micelle chamber. After loading the precursor and reducing, the resulting catalyst can selectively grow chiral carbon nanotubes such as (14,4). Among different surfactants, the catalyst obtained using cationic surfactant cetyltrimethylammonium bromide (CTAB) showed the highest selectivity for (14,4), about 53%. The reason may be that the surface charge of the aqueous micro-micelle chamber formed by different surfactant molecules varies, which determines the different ion adsorption on the surface of cobalt tungstate, and the different element distribution near the surface of the catalyst. The positive part of CTAB selectively adsorb WO_4^{2-} , making the catalyst surface rich in tungsten, which can resist the loss of tungsten during the reduction process and stabilize the structure of the catalyst. This work further demonstrates the potential of tungsten-based bimetallic alloys in chiral-selective synthesis of single-walled carbon nanotubes.

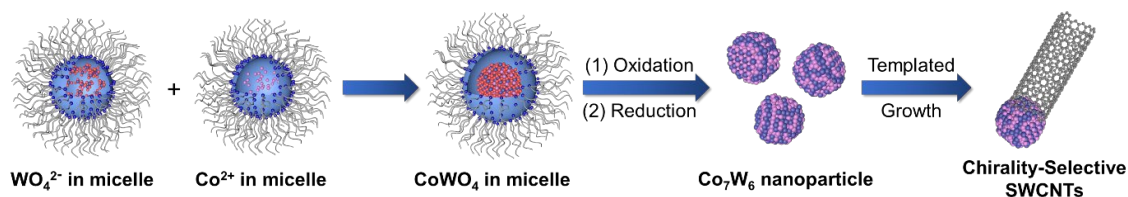


Figure caption: Scheme of selective growth of SWCNTs using CoWO_4 nanoparticles from microemulsion system as precursor.

References

- [1] F. Yang *et al.*, *Nature* **510**, 522–524 (2014).
- [2] F. Yang *et al.*, *J. Am. Chem. Soc.* **137**, 8688–8691 (2015).
- [3] F. Yang *et al.*, *ACS Nano* **11**, 186–193 (2017).
- [4] F. Yang *et al.*, *Acc. Chem. Res.* **49**, 606–615 (2016).

Collective modulation of solution-processed molybdenum disulfide for tunable electronics and optics

S. Liu¹, Y. Wen¹, J. Pei¹, Y. Liu^{1,2}, G. Hu¹

¹Department of Electronic Engineering, The Chinese University of Hong Kong (HKSAR, China), ²Shun Hing Institute of Advanced Engineering, The Chinese University of Hong Kong (HKSAR, China)

Molybdenum disulfide (MoS₂), with the electronic wavefunctions confined in a two dimension configuration breaking the longitudinal translational symmetry, allows a convenient modulation of the electronic structures with the external fields for tunable electronics and optics [1]. Solution-processing of MoS₂ emerges promising for scalable device fabrication. The state-of-art reports, however, show inferior device performance as a result of the discrete nature of the solution-processed nanoflake networks [2, 3]. In this work, we present collective modulation of the macroscopic electronic properties of solution-processed MoS₂ with the local electrostatic fields and explore its applications in tunable electronics and optics.

Through theoretical studies with density-functional theory calculations, we show that the local electrostatic fields can redistribute the charges in solution-processed MoS₂ nanoflakes, leading to a collective modulation of the macroscopic electronic properties of the nanoflake networks for tunable electronics fabrication. To investigate the effectiveness of this modulation approach, we fabricate devices from solution-processed MoS₂ coupled with ferroelectrics (e.g. BaTiO₃, P(VDF-TrFE)), where the ferroelectrics are employed to provide the local polarization fields for modulation. Particularly, we fabricate nonlinear MoS₂-ferroelectric junctions and ferroelectric transistor memory, with high device performance demonstrated, proving an effective collective modulation of the underlying macroscopic electronic properties of the solution-processed MoS₂. Beyond MoS₂, we show the modulation approach is applicable to the other solution-processed 2D materials, such as the other transition metal dichalcogenides (e.g. MoTe₂) and bismuth telluride (Bi₂Te₃). Beyond the electronic properties, we show that the modulation approach can alter the optical properties towards the fabrication of tunable optics. As an example, we demonstrate electro-optical modulator fabrication from the solution-processed MoS₂.

Given the scalability of solution-processing, as well as its adaptability to the CMOS processes and the emerging printing techniques for scalable device fabrication, this modulation approach and the enabled devices hold the potential to lead to practical scalable device applications [4]. As an example, we investigate reservoir computing realization with the nonlinear MoS₂-ferroelectric junctions devices. We implement an echo state network via a simulation study where the high-order nonlinear device characteristics are harnessed and incorporated in the network nodes for the nonlinear mapping of the input. The network successfully replicates the dynamical systems of Lorentz-63 and Mackey-Glass, showing the capability to unveil chaotic time-series signal patterns of, for instance, IoT sensors and brain-computer interfaces.

References

- [1] K. S. Novoselov, *et al.*, *Science*, **353**, 6298 (2016).
- [2] S. Conti, *et al.*, *Nat. Rev. Mater.*, **8**, 651-667 (2023).
- [3] A. G. Kelly, *et al.*, *Nat. Rev. Mater.*, **7**, 217-234 (2022).
- [4] A. C. Ferrari, *et al.*, *Nanoscale*, **7**, 4598-4810 (2015).

Colorimetric Paper with Inkjet-Printed Carbon Nanotube Chemiresistors for Detection of Liquid and Gas Phase Chemical Warfare Agents

Seongyeop Lim¹, Sanghwan Park¹, Seongwoo Lee², Cheongha Lee¹, Chang Young Lee^{1,3}

¹School of Energy and Chemical Engineering, ²Department of Materials Science and Engineering, ³Graduate School of Carbon Neutrality, Ulsan National Institute of Science and Technology (UNIST), Ulsan 44919, Republic of Korea (Republic of Korea)

Colorimetric papers have been widely used for the convenient and inexpensive detection of toxic chemicals, including chemical warfare agents (CWAs). The majority of colorimetric papers, however, only detect liquid phase analytes, exhibiting limited gas- sensing performance. In this study, we report a colorimetric paper capable of detecting and identifying CWAs in both liquid and gas phases, achieved by inkjet printing carbon nanotube (CNT)-based chemiresistors on the paper. The inkjet-printed CNTs generate electrical signals unique to liquid-phase CWAs (GB, VX) and their simulants, without affecting the colorimetric responses, thereby enabling more accurate analyte identification. Inkjet printing can also be employed to non-covalently functionalize CNTs with various receptors. We fabricated a gas sensor array on the colorimetric paper by inkjet printing three different receptors on the CNT chemiresistors, and demonstrated the identification of four CWA simulants based on the response patterns of the array. This hybrid sensing platform, exhibiting both colorimetric and electrical signals, potentially serves as an inexpensive alternative to existing analytical tools for the analysis of CWAs and other toxic chemical compounds.

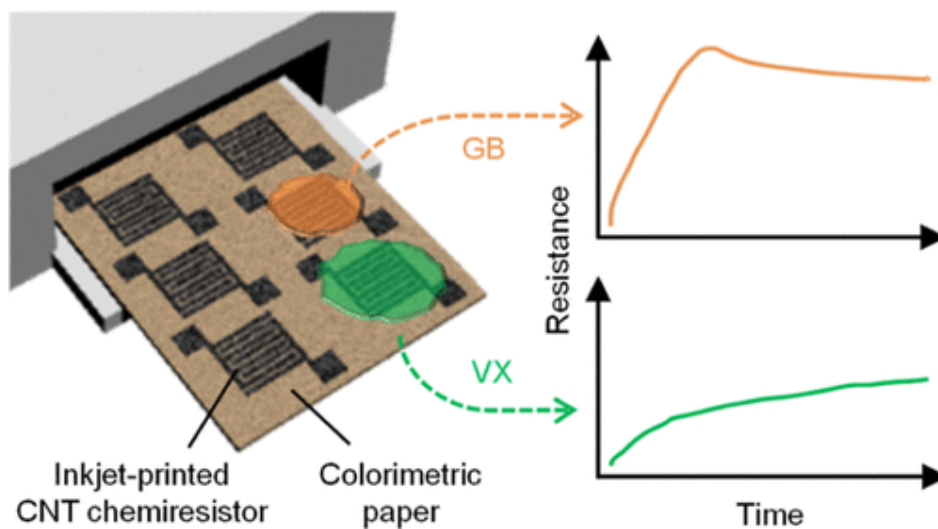


Figure 1 : Detection of liquid-phase CWAs (GB, VX) using colorimetric paper with inkjet-printed SWCNT chemiresistors. Schematic showing an array of SWCNT chemiresistors printed on colorimetric paper using a commercial inkjet printer, colorimetric and resistive responses to liquid-phase CWAs (GB, VX).

References

[1] Lim, Seongyeop et al, *ACS Applied Nano Materials*. 6.21, 19955-19962 (2023).

COMPLEX REFRACTIVE INDEX SPECTRA OF SINGLE-CHIRALITY CARBON NANOTUBE MEMBRANES WITH BIREFRINGENT OPTICAL RESPONSES

Hengkai Wu¹, Taishi Nishihara¹, Akira Takakura¹, Kazunari Matsuda¹, Takeshi Tanaka²,
Hiromichi Kataura², Yuhei Miyauchi¹

¹ Institute of Advanced Energy, Kyoto University (Japan), ² Nanomaterials Research Institute, AIST (Japan)

Membranes consisting of single-walled carbon nanotubes (SWCNTs) with a specific chirality have great potential in photonic [1] and thermo-optic [2] applications because of their strong and distinct light-matter interaction via excitons with high-temperature robustness. Generally, these membranes are fabricated via the vacuum filtration of single-chirality SWCNT dispersion [1], and SWCNTs are aligned two-dimensionally in the plane (Figure 1 (a)). The electric field component normal to the membrane surface (red arrow in Figure 1(b)) is always perpendicular to the tube axis of each SWCNT. Meanwhile, the optical properties of SWCNTs are anisotropic with respect to the tube axis [3, 4]. For these reasons, it is expected that the macroscopic responses of the membranes depend on the light-propagation direction. However, their anisotropic optical features and complete complex refractive index spectra remain to be unveiled, hindering the design of devices to deal with light propagating in arbitrary directions using SWCNT membranes as opto-functional materials.

Here, we report the birefringent optical response of a single-chirality SWCNT membrane [5], as examined using polarization- and angle-resolved reflection spectroscopy. We determined the ordinary (in-plane) and extraordinary (out-of-plane) complex refractive index spectra for it. The membrane was fabricated via the vacuum filtration of a (6,5) SWCNT dispersion prepared using gel chromatography [6], and the spectra were obtained in the near-infrared-to-visible region using homemade optical setups. All spectral features were consistent with a uniaxial birefringent membrane, reflecting the random in-plane orientations of SWCNTs. Figure 1 (c) shows the obtained complex refractive index spectra. The ordinary one presented a series of sharp resonances of parallel-polarized excitons while the extraordinary one is ~ 1.9 in with the small contribution from the cross-polarized exciton resonance (S_{cross}) which is indispensable for properly predicting angle-dependent optical responses of the membrane. The complete knowledge of the birefringence and complex refractive index spectra of the single-chirality SWCNT membrane facilitates the precise and diverse design of photonic and thermo-optic devices based on SWCNTs.

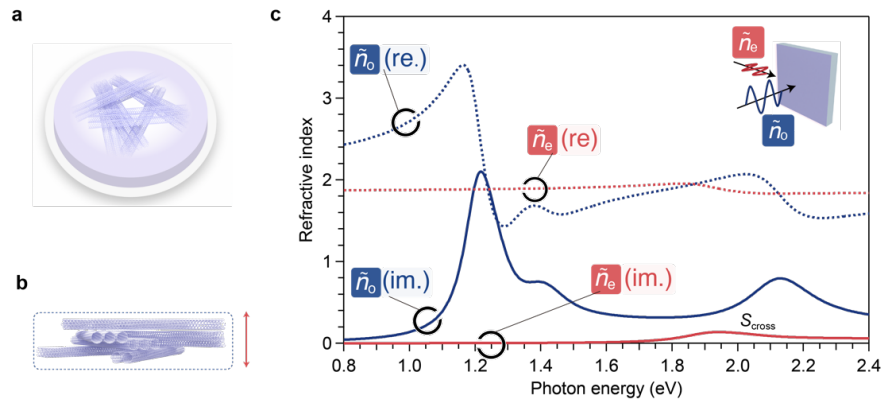


Figure 1: Schematic of the (a) top and (b) side views of a single-chirality SWCNT membrane fabricated via vacuum filtration. The arrow in (b) indicates the electric field component normal to the membrane surface. (c) Ordinary (\tilde{n}_o , blue) and extraordinary (\tilde{n}_e , red) complex refractive index spectra of the membrane. The dotted and solid curves represent real and imaginary parts, respectively. The inset shows a schematic light configuration corresponding to each complex refractive index. The blue and red wavy curves represent the electric field of light.

References

- [1] T. Nishihara *et al.*, *Nanophotonics* **11**, 1011-1020 (2022).
- [2] T. Nishihara *et al.*, *Nat. Commun.* **9**, 3144-3150 (2018).
- [3] H. Ajiki, T. Ando, *Phys. B: Condens. Matter* **201**, 349-352 (1994).
- [4] Y. Miyauchi *et al.*, *Phys. Rev. B* **74**, 205440-205445 (2006).
- [5] H. Wu *et al.*, *Carbon* **218**, 118720-118726 (2024).
- [6] Y. Yomogida *et al.*, *Nat. Commun.* **7**, 12056-12063 (2016).

CONFINEMENT-INDUCED NONLOCALITY AND CASIMIR FORCE IN TRANSDIMENSIONAL SYSTEMS

I. V. Bondarev,^{1*} M. D. Pugh,¹ P. Rodriguez-Lopez,² L. M. Woods,³ and M. Antezza^{4,5}

¹Department of Mathematics & Physics, North Carolina Central University, Durham, NC 27707, USA

²Área de Electromagnetismo and Grupo Interdisciplinar de Sistemas Complejos (GISC), Universidad Rey Juan Carlos, 28933 Móstoles, Madrid, Spain

³Department of Physics, University of South Florida, Tampa, FL 33620, USA

⁴Laboratoire Charles Coulomb (L2C), UMR 5221 CNRS-University of Montpellier, F-34095 Montpellier, France

⁵Institut Universitaire de France, 1 rue Descartes, F-75231 Paris Cedex 05, France

*Email: ibondarev@nccu.edu

We apply a confinement-induced nonlocal electromagnetic response model [1-5] to generalize the Lifshitz theory of the long-range Casimir force [6] for in-plane isotropic and anisotropic ultrathin transdimensional material slabs [7,8]. In the former case, we show that the confinement-induced nonlocality not only weakens the attraction of ultrathin slabs but also changes the distance dependence of the material-dependent correction to the Casimir force to go as inverse square root of distance contrary to inverse distance dependence of that of the local Lifshitz force (Fig.1, left). In the latter case, we use closely packed arrays of parallel aligned single-wall carbon nanotubes (SWCNs) in a dielectric layer of finite thickness (Fig.1, middle) to show the strong orientational anisotropy and crossover behavior for the inter-slab attractive force in addition to its reduction with decreasing slab thickness (Fig.1, right). We give physical insight as to why such a pair of ultrathin slabs prefers to stick together in the perpendicularly oriented manner, rather than in the parallel relative orientation as one would customarily expect.

This work is supported by the U.S. Army Research Office under award No. W911NF2310206 (I.V.B), URJC AYUDA PUENTE 2022 (P.R.-L.), the US Department of Energy under Grant No. DE-FG02-06ER46297 (L.M.W.), and the grant ‘‘CAT’’ No. A-HKUST604/20 (M.A.).

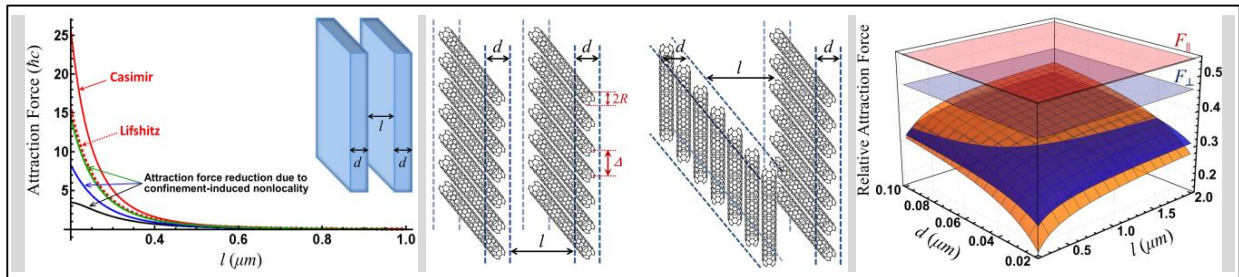


Fig. 1: Attraction force between in-plane isotropic (left) and anisotropic (middle & right) material slabs. Right panel shows forces as functions of slab thickness and inter-slab distance, relative to the Casimir force, for slabs packed with 2 nm-radius SWCNs oriented as shown in the middle (parallel planes indicate the asymptotic force values) [6].

References

- [1] S.-A. Biehs and I. V. Bondarev, Far- and near-field heat transfer in transdimensional plasmonic film systems, *Adv. Opt. Mater.* **11**, 2202712 (2023).
- [2] I. V. Bondarev, H. Mousavi, and V. M. Shalaev, Transdimensional epsilon-near-zero modes in planar plasmonic nanostructures, *Phys. Rev. Res.* **2**, 013070 (2020).
- [3] I. V. Bondarev, Finite-thickness effects in plasmonic films with periodic cylindrical anisotropy [Invited], *Opt. Mater. Express* **9**, 285 (2019).
- [4] I. V. Bondarev, H. Mousavi and V. M. Shalaev, Optical response of finite-thickness ultrathin plasmonic films, *MRS Commun.* **8**, 1092 (2018).
- [5] I. V. Bondarev and V. M. Shalaev, Universal features of the optical properties of ultrathin plasmonic films, *Opt. Mater. Express* **7**, 3731 (2017).
- [6] E. M. Lifshitz, The theory of molecular attractive forces between solids, *Soviet Physics* **2**, 73 (1956).
- [7] I. V. Bondarev, M. D. Pugh, P. Rodriguez-Lopez, L. M. Woods, and M. Antezza, Confinement-induced nonlocality and Casimir Force in transdimensional systems, *Phys. Chem. Chem. Phys.* **25**, 29257 (2023).
- [8] P. Rodriguez-Lopez, D.-N. Le, I. V. Bondarev, M. Antezza, and L. M. Woods, Giant anisotropy and Casimir phenomena: the case of carbon nanotube metasurfaces, *Phys. Rev. B* **109**, 035422 (2024).

Controlled growth of semiconducting SWNT arrays through a dual-ion-implantation strategy

Y. Xie^{1,§}, Y. Li^{2,§}, L. Qian¹, Z. Q. Zhao^{2,*}, J. Zhang^{1,*}

¹College of Chemistry and Molecular Engineering, Beijing Science and Engineering Center for Nanocarbons, Beijing National Laboratory for Molecular Sciences, Peking University, Beijing 100871, China, ²State Key Laboratory of Nuclear Physics and Technology, School of Physics, Peking University, Beijing 100871, P. R. China

Carbon nanotubes (CNTs) have been considered as one of the most promising materials for the next-generation electronic devices. The prerequisite of the application is the controlled synthesis of single-walled carbon nanotube (SWNT) arrays with high density and semiconducting purity. Selective etching the more reactive metallic CNTs by introducing oxidizing agents is a common method of enhancing semiconducting purity of SWNT arrays, but the traditional etching process is less effective and has poor controllability. [1,2] Herein, we develop a dual-ion-implantation strategy of growing semiconducting SWNT arrays. Iron ions as catalyst precursors and oxygen ions as etching precursors are implanted into the substrate together. During chemical vapor deposition (CVD) process, iron nanoparticles form and catalyze the growth of SWNT arrays. Oxygen ions are released together and etch metallic SWNTs in situ. The amounts of etchants are quantitative by setting ion implantation parameters. The process of etching is controllable by regulating growth parameters. Through the dual ion implantation strategy, SWNT arrays with controlled semiconducting purity can be prepared. This method shows the potential in customized synthesis of semiconducting SWNT arrays and can be easily extended to wafer-scale growth, which is significant to open up new applications of CNTs in the future.

References

- [1] X. J. Qian *et al.*, *Nano Lett.* **14**, 512–517 (2014).
- [2] W. W. Zhou, *J. Am. Chem. Soc.* **134**, 14019–14026 (2012).

COULD WE REPLACE DINOSAUR JUICE LUBRICANTS WITH DARK GREEN VEGAN PRODUCTS?

R.G. Jędrzyak¹, S. Ruczka¹, Ł. Wojciechowski², M. Skrzypek², S. Boncel¹

¹*Silesian University of Technology, Faculty of Chemistry, CONE, NanoCarbonGroup, (Poland),*

²*Poznan University of Technology, Institute of Machines and Motor Vehicles (Poland)*

The attempts to use alternative to fossil fuels energy sources continue to expand. Even if in the automotive or, generally, the machinery industry, hydrocarbons obtained from crude oil are not used solely as propellants, the petrochemically born lubricants are widely used in gear boxes and other elements exposed to wear as a result of friction of moving elements. This application probably will last in the case of entirely electric cars, in which it will enable the reduction of electricity consumption and overcome the fundamental problem of the limited range.

For automatic gear boxes, spermaceti oil was used. However, the ban on a sperm whale hunting introduced in the 1970s [1] made it necessary to replace it with other media. The use of mineral oils did not bring the expected results – the number of automatic transmission failures in the United States alone increased in late '70 from less than 1M to 8M per year. The solution was modified jojoba oil – the first step in the replacement of mineral and animal oils with products of plant origin.[2]

In our research, we indicate the possibility of using vegetable oils in combination with carbon nanotubes and their chemically modified derivatives in the preparation of lubricating oils. Such a combination is beneficial as extending the operation time of the lubricant by capturing free radicals,[3] increases thermal conductivity, and improves lubricating properties in metal-metal and metal-polymer tribo-pairs.

Acknowledgements

The authors are very grateful for the financial support from the National Science Centre (Poland) Grant No. 2020/39/B/ST5/02562 in the framework of the OPUS-20 program.

References

- [1] The Endangered Species Act of 1973, **16 U.S.C. § 1531.**
- [2] H. Gisser, J. Messina, D. Chasan, *Wear* **34**(1), 53-63 (1975).
- [3] T. Shimizu, R. Kishi, T. Yamada, K. Hata, *RSC Adv.* **10**, 29419 (2020).

Covalently Functionalized Carbon Nanotube-Based Nickel Complexes for Electrocatalytic Aryl Halide Coupling

T. N. Pioch¹, T. M. Swager¹

¹Massachusetts Institute of Technology (United States of America)

Carbon nanotubes (CNTs) have proven an attractive platform for electrocatalysis due to their unique electronic properties and adjustable reactivity via functionalization [1-3]. Previously, our group demonstrated that the conductive inner layers of multi-wall carbon nanotubes (MWCNTs) may serve as a “chemical wire” capable of accelerating the electron transfer from Pd(0) to Cu(II) centers in Wacker-type oxidation reactions [4]. Despite heavy covalent functionalization on the surface, the MWCNTs still served as effective electronic interconnects between the chemisorbed metal centers.

We have also shown that MWCNTs may be covalently functionalized with bidentate or tridentate chelating ligands by the 1,3-dipolar cycloaddition of nitrile oxides onto the nanotube surface to form isoxazolines [5]. The resulting ligand scaffold is capable of stabilizing low-nuclearity transition metal centers on the nanotube surface. An iridium-chelated isoxazoline-MWCNT system proved to be catalytically active toward the oxygen evolution reaction, but given the tunability of both the isoxazoline-based ligand scaffold and the metal center, this approach holds great potential to improve other catalytic processes as well. We have combined the robust chelation of our isoxazoline-MWCNT system with the capacity of MWCNTs to shuttle electrons from the working electrode to bound metal centers to develop a heterogeneous electrocatalyst for the reductive coupling of aryl halides to form biaryls. Nickel, a cost-effective alternative to palladium or platinum [6], is known to catalyze such cross-couplings through a complex, interconnected set of catalytic cycles involving Ni(0), Ni(I), Ni(II), and Ni(III) [7]. We have developed a heterogeneous, nickel-chelated, isoxazoline-functionalized MWCNT catalyst to improve the electron transfer kinetics of biaryl synthesis from aryl halides, especially when drop-casted onto a working electrode to provide electrochemical control of the reaction conditions.

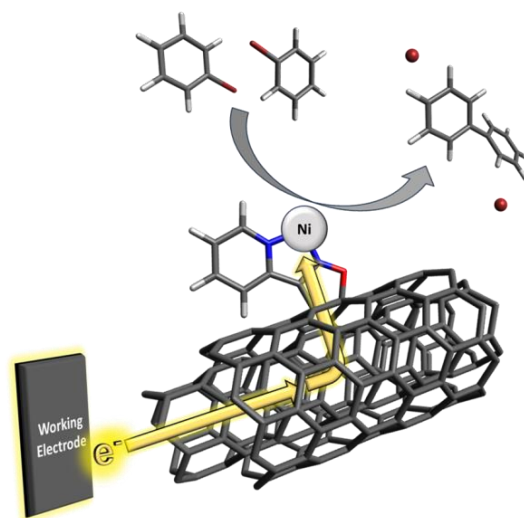


Figure 1: Nickel-chelated, isoxazoline-functionalized MWCNT serves as an electron transfer agent to accomplish nickel-catalyzed reductive coupling of aryl halides to form biaryl species.

References

- [1] K. Y. Cho *et al.*, *Carbon* **105**, 340–352 (2016).
- [2] K. Jiang *et al.*, *Nat. Commun.* **10**, 3997 (2019).
- [3] Y. Wu *et al.*, *Nature* **575**, 639–642 (2019).
- [4] J. M. Schnorr and T. M. Swager, *J. Mater. Chem.* **21**, 4768–4770 (2011).
- [5] S.-X. L. Luo *et al.*, *J. Am. Chem. Soc.* **143**, 10441–10453 (2021).
- [6] F.-S. Han, *Chem. Soc. Rev.* **42**, 5270–5298 (2013).
- [7] T. T. Tsou and J. K. Kochi, *J. Am. Chem. Soc.* **101**, 7547–7560 (1979).

Critical roles of Fe and Co binary catalysts in ACCVD growth of SWCNTs

Qingmei Hu¹, Ya Feng^{1,2}, Kunio Mori¹, Ryo Yoshikawa¹, Yongjia Zheng^{1,3}, Wanyu Dai¹, Ryotaro Kaneda¹, Aina Fitó Parera⁴, Wim Wenseleers⁴, Sofie Cambré⁴, Shohei Chiashi¹, Rong Xiang^{1,3}, Keigo Otsuka¹, Shigeo Maruyama^{1*}

¹ Department of Mechanical Engineering, The University of Tokyo (Japan), ² Key Laboratory of Ocean Energy Utilization and Energy Conservation of Ministry of Education, School of Energy and Power Engineering, Dalian University of Technology, (China), ³ School of Mechanical Engineering, Zhejiang University (China), ⁴ Department of Physics, University of Antwerp, (Belgium)

Abstract: Based on our previous exploration of an extended alcohol catalytic chemical vapor deposition (ACCVD) at a wide range of temperatures and pressures [1], we further investigated the catalyst recipe of iron (Fe) and cobalt (Co) for the synthesis of single-walled carbon nanotubes (SWCNTs) in an even wider parametric window. On one hand, we found that at a relatively low temperature of 600 °C, mono-metallic Co catalyst exhibited the most efficient synthesis of SWCNTs among five different Fe/Co ratios from 0% to 100% (Fig. 1(a) and (c)) [2]. On the other hand, at lower pressure, such as 50Pa, and higher temperature, such as 850 °C or 900 °C, bi-metallic catalyst with 25 % Co atomic ratio showed the best performance than any other atomic ratio, while the mono-metallic Co or Fe catalyst all became inactive (Fig. 1(a) and (d)). Meanwhile, at 900 °C, the chirality distribution varied depending on pressures, and lower pressure led to the formation of SWCNTs with larger diameters (Fig. 1(b)). At the same time, we analyzed the chirality distribution of SWCNTs grown from catalysts with different Fe/Co atomic ratios by conducting a comprehensive methodology for the fitting of SWCNTs absorption and photoluminescence (PL) spectra [3-4]. At a low temperature of 600 °C, the mono-metallic Co catalyst showed a narrow diameter distribution of SWCNTs (Fig. 1(e) and (f)). Furthermore, we have confirmed that under identical growth conditions, a fixed recipe can consistently induce the same chirality distribution in both particle-substrate (zeolite) and plane-substrate (silicon), as evidenced by the Raman spectrum in Fig. 1(g). The subsequent step necessitates the acquisition of transmission electron microscopy (TEM) measurements to evaluate the formation of Fe and Co bimetallic catalyst.

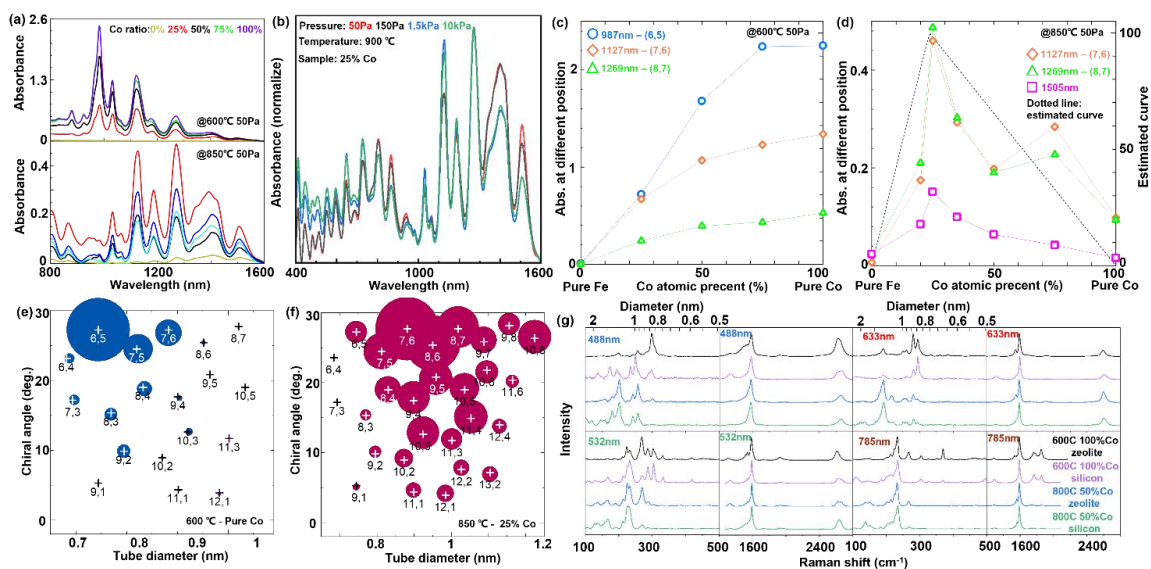


Fig.1 UV-Vis-NIR absorption spectrum of (a) all ratio's sample grown at 600°C and 850°C with 50Pa, (b) 25% Co grown at 900°C with different pressure; (c, d) The dependence of absorbance intensity at different wavelengths and Co atomic percentage; (e, f) The chirality distribution of pure Co at 600°C and 25% Co at 850°C; (g) The Raman spectrum of 100% Co at 600°C and 50% Co at 800°C grown on zeolite or silicon;

References: [1] B. Hou, *et al.*: *Carbon*, **119**, 502 (2017). [2] M. Liu, *et al.*: *Carbon*, **146**, 413-419 (2019).

[3] M. Pfohl, *et al.*: *ACS Omega*, **2**, 1163-1171 (2017). [4] A. Castan, *et al.*: *Carbon*, **171**, 968-979 (2021).

CROSS-LINKING OF CARBON NANOTUBES USING *s*-TETRAZINE DERIVATIVES

A. Blacha¹, S. Ruczka¹, P. Audebert², A. Terzyk³, S. Boncel¹

¹ Silesian University of Technology (Poland), ² Université Paris-Saclay, ENS Paris-Saclay, CNRS (France), ³ Nicolaus Copernicus University in Torun, Physicochemistry of Carbon Materials Group (Poland)

Carbon nanotubes (CNTs), due to their *quasi*-aromatic structure and thin-cylindrical shape at the high aspect ratio, are characterized by excellent electrical, thermal, mechanical, and optical properties [1]. Since discovery, their applicability, ranging from electronics to materials engineering to medicine, has either yet materialized or still awaits methods enabling an efficient transfer of superb characteristics from nano- to macroscale [2].

Generally, exohedral functionalization of CNTs ensures their enhanced solvent dispersibility and increased physicochemical compatibility with a variety of matrices, such as polymers, ceramics or metals. Therefore, there is a constant need to *de novo* design and develop modified CNTs (and other sp²-carbon nanomaterials) toward the target applications, while the controlled functionalization should make CNTs reproducibly processable. On the other hand, assembling CNTs into the desired forms and geometries, of the above-mentioned excellent electrical, thermal, and mechanical properties, would require ‘infinitely’ long CNTs. This function could be achieved, for example, by cross-linking of CNTs [3].

In this paper, we present a method of covalent cross-linking of CNTs using versatile *s*-tetrazine derivatives [4,5]. To achieve it, we have selected and synthesized several *s*-tetrazine derivatives containing aromatic and aliphatic substituents [6]. The so-obtained functionalized CNTs (f-CNTs) were comprehensively examined using thermogravimetric analysis (TGA), scanning and transmission electron microscopy (SEM, TEM), Raman and infrared spectroscopy (FTIR). Then, their novel nanocomposites and hybrid materials/coatings were manufactured, and their electrical, thermal, and mechanical properties were studied revealing enhanced characteristics of a high potential toward every-day-life applications.

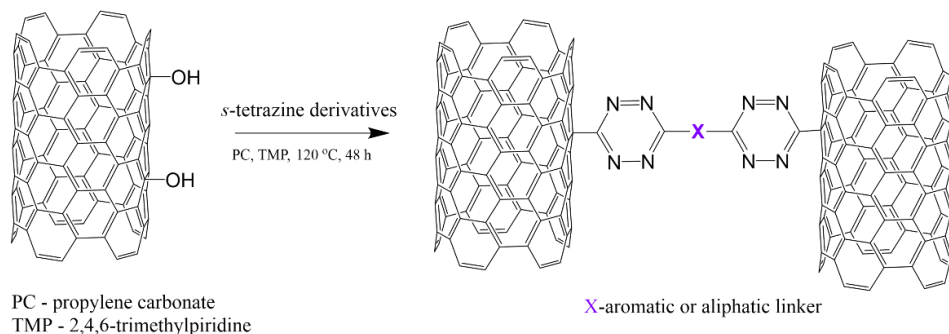


Figure 1: Schematics of cross-linking of CNTs using *s*-tetrazine derivatives

Acknowledgements

The authors are very grateful for the financial support from the National Science Centre (Poland) Grant No. 2021/41/B/ST5/00892 in the framework of the OPUS-21 program.

References

- [1] J. W. Mintmire and C. T. White, *Carbon* **33**, 893–902 (1995).
- [2] S. Rathinavel *et al.*, *Mater. Sci. Eng. B*, **268** 115095 (2021).
- [3] S. Boncel *et al.*, *ACS Nano* **5**, 9339–9344 (2011).
- [4] Y. Li *et al.*, *Chem. Mater.* **27**, 4298–4310 (2015).
- [5] M. Bosmi *et al.*, *ChemElectroChem* **11**, 2023004 (2024).
- [6] A. Blacha *et al.*, *in prep.*

Decoding Adaptive Plant Signaling: Mathematical Modeling Using Single-Walled Carbon Nanotube Fluorescence Sensing Data

Thomas K Porter¹, Michael N Heinz², Daniel J Lundberg¹, Tedrick TS Lew^{3,4}, Mervin CY Ang⁵, Duc T Khong⁵, Kevin S Silmore¹, Jolly M Saju⁶, Sarangapani Sreelatha⁶, Suh I Loh⁵, Song Wang⁵, Kien V Vu^{5,6}, Benny JR Sng^{5,6,7}, Ian KY Choi^{5,7}, Jianqiao Cui¹, Xun Gong¹, Nguyen H Nguyen^{5,6}, Minkyung Park¹, Riza Ahsim⁵, Hui J Chin^{5,6}, Mary B Chan-Park⁸, In-Cheol Jang^{5,6,7}, A Merritt Brooks¹, Volodymyr B Koman¹, Gajendra P Singh⁵, James W Swan¹, Rajani Sarojam^{5,6}, Nam-Hai Chua^{5,6} and Michael S Strano¹

¹Department of Chemical Engineering, Massachusetts Institute of Technology, Cambridge, MA, USA

²Department of Mathematics, University of California, Berkeley, CA, USA

³Department of Chemical and Biomolecular Engineering, National University of Singapore, Singapore

⁴Institute of Materials Research and Engineering (A*STAR), Singapore

⁵Disruptive and Sustainable Technologies for Agricultural Precision IRG, SMART, Singapore

⁶Temasek Life Sciences Laboratory Limited, Singapore

⁷Department of Biological Sciences, National University of Singapore, Singapore

⁸School of Chemical and Biomedical Engineering, Nanyang Technological University, Singapore

Recent progress in nanotechnology-enabled sensors that can be placed inside of living plants has shown that it is possible to relay and record real-time chemical signaling initiated by external stimuli. Here, we provide an overview of our recently developed carbon nanotube sensors for plant analytes, specifically highlighting our modeling efforts on their spatiotemporal dynamics and the insights we have uncovered. First, we highlight the application of our H₂O₂ sensor in understanding mechanical stress in plants and develop an autocatalytic propagation model to describe H₂O₂ waveforms immediately post-stress. We then expand on this model, using multiplexed data with sensors for the defense hormone salicylic acid (SA) to analyze stress responses in *Brassica rapa subsp. Chinensis* (Pak choy) plants subjected to different treatments, including light stress, heat stress, pathogen stress, and mechanical wounding. The timing of SA production in relation to the H₂O₂ wave, as well as the shape of the H₂O₂ waveform, are stress-dependent, providing a key insight into how plants differentiate between various types of stress. In addition to stress signaling related studies, we have also investigated auxin, a hormone involved in plant growth and shade avoidance. We developed a transport model describing dynamic changes in auxin distribution, and key features such as midvein impermeability and rapid leaf margin transport were mathematically described. Overall, this modeling enabled by nanosensor data facilitates the formulation of testable hypotheses regarding the underlying mechanisms and chemical species involved in plant signaling. The showcased efforts highlight advances in the application of nanosensors for understanding plant signaling mechanisms, as well as new approaches for analyzing and modeling nanosensor data.

Detection Sensitivity of a Carbon Nanotube based Crack Gauge

S. Kessler¹, C. Shubert Kabban² and Y. Stein³

¹Metis Design Corporation (USA), ²Air Force Institute of Technology (USA), ³Analog Devices Inc (USA)

Structural Health Monitoring (SHM) is defined as an in-situ implementation of non-destructive evaluation (NDE); essentially sensors are permanently installed on structure to facilitate inspection with minimal human intervention. In alignment with NDE, before an SHM system can be employed to manage structural integrity risk the detection sensitivity for a given method must be established, i.e. quantifying the statistical reliability of the system as a function of flaw size. The established consensus guidelines for determining detection sensitivity can be found in MIL-HDBK-1823A [1], which is generally followed by the US military and most commercial aircraft companies. This paper presents detection sensitivity results for a novel polymer nanocomposite (PNC) based crack gauge sensor. The crack gauge sensor itself is formed by blending carbon nanotube (CNT) with an epoxy binder to form a PNC, which is then sealed between flexible thermoplastic sheets along with silk-screened metallic electrodes. CNT are advantages for this application due to their resilience to corrosion, creep and fatigue, and offering a greater resistivity than metal traces resulting in higher precision measurements with common electronics. A design of experiment was established to quantify the effects of external factors on the gauge output, including temperature, strain, humidity and ageing. An in-situ compensation strategy was implemented, and proves effective in counteracting all studied external factors. A simple fatigue experiment was conducted on 60 aluminum bars with EDM notches to define the initiation point, and a PNC crack gauge was bonded to each bar. One hundred data points were collected during each experiment as the crack was grown up toward 2mm in length, and a probability of detection (PoD) curve was established using a hit/miss statistical model. The resulting $a_{90|95}$ value (smallest crack found with 90% probability and 95% confidence) was 0.32mm. Based on these PoD results, the PNC crack gauge participated in a high-g flight-test campaign on an F-15 through the U.S. Air Force.

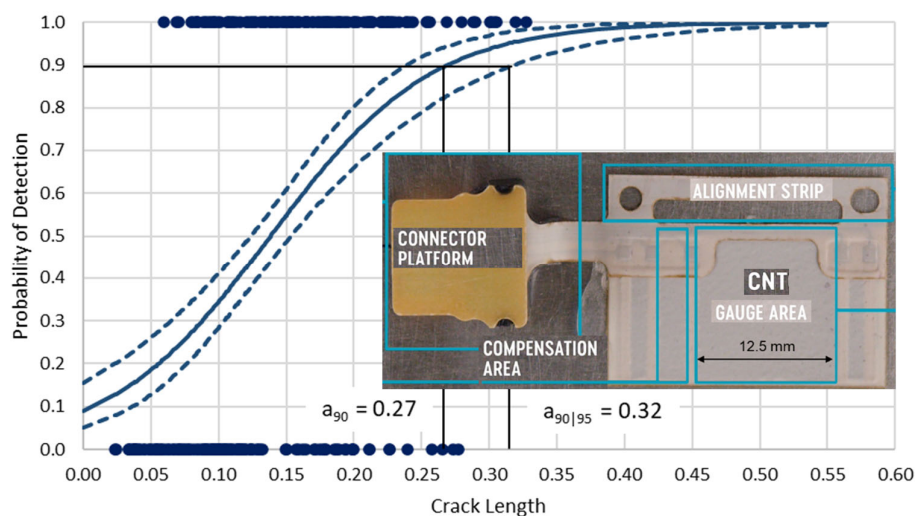


Figure 1: Probability of Detection (PoD) for a carbon nanotube crack gauge as a function of crack length.

References

- [1] MIL-HDBK-1823A, DoD Handbook: Nondestructive Evaluation System, Reliability Assessment (07 Apr 2009)
- [2] Lee J., Stein I.Y., Devoe M.E., Lewis D.J., Lachman N., Kessler S.S., Buschhorn S.T. and B.L. Wardle "Impact of carbon nanotube length on electron transport in aligned carbon nanotube networks." *Applied Physics Letters* 106, 053110 (2015)
- [3] Kessler, S.S., Raghavan A. and B.L. Wardle (2017). Multifunctional CNT-Engineered Structures (U.S. Patent No. 9,839,073). U.S. Patent and Trademark Office.
- [4] Stein Y., Kessler, S.S. and H. Primo (2023). Self-Calibrating Polymer Nano Composite (PNC) Sensing Element. (U.S. Patent No. 11,656,193). U.S. Patent and Trademark Office.
- [5] Kessler S.S., Thomas, G.A., Dunn C.T., Borgen M. and B.L. Wardle (2023). Multifunctional Assemblies (U.S. Patent No. 11,706,848). U.S. Patent and Trademark Office.

Diameter Control of Single-Walled Carbon Nanotubes Produced by Arc Discharge

Yixi Yao¹, Zeyao Zhang^{1,2,*}, Yan Li^{1,*}

¹Peking University, ²Institute of Carbon-Based Thin Film Electronics, Peking University, Shanxi (China)

zeyaozhang@pku.edu.cn; yanli@pku.edu.cn

Single-walled carbon nanotubes (SWCNTs) are considered to be the core material for the next generation carbon-based nanoelectronic devices due to their excellent electrical, thermal and mechanical properties. The intrinsic properties of SWCNTs are uniquely determined by their structures. According to the tight-binding model, the bandgaps of semiconducting SWCNTs is inversely proportional to the diameter d . To reduce the device performance fluctuations caused by the differences of bandgaps of SWCNTs, high-level devices require SWCNT samples with a narrow diameter distribution, and different devices require SWCNTs with different diameters. This places strict requirements on the diameter-controllable synthesis of prepared by arc discharge due to their higher degree of graphitization, fewer defects, and thus more excellent electrical and thermal properties. In this work, we applied the same anode components and obtained SWCNTs with different diameter distributions by adjusting the current and the pressure of helium during the arc discharge process. A larger current in an appropriate range led to an increase in the diameter of SWCNTs, as well as an increase in the content of SWCNTs. A higher pressure of helium also resulted in larger diameter and higher content of SWCNTs. Further, we found that the composition of the anode filler also has significant effects on the diameter distributions of SWCNTs. This work also demonstrates the practical potential for large-scale preparation of diameter-enriched SWCNTs using arc discharge.

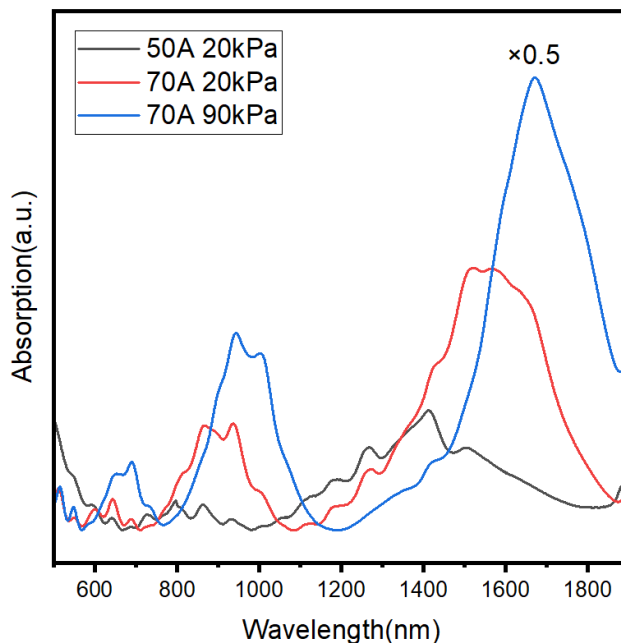


Fig. 1 Vis-NIR absorption spectra (normalized) of SWCNTs grown with different current and the pressure.

Diffusion ^1H -NMR (DOSY) for Analyzing 2D Polyaramid Polymers

M. Quien¹, M.S. Strano¹

¹*Department of Chemical Engineering, Massachusetts Institute of Technology (USA)*

The recent synthesis of two dimensional (2D) polyaramid (PA) polymers has shown that they exhibit remarkable mechanical and gas barrier properties. Herein, we use Diffusion ^1H -NMR analysis of the aromatic and proton end group regions to characterize polydisperse 2DPA-1 solutions. We introduce the concept of a q-window, which is the range of diffusivities that is detectable by a DOSY experiment, and which can be moved to view different portions of a polydisperse sample. Using a statistical analysis of the diameter distribution of a 2DPA-1 sample from TEM imaging, we compare the results from DOSY to elucidate how the q-window impacts the size range that is captured. We further highlight good practice and guidance to the reader on optimizing DOSY results.

Effect of Feedback Control Systems of Catalysts in Deep-Injection Floating Catalyst Chemical Vapor Deposition (DI-FCCVD)

Mingrui (Lily) Gong¹, Ana Victoria Benavides Figueroa², Eldar Khabushev¹, Arthur Sloan¹,
Glen Irvin¹, and Matteo Pasquali^{1,2,3}

¹*Department of Chemical and Biomolecular Engineering, ²Department of Chemistry, ³Smalley Curl Institute, Rice University (USA)*

Control over the catalyst particle formation and delivery rate is essential to improve the performance of floating-catalyst chemical vapor deposition (FCCVD). However, in most laboratory set-ups the delivery of the catalyst precursors is poorly characterized and regulated, especially when powdered ferrocene is used. Experimental iron (Fe) catalyst delivery rates are often approximated using the saturation equilibrium of ferrocene between vapor and solid phase, despite the possible variabilities in surface contact areas, pressure, and temperature across different types of sublimation methods.

To decrease such experimental variability, we introduced and developed a cost-effective feedback control system capable of maintaining an accurate and consistent ferrocene vapor delivery using real-time acoustic measurement of ferrocene concentrations. By controlling and tuning the iron delivery to our methane pyrolysis deep injection FCCVD process [1], we consistently synthesized long (>10 μm), highly crystalline (Raman G/D >50) FWCNTs with small diameters (1.42 ± 0.06 nm), at high rates (~ 1 g/hr), with minimal residual catalyst (< 5 wt%) and non-CNT carbon content (>90% CNTs), while also achieving extremely high single-pass methane conversions (>25%). Controlling catalyst delivery is critical to causal parameter studies that is foundational to the advancement of CNT synthesis.

Reference

[1] Sung-Hyun Lee. *et al.*, *Carbon* **173**, 901-909, (2021)

Effect of High Packing Aligned Carbon Nanotube Nanocomposites on Polysiloxane Thermal Protection Properties

P. B. Patel¹, S. Kim², N. Miller¹, J. Dai¹, J. Buffy³, J. H. Koo², B. L. Wardle¹

¹Massachusetts Institute of Technology (USA), ²The University of Texas at Austin (USA), ³Techneglas LLC (USA)

Aerospace polysiloxane ultra high temperature resin (UHTR), serves as an ablative material in thermal protection systems (TPS), specifically incorporated into the outermost layer of heat shields for re-entry space vehicles. The optimal functionality of TPS necessitates specific attributes in the ablative material, including low density, low thermal conductivity, high temperature resistance, and the capability to form a stable and robust char. In these applications, the aerospace industry commonly adopts fiber reinforced polymer composite materials due to their outstanding strength-to-weight ratio. Crystalline nanofibers, such as carbon nanotubes (CNTs) and boron nitride nanotubes (BNNTs), exhibit remarkable properties such as high specific strength, thermal stability, and unique electrical and thermal characteristics. This renders them potentially advantageous reinforcements for UHTRs as opposed to traditional carbon (micro)fibers (CF). However, prevalent methods employed for nanotube (NT)-reinforced resins often result in nanocomposites with voids, randomly oriented and agglomerated NTs, leading to insufficient packing density and limited enhancement in properties. Addressing this challenge, this study incorporates a novel bulk nanocomposite laminating process (BNL). The BNL technique integrates a straightforward NT orientation and densification method with the resin polymer infiltration process. Through this innovative approach, we successfully fabricate 6-ply CNT-polysiloxane laminates characterized by aligned CNTs, uniform CNT distribution, and a substantial CNT packing density above 30% by volume.

In preliminary studies, the oxyacetylene ablative test revealed better thermal protection properties achieved by the CNT-polysiloxane laminate when placed as a 60-micron thick coating on a CF-polysiloxane test specimen compared to a baseline CF-polysiloxane test specimen [1]. However, at the beginning of the test, the CNT-polysiloxane coating delaminated from the CF-polysiloxane specimen due to resin outgassing. To prevent delamination and for better thermal protection, in this experiment, a ceramic adhesive was used to secure the CNT-polysiloxane coating on the CF-polysiloxane specimen. Various property characterization techniques, including micro-computed tomography (μ CT), thermogravimetric analysis (TGA), and polarized Raman spectroscopy, were employed to characterize the properties of the CNT-polysiloxane laminates. The CNT-polysiloxane and CF-polysiloxane specimens were evaluated in an oxyacetylene test bed to assess their ablation properties.

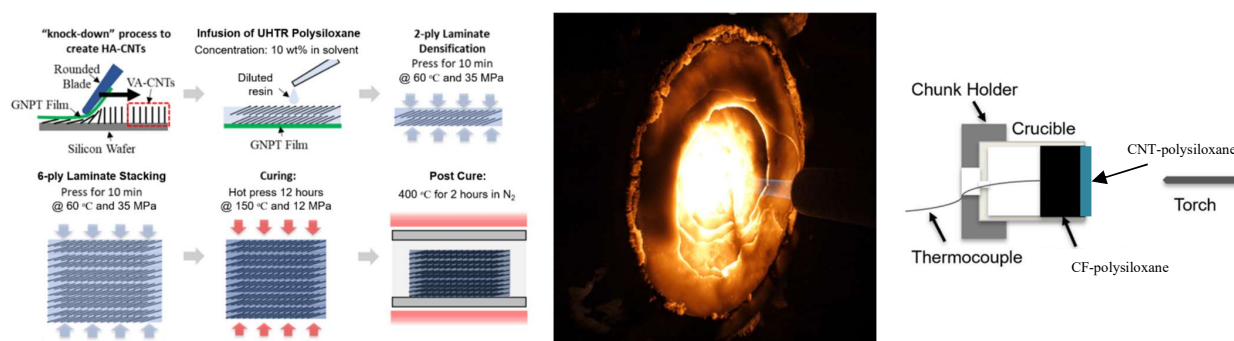


Figure: (left) Schematic depicting the bulk nanocomposite laminate (BNL) manufacturing for CNT-polysiloxane nanocomposite. (middle) Image of oxyacetylene torch testing the specimens. (right) Schematic of the oxyacetylene test bed for ablative testing. [1]

References

[1] P. B. Patel *et al.*, *AIAA Science and Technology*, 2024.

Effect of oxidation on water adsorption and dissociation in transition metal chalcogenides films epitaxially grown by molecular beam epitaxy

Hyuk Jin Kim¹, Young Jun Chang^{1,2,3*}

¹*Department of Physics, University of Seoul (Republic of Korea),*

²*Department of Smart cities, University of Seoul (Republic of Korea)*

³*Department of Intelligent Semiconductor Engineering, University of Seoul (Republic of Korea)*

Transition metal chalcogenides (TMCs) have been studied for their remarkable water splitting properties and have gained significant attention as earth-abundant and environmentally friendly materials. The HER process of water splitting involves the adsorption and dissociation of water molecules, so it is essential to understand these characteristics in order to elucidate the underlying reaction mechanism. However, most of the HER results in TMCs have been obtained from exfoliated samples or powders, which makes it difficult to control impurities and limits the rigorous analysis of the intrinsic water absorption and dissociation characteristics of the TMC materials. Due to the limitation, deep understanding of the evolution of surface oxidation states upon water exposure remains elusive, particularly water adsorption and dissociation characteristics. To reveal such critical information, both high quality sample preparation and in situ water exposure analysis are of great importance. Here, we will present the effect of oxidation on water adsorption properties on epitaxially grown VSe₂ and CoSe₂ films using APXPS under water vapor conditions. Rather than the Metal-Selenium bonding property, the Metal-Oxygen bonding property plays a significant role in enhancing the water adsorption characteristic. Our results can help to understand heterogeneous catalytic properties for water splitting applications.

* Corresponding author email address: yjchang@uos.ac.kr

EFFECT OF REACTOR ORIENTATION ON FCCVD SYNTHESIS OF FEW-WALLED CARBON NANOTUBES

A.V. Benavides-Figueroa¹, M. Gong², J. Junnarkar², G. Irvin², M. Pasquali^{1,2,3}

¹Department of Chemistry, ²Department of Chemical and Biomolecular Engineering, ³The Smalley-Curl Institute, Rice University (USA)

Floating catalyst chemical vapor deposition (FCCVD) is one of the most promising techniques for the commercial synthesis of high-quality few-walled carbon nanotubes (FWCNTs). FCCVD provides control over the morphology and structure of the produced material while allowing continuous operation. FCCVD reactors can be operated in horizontal or vertical configurations; often the selection is made based on laboratory space constraints. There are exhaustive reports on the effect of different carbon feedstocks, growth promoters, and catalysts on FCCVD synthesis of FWCNTs. [1] Yet, although the coupling of fluid dynamics and chemistry in the reactor is critical to the process, there are only a few studies of how reactor geometry affects synthesis.

Here, we study two almost identical FCCVD reactor systems with the only difference in orientation, horizontal and vertical, while maintaining the same reaction parameters. We introduce methane, ferrocene, and thiophene directly into the hot zone of the reactor via deep injection. [2] We find significant differences in methane conversion to FWCNTs (from 12 wt% to 20 wt%) between horizontal to vertical reactors while maintaining selectivity of ~ 95 wt% and high crystallinity ($G/D > 35$) for both configurations. Aspect ratio measurements show that FWCNTs made in the horizontal reactor are longer ($AR \sim 8500$) compared to those made in the vertical reactor ($AR \sim 6500$). Additionally, Computational Fluid Dynamics (CFD) simulations suggest differences in the fluid dynamics of both reactors, which results in different thermal and velocity profiles. Our results indicate that the orientation of both reactors may be producing different reaction environments, resulting in variances in process performance and FWCNTs characteristics. We believe our work contributes to a deeper understanding of FCCVD reactor working principles and could pave the way towards efficient knowledge transfer and faster industrial adoption of the FCCVD process for FWCNTs synthesis.

References

- [1] D. R. Chen, *et al.*, *Nano Life* **9**, no. 04, 1930002, (2019).
- [2] S. H. Lee, *et al.*, *Carbon* **173**, 901-909, (2021).

Efficient green-emitting 0D Mn²⁺-doped Cs₃CdBr₅ perovskite for WLEDs and X-ray imaging

Tongtong Kou¹, Liang Wang², William W. Yu^{1,*}

¹ School of Chemistry and Chemical Engineering, Key Laboratory of Special Functional Aggregated Materials, Ministry of Education, Shandong University, Jinan 250100, China.

² School of Integrated Circuits, Shandong University, Jinan 250101, China.

0D Cs₃CdBr₅ was synthesized at low temperature by manipulating the Cs/Cd molar ratio. It was then doped with 20% Mn²⁺ and a 520 nm green emission (520 nm) with 78.66% photoluminescence quantum yield was obtained. The WLEDs based on this 20% Mn:Cs₃CdBr₅ together with other phosphors exhibited warm white light; the color rendering index was 91 and the correlated color temperature was 4108 K. Further, this perovskite also demonstrated excellent x-ray scintillation properties with a low detection limit of 46.32 nGy_{air}·s⁻¹. The results show that Mn:Cs₃CdBr₅ is a promising candidate for solid-state lighting and low-dose high-resolution X-ray imaging.

Electrical characterization of SWCNT bundles

Abu Taher Khan¹, Nan Wei², Kimmo Mustonen³, Esko I. Kauppinen¹

¹Aalto University (Finland), ²Peking University (China), ³University of Vienna (Austria)

When carbon nanotubes grow in a floating catalyst CVD (FCCVD) reactor, they agglomerate due to Brownian diffusion [1] and form bundles as predicted by simple aerosol models [2]. Generally, as one third of as-synthesized SWCNTs are metallic, bundles, too, consist of a mixture of metallic and semiconducting tubes. While significant research efforts have been devoted to exploring the electrical performance of field effect transistors (TFT-FET) based on individual SWCNTs, less attention has been paid investigating the electrical performance variations that result from differences in SWCNT bundle dimensions and the underlying transport properties of the bundles [3,4].

In this work, we investigated transport behavior and electrical performance of two distinct sets of SWCNT bundles with mean diameters of 4.1 nm and 7.1 nm, and with mean tube diameters of 1.4 nm and 1.9 nm, respectively. Ideally, the transistor is expected to lose its switching efficiency (high off-state current) due to the presence of a metallic tube in the bundle. Thus, one would expect that all SWCNT bundles that contain metallic tubes (a clear majority of them), exhibit poor switching characteristics. Surprisingly, however, our data implies the opposite, and in fact, we observe a higher fraction of semiconducting devices than the fraction of semiconducting SWCNTs. In total we studied 4128 transistors from both small and large diameter bundles. Of the entire sample, approximately 70% exhibited semiconducting characteristics. The charge carrier mobility, a key performance metric, was extracted using both the peak transconductance method (μ_{PTC}) and the Y-function method (μ_{YFM}). The Ohmic contact single large bundle and large diameter SWCNT FETs demonstrated a mean μ_{PTC} value of $1853.93 \text{ cm}^2\text{V}^{-1}\text{S}^{-1}$ and a mean μ_{YFM} value of $5378.24 \text{ cm}^2\text{V}^{-1}\text{S}^{-1}$, while the single small bundle small diameter SWCNT FETs exhibited respective values of $1061.42 \text{ cm}^2\text{V}^{-1}\text{S}^{-1}$ and $2817.48 \text{ cm}^2\text{V}^{-1}\text{S}^{-1}$. To our best understanding, these mobility values are higher than those previously reported by others. Furthermore, large bundle large diameter SWCNT FETs exhibited I_{on}/I_{off} ratio distribution ranges between 10^3 and 10^8 , whereas small bundle small diameter SWCNT FETs displayed narrow distribution ranges between 10^6 and 10^8 . SWCNT bundle transistors demonstrate excellent control over switching efficiency making them ideal for high-speed digital electronics.

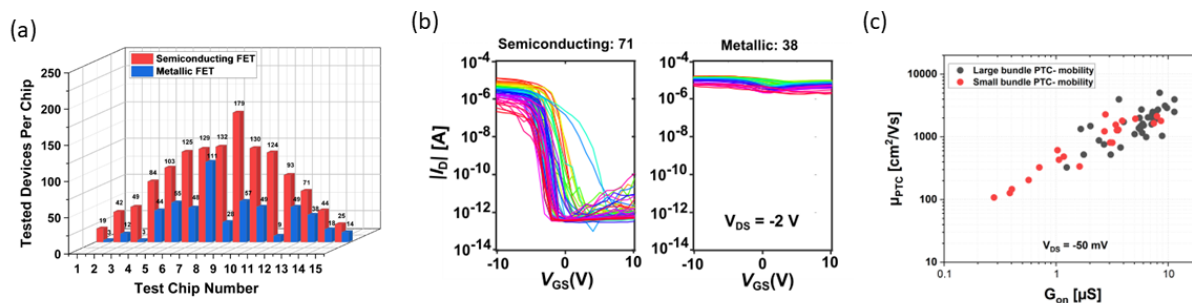


Figure: Electrical characterization of SWCNT bundle FETs. a) Bar chart shows the fraction of semiconducting and metallic FETs on fifteen chips. b) The transfer curves of semiconducting and metallic devices at $V_{DS} = -2 \text{ V}$ measured from one chip fabricated from small diameter SWCNT forming small diameter bundles. c) The peak transconductance mobility of fifty-five Ohmic contact FETs extracted at $V_{DS} = -50 \text{ mV}$.

References

- [1] A. Moaisala *et al. Chem. Eng. Sci.* **61**(13), 4393–4402 (2006).
- [2] K. Mustonen *et al. Phys. Lett.* **107**, 013106 (2015).
- [3] A. Kaskela *et al. Appl. Mater. Inter.* **7**, 28134–28141 (2015).
- [4] P. Laiho *et al. Appl. Mater. Inter.* **9**, 20738–20747 (2017).

Electronic Properties of One-Dimensional Titanate Nanofilaments and their Dye-Sensitization Behavior

Adam D. Walter, Gregory R. Schwenk, Jacob Cope, Kaustubh Sudhakar, Mary Qin Hassig, Lucas Ferrer, Andrea Mininni, Andrew J. Lindsay, and Michel W. Barsoum

Drexel University, Philadelphia, PA, 19104

This presentation will focus primarily on the published work by our group on the self-sensitization [1] of novel low-dimensional titanate materials, or 1DLs, supplemented with work from our collaborators on the electronic structure [2]. These materials have had over 10 papers published in just 2 years since its discovery [3,4], with many more on the way. A key aspect of this work is the simplicity of the fabrication process of 1DLs. This is a highly scalable process that provides a method of obtaining 1DL colloid, free of all precursor powders.

Although the only published paper on this work is regarding Rh6G and CV, some further results that are currently in the draft stage will be included. This primarily focuses on malachite green (MG) a more technically viable product than Rh6G and CV. 1DLs exhibit self-sensitization behavior with both Rh6G and CV (Figure 1), with similar performance with MG (not shown). It must be noted that self-sensitization of a semiconductor by CV has not been previously reported. In all cases, on the order of 30 minutes P25, the standard titania photocatalyst, exhibits no self-sensitization, while 1DLs decolorize much of the dye.

After discussing these results, the potential applications of dye-sensitized 1DLs will be introduced, as well as the benefits of low-dimensional titanate materials over traditional titania. This will be focused around the calculated (in-draft) and experimentally determined band locations of 1DLs [2] and how they impact the overall properties of 1DLs.

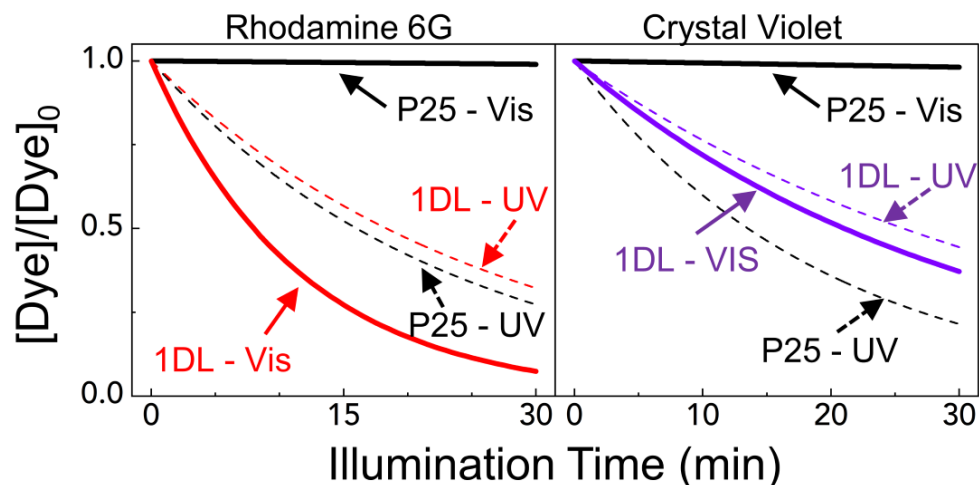


Figure 1: Decolorization of Rh6G, and CV over 1DL and P25. Solid lines denote activity with visible light only. Dashed lines denote activity with UV light only. Lines correspond to the average pseudo-first order kinetics over the 3 runs. Note that P25 is totally inactive in the visible range. Dyes were in a 1:1 mass ratio to 1DLs; starting dye concentration was 10 mg/L. Concentrations are normalized by concentration after 30 min in the dark, $[\text{Rh6G}]_0$ and $[\text{CV}]_0$. Adapted from ref [1].

References

- [1] Walter, A. D. et al. *Matter* 2023, 6 (11), 4086-4105. DOI: <https://doi.org/10.1016/j.matt.2023.09.008>.
- [2] Colin-Ulloa, E. et al. *J. Phys. Chem. C* 2023. DOI: 10.1021/acs.jpcc.2c06719.
- [3] Badr, H. O. et al. *Mater. Today*. 2022, 54, 8-17. DOI: 10.1016/j.mattod.2021.10.033.
- [4] Badr, H. O. et al. *Matter* 2022. DOI: <https://doi.org/10.1016/j.matt.2022.10.015>.

Electronic transport properties of the carbon nanotubes with the porphyrin-like substitutional defect

Jinwoong Chae and Gunn Kim*

Department of Physics and HMC, Sejong University (Republic of Korea)

*Corresponding author: gunnkim@sejong.ac.kr

Quantum transport properties of nanomaterials have significant implications for device physics and nanotechnology. In this research, we explore the potential of carbon nanotubes (CNTs) containing metalloporphyrin-like substitutional defects as sensors for toxic molecules, based on their altered electronic behavior. Utilizing the nonequilibrium Green's function method, we investigate the electron transport characteristics of CNTs with these novel defects.

The defect structure is engineered by removing two carbon atoms, forming a nanohole, and subsequently replacing four neighboring carbon atoms with nitrogen atoms. An iron (Fe) atom is then positioned at the nanohole's center. Our findings reveal that the transmission of CNTs with these substitutional defects exhibits spin-dependent behavior. Within specific energy regions, the metalloporphyrin-like defect act as a scattering center, significantly influencing electron transport.

Transmission through a pristine armchair CNT via the π and π^* channels near the Fermi level approaches $2G_0$ ($G_0 = 2e^2/h$). However, the introduction of these defects reduces the transmission below G_0 in certain energy ranges, suggesting complete backscattering within the eigenchannels induced by the porphyrin-like defect.

Furthermore, we investigate the interaction of two representative toxic radicals, cyanide ($\text{N}\equiv\text{C}^-$) and sulfanyl (HS^\bullet) groups, bonded with the iron atoms located within the defective CNTs. Compared to the bare defective CNTs, the adsorption of these radicals noticeably alters the transmission spectra.

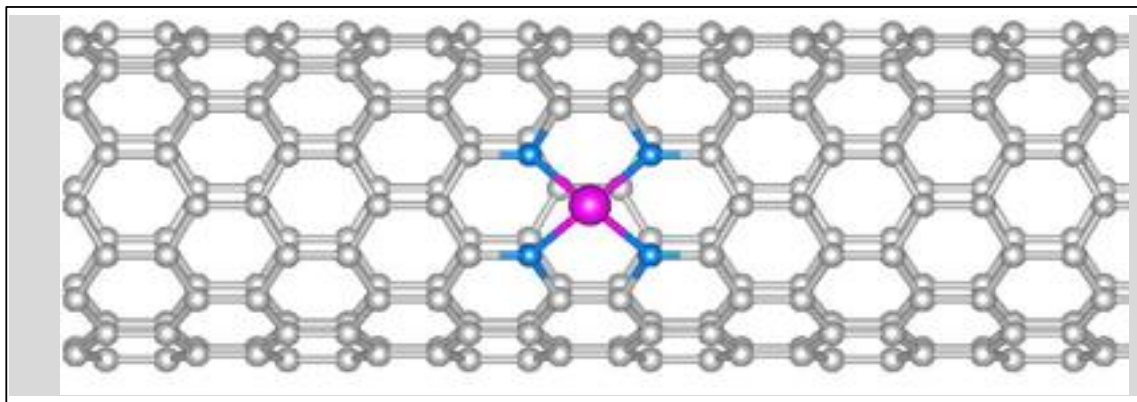


Figure: An armchair carbon nanotube with a metalloporphyrin-like defect.

Electrothermal free-form additive manufacturing of nanotube-loaded thermosets

Anubhav Sarmah, Ethan M. Harkin, Micah J. Green

Artie McFerrin Department of Chemical Engineering, Texas A&M University, College Station, TX, 77843, USA

Despite the extensive use of thermosetting resins, additive manufacturing of such materials is extremely limited. Traditional processing requires either (i) long curing schedules to avoid the collapse of an uncured printed part or (ii) changes to the resin chemistry and curing mechanism. This work demonstrates a material-extrusion based setup capable of printing and curing any industry-standard thermoset resin loaded with carbon nanotubes. First, we use a conventional Direct Ink Writing (DIW) printer to deposit the uncured resin ink. After each layer is deposited, the nanotube-loaded part is exposed to radio frequency (RF) fields generated by a coaxial applicator suspended over the part. The resulting current generates heat rapidly and volumetrically, curing the resin, preventing part collapse, and enabling further printing. This methodology enables rapid additive manufacturing of arbitrarily large structures with low viscosity resins that are otherwise impossible to print.

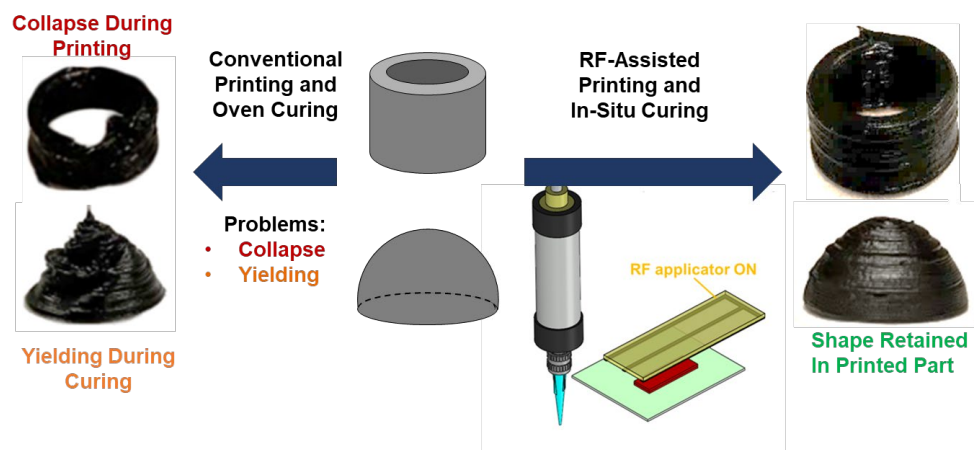


Figure: A methodology for additive manufacturing and in-situ curing of CNT-epoxy composites is presented. During direct ink writing, low power radio-frequency fields are applied to deposited thermoset ink, causing current generation through the CNT-filled resin, volumetrically heating the part, and inducing curing. This methodology can be easily applied to other resin systems.

Elucidating the Prominent Role of Non-Electrostatic Barriers in the Stabilization of Individual Carbon Nanotubes in Water using Bile Salt Surfactants

Rahul Prasanna Misra^{1†}, Peng Wang^{2†}, Chiyu Zhang², YuHuang Wang^{2,3}, and Daniel Blankschtein¹

¹*Department of Chemical Engineering, Massachusetts Institute of Technology, Cambridge, Massachusetts 02139, United States*

²*Department of Chemistry and Biochemistry, University of Maryland, College Park, Maryland 20742, United States*

³*Maryland NanoCenter, University of Maryland, College Park, Maryland 20742, United States*

[†]*These authors contributed equally to this work*

Traditional ways of dispersing single-walled carbon nanotubes (SWCNTs) and other nanomaterials using surfactants typically involve high surfactant concentrations, often in the range of 1–2 wt/v% of the solution. Here, we develop a sonification-free method called superacid-surfactant exchange (S2E) to stabilize individual carbon nanotubes at substantially lower surfactant concentrations of approximately 0.08 wt/v%, near the critical micelle concentration (CMC) of the surfactants [1]. Among the diverse ionic surfactants and charged biopolymers explored, we demonstrate that the bile salt surfactant, sodium deoxycholate (DOC), exhibits the highest dispersion efficiency, outperforming sodium cholate (SC), a structurally similar bile salt surfactant containing just one additional oxygen atom compared to DOC. The molecular mechanism of surfactant-aided SWCNT stabilization is uncovered using all-atomistic molecular dynamics (MD) simulations. To this end, MD simulations are first carried out to obtain the change in the Helmholtz free energy as a DOC/SC surfactant molecule is transferred from the bulk solution to the SWCNT/water interface. Subsequently, this free energy profile is utilized in conjunction with the Langmuir adsorption model to show that at bulk surfactant concentrations close to the CMC, the SWCNTs are covered by surfactants corresponding to their saturated surface coverage. Next, MD simulations are carried out to obtain the change in the Helmholtz free energy as two surfactant-covered SWCNTs at the saturated surface coverage approach one another from the bulk solution. These simulations yield two key insights: (i) both the DOC and SC surfactants efficiently penetrate the space between the interacting nanotubes with the dispersion efficiency of the S2E process being governed by a free energy barrier, non-electrostatic in origin, which is associated with the free energetic cost of removing the last layer of surfactant molecules intercalated between the SWCNTs, and (ii) a substantially larger free energy barrier is obtained for DOC due to its relatively stronger interaction with the nanotube wall, consistent with the experiments. Crucially, our MD simulations also reveal that the free energy barrier in the presence of Na⁺ and Cl⁻ ions, which are generated during the S2E process, does not obey the classical Derjaguin–Landau–Verwey–Overbeek (DLVO) theory of colloidal stability, underscoring the important role of non-electrostatic dispersion and hydration interactions at the nanoscale, even in the case of ionic surfactants like DOC. These molecular insights advance our understanding of surfactant chemistry at the bare nanotube limit and suggest a low-energy, surfactant-efficient solution processing method for SWCNTs and potentially other nanomaterials.

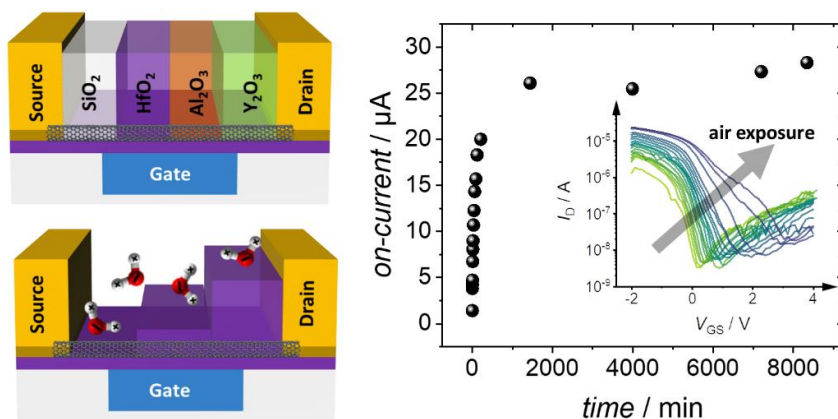
- [1] Wang, P., Misra, R. P., Zhang, C., Blankschtein, D. & Wang, Y. Surfactant-Aided Stabilization of Individual Carbon Nanotubes in Water around the Critical Micelle Concentration. *Langmuir* **40**, 159–169 (2024). (featured as the cover story in the 40th anniversary issue of *Langmuir*)

Encapsulation of High-Frequency CNT-based FETs for RF Communication

M. Hartmann, M. Ernst, S. Böttger, S. Hermann

Center for Microtechnologies, Chemnitz University of Technology, Chemnitz, Germany
Center for Materials Architecture and Integration of Nanomembranes, Chemnitz University of Technology, Chemnitz, Germany
martin.hartmann@zfm.tu-chemnitz.de

High frequency carbon nanotube-based field effect transistors (CNT-FET) are a highly promising candidate to enhance future communication electronics due to their high charge carrier mobility and low intrinsic capacitance. It has already been shown in 2019 that this technology surpassed comparable silicon-based radio frequency (RF) FETs *e.g.* in terms of their extrinsic current gain cut-off frequencies as well as maximum frequencies of oscillation [1]. Moreover, in recent years their performance was further increased approaching the THz region [2]. Nevertheless, this technology is still at its infancy and technological improvements of the device geometry, the CNT to metal contacts, the CNT alignment and density, the CNT quality and the CNT encapsulation/ doping will enhance the HF CNTFET properties further. Within this study we report on the impact of different CNT encapsulation layers as well as their deposition processes onto the properties of CNTFETs. Especially interface phenomena such as electrostatic doping (ED) and charge transfer doping (CTD) between the CNTs and their direct environment will be discussed. Therefore, initially the barrier properties of the encapsulation layers against the ambient were studied to differentiate between ED / CTD and water / oxygen induced doping.



Overview of different CNTFET passivation approaches and device designs (left) and electrical measurements of the time stability of a CNTFET with 5 nm HfO₂ passivation

References

- [1] C. Rutherglen *et al.*, *Nature Electronics* **2**, 530–539 (2019).
- [2] J. Zhou *et al.*, *IEEE Electron Device Letters* **44** (2), 329–332 (2023).

Engineering Organic Color Centers along Single-Walled Carbon Nanotubes with DNA

Abhindev Kizhakke Veetil¹, Xiaojian Wu¹, Mijin Kim^{1,2}, Lucy J. Wang¹, YuHuang Wang^{1,*}

¹Department of Chemistry and Biochemistry, University of Maryland, College Park, MD 20742 (USA), ²School of Chemistry and Biochemistry, Georgia Institute of Technology, Atlanta, GA 30332 (USA)

Organic color centers (OCCs) hold substantial potential to advance multiple research fronts, including imaging, sensing, and quantum information science. However, it has been challenging to program the synthesis of these chemical defects. In this work, we introduce a DNA-based approach to create sp^3 defect sites in the sp^2 lattice of SWCNTs. By replacing DNA bases with photosensitive, modified RNA bases, we incorporate reactive sites in single-stranded DNA that wraps around the nanotube. Photoexcitation of this system leads to the generation of sp^3 defects along SWCNTs. These sp^3 centers, which act as deep exciton traps in SWCNTs, are characterized by pronounced photoluminescence peaks red-shifted from pristine nanotube emission in the near-infrared (NIR). Furthermore, the DNA sequences were engineered with inert spacers to control the position and density of defects along the nanotube. This method, which integrates carbon nanotubes and OCCs with DNA, a polymer central to biological systems, marks a crucial step in utilizing these molecularly tunable color centers in various potential applications.

Enhancing VRFB Performance: Horizontally Aligned CNT Nanocomposites Bipolar Plates

Jae-Moon Jeong¹, Jingyao Dai², Luiz Acauan², Hyunsoo Hong¹, Brian L Wardle^{2,3}, Seong Su Kim¹

¹ Department of Mechanical Engineering, Korea Advanced Institute of Science and Technology (Korea),

² Department of Aeronautics and Astronautics, Massachusetts Institute of Technology (USA),

³ Department of Mechanical Engineering, Massachusetts Institute of Technology (USA)

Bipolar plates (BPs) are integral components in vanadium redox flow batteries (VRFBs), serving as multifunctional elements crucial for efficient charge transfer, mechanical support, and electrochemical stability [1]. Therefore, conventional BPs based on graphite sheets have garnered attention for their impressive tensile strength, stiffness, electrical conductivity, and corrosion resistance [2]. However, a major obstacle remains in resolving the consistent formation of resin-rich areas and voids between graphite sheets, resulting in reduced electrical conductivity along the thickness. In this study, we introduce a novel concept of horizontally aligned carbon nanotube nanocomposite BPs (HACN-BP). Utilizing a manufacturing process involving hot press and co-cure techniques, HACN-BP obtained a remarkable 59.9% CNT volume fraction, by knocking down vertically aligned carbon nanotubes (VA-CNT) [3-5]. This design ensures superior electrical conductivity in both in-plane and thickness directions, while maintaining low permeability. Furthermore, numerical simulations evaluating the electrochemical characteristics of VRFB cells equipped with integrated HACN-BP and current collectors demonstrate effective mitigation of ohmic losses, resulting in a significant reduction in potential drop. The utilization of the integrated HACN-BP in VRFB single-cell tests demonstrated a remarkable improvement, showing a 6% increase in energy efficiency and a 15% increase in capacity compared to the conventional BP.



Figure: Horizontally Aligned CNT Nanocomposite Bipolar Plate

References

- [1] J.-M. Jeong, et al, Applied Materials Today, 24, 101139 (2021).
- [2] K.I. Jeong, et al, Composites Part B: Engineering, 233, 109657 (2022).
- [3] A.L. Kaiser, et al, ACS Applied Nano Materials, 5, 9008-9023 (2022).
- [4] C.X. Li, et al AIAA SCITECH 2024 Forum. Publisher. (2024)
- [5] C. Curtis-Smith, et al AIAA SCITECH 2023 Forum. Publisher. (2023)

Evaluation of p-n junctions in graphene nanoflakes via carrier density mapping with Kelvin Probe Force Microscopy

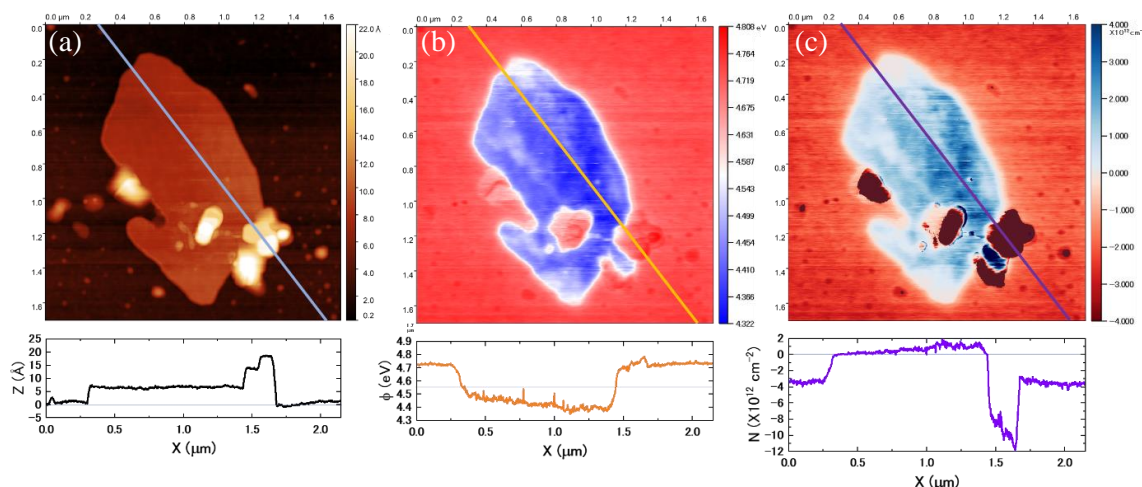
M. Ashino, H. Okabayashi, K. Sakai, H. Shimamura, K. Ishibashi

Kanazawa Institute of Technology (Japan)

Substantially important to modern civilization, semiconductor devices are constructed upon the p-n junction. Graphene, a two-dimensional material with a thickness of a single carbon atom, is the most promising candidate for semiconductor materials of the next generation. Ongoing endeavors are being made to fabricate and assess p-n junctions on graphene [1]. It is common knowledge that graphene on oxidized films of silicon (SiO_2/Si) substrates is p-type doped in air [2]. Conversely, n-type doping can be accomplished by inducing electrons into graphene through the electric field effects or by adsorbing other substances on the surface or by mixing them in during chemical vapor deposition. By extension, p-n junctions have been formed in the in-plane direction and at the interface with the stacked overlayers, but those methods require large-scale equipment or have stability or performance issues [1].

Our group have postulated that graphene nanoflakes (GNFs), smaller than $1 \mu\text{m}^2$ in size, formed on the SiO_2/Si substrate in air by mechanical exfoliation would not necessarily be p-type doped. To investigate this hypothesis, we concurrently observed the surface topography (Fig. (a)) and electric potentials of GNFs using frequency-modulated Kelvin probe force microscopy (FM-KPFM) [3]. From the pre-determined work function value of the probe tip, the surface potential images obtained on the GNFs have been converted to work function images (Fig. (b)). Furthermore, the carrier density images of the entire GNFs (Fig. (c)) have been obtained by applying the method of deriving the carrier density of the single-layer and stacked overlayer regions [4,5] to the work function images based on the correspondence relationship with the topography images obtained simultaneously (Fig. (a)). This method allows for revealing not only the existence of intrinsic and n-type regions but also the formation of p-n junctions in the same plane of the single layer and at its interface with the stacked overlayers.

Here, we report a quantitative evaluation of the "depletion region widths" and "work function differences" by applying the Poisson equation to the "depletion regions" in the p-n junctions and simulating the surface electric potentials after studying the formation model of each region and interface including the intrinsic regions.



Carrier density mapping with FM-KPFM: Topography (a), work function (b), and carrier density (c) images ($1.7 \times 1.7 \mu\text{m}^2$) and their line profiles (below) of graphene nanoflakes on a SiO_2/Si substrate.

References

- [1] P. Tian et al., *Adv. Mater. Technol.* **4**(7), 1900007 (2019).
- [2] K. S. Novoselov et al., *Science* **306**, 666–669 (2004).
- [3] V. Panchal et al., *Sci. Rep.* **3**, 2597 (2013).
- [4] Y.-J. Yu et al., *Nano Lett.* **9**, 3430–3434 (2009).
- [5] D. Ziegler et al., *Phys. Rev. B* **83**, 235434 (2011).

Evolving the Synthesis of Horizontally Aligned Carbon Nanotube Arrays: AI-Driven Catalyst Innovation and Density Control

Yue Li^{1,2#}, Shurui Wang^{1#}, Zhou Lv¹, Ziqiang Zhao², Yaodong Yang^{3*}, Liu Qian^{1*}, Jin Zhang^{1,2*}

¹*School of Material Science and Engineering, Peking University (China),*

²*State Key Laboratory of Nuclear Physics and Technology, School of Physics, Peking University (China),*

³*School of Intelligence Science and Technology, Peking University (China),*

The controlled synthesis of horizontally aligned carbon nanotube (HACNT) arrays presents a complex challenge, spanning over a dozen dimensions from a single nanoscale catalyst to wafer-scale samples. Traditional research paradigms struggle to address such multi-dimensional complexity.

In this presentation, we unveil a groundbreaking system for the synthesis of HACNT arrays, distinguished by its integration of artificial intelligence and automation. Central to our system are two large language models, Carbon_GPT and Carbon_BERT. These models, functioning as an advanced AI 'brain', are aligned with literature on carbon materials based on GPT and BERT, driving innovation in experimental design. Complementing these AI models is an automated chemical vapor deposition (CVD) system, which acts as the 'physical extension' of the AI, enabling around-the-clock experiments and significantly boosting the efficiency and stability of carbon nanotube array production.

Our system's capabilities are showcased in two key applications: catalyst prediction and density-controllable synthesis of HACNT arrays. First, leveraging the analytical and predictive power of our AI models, we identified novel catalyst combinations that enhance the growth of carbon nanotube arrays. This innovation was validated through high-throughput, automated experiments, demonstrating the AI's capability in generating creative solutions. Secondly, we employed a digital twin technology in conjunction with our extensive process-performance database to precisely control the density of the carbon nanotube arrays. This aspect of our work exemplifies the precision and accuracy achievable through our integrated AI and automated system.

Throughout the presentation, we will explore the synergistic relationship between the AI models and the automated CVD system, detailing how this integration not only facilitates innovative catalyst discovery but also enables precise control over the material synthesis process. Our approach represents a paradigm shift in nanomaterials synthesis, illustrating the potent combination of AI and automation in advancing material science.

Excitonic Fano Line Shape in Scattering of Surfactant-Wrapped Carbon Nanotube Dispersion

In-Seung Choi, Seongjoo Hwang, and Sang-Yong Ju*

Department of Chemistry, Yonsei University, 50 Yonsei-ro, Seodaemun-Gu, Seoul 03722, Republic of Korea

The optical characteristics of single-walled carbon nanotubes (SWNTs) are fundamentally excitonic, yet the dynamics of excitonic scattering in the presence of surfactants are not fully understood. In this study, we explore the excitonic scattering patterns of both single-chirality and mixed-chirality SWNTs utilizing an integrating sphere that allows for the separation of scattering from extinction and absorption. For single-chirality SWNTs, the extinction spectrum displays additional peaks due to exciton-phonon interactions, flanking the main excitonic transitions. This leads to a scattering spectrum characterized by distinctive, heartbeat-like inelastic Fano resonances at each exciton and exciton-phonon interaction point, layered atop a baseline scattering trend. The appearance and shape of these Fano resonances, indicative of the interaction between excitons and free charges in the continuum, are influenced by the Fano parameter. This parameter is largely influenced by the variance in the dielectric constants between the SWNT's surface and the surfactant's headgroup that interacts with the SWNT.

Excitonic-Optics Study of 2D Chalcogenides Layered Semiconductors

Ching-Hwa Ho¹

¹Graduate Institute of Applied Science and Technology, National Taiwan University of Science and Technology, Taipei 106, Taiwan

E-mail address: chho@mail.ntust.edu.tw,

The excitonic state or many-body effect (like trion) is an important physical phenomenon for studying optical property of two-dimensional (2D) semiconductors. The most important example is the case of GaN or ZnO, whose band-edge excitons are available for light emission and photodetection. The advantage of 2D semiconductors is the reduced dimensionality could decrease the dielectric screening effect between layer by layer and which renders the existence of excitons and many-body particles in the compound for further optoelectronics application. The 2D semiconductors exhibit immense functionalities and practicalities of large area, ultra-thin smooth surface, high carrier mobility, flexible layers, and thickness-tunable band-gap modulation that have gradually received blooming attention in semiconductor technological studies and development in the post-silicon era. Among the 2D semiconductors, transition-metal dichalcogenides (TMDCs) MX_2 ($M = W, Mo, Re$ and $X = S, Se$) comprising a monolayer structure with $X-M-X$ and layered III-VI compounds NX ($N = Ga, In$ and $X = S, Se, Te$) that are composed of fundamental units of $X-N-X$ might be two of the important braches of 2D materials that require further research and development in electronics and optoelectronics devices applications. There is also another group of van der Waals gapped chalcogenides, metal thio(seleno) phosphates MTPs which possess a monolayer structure combining both types of TMDs and III-VI monochalcogenides have been gradually bloomed, *e.g.* $NiPS_3$ and $CuInP_2S_6$. These MTPs layers can be the potential candidates for ferroelectric and ferromagnetic memories applications.

In this study, we grow high-quality layered chalcogenides crystals of TMDCs, III-VI, and MTPs, etc. and do optical measurements of micro-thermoreflectance (μ TR), micro-photoluminescence (μ PL), time-resolved-photoluminescence (TRPL), and fluorescence-lifetime-image mapping (FLIM), and area-fluorescence wavelength mapping (AFWM), *etc.* for excitonic and band-edge characteristics of the exfoliated multilayer chalcogenides samples. Meanwhile, the potential usages for the 2D layered chalcogenides with strong many-body excitonic effects are also proposed and demonstrated.

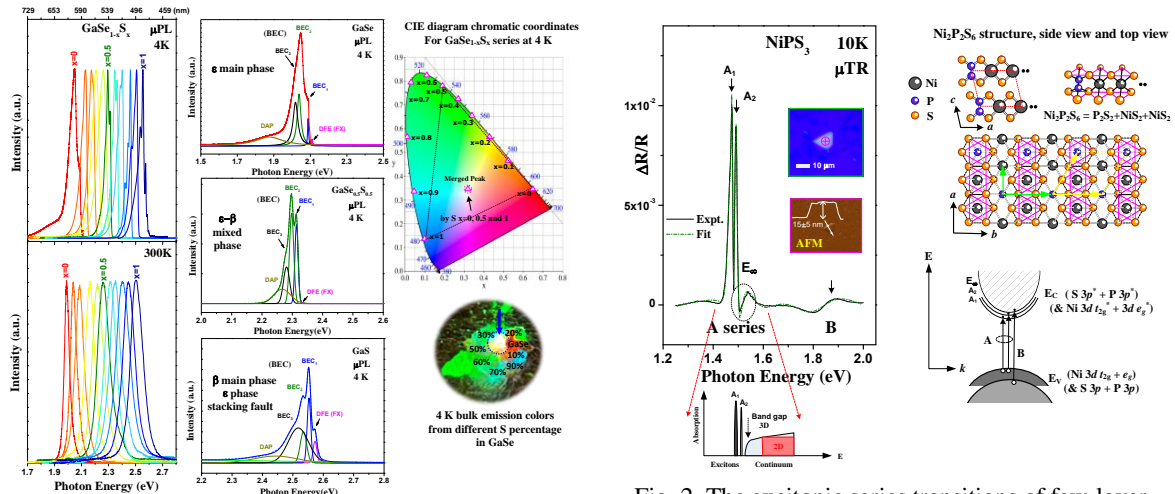


Fig. 1. Full-wavelength visible white-light emission from multilayered $GaSe_{1-x}S_x$ ($0 \leq x \leq 1$)

Fig. 2. The excitonic series transitions of few-layer $NiPS_3$ observed by μ TR measurement at 10 K and its atomic and band-edge schemes.

References

- [1] C. H. Ho, Z. Z. Liu, Nano Energy **56**, 641-650 (2019).
- [2] C. A. Chuang, F. H. Yu, B. X. Yeh, A. M. Ummah, A. S. Rosyadi, C. H. Ho, Adv. Optical Mater. **11**, 2301032 (2023).
- [3] C. H. Ho, T. Y. Hsu, L. C. Muhimma, npj 2D Mater. & Appl. **5**, 8 (2021).

Experimental and Theoretical Calculations of Fluorinated Few-layer Graphene/epoxy Composite Coatings for Anticorrosion Applications

Hao-Hsuan Hsia,¹ Geng-Hua Li,¹ Yun-Xiang Lan,² Ria Kunwar,³ Liang-Yin Kuo,^{3,*} Jui-Ming Yeh^{2,*} and Wei-Ren Liu^{1,*}

¹ Department of Chemical Engineering, R&D Center for Membrane Technology,

Research Center for Circular Economy, Chung Yuan Christian University Taoyuan 32023, Taiwan

² Department of Chemistry, Center for Nanotechnology, Chung Yuan Christian University, Taoyuan 32023, Taiwan

³ Department of Chemical Engineering, Ming Chi University of Technology, No. 84, Gungjuan Rd., Taishan Dist., New Taipei City 243303, Taiwan

Corrosion protection technology plays a crucial role in preserving infrastructure, ensuring safety, reliability and promoting long-term sustainability. In this study, we combined experiments and density functional theory (DFT) to investigate the mechanism of corrosion for fluorine-doped few-layer graphene (F-FLG). We introduced a facile approach that combines environmentally friendly jet cavitation with hydrothermal processes to synthesize hydrophobic and anti-corrosive F-FLG from graphite (G), shown in Fig. 1. By coating F-FLG/epoxy composite film (F-FLG/EP) on the surface of cold-rolled steel (CRS), we found that the addition of F dopant enhanced the hydrophobicity of the F-FLG/EP coating from 78.89° to 106.3°. Notably, the corrosion rate of the F-FLG/EP coating is 8.279×10^{-3} $\mu\text{m}^2/\text{year}$, which exhibits four orders of magnitude lower than that of the CRS substrate. The DFT calculations indicate an increased band gap for F-FLG. Moreover, the energy barrier for the oxygen diffusion through F-FLG is larger than that for FLG, indicating improved oxygen resistance for F-FLG. These results indicate the high efficiency and potential of F-FLG as a highly promising agent for preventing corrosion in various commercial applications.

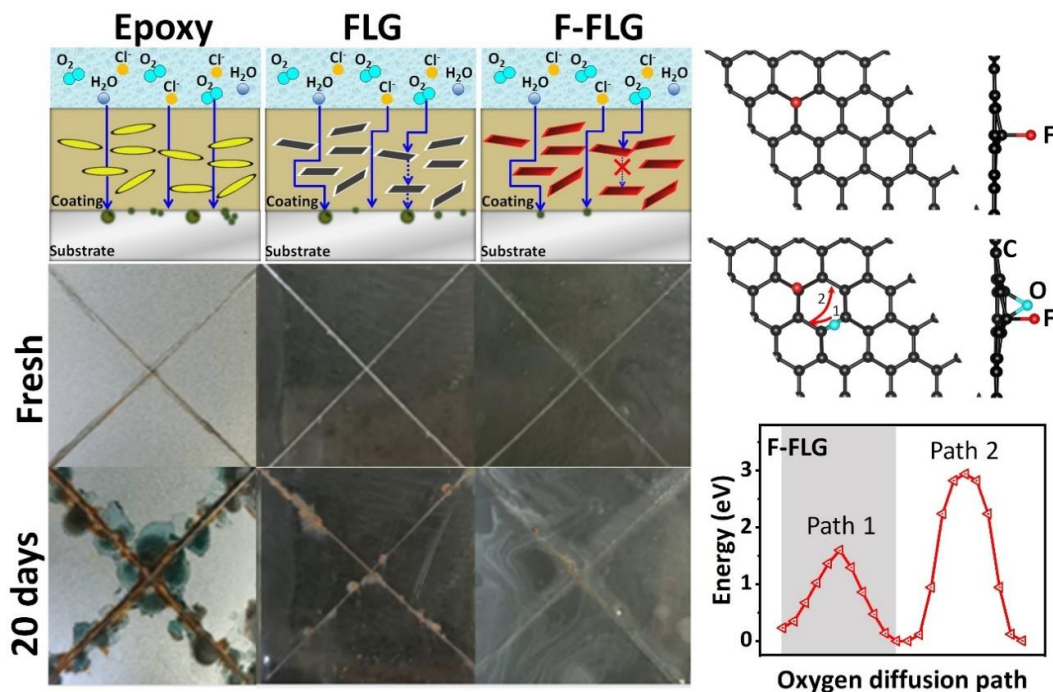


Figure 1: Anticorrosion mechanism of F-FLG/EP composite film, salt spray tests and DFT results.

Reference

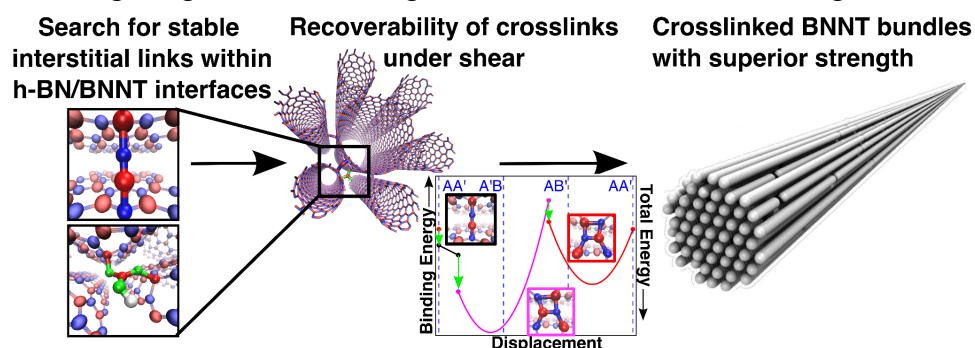
- [1] Hao-Hsuan Hsia, Geng-Hua Li, Yun-Xiang Lan, Liang-Yin Kuo, Jui-Ming Yeh* and Wei-Ren Liu,* "Experimental and Theoretical Calculations of Fluorinated Few-layer Graphene/epoxy Composite Coatings for Anticorrosion Applications," *Carbon*, **217** (2024) 118604.

Exploration into Interstitial Crosslinks Capable of Strengthening Boron Nitride Nanotube Bundles

N. Tjahjono^{1*}, E.S. Penev¹, V. Yamakov², C. Park³, B.I. Yakobson¹
¹Rice University- Houston (United States) ²National Institute of Aerospace- Hampton
(United States). ³NASA Langley Research Center- Hampton (United States)
*email: nt21@rice.edu

Boron nitride nanotubes (BNNTs) are strong, lightweight, and piezoelectric nanomaterials, whose unique properties lend themselves to a wide variety of applications ranging from vibration sensing to resilient aerospace materials with radiation shielding capabilities [1]. However, the superior mechanical properties of individual nanotubes [2] and ultrahigh interlayer friction within multi-walled BNNTs [3] have yet to be manifested in practical macroscale BNNT bundles: despite their partially ionic B-N bonds, synthesized BNNT bundles [4] have not exhibited strengths substantially higher than carbon nanotube bundles.

Here, we use *ab initio* calculations to search for interstitial species that can strengthen BNNT bundles via the formation of interlayer crosslinks. Density-functional theory (DFT) calculations indicate that small species present in the laser ablation synthesis of BNNTs [5,6], such as BN dimers, form stable links between h-BN bilayers, with binding energies greater than 2 eV. Additional *ab initio* molecular dynamics (AIMD) and DFT calculations suggest that larger species found during BNNT purification [7] (such as deprotonated forms of boric acid), can form covalent bridges within small-diameter BNNT bundles. Full enumeration of low-energy interstitial configurations within various h-BN bilayer stacking modes reveals that these interstitials prefer to bridge the layers in their ground states. These results demonstrate not only the recoverability and stability of these links under shear, but also the potential for high friction [8] as crosslinks transition between their ground states. Moreover, this suggests that links can strengthen BNNT bundles by orders of magnitude, thereby providing a path to bolster BNNT fibers up to the long-sought intrinsic strength of individual tubes, in the range of tens of GPa [2].



Schematic of *ab initio* study into interstitials capable of strengthening BNNT bundles. Stable interstitial links include BN (top left) and HBO_3 , a doubly-deprotonated form of boric acid (bottom left). The plot depicts ground state transitions of BN across the AA' armchair shearing direction. Rightmost image is adapted from ref. [8].

References

- [1] J. H. Kang et al., *ACS Nano* **9**, 11942–11950 (2015).
- [2] X. Wei et al., *Advanced Materials* **22**, 4895–4899 (2010).
- [3] A. Niguès et al., *Nature Materials* **13**, 688–693 (2014).
- [4] C. J. Simonsen Ginestra et al., *Nature Communications* **13**, 3136 (2022).
- [5] J. H. Kim et al., *Scientific Reports* **9**, (2019).
- [6] S. Yatom et al., *Physical Chemistry Chemical Physics* **22**, 20837–20850 (2020).
- [7] D. M. Marincel et al., *Chemistry of Materials* **31**, 1520–1527 (2019).
- [8] N. Gupta, J.M. Alred, E.S. Penev, B.I. Yakobson, *ACS Nano* **15**, 1342–1350 (2021).

Exploring polymer contamination cleaning and characterization approaches for aligned CNT material.

Marina Y. Timmermans¹, Carlos R. Cunha^{1,2}, Luca Mana¹, Xiangyu Wu¹, Dennis Lin¹, Himanshu Sharma¹, Pieter-Jan Wyndaele^{1,3}, Lijun Liu^{1,3}, Katherine R. Jinkins⁴, Michael S. Arnold⁴, Steven Brems¹, Cesar J. L. de la Rosa¹, Gouri S. Kar¹, Jean-Francois de Marneffe¹

¹imec, Kapeldreef 75, 3001 Leuven (Belgium), ²Intituto Superior Tecnico, Av. Rovisco Pais, Lisbon, 1049-001 (Portugal), ³KU Leuven, Celestijnenlaan 200D, 3001 Leuven (Belgium), ⁴SixLine Semiconductor, Inc., 5262 Bishops Bay Pkwy, 53597 Middleton, WI (USA)

Aligned single-walled carbon nanotubes (SWCNTs) are a promising material candidate for next-generation field-effect transistors (FETs). The ideal CNT material system for high-performance FETs consists of well-aligned densely packed CNTs with a consistent pitch (>200 CNTs/ μm), a semiconducting purity $>99.9999\%$ and a narrow chirality distribution. With the recent progress in CNT purification, aligned assembly and subsequent integration in devices, CNTs show to be not only a scientifically attractive material but offer a technologically feasible solution towards high-performance and ultimately scaled transistors [1-4]. However, there are still a number of challenges on their way from the lab to the fab.

In this work we explore the post-deposition processing of semiconducting SWCNTs which were aligned into a dense array by means of 2D nematic tangential flow interfacial self-assembly (TaFISA) [2]. The extraction of high purity semiconducting CNTs and their assembly into aligned arrays require the use of conjugated polymers which need to be removed without damaging CNTs after their deposition on the substrate. We explore various CMOS compatible approaches to remove the polymer residue including downstream remote plasma etching, thermal anneal and UV cure. We apply different material characterization techniques to assess the efficiency of the cleaning and its effect on the CNT material quality. Further, we fabricate bottom gate CNT FETs with L_g down to 50 nm and present the electrical performance of the aligned CNT material.

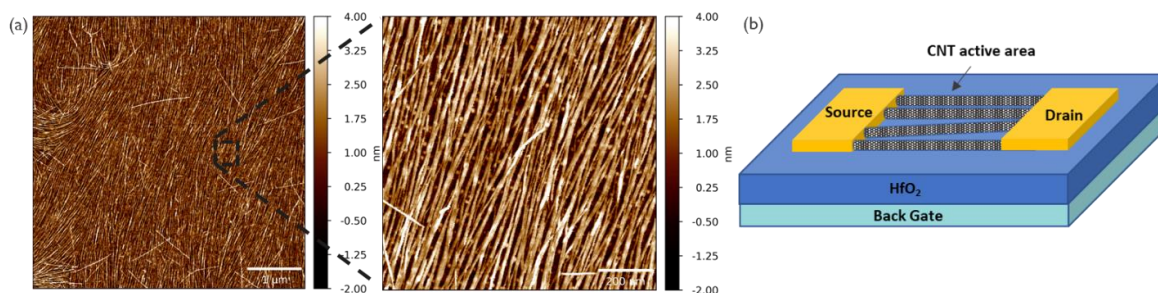


Figure: (a) AFM images of aligned CNT arrays deposited by TaFISA. (b) Schematic illustration of back gated CNT FET.

References

- [1] Liu et al, Science **368**, 850 (2020)
- [2] Jinkins et al, Sci. Adv. **7** (2021)
- [3] Bishop et al, Nat. Electron. **3** **492** (2020)
- [4] Lin et al, Nat. Electron, **6** (2023)

Fabrication of SWCNT thin films at the interface of liquid-liquid phase separation

Seiya Nishida¹, Yusaku Shimada¹, Tsuyoshi Endo¹, Ryotaro Kaneda¹, Keigo Otsuka¹,
Shigeo Maruyama¹, and Shohei Chiashi¹

¹Department of Mechanical Engineering, The University of Tokyo, Tokyo, 113-8656, Japan

chiashi@photon.t.u-tokyo.ac.jp

Applications that take advantage of the high conductivity of SWCNTs are critically important in the field of SWCNT research. Generally, SWCNTs are synthesized in a highly entangled state, so technology is required to untangle and shape them into the desired configurations. In particular, SWCNT thin films, which are anticipated to exhibit excellent electrical conductivity, often fall short of the conductivity demonstrated by individual SWCNTs. There are various reasons for this, but one of the causes is dispersion in water with surfactants, which are often used when producing thin films. Surfactants and dispersion treatments are known to reduce the electrical conductivity of SWCNTs, so it is imperative to develop techniques that can effectively untangle SWCNTs and create uniform thin films without surfactants.

In this study, we developed a method for forming a SWCNT thin film using an organic solvent dispersion and investigated the mechanism of the thin film formation. Dimethylformamide (DMF) was used as an organic solvent with miscibility with water. It has a relatively high dispersibility of SWCNTs, while the dispersibility is not as good as that of surfactant water [1]. So, the concentration of SWCNT/DMF dispersion was lower than that of surfactant water solution. Commercially available SWCNTs were dispersed in DMF by using an ultrasonic disperser, and the dispersion was mixed with additives such as PDMS. This additive is soluble in DMF, but not in water. When the SWCNT/DMF dispersion was gently poured into water, liquid-liquid phase separation occurred due to the presence of the additive. Since the liquid-liquid phase separation is not stable, DMF gradually diffused into the water below, resulting in the increase of SWCNT concentration in the upper DMF layer. Then SWCNTs precipitated uniformly at this liquid-liquid interface, and uniform SWCNT thin films were obtained. Figure 1 shows an optical image of the liquid-liquid phase separated state. If a substance with high vapor pressure is used as an additive instead of PDMS, it was easily removed from the SWCNT thin film. Due to its hydrophobic nature, SWCNTs formed on the water surface was easily picked up and transferred to any substrate. In addition, it was possible to fabricate SWCNT thin films with extremely low density.

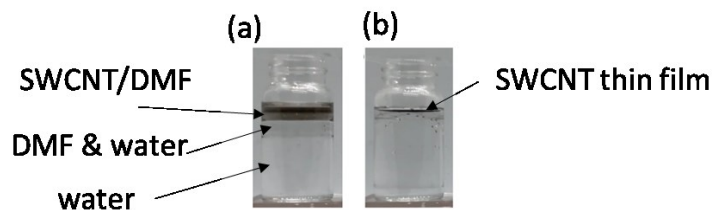


Figure 1: Optical images of (a) liquid-liquid phase separation state of SWCNT/DMF and water, and (b) SWCNT film formed after whole DMF diffused into the water layer.

Reference

[1] S. Manzetti & J.-C. P. Gabriel, *Int. Nano Lett.*, **9**, 31-49 (2019).

Facilitating Quasi-van der Waals Epitaxy of WS₂ on Sapphire through Tungsten Oxide

A. Cohen^{1,2}, P.K Mohapatra¹, S. Hettler^{3,4}, A. Patsha¹, K.V.L.V. Narayanachari⁵, P. Shekhter¹, J. Cavin⁵, J.M. Rondinelli⁴, M. Bedzyk⁵, O. Dieguez¹, R.Arenal^{3,4} and A. Ismach¹.

¹ Tel Aviv University (Israel), ² Technion (Israel), ³ Tel Aviv University (Israel), ⁴ Universidad de Zaragoza, (Spain), ⁵ CSIC-Universidad de Zaragoza, (Spain), ⁵ Northwestern University (United States).

Abstract

The current state-of-the-art in semiconductor technology heavily relies on traditional epitaxy for precise control of thin films and nanostructures at the atomic level. These components serve as essential building blocks for various applications, including nanoelectronics, optoelectronics, and sensors. Approximately four decades ago, the terms "van der Waals" (vdW) and "quasi-vdW (Q-vdW) epitaxy"¹ were introduced to describe the oriented growth of vdW layers on 2D and 3D substrates, respectively.

In this research, a novel approach is employed for the growth of WS₂ by exposing metal and chalcogen precursors sequentially in a metal-organic chemical vapor deposition (MOCVD) system². This method incorporates a metal-seeding stage before the actual growth process. The precise control over precursor delivery allows for the investigation of the formation of a continuous and seemingly ordered WO₃ mono- or few-layer on the surface of a c-plane sapphire. Significantly, this interfacial layer is revealed to exert a strong influence on the subsequent quasi-vdW epitaxial growth on sapphire, marking a pivotal advancement in the field by elucidating a new epitaxial growth mechanism³.

Furthermore, the study demonstrates the capability of epitaxial growth of WS₂ at relatively low temperatures, extending up to 300°C, and provides insights into the underlying mechanisms⁴. These findings open the door to the possibility of rational epitaxial growth on a diverse range of material systems, showcasing the potential for broader applications in semiconductor technology.

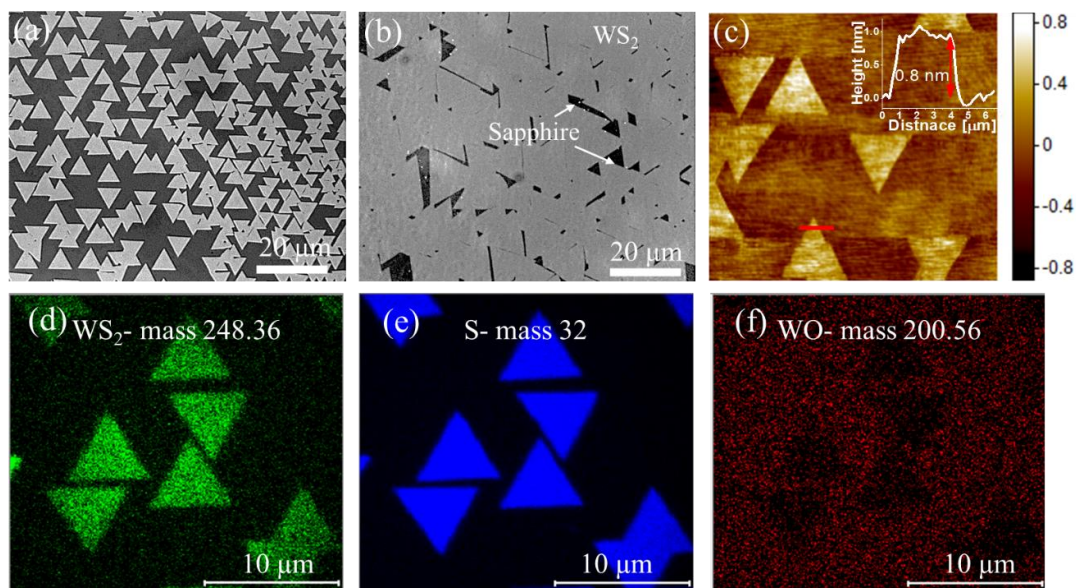


Figure caption: WS₂ epitaxial growth on sapphire (a-b) optical image; (c)AFM image;(d-f) TOF-SIMS analysis showing the domain and the WO_x interface layer between WS₂ to the sapphire.

References

- Koma, Journal of Crystal Growth, Issue 201-202, [pp. 236-241] (1999).
[1] Assael Cohen et al., ACS Nano, vol.15, no. 1, [pp. 526–538], (2021).
[2] Assael Cohen et al., ACS Nano, vol. 17 no. 6, [pp. 5399-5411], (2023).
[3] Assael Cohen (soon to be published)

FROM DOTS TO TUBES – THE *REVERSE* SCENARIO OF BOTTOM-UP CATALYST-FREE SYNTHESIS OF *N*-DOPED CNTs

S. Boncel¹, A. Kolanowska¹

¹Silesian University of Technology, CONE, NanoCarbon Group (Poland)

In 2004, the family of carbon nanoallotropes, with the reborn in 1991 1D carbon nanotubes (CNTs), grew to include 0D carbon quantum dots (CQDs) [1]. While intrinsically fluorescent CQDs vary in their chemical nanoarchitecture, one of their most important representatives is nanoparticles with a nanocarbon core and polar, shell O/N functionalities. In general, CQDs, as carbon nanomaterials unique *per se*, might serve as fluorescent probes, drug delivery systems, sensors, light emitters, and photocatalysts [2], but they are generally not considered as versatile substrates in the synthesis. At the same time, nitrogen-doped CNTs (*N*-CNTs), including *n*-doped, i.e., electron-enriched single-walled CNT semiconductors, can be applied as supercapacitors, electrodes, active 1D fillers of reinforced, thermo- and electroconductive composites, separation membranes, superhydrophobic surfaces, and sensors [3].

The synthetic interrelationships between CQDs and CNTs have been represented so far only by a top-down strategy based on progressive, oxidation-driven degradation of CNTs toward CQDs [4]. Indeed, there are no reports on the synthesis of *N*-CNTs from CQDs: only the *reverse* scenario was realized. And although the synthesis of CNTs and *N*-CNTs has been studied for more than three decades, the catalyst-free methods were elaborated almost exclusively for CNTs.

Here, we report a novel, sustainable method for the synthesis of *N*-CNTs from amino-acid-derived CQDs in the absence of an external catalyst [5]. *Yucca*-like *N*-CNTs, containing from 4 to 26 at.% of N, were comprehensively analyzed using complementary methods, such as SEM, EDX, TEM, XPS, Raman spectroscopy, and ICP-AES. The elaborated strategy enables protocols for the synthesis of novel materials applicable as, for instance, from-transparent-to-translucent electrodes, multifunctional coatings/self-standing films of enhanced electroconductivity [6], and needle-like drug delivery systems, while the above list has rather only a tentative character.

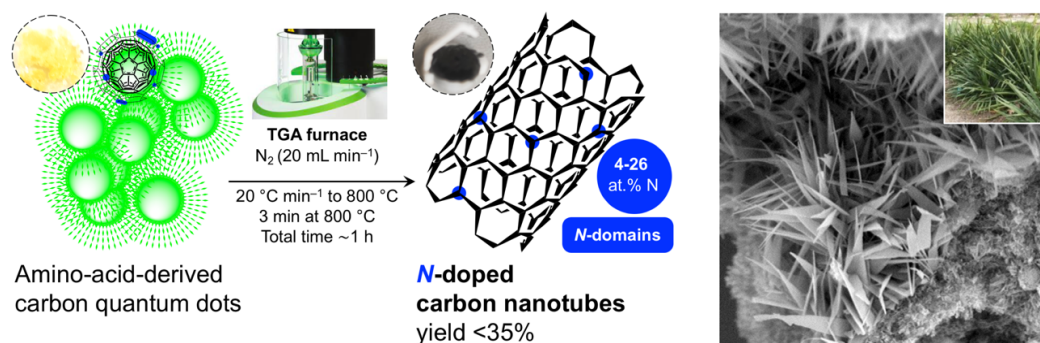


Figure: Synthesis of *N*-CNTs from amino-acid-derived CQDs (*left*); SEM image of *Yucca*-like *N*-CNTs (*right*)

Acknowledgements

The authors are very grateful for the financial support from the National Science Centre (Poland) Grant No. 2021/43/B/ST5/00421 in the framework of the OPUS-22 program.

References

- [1] S. Y. Lim *et al.*, *Chem. Soc. Rev.* **44**, 362–381 (2015).
- [2] A. Kolanowska *et al.*, *ACS Omega* **7**, 41165–41176 (2022).
- [3] S. Boncel *et al.*, *Beilstein J. Nanotechnol.* **5**, 219–233 (2014).
- [4] A. Kolanowska *et al.*, *RSC Adv.* **9**, 37608–37613 (2019).
- [5] A. Kolanowska *et al.*, *Chem. Commun.* **59**, 7659–7662 (2023).
- [6] S. Boncel *et al.*, *ACS Appl. Nano Mater.* **5**, 15762–15774 (2022).

Functional materials based on wood, carbon nanotubes, and graphene

A. Lekawa-Raus¹, D. Łukawski²

¹ Warsaw University of Technology (Poland), ² Poznan University of Technology (Poland)

The recent search for sustainable and low-carbon footprint materials has increased the interest of materials scientists in wood. Wood is a robust, porous, lightweight, and easily processable material. Simultaneously, it is natural, widely available, renewable, and biodegradable. It can be used as a raw material or turned into a wide range of composites and derivatives of varying properties.

Enriching this carbon-based material and its composites and derivatives with carbon nanotubes (CNTs) and graphene can lead to the development of many novel applications, and significantly change the functionality and performance. Our earliest works have shown that wood can be coated with CNTs and graphene using standard printing and coating techniques, but interestingly, CNTs and graphene can also be deposited on wood without the use of binders [1,2]. Depending on the chosen technique of deposition and coating material we turned wood superhydrophobic and antistatic. Moreover, we have shown a range of electronic applications such as wood-based flood sensors, motion sensors, temperature sensors, integrated floor heaters or wood dryers. Further studies have shown that carbon nanomaterials can be easily integrated into wood binders and produce electroactive particleboards, which keep the international standards set for the reference composites [3,4]. The most recent study considers the use of CNT-enriched wood sponges as medical electrodes. However, the combination of wood, CNTs and graphene can provide many more interesting solutions. Our recent reviews analyze current progress in this area and indicate directions for future development [5,6].

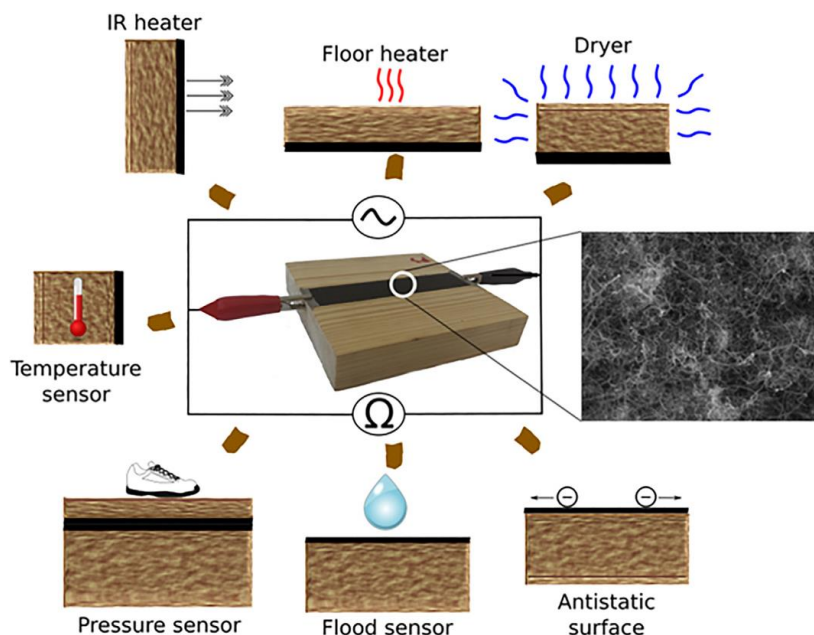


Figure 1 Electronic wood composites [2]

References (if desired)

- [1] D. Łukawski et al., *Prog. Org. Coat.* 125, 23 (2018).
- [2] D. Łukawski et al., *Compos. Part A*, 127, 105656 (2019).
- [3] D. Łukawski et al., Phenol-formaldehyde resin enriched with graphene nanoplatelets as an electroconductive adhesive for wood composites, under review in *International Journal of Adhesion and Adhesives*
- [4] D. Łukawski et al., *Drewno*, 62, 203 (2019).
- [5] D. Łukawski et al. *Wood. Sci. Tech* 57, 989 (2023)
- [6] D. Łukawski et al. *Polymers*, 14, 745 (2022)

Giant Second-Harmonic Generation from Aligned Enantiomer-Enriched Carbon Nanotube Films

J. Doumani¹, R. Xu¹, N. Hong³, F. Tay¹, W. Gao⁴, R. Saito^{2,6,7}, Y. Yomogida², K. Yanagi², V. Perebeinos⁵, A. Baydin¹, J. Kono¹, and H. Zhu^{1,*}

¹Rice University (USA), ²Tokyo Metropolitan University (Japan), ³J.A. Woollam Co. (USA), ⁴University of Utah (USA), ⁵University at Buffalo (USA), ⁶Tohoku University (Japan), ⁷National Taiwan Normal University (Taiwan)

Recent years have witnessed the emergence of novel systems that exhibit broken mirror symmetry, i.e., chirality [1-5]. The chiral motion of charged particles can couple with other degrees of freedom, such as photons [4] and spins [3,6], and chiral molecules and materials are optically active. They can be utilized in diverse technologies, including quantum-photonics sources, secure communications, and biosensing. In carbon nanotubes (CNTs), there are two types of chirality: molecular chirality and synthetic chirality. The latter has been recently achieved at wafer scales in ordered CNT films [7]. However, molecular chirality has yet to be explored in macroscopic architectures except for observations of circular dichroism in aqueous suspensions of individualized single-enantiomer CNTs [8-10]. Here, we report the first observation of second-harmonic generation (SHG) from a film of aligned enantiomer-enriched single-chirality CNTs.

Theoretical projections foresaw strong second-order nonlinearities in chiral species of single-wall CNTs, where the chirality indices (n,m) satisfy $n > m > 0$. The predicted values of the second-order nonlinear optical susceptibility $\chi^{(2)}$ have been as large as a few nm/V [11], due to enhancement through the van Hove singularities inherent in the electronic density of states in CNTs. Yet, to date, the observation of faint SHG signals in single CNTs and thin CNT films underscored challenges arising from insufficient enantiomer purity and sample crystallinity. Both enantiomer enrichment and alignment are crucial for observing SHG since the co-existence of an equal number of right-handed and left-handed CNTs, as well as the lack of macroscopic alignment, will prevent inversion-symmetry breaking.

By implementing enantiomer purification of CNT species, combined with nanotube alignment, we demonstrated giant SHG from an aligned film of (6,5)- single-enantiomer-enriched CNTs, a validation of the theoretical predictions. Utilizing mixed-surfactant gel chromatography [9] and controlled vacuum filtration [12], we achieved enantiomer purification and nanotube alignment, resulting in a resonance-enhanced $\chi^{(2)}$ of ~ 1.5 nm/V when the fundamental photon frequency was at the E₁₁ exciton transition. This value rivals the $\chi^{(2)}$ of small-area 2D semiconductors of few nm/V like Te, InSe, GaS, and 2H-MoTe₂ [13]. Our approach attains nonlinearity at wafer scales, presenting a promising avenue for practical applications in quantum information processing, biomedical imaging, short-wavelength lasers, and frequency conversion.

References

- [1] H. Zhu *et al.*, *Science* **359**, 579-582 (2018).
- [2] F. G. G. Hernandez *et al.*, *Sci. Adv.* **9**, eadj4074 (2023).
- [3] S. Das *et al.*, *Nano. Lett.* **23**, 6602-6609 (2023).
- [4] P. Lodahl *et al.*, *Nature* **541**, 473-480 (2017).
- [5] J. Luo *et al.*, *Science* **382**, 698-702 (2023).
- [6] R. Naaman *et al.*, *J. Phys. Chem. Lett.* **3**, 2178-2187 (2012).
- [7] J. Doumani *et al.*, *Nat. Commun.* **14**, 7380 (2023).
- [8] S. Ghosh *et al.*, *Nat. Nanotechnol.* **5**, 443-450 (2010).
- [9] X. Wei *et al.*, *Nat. Commun.* **7**, 12899 (2016).
- [10] G. Ao *et al.*, *J. Am. Chem. Soc.* **138**, 16677-16685 (2016).
- [11] G. Y. Guo *et al.*, *Phys. Rev. B* **69**, 205416 (2004).
- [12] X. He *et al.*, *Nat. Nanotechnol.* **11**, 633-638 (2016).
- [13] Q. Fu *et al.*, *Adv. Mater.* **35**, 2306330 (2023).

Growth of Nanostructured Molybdenum Disulfide (MoS₂) Thin Film Using the Plasma-Enhanced Atomic Layer Deposition for the Application of Electronic Materials

Ibraheem Giwa¹, Fabian Sanchez¹, Elton Mawire¹, Qunying Yuan², and Zhigang Xiao^{1*},

¹Department of Electrical Engineering, Alabama A&M University, Normal, AL 35762

²Department of Biological and Environmental Science, Alabama A&M University, Normal, AL 35762

(*Email: zhigang.xiao@aamu.edu)

Abstract

We report the fabrication of molybdenum disulfide (MoS₂) thin films–based electronic devices. Nanostructured molybdenum disulfide (MoS₂) thin films are grown as the active semiconducting channel material for the fabrication of MoS₂-based field-effect transistors using plasma-enhanced atomic layer deposition (PE-ALD). MoS₂-based electronic devices such as MoS₂ field-effect transistors, inverters, and ring-oscillators are fabricated with the ALD-grown MoS₂ film using the clean room-based micro- and nano-fabrication techniques. Hydrogen sulfide (H₂S) gas is used as the S source in the growth of molybdenum disulfide (MoS₂) while molybdenum (V) chloride (MoCl₅) powder is used as the Mo source. The MoS₂ film is analyzed by the high-resolution tunnel electron micrograph (HRTEM), scanning electron micrograph (SEM), X-ray photoelectron spectroscopy (XPS) analysis and Raman spectrum analysis. The fabricated MoS₂ device wafer is annealed at high-temperatures (800 – 900 °C), and the electrical property of the MoS₂-based electronic devices is measured before and after the high-temperature annealing and is compared. The characterization results of the nanostructured molybdenum disulfide (MoS₂) thin films and the measurement results on the fabricated MoS₂-based electronic devices will be reported in the ICMCTF 2024 Conference.

Acknowledgements: The research is supported by National Science Foundation under Grant No. ECCS-2100748.

Heavy Anchoring of Silver Nanoparticles on Carbon Nanotubes

Jen-Hung Fang¹, Luiz Acauan¹, Aniruddha Ghosh¹, Yosi Stein², and Brian L. Wardle^{1*}

¹Massachusetts Institute of Technology (USA), ²Analog Devices, Inc. (USA)

Conductive composites have garnered considerable attention for their diverse industrial applications. In this study, we employed a strategic approach by incorporating silver nanoparticles (Ag NPs) into carbon tubes (CNTs) to achieve enhanced electrical conductivity. Initially, untreated CNTs were coated with benzyl mercaptan (BnSH) through π - π interactions, introducing thiol functional groups. This coating facilitated the creation of numerous nucleation sites for the growth of Ag NPs. By doing so, we maximized the quantity of Ag NPs on the CNTs, mitigating attachment issues arising from the steric hindrance of larger silver nanoparticles. In essence, this method overcame challenges that would arise if Ag NPs were to grow directly on BnSH molecules without CNTs, preventing the spatial blockage of adjacent attachment sites on the CNTs. Looking ahead, the integration of Ag NPs onto CNTs holds promise for applications in structural electronics, enabling the replacement of current copper-based electronics.

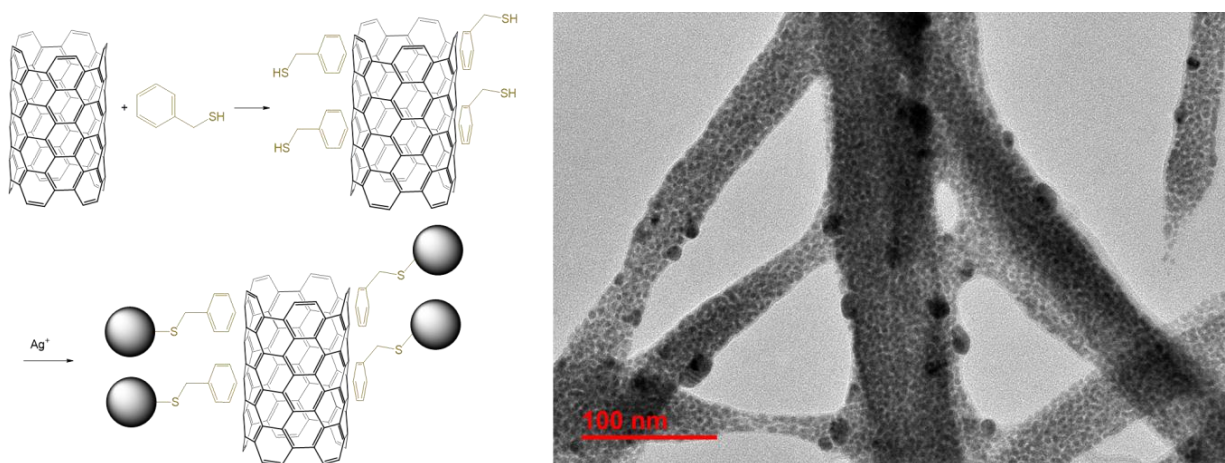


Figure: Mechanism (left side) for high loading of Ag NPs on carbon nanotubes (right side).

Hierarchical Mesostructures of Anatase Nanoparticles for Photodegradation of Bisphenol-A

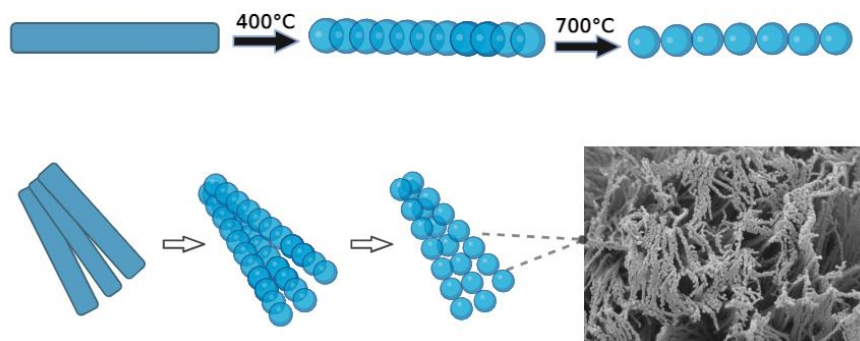
Treesa Reji¹, Adam D. Walter¹, Yasunori Hioki², Mohamed Ibrahim¹, Gregory R. Schwenk¹, Hussein O. Badr¹, Michel W. Barsoum¹

¹Department of Materials Science and Engineering, Drexel University, Philadelphia, PA, USA

²MuRata Corporation, Kyoto, JP

Phase transition from one-dimensional lepidocrocite (1DL) TiO₂ nanofilaments to anatase phase resulted in a new hierarchical mesostructure of TiO₂ anatase nanoparticles. These hierarchical structures of anatase nanoparticles exhibit potential for the photodegradation of a water-soluble, endocrine disruptor organic compound, bisphenol-A (BPA). 1DL mesopowders are subjected to annealing at different ranges of temperatures (200°C – 700°C), and the phase transformation is studied. Mesostructures remain after annealing and the 1DL nanofilaments turn into anatase nanoparticles. These phases are employed to study the photodegradation of BPA in water and compared. The structural and phase transformation to anatase has been analyzed and verified using different characterization tools. Rapid degradation of BPA solution in a short duration of time is an advancement in the environmental remediation.

X-ray diffraction analysis confirmed the transformation of 1DL TiO₂ lepidocrocite to the anatase phase. Characteristic peaks for anatase TiO₂ start to appear for 400°C-1DL, and the high-intensity crystalline peaks of 700°C-1DL mark the complete 1DL-anatase phase transition. The kinetics of degradation were studied using liquid phase ultraviolet-visible spectroscopy (UV-Vis) and total organic carbon (TOC) analysis. Optical band gap of the prepared anatase nanoparticles calculated using Solid State UV-VIS Analysis is 3.24 eV. The impact of thermal processing on the morphological change of the 1DL TiO₂ nanostructures was imaged by scanning electron microscope (SEM). Sphere-shaped particles can be seen aligned only in one dimension, as each TiO₂ particle is separated from the other, resembling the beads in a long chain.



Graphical Abstract: Temperature induced phase change and spheroidization of 1DL nanofilaments into anatase hierarchical structures.

References

- [1] Kaushik, R., Daniel, P. V., Mondal, P., & Halder, A. (2019). Transformation of 2-D TiO₂ to mesoporous hollow 3-D TiO₂ spheres-comparative studies on morphology-dependent photocatalytic and anti-bacterial activity. *Microporous and Mesoporous Materials*, 285, 32-42
- [2] Ge, M., Cao, C., Huang, J., Li, S., Chen, Z., Zhang, K. Q., ... & Lai, Y. (2016). A review of one-dimensional TiO₂ nanostructured materials for environmental and energy applications. *Journal of Materials Chemistry A*, 4(18), 6772-6801.
- [3] Ge, M., Cao, C., Huang, J., Li, S., Chen, Z., Zhang, K. Q., ... & Lai, Y. (2016). A review of one-dimensional TiO₂ nanostructured materials for environmental and energy applications. *Journal of Materials Chemistry A*, 4(18), 6772-6801.
- [4] Do, H. H., Nguyen, D. L. T., Nguyen, X. C., Le, T. H., Nguyen, T. P., Trinh, Q. T., ... & Van Le, Q. (2020). Recent progress in TiO₂-based photocatalysts for hydrogen evolution reaction: A review. *Arabian Journal of Chemistry*, 13(2), 3653-3671.

High Performance Dielectric Elastomer Actuators with Carbon Nanotubes

Suhan Kim, YuFeng (Kevin) Chen

Research Laboratory of Electronics, Massachusetts Institute of Technology (USA)

Dielectric elastomer actuators (DEAs) are a class of soft artificial muscles applied in a wide range of robotics systems including haptics, wearables, biomimetics, and aerial robots. The structure of a DEA consists of a thin elastomer layer sandwiched between two compliant electrode layers. When an input voltage is applied across the electrode layers, the electrostatic force induces the contraction of the elastomer layer, which results in the expansion along orthogonal directions. Performance characteristics, such as electrical resistance/capacitance, frequency behaviors (e.g. time constant, hysteresis), and actuation range/force, are strongly dependent on material selection of the elastomer and the electrodes. To develop aerial robots, we aim to achieve high bandwidth (>300 Hz) and high power density (>700 W/kg) in soft actuators. These functional requirements guide our selection of elastomer and electrode materials. We choose the multilayer composite of Elastosil P7670 with single-walled carbon nanotubes (SWCNTs) [1], which exhibits the best performance as flying muscles.

In this report, we describe the unique benefits of SWCNTs as DEA electrodes. To be specific, when there is a local defect inside the DEAs, SWCNTs are capable of selectively isolating this area under a high voltage input. By disconnecting the defects that would cause early dielectric breakdown, the actuator can endure higher electric field (~ 60 V/ μm), which enhances both actuation range and force. By resolving the issues caused by inherent fabrication defects, we were able to fabricate DEAs with thinner elastomer layers that can actuate at lower operation voltages and exhibit substantially longer lifetime [2]. Furthermore, we found this phenomenon to be effective on isolating severe external damage such as piercing and burning [3]. We demonstrated damage resilience by showing that the flying robot maintains its flying capability after suffering significant amount of piercing damage. Under the piercing damage of more than 100 punctures, our DEA was still able to support controlled hovering flight. These results highlight the potential of applying SWCNT-based DEAs for broader application toward robotic and mechatronic systems.

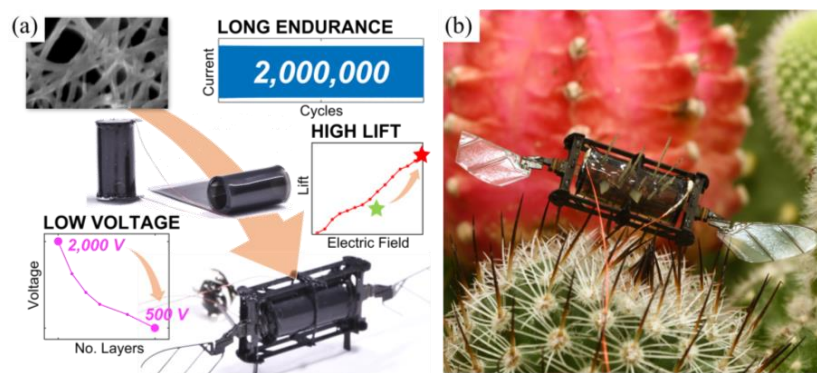


Figure caption: Conceptual representation of the impact of SWCNTs on **a)** the lifetime, power-density, operation voltage [2], and **b)** damage resilience of the robot [3].

References

- [1] Y. Chen, *et al.*, *IEEE Transactions on Robotics* **37.5**, 1752-1764 (2021).
- [2] Z. Ren, *et al.*, *Advanced Materials* **34.7**, 2106757 (2022).
- [3] S. Kim, *et al.*, *Science Robotics* **8.76**, eadf4278 (2023).

High-Precision Sorting of Single-Walled Carbon Nanotubes Using the Aqueous Two-Phase Extraction Method

B. Podlesny¹, D. Janas¹

¹*Silesian University of Technology, Gliwice (Poland)*

Despite the passage of time, single-walled carbon nanotubes (SWCNTs) remain among the most extensively researched materials of our times. Unfortunately, they are still produced as polydisperse mixtures containing many different types of SWCNTs with dissimilar characteristics. Consequently, such blends must be sorted to obtain a material of the properties tailored for a specific application. Across a spectrum of SWCNT sorting techniques, the aqueous two-phase extraction method is particularly attractive. It does not require sophisticated apparatus or niche chemical compounds, making it highly useful even for non-specialists [1]. Besides that, it has considerable application potential for purifying many classes of nanomaterials.

However, the mechanism of this process is still unclear, which limits its potential. This contribution will display our efforts to solve this problem. We synthesized a new Pluronic/Dextran system and comprehensively analyzed its *modus operandi* by sorting polychiral mixtures of SWCNTs [2]. The results revealed that the phase-forming compounds, commonly regarded as passive participants of the process, actively engage in purification. Moreover, the combination of novel experimental pathways with molecular dynamics unraveled the impact of surfactants on SWCNT partitioning. Previously unreported differences were uncovered between widely employed sodium dodecylbenzene sulfonate and sodium dodecyl sulfate, which determine their interactions with SWCNTs.

Having obtained a deeper understanding of the nature of biphasic systems, we embarked on enhancing its capacity for differentiating SWCNTs. Consequently, we isolated (7,5) [3] and (6,4) [4] SWCNTs in a single step. The developed method is highly robust, which is proven by isolating monochiral SWCNTs from several raw SWCNT materials, including SWCNT waste generated over the years in the laboratory. Importantly, the application of previously unrecognized non-ionic surfactants and modeling enabled us to discover the affinity of surfactants for specific SWCNT species [3,4]. These newly noted relations may facilitate sorting of SWCNTs using a broad spectrum of techniques, possibly bringing this material closer to the application phase.

The authors would like to thank the National Science Centre, Poland (under the OPUS program, Grant agreement UMO-2019/33/B/ST5/00631).

References

- [1] J. Fagan, Aqueous two-polymer phase extraction of single-wall carbon nanotubes using surfactants, *Nanoscale Advances* **1** (2019) 3307–3324.
- [2] P. Tiwari, B. Podlesny, M. Krzywiecki, K.Z. Milowska, D. Janas, Understanding the partitioning behavior of single-walled carbon nanotubes using an aqueous two-phase extraction system composed of non-ionic surfactant and polymer, *Nanoscale Horizons* **8** (2023) 685–694.
- [3] B. Podlesny, B. Olszewska, Z. Yaari, P.V. Jena, G. Ghahramani, R. Feiner, D.A. Heller, D. Janas, En route to single-step, two-phase purification of carbon nanotubes facilitated by high-throughput spectroscopy, *Scientific Reports* **11** (2021) 10618.
- [4] B. Podlesny, K.R. Hinkle, K. Hayashi, Y. Niidome, T. Shiraki, D. Janas, Highly-Selective Harvesting of (6,4) SWCNTs Using the Aqueous Two-Phase Extraction Method and Nonionic Surfactants, *Advanced Science* **10** (2023) 2207218.

High-yield liquid phase exfoliation of graphene utilizing low boiling co-solvent solutions and ammonia

Martin Nastran^{1*}, Paul Peschek¹, Izabela Walendzik¹, Jakob Rath¹, Bernhard Fickl¹, Jasmin Schubert¹, Gabriel Szabo², Richard A. Wilhelm², Jochen Schmidt³, Dominik Eder¹, Bernhard C. Bayer¹

¹Technische Universität Wien, Institute of Materials Chemistry, Austria ² Technische Universität Wien, Institute of Applied Physics, Austria ³ Carbon-Solutions Hintsteiner GmbH, Austria

Graphene is a two-dimensional carbon material with unique chemical, electrical and mechanical properties that has a wide range of potential applications in various fields. One of the most effective methods of producing graphene is liquid phase exfoliation (LPE), in which bulk graphite is broken down into its individual layers while suspended in a suitable suspension medium ('solvent'). However, this exfoliation process can be challenging due to the complex effects of the solvent system on exfoliation, dispersibility and yield.

To overcome these challenges, and extending previous findings by Arao et al. [Carbon 118, 18–24 (2017)], we have developed a highly efficient method for exfoliation of graphite to graphene using a cosolvent system of low boiling point organic solvents in combination with water and ammonia (NH₃) as additive. Our method results in high yields of graphene and, importantly, all suspension components including the ammonia additive are also readily removable. Our work thus demonstrates a facile route to improved graphene LPE yields by introducing a very easily removable additive (NH₃) in a wide range of solvent mixtures (including low boiling point and benign mixtures), thus providing a framework for simpler, more flexible and safer 2D graphene LPE development. Such produced nanographite flakes were furthermore compared with other (nano-)carbon fillers for electrically conductive coatings with various polymer binders. The high electrical conductivity values achieved enable a wide range of applications as a lightweight, conductive coating.

High-Yield Separation of Single-Walled Carbon Nanotubes Using Conjugated Polymer Extraction

D. Just¹, D. Janas¹

¹*Silesian University of Technology, Gliwice (Poland)*

Recent advancements in extractive purification techniques of single-walled carbon nanotubes (SWCNTs), such as aqueous two-phase extraction (ATPE) and conjugated polymer extraction (CPE), have addressed the challenge of obtaining single types of the material from polychiral mixtures¹. However, the yield or purity of the resulting fractions often remains unsatisfactory and, typically, one needs to sacrifice one of these parameters. As a result, either substantial amount of SWCNTs with inferior purity are generated or structurally-homogeneous fractions of dissatisfying concentration are harvested²⁻⁴. To alleviate this problem, the agitation/extraction process can be conducted for a prolonged time⁵⁻⁶ or repeatedly, but this reduces the potential of this technology.

Through the incorporation of small molecular enhancers and selective polymers like poly(9,9'-dioctylfluorenyl-2,7-diyl-alt-6,6'-(2,2'-bipyridine)) [PFO-BPy6,6'] and poly(9,9'-dioctylfluorenyl-2,7-diyl) [PFO], we increased the concentration of harvested SWCNTs dramatically, while maintaining monochiral purity⁷⁻⁸. Besides that, we elucidated the importance of specific motifs in the polymers, enabling much more facile extraction of SWCNTs. The carried-out modeling illustrated the mechanism responsible for the sorting yield enhancement, uncovering the interplay of polymer and solvent molecules with SWCNTs at the nanoscale. Besides the practical merits of these achievements, they shed more light into the elusive mechanism of the CPE approach.

The authors would like to thank the National Science Centre, Poland (under the SONATA program, Grant agreement UMO-2020/39/D/ST5/00285).

References

- [1] Janas, D. Towards Monochiral Carbon Nanotubes: A Review of Progress in the Sorting of Single-Walled Carbon Nanotubes. *Materials Chemistry Frontiers*. Royal Society of Chemistry 2018, pp 36–63. <https://doi.org/10.1039/c7qm00427c>.
- [2] Ouyang, J.; Shin, H.; Finnie, P.; Ding, J.; Guo, C.; Li, Z.; Chen, Y.; Wei, L.; Wu, A. J.; Moisa, S.; Lapointe, F.; Malenfant, P. R. L. Impact of Conjugated Polymer Characteristics on the Enrichment of Single-Chirality Single-Walled Carbon Nanotubes. *ACS Appl Polym Mater* 2022, 4 (8), 6239–6254. <https://doi.org/10.1021/acsapm.2c01022>.
- [3] Ozawa, H.; Ide, N.; Fujigaya, T.; Niidome, Y.; Nakashima, N. One-Pot Separation of Highly Enriched (6,5)-Single-Walled Carbon Nanotubes Using a Fluorene-Based Copolymer. *Chem Lett* 2011, 40 (3), 239–241. <https://doi.org/10.1246/cl.2011.239>.
- [4] Dzienia, A.; Just, D.; Taborowska, P.; Mielanczyk, A.; Milowska, K. Z.; Yorozuya, S.; Naka, S.; Shiraki, T.; Janas, D. Mixed-Solvent Engineering as a Way around the Trade-Off between Yield and Purity of (7,3) Single-Walled Carbon Nanotubes Obtained Using Conjugated Polymer Extraction. *Small* 2023. <https://doi.org/10.1002/sml.202304211>.
- [5] Graf, A.; Zakharko, Y.; Schießl, S. P.; Backes, C.; Pfohl, M.; Flavel, B. S.; Zaumseil, J. Large Scale, Selective Dispersion of Long Single-Walled Carbon Nanotubes with High Photoluminescence Quantum Yield by Shear Force Mixing. *Carbon N Y* 2016, 105, 593–599. <https://doi.org/10.1016/j.carbon.2016.05.002>.
- [6] Lindenthal, S.; Settele, S.; Hellmann, J.; Schmitt, K.; Zaumseil, J. A Hands-On Guide to Shear Force Mixing of Single-Walled Carbon Nanotubes with Conjugated Polymers. 2023. <https://doi.org/10.11588/heidok.00033977>.
- [7] Just, D.; Dzienia, A.; Milowska, K. Z.; Mielanczyk, A.; Janas, D. High-Yield and Chirality-Selective Isolation of Single-Walled Carbon Nanotubes Using Conjugated Polymers and Small Molecular Chaperones. *Mater Horiz* 2023. <https://doi.org/10.1039/d3mh01687k>.
- [8] Just, D.; Wasiak, T.; Dzienia, A.; Milowska, K. Z.; Mielanczyk, A.; Janas, D. Two-component systems for the separation of (7,5) single-walled carbon nanotubes (in preparation).

Hysteresis in the transfer characteristics of graphene field-effect transistors elucidated by nitrogen vacancy centers in nanodiamonds

Kazuki Nishibara, Seiji Akita, and Takayuki Arie

Department of Physics and Electronics, Osaka Metropolitan University, Osaka 599-8531 (Japan)

Hysteresis in the transfer characteristics of graphene field-effect transistors (GFETs) is a well-known phenomenon [1]. The underlying cause of the hysteresis in long-channel GFETs is attributed to the occurrence of oxidation-reduction reactions at the graphene/SiO₂ interface [2, 3]. In this study, we report the hysteresis observed by measuring the local current density in the graphene channel of GFET using optically detected magnetic resonance (ODMR) method with nanodiamonds (NDs) containing nitrogen-vacancy (NV) centers.

Cr/Au electrodes were evaporated on a Si/SiO₂ substrate using photolithography, followed by the transfer and formation of the CVD-grown graphene channels to fabricate GFETs. NDs were then drop-cast onto the graphene channels. Transfer characteristics of graphene and ODMR spectra of the NDs on the channel were simultaneously measured at the various gate voltages V_{GS} (+40 V ~ -40 V ~ +25 V) with I_{DS} fixed to be 0.5 mA. Oersted magnetic field was estimated from the Zeeman splitting of ODMR spectra. Under the constant electric current through the channel, the measured magnetic field is anticipated to remain constant regardless of V_{GS} . Therefore, the modulation of magnetic field is attributed to the current modulated by interactions between the NDs and the graphene channel. Measurements were done under ambient conditions with the external magnetic field applied along the channel width.

From the transfer characteristics of GFETs fabricated in our laboratory, the graphene channel is doped with positive charge carriers, and the predominant conducting carriers are holes throughout the measurement. Hysteresis was observed in both the transfer and Oersted magnetic field (Fig. 1) characteristics of GFET. The hysteresis in this GFET can be explained by the occurrence of the reaction, $4OH^- \rightarrow O_2 + 2H_2O + 4e^-$, which proceeds during the measurement. Consequently, the hole carriers decrease, which leads to an increase in resistivity of the channel. The Oersted magnetic field continuously decreases, which indicates the relative increase in the resistivity of the channel in the vicinity of NDs. This implies that the redox reaction is suppressed under NDs, or another reaction that increases the resistivity of the channel under NDs exists.

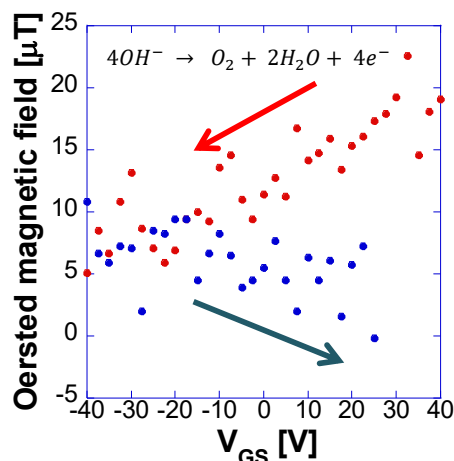


Fig. 1: The Oersted magnetic field of the GFET as a function of V_{GS}

References

- [1] H Wang et al., *ACS Nano* **4**(12) 7221–7228 (2010)
- [2] Xu, H. et al., *Small* **8**, 2833-2840 (2012)
- [3] Jiawei Wei et al., *Carbon* **156**, 67-76 (2020).

ICEPHOBIC AND SELF-HEALING HYDROXY-NANOCARBON COMPOSITES

M. Tarnowska¹, E. Korczeniewski², A. P. Terzyk², S. Boncel¹

¹Silesian University of Technology, NanoCarbon Group (Poland), ²Nicolaus Copernicus University in Torun, Physicochemistry of Carbon Materials Group (Poland)

The last two decades have witnessed a rapid development of new icephobic coatings. This interest was translated into the improvement in the fields of nanomaterials, including novel coating methods and an in-depth understanding of ice nucleation and ice adhesion. Anti-icing properties of carbon nanotubes (CNTs), graphene(s), and its oxide(s) are well-known, and seem to be the most promising in the field of icephobic coatings [1]. Never applied before, but promising for this purpose, modern carbon nanomaterials like pristine and hydrogenated single-walled carbon nanohorns (SWCNHs), nanosized graphane, or fluorographane, exhibit high hydrophobicity. At the same time, formation of surface cracks and scratches cannot be neglected during design and manufacturing of the ice-repellent coatings. Nature-inspired, self-healing materials represent a promising solution for this problem [2]. For instance, polydimethylsioxane vitrimers combined with boric acid were proven to act as a prospective component of recovering materials [3].

Here, we have synthesized self-healing and icephobic composites based on polydimethylsiloxane (PMDS) vitrimers combined with, the thereto embedded, carbon nanomaterials, such as single-walled (SW-), multi-walled (MW-) CNTs, SWCNHs, and/or carbon nanofibers. As the initial modification of carbon nanomaterials, Fenton hydroxylation was applied [4], for which quantification of oxygen functionalities was performed by Boehm titration, thermogravimetric analysis, and Raman spectroscopy. As a result, the highest level of functionalization was obtained for SWCNTs (7.8 mmol g⁻¹), while for SWCNHs 3.0 mmol g⁻¹. Summing up, all carbon nanomaterials were successfully hydroxylated and may undergo further processing aimed at the self-healing and icephobic composites.

Acknowledgements

The authors are very grateful for the financial support from the National Science Centre (Poland) Grant No. 2021/43/B/ST5/00421 in the framework of the OPUS-22 program.

References

- [1] E. Korczeniewski *et al.*, *Chem. Eng. J.* **462**, 142237 (2023).
- [2] E. Korczeniewski *et al.*, *Chem. Eng. J.* **482**, 148777 (2024)
- [3] J. Ma *et al.*, *Nat. Commun.* **12**, 5210 (2021).
- [4] A. Zniszczol *et al.*, *Enzyme Microb. Technol.* **87–88** 61–69 (2016).

Improving Energy Dissipation for Ballistic Impacts

by Ion Irradiation of MWCNT Mats

Edwin L. Thomas, Kailu Xiao

*Department of Materials Science and Engineering, Texas A & M University,
College Station, TX, 77843*

Highly porous, planar isotropic multiwall carbon nanotube (MWCNT) mats were irradiated with high energy carbon ions to explore the effect of ion irradiation-induced new sp^3 bonds and defects introduced into the sp^2 bonding on the ultra-high strain rate mechanical properties. Energy dissipation of pristine vs. ion irradiated mats was measured using the laser-induced micro-projectile impact test (LIPIT). Specific penetration energy E_p^* increased strongly, over 200%, with ion irradiation with a maximum E_p^* of ~ 26 MJ/kg occurring at an impact velocity of 650 m/s for a 245 nm thick film irradiated with an ion dose of 10^{13} ions/cm². This is a factor of over 10 times higher specific energy absorption than present armor materials and other materials tested by microscale LIPIT experiments. The perforation morphologies observed by scanning and transmission electron microscopy reveal a much larger deformed network region around the impact site for the ion irradiated sample compared to the pristine sample. The increased damage zone is due to the ion-induced sp^3 bonding creating greatly improved load transfer between tubes and tube bundles while defects in the sp^2 tube structure also introduced by the radiation caused substantially more tube and bundle clean break fractures. Together these effects lead to significantly enhanced energy dissipation. Our present study provides insight into improvements of the extreme rate dynamical performance of MWCNT mats.

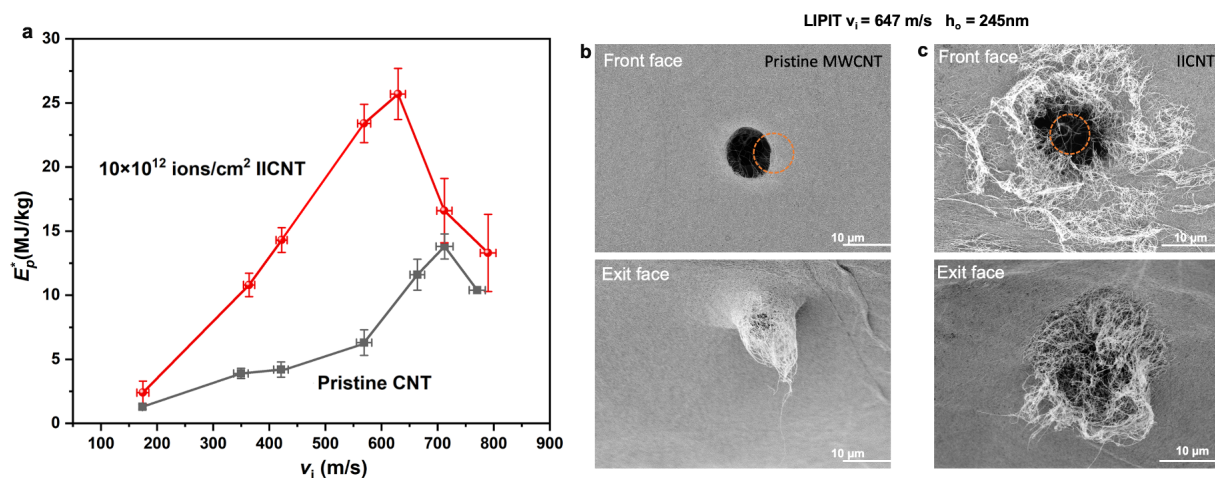


Fig. 1 (a) Specific penetration energy (E_p^*) of $h_0 = 245$ -nm-thick IICNT mats impacted with 7.4 micron diameter alumina spherical projectiles, showing dramatic improvement after irradiation with a strong correlation with impact velocity, v_i . (b) and (c) SEM micrographs of the front and exit mat faces showing the failure morphology of pristine CNT mat and the 10^{13} ions/cm² irradiated mat.

***In situ* observation of vapor-liquid-solid growth of monolayer WS₂ in confined space of substrate-stacked microreactor for crystallinity control**

Hiroo Suzuki^{1,2}, Shuhei Aso², Koki Tanaka², Yutaro Senda², Yasuhiko Hayashi^{1,2}

¹*Life, Natural Science and Technology, Institute of Academic and Research, Okayama University (Japan),*

²*Department of Electrical and Communication Engineering, Faculty of Engineering, Okayama University (Japan)*

Transition metal dichalcogenides (TMDCs), one of the two-dimensional semiconducting materials, have attracted attention for optoelectronic device applications due to their high flexibility, light absorption, and emission coefficient with direct band-gap. The growth of high crystalline TMDC crystals is critical to realize their various applications. We have reported the chemical vapor deposition (CVD) growth of monolayer WS₂ based on the vapor-liquid-solid (VLS) method with metal salt employing the microreactor constructed with two growth substrates [1]. We have grown extremely large WS₂ crystals up to ~1100 μm. The growth mechanism of monolayer WS₂ has been investigated based on the energetical estimation of the rate-limiting step. We have found that the growth mechanism is governed by the surface diffusion-limited process of sulfur atoms in the confined space. In addition, we have found that the growth temperature strongly affects on the photoluminescence (PL). Furthermore, we have recognized the various distributions of the PL properties, such as peak intensity, width, and energy. Such PL properties could relate to the growth dynamics, such as growth velocity and growth regime (*e.g.* fractal growth), however, we have not directly observed the growth of monolayer WS₂.

In situ observation of crystal growth is a strong tool to investigate the growth mechanism. In this research, therefore, we constructed a CVD system with an *in situ* observation system using an optical microscope. Using this system, we succeeded in the direct observation of VLS growth of monolayer WS₂ which involves the dynamic motion of molten liquid, nucleation, and WS₂ lateral growth (Figure 1). The direct *in situ* observation enables us to determine the growth velocity of WS₂ in the microreactor. Furthermore, we investigated the relationship between the growth velocity and PL properties in a single crystal and found the trend which PL intensity decreases with increasing growth velocity. This research will contribute to the understanding of the growth mechanism and finding the method to improve the crystallinity and optical properties of the monolayer WS₂ crystal.

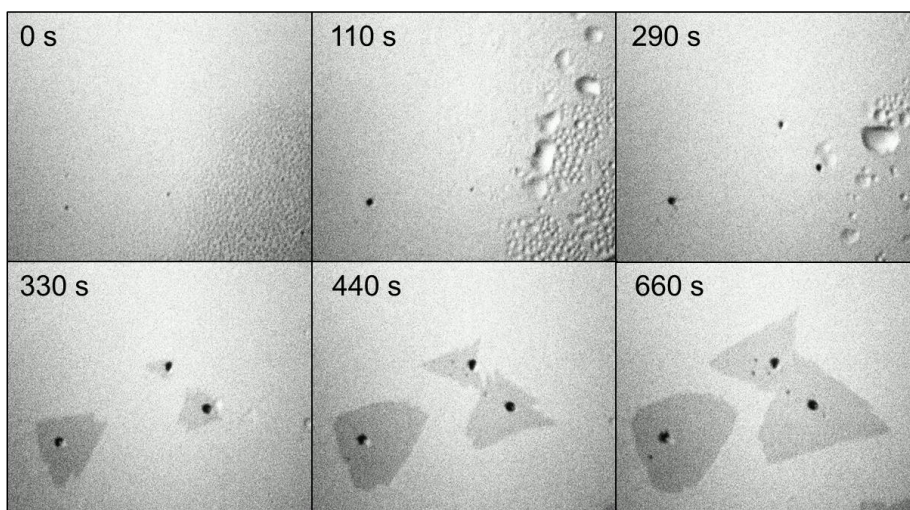


Figure 1: *In situ*-observed microscope images during CVD growth at different growth times.

Reference

[1] H. Suzuki *et al.*, *ACS Nano* **16**, 11360 (2022).

***In vivo* and *ex vivo* imaging with near-infrared emitting graphene quantum dots**

Alina Valimukhametova¹, Natalia Castro Lopez², Floyd Wormley², Anton Naumov¹

¹ *Physics and Astronomy Department, Texas Christian University (USA)*, ² *Department of Biology, Texas Christian University (USA)*

Near-infrared (NIR) imaging is one of the most rapidly developing techniques in biomedical diagnostics due to the high tissue penetration depth of NIR light compared to visible, enabling *in vivo* and *ex vivo* fluorescence tracking. However, the most developed NIR fluorophores do not have therapeutic delivery capabilities, exhibit low photostability, and are poorly excreted from live animals, raising toxicity concerns. To address these issues, we have developed biocompatible graphene quantum dots (GQDs) exhibiting spectrally-separated fluorescence in the NIR range of 928 – 1053 nm with NIR excitation (808 nm and 980 nm) *in vitro*, demonstrating high photostability and ability to attach a therapeutic material [1]. In this work, we demonstrate GQD NIR fluorescence *in vivo* and *ex vivo*. GQD optical properties in the NIR are attributed to either rare-earth metal dopants (Yb-NGQDs, Nd-NGQDs) or defect states (RGQDs). We introduce different concentrations of GQDs intravenously to Balb/C mice to perform fluorescence imaging in live sedated animals without having to sacrifice those at 1, 6, 12, 24, 48 h time points by utilizing IR VIVO animal imager from Photon etc. GQD distribution in the spleen, kidneys, liver, lungs, heart, and brain is assessed from NIR fluorescence in live mice. The NIR fluorescence from the excised whole-organ and organ tissue slices are further analyzed to confirm accumulation/excretion of GQD within the organs. This capability of NIR fluorescence imaging to detect RGQDs, Nd-NGQDs, and Yb-NGQDs in real-time in live mice makes them appealing candidates for both *in vivo* and *ex vivo* theragnostic applications.

References

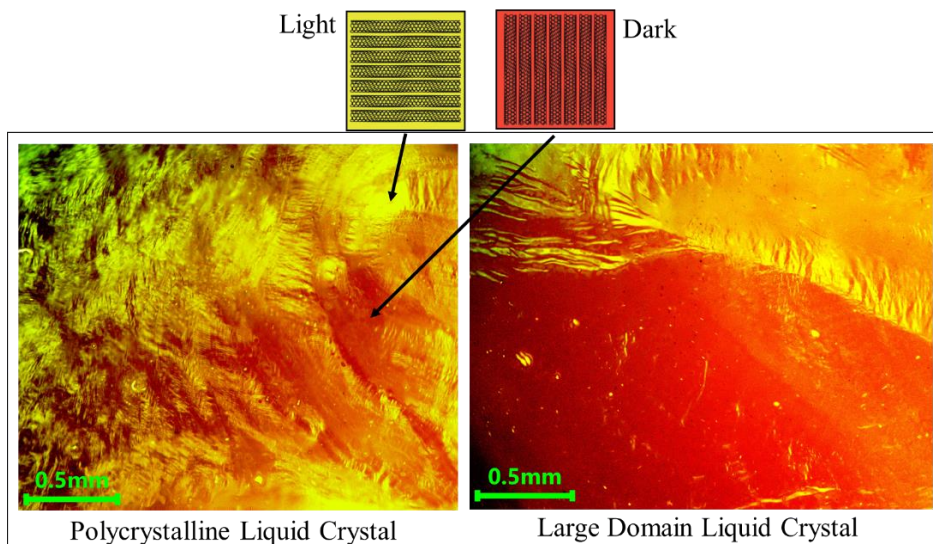
[1] A. Valimukhametova *et al.*, *2D Materials* (2024).

IN-SITU MICROSCOPY OF 2-DIMENSIONAL CARBON NANOTUBE LIQUID CRYSTALS AT LIQUID/LIQUID INTERFACES

James Unzaga¹, Evan Wehbe¹, and Dr. Michael Arnold¹

¹Department of Materials Science and Engineering, University of Wisconsin–Madison (United States)

Densely packed arrays of aligned semiconducting carbon nanotubes (CNTs) are expected to yield up to 10x gains in speed/energy-efficiency over Si in logic microprocessors in a single layer of transistors and up to 1000x gains once integrated into 3D architectures. There has been a burst of activity over the last five years in driving the self-assembly of CNTs into such dense arrays by accumulating the CNTs at liquid-liquid interfaces, which induce CNT alignment. It has been hypothesized that CNTs collected at liquid/liquid interfaces form two-dimensional nematic liquid crystals (2D-LCs). However, the presence of these 2D-LCs has never been directly confirmed. Here, we prove the existence of 2D-CNT LCs directly at the interface. We show that CNTs' birefringent nature allows 2D-LCs of CNTs to be imaged *in-situ* using cross-polarized optical microscopy at the liquid/liquid interface. This approach allows for the microscopic ordering (e.g., LC domain size and orientation) of these liquid crystals to be quantified nondestructively in real time. To create this liquid/liquid interface, a droplet of CNT ink is dispensed into a petri dish containing water. This ink consists of sorted arc-discharge CNTs wrapped with poly[(9,9-dioctylfluorenyl-2,7-diyl)-alt-(6,6'-{2,2'-bipyridine})] (PFO-BPy), suspended in chloroform. After the ink droplet is formed in the water, CNTs rapidly collect and form a polycrystalline 2D-LC at the liquid/liquid interface with 200 μm domains. With the introduction of small amounts of impurity molecules such as ethanol, PFO-BPy, or polymethyl methacrylate (PMMA) into the CNT ink, flow is induced due to Marangoni effects, ultimately leading to larger 2D-LC domains as large as 2 mm. Once formed, the 2D-LCs can be collected onto substrates and studied on the nanoscale using scanning electron microscopy. This work opens the door to more in-depth studies of the factors that lead to improved ordering and packing of CNTs at liquid-liquid interfaces and thus the development of CNT arrays with superior ordering and microstructure for next-generation microelectronics.



INTEGRATION OF PIEZORESISTIVE SENSORS WITH REINFORCED FIBER POLYMER COMPOSITE: METHODOLOGY AND MECHANISM

A. Alrai^{1,2}, A. Yildiz^{1,2}, F. Ç. Cebeci^{3,4}, K. Yildiz^{2,5}, D. Köken⁶, H. Cebeci^{1,2}

¹ Department of Aeronautics and Astronautics, Istanbul Technical University (Turkey), ² Aerospace Research Center, Istanbul Technical University (Turkey), ³ Faculty of Engineering and Natural Sciences, Sabanci University (Turkey), ⁴ Sabanci University SUNUM Nanotechnology Research Center (Turkey), ⁵ Aviation Institute, Istanbul Technical University (Turkey), ⁶ Turkish Aerospace Industry (Turkey)

Reinforced fiber polymer (RFP) composites are increasingly utilized across various applications; however, due to their complex failure mechanisms, the continuous monitoring of the composite part's health becomes essential for high end applications, particularly in aerospace. The integration of piezoresistive sensors with RFP composites enables the collection of data in real-time and monitors the health of the composite part. Herein, we aim to integrate carbon nanomaterial-based piezoresistive sensors into and onto glass reinforced fiber polymer (GRFP) composites. We printed a specific geometrical pattern using carbon nanotube (CNT) and graphene onto GRFP composite. After subjecting the composites to various mechanical stimuli and collecting the electrical responses of the integrated piezoresistive sensors, we studied the electromechanical performance of the sensors. The electromechanical testing consisted of cyclic tensile loading and ball-drop impact tests. The results obtained from the electromechanical testing have allowed us to study the piezoresistive response of the integrated sensors in terms of their sensitivity, reliability, and linearity. The integrated sensors showed a sensitivity of 2.5, a linearity of 98%, and exhibited reliable performance for at least 50 cycles. In conclusion, this work contributes into the understanding of the piezoresistive properties of integrated carbon nanomaterial-based sensors within composites and their practical applications for monitoring the health of the host composites, emphasizing the importance of sensitivity and reliability in capturing real-time data. Finally, the findings provide insights into the development and optimization of carbon nanomaterial-based piezoresistive sensors.

Intershell Locking of Double-walled Carbon Nanotubes Resulting from Enhanced Intershell Friction at High Shear Rates

Hongjie Yue, Fei Wei

Beijing Key Laboratory of Green Chemical Reaction Engineering and Technology,

Department of Chemical Engineering, Tsinghua University

Beijing 100084, China

E-mail: yue-hj23@mails.tsinghua.edu.cn

Abstract

Friction is a pervasive phenomenon in various mechanical processes, especially in systems involving high-speed motion where friction has a great impact on energy dissipation and mechanical transmissions. Meanwhile, friction in some nanomaterials exhibits velocity-dependent phenomena that are different from macroscopic friction, suggesting that friction has a significant impact on nanoscale systems involving high-speed motion. However, the measurement of nanoscale-friction at high sliding velocities has remained elusive due to the limitations in temporal and spatial resolution associated with nanomanipulation techniques in electron microscopes. Here, we developed a non-contact photocatalytic cut-off method specifically tailored for the outer shells of double-walled carbon nanotubes (DWCNTs), and captured the motion of the outer shells as they slide along the inner shells subsequent to fracture under an optical microscope. The result indicates that the intershell friction is independent of the

overlap length but linearly related to the sliding velocity. At velocity of 977 mm/s or shear rate of 10^9 s^{-1} , the intershell friction reaches 195 nN—comparable in scale to tensile stress. Moreover, the linear increase of shear stress with shear rate presents a quasi-Newtonian fluids sliding behavior, wherein the shear viscosity exhibits a decrease from 2 mPa·s to 0.06 mPa·s and then maintains a relatively constant value at high shear rates. Such enhanced intershell friction leads to locking of the inner and outer tubes when the DWCNTs undergo high-speed fracture, thus improving the resistance of DWCNTs to high-speed impacts.

Introduction and properties of mass-producible CNT-CF-hybrid structural materials

K. Ishizeki¹ and F. Deng¹,

¹CARBON FLY, Inc. (Japan)

In order to apply the exceptional physical properties of carbon nanotube (CNT), which include high tensile strength and elastic modulus while being lightweight, to newer structural materials, carbon nanotube (CNT)-based composites have been studied. Numerous investigations revealed that CNT-based nano compotes exhibited superior structural qualities compared to materials made of carbon fiber (CF). However, from the perspective of industrial mass production, scaling up the production quantity presented certain difficulties.

Using CNT thin films made using a dry-fabric formation technique, we created unique CNT-CF-hybrid structural materials in this work, such as preregs. The next-generation CNT structural materials are distinguished from conventional ones with only CF by having superior structural properties (such as higher tensile strength, elastic modulus, and impact resistance) and the ability to be produced continuously for industrial mass production. In our presentation, we will present our new product, the CNT structural materials, covering everything from the fundamental characteristics of CNT to their structural attributes.

Overview of the products



Figure 1: Described in brief as our new CNT-CF hybrid structural materials.

INVESTIGATING CHIRALITY PREFERENCE OF THE GROWTH OF SINGLE-WALLED CARBON NANOTUBES WITH MACHINE-LEARNING FORCE FIELDS

S. Sun¹, Y. Li^{1,*}

¹College of Chemistry and Molecular Engineering, Peking University (China)

A long-unsolved mystery in carbon nanotube growth theory is that, in many cases, single-walled carbon nanotubes (SWCNTs) tend to grow towards $(n,n-1)$ chirality [1,2]. It is generally considered to be a kinetically controlled process from the screw dislocation theory [3]; Recent arguments based on configurational entropy [4], however, can show that the SWCNT edge evolution deviates from the screw dislocation scheme, and the preference is kind of thermodynamically controlled.

Using a home-developed machine-learning force field (MLFF) of the cobalt-carbon system, we performed extensive molecular dynamics simulations of the SWCNT growth process over a cobalt cluster. The energy and force RMSEs of the MLFF are 8.4 meV/atom and 0.28 eV/Å from a 11-fold cross-validation over the training set. The chirality preference towards (6,5) was successfully reproduced for a sample size of $N = 209$. By analyzing the chirality evolution and the edge pattern distribution, we discovered that the nucleation phase consists of frequent chirality-switching processes, possibly indicating a thermodynamically controlled scheme. Also, while a considerable fraction of the edges can exist without corresponding to any chirality, the distribution of those edges with a fixed chirality can deviate significantly from the configuration that maxes out the mixing entropy of the A and Z edge units. Further investigations of the underlying thermodynamics and kinetics are still being worked on.

References

- [1] F. Yang *et al.*, *Acc. Chem. Res.* **49**, 606–615 (2016).
- [2] X. Zhao *et al.*, *Acc. Chem. Res.* **55**, 3334–3344 (2022).
- [3] V. Artyukhov *et al.*, *Nat. Commun.* **5**, 4892 (2014).
- [4] G. D. Forster *et al.*, *ACS Nano* **17**, 7135–7144 (2023).

Iron Nanoparticles Evolution in FCCVD: Kinetic Modelling and Experimental Validation

C. Giudici¹, M. Vazquez-Puffleau², M. Maestri¹, M. Pelucchi¹, J. J. Vilatela²

¹Politecnico di Milano – Milano (Italy), ²IMDEA Materials Institute - Getafe, Madrid (Spain)

The Floating Catalyst Chemical Vapor Deposition (FCCVD) method holds promising potential for large-scale synthesis of high-quality carbon nanotubes (CNTs) and their assembly into macromaterials [1,2], but effective control of the synthesis process poses a significant challenge. One of the primary difficulties is gaining a comprehensive understanding of the evolution of catalytic nanoparticles (NPs) formed during the process, as they play a crucial role in the subsequent growth of nanotubes. Correlating process variables with the resultant iron particle size distribution (PSDs) is therefore essential to understand the growth mechanism under FCCVD, to optimize the process in terms of CNT diameter and length control, and to scale up the process through increases in conversion and solid product concentration.

On the one hand, we experimentally investigated the effect of reactor temperature, residence time, and the amount of sulfur injected on the evolution of iron PSDs across the reactor, through NP characterization using a Differential Mobility Analyzer (DMA). On the other hand, we developed a detailed kinetic model describing the decomposition of ferrocene into iron atoms and the subsequent nucleation and growth of the catalyst particles through agglomeration of the produced iron atoms. The model is based on the discrete sectional method and comprises 20 discrete sections to cover the diameter range experimentally observed (i.e., 1-100 nm). The close agreement between experimental results and simulations (Figure 1) highlights the effectiveness of the model in reproducing the main experimental trends. The model accurately replicates the evolution of catalytic nanoparticles in terms of spatial distribution and number concentration as a function of key process variables, demonstrating significant potential for advancing controlled CNT synthesis.

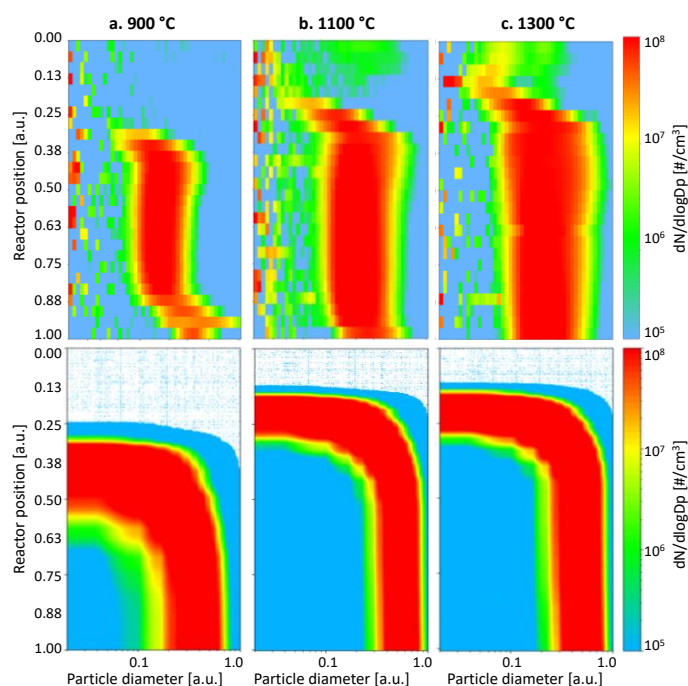


Figure 1: Comparison between in-situ measurements (upper) and simulation results (lower panels) of the iron catalyst PSD for different furnace temperature set-points (a. 900, b. 1100, c. 1300 °C) at a bulk hydrogen flowrate of 1.42 slpm. X and y axes are in normalized arbitrary units.

References:

- [1] M. Sehwat *et al.*, *Carbon*, 118747 (2023).
- [2] I. Gómez-Palos *et al.*, *Nanoscale* 324, 15, 6052-6074 (2023).

ISOXAZOLE-FUNCTIONALIZED CARBON NANOTUBES: SYNTHESIS AND ELECTROOPTICAL PROPERTIES

Z. Amjad¹, S. Boncel¹

¹*Silesian University of Technology, NanoCarbon Group (Poland)*

Carbon nanotubes (CNTs) are 1D nanoallotropes known for their exceptional mechanical, electrical, and optical properties. However, targeted applications of CNTs demand fine-tuning of their structure. Multiple functionalization strategies are widely explored to harvest the potential of CNTs for applications ranging from drug delivery to electronics [1].

Here, we focus on the covalent functionalization of single-walled CNTs (SWCNTs, Tuball™) and multi-walled CNTs (MWCNTs) (Nanocyl NC7000™ and in-house CVD grown, ultralong MWCNTs) using the isoxazole (1,2-oxazole) moieties, while minimizing the impact of such a modification on the CNT framework. The target functionalized CNTs (f-CNTs) were obtained by the optimized reaction of the above CNTs, bearing an *N*-nitrile oxide motif [2], with both an aromatic and aliphatic alkyne [3]. Additionally, considering the importance of the pi-conjugated macromolecular systems [4], theoretical investigations of the optical properties of (5,5)-armchair pristine and functionalized SWCNTs, conducted on B3LYP-631G (d, p) ++ theory level, were performed, and the effect of functionalization on the charge transport properties of f-SWCNTs is discussed.

Acknowledgements

The authors are very grateful for the financial support from the National Science Centre (Poland) Grant No. 2021/41/B/ST5/00892 in the framework of the OPUS-21 program.

References

- [1] N. Karousis *et al.*, *Chem. Rev.* **116**, 4850–4883 (2005).
- [2] A. Kolanowska, *RSC Adv.* **7**, 51374–51381 (2017).
- [3] Z. Amjad, S. Boncel, *in prep.*
- [4] R. Oshi *et al.*, *Comp. Theor. Chem.* **1099**, 209–215 (2017).

Joule heating as a high-temperature out-of-oven manufacturing technique for nanocarbon/inorganic composites

S.T. Upama¹, A. Mikhalchan², L. Arévalo², A. Pendashteh², J.J. Vilatela², M.J. Green¹.

¹Texas A&M University (USA), ²IMDEA Materials Institute (Spain)

Composites of transition metal oxides and nanocarbons such as carbon nanotubes (CNTs) have applications in diverse fields ranging from electrochemical energy conversion and storage to catalysis and sensing. In order to maximize the electrochemical performance of these composites, it is important for the CNTs to be connected to each other to form a conductive network – non-woven, unidirectional CNT fabrics (CNTf) are ideal as such a conductive network. The electrochemical performance of the composites can also be enhanced by uniformly distributing the redox active inorganic phase uniformly within the composite

Previously, we have shown that inorganic phases such as MnO₂ [1] and MoS₂ [2] can be uniformly coated onto a conductive network of CNTf to form nanostructured composites with application as flexible battery electrodes. Additionally, we have shown that the underlying conductive network can be Joule heated [3] to generate current-induced heating within the CNTf and, in turn, the composite, as a rapid out-of-oven thermal processing technique to crystallize the inorganic phase.

Now, we seek to push the Joule heating processing limits for CNTf/inorganic composites for high-temperature (>1000 °C) processing, using vanadium oxide (VO_x) and manganese oxide (MnO_x) as model inorganic phases. First, we utilize thermogravimetric analysis and Joule heating in controlled atmospheres (air and inert) to study how the presence of the metal oxide affects CNT thermal stability. Then, we introduce a reducing atmosphere to extend the thermal processing window for metal oxide matrices. We envision that our approach, combining reduced annealing time with high processing temperatures, may be generalized to thermally process industrially important nanocarbon/inorganic composites that are otherwise difficult or time- and energy-consuming.

References

- [1] M. Rana *et al.*, *J. Mater. Chem. A* 2019,**7**, 26596-26606.
- [2] M. Rana *et al.*, *ACS Appl. Energy Mater.* 2021, **4**, 6, 5668–5676.
- [3] S. Upama *et al.*, *ACS Appl. Mater. Interfaces* 2023, **15**, 5590–5599

Large-Area Fabrication of Isolated Suspended Single-Walled Carbon Nanotube Arrays for Heteronanotube Growth

T. Inoue¹, M. Shimizu¹, Y. Kobayashi¹

¹Osaka University (Japan)

Heteronanotubes (HeteroNTs), in which different types of nanotubes are coaxially combined [1], can realize a variety of electronic devices through the design of nested structures [2-4]. To achieve coaxial growth of outer walls by chemical vapor deposition, it is imperative to employ isolated nanotube segments that do not make contact with substrates or other nanotubes, serving as a template [5]. In addition, an aligned array structure [6] is required for applications in high-performance electronics. In this study, we developed the large-area fabrication of isolated suspended single-walled carbon nanotube (SWCNT) arrays that are suitable for growth of aligned heteroNTs. Horizontally aligned SWCNTs synthesized on a crystal quartz substrate (Fig. 1(a)) were transferred onto a trench-patterned Si substrate using a polymer film. Critical point drying (CPD) [7,8] was employed to prevent the bundling of SWCNTs induced by surface tension after the polymer dissolution process. In the case of natural drying instead of CPD, SWCNT bundles were frequently formed. In contrast, the use of CPD resulted in suspended SWCNT segments with well-aligned and less-bundled structures across the entire substrate ($> 10 \times 10 \text{ mm}^2$) (Fig. 1(b)). When the trench length was $\sim 2 \mu\text{m}$, a suspended array with a minimal intertube distance of $\sim 70 \text{ nm}$ was obtained, suggesting the possibility of forming high-density arrays of suspended SWCNTs by controlling the trench length and other factors. By using the suspended arrays as the template, we synthesized heteroNTs consisting of SWCNTs and boron nitride nanotubes (BNNTs) (Fig. 1(c)). Raman spectroscopy revealed an upshift in the G-band, supporting outer wall BNNT growth on the SWCNTs in the array form.

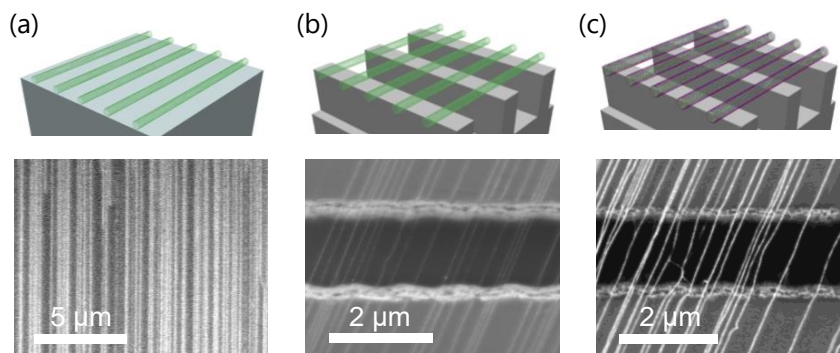


Fig. 1: Schematic and SEM images of (a) an SWCNT array on a crystal quartz substrate, (b) a suspended SWCNT array over a trench-patterned substrate, and (c) an array of BNNT-wrapped SWCNTs.

References

- [1] R. Xiang et al., *Science* **367**, 537 (2020).
- [2] Y. Feng et al., *ACS Nano* **15**, 5600 (2021).
- [3] K. Otsuka et al., *Nano Res.* **16**, 12840 (2023).
- [4] M. Kato et al., *Appl. Phys. Express* **16**, 035001 (2023).
- [5] Y. Zheng et al., *Proc. Natl. Acad. Sci.* **118**, e2107295118 (2021).
- [6] S. Matsushita et al., *ACS Appl. Mater. Interfaces* **15**, 10965 (2023).
- [7] E. D. Minot et al., *Phys. Rev. Lett.* **90**, 4 (2003).
- [8] K. I. Bolotin et al., *Solid State Commun.* **146**, 351 (2008).

Large-area synthesis of SWCNT forests in a bulk-diffusion-dominated kinetic regime

S. J. Park¹, K. E. Moyer-Vanderburgh¹, F. Fornasiero¹

¹ Lawrence Livermore National Laboratory (USA)

Robust synthesis of vertically aligned carbon nanotubes (VACNT) at large scale is required to accelerate deployment of numerous cutting-edge devices to emerging commercial applications [1]. Large-area single-walled (SW) CNT forests with high densities and small diameters are especially important for many applications, yet they are conspicuously absent from the literature due to reproducibility and synthesis challenges, which are further exacerbated when flexible metal foils are used as support instead of traditional Si or quartz wafers. To address this need, we demonstrate that the structural characteristics of SWCNTs produced in a growth regime dominated by bulk diffusion of the gaseous carbon precursor are remarkably invariant over a broad range of process conditions [2]. Forests structural properties are also preserved when growth is transitioned from Si wafers to Inconel metal foils [3]. We show that a simple growth kinetics model that accounts for both reactant bulk diffusion and competing byproduct formation in the presence of excess hydrogen quantitatively reproduces the experimental data in the entire isothermal parameter space. The model enables critical predictions for process scale-up optimization including a potential 6-fold increase in CNT production rate, a $\sim 90\%$ carbon conversion efficiency in select conditions, and elimination of reaction rate decay observed at high pressures by using a hydrogen-free growth environment. This model-guided opportunity to substantially improve synthesis throughput and efficiency, in conjunction with the remarkably invariant CNT properties on both metal and insulating substrates, is appealing for reliable VACNT device fabrication at both small and industrial scales.

This work was performed under the auspices of the U.S. Department of Energy by Lawrence Livermore National Laboratory under Contract DE-AC52-07NA27344.

References

- [1] R. Rao, et al., *ACS Nano* **2018**, *12*, 11756.
- [2] S. J. Park, et al., *Carbon* **2023**, *201*, 745.
- [3] K. Moyer-Vanderburgh, et al., *ACS Appl Mater Interfaces* **2022**, *14*, 54981.

Lepidocrocite Titanium Oxide 1D Nanofilaments: A New Form of Titania for Photochemical Hydrogen Production and Electrochemical Oxygen Evolution Reaction

Hussein O. Badr¹, Michel Barsoum¹

¹Department of Material Science and Engineering, Drexel University, Philadelphia, PA, USA

An essential part to the growth of the green hydrogen economy is the development and integration of active, stable, and inexpensive electrode materials for the generation of hydrogen from water. While activity targets, as measured by the required overpotential to reach a desired reaction rate (i.e. current density), have been met by numerous non-platinum group metal (non-PGM) catalysts for oxygen evolution reaction (OER) in alkaline electrolytes, durability is too often treated with little concern, assuming that the high pH electrolyte will ensure stable passivation of the catalyst surface. Recently, we developed a bottom-up synthesis approach that enables the low-cost, large-scale – in the kilogram range – production of metal oxide-based low-dimensional nanostructures at near ambient conditions.⁽¹⁻⁷⁾ In one case, we converted a dozen Ti-containing carbides, nitrides, borides, and other compounds into one-dimensional lepidocrocite titanate-based nanofilaments henceforth referred to as 1DLs.⁽¹⁻³⁾ With cross-sections in the $5 \times 7 \text{ \AA}^2$ and a band gap energy of 4 eV, these 1DLs represent a new and thus patentable type of titania never reported on before.⁽⁸⁾ In photocatalytic water splitting, 1DLs showed an apparent quantum yield as high as 11.7% along with high stability in water for > 6 months, 300 hours of which were under illumination.⁽⁹⁾ In OER, our results showed that incorporating Ni and Fe traces in 1DLs renders them not only as active as, but also more durable than IrO_2 nanomaterials and NiFe layered double hydroxides (LDH) in alkaline electrolytes.⁽¹⁰⁾ The developed synthesis protocol of 1D materials in bulk-scale at near ambient conditions is paradigm shifting and will undoubtedly open new and exciting avenues of research and applications.

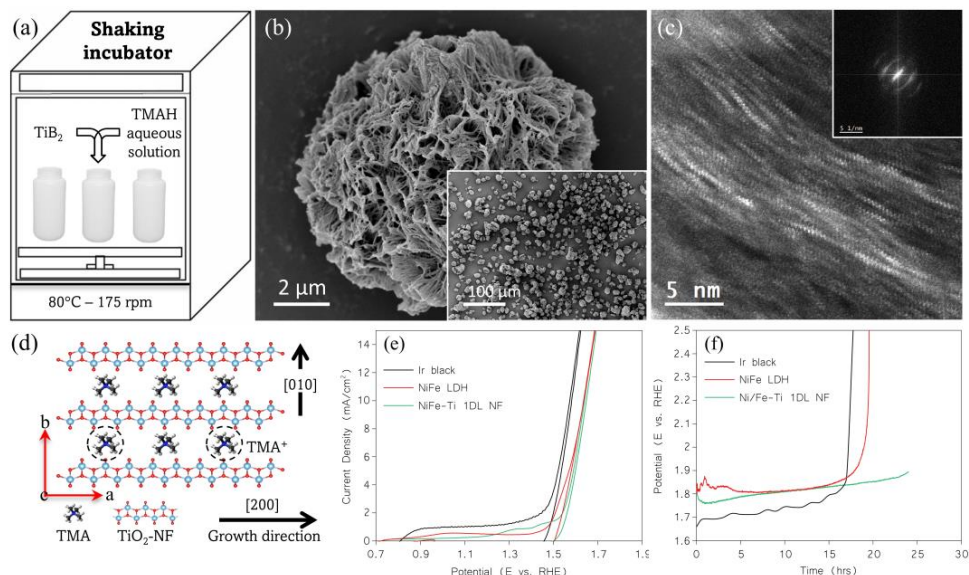


Figure 1: Synthesis, characterization and electrocatalytic OER application of 1DLs nanofilaments. (a) Schematic of temperature-controlled shaker used to convert 15 different Ti-containing powders into 1DLs nanofilaments. (b) and inset in (b) Typical SEM micrographs of free-flowing and non-agglomerating 1DLs-based mesoporous particles with particle sizes of 5-30 μm . (c) STEM imaging of 1DLs that are 2 Ti-atoms wide with a zigzag pattern. Inset in (c) shows FFT produced from NFs bundles shown in (c). (d) DFT-generated lepidocrocite titanate structure showing ribbons 2 Ti-atoms thick growing along [100] and stacking along [010] (viz., the a and b crystallographic directions, respectively). (e) OER polarization curves in Ar-saturated 0.1M KOH at 20 mV/s and 1600 rpm for NiFe-TiO₂ 1DL NFs (green), Ir black (black), and Ni/Fe LDH (red). (f) Constant current (10 mA/cm²) durability test for Ni/Fe-TiO₂ 1DL NFs (green), Ir black (black), and Ni/Fe LDH (red).

References

1. H. O. Badr *et al.*, Bottom-up, scalable synthesis of anatase nanofilament-based two-dimensional titanium carbo-oxide flakes. *Mater. Today* **54**, 8-17 (2022).
2. H. O. Badr *et al.*, On the Structure of One-Dimensional TiO₂ Lepidocrocite. *Matter* **6**, 128-141 (2023).
3. H. O. Badr *et al.*, Titanium Oxide-based 1D Nanofilaments, 2D Sheets, and Mesoporous Particles - Synthesis, Characterization, and Ion Intercalation. *Matter*, (2023).
4. K. Sudhakar *et al.*, One-dimensional, Lepidocrocite-based Nanofilaments and Their Self-Assembly. *Matter* **6**, 3538-3554 (2023).
5. H. O. Badr *et al.*, Scalable, inexpensive, one-pot, facile synthesis of crystalline two-dimensional birnessite flakes. *Matter* **5**, 2365–2381 (2022).
6. K. Sudhakar *et al.*, One pot, scalable synthesis of hydroxide derived ferrite magnetic nanoparticles. *J. Magn. Magn. Mater.* **582**, 170986 (2023).
7. Mary Qin Hassig *et al.*, Reacting Mn₃O₄ powders with quaternary ammonium hydroxides to form two-dimensional birnessite flakes. *Ceram. Int.* **49**, 33537-33545 (2023).
8. E. Colin-Ulloa *et al.*, Electronic Structure of 1D Lepidocrocite TiO₂ Quat-Derived Nanomaterial, QDN, as Revealed by Optical Absorption and Photoelectron Spectroscopy. *Phys. Chem. C* . **127**, 7275–7283 (2023).
9. H. Badr *et al.*, Ultra-stable, 1D TiO₂ Lepidocrocite for Photocatalytic Hydrogen Production in Water-Methanol Mixtures. *Matter*, (2023).
10. N. Carpentieri *et al.*, Two-Dimensional Aggregates of Lepidocrocite TiO₂ Nanofilaments with Ni/Fe Active Sites for Durable Oxygen Evolution Electrocatalysis. *ACS Appl. Eng. Mater.*, (2023).

Liquid Metal Spreading on Metallic Surfaces Suppressed by Carbon Nanotubes

Authors: Anar Zhexembekova¹, Chang Young Lee^{1,2}

¹*School of Energy and Chemical Engineering, Ulsan National Institute of Science and Technology, Ulsan 44919 (Republic of Korea)*

²*Graduate School of Carbon Neutrality, Ulsan National Institute of Science and Technology, Ulsan 44919 (Republic of Korea)*

Gallium-based liquid metal alloys, particularly eutectic gallium-indium (eGaIn), are widely utilized and have become key materials in producing soft, stretchable devices due to their high conductivity and fluidity at room temperature. However, the extensive application of eGaIn is hindered by its selective wettability, adhesion to specific surfaces, and wetting-induced spreading, which can lead to device failures. Gallium oxide, often a component in eGaIn, tends to adhere to various surfaces, causing embrittlement or dissolution of solid/metallic contacting parts. Therefore, understanding and controlling these interactions is crucial for practical applications. In this study, we present a straightforward method to suppress the spreading of eGaIn using carbon nanotubes (CNTs). We demonstrate that dispersing functionalized CNTs homogeneously in eGaIn suppresses its spreading on metallic surfaces. Additionally, the agglomeration of CNT bundles within the eGaIn influences the surface tension of the composite. A higher concentration of CNTs in the resulting CNT/eGaIn liquid-state composite inhibits spreading for up to 30 days. Employing the CNT/eGaIn interconnect as a proof of concept, we observed that this interconnect exhibits mechanical longevity and electrical stability, demonstrating the long-term stability of the device. Furthermore, this work elucidates the general mechanism in the reaction-diffusion-spreading process for gallium-based liquid metal alloys and metal (eGaIn-Pt) systems. In this system, CNTs act as an inhibitor, restricting gallium diffusion and spreading. This study proposes an alternative method for controlling the wetting and spreading of eGaIn using CNTs on metallic surfaces.

Liquid processing of high aspect ratio nanowires into macrostructures

D. Tilve-Martinez, J.J. Vilatela

IMDEA Materials, C/ Eric Kandel 2, 28906 Getafe, Madrid, Spain.

Synthesis by Float catalyst chemical vapor deposition (FCCVD) allows to create 1D inorganic nanoparticles with few microns length in seconds [1]. Among them are silicon nanowires (SiNW), which generate great interest due to their potential applications in catalysis, energy storage, optoelectronics, and reinforcement in composites [2,3,4]. The formation of macrostructures with controlled structure and aggregation could lead to a new family of multifunctional materials with low dimensionality. One of the methods to assemble 1D inorganic nanowires/nanotubes into macromaterials is by taking advantage of their aggregation in the gas phase during synthesis by FCCVD, to form macroscopic continuous networks. This has proven suitable to make transparent conductors, high-performance fibres, electrodes, etc.

However, it is also of interest to leverage wet-chemical methods to process these high aspect ratio nanomaterials. This enables not only integration using soft chemical processing routes (3D printing, ink printing, etc) , but also to produce model systems of nanowires, for example that provide insights into their size, aggregation and properties as ultra-aligned systems. In this work, we study the stabilization of individual Si_{nw} in various solvents. We determine the stability of dispersion in different liquids and provide preliminary results on the controlled aggregation of nanowires upon solvent removal, as a step towards wet-processing of macromaterials of NWs.

References

- [1] R. S. Schäufele *et al.*, *Nanoscale*. **14**, 55–64 (2022).
- [2] I. Gómez-Palos, *Nanoscale*. **13**, 6052–6074 (2022).
- [3] M. Rana, *Adv. Energy Mater.* **12**, 2103469 (2022).
- [4] Pendashteh *et al.*, *Adv. Energy Mater.* 2304018 (2024).

LOAD-BEARING CARBON CEMENT SUPERCAPACITORS FOR STRUCTURAL ENERGY STORAGE SYSTEMS

D. Stefaniuk¹, J.C. Weaver², A. Masic¹, F.-J. Ulm¹

¹Department of Civil and Environmental Engineering, Massachusetts Institute of Technology (USA)

²Wyss Institute for Biologically Inspired Engineering, Harvard University (USA)

Traditionally, cementitious materials primarily serve as load-bearing elements, while battery/supercapacitor technology is employed for electrical energy storage. Through the implementation of electron-conducting carbon concrete (EC³) [1] with 'Oreo'-like shaped structures, we create a symbiotic relationship between structural support and energy storage. For this purpose, we incorporate inexpensive, abundant, and widely available resources, i.e., a blend of nano carbon black, cement, and an electrolyte, to create electrodes which can then be stacked in series to form a functional supercapacitor. Herein, we present a 12V meso-scale EC3 column (Figure 1a) that, based on cyclic-voltammetry tests at different scan rates (Figure 1b), enables the evaluation of a rate-independent volumetric capacitance of 42.9F, equivalent to an energy storage of 260 Wh/m³ (Figure 1c). The invention can be employed to shape various types of large-scale structures such as columns, piles, foundations, arches, just to name a few, in an 'Oreo'-like shape with a desired energy capacity. Our technology has the potential to significantly diminish the reliance on currently employed batteries/supercapacitors, such as those made of lithium-ion material, and to facilitate the urgent transition from a fossil fuel-based economy to one based on renewables.

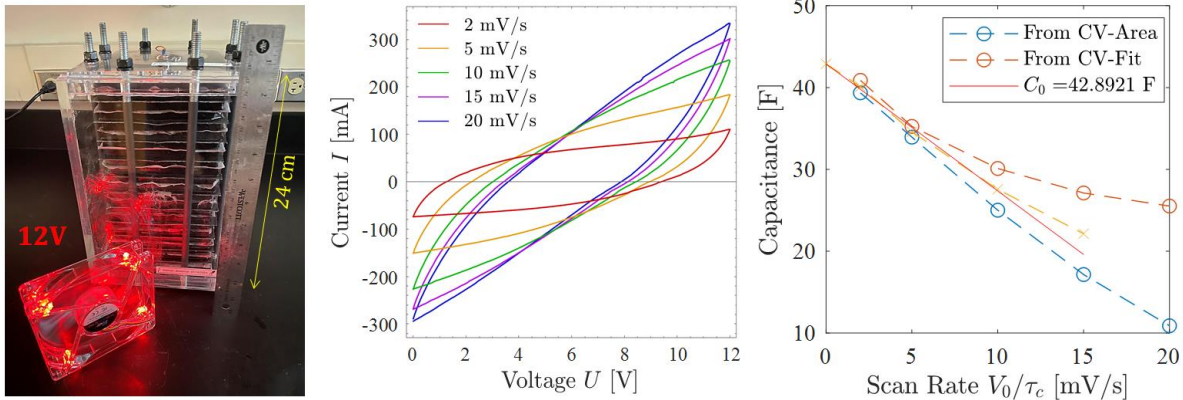


Figure caption: The prototype of a load-bearing carbon cement supercapacitor: (a) 12V meso-scale column, (b) its cyclic-voltammetry test results at different scan rates, and (c) an evaluation showing a rate-independent volumetric capacitance (C_0) of 42.9F.

References

- [1] Chanut, N., Stefaniuk, D., Weaver, J.C., Zhu, Y., Shao-Horn, Y., Masic, A., Ulm, F.-J. (2023). Carbon-cement supercapacitors as a scalable bulk energy storage solution. *Proceedings of the National Academy of Sciences*, 120, e2304318120. (2009).

LOW TEMPERATURE SYNTHESIS AND CHARACTERIZATION OF HIGH ENTROPY OXIDE NANOPARTICLES FOR VARIOUS APPLICATIONS

I. B. Algan Simsek^{1,2}, H. O. Badr¹, M. W. Barsoum¹
¹ Drexel University (USA), ² Gazi University (Turkey)

High entropy oxide (HEO) consists of five or more metallic elements with equal or near-equal stoichiometric ratios. This novel material group has a sluggish diffusion effect that allows single-phase solid solution formation unlike the phase separation encountered in traditional element doping strategies [1]. HEOs can be synthesized by different methods like solid state, hydrothermal, solvothermal, and sol-gel. However, simplicity of synthesis method, less energy and time consumption are quite important in terms of availability of HEO, especially for new generation materials [2,3]. For this reason, wet chemical synthesis methods like-sol gel and low temperatures offer a lot of advantages. This study mainly aims to determine our low temperature synthesis of single-phase spinel structure HEOs including earth abundant transition metals (Fe, Ni, Co, Cu, Zn) as well as their promising trends in various applications including Li-ion battery, dye degradation, and photo excitations performances.

References

- [1] Liu, Z. Y. et al., *Green Energy & Environment*, **8**, 1341-1357 (2023).
- [2] Zhao, B. et al., *Advanced Functional Materials*, **33**, 2209924 (2023).
- [3] Pan, Y. et al., *Chemical Engineering Journal*, **451**, 138659 (2023).

Low-temperature Synthesis of Linear Carbon Chain inside Single-walled Carbon Nanotubes

Bowen Zhang¹, Xiyang Qiu¹, Qingmei Hu¹, Ya Feng², Aina Fitó Parera³, Yongjia Zheng⁴, YuHuang Wang⁵, Yutaka Matsuo⁶, Shohei Chiashi¹, Rong Xiang⁴, Sofie Cambré³, Wim Wenseleers³, Slava V. Rotkin⁷, Keigo Otsuka¹, and Shigeo Maruyama¹

1. The University of Tokyo 2. Dalian University of Technology 3. University of Antwerp 4. Zhejiang University 5. University of Maryland 6. Nagoya University 7. Pennsylvania State University

Linear carbon chains (LCCs) have attracted much interest due to their unique structure and potential technological applications. LCCs possess higher strength, elastic modulus, and stiffness than any known materials, which provides a possibility for LCC as a new composite material. Yet, their chemical stability remains an issue [1], and efficient synthesis of LCCs has not been fully realized. A landmark study on LCC synthesis has been achieved using double-walled carbon nanotubes (DWCNTs) as the template, but a high-temperature annealing treatment at 1460°C is required to attain long chains composed of more than 6,000 carbon atoms [2]. Besides DWCNTs, single-walled carbon nanotubes (SWCNT) were also exploited as the templates. However, given the instability of SWCNTs at higher temperatures [2], the synthesis efficiency is not as optimal as DWCNTs. To our knowledge, there is still no report on an efficient LCC synthesis inside SWCNTs. Herein, we report efficient LCC synthesis using SWCNTs as the templates at low temperatures (400°C) for the first time.

To this end, a SWCNT dispersion [3] underwent a surfactant exchange process and was fabricated into a SWCNT film by filtration. The SWCNT film was annealed under 400°C in an argon atmosphere to synthesize LCC. Raman spectroscopy (laser wavelength 532 nm) was used to characterize the efficiency of the LCC synthesis. A strong peak at 1863 cm⁻¹ appeared after annealing, originating from the well-known C-mode of the linear carbon chain [4], thereby confirming its existence inside SWCNTs. SWCNTs synthesized by a low-pressure alcohol catalytic chemical vapor deposition (ACCVD) method [5] were also adopted for the LCC synthesis template, resulting in a similar LCC Raman peak at 1863 cm⁻¹. We attribute this successful low-temperature LCC synthesis to the appropriate surfactant that could be encapsulated inside CNTs and converted to LCC during annealing.

Keywords: Linear Carbon Chain, Single-walled Carbon Nanotubes, Surfactants

References:

- [1] M. Liu et al., *ACS Nano* **7**, 10075–10082 (2013).
- [2] S. Lei et al., *Nature Mater* **15**, 634–639 (2016).
- [3] T. Tanaka et al., *Nano Lett.* **9**, 4, 1497–1500 (2009).
- [4] M. Martinati et al., *Carbon* **189**, 276–283 (2022).
- [5] S. Maruyama et al., *Chem. Phys. Lett.* **360**, 229–234 (2002).

Lyotropic Liquid Crystalline Behavior of Boron Nitride Nanotubes in Aqueous Sodium Deoxycholate Dispersions

J. F. Khoury^{1,2,3}, E. Khabushev^{1,2,3}, M. Gong^{1,2,3}, A. Benavides-Figueroa^{2,3,4}, A. Chow⁴, L. R. Scammell⁵, C. Park⁶, A. A. Marti^{2,4,7,8}, and M. Pasquali^{1,2,3,4,8}

¹Department of Chemical and Biomolecular Engineering, Rice University (USA), ²The Smalley-Curl Institute, Rice University (USA), ³Carbon Hub, Rice University (USA), ⁴Department of Chemistry, Rice University (USA), ⁵BNNT, LLC (USA), ⁶Advanced Materials and Processing Branch, NASA Langley Research Center (USA), ⁷Department of Bioengineering, Rice University (USA), ⁸Department of Materials Science and Nanoengineering, Rice University (USA).

In the emerging field of nanotechnology research, boron nitride nanotubes (BNNTs) have been gaining a significant interest due to their outstanding mechanical and thermal properties. Controlling the alignment of BNNTs in macroscopic assemblies is essential in translating these properties into the final macroscopic materials. One approach involves preparing dispersions of BNNTs that exhibit a liquid crystal (LC) phase. This study investigates the behavior of BNNTs in aqueous solutions of sodium deoxycholate (SDC), identified as a good dispersing agent for BNNTs [1], particularly examining the effect of purity and concentration on the formation of LC phases. We attain high concentration of BNNT, up to 15 wt%, dispersions in surfactant. Our investigation of these dispersions via polarized light microscopy reveals the formation of nematic liquid crystals. We detail the phase transition from isotropic state to the presence of locally ordered nuclei, or “swarms”, which are larger at higher concentrations, to the fully nematic LC phase. We examine the effect of BNNT purity and BNNT-SDC concentrations on the phase behavior and phase transition. Additionally, we demonstrate the feasibility of fabricating aligned BNNT films from these dispersions, using shear alignment followed by coagulation in ethanol. This approach marks a significant advancement in the field, offering a pathway to translate the unique properties of BNNTs into macroscopic materials. Our findings contribute to the growing knowledge on BNNT liquid crystals, providing insights that are crucial for the development of BNNT-based technologies in electronics and aerospace applications.

References:

- [1] J. F. Khoury, J. C. Vitale, T. L. Larson, and G. Ao, Boron Nitride Nanotubes Enhance Mechanical Properties of Fibers from Nanotube/Polyvinyl Alcohol Dispersions, *Nanoscale Adv*, **2021**.

MAGNETIC PROPERTIES OF COORDINATION POLYMERS

S.A. Siddiqui¹, H. Shiozawa^{1,4}

¹Faculty of Physics, University of Vienna & VDSP, (Austria), ⁴J. Heyrovsky Institute of Physical Chemistry (Czech Republic)

Coordination polymers refer to solid state structures that comprise of repeating coordination units forming diverse structures like 1D extended chains, 2D sheets or 3D frameworks. The versatility of combining different organic ligands (Lewis base) with the metal ion (Lewis acid) enables diverse applications in catalysis, optics, electronics, energy transfer and spintronics.

Our research deals with the study of synthesis, structure, electronic and magnetic properties of transition metal, e.g. iron and copper, coordination polymers with different organic ligands such as 1H-1,2,4-Triazole and melamine.

Iron coordination polymer $[\text{Fe}(\text{Htrz})_2(\text{trz})](\text{BF}_4)$ shows spin transition from low spin (LS) to high spin (HS) state accompanied by thermochromism. Spin transition or spin crossover is a phenomenon wherein the coordination polymer changes its form from a LS state to a HS state under the influence of external factors such as temperature, pressure or external stimuli. This change can be examined using Raman spectroscopy [1].

Two different structures : (Cu₂M1) and (Cu₄M1) made of Cu(II) and melamine can be synthesized by adjusting the molar ratios of the precursors [2]. The single crystal diffraction on the Cu₂M1 crystal reveals a dimer structure whereas Cu₄M1 is a 1D coordination polymer consisting of copper-chlorine chains. The magnetic properties are explained using spin-1/2 dimer (Bleaney – Bowers) model and spin-1/2 one dimensional chain (Bonner – Fisher model). The high-quality single crystals have great impetus in future research on spintronics.

In our recent work, a one-dimensional coordination polymer and a metal-organic framework are synthesized using copper chloride and 1H-1,2,4-triazole in different conditions. The magnetic properties of the coordination polymer can be explained based on the Ising model, while the metal-organic framework exhibits spin frustration in the triangular motif.

References

- [1] S. A. Siddiqui et al., *J. Mater. Chem. C* **9**(3), 1077–1084 (2021).
- [2] I. B. Virseda et al., *RSC Adv.* **11**(39), 23943–23947 (2021).

MECHANICAL AND PIEZORESISTIVE RESPONSES OF CARBON NANOTUBE YARNS ALONG AXIAL AND TRANSVERSE DIRECTIONS

I. Garcia Guerra¹, D. Feria Garnica², G. Marcati², J.L. Abot¹, I. Pereyra², M.N. Carreño Paez².

¹The Catholic University of America (USA), ²Universidade de São Paulo (Brasil).

The inherent hierarchical arrangement and microscale dimensions found in carbon nanotube yarns (CNTYs) make them highly promising for diverse integrated sensing applications, attributed to their distinct mechanical and electrical characteristics. Piezoresistivity, characterized by changes in electrical resistance in response to mechanical strain, constitutes a fundamental mechanism employed in the strain sensing capabilities of CNTYs. Consequently, a thorough understanding of the diverse electromechanical responses exhibited by CNTYs, encompassing both tension and compression, and addressing both the axial and the transversal directions of the yarn, becomes imperative. This understanding would enable the deployment of CNTYs across a broad spectrum of applications.

Regarding the axial piezoresistive response, a single CNTY embedded into a polymeric resin (CNTY monofilament composite) was investigated under compressive forces in the axial direction of the yarn and correlated with prior and new results of the response under axial tensile loading. The results suggest that the CNTY exhibits a strong positive piezoresistive response, with correspondence between strain and electrical resistance change over multiple cycles indicating a predictable piezoresistive response of the CNTY. This predictability underscores the potential of the CNTY monofilament composite as a reliable and robust piezoresistive sensor. The monofilament composites showed a sensitivity or gauge factor values in the order of 0.4–0.5, with slightly lower values under compression loading.

The axial properties of the yarn have been thoroughly investigated; however, the transverse or radial properties, orthogonal to the fiber axis, remain relatively unknown due to the challenges associated with their measurement. In this study, the transverse elastic modulus of CNTYs was determined using Atomic Force Microscopy (AFM). This modulus would enable the calculation of the lateral piezoresistive response. Quantifying transverse properties in fibrous materials presents formidable challenges owing to their inherent anisotropy, whereby mechanical characteristics exhibit directional disparities, i.e., the properties in the transverse direction are several orders of magnitude smaller than in the axial direction. Another challenge for the assessment of transverse properties can be attributed to the elevated aspect ratio of the CNTY. To overcome these difficulties, AFM can be used to enable high-resolution capabilities for imaging and mechanical characterization at the nanoscale level. AFM was utilized to perform nanoindentation experiments, where a tipless flexible cantilever probe was used to apply a controlled force to the fiber surface. The resulting indentation depth was then analyzed to determine the transversal elastic modulus. Preliminary findings indicate that the transverse elastic modulus of the CNTYs varies significantly with the strain level and ranges from 100-700 kPa for deformations to the microstrain level.

References

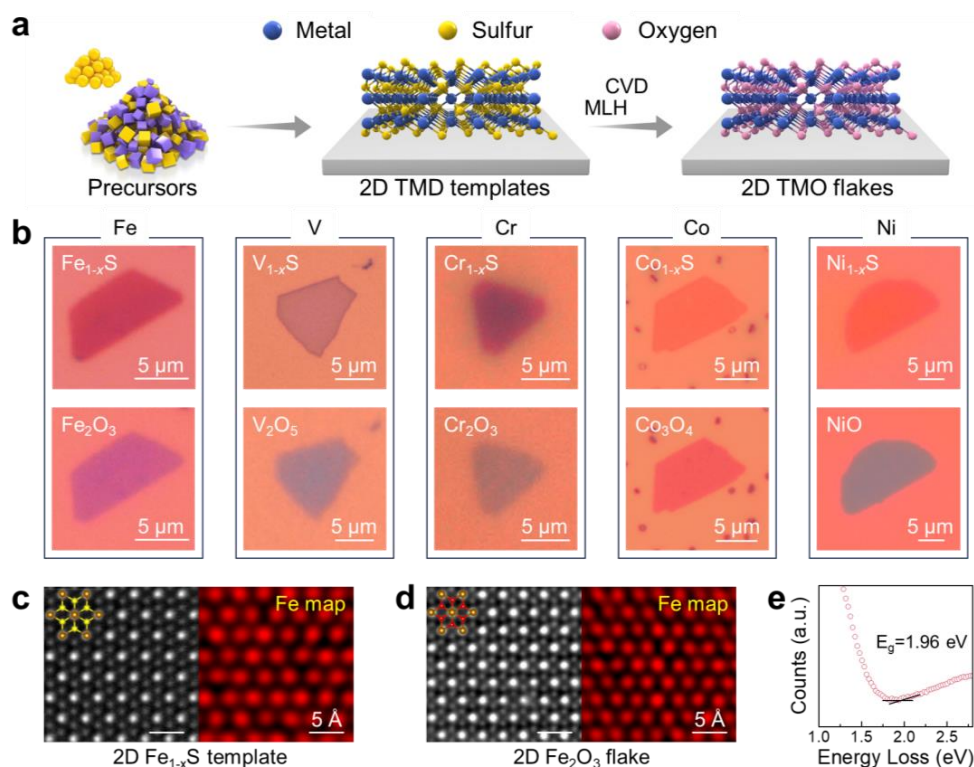
[1] I. Garcia Guerra, T. Tayyarian, O. Rodríguez-Uicab & J.L. Abot. (2023). Piezoresistive response of carbon nanotube Yarn Monofilament Composites under axial compression. *C*, 9(4), 89.

Metal-lattice-heredity conversion for universal synthesis of 2D transition metal oxides

Junyang Tan¹, Jingwei Wang¹, Bilu Liu¹, Hui-Ming Cheng^{1,2}

¹Shenzhen International Graduate School, Tsinghua University (China), ²Shenzhen Institute of Advanced Technology, Chinese Academy of Sciences (China)

Two-dimensional (2D) transition metal oxides (TMOs) have sparked much interest due to their intriguing properties and high stability in ambient environments. However, due to the strong covalent bonds and large electronegativity difference between metal and oxygen atoms, the direct synthesis of high-quality 2D TMOs is challenging. Here, we propose a metal-lattice-heredity (MLH) conversion strategy for the controllable preparation of 2D TMOs. This approach utilizes 2D transition metal chalcogenides (TMDs) as a host matrix, where the target 2D TMOs are obtained after a confined sulfur-to-oxygen substitution reaction. As a proof-of-concept, we convert 2D Fe_{1-x}S to 2D Fe_2O_3 with an ultrathin thickness (2 nm) and a flat surface (roughness < 1 nm). The Fe atoms retain their hexagonal arrangement throughout the MLH process, resulting in the single-crystalline Fe_2O_3 . In addition, this method has been extended to V, Cr, Co, and Ni-based 2D TMOs, providing rich candidates with bandgaps ranging from near-infrared region to near ultraviolet region. This work develops a universal method for preparing high-quality 2D TMOs, paving the way for their applications, such as in high-temperature electronic devices.



The metal-lattice-heredity conversion method: (a) Schematic of the method. (b) Optical microscopy images of the five types of TMD templates and the corresponding converted TMO flakes. (c) HAADF-STEM image and the Fe elemental map of 2D Fe_{1-x}S template. (d) iDPC image and the Fe elemental map of the converted 2D Fe_2O_3 . (e) Bandgap measurement of 2D Fe_2O_3 based on valence-EELS spectrum.

References

- [1] Z. Cai *et al.*, *Chem. Rev.* **118**, 6091–6133 (2018).
- [2] L. Tang *et al.*, *Acc Mater Res.* **2**, 36–47 (2021).
- [3] J. Tan *et al.*, *Sci. Bull.* **67**, 1649–1658 (2022).
- [4] J. Wang, *et al.*, *Adv. Powder Mater.* **3**, 100164 (2024).

Micro-scale Metal Plating on Carbon Nanotubes

Yuanqi Wei¹, Dalue Tang², Kaili Jiang¹

¹ State Key Laboratory of Low-Dimensional Quantum Physics, Department of Physics, Tsinghua University, Beijing, China.

² Department of Materials Science and Engineering, McMaster University, 1280 Main St West, Hamilton, ON, Canada, L8S4L8.

Corresponding author(s): jiangkl@mail.tsinghua.edu.cn

Metal plating on carbon nanotube at micro-scale was carried out by using a home-made instrument. It is found that a variety of metals can be deposited on the surface of carbon nanotubes. Compared with traditional plating method, the current approach enables accurate electroplating within a few microns, which is very helpful for fabricating metallic micro stripes precisely. It was also used to weld carbon nanotubes to electrodes to get better electrical contact and less contact resistance. This approach might also be utilized in other nanomaterials, such as 2D materials to directly printing electrodes on them.

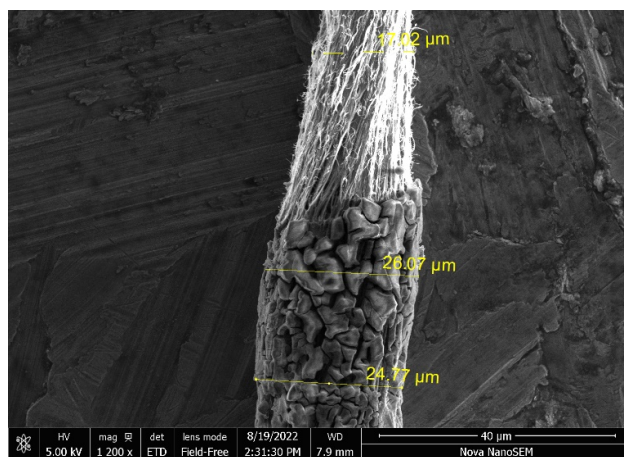


Fig.1 Copper plating on the carbon fiber made of carbon nanotubes.

MICROSTRUCTURE, MECHANICAL PROPERTIES, AND TRIBOLOGICAL BEHAVIOR OF CU-NANO TiO₂-MWCNT COMPOSITE SINTERED MATERIALS

A. Marek¹, S. Boncel¹, A. Piasecki²

¹Silesian University of Technology, NanoCarbon Group (Poland), ²Poznan University of Technology (Poland)

The pursuit for new materials with tribological properties is burning from the point-of-view of practical and economic applications. Tribological wear is one of the most common causes of material wear, leading to damage of the machine parts or tools. This phenomenon has a large economic effect related to the downtime of the devices and a period of time required for the replacement of parts. Therefore, the search for new materials with a higher wear resistance is particularly important, allowing for the longer operational stability [1].

Here, we present the results of microstructure, mechanical, and tribological tests of copper matrix sinters with the addition of nano-TiO₂ and Cu-decorated multi-walled carbon nanotubes (MWCNTs) [2]. A powder metallurgy was used to produce composite materials. The aim of the work was to determine the properties and wear mechanism of the produced sinters with single additives and to investigate the synergistic interaction of TiO₂ and CNTs. The main wear mechanisms of the friction pairs tested at room temperature and 600 °C were adhesive, abrasive, and oxidation wear. Furthermore, at the test temperature of 600 °C, the formation of a tribofilm was observed on the surface of the friction pairs, which reduced the friction wear. The introduced additions to the copper matrix increased its hardness, stiffness, work of axial deformation, and the wear resistance. Moreover, the additions decreased the relative value of the thermal expansion coefficient of the sintered copper. It has been shown that the friction pair (Cu + 1 wt.% MWCNTs – Inconel[®]625) was characterized by the lowest coefficient of friction at room temperature and 600 °C, of approximately 0.62 and 0.56, respectively. The sintered composite material of Cu – 10 wt.% nano-TiO₂ – 1 wt.% MWCNTs was characterized by the highest mechanical properties and the lowest wear.

Acknowledgements

The authors are very grateful for the financial support from the National Science Centre (Poland) Grant No. 2020/39/B/ST5/02562 in the framework of the OPUS-20 program.

References

- [1] M. Tonk, *Mater. Today: Proceedings* **37**, 3275–3278 (2021).
- [2] A. Piasecki *et al.*, *Wear* **522**, 204834 (2023).

Mixed-Scale Fabrication of a Carbon Nanotube based Corrosivity Gauge

S. Kessler¹, E. Kalfon Cohen¹, L. Acauan², B. Wardle² and Y. Stein³

¹Metis Design Corporation (USA), ²Massachusetts Institute of Technology (USA), ³Analog Devices Inc (USA)

A decade ago, the global cost of corrosion was estimated to be US\$2.5 trillion, which was equivalent to 3.4% of the global GDP. By deploying a means for witnessing and quantifying the true corrosive potential of a given environment, more effective, informed and timely mitigation, maintenance, repair and replacement strategies can be implemented with the potential to save billions by avoiding down-time and structural damage. Thus, a novel corrosivity gauge was developed, to capture the effects of environmental conditions such as temperature, humidity, atmospheric chemical composition in addition to mechanical strain over time. The gauge was fabricated by combining a mix of common manufacturing techniques of various length-scales. One key element was a polymer nanocomposite (PNC) created by thoroughly blending a durable epoxy with carbon nanotubes (CNT), which was then silk-screened on a thermoplastic substrate to obtain a desired geometric shape and electrical resistance. Similarly metallic electrodes were patterned on top of the PNC to steer electrical current. The entire assembly was sealed between thermoplastic layers using laser-cut film-adhesive layers. The final step in the process was a selectively sputtered nano-thin layer of metal that serves as the principal witness material. In practice, the PNC layer provides a base resistance that can be precisely measured with common electronics, which is itself resistant to most environmental factors (such as corrosion) and employs in-situ features to compensation for the effects of temperature and strain. The sputtered metal layer acts as a thin-film parallel resistor to locally reduce the resistance of a portion of the PNC network. Consequently, as the environment being witnessed attacks the metal film over time, the overall network resistance would increase by as much as a factor of 10, which still can be precisely measured. The intent is for gauges and representative host materials to be subjected to the same accelerated environments to establish a mapping between corrosivity gauge output and respective material damage metric (e.g. pitting depth or mass loss). Much of this paper is devoted to overcoming the challenges of mixed-scale fabrication, most notably the 3-dimensional shaping of a PNC, and the surface-roughness effects on sputtering of nano-scale metal films layers onto a polymer, and characterization of the resulting electrical and mechanical properties.

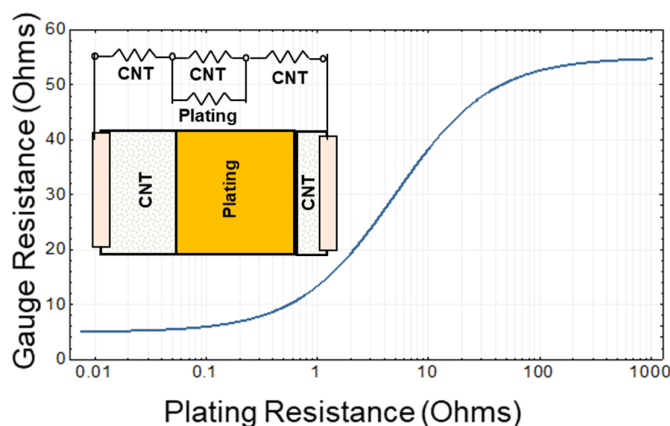


Figure 1: Change in carbon nanotube network resistance as a function of increasing plating layer resistance.

References

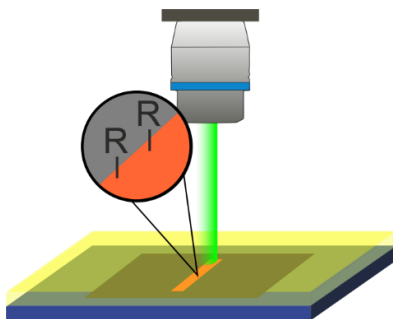
- [1] Lee J., Stein I.Y., Devoe M.E., Lewis D.J., Lachman N., Kessler S.S., Buschhorn S.T. and B.L. Wardle "Impact of carbon nanotube length on electron transport in aligned carbon nanotube networks." *Applied Physics Letters* 106, 053110 (2015)
- [2] Kessler, S.S., Raghavan A. and B.L. Wardle (2017). Multifunctional CNT-Engineered Structures (U.S. Patent No. 9,839,073). U.S. Patent and Trademark Office.
- [3] Kessler, S.S., Dunn C.T. and Y. Stein (2019). Disposable Witness Corrosion Sensor (U.S. Patent No. 10,502,676). U.S. Patent and Trademark Office.
- [4] Stein Y., Kessler, S.S. and H. Primo (2023). Self-Calibrating Polymer Nano Composite (PNC) Sensing Element. (U.S. Patent No. 11,656,193). U.S. Patent and Trademark Office.
- [5] Kessler S.S., Thomas, G.A., Dunn C.T., Borgen M. and B.L. Wardle (2023). Multifunctional Assemblies (U.S. Patent No. 11,706,848). U.S. Patent and Trademark Office.

Modular Chemical Patterning of Graphene by Direct Laser Writing Using λ^3 -iodanes

K. Gerein,¹ F. Hauke,¹ A. Hirsch,¹ and T. Wei¹

¹Department of Chemistry and Pharmacy & Center of Advanced Materials and Processes (ZMP)
Friedrich-Alexander-University of Erlangen-Nürnberg
Nikolaus-Fiebiger-Strasse 10, 91058 Erlangen, Germany
kevin.gerein@fau.de

Covalently binding addends on graphene represents a viable option to address the challenge of the material's lacking band gap and is accompanied by additional benefits, such as fine-tuning its chemical properties by introducing functional moieties.[1] These functionalities augment the outstanding properties of graphene and can enable molecular recognition, catalysis or tailored wettability behavior.[2, 3] Precise control over the entire process localized to the specific graphene surface regions extends the flexibility of the material and allows for the development of surfaces and devices tailored for specific demands. The emerging laser writing represents an efficient and promising strategy for covalent 2D patterning of graphene, yet remains a challenging task due to the lack of applicable reagents. Here, we present a versatile approach for the covalent laser patterning of graphene using a family of trivalent organic iodine compounds as effective reagents, allowing for the engraving of a library of functionalities onto the graphene surface. The relatively weak iodine-centered bonds within these compounds can readily undergo a laser-induced cleavage to *in situ* generate radicals localized to the irradiated regions for graphene binding, thus completing the covalent 2D structuring of this 2D film. The tailor-made attachment of distinct functional moieties with varying electrical properties as well as their thermally reversible binding manner enables programming the surface properties of graphene. With this delicate strategy, the bottleneck of a limited scope of functional groups patterned onto the graphene surface upon laser writing is tackled.



Scheme 1: Schematic representation of the laser writing procedure.

References

- [1] D. C. Elias *et al.*, *Science* **323**, 610–613 (2009).
- [2] K. F. Edelthammer, *et al.*, *Angew. Chem. Int. Ed.* **59**, 23329-23334 (2020).
- [3] L. Bao *et al.*, *Adv. Mater. Interfaces* **9**, 2200425 (2022).

Molecular Impermeability of Irreversibly Bonded Two-Dimensional Polyaramid (2DPA-1) Nanofilms

C.L. Ritt¹, M. Quien¹, Z. Wei¹, K. Altmisdort², Y.-M. Tu¹, J.S. Bunch^{2,3}, M.S. Strano¹

¹Massachusetts Institute of Technology (USA), ²Boston University (USA)

The climate crisis necessitates a large-scale transition from energy technologies based on fossil fuels to renewables, including hydrogen (H₂). Achieving this requires new materials that restrict the molecular transport of H₂ to enable infrastructure for its safe storage and transportation. Many nanofluidic platforms of interest for H₂ storage involve molecularly thin two-dimensional (2D) materials. Our recent synthesis of irreversibly bonded 2D polyaramid (2DPA-1) is a solution-processable version of such a material that has potential to scale 2D nanopores and fluidics beyond the limits of conventional materials. Here, we report spin-coated 2DPA-1 films, between 3 to 35 nm in thickness, with gas permeabilities approaching the measurement detection limit ($\mathcal{O} \sim 10^{-8}$ Barrer). Gas permeation measurements are enabled by atomic force microscopy (AFM) of pressurized bulges suspended over microwells. We find the gas barrier properties of 2DPA-1 thin films are commensurate with graphene despite their non-crystalline nature. Further, the inflation of 3-nm-thick bulges suspended across microwells indicates the absence of defects (e.g., pinholes) that commonly plague graphene and other molecularly thin films. Despite the intrinsic porosity of a single 2DPA-1 platelet, the impermeability, negligible BET surface area, and orientation-dependent fluorescence of its films suggests 2DPA-1 platelets align anisotropically in a tightly packed and staggered order that prevent molecular transport. The immutable nature of bulges pressurized in a 200 kPa-H₂ environment mirror the behavior of air trapped within the microwells upon film transfer, suggesting possible translation of this material as a H₂ barrier and warranting further exploration of 2DPA-1 films as nanofluidic platforms.

MOLECULE SUPER-TRANSPORT THROUGH MACROSCOPIC LENGTH OF INDIVIDUAL CARBON NANOTUBE

Jingwei WU¹, Silei SUN¹, Fei WEI¹

¹Tsinghua University (China)

The flow and transport in nanoscale channel pose challenges to the classic models. Herein, we establish a mass spectroscopy system to research the molecule transport in single ultra-long carbon nanotube. The measured water flow exceeds the values calculated from Poiseuille flow by more than six orders of magnitude. The measured gas flow exceeds predictions of Knudsen diffusion by more than an order magnitude. This surprising result highlights that the phenomenon of molecule super-transport is still efficient at the macroscopic length scales, reflecting a frictionless fluid-carbon interface. This work provides new insights into the super-transport of macroscopic length and demonstrates the possibility of a low energy-consumed process.

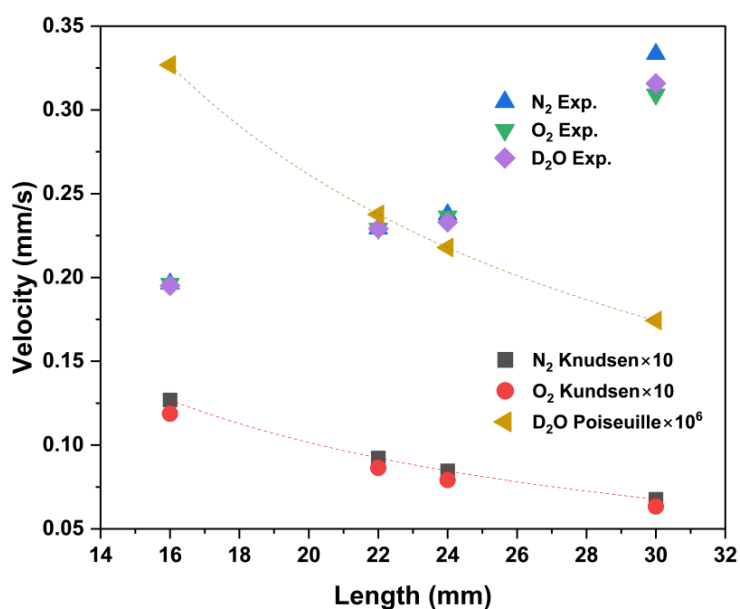


Figure 1: Dependence of flow velocity on the length of individual carbon nanotube

Morphology Changes and Stoichiometry Based MoS₂ Growth by Chemical Vapor Deposition using Kinetic Monte Carlo (KMC) Simulation

Yoonbeen Kang, Sang-Yong Ju*

Department of Chemistry, Yonsei University, Seoul, 03722, Korea

* Corresponding author e-mail: syju@yonsei.ac.kr

MoS₂ is one of the transition metal dichalcogenides (TMDs). The atomic structure of MoS₂ is in a sandwich with a hexagonal configuration where Mo is surrounded by S. Among the various methods to obtain MoS₂, chemical vapor deposition (CVD) method utilizes a bottom-up approach using Mo and S precursors, and displays high-quality large-area growth. The exact mechanism of MoS₂ growth has not been elucidated by the conventional synthesis method such as CVD. Recently, Wang *et al.*, [1] reported that the shapes of MoS₂ are evolved from inverted triangle, hexagon, and upright triangle which is determined by gaseous sulfur concentration.

In this poster, we use KMC to simulate the growth of MoS₂ crystal. Especially, this simulation was performed using the initial Mo seed. For this, we utilize vapor-solid growth mechanism in which gaseous precursors adsorb on a substrate and diffuse to form MoS₂ crystals. By using the reported energies for adsorption, desorption, diffusion, and enthalpy by density functional theory, we obtained the atomic morphology change of MoS₂ during the course of time. In addition, stoichiometry based MoS₂ was obtained by changing the ratio of Mo and S. Analysis of the KMC simulation displays that incorporating the desorption energy induces to the larger crystals growth with relatively smooth edges and the disappearance of energetically-unstable small crystals, as compared to the case considering adsorption energy. This method provides insight for the effect of growth parameters on the shape change of TMC for various applications.

Reference

[1] S. Wang *et al.*, *Chem. Mater.*, **2014**, 26(22), 6371–6379

Multifunctional Carbon Nanotube-based Composite Carbon Fibers for Enhanced Mechanical Properties

Junghwan Kim¹, So Jeong Heo¹, Seo Gyun Kim^{1*}, Bon-Cheol Ku^{1*}

¹Korea Institute of Science and Technology (KIST), Republic of Korea

*E-mail; seogyun.kim@kist.re.kr and cnt@kist.re.kr

The increasing significance of high-performance carbon fibers (CFs) has prompted extensive research across various applications such as aerospace, automotive, and batteries. Traditional CFs, derived from polyacrylonitrile(PAN), pitch, and cellulose, typically exhibit either high tensile strength or high modulus properties due to inherent structural limitations. Consequently, the simultaneous achievement of both tensile strength and modulus with high conductivity poses a significant challenge. Numerous studies have thus been undertaken to develop multifunctional CFs with superior performance [1]. Notably, 1-dimensional carbon nanotubes (CNTs) have become a common choice for CF fabrication due to their exceptional mechanical and conductive properties [2]. This presentation introduces CNT-based composite CFs, focusing on CNT-poly(*p*-phenylene sulfide) (PPS) and CNT-polyimide (PI) composite fibers [3-4]. These fibers exhibit outstanding mechanical properties while reducing production costs through the incorporation of low-cost polymers such as PPS and PI. Additionally, the presentation explores mechanism-based approaches aimed at elucidating the improvements in mechanical properties resulting from polymer integration. Ongoing efforts are directed towards the creation of high-performance CFs by combining diverse carbon nanomaterials and polymers, potentially finding applications in aerospace, defense, and other industries.

References

- [1] D. Lee *et al.*, *Funct. Compos. Struct.* **5**, 045007 (2023).
- [2] D. Lee *et al.*, *Sci. Adv.*, **8**, eabn0939 (2022)
- [3] J. Kim *et al.*, *Carbon* in press (2024)
- [4] S. Kim *et al.*, *Compos Part B*, **247**, 110342 (2022)

MXENE / METAL NANOMATERIALS FOR ENERGY CONVERSION APPLICATION

S. A. Sergiienko

University of Chemistry and Technology Prague, Technick'a 5, 166 28 Prague 6, Czech Republic

The emergence of new multifunctional materials continuously increases the expectations for the performance of energy conversion and storage devices. MXenes, a family of two-dimensional transition metal carbides has been discovered as an exciting candidate for these applications [1]. Transition metal-based electrodes are commonly used as cathodes in alkaline electrolysers for hydrogen production, provided by their low cost, appropriate electrocatalytic activity and corrosion resistance [2]. This work explores the possibilities for the processing of Ni, MAX phase and MXene-containing composite electrodes for H₂ production. Synthesis of powder mixtures with extra Ni and Al content (e.g. Ni:Mo:Ti:Al:C = 1:2:1:7:2) resulted in products containing modified molybdenum- and titanium-based MAX phase material and metal-Al alloys [2]. The presence of Ni in the initial reactional mixture allowed to reduce Al evaporation rate during the MAX phase synthesis and to increase the density of final products. The intentional excess of aluminium in the reaction mixture compared to the nominal composition of the MAX phases resulted in the formation of various metal–Al alloys (Mo₃Al₈, Ni₂Al₃, Al₅Mo₂Ni) segregated in the space between the modified MAX phase crystals. It was found that the presence of Ni and Al excess in the reaction mixture promotes the formation process of conventional (Mo₂Ti₂AlC₃, Mo₂TiAlC₂) and modified (probably Mo₂TiAl₂C₂) MAX phases due to generating Al-rich metal-Al alloys (intermediates) with a lower melting point e.g. Ni₂Al₃ that accelerates the formation of final products (MAX phases) and reduce the content of intermediate compounds. Further etching of these products in 10M NaOH allowed the direct formation of electrodes with active surface containing MAX phase, MXene and nanoporous metal composites [2, 3]. The proposed methodology allows producing a composite electrode with a well-developed 3D porous MAX phase-based structure acting as a support for electrocatalytic species, including MXene, and nano-metal possessing good mechanical integrity [2]. Several factors contributed to this performance, including the intrinsically high electrocatalytic activity of the above phases, high specific surface area and intercrystallite porosity, promoted by compositional design facilitating the etching. The presence of nickel provided an additional important contribution, improving the electrical connection of the MAX phase and MXene crystals and the integrity of the obtained electrodes with a 3D structure. Electrochemical tests have shown a high electrochemical activity of such electrodes towards the hydrogen evolution reaction (HER), combined with a relatively high areal capacitance (up to 10 F cm⁻²). The guidelines for the processing of MXenes under fluorine-free conditions are proposed and discussed.

References

- [1] Y. Gogotsi *et al.*, *ACS nano* **13**, 8491–8494 (2019).
- [2] S. A. Sergiienko *et al.*, *RSC advances* **14**(5), 3052–3069 (2024).
- [3] S. A. Sergiienko *et al.*, *Int. J. of Hydrogen Energy* **46**(21), 11636–11651 (2021).

Near-Infrared Fluorescent Carbon Nanotube Sensors for the Plant Hormone Family Gibberellins

Boonyaves, K.,⁺¹ Ang, M.C.Y.,⁺² Park, M.,⁺³ Cui, J.,³ Khong, D.T.,² Singh, G.P.,² Koman, V.B.,³ Gong, X.,³ Porter, T.K.,³ Choi, S.W.,³ Chung, K.,³ Chua, N.-H.,² Urano, D.,^{*2} and Strano, M. S.^{*3}

¹Mahidol University (Thailand)

²Disruptive and Sustainable Technologies for Agricultural Precision (Singapore)

³Massachusetts Institute of Technology (U.S.A.)

[†] These authors contribute equally

^{*} Corresponding authors

Gibberellins (GAs) are a class of phytohormones, important for plant growth, and very difficult to distinguish because of their similarity in chemical structures. Herein, we develop the first nanosensors for GAs by designing and engineering polymer-wrapped single-walled carbon nanotubes (SWNTs) with unique corona phases that selectively bind to bioactive GAs, GA₃ and GA₄, triggering near-infrared (NIR) fluorescence intensity changes. Using a new coupled Raman/NIR fluorimeter that enables self-referencing of nanosensor NIR fluorescence with its Raman G-band, we demonstrated detection of cellular GA in Arabidopsis, lettuce, and basil roots. The nanosensors reported increased endogenous GA levels in transgenic Arabidopsis mutants that overexpress GA and in emerging lateral roots. Our approach allows rapid spatiotemporal detection of GA across species. The reversible sensor captured the decreasing GA levels in salt-treated lettuce roots, which correlated remarkably with fresh weight changes. This work demonstrates the potential for nanosensors to solve longstanding problems in plant biotechnology.

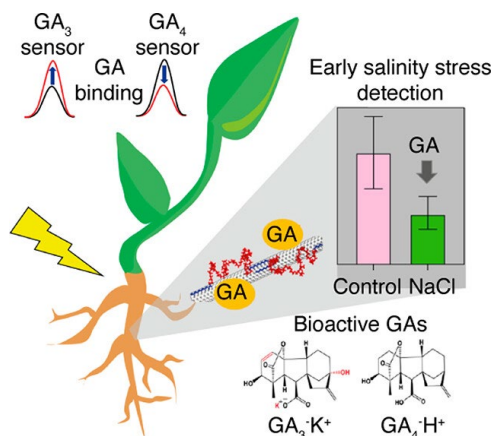


Figure caption: Schematic of GA₃ and GA₄ sensor in plant roots to detect the onset of salinity stress.

New Architectures for Heat Sink Less Carbon Nanotube Film Thermoelectric (TE) Devices Inspired by Kirigami

C. Zeng¹, E. Bilotti¹

¹Department of Aeronautics, Imperial College London, Exhibition Road, London, SW7 2AZ (UK)

Thermoelectric (TE) technology [1] presents a unique opportunity to convert waste heat directly into electricity, offering a promising solution to address energy harvesting and sustainability challenges. However, conventional TE devices with π -type structures always need a heat sink to thermally link to the air during operation which remains a significant limitation for their practical applications.

Herein, we report a new configuration of a TE device that has a built-in heat sink for the first time. Furthermore, the device modified with shape-memory polymer films can be self-folded into a hexagonal structure via heating above its glass transition temperature. We demonstrate the feasibility of our design through experimental characterization and modelling. The device with built-in fins exhibits superior thermoelectric performance with both organic (carbon nanotube veils) and inorganic (bismuth telluride, BiTe) TE materials. The maximum power output of the BiTe-based device can reach 180 μW , which is 4.4 times higher than that of the carbon-based device (41 μW) when the temperature difference is 43 K and airflow is 1.5 m s^{-1} . BiTe-based devices show better TE performance but less stability compared to carbon-based devices. Moreover, carbon-based devices can be self-folded via external temperature stimulus and keep resistance no change (95 Ω) while BiTe-based devices cannot.

This work provides a path to optimize the thermoelectric performance of TE devices by designing rational structures. This approach has the potential to reduce the cost, mass, and volume of TE devices, making them more attractive for a wide range of applications, such as waste heat recovery, energy harvesting, and thermal management.

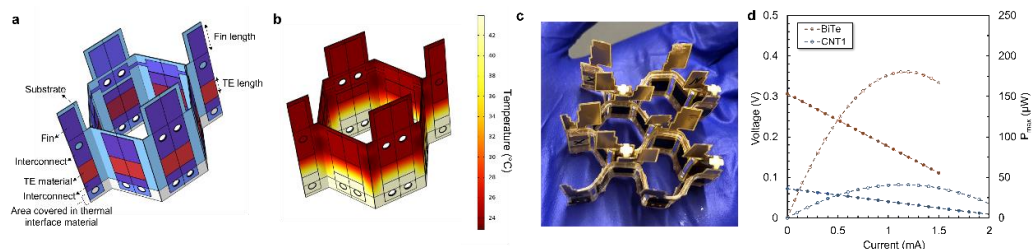


Figure 1 Design and performance of carbon nanotube film-based TE devices.

References

[1] T. Sun, B. Zhou, Q. Zheng, L. Wang, W. Jiang, G.J. Snyder, Nature Communications, 11, 572 (2020)

Nonadiabatic Dynamics for Assessing Yield of Emission of sp^3 defect carbon nanotubes

Semiconducting single-walled carbon nanotubes (SWCNTs) hold promise as single-photon emitters. Incorporating quantum defects into the sidewalls of SWCNTs through covalent bonding is a route to predictably modify electronic structures, optical properties and develop optoelectronic functionality. To narrow down the list of monochromatic emitters require selectivity in binding conformation of defects on the sidewalls of SWCNTs. The brightening and red-shift of photoluminescence is modeled as a function of selective aryl functionalization of (11,0) SWCNTs. First principles modeling and nonadiabatic dynamics simulation reveals the emitting signatures functionalized nanotubes specific to defect geometry. The value of red-shifted of photoluminescence, lifetime, and higher photoluminescence quantum yield are correlated to details of binding geometry.

The work is supported by DE-SC0021287 for exploring IR-emission of carbon nanotubes.

NON-COVALENTLY FUNCTIONALIZED COBALT-PHTHALOCYANINE TRANSITION METAL DICHALCOGENIDE NANOSHEET NETWORKS

Elena A. Mack¹, Alejandro Cadranel¹, Kevin Synnatschke², Leandro Lourenço³, Dirk M. Guldi¹

¹Friedrich-Alexander-Universität (Germany), ²Technische Universität Dresden (Germany), ³University of Aveiro (Portugal)

Solution-processed nanosheet networks (NN) of exfoliated transition metal dichalcogenides (TMDs) have attracted immense interest which is partially attributed to their compatibility with printing techniques, suitable for large area processing. The electrical characteristics of the NN obtained from liquid–liquid interface deposition, demonstrate an electron mobility of $10 \text{ cm}^2\text{V}^{-1}\text{s}^{-1}$ for networks of molybdenum disulfide nanosheets [1].

The TMD NN's semiconducting nature offers opportunities for adjusting electronic properties through functionalization, especially with pyridyl-cobalt phthalocyanines (CoPcs). These molecular building blocks have previously demonstrated effectiveness as carbon dioxide capture and reduction photocatalysts [2].

Here, we report on non-covalent functionalized TMD NN with CoPcs immobilized on the exposed basal plane surface of the NN [3]. The appearance of charge transfer (CT) steady-state extinction bands imply a strong ground state interaction between the TMD and the CoPc. The interfacial CT states have electronic matrix coupling elements of about 1000 cm^{-1} , typical for strongly coupled CT systems. Electrochemical characterizations show distinct peaks for the functionalized films, confirming that the CoPcs act as electrochemically active sites on the surface of the NN. Furthermore, charge separation was corroborated by femtosecond transient absorption spectroscopy [4] supported by steady-state spectroelectrochemistry of the CoPcs. We hence conclude that these functionalized NNs exhibit promising characteristics for the design of carbon dioxide photocatalytic systems.

References

- [1] Kelly, A. G., O'Suilleabhain, D., Gabbett, C., & Coleman, J. N., *Nature Reviews Materials*, **7**, 217–234 (2022).
- [2] Roy, S., Miller, M., Warnan, J., Leung, J. J., Sahm, C. D., & Reisner, E., *ACS Catalysis*, **11**, 1868–1876, (2021).
- [3] Wibmer, L., Lourenço, L. M. O., Roth, A., Katsukis, G., Neves, M. G. P. M. S., Cavaleiro, J. A. S., Tomé, J. P. C., Torres, T., & Guldi, D. M., *Nanoscale*, **7**, 5674–5682 (2015).
- [4] Scharl, T., Binder, G., Chen, X., Yokosawa, T., Cadranel, A., Knirsch, K. C., Spiecker, E., Hirsch, A., & Guldi, D. M., *Journal of the American Chemical Society*, **144**, 5834–5840 (2022).

OBTAINING BAMBOO STRUCTURE USING MWCNT

Obtaining the Bamboo structure, nanotube with multiple walls, using the pyrolytic spraying method

Carbon nanotubes (CNTs) are an allotropic form of carbon, apart from diamond and graphite. CNTs are extraordinary materials that have attracted much research interest. They were discovered in 1991 by Iijima [1] and could be particularly useful in electronic devices due to their unique properties [2].

It is possible to influence the mechanical, electronic, vibrational, chemical properties of CNT by replacing some carbon atoms, either boron or nitrogen atoms [3]. Thus, if a few boron atoms replace C atoms in the graphite sheet (sp² carbon system), it results in p-type states in the valence band, while when nitrogen atoms replace C atoms, electrons are injected into conduction band, and an n-type material appears.

Using theoretical calculations [4], it was discovered that CNTs doped with boron are uniformly metallic. Nitrogen-doped CNTs are either metallic type or have a narrow bandgap, typical of semiconductors [5].

So far, CVD synthesis has been the most promising in producing MWCNTs doped with nitrogen and having a bamboo structure.

We characterized our samples using TEM, HRTEM.

Experimental

We investigated the influence of the nature of the carrier gas and the composition of the benzene-pyridine mixture on the quantity and quality of MWCNTs.

TEM and HRTEM methods were used to characterize the final product. TEM investigations provide important data regarding the characteristics of CNTs, their inner and outer diameters, as well as an estimate of the level of graphitization of the multiple walls of the nanotubes.

Results and discussion

We studied the effect of the quantity of pyridine in the pyridine-benzene mixture, used as a carbon source, and the effect of the carrier gas on the quantity and quality of CNT thus obtained.

During the synthesis, the characteristic values of the experimental parameters were: the carrier gas flow rate is 500 l/h, at a temperature of 875 °C in the reactor, the solution flow rate is 1 ml/min, the catalyst concentration is 3.5 g ferrocene in 50 ml carbon source liquid.

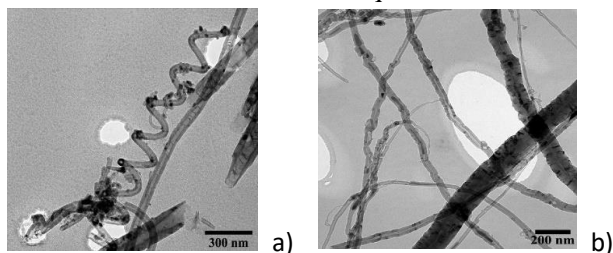


Figure 4.1. TEM images of CNT obtained from pyridine as carbon source.

- a) TEM image of sample S105 (using argon as carrier gas),
- b) showing a spiral of the nanotube;
- b) sample S105 after purification;
- c) sample S106 (using nitrogen as carrier gas), after purification.

The quality of the obtained nitrogen-doped CNTs was investigated by TEM and HRTEM.

TEM images of CNTs are presented in Figures a) and b).

The content in multi-walled nanotubes with a bamboo structure increases with increasing pyridine content in the carbon source. Spiral CNTs were observed.

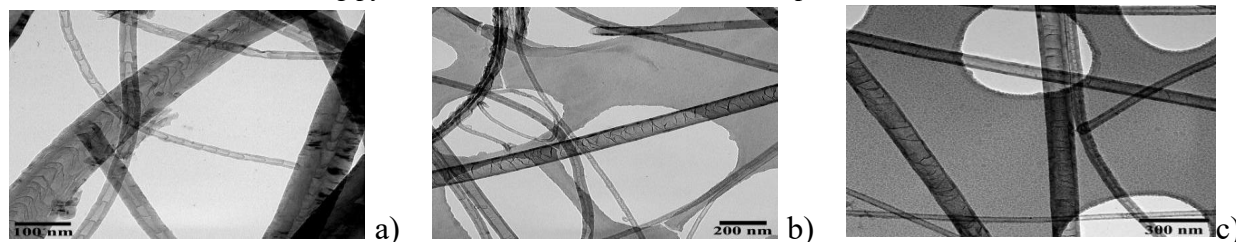


Figure 4.2. Characteristic of TEM images of CNTs obtained from

- a) benzene (sample S133); b) pyridine-benzene mixture (sample S129, pyridine concentration vol. 25%);

c) pyridine-benzene mixture (sample S87, pyridine concentration vol. 50.%). Images were taken after sample purification

Bibliography

[1] S. Iijima, Nature (London) **354**, 56 (1991).

[2] M. S. Dresselhaus, G. Dresselhaus, P. C. Eklund, Science of Fullerenes and Carbon Nanostructures, Academic Press, San Diego, 1996.

[3] L. P. Biró, C. A. Bernardo, G. G. Tibbets, Ph. Lambin Eds., Carbon Filaments and Carbon [41],[42] .

One-Dimensional, Titania-Based Lepidocrocite Nanofilaments: Large Scale Production, Characterization, Properties and Potential Applications

Hussein O. Badr¹, Michel W. Barsoum¹

¹Department of Material Science and Engineering, Drexel University, Philadelphia, PA, USA

Titania nanostructures have been, and remain, of significant commercial and research interest due to their potential use in a wide range of fields including paints, catalysis, photocatalysis, among many more. Conventionally, bulk synthesis of titania nanostructures has predominantly been through autoclaving safety hazardous chemicals at elevated temperature and pressure. Recently, we developed a solution processing-based protocol to convert 15 different cheap and earth abundant Ti-containing powders (carbides, borides, nitrides, etc) into one-dimensional lepidocrocite titania-based nanofilaments, referred to as 1DL NFs. Our method entails mixing the precursor powders with a common base, tetramethylammonium hydroxide, in plastic bottles at 80°C for a few days under ambient pressure.(1, 2) With a band gap energy of ≈ 4 eV, the resulting NFs are the first to truly fit the quantum mechanical definition of one dimensionality for titania nanostructures.(3) Morphologically, the NFs self-assemble in a plethora of nanostructures, viz. two-dimensional flakes, nanobundles or mesoporous particles, when dispersed in different solvents.(4, 5) Chemically, we showed that the NFs can be readily ion exchanged with various mono- and divalent cations including TMA⁺, H₃O⁺, Li⁺, Na⁺, Mg²⁺, Mn²⁺, Fe²⁺, Co²⁺, Ni²⁺, or Zn²⁺ ions.(1, 4) The resulting 1DLs showed outstanding performance in a diversity of energy, environmental, and biomedical fields such as photo- and electrocatalytic water splitting, lithium-sulfur and lithium-ion batteries, water purification, dye degradation, cancer therapy, and polymer composites.(1, 6-11) Beyond 1DLs, we showed that hydroxides aqueous solutions are quite powerful in preparing other metal oxides nanostructures including magnetic Fe₃O₄ nanoparticles and MnO₂ birnessite-based crystalline two-dimensional flakes.(12-15)

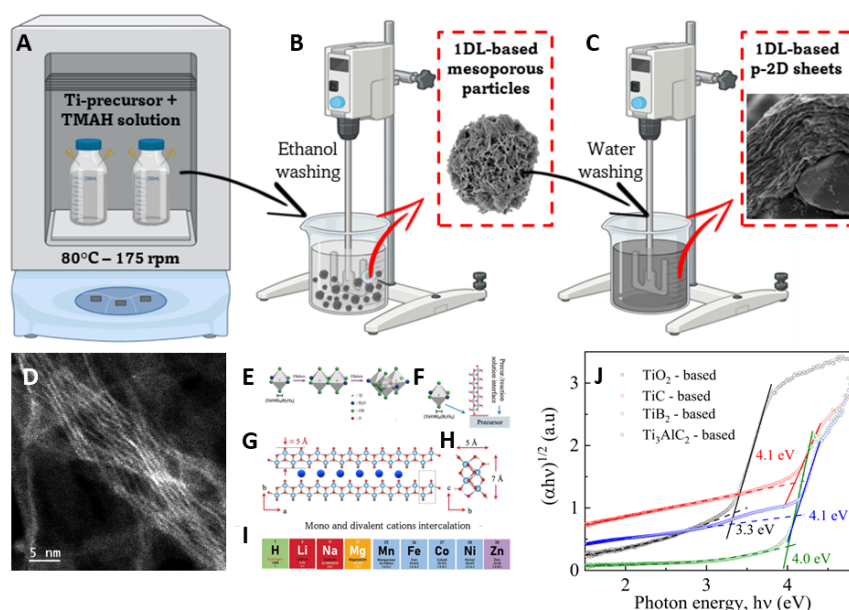


Figure 1: Schematic showing 1DL NFs (A) Processing in temperature-controlled shaker, and (B)-(C) Subsequent washing steps in ethanol and water, respectively. Dashed red rectangles in (B) and (C) illustrate the resulting 1DL-based morphologies (mesoporous particles and two-dimensional sheets, respectively). (D) High resolution STEM image of 1DLs bundle. (E) Olation reaction leading to formation of a plethora of TiO₂ structures including 1DLs, (F) Schematic of a monomer being inserted between the solid precursor surface and reaction solution. This explains how the NFs grow from the base. (G) DFT generated 2 Ti-atom wide, lepidocrocite-based structure formed. NFs stack in b-direction and grow in a-direction. (H) Smallest possible cross-section of NFs that is DFT stable. 1DL NFs are readily ion exchangeable with various mono- and divalent cations shown in (I). (J) Tauc plots of TiC-, TiB₂- and Ti₃AlC₂-derived NFs depicting characteristic band gap (~ 4 eV) of the resulting 1DL NFs. Black curve is a Tauc plot of TiO₂ sample processed similarly in TMAH solution and showing $E_g \sim 3.3$ eV that aligns with bulk anatase.

References

1. H. O. Badr *et al.*, Bottom-up, scalable synthesis of anatase nanofilament-based two-dimensional titanium carbo-oxide flakes. *Mater. Today* **54**, 8-17 (2022).
2. H. O. Badr *et al.*, On the Structure of One-Dimensional TiO₂ Lepidocrocite. *Matter* **6**, 128-141 (2023).
3. E. Colin-Ulloa *et al.*, Electronic Structure of 1D Lepidocrocite TiO₂ Quat-Derived Nanomaterial, QDN, as Revealed by Optical Absorption and Photoelectron Spectroscopy. *Phys. Chem. C* . **127**, 7275–7283 (2023).
4. H. O. Badr *et al.*, Titanium Oxide-based 1D Nanofilaments, 2D Sheets, and Mesoporous Particles - Synthesis, Characterization, and Ion Intercalation. *Matter*, (2023).
5. K. Sudhakar *et al.*, One-dimensional, Lepidocrocite-based Nanofilaments and Their Self-Assembly. *Matter* **6**, 3538-3554 (2023).
6. N. Cardoza, H. O. Badr, R. Pereira, M. Barsoum, V. Kalra, One-Dimensional, Titania Lepidocrocite-based, Nanofilaments and Their Polysulfide Anchoring Capabilities in Lithium Sulfur Batteries. *ACS Appl. Mater. Interfaces*, (2023).
7. N. Carpentieri *et al.*, Two-Dimensional Aggregates of Lepidocrocite TiO₂ Nanofilaments with Ni/Fe Active Sites for Durable Oxygen Evolution Electrocatalysis. *ACS Appl. Eng. Mater.*, (2023).
8. H. Badr *et al.*, Ultra-stable, 1D TiO₂ Lepidocrocite for Photocatalytic Hydrogen Production in Water-Methanol Mixtures. *Matter*, (2023).
9. L. Wang *et al.*, Unique Hierarchical Structures of One Dimensional Lepidocrocite Titanate with Cation-Exchangeable Sites for Extraordinary Selective Actinide Capture for Water Purification. *Chem. Eng. J.* **474**, 145635 (2023).
10. O. R. Wilson *et al.*, Repairable reinforced composites of 1D TiO₂ lepidocrocite mesoparticles and thiol-yne click networks via alkylborane-initiated in situ polymerization. *Cell Rep.* **4**, 101434 (2023).
11. Adam D Walter *et al.*, Adsorption and self-sensitized, visible-light photodegradation of rhodamine 6G and crystal violet by one-dimensional lepidocrocite titanium oxide. *Matter* **6**, 4086-4105 (2023).
12. H. O. Badr *et al.*, Scalable, inexpensive, one-pot, facile synthesis of crystalline two-dimensional birnessite flakes. *Matter* **5**, 2365–2381 (2022).
13. Mary Qin Hassig *et al.*, Reacting Mn₃O₄ powders with quaternary ammonium hydroxides to form two-dimensional birnessite flakes. *Ceram. Int.* **49**, 33537-33545 (2023).
14. K. Sudhakar *et al.*, One pot, scalable synthesis of hydroxide derived ferrite magnetic nanoparticles. *J. Magn. Magn. Mater.* **582**, 170986 (2023).
15. W. Zheng *et al.*, MXene//MnO₂ Asymmetric Supercapacitors with High Voltages and High Energy Densities. *Batteries & Supercaps* (2022).

One-step hydrothermal Synthesis of 3D Garland BiOI, Spherical ZnO, and CNFs for advancing Supercapacitor Performance with Enhanced Electrochemical Properties

Nallapureddy Jyothi^{1,a}, Ramesh Reddy Nallapureddy^{2,b}, Mohan Reddy Pallavolu^{2,b} and Sang W. Joo^{1,c}

¹School of Mechanical Engineering, Yeungnam University, Gyeongsan 38541, the Republic of Korea

²School of Chemical Engineering, Yeungnam University, Gyeongsan 38541, the Republic of Korea

^anjyothi94@yu.ac.kr, ^brameshsun999@gmail.com, ^bpmreddy@yu.ac.kr, ^cswjoo@yu.ac.kr

Abstract

In this study, we present a different approach for the one-pot hydrothermal synthesis of 3D garland BiOI, spherical ZnO, and carbon nanofibers on a Ni foam substrate, aimed at improving the supercapacitor performance with enhanced electrochemical properties. Owing to the efficient utilization of pseudoactive species, fast ion/electron transfer, and strong interactions between the electrode materials, the synthesized nanocomposites exhibited high specific capacitance of 1073 g⁻¹ at a current density of 1 A/g and excellent cycling stability, with 88.6% retention of the original capacity after 5000 cycles in a 2M KOH aqueous solution. These findings highlight the potential of the developed 3D garland BiOI, spherical ZnO, and CNF-on-Ni foam nanocomposites as promising electrode materials for advanced supercapacitors, offering significant improvements in energy storage capabilities. The outstanding electrochemical performance observed in our 3D garland BiOI, spherical ZnO, and CNF-on-Ni foam nanocomposites highlights their promise as advanced electrode materials for supercapacitors. These materials not only surpass existing counterparts in specific capacitance but also offer significant advancements in energy storage capabilities. This study paves the way for the development of high-performance supercapacitors with enhanced energy storage, emphasizing the importance of tailored nanostructures and composite materials in advancing energy storage technologies.

One-Zone Chalcogenization for Fabrication of Few-Layer Transition Metal Dichalcogenide Films

M. Sojková,^{1*} J. Hrdá,¹ L. Pribusová Slušná,¹ P. Hutár,¹ K. Vegso,^{2,3} E. Dobročka,¹ P. Siffalovic^{2,3} and M. Hulman¹

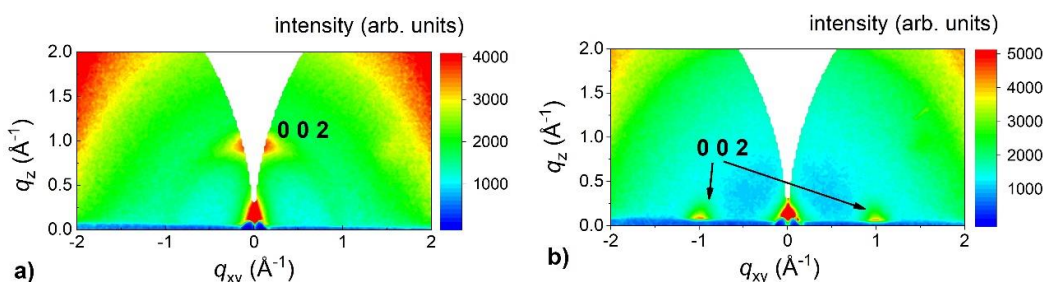
¹ Institute of Electrical Engineering, SAS, Dúbravská cesta 9, 841 04 Bratislava, Slovakia

² Institute of Physics, Slovak Academy of Sciences, Dúbravská cesta 9, 84511 Bratislava, Slovakia

³ Centre for advanced materials application (CEMEA), Slovak Academy of Sciences, Dúbravská cesta 5807/9, 84511 Bratislava, Slovakia

Layered materials, exhibiting a weak out-of-plane van der Waals interaction, have been a subject of significant interest for decades. Two-dimensional transition metal dichalcogenides (TMDCs) represent a burgeoning class of materials with properties that render them highly appealing for exploring novel physical phenomena and applications spanning nanoelectronics, nanophotonics, sensing, and nanoscale actuation. While various methods exist for fabricating monolayer or few-layer films within this material group, achieving large-area TMDC films with few layers remains a challenging task. Among the methods facilitating the growth of extensive films, chalcogenization of pre-deposited metal or metal oxide layers stands out. The spatial orientation of TMDC layers is crucial for their envisioned applications. Depending on the synthesis conditions, TMDC films can grow horizontally or vertically. In horizontal alignment, the basal planes align parallel to the substrate surface, with the crystallographic *c*-axis oriented along the surface normal. Conversely, in vertical alignment, the basal planes stand upright on the substrate, and the *c*-axis is perpendicular to the surface normal.

In this work, we present a custom-designed chalcogenization process suitable for growing various TMDC films, including molybdenum disulfide, [1,2] tungsten disulfide [3], platinum diselenide, [4,5] niobium diselenide, or palladium diselenide. Characterization of the prepared films involves various techniques such as GIWAXS, AFM, Raman spectroscopy, and electrical measurements. We demonstrate how synthesis conditions impact film orientation, as well as the structural and electrical properties of the resulting TMDC films.



GIWAXS reciprocal space maps of MoS₂ layers prepared from Mo films with the nominal thickness of (a) 1 nm and (b) 3 nm sulfurized at 800 °C / 30 min.

References (if desired)

- [1] M. Sojková *et al.*, RSC Advances 9, 29645 (2019).
- [2] M. Sojková *et al.*, Scientific Reports 9, (2019).
- [3] I. Hotovy *et al.*, Applied Surface Science 544, 148719 (2021).
- [4] M. Sojková *et al.*, Applied Surface Science 538, 147936 (2021).
- [5] M. Sojková *et al.*, Appl. Phys. Lett. 119, 013101 (2021).

Optimized Purification of Efficiently-synthesized Carbon Nanotubes for Fiber Spinning

M. Durán-Chaves¹, O.S. Dewey², A.V. Benavides-Figueroa¹, M. Gong², K. Dale¹, A. Dantzler², M. Pasquali^{1,2,3,4}

¹Department of Chemistry, ²Department of Chemical and Biomolecular Engineering, ³The Smalley-Curl Institute, ⁴Carbon Hub, Rice University (USA)

Carbon nanotubes (CNTs) strongly bundle together via van der Waals forces to form lightweight macromaterials with remarkable properties, including high electrical conductivity, thermal conductivity, and tensile strength. There is great interest in developing wet spun CNT fibers to utilize these unique nanomaterials in applications such as cabling, wearable electronics, and biomedical devices. The macroscopic properties of CNT fibers depend on CNT intrinsic properties, including aspect ratio (L/d), crystallinity, and purity [1]. The best wet-spun fiber properties reported in the literature [2-4] have been achieved by wet spinning at low CNT concentrations in superacid (0.25 - 0.50 wt%), which limits commercial adoption. The production of fibers at high concentrations could increase the process efficiency and reduce its environmental impact. CNT fibers can be solution-spun at high concentration when using shorter CNTs or by aggressive purification of as-synthesized samples, which is known to oxidize and cut the CNTs, leading to property degradation [5-7].

We study the coupled synthesis, purification, and wet spinning of CNT fibers. We synthesize CNTs with high aspect ratio (~ 6000), crystallinity (G/D > 20), and purity (95 % selectivity); we find that, however, the as-synthesized material requires additional purification to obtain homogeneous solutions at high concentrations. We studied thermal oxidation to determine the minimal purification needed for superacid dissolution at high CNT concentration. We find that purification can be optimized to produce spinnable dopes while limiting carbon mass loss to below 10%. The resulting CNT fibers showed properties that are competitive with the best properties previously obtained. The production of CNT fibers at higher concentrations improves throughput of the wet-spinning process and lowers cost and environmental footprint of the process.

References

- [1] Tsentelovich et al., *ACS applied materials & interfaces*, **9**(41), 36189-36198 (2017).
- [2] Taylor et al., *Carbon*, **171**, 689-694 (2021).
- [3] Kim et al., *Carbon*, **196**, 59-69 (2022).
- [4] Lee et al., *small*, **13**, 1701131 (2017).
- [5] Ericson et al., *Science*, **305**, 1447-1450 (2004).
- [6] Davis et al., *Nature Nanotechnology*, **4**, 830-834 (2009).
- [7] Behabtu et al., *Science*, **339**, 182-186 (2013).

Oxygen-Rich Amorphous Carbon as a Functional Interphase in Industrial Carbon Nanotube Yarn Networks

Durso, M. N.¹, Hart, A. J.²

¹Department of Materials Science & Engineering, Massachusetts Institute of Technology (United States of America),

²Department of Mechanical Engineering, Massachusetts Institute of Technology (United States of America)

The presence of amorphous carbon as a contaminant phase in carbon nanotube (CNT) and continuous CNT yarn networks is well-established, and numerous purification strategies have been outlined in the literature that target it (and retained iron catalyst particles), relying on the phase's lower thermal and chemical stability versus crystalline CNTs[1], [2], [3]. Despite its ubiquity in various CNT materials, limited research exists regarding the interfacial and microstructural role of amorphous carbon as it exists in a hierarchically-assembled network of CNTs (as in yarn and sheet materials). However, it has been recognized as a potential CNT reinforcement: amorphous carbon was treated by Jensen et al. as a model system for predicting the properties of fully-dense CNT composites[4], in part due to its presence in real CNT networks.

Recent work from our team investigates the effects of amorphous carbon in industrially-produced yarns, which suggests it exists in-situ at the mesoscale inside and between dense CNT bundles. Here, this phase does behave analogously to polymer reinforcement, and in purified yarns, we find both reduced tensile properties and greater pore network accessibility[1], [5]. Further, we demonstrate that the hygroscopic, oxygen-functionalized amorphous carbon surface[1], [5], [6] may enhance interfacial properties in composites[1], [7]. The existence and effects of this phase must therefore be considered for processes that modify the yarn network in-situ, such as functionalization, and suggests optimization of this phase's chemical moieties and spatial distribution may improve their properties in record-breaking, bulk CNT yarn composites[8].

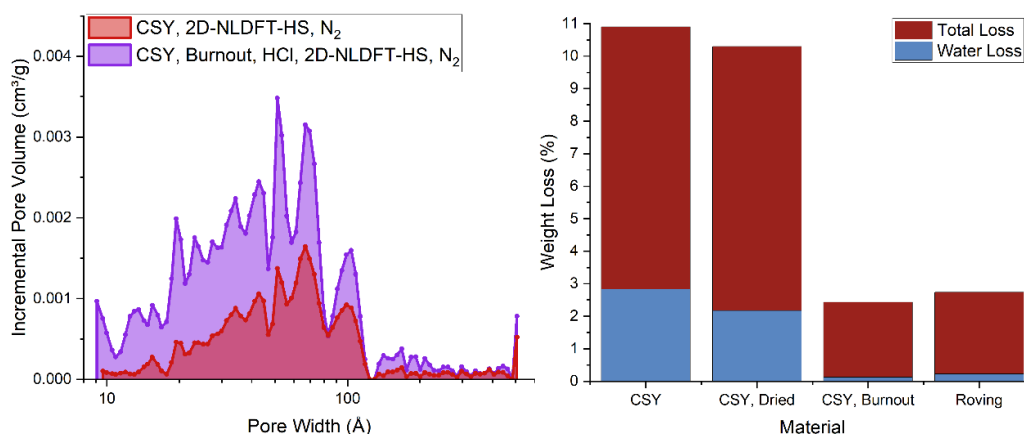


Figure 1: Mesoscale spatial distribution of amorphous carbon by gas adsorption analysis (left) and hygroscopic behavior from water loss (right) in CNT yarns. “Burnout” and “roving” yarns possess no amorphous carbon.

References

- [1] M. N. Durso and A. J. Hart, “Purification of dense carbon nanotube networks by subcritical hydrothermal processing,” *Carbon Trends*, vol. 9, p. 100206, Oct. 2022, doi: 10.1016/J.CARTRE.2022.100206.
- [2] T. Q. Tran *et al.*, “Purification and Dissolution of Carbon Nanotube Fibers Spun from the Floating Catalyst Method,” *ACS Appl Mater Interfaces*, vol. 9, no. 42, pp. 37112–37119, Oct. 2017, doi: 10.1021/acsami.7b09287.
- [3] Y. Lin, J.-W. Kim, J. W. Connell, M. Lebrón-Colón, and E. J. Siochi, “Purification of Carbon Nanotube Sheets,” *Adv Eng Mater*, vol. 17, no. 5, pp. 674–688, May 2015, doi: 10.1002/adem.201400306.
- [4] B. D. Jensen, G. M. Odegard, J. W. Kim, G. Sauti, E. J. Siochi, and K. E. Wise, “Simulating the effects of carbon nanotube continuity and interfacial bonding on composite strength and stiffness,” *Compos Sci Technol*, vol. 166, pp. 10–19, Sep. 2018, doi: 10.1016/J.COMPOSITECH.2018.02.008.
- [5] M. N. Durso, W. J. Sawyer, and A. J. Hart, “Reinforcing Amorphous Carbon Phases and Network Morphology in CNT Yarn Composites”, *under review*.
- [6] B. Alemán, M. Vila, and J. J. Vilatela, “Surface Chemistry Analysis of Carbon Nanotube Fibers by X-Ray Photoelectron Spectroscopy,” *physica status solidi (a)*, vol. 215, no. 19, p. 1800187, Oct. 2018, doi: 10.1002/pssa.201800187.
- [7] M. N. Durso, W. J. Sawyer, and A. J. Hart, “Polyetherimide Carbon Nanotube Composites by In-Situ Interfacial Polymerization”, *under review*.
- [8] C. E. Evers *et al.*, “Scalable High Tensile Modulus Composite Laminates Using Continuous Carbon Nanotube Yarns for Aerospace Applications,” *ACS Appl Nano Mater*, vol. 6, no. 13, pp. 11260–11268, Jul. 2023, doi: 10.1021/ACSANM.3C01266

Pristine SWCNT-based composite materials for Lithium battery applications.

Oleg A Kuznetsov, Avetik R Harutyunyan

Honda Research Institute USA, Inc. San Jose, CA 95134

We have developed a new type of composite materials consisting of powdered materials embedded into a 3-dimensional network of pristine individual or a few-bundled single wall carbon nanotubes (SWNTs). A wide selection of powdered materials can be used, and SWNT content can be varied in a broad range. This uniform dispersion has been achieved by *in-situ* mixing of aerosols of pristine, as-grown SWNTs and the particle aerosol. The resulted composite materials typically are self-standing, mechanically robust and with electrical conductivity 10^1 - 10^5 S/m, depending on the material composition and density. The composites demonstrate anomaly high Poisson's ratio (~ 0.8) and high piezoresistivity (gauge factor 3-6).

We have been using this technology to create composites of Li-ion battery materials for self-standing, binder and collector free battery electrodes. Application of these electrodes allows to increase battery energy density up to 40% and increase specific energy up to 70%. High power density designs are also possible with this architecture for high C-rate applications (up to 20C), making such battery architecture attractive for EV/EVTOL batteries. Remarkably, the free-standing electrodes can also serve as "built-in" sensors for *operando* monitoring of battery health utilizing their intrinsic piezoresistivity, making the batteries "smart", capable of monitoring battery condition throughout its lifecycle. We have demonstrated that such sensors can detect mechanical bending or stretching of the battery or electrode(s). The possibility of using these composites for *operando* sensing of the battery pressure and gas evolution in the battery will be discussed.

- [1] O.A. Kuznetsov, S. Mohanty, E. Pigos, G. Chen, W. Cai, A.R. Harutyunyan, High energy density flexible and ecofriendly lithium-ion smart battery. *Energy Storage Materials*, 2023 (54) 266-275, ISSN 2405-8297, doi.org/10.1016/j.ensm.2022.10.023

Proper Electrolytes and Reaction Conditions for Prelithiation of SiO-Carbon Nanotube Sponge Anode for Lithium-Ion Batteries

B. Huang¹, T. Mae¹, S. Noda^{1,2,*}

¹ Department of Applied Chemistry, Waseda University, 3-4-1 Okubo, Shinjuku-ku, Tokyo, 169-8555, (Japan),

² Waseda Research Institute for Science and Engineering, Waseda University, 3-4-1 Okubo, Shinjuku-ku, Tokyo, 169-8555, (Japan).

Carbon nanotube (CNT) can be used to support various cathode and anode materials to build the lightweight electrodes for lithium-ion batteries (LIBs) with high energy density [1,2]. Silicon monoxide (SiO) shows high capacity when combined with CNT for anodes. However, SiO and CNT cause active lithium loss due to lithium silicate formation from SiO and solid electrolyte interphase (SEI) formation on the surfaces of SiO and CNT [3]. Herein, the SiO-CNT electrodes were prepared via the simple dispersion-filtration method [3], prelithiated using three types of electrolytes and Li foils, and the electrochemical performance was studied by making half cells with Li foil counter electrodes.

The SiO-CNT electrode without prelithiation had a good reproducibility with 1st delithiation capacity as high as 1600–1700 mA h g_{SiO}⁻¹ (Fig. 1a). However, they showed the initial irreversible capacity as large as ~1200 mA h g_{SiO}⁻¹, causing the depletion of active Li in case of full cells [4]. Whereas the prelithiated electrodes showed much smaller irreversible capacity, meaning that the consumption of active Li had been completed during the prelithiation process (Fig. 1b,c). 1 M LiPF₆ in EC/DEC resulted in better reproducibility (Fig. 1b) compared to 3.47 M LiFSI in DME (Fig. 1c) possibly because the latter had higher viscosity that resulted in insufficient wetting of the electrode with the electrolyte. CNTs were thin in the electrode without prelithiation (Fig. 1d) while got thicker after prelithiation (Fig. 1e,f) because of the SEI covering the CNT surface. Once the surfaces of SiO particles and CNTs were covered with SEI, then the irreversible capacity can be reduced in the half cells (Fig. 1b,c). But the too thick SEI found in the electrode prelithiated using 3.47 M LiFSI (Fig. 1f) could inhibit the Li⁺ diffusion, causing the increased overvoltage and poor reproducibility of the electrode (Fig. 1c). Various combinations of electrolytes for prelithiation and cell fabrication will be discussed toward rational design of the full cells using the SiO-CNT anode and various cathodes.

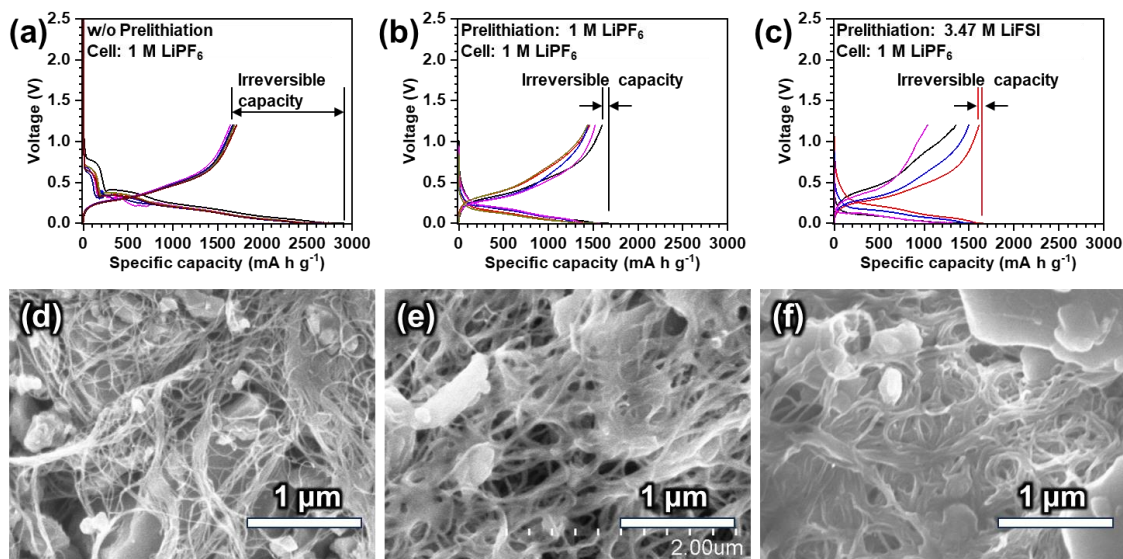


Fig. 1. The 1st lithiation and delithiation curves (a–c) and plan-view SEM images of the SiO-CNT electrodes without prelithiation (a,d) and after prelithiation using electrolytes of 1 M LiPF₆ in EC/DEC (b,e) and 3.47 M LiFSI in DME (c,f). Experiments were conducted 4–5 times for each condition in (a–c).

References

[1] K. Kaneko, et al., *Carbon*, **2020**, *167*, 596. [2] K. Hori, et al., *Carbon* **2020**, *161*, 612. [3] T. Mae, et al., *Carbon*, **2023**, *209*, 118014. [4] T. Mae, et al., *Carbon*, **2024**, *218*, 118663.

Quantum defects in carbon nanotubes for functionalization and sensing

S. Kruss¹

¹*Ruhr Universität Bochum, Germany*

Single wall carbon nanotubes (SWCNTs) are 1D nanomaterials that fluoresce in the near infrared (NIR, >800nm). They have been assembled non-covalently with biopolymers such as DNA to form highly sensitive molecular sensors. Such sensors change their fluorescence when they interact with analytes. In the past, covalent chemistry was less explored to functionalize SWCNTs as it impairs NIR emission. However, certain covalent modifications in the carbon lattice have emerged that preserve NIR fluorescence and even introduce new redshifted emission peaks. Here, we show that quantum defects are versatile tools to modify SWCNT surface chemistry and tailor molecular sensing. First, we show in single molecule experiments that the number of sp³ quantum defects of fluorescent SWCNTs is in the range of 1-3. Additionally, we demonstrate how both sp³ as well as guanine quantum defects can be used to attach recognition units such as boronic acids as well as aptamers for sensing of molecules. In summary, we show that quantum defects provide the next level of control over SWCNT surface chemistry and sensing [1-3].

References (if desired)

- [1] Metternich et al. JACS 2023
- [2] Chen et al. ACS Nano 2023
- [3] Chen et al. ChemRxiv 2023

Rapid Degradation of Single-Wall Carbon Nanotubes via Sodium Hypochlorite and UV-Light Irradiation

○Minfang Zhang, Mei Yang, Yoko Iizumi, Toshiya Okazaki, Don Futaba

National Institute of Advanced Industrial Science and Technology (AIST) (Japan)

With the growing usage of carbon nanotubes in industry, concerted efforts must be directed toward the efficient and effective handling of waste materials, with a specific focus on water, to ensure sustainable and responsible practices in the rapidly advancing field of nanotechnology. In this area, carbon nanotubes (CNTs) present a unique challenge for safe disposal due to their inherent structural stability. In this study, we report a novel method for the accelerated degradation of single-wall carbon nanotubes (SWNTs) into carbon dioxide at room temperature without the use of environmentally or toxic materials [1]. This approach leverages the combination of sodium hypochlorite (NaClO) and UV-light irradiation (UV/NaClO), resulting in a remarkable reduction in degradation time from over a week to 1-2 hours. Structural and chemical analyses revealed that, upon UV light irradiation, the NaClO induced radical oxygen species that rapidly reacted with CNTs in a multi-step oxidation (Figure 1). The reaction involved the generation of epoxy and ether groups on SWNTs, leading to the formation of carboxylic groups and the introduction of defects. Carboxylic and/or ether groups underwent direct transformation into carbon dioxide or intermediate products like ethylene glycols, providing crucial insights into the degradation pathway. Beyond its scientific contributions, this study introduces a practical and cost-effective approach to address challenges in CNT wastewater treatment, offering solutions for safe handling, disposal, and risk management in the rapidly expanding CNT industry.

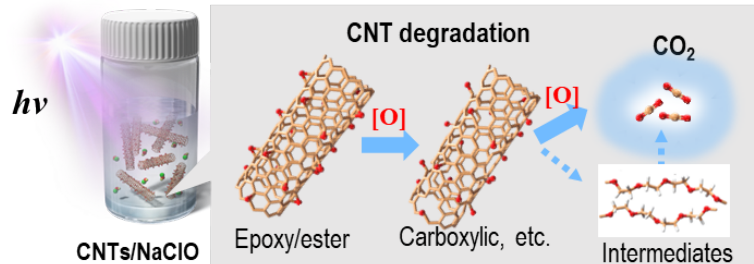


Figure 1: Scheme for the process of CNTs degradation by oxygen radicals $[O]$.

References

- [1] M. Zhang, et al. *Sci Rep* **9**, 1284 (2019).
- [2] M. Yang, M. Zhang, et al. *Carbon* **208**, 238–246 (2023).

Recent Advances in 2D Nanomaterials-Based Triboelectric Nanogenerators: Structure, Properties, Performance, and Device Applications

Prasanjit K. Dey¹

¹*Department of Metallurgical Engineering and Materials Science, Indian Institute of Technology Bombay (India)*

Abstract text: In recent developments, two-dimensional (2D) nanomaterials have become increasingly prominent in triboelectric nanogenerators (TENGs) construction. TENGs, known for their high-power output, versatility in material choice, and cost-effective manufacturing, are influenced by various factors like material selection, surface enhancement techniques, and dielectric properties. The present paper discusses on the state-of-the-art advancements of 2D nanomaterials-based TENGs concerning their structure type, properties, and performance for various device applications. It highlights distinctive features of layered nanomaterials that can boost the performance and efficiency of TENGs. The paper also covers a range of device applications, from energy harvesting to wearable electronics and sensing technologies. Finally, it looks at emerging trends and addresses potential challenges in the field, offering insights into future developments and applications of 2D nanomaterial-based TENGs in nanotechnology.

Reconfigurable Chiro-optical Response in Twist Stacks of Aligned Carbon Nanotubes and Phase Change Material Heterostructure

Jichao Fan¹, Minhan Lou¹, Ruiyang Chen¹, Nina Hong², and Weilu Gao^{1,*}

¹Department of Electrical and Computer Engineering, The University of Utah, Salt Lake City, UT, USA,

²J.A. Woollam Co., Lincoln, NE, USA.

*weilu.gao@utah.edu

Twist stacks of aligned carbon nanotubes (CNTs) have been emerging as a new chiral matter platform [1], which not only possesses strong chiro-optical responses from quantum-confinement-induced properties but also can be manufactured using low-cost, scalable self-assembly processes. Although their chiro-optical responses, such as circular dichroism (CD), can be engineered by adjusting CNT film thickness, rotation angles, and band structures, these responses cannot be dynamically changed after fabrication. Here, we experimentally demonstrated a heterostructure consisting of twist stacks of aligned CNTs, thin films of Ge₂Se₂Te₅ (GST) phase change material, and other oxide thin films, as illustrated in Fig. 1a. GST material features ultrafast and non-volatile phase transition between amorphous and crystalline states under thermal or electrical stimulus, and huge change of refractive indices on the order of unity. Hence, under the GST phase transition, the CD response of the heterostructure can be reconfigured and programmed. The incorporation of other oxide layers aims to enhance the tunability range of CD response through photonic-cavity-like effects. To design the heterostructure structural parameters to maximize such tunability, we have developed a deterministic inverse design framework based on the generalized transfer matrix method and the backpropagation algorithm. The simulations and experimental results of optimized heterostructures show excellent agreement; see Fig. 1b.

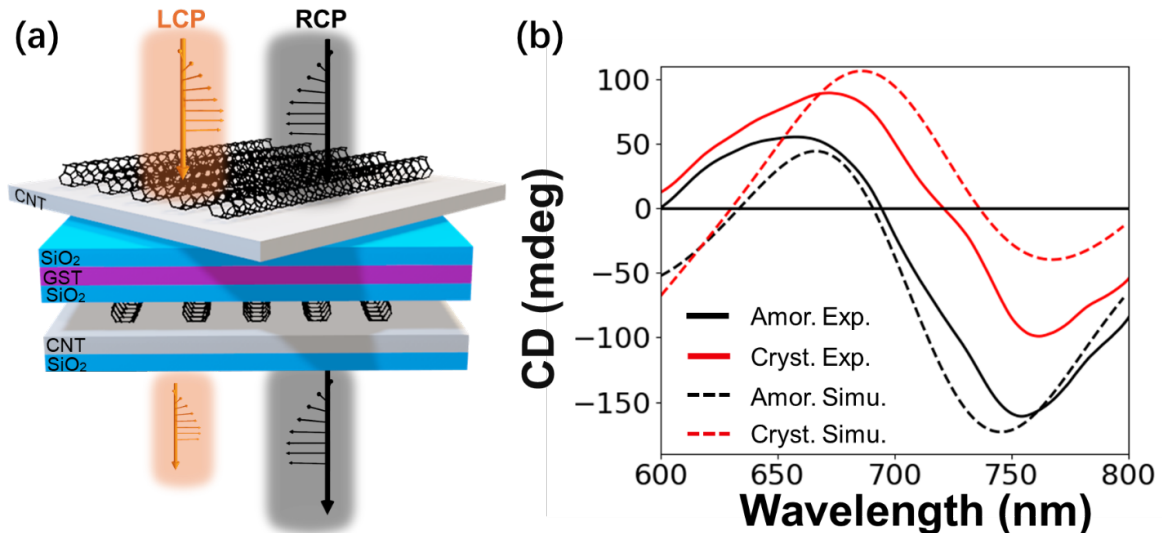


Figure 1: (a) Schematic of wafer-scale twisted stacks of CNT-GST heterostructures for reconfigurable CD. (b) The experimental and simulation CD spectra.

References

[1] Doumani, J., *et al.*, Nat. Commun. **14**, 7380 (2023).

RECONFIGURABLE NONLINEAR LOSSES OF NANOMATERIAL COVERED WAVEGUIDES

Ayvaz Davletkhanov^{*1}, Aram Mkrtchyan¹, Alexey Bunkov¹, Dmitry Chermoshentsev¹, Mikhail Shashkov², Daniil Ilatovskii¹, Dmitry Krasnikov¹, Albert Nasibulin¹, Yuriy Gladush¹

^{*}Present affiliation: Institute of Quantum Materials and Technologies, Karlsruhe Institute of Technology (Germany)

¹Skolkovo Institute of Science and Technology (Russia), ²Boriskov Institute of Catalysis SB RAS (Russia),

Devices for controlling propagating light are a necessity in all optical systems, spanning from optical communications to all-optical computing systems. In systems where light travels in waveguides, one effective method for light control involves covering the waveguide with nanomaterial. The idea of nanomaterial covered waveguides has already led to many practical demonstrations from saturable absorbers and modulators to optical sensors [1, 2]. Further development of this approach implies the creation of reconfigurable devices granting more freedom for light manipulation. In the present study, we show that the nonlinear response of the nanomaterial covered waveguide, exemplified by the case of a polished optical fiber covered with single-walled carbon nanotube film, can be reversed to act as an optical limiter, which means increased losses at higher intensities [3]. This behavior is rather unexpected and uncommon, as the carbon nanotube film is well-known as a saturable absorber material, implying reduced losses at higher intensities. Moreover, the device can exhibit a non-monotonic dependence of losses on intensity, which is adjustable by varying the film thickness. By utilizing electrochemical gating of the nanotube film, we demonstrate the applicability of the observed effect by fabricating the device whose nonlinear optical response can be controllably switched between saturable absorbing and optical limiting. The findings are supported by an analytical approach extending the phenomenon to planar waveguides and revealing the conditions for its observation. It should be emphasized that the effect under consideration is a general phenomenon that can be observed in various waveguide types and covering materials, once the requirements on material thickness and refractive index are met. These introduce possibilities for engineering the complex nonmonotonic nonlinear optical response of nanomaterial covered waveguides, which, for example, could be implemented in all-optical computing and neuromorphic integrated photonic systems. In addition, our study highlights the importance of optimization of the parameters of saturable absorbers on a waveguide and presents a theoretical framework for it.

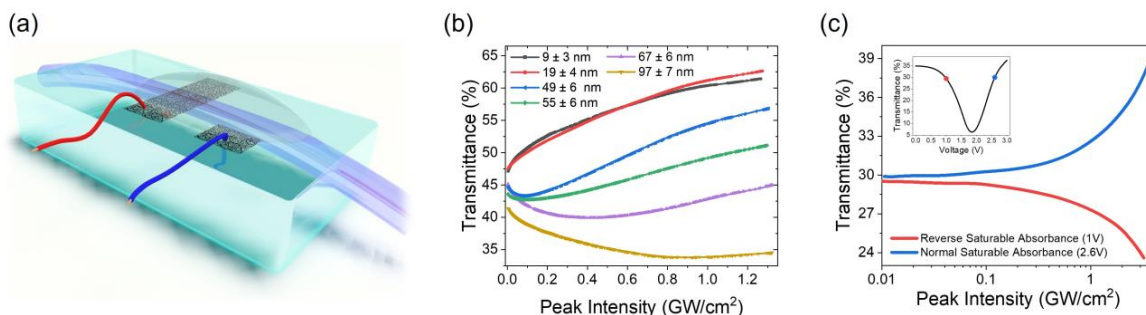


Figure caption: (a) Graphical illustrations of the polished fiber with carbon nanotube film gated with ionic liquid, (b) nonlinear transmittance curves for different film thicknesses and (c) gate voltage.

References

- [1] Zhipei Sun *et al.*, *Nat. Photonics* **10**, 227–238 (2016).
- [2] Yong-Won Song, *Opt. Lett.* **32**, 148–150 (2007).
- [3] Ayvaz Davletkhanov *et al.*, *Nanophotonics* **12**, 4229–4238 (2023).

Remote-contact catalysis for high-purity semiconducting carbon nanotube array

Jiangtao Wang^{1,‡}, Xudong Zheng^{1,‡}, Gregory Pitner², Xiang Ji¹, Tianyi Zhang¹, Aijia Yao¹, Jiadi Zhu¹, Tomás Palacios¹, Lain-Jong Li³, Han Wang², Jing Kong^{1,*}

¹ Department of Electrical Engineering and Computer Science, Massachusetts Institute of Technology, Cambridge, Massachusetts, USA, ² Taiwan Semiconductor Manufacturing Company, Corporate Research, San Jose, California, USA, ³ Taiwan Semiconductor Manufacturing Company, Corporate Research, Hsinchu, Taiwan

Electrostatic catalysis has been an exciting development in chemical synthesis (beyond enzymes catalysis) in recent years, boosting reaction rates and selectively producing certain reaction products. Most of the studies to date have been focused on using external electric field (EEF) to rearrange the charge distribution in small molecule reactions such as Diels-Alder addition, carbene reaction, etc. However, in order for these EEFs to be effective, a field on the order of 1 V/nm (10 MV/cm) is required, and the direction of the EEF has to be aligned with the reaction axis. Such a large and oriented EEF will be challenging for large-scale implementation, or materials growth with multiple reaction axis or steps. Here, we demonstrate that the energy band at the tip of an individual single-walled carbon nanotube (SWCNT) can be spontaneously shifted in a high-permittivity growth environment, with its other end in contact with a low-work function electrode (e.g., hafnium carbide or titanium carbide). By adjusting the Fermi level at a point where there is a substantial disparity in the density of states (DOS) between semiconducting (s-) and metallic (m-) SWCNTs, we achieve effective electrostatic catalysis for s-SWCNT growth. This approach enables the production of high-purity (99.92%) s-SWCNT horizontal arrays with narrow diameter distribution (0.95 ± 0.04 nm), aided by weak EEF perturbation (20 V/mm). These findings highlight the potential of electrostatic catalysis in materials growth, especially for s-SWCNTs, and pave the way for the development of advanced SWCNT-based electronics for future computing.

RESONANCE FLUORESCENCE ANISOTROPY OF A DIPOLE EMITTER NEAR AN ULTRATHIN ALIGNED CARBON NANOTUBE FILM

M. D. Pugh, F. I. Seikh, and I. V. Bondarev*

Department of Mathematics & Physics, North Carolina Central University, Durham, NC 27707, USA

*Email: ibondarev@ncsu.edu

We use the medium-assisted Quantum Electrodynamics (QED) approach to study spontaneous emission (SE) and resonance photoluminescence (PL) for a quantum two-level dipole emitter (DE) near an ultrathin closely packed periodically aligned single-wall carbon nanotube (SWCN) film of variable thickness. Periodically aligned SWCN film systems present an example of flexible metasurfaces with highly tunable optical properties [1-5] that are now available experimentally [5-8]. SE and PL intensity profiles are derived analytically and computed numerically as functions of DE excitation frequency and parameters of the film such as SWCN composition and thickness, to show that the SWCN in-plane periodic alignment provides an additional measure for the dipolar SE and PL rate control of the DE located nearby. The SE and PL rates are shown to be strongly enhanced and highly anisotropic relative to the SWCN alignment direction (Fig.1), breaking the commonly believed viewpoint of their uncontrollably random directionality. The model system we study mimics a single-atom detector or a single-photon source device. Knowledge of the features we predict is advantageous for the new application development with SWCN metasurfaces for solid-state single-photon source and single-atom detector engineering.

Work supported by the U.S. Army Research Office under award No. W911NF2310206 (I.V.B.)

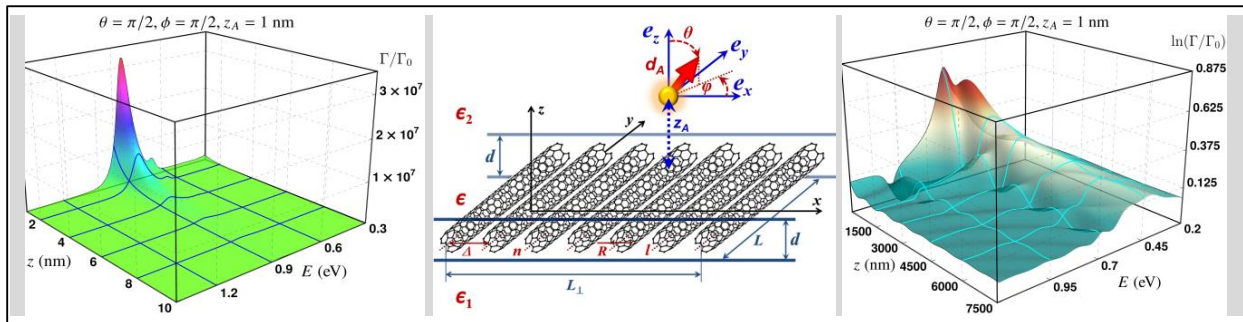


Fig.1: Short-range SE (left) and long-range PL (right) rates relative to vacuum computed for a DE placed 1 nm above 10 nm-thick weakly inhomogeneous SWCN film (sketch in the middle) with the dielectric response derived and reported in Ref.[1]. Shown are the (strongest) rates of emission in the direction perpendicular to the plane of the film.

References

- [1] I. V. Bondarev and C. M. Adhikari, Collective excitations and optical response of ultrathin carbon-nanotube films, *Phys. Rev. Appl.* **15**, 034001 (2021).
- [2] P. Rodriguez-Lopez, D.-N. Le, I. V. Bondarev, M. Antezza, and L. M. Woods, Giant anisotropy and Casimir phenomena: the case of carbon nanotube metasurfaces, *Phys. Rev. B* (accepted, arXiv2311.05001).
- [3] I. V. Bondarev, M. D. Pugh, P. Rodriguez-Lopez, L. M. Woods, and M. Antezza, Confinement-induced nonlocality and Casimir Force in transdimensional systems, *Phys. Chem. Chem. Phys.* **25**, 29257 (2023).
- [4] C. M. Adhikari and I. V. Bondarev, Controlled exciton-plasmon coupling in a mixture of ultrathin periodically aligned single-wall carbon nanotube arrays, *J. Appl. Phys.* **129**, 015301 (2021).
- [5] P.-H. Ho, D. B. Farmer, G. S. Tulevski, S.-J. Han, D. M. Bishop, L. M. Gignac, J. Bucchignano, P. Avouris, and A. L. Falk, Intrinsically ultra-strong plasmon-exciton interactions in crystallized films of carbon nanotubes, *Proc. Natl. Acad. Sci. USA* **115**, 12662 (2018).
- [6] S. Zhu, W. Li, S. Yu, N. Komatsu, A. Baydin, F. Wang, F. Sun, C. Wang, W. Chen, S. C. Tan, H. Liang, Y. Yomogida, K. Yanagi, J. Kono, and Q. J. Wang, Extreme polarization anisotropy in resonant third-harmonic generation from aligned carbon nanotube films, *Adv. Mater.* **35**, 2304082 (2023).
- [7] J. A. Roberts, S.-J. Yu, P.-H. Ho, S. Schoeche, A. L. Falk, and J. A. Fan, Tunable hyperbolic metamaterials based on self-assembled carbon nanotubes, *Nano Lett.* **19**, 3131 (2019).
- [8] X. He, W. Gao, L. Xie, B. Li, S. Lei, J. M. Robinson, E. H. Házor, S. K. Doorn, W. Wang, R. Vajtai, P. M. Ajayan, W. W. Adams, R. H. Hauge, and J. Kono, Wafer-scale monodomain films of spontaneously aligned single-walled carbon nanotubes, *Nat. Nanotechnol.* **11**, 633 (2016).

Single-Walled Carbon Nanotube Film as an Efficient Conductive Network for Si-based Anodes

Ziying He¹, Fei Wei^{1*}

¹Department of Chemical Engineering and Technology, Tsinghua University, Beijing 100084 (China)

Silicon-based anodes are considered ideal candidate materials for next-generation lithium-ion batteries (LIBs) due to their high capacity. However, the low conductivity and large volume variations during cycling inevitably result in inferior cyclic stability. Herein, a dry method without binders is designed to fabricate Si-based electrodes with single-walled carbon nanotubes (SWCNTs) network and to explore the different mechanisms between SWCNT and multiwalled carbon nanotubes (MWCNTs) as conductive network. As expected, higher initial discharge capacity (1785 mAh·g⁻¹), higher initial coulombic efficiency (ICE, 81.52%) and outstanding cyclic stability are obtained from the SiO_x@C|SWCNT anodes. Furthermore, its lithium-ion diffusion coefficient (D_{Li⁺}) is 3-4 orders of magnitude higher than that of SiO_x@C|MWCNT. The underlying mechanism is clarified by in situ Raman spectroscopy and theoretical analysis. It is found that the SWCNTs can maintain good contact with SiO_x@C even under tensile stresses up to 6.2 GPa, while the MWCNTs lose electrical contact due to alternating compressive stress up to 8.9 GPa and tensile stress up to 2.5 GPa during long-term cycling. Under such very large stresses, the more flexible SWCNTs and their stronger van der Waals forces ensure that SiO_x@C still has good contact with SWCNTs.

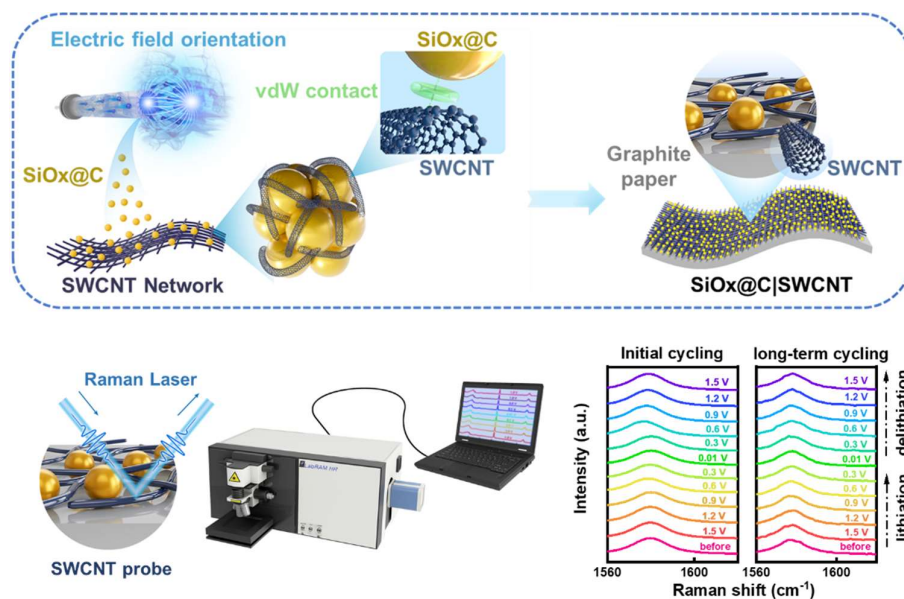


Fig. 1 The fabrication and characterization of the SiO_x@C|SWCNT anode

References (if desired)

- [1] Ziying He, F. Wei, et al. Single-Walled Carbon Nanotube Film as an Efficient Conductive Network for Si-based Anodes, *Adv. Funct. Mater.* 2023, 33, 2300094.
- [2] Qian Liu, Zhang Jin, et al. Building a Bridge for Carbon Nanotubes from Nanoscale Structure to Macroscopic Application, *JACS* 2021, 143, 18805.
- [3] Park Sang-Hoon, Nicolosi, Valeria, et al. High areal capacity battery electrodes enabled by segregated nanotube networks, *Nat. Energy* 2019, 4, 560.

Role of Spin-orbit coupling on Chiral-induced Spin Selectivity in Carbon Nanotube Networks

Seyedamin Firouzeh¹, Sandipan Pramanik¹

¹Department of Electrical and Computer Engineering, University of Alberta, Alberta, T6G 1H9 (Canada)

Chiral-induced spin selectivity (CISS) is a fascinating phenomenon in which chiral molecules act as spin filters during charge transfer [1]. In this effect, depending on the handedness (left- or right-handed) of the molecules, only one type of spin (either up or down) preferentially transfers through the system, as shown in Figure 1(a). This effect holds promising potential for spintronics because it may allow non-magnetic, molecular-scale spin filters for further miniaturization of spintronic devices. The physical origin of CISS is often a subject of debate, and here, we shed light on this topic by using chiral peptide (Fmoc-FF L/D; Fmoc: N-Fluorenylmethoxycarbonyl; FF: diphenylalanine) functionalized carbon nanotubes (CNTs) as the chiral medium.

In CISS experiments, commonly chiral organic molecules such as DNA, amino acids etc. are used as transmission media due to their intrinsic chirality. However, their insulating nature imposes limitations on their practical application in electronic devices. To address this constraint, carbon nanotubes (CNTs) have emerged as a focal point. CNTs act as one-dimensional molecular conductors and can be functionalized with a variety of chiral molecules, and molecular chirality can be transferred to the CNTs. The potential for observing the CISS effect in CNTs was investigated both theoretically [2] and experimentally [3-4], typically probing a few CNTs, where significant signals are observed at low temperatures.

Despite advances in this field, the theoretical understanding of CISS remains challenging, although three necessary ingredients have been identified: spin-orbit coupling (SOC) of a chiral medium, structural inversion asymmetry, and time reversal asymmetry. Traditionally, the presence of SOC in a chiral medium has been considered crucial for the manifestation of the CISS effect. However, some recent studies claim that CISS can occur in chiral media even without SOC [5].

We demonstrated the impact of SOC of a chiral medium on the CISS effect by employing a chiral peptide functionalized CNT network connected between Au and a Ni spin detector, as shown in Figure 1(b). In this medium, charge transport occurs through the CNTs due to the insulating nature of the attached chiral molecules, and the carriers are subject to the SOC of the CNTs. The SOC of CNTs, however, can be changed by varying CNT diameter, as CNT SOC is inversely related to the diameter of the CNTs [6]. We systematically altered the nanotube diameter, and in all cases observed tell-tale signs of the CISS effect, as shown in Figure 1(c-d). Our findings illustrate that an increase in the CNT diameter (and a concomitant weakening of the SOC effect), diminishes the CISS signal, as shown in Figure 1(e). This correlation between SOC strength and the CISS signal shows that the chiral medium's SOC indeed plays a critical role in CISS.

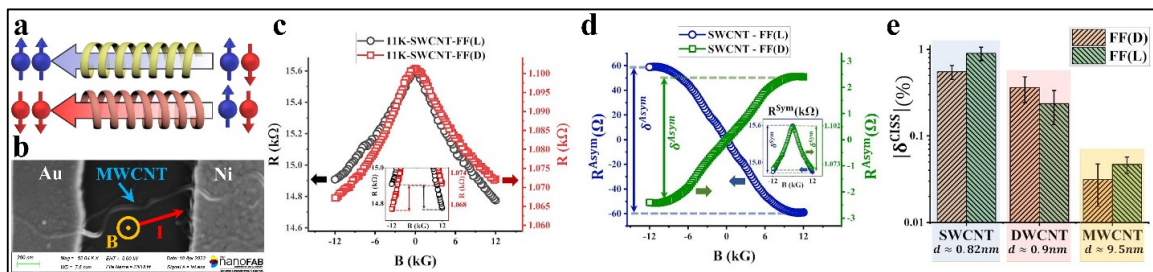


Figure 1: (a) Schematic of CISS (b) Scanning Electron Microscopic (SEM) image of the device (c) Chirality-dependent magnetoresistance (MR) effects (d) Asymmetric and symmetric components of the MR responses (e) CISS signal as a function of tube diameter.

References

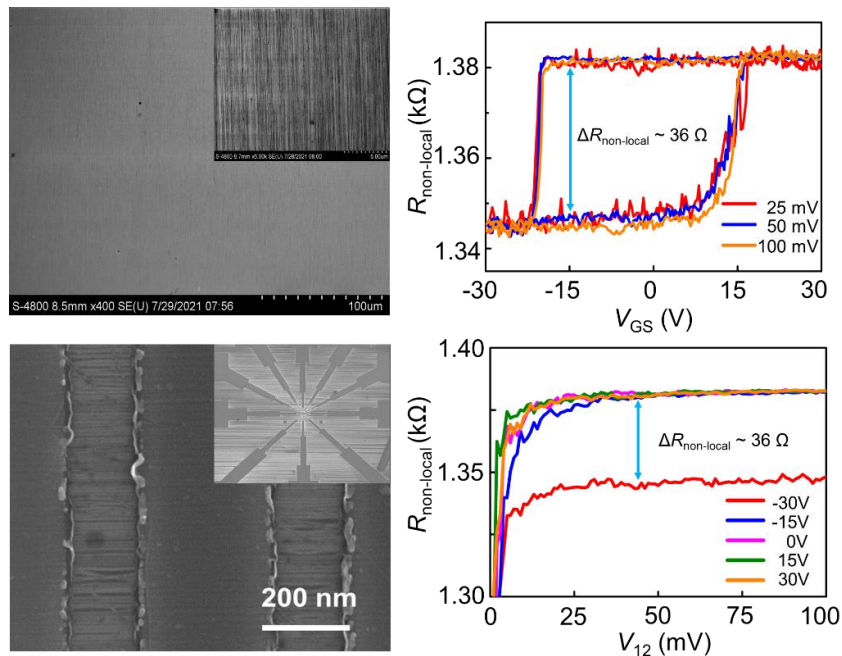
- [1] F Evers *et al.*, *Adv. Mater.* **34**(13), 2106629 (2022).
- [2] G.S. Diniz *et al.*, *Phys. Rev. Lett.* **108**(12), 126601 (2012).
- [3] Md.W. Rahman *et al.*, *ACS Nano* **14**(3), 3389–3396 (2020).
- [4] Md.W. Rahman *et al.*, *ACS Nano* **15**(12), 20056–20066 (2021).
- [5] J. Xiao *et al.*, *arXiv e-prints*, 2201.03623 (2022)
- [6] Perltitz, Y *et al.*, *Phys. Rep.* **B 98**(19), 195405 (2018).

Room-temperature spin field effect transistor based on carbon nanotube array

Zhisheng Peng¹, Yi Xie¹, Liu Qian¹, Jin Zhang^{1,2}

¹ Schools of Materials Science and Engineering, Peking University, (China), ² Center for Nanochemistry, Beijing National Laboratory for Molecular Sciences, State Key Laboratory for Structural Chemistry of Unstable and Stable Species, College of Chemistry and Molecular Engineering, Peking University, (China)

In silicon-based very large-scale integrated circuits (IC), the core component is a complementary metal oxide semiconductor field effect transistor.[1] As the silicon-based IC enters sub-5-nanometer technology nodes, developing core devices in the post-Moore era has become an important issue attracting widespread attention. Constructing spin transistors utilizing the spin properties of electrons, especially gate-tunable spin field-effect transistors, represents a key challenge and development direction for a new type of integrated circuit based on spintronics.[2,3] Owing to weak spin-orbit coupling and hyperfine interactions at room temperature, single-walled carbon nanotubes (SWNTs) can exhibit spin diffusion lengths on the order of micrometers.[4,5] This makes SWNT a potential candidate for its applications in spintronics, especially horizontally aligned SWNT array. A four-terminal spin FET based on high-density horizontally aligned SWNT array was designed and constructed. The spin signal of this four-terminal FET can be modulated by gate voltages and external magnetic field. And the resistance of SWNT array exhibits negative magnetoresistance with external magnetic field. These are manifested that the spin FET based on SWNT array has the advantages of in-memory computing, which may open up a new path for carbon-based spintronics.



SEM images and transfer characteristics of a typical spin FET based on high-density horizontally aligned SWNT array.

References

- [1] M. M. Waldrop, *Nature* **530**, 144-147 (2016).
- [2] P Barla et al., *Journal of Computational Electronics* **20**, 805-837 (2021).
- [3] Yang H et al., *Nature*, **606**, 663-673 (2022).
- [4] Avsar A et al., *Reviews of Modern Physics* **92**, 021003 (2020).
- [5] L. E. Hueso et al., *Nature* **445**, 410-413 (2007).

Selective Formation of Analyte-Matrix Cocrystals on the Surface of Carbon Nanomaterials for MALDI Mass Spectrometry of Neuropeptides

Cheongha Lee¹, Sanghwan Park¹, and Chang Young Lee^{1,2}

¹*School of Energy and Chemical Engineering, ²Graduate School of Carbon Neutrality, Ulsan National Institute of Science and Technology (Republic of Korea)*

Matrix-assisted laser desorption/ionization mass spectrometry (MALDI-MS) is a powerful tool for analyzing peptides and proteins due to its sensitivity, accuracy, and high salt tolerance. However, biological samples are often limited in quantity, being as low as femtomole to attomole levels. Therefore, preconcentration of analytes is required to obtain sufficient mass intensity. Herein, we demonstrate a novel approach for preconcentration by selectively forming matrix-analyte cocrystals on the surface of carbon nanomaterials (graphene or carbon nanotubes). A CHCA (α -cyano-4-hydroxycinnamic acid) matrix solution containing analytes forms cocrystals uniformly and selectively on the surface of carbon nanomaterials. Unlike the random crystal formation observed on bare silicon or glass substrates, patterning with carbon nanomaterials enables precise and reproducible crystallization at targeted locations. This is evidenced by fluorescence microscope images, which reveal uniform and controlled cocrystal formation specifically in the carbon nanomaterial regions. This targeted enrichment is validated by the significantly enhanced MALDI-MS signals from these areas, demonstrating the effectiveness of our approach in concentrating analytes for MALDI-MS analysis. Such precision makes our method particularly advantageous for the analysis of cell-to-cell signaling molecules such as neuropeptides released from single cells.

Self-assembling Semiconducting Conjugated Polymers for SWCNT Separation

B. McLean^{1,*}, Luke C. B. Salter², Molly M. Stevens^{2,3}, I. Yarovsky¹

¹RMIT University, Melbourne (Australia), ²Imperial College London, London (United Kingdom), ³University of Oxford, Oxford, (United Kingdom)

*email: ben.mclean2@rmit.edu.au

Conjugated semiconducting polymers have proven effective in sorting SWCNTs suspensions [1]. Semiconducting SWCNTs can be selectively extracted from the solvent, with their chirality and diameter correlated with polymer shape, size, and structure. The semiconducting polymers act by wrapping around the SWCNT. Additionally, SWCNTs have been observed to enhance semiconducting polymer films in light-emitting field-effect transistors (LEFETs) [2]. Recent experimental strategies have demonstrated attachment of functional groups to conjugated polymers, affording semiconducting graft copolymers that retain tunable optoelectronic and mechanical properties [3], which may offer additional functionality when combined with SWCNTs. These novel systems, however, are complex and their assembly process and molecular origins of the properties require further experimental and theoretical investigation to enable the rational design of semiconducting copolymers for SWCNT application. This work aims to model the self-assembly mechanisms of poly(9,9-dioctylfluorene-alt-benzothiadiazole) (F8BT) modified with polyethylene glycol (PEG) (Fig. 1a) using fully atomistic molecular dynamics (MD) simulations. F8BT polymers modified with PEG explicitly solvated in cubic periodic cells in pure aqueous and mixed THF-water solvents of varying concentration. Small-angle neutron scattering (SANS), atomic force microscopy (AFM), and cryogenic transmission electron microscopy (cryo-TEM) data reveals the self-assembly of dendritic, fractal-like networks depending on the THF:H₂O solvent ratio. This work explores first the solvation structure of these semiconducting copolymers, guiding their application in optoelectronic devices and provides understanding of how they may be applied to the sorting of SWCNT suspensions.

References

- [1] F. Yang *et al.*, *Chem. Rev.* **120**, 2693-2758 (2020).
- [2] M. Gwinner *et al.*, *ACS Nano* **6**, 539-548 (2012).

SEM imaging of insulating specimen through a transparent conducting veil of carbon nanotube

Xinyu Gao¹, Guo Chen¹, He Ma², Yuchen Ju¹, Ke Zhang¹, Lin Cong¹, Wen Ning¹, Zi Yuan¹, Zebin Liu¹, Lina Zhang¹, Peng Liu¹, Shoushan Fan¹, and Kaili Jiang^{1,3,4}

¹State Key Laboratory of Low-Dimensional Quantum Physics, Department of Physics and Tsinghua-Foxconn Nanotechnology Research Center, Tsinghua University, Beijing 100084 (China), ²College of Applied Sciences, Beijing University of Technology, Beijing 100124 (China), ³Frontier Science Center for Quantum Information, Beijing 100084 (China), ⁴Beijing Advanced Innovation Center for Future Chips, Beijing 100084 (China).

Abstract text.

Observing the morphology of insulating specimen in scanning electron microscope (SEM) is of great significance for the nanoscale semiconductor devices and biological tissues. However, the charging effect will cause image distortion and abnormal contrast when observing insulating specimen in SEM. A typical solution to this problem is using metal coating or water-removable conductive coating. Unfortunately, in both cases the surface of the specimen is covered by a thin layer of conductive material which hides the real surface morphology and is very difficult to be completely removed after imaging. Here we show a convenient, residue-free, and versatile method to observe real surface morphology of insulating specimen without charging effect in SEM with the help of a nanometer-thick film of super-aligned carbon nanotube (SACNT). This thin layer of SACNT film, like metal, can conduct the surface charge on insulating specimen through the sample stage to the ground, thus eliminating the charging effect. SACNT film can also be used as the conductive tape to carry and immobilize insulating powder or particles during SEM imaging. Different from the metal coating, SACNT film is transparent, so that the real microstructure of the insulating specimen surface can be observed. In addition, SACNT film can be easily attached to and peeled off from the surface of specimen without any residue. This convenient, residue-free, and versatile method can open up new possibilities in non-destructive SEM imaging of a wide variety of insulating materials, semiconductor devices, and biological tissues.

SIMULATION OF THE SULFUR EFFECT ON THE CATALYTIC GROWTH OF SWCNTS BY REACTIVE MOLECULAR DYNAMICS

Morinobu Endo,^{1,2} Rodolfo Cruz-Silva,³ Aaron Morelos-Gomez,^{1,2} Juan Fajardo-Diaz,^{1,2} Jono Ryota,⁴ Syogo Tejima⁴

¹ Sustainable and Green Carbons Institute, Faculty of Engineering, and ² Research Initiative for Supra-Materials, Interdisciplinary Cluster for Cutting Edge Research, Shinshu, University, 4-17-1 Wakasato, Nagano-city 380-8553, Japan. ³ Center for Applied Research in Chemistry, Plastic transformation department, Enrique Reyna H. 140, San José de los Cerritos, 25294 Saltillo, Coah., Mexico. ⁴ Research Organization for Information Science and Technology, Sumitomo Hamamatsucho, Building, 1-18-16, Hamamatsucho, Minato-ku, Tokyo, 105-0013, Japan.

Catalysts for the growth of single and multiwalled carbon nanotubes have been studied extensively in the last 40 years yet the mechanism of growth is not completely understood.[1,2] In this work, we used reactive molecular dynamics as a tool to investigate the carbon nanotubes mechanism of growth at the atomic and molecular level in an attempt to shed some light on the process. Among the different computational methodologies, reactive molecular dynamics using the reaxff method has become popular because it combines computational speed and chemical accuracy. Here, we used this method to study the dynamics of small clusters of iron and sulphur with different chemical compositions at high temperature, conditions where they are known to behave as catalyst for the growth of single walled carbon nanotubes. We were able to reproduce the reduction of the melting point of iron and iron sulfide nanoparticles, which are not well described by current Fe-S bulk phase diagrams. We found that the reax force fields currently available are not accurate enough to reproduce the basic reactions and equilibrate the typical materials involved in the carbon nanotube chemical vapor deposition. We believe it is necessary to address the limitations of reactive molecular dynamics for simulations of nanotube growth and develop more accurate force fields or even new methods for this particular reaction. These results can contribute to further development of new force fields or new computational methods to study the SWCNT growth simulation, which can be useful for large-scale nanotube production.

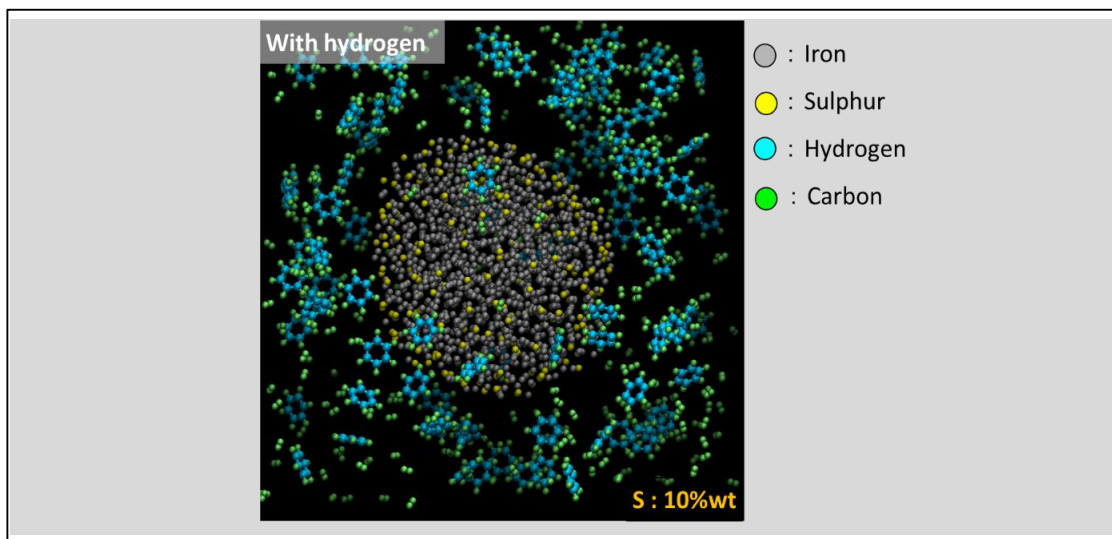


Figure S9. Cells showing the simulation of benzene decomposition over an iron sulfide nanoparticle in of hydrogen.

References

- [1] Oberlin, A.; Endo, M.; Koyama, T. Filamentous growth of carbon through benzene decomposition. *Journal of Crystal Growth* 1976, 32 (3), 335-349.
- [2] Endo, M. Grow carbon fibers in the vapor phase. *Chemtech* 1988, 18 (9), 568-576.

Single-chirality nanotube synthesis by guided evolutionary selection

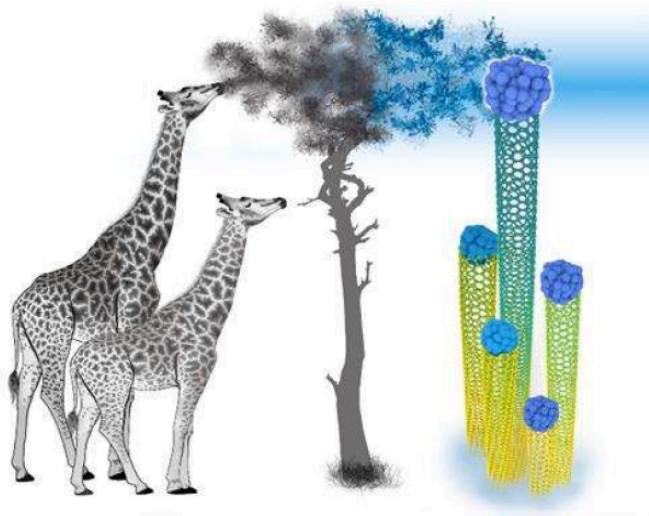
Ksenia V. Bets, Ting Cheng, Boris I. Yakobson

Rice University (USA)

Over the decades since the discovery of CNT, they became a quintessential nanomaterial. Possessing a relatively simple, cylindrical structure characterized by the helical symmetry type colloquially called “chirality” [1], they became a prime example of structure-property correlation typical for nanomaterials. The entire range of properties - mechanical, electronic, optical, etc. - is fully defined by the chiral angle $0 < \chi < 30^\circ$ or a pair of chiral indexes (n, m) . Any practical use of CNTs calls for chirality-pure samples, demanding an efficient process for chirality-selective growth. To date, the single chirality and even more so *selected* chirality, growth remains elusive.

Over time, the experimental observation of the controlled distribution of nucleated CNTs based on the catalyst size and type, the long defect-free growth through the kite mechanism, and CNT termination through underfeeding due to varying CNT kinetics advanced our understanding of the underlying processes, suggesting different ways for growth control. In particular, a clear appreciation that the CNT growth speed is an explicit function of its chirality and feedstock concentration allowed us to propose a selective CNT synthesis based on nonlinear feedback built in this function [2]. The suggested technique relies on the localized and moving feeding zone, continuously supplying building units to the CNTs, but only those that are capable of growing fast enough to “keep up,” while allowing all slower “species” to die out, effectively imposing a lower cutoff for the growth speed on the nanotube population. The second part of the approach similarly uses a dissolution process, eliminating all tubes growing faster than the target chirality. This way, careful control over the reaction zone speed would allow the elimination of all undesirable CNTs through the guided evolutionary selection process, achieving targeted chirality synthesis.

Figure 1: Proverbial Lamarck giraffes, and CNTs, illustrating evolution based on selective feeding.



The synthesis of BN nanotubes remains significantly behind its carbon counterparts, with basic principles still under investigation. To lay the foundation, we investigate the immediate precursor - a molecule directly participating in growth - through the exploration of the gas-phase and substrate-induced processes on ammonia borane (AB) that is commonly used as feedstock that precedes the reaction with the BNNT edge [3]. In both cases, the AB molecule undergoes significant de-hydrogenation. The gas phase processes demonstrate significant kinetic barriers that are somewhat lowered by the presence of BH_4^- and NH_4^+ ions to 1.5 eV with HBNH as the immediate precursor. The presence of the catalyst particles, both Ni and B, lowers the barrier to 1.3 eV and leads to the formation of BNH and BN. Our study maps out three typical experimental conditions for the dissociation of AB-precursor, providing insights into the underlying reaction mechanisms of gas-phase precursors, and uncovering crucial details of the BNNT formation.

References

- [1] H. Zhu and B. I. Yakobson, *Perspective: Creating chirality in the nearly-two dimensions*, Nature Materials, doi.org/10.1038/s41563-024-01814-2 (2024).
- [2] B. I. Yakobson and K. V. Bets, *Single-Chirality Nanotube Synthesis by Guided Evolutionary Selection*, Sci. Adv. **8**, eadd4627 (2022).
- [3] T. Cheng, K. V. Bets, and B. I. Yakobson, *Synthesis Landscapes for Ammonia Borane CVD of H-BN and BNNT: Unraveling Reactions and Intermediates from First Principles*, submitted (2024).

SINGLET AND TRIPLET EXCITATIONS IN CHEMICIALLY FUNCTIONAL- IZED SINGLE-WALLED CARBON NANOTUBES

Dinesh Thapa¹ and Svetlana Kilina¹

¹*Department of Chemistry and Biochemistry, North Dakota State University, Fargo ND 58108*

The study of optical properties of functionalized, semiconducting single-walled carbon nanotubes (SWCNTs), has recently garnered significant attention due to potential applications in optoelectronics, telecommunications, and quantum technology. These functionalizations introduce organic color centers on the surface of the nanotubes. As a result, the lowest energy electronic excitation becomes optically active and is localized around these defect sites. Experimental efforts have extensively utilized aryl groups to functionalize SWCNTs at different positions along the tube's surface, thereby creating color centers in the form of sp³ defects within the sp² carbon lattice. In this context, we have used density functional theory to study electronic and optical properties in functionalized (11,0) zigzag SWCNT employing periodic boundary conditions. Our simulations predict red shifted bright emission peaks well below the band edge transition in ortho and para defect configurations compared to pristine nanotube which is in agreement with experimental evidences. Additionally, our simulations reveal a minor singlet-triplet splitting, falling within the range of tens of millielectronvolts. This enables us to quantify the electron-hole exchange interaction's effects, which surpasses that of the electron-electron exchange interaction. Furthermore, our findings elucidate the quantitative aspects of electron-electron exchange interaction in parallel and anti-parallel couplings for the (11,0) zigzag nanotube. These insights can help applications of carbon nanotubes modified with color centers to photonic applications such as single-photon sources operating at room temperature boosting energy transfer from triplet to singlet states through upconversion processes.

Single-walled carbon nanotube growth with high entropy alloy catalysts composed of platinum-group metals

T. Maruyama^{1,2}, S. Matsuoka², Kamal P. Sharma², T. Saida^{1,2}, K. Kusada^{3,4}, H. Kitagawa³

¹Department of Applied Chemistry, Meijo University (Japan), ²Meijo University Nanomaterial Research Center (Japan), ³Division of Chemistry, Graduate School of Science, Kyoto University (Japan), ⁴The Hakubi Center for Advanced Research, Kyoto University (Japan)

High-entropy alloys (HEAs) consist of five or more metals in almost equal proportions [1-3]. Recently, HEA nanoparticles (NPs) have attracted significant attention in several fields because of their unique structures and properties; they exhibit structural durability in harsh environments and sometimes exhibit new catalytic functions. In this study, we investigated the catalytic activity of HEA NPs in the growth of single-walled carbon nanotubes (SWCNTs). Using HEA NPs composed of five platinum-group metals (5PGM), Ru, Rh, Pd, Ir, and Pt, as catalysts, we succeeded in growing SWCNT via chemical vapor deposition (CVD). After CVD growth with C₂H₂ feedstock at 750 °C for 10 min, high-density SWCNTs with lengths of 1 μm or more were grown from 5PGM HEA NPs. Raman spectra showed that the diameters of most SWCNTs grown from 5PGM HEA NPs were in the range of 0.84–1.1 nm, exhibiting the growth of small-diameter SWCNTs. Compared with monometal PGM catalysts (Ru, Pd, Ir, and Pt), the SWCNT yield with the 5PGM HEA NP catalysts was much higher and was compatible even with those with Fe and Co, which are the most common catalysts for obtaining high-yield SWCNTs. Scanning transmission electron microscopy and energy-dispersive X-ray spectroscopy mapping showed that even after SWCNT growth, each element was homogeneously distributed in the 5PGM HEA NPs, confirming their robustness during chemical reactions through SWCNT growth. Our results demonstrate that the 5PGM HEA NPs act as highly active catalysts for obtaining small-diameter SWCNTs.

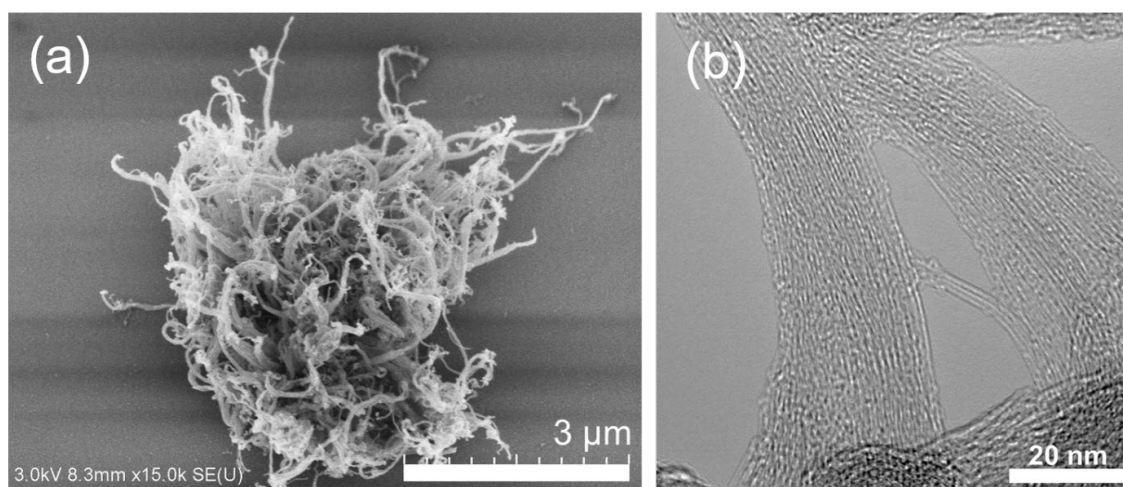


Figure: (a) SEM and (b)TEM images of SWCNTs grown at 750°C from 5PGM HEA NPs.

References

- [1] K. Kusada, D. Wu and H. Kitagawa, *Chem. Eur. J.* **26**, 5105-5130 (2020).
- [2] K. Kusada, H. Kitagawa *et al.*, *J. Phys. Chem. C* **125**, 458-463 (2021).
- [3] D. Wu, K. Kusada, H. Kitagawa *et al.*, *J. Am. Chem. Soc.* **142**, 13833-13838 (2020).
- [4] D. Wu, K. Kusada, H. Kitagawa *et al.*, *J. Am. Chem. Soc.* **144**, 3365-3369 (2022).

Single-walled Carbon Nanotubes Synthesized by Laser Ablation from Coal

Shaochuang Chen¹, Zeyao Zhang^{1,2,*}, Yan Li^{1,*}

¹Peking University, ²Institute of Carbon-Based Thin Film Electronics, Peking University, Shanxi (China)

zeyaozhang@pku.edu.cn; yanli@pku.edu.cn

Developing methods to synthesize single-walled carbon nanotubes (SWCNTs) in a greener way is of long-term interests. Laser ablation, developed in 1995, is an important method to synthesize SWCNTs. However, different from chemical vapor deposition and arc discharge, it uses solid carbon sources without preference in conductivity. This endows a great flexibility in carbon source selection for laser ablation. Using coal as the carbon source and Co/Ni as the catalyst, we synthesized high-quality SWCNTs (Fig. 1a, 1b). We studied the effects of temperature, pressure, Ar flow rate, and the ratio of Co/Ni on the yield and diameter distribution of SWCNTs. Separations based on diameter and conductivity were realized by aqueous two-phase extraction. Semiconducting SWCNTs sorted by PCz (poly[9-(1-octylonoyl)-9H-carbazole2,7-diyl]) were used to fabricate high-performance field effect transistors (Fig. 1c).

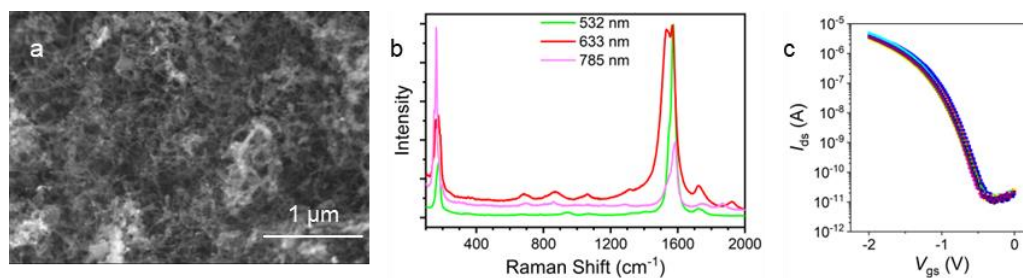


Fig.1 Characterizations of SWCNTs synthesized by LA from coal. (a) SEM image. (b) Raman spectra with different excitation wavelengths. (c) Transfer characteristics of the field effect transistors fabricated by SWCNTs sorted by PCz.

Small-load rGO as partial replacement for the large amount of zinc dust in PU zinc-rich composites applied in heavy-duty anticorrosion coatings

Yun-Xiang Lan, Yu-Ting Tseng, Jui-Ming Yeh*

Department of Chemistry, Center for Nanotechnology at Chung Yuan Christian University, Chung Li, 32023, Taiwan, Republic of China

Abstract

A small load (e.g., 0.5 wt%) of reduced graphene oxide (rGO) was used to replace a large amount (e.g., 25 wt %) of zinc dust (ZD) in solvent-based zinc-rich polyurethane (PU) composite coatings (PCCs) to maintain similar anticorrosion, as well as to promote the adhesion/wear resistance of the corresponding coatings simultaneously.

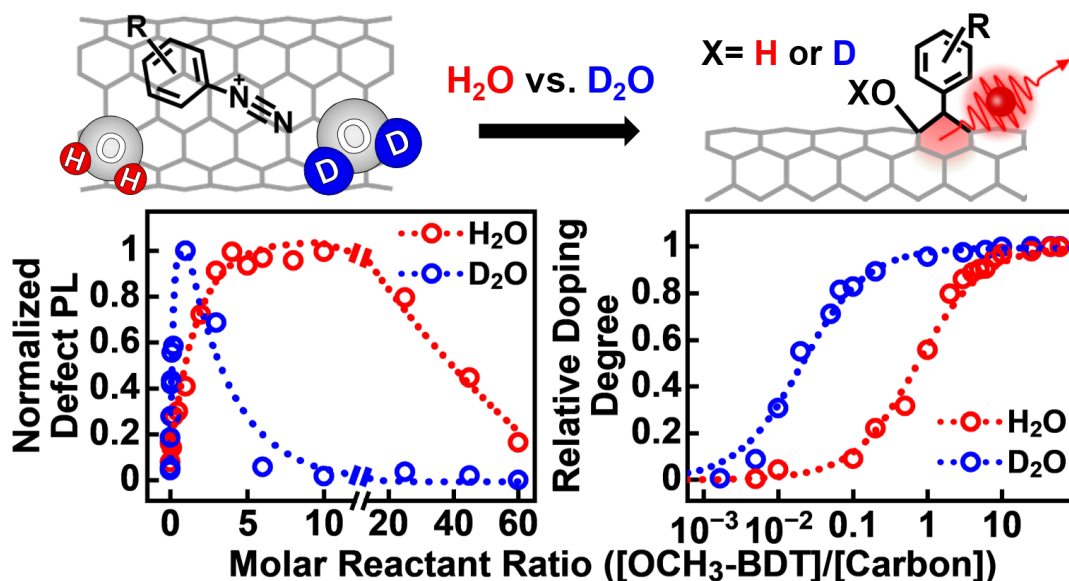
First, the corrosion protection of zinc-rich PCCs containing 20, 40, and 80 wt% of ZDs (denoted as DZ-20, DZ- 40, and DZ-80, respectively) was investigated by performing a series of electrochemical measurements. The corrosion protection of PCCs was found to decrease in the order DZ-80 > DZ-40 > DZ-20. However, wear- resistance and adhesion tests of PCCs had the opposite trend of DZ-80 < DZ-40 < DZ-20 based on the method of ASTM 3359 and ASTM D4060, respectively. Subsequently, the small-load calcined GO at the operational temperatures of 300° C (denoted as rGO-300) was further incorporated into PCCs to partially replace large amounts of ZD and maintain similar anticorrosion performance and enhance the wear resistance and adhesion of the corresponding ECCs. This finding indicated that incorporating a small load of 0.5 wt% of rGO-300 can partially replace 25 wt% of ZD load, respectively, in PCCs. Accelerated salt-spray corrosion assays of scrapped test panels with and without coatings in an aggressive solution medium were used to evaluate corrosion resistance according to ASTM B-117. Results from the salt-spray assays of PCCs were consistent with those from the electrochemical measurements.

Solvent Isotope Effects on the Formation of Fluorescent Quantum Defects in Carbon Nanotubes via Aryl Diazonium Chemistry

Brandon J. Heppe,¹ Nina Dzombic,¹ Joseph M. Keil,² Xue-Long Sun,^{1,2*} Geyou Ao^{1*}

¹Department of Chemical and Biomedical Engineering, Washkewicz College of Engineering, Cleveland State University (USA), ²Department of Chemistry, Center for Gene Regulation in Health and Disease (GRHD), Cleveland State University (USA)

The combination of aryl diazonium and carbon nanotube chemistries has offered rich and versatile tools for creating nanomaterials with tunable optical and electronic properties. The diazonium reaction with single-wall carbon nanotubes (SWCNTs) is known to proceed through radical or carbocation mechanism in aqueous solutions, with deuterated water (D_2O) being the frequently used solvent. Here, we show the significant impact of water solvent isotopes on the aryl diazonium reaction with SWCNTs for creating fluorescent quantum defects using water (H_2O) and D_2O . We found a deduced reaction constant of ~ 18.2 times larger value in D_2O than in H_2O , potentially due to their different chemical properties. We also observed the generation of new defect photoluminescence over a broad concentration range of diazonium reactants in H_2O , as opposed to a narrow concentration window in D_2O under UV excitation. Without UV light, aryl diazonium physically adsorbed to the SWCNT surface, leading to the fluorescence quenching of nanotubes. These findings provide important insights into the aryl diazonium chemistry with carbon nanotubes for creating material platforms in a controllable fashion for optical sensing, imaging, and quantum communication technologies.



STABLE DISPERSIONS OF CARBON NANOMATERIALS IN IONIC AND NON-IONIC LIQUIDS

S. Ruczka¹, R. Jedrysiak¹, S. Boncel¹

¹Silesian University of Technology, NanoCarbon Group (Poland)

Carbon nanomaterials (CNMs) constitute a large collection of nanoparticle-based systems with a various dimensionality, and hence, morphology, and physicochemical properties. Many years of research on the *strictly* pure carbon nanoallotropes have identified a number of factors correlating the chemical structure with the desired physicochemical properties. Those interrelationships enabled not only potential, but, now, realistic applications [1]. However, a recently conducted market research has indicated a low share in the ready-to-use ‘nanoproducts’ based on 1D and 2D CNMs, such as carbon nanotubes (CNTs), nanodiamonds, or graphene [2]. This outcome stems from the fact that, in general, nanoparticles tend to agglomerate due to the intermolecular interactions, i.e., van der Waals forces, π - π stacking, etc., as ‘overexpressed’ at the strongly developed specific surface area. Overall, the main obstacle toward the industrial use of 1D and 2D CNMs is the necessity to use complex dispersing procedures, which generates a significant increase of the production costs. Hence, there is a constant need to produce operationally stable nanodispersions in the final products.

Here, we aim to design, elaborate, and develop protocols toward formation of stable CNM dispersions in ionic and non-ionic liquids – preferentially, by using possibly the smallest amounts of additives, such as surfactants [3]. The obtained nanosystems of an excellent homogeneity measured under optical microscopy and Dynamic Light Scattering (DLS). New nanosystems emerge as promising superlubricants achieving different coefficient of friction (COF), viscosity in the POM-Steel, polymer-metal tribo-pairs [4].

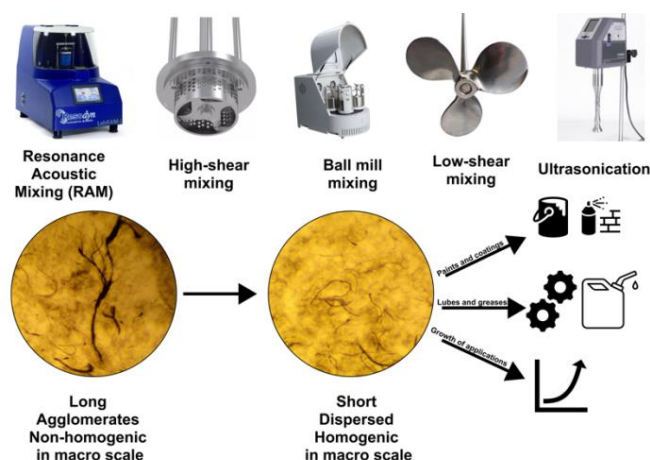


Figure 1: Different ways of mixing CNTs and base fluids toward stable dispersions

Acknowledgments

The authors are very grateful for the financial support from the National Science Centre (Poland) Grant No. 2020/39/B/ST5/02562 in the framework of the OPUS-20 program.

References

- [1] S. Talebian *et al.*, *ACS Nano* **15**, 15940–15952 (2021).
- [2] C. Pramanik *et al.*, *ACS Nano*, **11**, 12805-12816 (2017).
- [3] S. Boncel *et al.*, *J. Mol. Liq.* **391**, 1232151 (2023).
- [4] L. Wojciechowski *et al.*, *Tribol. Int.* **191**, 109203 (2024).

Stacked 2D Materials For Temporal Gating of Ion Transport Through Nanopores

M. Schiel¹, E. Cao¹, A.H. Barajas-Aguilar¹,
J.D. Sanchez-Yamagishi¹, and Z.S. Siwy¹

¹*University of California Irvine (USA)*

Transport properties of nanopores can be controlled by chemical modification, electrolyte conditions, or placing a gate near or in the pore. All the systems reported thus far operate with the classical Debye layer such that the changes are slow and allow a electrical double-layer (EDL) to form. Here, we present a nanopore system with 2D gates whose electrical potential will be gated with GHz frequencies. We have drilled single sub-10nm nanopores by TEM in stacked 2D materials (hBN and graphene) positioned over a 5 μ m diameter micropore in the center of a silicon nitride membrane on a silicon chip. We have tested these nanopores drilled in single hBN flakes as well as in hBN-graphene-hBN stacks, where a ~1nm conducting layer of graphene is encapsulated in between two insulating hBN flakes. We were then able to measure ionic current through the pores with varying KCl concentration using a PDMS conductivity cell. The nanopores exhibit a low concentration conductance saturation indicative of surface charges on walls inside the pore. At the same time we developed a thin polyimide printed circuit board (PCB) to go in the middle of our PDMS conductivity cell with coaxial connections to apply high frequency voltages to the chip. To contact the PCB we added metal electrodes to the chip and fine metal contacts to the graphene layer of an hBN-graphene-hBN stack. Finally, we deposited a PMMA layer over the chip, except for a square over the 2D material. We showed this layer insulates the electrodes from the fluid and we are able to apply voltages with low resistance to the electrodes on the chip, allowing us to test non-equilibrium EDL gating.

Strong Artificial Muscle Fibers by Carbon Nanotube@Double Network Liquid Crystal Elastomer

Guang Yang^{1,2}

¹ University of Science and Technology of China (China), ² Suzhou Institute of Nano-Tech and Nano-Bionics, Chinese Academy of Sciences (China)

Fibers of liquid crystal elastomers (LCEs) as the promising artificial muscle show ultralarge, and reversible contractile strokes. However, the contractile force and load bearing capability are still seriously limited by the poor mechanical properties of LCE fibers. Herein, we report the preparation of high-strength LCE fibers by introducing a rigid secondary network into the single network LCE. The double-network LCE (DNLCE) showed considerable improvements in tensile strength and maximum actuation, which are 313.9% and 342.8% of those of the pristine LCE fibers, respectively. To facilitate the controllability and application, a coiled artificial muscle fiber consisting of DNLCE coated carbon nanotube (CNT) fiber is prepared. When electrothermally driven, the artificial muscle fiber outputs high actuation performance (59.9% maximum contraction, 26.7 MPa maximum isometric contractile stress, and 58 MPa maximum actuation load). Furthermore, by knitting the artificial muscle fibers into origami structures, an intelligent gripper and a crawling inchworm robot have been demonstrated. These demonstrations provide promising application scenarios of artificial muscle fibers for advanced intelligent structures and systems in the future.

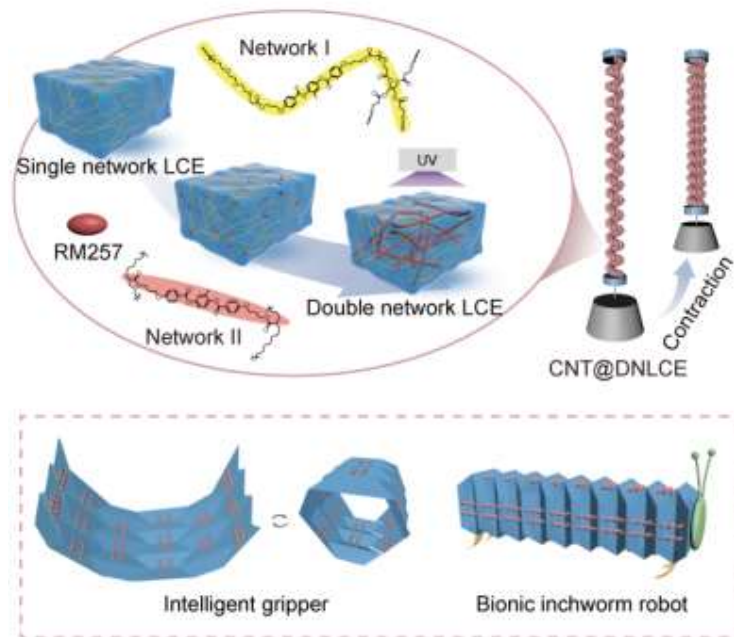


Figure caption: (a) Schematic illustration of the preparation of the CNT@DNLCE artificial muscle fiber. (b) Application of the CNT@DNLCE artificial muscle fibers.

Structure and Charge Transfer in Fibers of Carbon Nanotube Intercalation Compounds

A. I. de Isidro-Gómez^{1,2}, A. Mikhachan¹, V. Vassilev-Galindo¹, H. Terrones^{1,3}, J. Llorca^{1,4}, J. Christensen¹, J. J. Vilatela¹

¹IMDEA Materials (Spain), ²Universidad Autónoma de Madrid (Spain), ³Department of Physics, Rensselaer Polytechnic Institute (USA), ⁴Department of Materials Science, Polytechnic University of Madrid (Spain)

Continuous fibres of carbon nanotube intercalation compounds (CNTIC) feature aligned carbon nanotubes with intercalated species, such as FeCl₃ or Br, organized between them, forming extended domains of periodic intercalation. [1][2] Previously, we found that introducing intercalants into carbon nanotubes (CNTs) increases bulk fibre to levels close to copper or aluminium on a mass basis, while maintaining the exceptional mechanical properties of CNT fibres. [3] This makes intercalated CNTs promising lightweight conductors superior to most metals and graphite intercalation compounds.

The aim of this work is to identify the structure of the intercalate, its relation to the CNT channel size and the effect on charge transfer and electronic structure of the intercalation compound. The structure of the intercalation compound is directly characterized using high-resolution transmission electron microscopy (HRTEM). Polarized Raman spectroscopy with various laser energies assesses charge transfer between intercalate and DWCNTs, and enables discrimination of different intercalate species, among dimers and polyanions. These results are combined with WAXS measurements, which probe a large DWCNTIC fibre volume and show different Br species in the compound, forming elongated domains that run parallel to the channel.

We perform DFT simulations on a model system of SWCNTs with intercalated Br. This system, with a reduced size, enables cell and geometry relaxations within feasible computational times. We observe that bromine adopts an energetically stable configuration by forming polyanions oriented primarily along the channels between nanotubes. The resulting DOS of the intercalation compound shows new electronic states and a negative shift of the Fermi level with respect to the starting SWCNTs, confirming the experimentally observed p-type doping process.

Finally, we introduce cross-sectional compositional maps that enable confirmation of intercalation, determination of the periodic distribution of the intercalant strings within the host, and aids in visualizing the intercalant diffusion process, thereby improving our understanding of the intercalation mechanisms in CNT fibres.

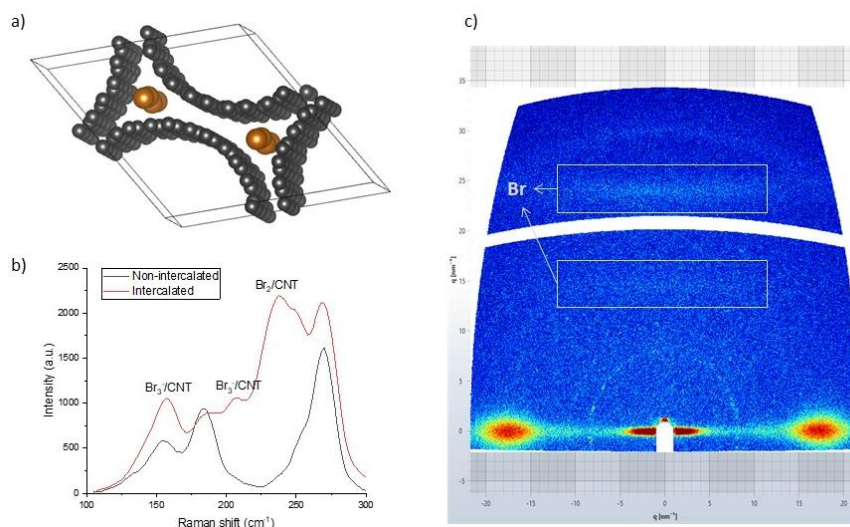


Figure 1: Charge transfer and structure simulation and characterization of Br-intercalated fibres of DWCNT. a) DFT simulation of the Br structure in the channels between SWCNTs. b) Raman spectra of Br-intercalated DWCNTs displaying the characteristic peaks of Br dimers and polyanions. c) WAXS pattern of an intercalated DWCNT fibre with periodic structures of Br alongside the inter-CNT channels.

References

- [1] C. Madrona, *et al.*, *Carbon*, **173**, 311-321 (2021).
- [2] C. Madrona, *et al.*, *Carbon*, **204**, 211-218 (2023).
- [3] Dongju Lee *et al.*, *Sci. Adv.* **8**, 16 (2022)

Study of thermal resistance at the metal-CNT interface through thermal structure function measurements

Kosuke Hayashi, Takayuki Nakano, Yoku Inoue

Shizuoka University (Japan)

Due to their high thermal conductivity, carbon nanotubes (CNTs) are extensively studied for thermal interface material (TIM) applications. In this study, we measured the thermal resistance (R_{th}) of CNT forests grown and transferred onto Al substrates, focusing on the CNT/Al system and estimating R_{th} through the thermal structure function using transient thermal response.

The measurement system is considered a ladder circuit of R_{th} and thermal capacitance of layered materials. R_{th} of the CNT sample was deduced from the corresponding step width in the structure function. CNT samples were located between a test element group (TEG) chip and a cold plate, where the TEG chip served as both a heat source and a temperature sensor (Figure 1).

Figure 2 compares the structure function curves measured for transferred-on-Al and grown-on-Al CNT forests. The measured R_{th} results from the sum of CNT specimens and TEG/CNT, CNT/Al, and Al/cold plate interfaces. We observed that directly grown CNTs exhibit a lower R_{th} ($4.78 \text{ cm}^2\text{K/W}$) than transferred CNTs ($5.48 \text{ cm}^2\text{K/W}$). This apparent decrease suggests the suppression of phonon scattering from CNTs to Al at the CNT/Al interface. We further studied the methods to suppress phonon scattering at the CNT/Al interface.

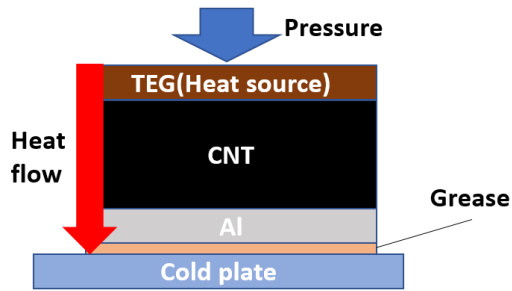


Figure.1: R_{th} measurement system

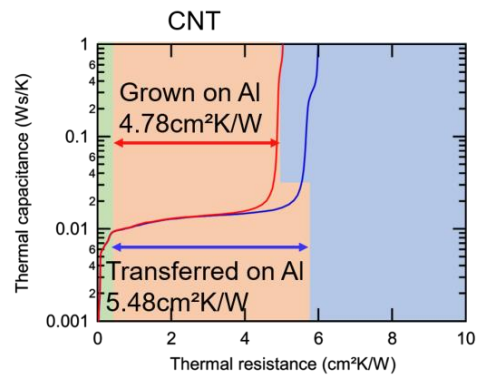


Figure.2: Comparison of thermal structure function of transferred-on-Al and grown-on-Al CNT forests.

SUPERHYDROPHOBIC HYDROGENATED NANOCARBONS

M. Małecka¹, A. Marek¹, E. Korczeniewski², A. P. Terzyk², S. Boncel¹

¹Silesian University of Technology, NanoCarbon Group (Poland), ²Nicolaus Copernicus University in Torun, Physicochemistry of Carbon Materials Group (Poland)

Superhydrophobicity is the *sine qua non* characteristic of anti-icing, anti-fogging, anti-wetting, and water-oil separation materials. Intrinsic anti-wetting properties of nanocarbon materials can be further enhanced by numerous approaches. The fundamental methods of the nanocarbon extra-hydrophobization involve covalent and non-covalent functionalization, *in situ* or *post factum* alignment of pristine or functionalized materials, coating by other (super)hydrophobic surfaces, and formation of hybrid/composite materials. One of the most prospective modifications of pristine nanocarbons toward superhydrophobicity is hydrogenation [1]. During this process, the nanocarbon is purified from iron-based compounds and amorphous carbons [2], the chemical structure of the C-framework changes (to a varied extent) from sp²- to sp³-hybridization, and morphology of the product can adopt a re-ordered geometry.

Here, hydrogenation of various carbon nanomaterials, i.e., carbon nanotubes (CNTs) of a different morphology, graphene, and single-walled carbon nanohorns (SWCNHs), was performed *via* two methods [3]. The first method was based on the electrochemical reduction in the optimized H₂O/MeOH media. The second approach involved scalable, high-pressure hydrogenation in an autoclave, at elevated temperature. The products were cross-characterized by SEM, TEM, elemental analysis, TGA, XPS, Raman and FT-IR spectroscopy. The wetting properties of hydrogenated *versus* non-hydrogenated nanocarbons were evaluated by water contact angle (WCA) measurements of the isotropic coatings obtained under fully reproducible protocols.

The hydrogenated carbon nanomaterials, due to their tunable morphology and surface physicochemistry accompanied by the excellent anti-wetting properties, including superhydrophobicity with WCA as high as >160°, emerge as promising candidates in numerous applications, such as anti-fogging and anti-icing surfaces or technologies for oil separation from the spillages.

Acknowledgements

The authors are very grateful for the financial support from the National Science Centre (Poland) Grant No. 2021/43/B/ST5/00421 in the framework of the OPUS-22 program.

References

- [1] L. Zheng *et al.*, *Chem. Commun.* **47**, 1213–1215 (2011).
- [2] D. Janas *et al.*, *J. Mater. Sci.* **49**, 7231–7243 (2014).
- [3] M. Małecka *et al.*, *in prep*

Surface Engineering of MXene and its Applications in light-Driven Actuation

D. Silva-Quinones¹, H. Wang¹

¹ *Electrical and Computer Engineering Department, Duke University, Durham, NC 27708, USA*

$Ti_2C_3T_x$, the first discovered MXene, has attracted attention for its unique properties such as adjustable electrical conductivity, high mechanical stability, and versatile responsiveness, offering a huge potential for advancing soft robotics and sensing. However, the performance of the MXene-based soft actuator is limited by uncontrollable surface terminations (-OH, -F, etc) induced in the synthesis process. Modifying these surface functional groups allows for customizing $Ti_2C_3T_x$ to possess desired properties.

In this work, we propose an innovative approach to engineer the surface termination of $Ti_2C_3T_x$ using plasma treatment. The $Ti_2C_3T_x$ flakes were exposed to different plasma conditions, with the resulting change in surface termination characterized by X-ray Photoelectron Spectroscopy (XPS). The morphology of $Ti_2C_3T_x$ is evaluated using Scanning Electron Microscopy (SEM) and Atomic Force Microscopy (AFM). Furthermore, we fabricated $Ti_2C_3T_x$ /cellulose actuators using $Ti_2C_3T_x$ with controlled surface terminations. In addition, cellulose in the nanocrystal, nanofiber, and microfiber phases are utilized and compared to obtain the best actuation performance. We observe that our $Ti_2C_3T_x$ /cellulose actuator demonstrates strong responses to light and moisture, which can be applied in soft robotics and sensing applications. The mechanism of controlled surface terminations contributing to the multi-responsive actuator will also be discussed.

Surface-Enhanced Raman Spectroscopy of Twisted Bilayer hBN

Xinyue Li¹, Cong Su^{1,2}

¹*Department of Applied Physics, Yale University (USA),* ²*Department of Mechanical Engineering & Materials Science, Yale University (USA)*

Recent advances in two-dimensional (2D) material have drawn great interest in exploring fundamental properties and potential applications of 2D heterostructures [1–4]. The novel physical phenomena of these layered materials provide a platform in studying artificial 2D with various physical properties. Raman, a powerful tool in characterizing structure of materials, has been heavily used to study moiré patterns which emerge when two periodic structures are overlaid with a slight twist [5,6]. Extra modes due to moiré patterns and double-resonance Raman scattering can be observed by Raman spectra revealing atomic structures associated with different twist angles [7,8]. The vibrational modes of hexagonal boron nitride (hBN), as well as the twisted structure, is particularly interesting due to the burgeoning of quantum emitters in hBN, whose emission is coupled with the lattice vibration through vibronic spectroscopy. However, studying twisted hBN by Raman is challenging due to limited exfoliation procedures, difficulty to isolate large monolayers, and relatively weak intensity of Raman signals [9-11]. As has been shown, graphene can be used as a substrate for enhancing Raman signals of adsorbed molecules [12-15], which is due to the reduced distance and charge transfer between the molecule and substrate [16]. In this work, we focus on enhanced Raman signal observed in freestanding twisted bilayer hBN capped by a monolayer graphene, offering potential insights into the new vibrational modes of this new lattice. The heterostructure demonstrates a remarkable enhancement in Raman signals, attributed to the unique vibrational properties emerging from the interlayer coupling and the angle-dependent moiré patterns formed by the twisted layers. Freestanding sample is required for determining the twist angles between the layers, but the preparation of such is challenging due to many factors such as uniformity, coverage, and cleanliness. To overcome these challenges, we are currently exploring a specific fabrication process to prepare freestanding bilayer hBN samples with various twisted angles. Moreover, we interpret our results with detailed analysis on detecting atomic reconstruction and correlation between moiré period and emerging optical and electronic properties. Our work shows the twist-dependent phonon scattering pathway in hBN and offers more possibilities for the development of novel photonic devices.

References

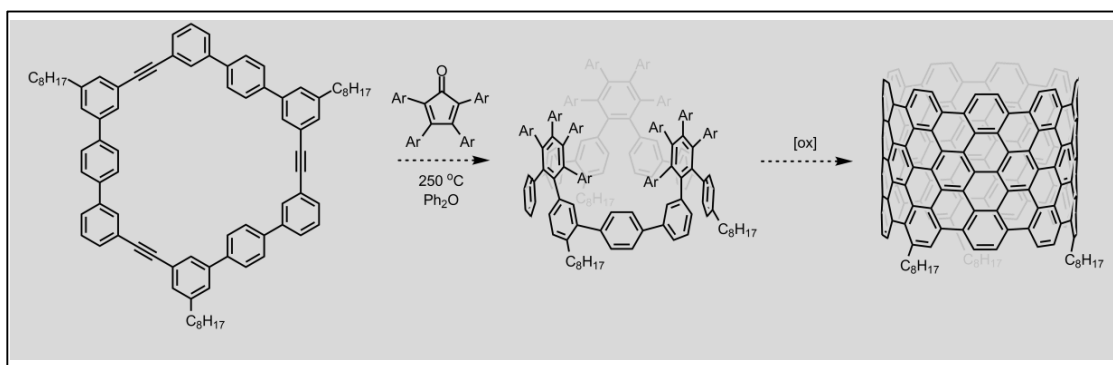
- [1] Liu Y. *et al.*, *Nat. Rev. Mater.* 1, 16042 (2016)
- [2] Kai L. *et al.*, *Adv. Mater.* 33, 2008333 (2021)
- [3] Jiang Y. *et al.*, *Light Sci. Appl.* 10, 72 (2021)
- [4] Qing Z. *et al.*, *Adv. Electron. Mater.* 4, 17003335 (2018)
- [5] Chang L. *et al.*, *J. Phys. Chem. Lett.* 14 (24),5573-5579 (2023)
- [6] M. V. O. *et al.*, *C.* 7,10 (2021)
- [7] A. R., *et al.*, *Phys. Rev. B* 84, 241409 (2011)
- [8] A. K. G. *et al.*, *Phys. Rev. B* 82, 241406 (2010)
- [9] Xi L. *et al.*, *Nano Lett.* 14, 3033-3040 (2014)
- [10] A. J. *et al.*, *Nano Lett.* 16, 5, 3360-3366 (2016)
- [11] R. V. G. *et al.*, *small* 7, 4, 465-468 (2011)
- [12] Xi L. *et al.*, *Nano Lett.* 10, 2, 553–561 (2010)
- [13] Xi L. *et al.*, *J. Phys. Chem. C* 117,5,2369-2376 (2013)
- [14] R. W. H. *et al.*, *Nano Lett.* 12, 3162-3167 (2012)
- [15] Wei X. *et al.*, *PNAS* 109 (24), 9281-9286 (2012)
- [16] N. B. *et al.*, *Nanomaterials*, 11(3), 622 (2021)

Synthesis and Cycloadditions of Cyclooligo(3,3'-*para*-terphenylene ethynylene)s: Precursors of Armchair Carbon Nanobelts

K. Murray¹, L. Sodergren¹, T. S. Hughes¹

¹Department of Chemistry and Biochemistry, Siena College, Loudonville, NY, (USA)

Cyclooligo(phenylene ethynylene) macrocycles were prepared by Sonogashira cross coupling of 3-iodo-3''-alkynylterphenyl and 3-iodo-3'-alkynylbiphenyl monomers. These monomers were synthesized from 3-iodo-5-bromoalkylbenzene via a series of Suzuki or Sonogashira cross couplings to join the alkynyl and aryl subunits together. The alkyl side chain is required to allow the solubility of the macrocycles. These fluorescent shape-persistent macrocycles aggregate in solution. Diels-Alder cycloadditions were attempted on the alkyne macrocycles to give cyclooligophenylenes. The sequence of cycloadditions required to give the nanotube precursors was modeled computationally, as was the subsequent cyclodehydrogenative oxidation that fuses the pendant phenyl rings of the Diels-Alder cycloadduct into a fully conjugated nanobelt.



Synthesis and optical characterization of NbS₂ based van der Waals heterostructures

Wanyu Dai¹, Yongjia Zheng^{1,2}, Akihito Kumamoto³, Mina Maruyama⁴, Susumu Okada⁴, Slava V. Rotkin⁵,

Esko I. Kauppinen⁶, Keigo Otsuka¹, Yuichi Ikuhara³, Rong Xiang^{1,2}, Shigeo Maruyama¹

¹ Department of Mechanical Engineering, The University of Tokyo, Tokyo 113-8656, Japan

² School of Mechanical Engineering, Zhejiang University, Hangzhou 310003, China

³ Institute of Engineering Innovation, The University of Tokyo, Tokyo 113-8656, Japan

⁴ Institute of Pure and Applied Sciences, The University of Tsukuba, Tsukuba 305-8571, Japan

⁵ Materials Research Institute, The Pennsylvania State University, Pennsylvania 16802, The United States of America

⁶ Department of Applied Physics, Aalto University School of Science, Tiilenlyöjankuja 9A SF-01720 Vantaa, Finland

The first demonstration of one-dimensional (1D) van der Waals (vdW) heterostructures which include single-walled carbon nanotubes (SWCNTs), boron nitride nanotubes (BNNTs), and molybdenum disulfide nanotubes (MoS₂NTs) was proposed in 2020, indicating the great potential of acquiring 1D forms of candidate materials from 2D vdW heterostructures [1-3]. As MoS₂/WS₂ are semiconducting materials, BNNT being insulating material, introducing metallic materials into the 1D vdW heterostructures would be of great research interest for potential device applications of 1D vdW heterostructures.

In this work, we demonstrated the experimental synthesis of 1D NbS₂ and investigated the optical properties of as acquired SWCNT-BNNT-NbS₂ heterostructures. As a metallic TMDC material, NbS₂ shows greatly different optical properties compared with MoS₂/WS₂-based 1D vdW heterostructures. Also, the statistical layer number distribution of as synthesized NbS₂ nanotubes indicated a double layer preference, which is unique than other 1D TMDCs such as MoS₂, WS₂, MoSe₂, etc. The investigation via the structural and spectral analysis reveals the electronic characteristics and extends the knowledge of intrinsic properties of NbS₂ vdW heterostructures based on SWCNT-BNNT, helping the future fabrication of more complicated 1D vdW hetero-structures and device development.

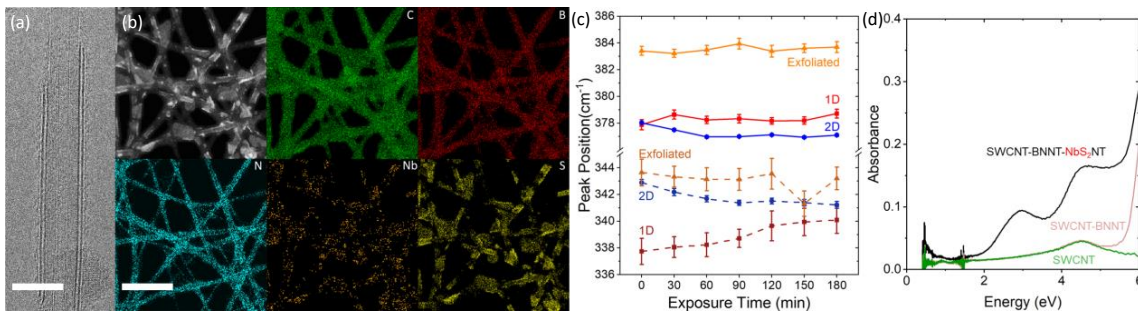


Fig. 1(a) TEM image of bilayer NbS₂ nanotube over coaxial SWCNT-BNNT, scale bar 5nm. (b) HAADF image and EDS mapping of as synthesized SWCNT-BNNT-NbS₂, scale bar 100 nm. (c) Raman decay of 1D and 2D NbS₂ @SWCNT-BNNT and exfoliated NbS₂@Si/SiO₂ substrate as exposed in the atmosphere. (d) UV-vis-NIR absorbance of NbS₂ based 1D vdW heterostructures

[1] R. Xiang, *et al.*, Science, **367**, 537 (2020).

[2] Y. Zheng, *et al.*, PNAS, **118**, e2107295118 (2021).

[3] S. Cambre, *et al.*, Small, **17**, 2102585 (2021)

Corresponding Author: S. Maruyama

Tel: +81-3-5841-6421, Fax: +81-3-5800-6983

E-mail: maruyama@photon.t.u-tokyo.ac.jp

Synthesis of carbon nanotubes using higher alkanes as a carbon source

L. Nowicki¹, S. Lepak-Kuc^{1,2}, A. Lekawa-Raus¹

¹Centre for Advanced Materials and Technologies (CEZAMAT) Warsaw (Poland), ²Faculty of Mechanical and Industrial Engineering, Warsaw University of Technology (Poland)

Although investigated for a long time now the synthesis of CNTs is still highly challenging. The game changer for further development of CNT applications would be the bulk production of CNTs with precisely controlled chirality, diameter, number of layers, and length [1-4]. In the following work we used a purpose designed Floating Catalyst Chemical Vapour Deposition (FC-CVD) method to perform a systematic study on the effect of the use of higher alkanes of increasing chain lengths as a carbon source in the synthesis CNTs, which to the best of our knowledge has not been reported by now. [5-9]. FC-CVD is a versatile method enabling a high yield synthesis of both MWCNTs and SWCNTs and their different assemblies [10-11]. Our purpose designed reactor enables the precise control of all basic synthesis parameters such as temperature, time of reaction or speed of injection and is set to manufacture CNT arrays. In this study we tested 6 higher alkanes - hexane, octane, decane, dodecane, tetradecane and hexadecane and investigated their decomposition at 4 different temperatures from 760°C - 1060°C. The feedstock comprised also ferrocene as a catalyst source and argon was used as carrier gas. The analysis of obtained materials showed clear differences in CNTs diameters, height of arrays, and amount of material, and temperature of decomposition in thermogravimetric analysis (TGA).

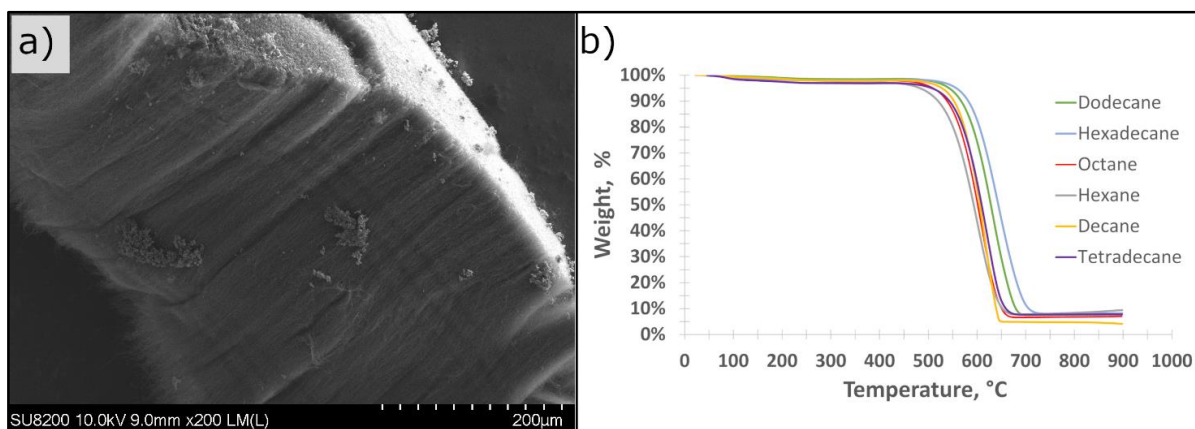


Figure 1: a) CNTs arrays with Octane as a carbon source. b) TGA for all tested alkanes synthesized in 760°C

References

- [1] S. Wang et al., *Nano Res.* **16**, 10342–10347 (2023)
- [2] A. Aghaei, M. Shaterian, H. Hosseini-Monfared, and A. Farokhi, *Chem. Pap.* **77**, 249–258 (2023)
- [3] X.-X. Lim, S.-C. Low, and W.-D. Oh, *Fuel Process. Technol.* **241**, 107624 (2023)
- [4] M. J. Giannetto et al., *ACS Nanosci. Au* **3**, 182–191 (2023)
- [5] S. S. Meysami, A. A. Koós, F. Dillon, and N. Grobert, *Carbon* **58**, 159–169 (2013)
- [6] N. Sonoyama et al., *Carbon* **44**, 1754–1761 (2006)
- [7] M. W. Brenner, V. M. Boddu, and A. Kumar, *Appl. Phys. A* **117**, 1849–1857 (2014)
- [8] H. W. Zhu, C. L. Xu, D. H. Wu, B. Q. Wei, R. Vajtai, and P. M. Ajayan, *Science* **296**, 884–886 (2002)
- [9] H. Li, D. He, T. Li, M. Genestoux, and J. Bai, *Carbon* **48**, 4330–4342 (2010)
- [10] T. Zhao et al., *Appl. Surf. Sci.* **357**, 2136–2140 (2015)
- [11] J. H. Park, J. Park, S.-H. Lee, and S. M. Kim, *Carbon Lett.* **30**, 613–619 (2020)

Telecom-band Light-emitting Diodes based on Chirality-sorted (10, 5) Carbon Nanotube Films

Bing Han¹, Yahui Li², Song Qiu^{*2}, Xiaowei He^{*1}, Sheng Wang^{*1}

¹Key Laboratory for the Physics and Chemistry of Nanodevices and Center for Carbon-Based Electronics, School of Electronics, Peking University, Beijing 100871, China

²Key Laboratory of Nanodevices and Applications, Suzhou Institute of Nano-Tech and Nano-Bionics, Chinese Academy of Science, Suzhou 215123, P.R. China

An important goal in carbon nanotube optoelectronics is to achieve a high-performance near-infrared (NIR) light source. But there are still many challenges such as the purity of SWCNT chirality, nonradiative defects, thin film quality and device structure design. Here, we realize infrared light-emitting diodes (LEDs) based on chirality-sorted (10, 5) single-walled carbon nanotube (SWCNT) network films, which operates at a low bias voltage and emits at the telecom O band of 1290 nm. Asymmetric palladium (Pd) and hafnium (Hf) contacts are used as electrodes for the hole and electron injection, respectively. However, the large Schottky barrier at the interface of the SWCNTs and the Hf electrode, primarily resulting from the polymer wrapped on the nanotube surface during the sorting process, leads to inefficient electron injection and thus a low electroluminescence (EL) efficiency. We find that the efficiency of electron injection can be improved by the local doping of the nanotubes with dielectric layers of YO_x-HfO₂, which reduces the Schottky barrier at the SWCNTs/Hf interface. Accordingly, the (10, 5) SWCNT film-based LED achieves an external quantum efficiency (EQE) of larger than 0.05% without any optical coupling structure. With further improvement, we expect that such an infrared light source will have great application potential in the carbon nanotube monolithic optoelectronic integrated system and on-chip optical interconnection, especially in the field of short distance optical fiber communications and data center.

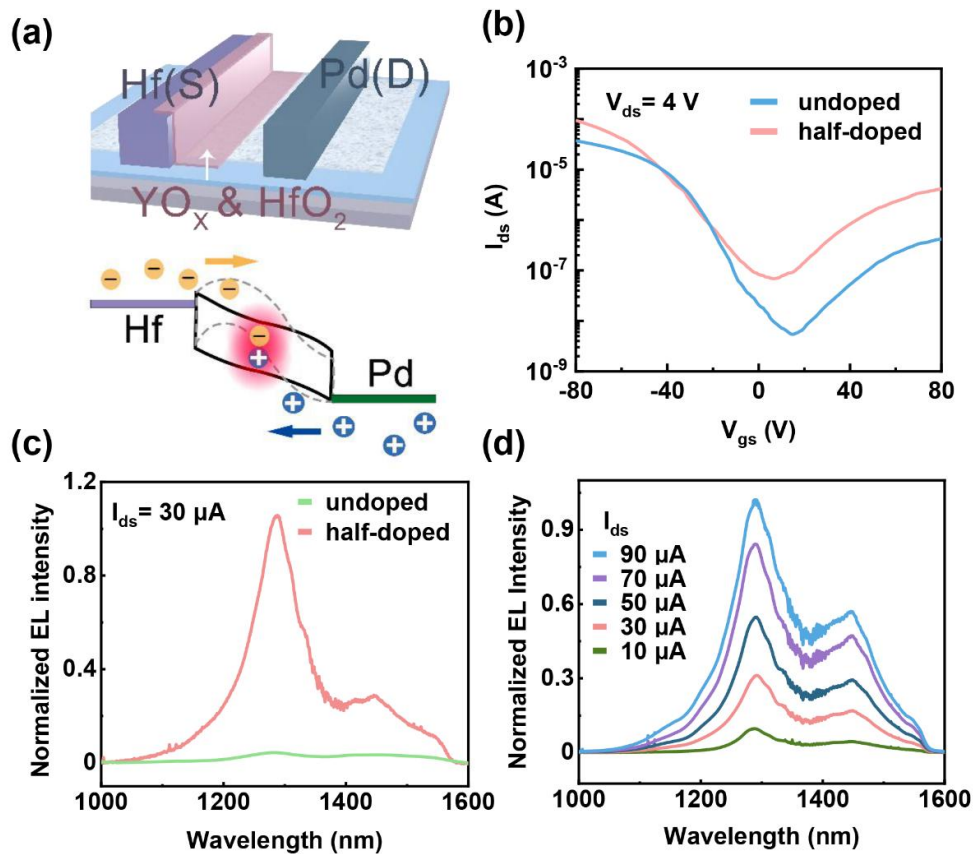


Fig.1 Structure and characterization of half-doped LEDs. (a) Schematic of half-doped LED. (b) (c) Comparison of transfer curves (b) and EL spectra (c) before and after doping. (d) EL spectra of half-doped devices under different currents.

References

[1] B. Han, Y. Li, W. Wu, X. Cai, S. Qiu, X. He, S. Wang. *ACS Applied Materials & Interfaces* Article DOI: 10.1021/acsami.3c11990

THE EFFECT OF DOPANT ORDERING IN CHARGE TRANSFER TO GRAPHITIC INTERCALATION COMPOUNDS – A CASE OF STUDY

Cristina Madrona¹, Juan J. Vilatela², José M. Guevara-Vela³

¹ICMol – Universidad de Valencia (Spain), ²IMDEA Materials (Spain), ³UAM (Spain)

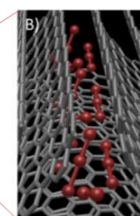
Lazzeri and Mauri theoretically showed that there is a master curve for G-shifts as a function of charge transfer in graphite intercalation compounds (GICs) [1]. The possibility of having a similar curve for intercalated CNTs was proposed by Puech et al. by intercalating H₂SO₄ in DWCNTs and extracting charge transfer through a novel approach using Raman spectroscopy [2]. We corrected this model for obtaining a more accurate charge transfer value [3] and further confirmed the existence of such a master curve by intercalating both rounded and collapsed DWCNTs with FeCl₃ and Br₂. This allows for direct calculation of charge transfer by just deconvoluting the G peak of the Raman spectra into the inner and outer contributions.

In this work, we compare three types of intercalated graphitic materials, Br-DWCNT fiber, stage 4 Br-K1100 carbon fiber, and Br-collapsed DWCNT fiber. These materials are ‘equivalent’ in the sense that each of the graphitic layers in contact with the dopant (outer/bounding) has an adjacent unintercalated layer (inner/interior). At comparing charge transfer, f , obtained for these systems, we find the following relations:

$$f(\text{Br-DWCNTs}) < f(\text{stage 4 Br-K1100}) < f(\text{Br-collapsed DWCNTs})$$

Our hypothesis is that the smaller charge transfer of stage 4 Br-K1100 with respect to Br-collapsed DWCNTs stems from the ordering of the dopant in AB stacked K1100 (as observed in WAXS), which increases the interaction between bromine species, thus decreasing charge transfer to the graphitic layers, similar to what happens in Br-DWCNTs, where formation of a 1:1 ratio of tribromide chains and molecular bromine not only does not increase charge transfer (expected for the formation of anionic chains), but decrease it with respect to lower concentrations of only molecular bromine (see Table 1).

Br Mass fraction (%)	4.8	9.2	13.1	16.8	20.1	23.2	26.1
Charge transfer per carbon atom*	-0.0004	-0.0007	-0.0012	-0.0019	-0.0016	-0.0026	-0.0029
Molar ratio Br ₃ ⁻ /Br ₂	0	0	0	0	1	0.67	0.5



* The result takes into account the average of 264 C atoms.

Table 1: Charge transfer from simulation of CNT-IC with different Br mass fractions.

References

- [1] Lazzeri, M., & Mauri, F. (2006). *Phys. Rev. Lett.*, **97**(26), 266407.
 [2] Puech, P., et al. (2012). *Phys. Rev. B*, **85**(20), 205412
 [3] Madrona, C., Vila, M., Oropeza, F. E., Víctor, A., & Vilatela, J. J. (2021). *Carbon*, **173**, 311-321

The Impact of Oxidized Ferrocene (Ferrocenium) Catalyst on Chiral Distribution of SWCNT TCFs in FCCVD Synthesis

Anastasios Karakassides¹, Hirotaka Inoue^{1,2}, Hua Jiang¹, Ghulam Yasin¹, Esko I. Kauppinen¹

¹Aalto University (Finland), ²Sumitomo Electric Industries (Japan)

The exceptional optoelectronic properties exhibited by single-walled carbon nanotubes (SWCNTs) have rendered them as excellent candidates for transparent conducting films (TCFs) in recent years [1,2]. Considerable effort has been dedicated to exploring innovative catalysts for the synthesis of SWCNTs with the aim of controlling their structure and achieving targeted selective growth. Within this context, our research group has investigated a novel catalyst—ferrocenium (oxidized ferrocene)—for SWCNT synthesis. The synthesis involved utilizing $\text{Cu}(\text{NO}_3)_2$ in a ferrocene/ethanol solution, leading to the partial oxidation of ferrocene. All samples underwent thorough characterization using advanced optical and microscopy techniques, with the chiral angles determined through TEM electron diffraction patterns (ED) [3]. Our findings highlight the significant impact of incorporating ferrocenium as a catalyst, effectively influencing the chiral distribution of the synthesized nanotubes. This represents a notable advancement towards achieving selective growth of SWCNTs.

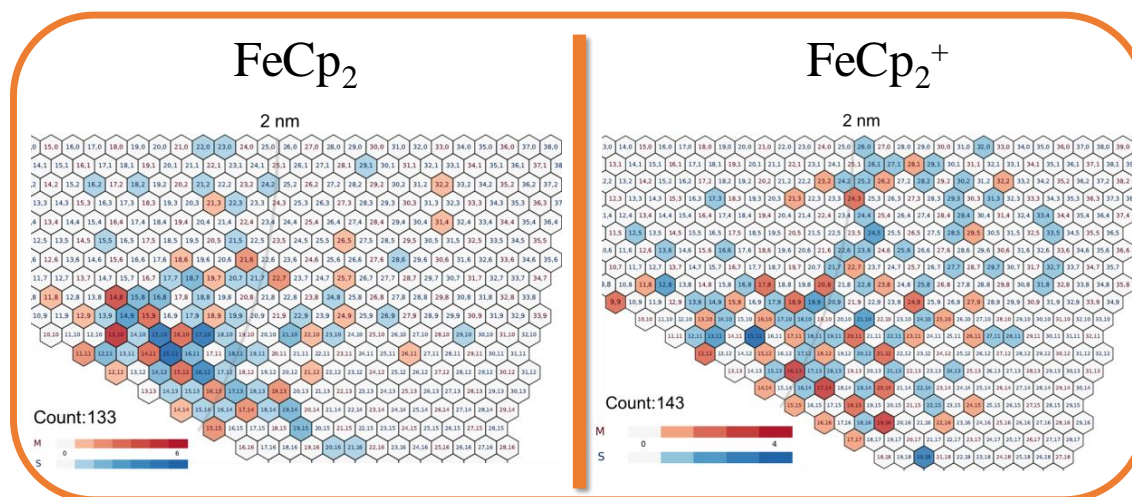


Figure 1. Chirality distribution of FeCp_2 and FeCp_2^+ CNT films.

References

- [1]. E.-X. Ding *et al.*, *Nanoscale* 9, 17601–17609 (2017).
- [2]. Q. Zhang *et al.*, *Topics in Current Chemistry* 375(6), 90 (2017).
- [3]. H. Jiang *et al.*, *Carbon* 45, 662 (2007).

The Important Role of Ethylene in Floating Catalyst Chemical Vapor Deposition for Tuning of Carbon Nanotube Chirality Distribution

Hiroataka Inoue^{1,2}, Anastasios Karakassides², Ghulam Yasin², Hua Jiang², Takamasa Onoki¹, Toshihiko Fujimori^{1,3}, Akira Takakura¹, Soichiro Okubo¹, Daisuke Tanioka¹, Esko I. Kauppinen²

¹Sumitomo Electric Industries (Japan), ²Aalto University (Finland), ³University of Tsukuba (Japan)

Carbon nanotube (CNT) has been expected as a promising material for next-generation lightweight electric wires due to their unique properties such as electrical properties, mechanical tolerance, and chemical stability, which strongly depend on their chirality. One of the most challenging problems for CNT electric wires is the control of chirality structure of CNTs. In the floating catalyst chemical vapor deposition (FC-CVD), which is believed to be suitable for industrial applicability due to its capability for continuous synthesis of CNTs, there are several reports on chirality control [1-3]. However, in the FCCVD process, the precursor decomposition of catalyst/carbon source, nanoparticle formation, and CNT growth occur within a few seconds, resulting in a highly intricate interplay among control parameters. Consequently, the correlation between synthesis parameters and the generated CNT structures has not been fully understood.

In this study, we demonstrate the important roles of the ethylene amount in the FC-CVD system. A specific amount of ferrocene and thiophene were dissolved in a methanol/citric acid solution, and the mist of the solution, generated by a nebulizer, was introduced to the reactor by carrier gas flow of nitrogen. Therefore, ethylene, methanol, and citric acid are potential carbon sources for CNT growth in this system. Chirality distributions of generated CNTs were carefully checked by UV-Vis spectroscopy and electron diffraction analysis using a high-resolution transmission electron microscope [4]. Fig. 1 shows the chirality distributions of CNTs produced with different of ethylene. Interestingly, the chirality shows noticeable narrow distribution with the specific amount of ethylene (5 sccm). The detailed mechanism of these results will be discussed during the presentation. Especially we will focus on the difference in the decomposition region for each potential carbon source in the reactor.

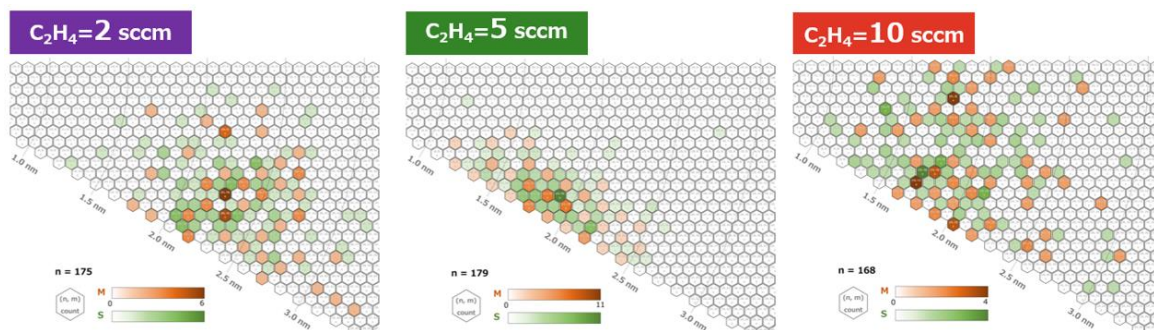


Figure 1: The relationship between ethylene amount and CNT chirality distribution.

References

- [1] P.-X. Hou *et al.*, *ACS Nano* **8** (7), 7156–7162 (2014).
- [2] Y. Liao *et al.*, *J. Am. Chem. Soc.* **140** (31), 9797–9800 (2018).
- [3] P. Liu *et al.*, *Adv. Electron. Mater.* **9** (7), 2300196 (2023).
- [4] H. Jiang *et al.*, *Carbon* **45**, 662 (2007).

The Role of Many-Body Polarization Interactions in the Interfacial Behavior of Hexagonal Boron Nitride

Shuang Luo¹, Rahul Prasanna Misra¹, Daniel Blankschtein¹
*Department of Chemical Engineering, Massachusetts Institute of Technology,
Cambridge, Massachusetts 02139, United States*

Understanding how water molecules and salt ions interact with hexagonal boron nitride (hBN) is crucial for practical applications such as seawater desalination and energy generation. When these water molecules and ions approach hBN surfaces, they generate strong electric fields, significantly polarizing the electron clouds of the boron and nitrogen atoms in hBN. This polarization energy is inherently non-additive due to the directional nature of the electric fields, resulting in complex many-body interactions [1]. However, the full extent of these polarization effects on the interface of water and salt ions with hBN is not completely understood.

In this study, we formulate a theoretical framework [1,2] that introduces new all-atomistic polarizable force fields to accurately model the anisotropic polarizability tensor of hBN and its interactions with water and ions. The new force fields incorporate a self-consistent modeling of the electric field-induced polarization of hBN using the classical Drude oscillator model, resulting in hBN-water binding energies which are in excellent agreement with the predictions from benchmark Diffusion Monte Carlo (DMC) simulations [3]. Through Molecular Dynamics (MD) simulations with our new polarizable force field, we explored the impact of many-body polarization interactions on the wetting behavior of hBN surfaces by water [2]. Our findings indicate that the new force field accurately predicts the water contact angle on multilayered hBN, consistent with recent experimental data [4, 5]. In contrast, using an implicit model based on the Lennard-Jones (LJ) potential — a common approximation in prior MD simulation studies, resulted in a significantly lower water contact angle. Additionally, we observed an increase in the fraction of interfacial water molecules adopting a 1 Leg orientation (with the -OH bond facing the hBN layer) when incorporating the polarization response of the hBN layer. This leads to a notable energy-entropy compensation in the calculated work of adhesion between hBN and water. When the hBN-water polarization is modeled implicitly using the LJ potential, this compensation effect is less pronounced. Furthermore, the modeling tools that we developed for simulating the polarization interactions between pure water and hBN have been extended to investigate the thermodynamic aspects of adsorption phenomena involving salt ions of various types and valences at the hBN/water interface. Overall, our results highlight the pivotal role of polarization effects in influencing water molecule orientation, wetting behavior, and the solvation process of ions at the hBN/water interface.

References

- [1] Misra, R. P.; Blankschtein, D. Insights on the Role of Many-Body Polarization Effects in the Wetting of Graphitic Surfaces by Water. *J. Phys. Chem. C* **2017**, 121(50), 28166–28179.
- [2] Luo, S.; Misra, R. P.; Blankschtein, D. Water Electric Field Induced Modulation of the Wetting of Hexagonal Boron Nitride: Insights from Multiscale Modeling of Many-Body Polarization. *ACS Nano* **2024**, 18, 1629–1646.
- [3] Al-Hamdani, Y. S.; Ma, M.; Alfè, D.; Von Lilienfeld, O. A.; Michaelides, A. Communication: Water on Hexagonal Boron Nitride from Diffusion Monte Carlo. *J. Chem. Phys.* 2015, 142 (18), 18s1101.
- [4] Zhang, X.; Cai, X.; Jin, K.; Jiang, Z.; Yuan, H.; Jia, Y.; Wang, Y.; Cao, L.; Zhang, X. Determining the Surface Tension of Two-Dimensional Nanosheets by a Low-Rate Advancing Contact Angle Measurement. *Langmuir* **2019**, 35(25), 8308–8315.
- [5] Keerthi, A.; Goutham, S.; You, Y.; Iamprasertkun, P.; Dryfe, R. A. W.; Geim, A. K.; Radha, B. Water Friction in Nanofluidic Channels Made from Two-Dimensional Crystals. *Nat. Commun.* **2021**, 12(1), 3092.

The underappreciated importance of polymer characteristics in extractive purification of single-walled carbon nanotubes

A. Dzienia¹, D. Just¹, T. Wasiak¹, D. Janas¹

¹ *Silesian University of Technology (Poland)*

Separating single-walled carbon nanotubes (SWCNTs) from raw soot into specific chiralities is critical for the production of tailor-made nanomaterials. Conjugated polymer extraction (CPE) in organic solvents stands out in this field due to its numerous merits [1]. However, due to the intricate nature of the process, only a handful of highly effective methods for isolating (6,5) and (7,5) chirality have been identified. A comprehensive understanding of the interplay between polymer structure, macromolecular parameters, mixture composition, and extraction protocol is essential for widespread application.

Recent studies have made significant strides in deciphering the mechanism of this process [2, 3, 4]. Investigation into factors like polymer molecular weight, solvent choice, process mixture composition, and isolation conditions has led to innovative chirality-selective sorting procedures. This breakthrough has substantially enhanced the efficiency of preparing monochiral dispersions of (6,5) and (7,5) SWCNTs. Additionally, a pioneering method for isolating the rare (7,3) chirality, previously unavailable in organic solvents, has been developed.

Our findings emphasize the challenges posed by PFO, requiring both a medium- or high-molecular-weight batch and a suitable methodology for effective use. Although optimisation of process methodology and composition can effectively mask the disadvantages of suboptimal batches. The application of our revised methodology allows high isolation yields for (7,5) SWCNTs with exceptional purity of around 90%. Conversely, PFO-BPy shows remarkable robust performance in this context, as it is much less affected by process parameters. Nonetheless, process performance still varies significantly in terms of the amount or purity of the harvested SWCNTs. Skillful utilization of polymer advantages yields highly-concentrated SWCNT dispersions of monochiral character.

The authors thank for the support National Science Centre, Poland (under the SONATA programme, Grant agreement UMO-2020/39/D/ST5/00285) and Initiative of Excellence – Research University (IDUB) programme carried out at the Silesian University of Technology 2023-2024 (grant agreement 04/020/SDU/10-4-01)).

References:

- [1] D. Janas, Towards monochiral carbon nanotubes: a review of progress in the sorting of single-walled carbon nanotubes, *Materials Chemistry Frontiers*, 2018, 2, 36-63
- [2] A. Dzienia, D. Just, P. Taborowska, A. Mielanczyk, K.Z. Milowska, S. Yorozyua, S. Naka, T. Shiraki, D. Janas, Mixed-Solvent Engineering as a Way around the Trade-Off between Yield and Purity of (7,3) Single-Walled Carbon Nanotubes Obtained Using Conjugated Polymer Extraction, *Small*, 2023, 19(46), 2304211
- [3] A. Dzienia, D. Just, D. Janas, Solvatochromism in SWCNTs suspended by conjugated polymers in organic solvents. *Nanoscale* 2023, 15 (21) , 9510-9524
- [4] D. Just, A. Dzienia, K. Z. Milowska, A. Mielanczyk, D. Janas, High-yield and chirality-selective isolation of single-walled carbon nanotubes using conjugated polymers and small molecular chaperones, *Materials Horizons*, 2024, 11, 758-767

Thermal conductivity of twisted CNT yarns and continuous ultra-long CNT

Haruto Kurono¹, Takayuki Nakano¹, Hisashi Sugime², Hayate Suzuki¹, Takumi Mochizuki¹, Hiromu Hamasaki¹, Hiroya Ikeda¹, Yoku Inoue¹

¹Shizuoka University (Japan), ²Kindai University (Japan)

The thermal conductivity of carbon nanotubes (CNTs) and CNT yarns has been extensively measured, showing results ranging from tens to thousands of W/mK. In this study, we developed a macroscopic method to measure the thermal conductivity of one-dimensional materials and examined CNT yarns and long continuous CNTs.

Dry spinnable CNT forests were synthesized using the chemical vapor deposition (CVD) method on a Si substrate with Fe as a catalyst layer and Al₂O₃ as a support layer. CNT webs drawn from these forests produced twisted CNT yarns. Additionally, long CNTs (>10 cm) were grown using cold-gas CVD with the addition of ferrocene and aluminium isopropoxide [1].

For thermal conductivity measurement, we estimated the thermal diffusivity α by analyzing the transient response of temperature decay in CNT specimens irradiated with an electron beam as a heat source (see Figure 1(a)). Subsequently, thermal diffusivity was determined by fitting the decay with a one-dimensional heat transport equation (see Figure 1(b)). The specific heat C of CNTs was measured using a differential scanning calorimeter (DSC). The thermal conductivity κ was then derived as $\kappa = \alpha\rho C$, using the weight density ρ of the measured samples.

The resulting thermal conductivity of the discontinuous CNT was 30 W/mK, while that of the continuous CNT was 160 W/mK. Interestingly, the thermal conductivity of yarns with numerous CNT-CNT interfaces is not significantly different from that of continuous crystalline materials. The influence of crystallinity on thermal conduction properties was also studied.

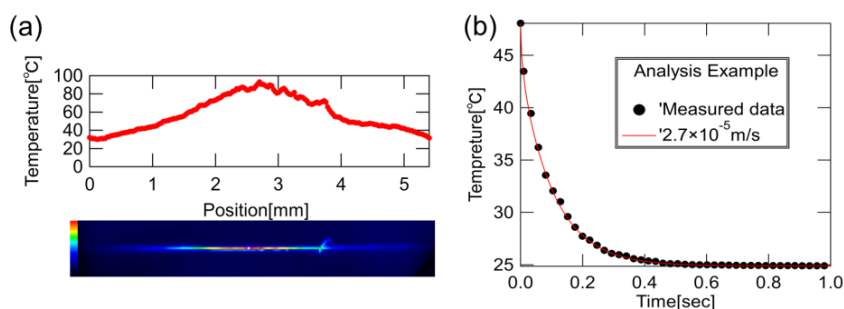


Figure 1 (a) Thermographic image and a temperature profile of CNT yarn irradiated with an electron beam in the center. (b) Derivation of thermal diffusion coefficient by fitting transient temperature decay using one-dimensional heat transport equation

References

[1]H.Sugime *et al.* Carbon **172**, 772–780 (2021).

Thermoelectric devices with carbon nanomaterials

F. van Veen¹, O. Braun¹, M Stiefel¹, Gabriela Borin-Barin¹, G. Blasi²,
G Haack², R. Fasel¹, H. van der Zant³, M. Calame¹, M. Perrin¹,

¹ Empa, Swiss Federal Laboratory for Materials Science and Technology

² University of Geneva

³ Kavli Institute of Nanoscience, Delft University of Technology

Thermoelectric effects at the nanoscale are of great interest for both energy-harvesting applications and fundamental studies of quantum materials [1,2, 3]. Here we report on the implementation of various carbon nano-materials into thermoelectric devices, which we thermoelectrically characterise while varying both the electrostatic potential and applied bias voltage using a recently developed measurement technique [1].

Remarkably, we find that films of bottom-up synthesized graphene nanoribbons exhibit very large thermoelectric responses, with measured equivalent Seebeck coefficients as high as 4 mV/K. Similar to previous studies on films of organic semiconductors, the charge transport through our GNR film fits very well to existing models describing the transport as temperature-activated hopping with additional polaron-assisted tunnelling. While the conductance increases exponentially with temperature, we find that the equivalent Seebeck coefficient remains constant. Finally, we show that our thermoelectric measurements can be numerically explained by including a strong bias dependence in the width of the electronic density of states.

Our results demonstrate the great potential of carbon nanomaterials for thermoelectric energy conversion devices, and indicate that new models are required to understand their operation at finite bias.

[1] P. Gehring *et al.*, Complete mapping of the thermoelectric properties of a single molecule, *Nature Nanotechnology*, 16, 426-430 (2021)

[2] C. Hsu *et al.*, Magnetic-Field Universality of the Kondo Effect Revealed by Thermocurrent Spectroscopy, *Phys. Rev. Lett.* 128, 147701 (2021)

[3] M. Josefsson *et al.*, A quantum-dot heat engine operating close to the thermodynamic efficiency limits, *Nature Nanotechnology* 13, 920-924 (2018)

Transforming Dairy Waste into High-Value Carbon Dots for Biomedical Applications

M.L. Fanarraga, R. Valiente, J. González, M.T. Candela, L. García-Hevia.

¹The Nanomedicine Group, IDIVAL- Universidad de Cantabria (Spain)

Carbon nanomaterials have become pivotal in the field of cancer nanomedicine, and among them, carbon dots (CDots) stand out as a secure and biocompatible option with substantial potential for various biomedical applications. These applications include drug and gene delivery, toxin absorption, nanosensors, and hyperthermia. CDots are semiconductor nanoparticles with diameters ranging from 2 to 10 nm which exhibit outstanding biocompatibility, optical absorption, chemical stability, low toxicity, and resistance to radiation, making them particularly promising for cancer treatment.

This project specifically envisions the utilization of CDots in bioimaging for diagnosing brain cancer and as theranostic agents for treating cancer through photo-hyperthermia in preclinical models of brain cancer. The study explores the transformation of dairy waste by-products into CDots using green chemistry, focusing on whey due to its uniform composition and high protein content, including essential amino acids like cysteine and methionine as a source of nitrogen and sulfur. These amino acids play a key role in enhancing CDot quantum yield, surface functionalization, and catalysis during a one-step synthesis process.

The primary objective is to produce CDots with tunable fluorescence emission. This comprehensive approach aims to unlock the potential of CDots derived from whey, presenting a versatile solution in the ongoing pursuit of safer and more effective biomedical interventions in cancer nanomedicine.

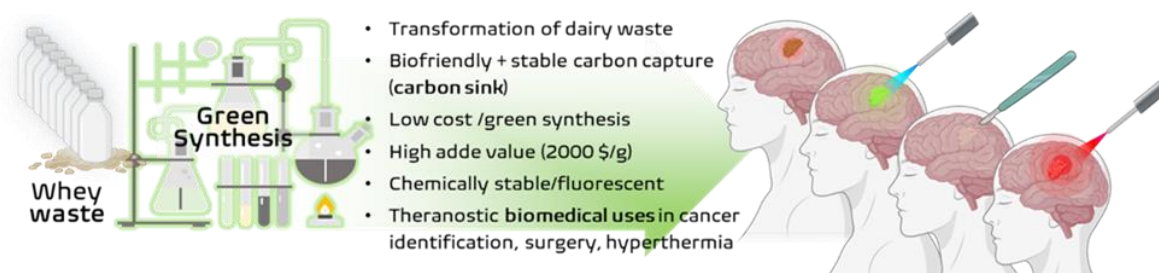


Figure 1: Vision of the study

TWISTED 2D MATERIALS FOR POLARIZATION OPTICS

K. Khaliji^{1, *}, L. Martín-Moreno^{2, 3}, P. Avouris^{1, 4}, S.-H. Oh¹, and T. Low¹

1 Department of Electrical and Computer Engineering, University of Minnesota, USA

2 Instituto de Nanociencia y Materiales de Aragon (INMA), CSIC-Universidad de Zaragoza, Spain

3 Departamento de Física de la Materia Condensada, Universidad de Zaragoza, Spain

4 IBM T. J. Watson Research Center, Yorktown Heights, USA

** kaveh.khaliji@gmail.com*

The ability to control light polarization state is critically important for diverse applications in information processing, telecommunications, and spectroscopy. Here, we show that a stack of anisotropic van der Waals materials can facilitate the building of optical elements with designer Jones matrices. Our results demonstrate that it is possible to control the Jones matrix elements of such stratified structures by adjusting the doping, twist angle, and stacking order of anisotropic 2D layers. As an example, we discuss an electrostatic-reconfigurable stack which can be tuned to operate as four different polarizers and be used for Stokes polarimetry.

References:

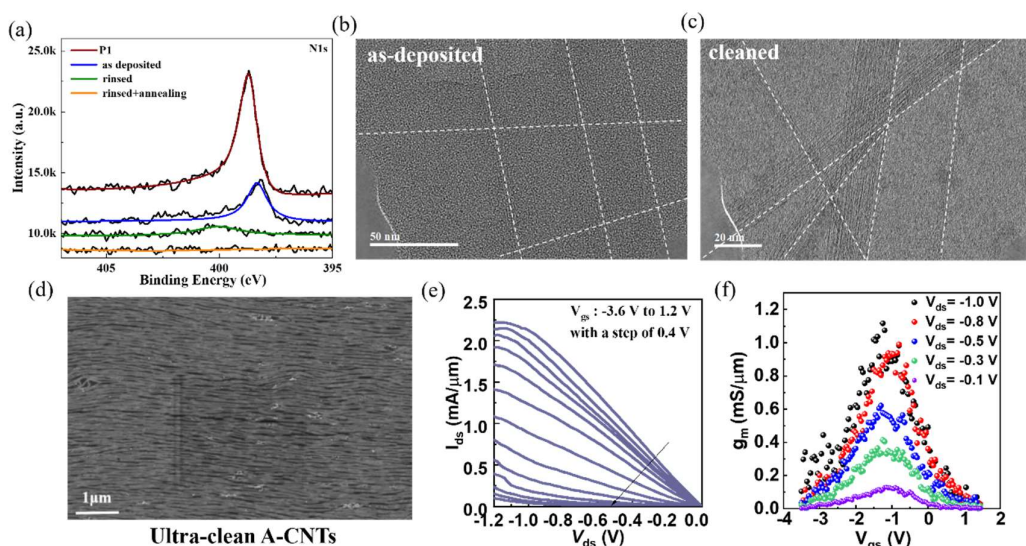
- [1] **K. Khaliji**, L. Martín-Moreno, P. Avouris, S.-H. Oh, & T. Low, *Physical Review Letters*. **128**, 193902 (2022).

Ultra-Clean and High-Semiconducting-Purity Carbon Nanotube Arrays for High-Performance Electronics

Lan Bai^{1,2}

¹Peking University, Beijing (China), ²Shanxi Institute of Carbon-Based Thin Film Electronics, Peking University (SICTFE-PKU), Taiyuan (China)

Semiconducting carbon nanotubes (S-CNTs) are promising channel materials for field-effect transistors (FETs) due to their unique one-dimension structure and excellent electronic and thermal properties. High-density and high-semiconducting-purity aligned carbon nanotubes (A-CNTs) are required for high performance electronics. Wafer-scale A-CNTs are usually self-assembled based on high-semiconducting-purity CNT solutions prepared by conjugated polymer wrapping. The polymer wrapper should ideally be completely removed from the A-CNTs as it hampers the intrinsic electronic performance of s-CNTs, but existing methods such as reducing excessive polymer concentration in s-CNT solutions and post-deposition solvent rinsing/annealing show little efficiency. Degradable conjugated polymers are proposed but few is compatible with available self-assembly techniques to prepare A-CNTs, and their effectiveness is indirectly judged by spectroscopy characterizations which cannot reflect the real scenario/degree of polymer removal due to limit of detection. In this work, a degradable conjugated polymer (P1) which could selectively separate s-CNTs with high purity and is also available with a wafer-scale self-assembly technique to prepare high-density A-CNTs is designed. As N is on the skeleton structure of the P1, the X-ray photoelectron spectroscopy (XPS) N1s peaks gradually reduce until disappear with the developed cleaning procedure, corresponding to the nearly complete removal of polymer. In addition, transmission electron microscopy (TEM) characterizations give direct evidence that the polymer wrapper could be removed from s-CNTs to obtain ultra-clean CNTs. Top-gated FETs based on the ultra-clean A-CNTs with a 45 nm channel length exhibit an on-state current (I_{on}) of 2.2 mA/ μm , a peak transconductance (g_m) of 1.1 mS/ μm , low contact resistance (R_c) of 191 $\Omega\cdot\mu\text{m}$ and negligible hysteresis, showing the great potential for high-performance electronics.



Ultra-dense CNT forests by adding ferrocene and aluminum isopropoxide to the growth process

Sota Goto¹, Takayuki Nakano¹, Hisashi Sugime², Yoku Inoue¹

¹Shizuoka University (Japan), ²Kindai University (Japan)

High-density carbon nanotube (CNT) forests hold potential applications in thermal interface materials and interconnects. However, during the growth of long CNT forests, catalytic activity tends to decrease due to structural changes in catalytic nanoparticles, leading to lower mass density [1]. Our recent work demonstrated ultra-long CNT forests by preventing catalyst deactivation by adding Fe (ferrocene, Fc) and Al (aluminum isopropoxide, AIP) in the growth process [2]. This study further achieves ultra-dense CNT forests by incorporating Fc and AIP into the CNT growth process.

Figure 1(a) illustrates the relationship between forest length and mass density with and without Fc and AIP. The high-density CNT forests reported to date are located near the trade-off line in Figure 1, with no cases significantly exceeding it. CNT forests lacking Fc or AIP exhibit behavior similar to the trade-off line, while those adding Fc or both Fc and AIP outperform it. Adding Fc and AIP increased the mass density of 1.3 mm CNT forests by 3.6 times, from 41.5 mg/cm³ to 150 mg/cm³. Figure 1(b)-(e) presents SEM images highlighting differences in CNT forest structure with and without Fc and AIP. Forests lacking Fc or AIP show a substantial reduction in density and loss of alignment. In contrast, those with Fc and AIP maintain alignment and density. This suggests that Fc and AIP supplement the catalyst and inhibit the thermal aggregation of catalyst particles, respectively. The results of electrical resistance measurements at each forest length will be presented.

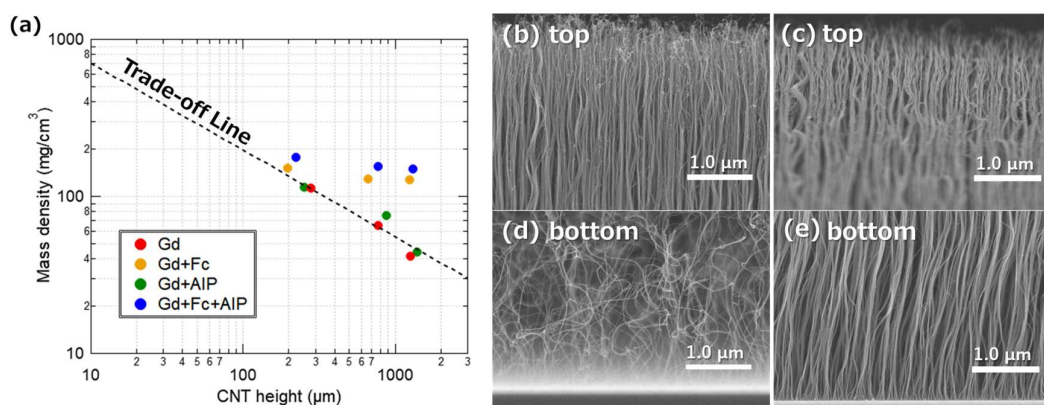


Fig.1 (a) Relationship between mass density and length of CNT forests with Gd+Fc, with Gd+AIP and with Gd+Fc+AIP, and SEM images of CNT forests grown without Fc and AIP (b) top and (d) bottom part, and with Fc and AIP (c) top and (e) bottom part.

References

- [1] K. Tabata et al. *J. Phys. Chem. C* **126**, 20448 (2022).
- [2] H. Sugime et al. *Carbon* **172**, 772-780 (2021).

Ultrafast and CMOS-compatible transfer of carbon nanotube horizontal arrays and other van der Waals materials

Xudong (Sheldon) Zheng¹, Jiangtao Wang¹, Jing Kong¹

¹Massachusetts Institute of Technology (United States)

The preparation of pure semiconducting single-walled carbon nanotube (s-SWCNT) horizontal arrays on silicon wafer is a key limiting factor for their application in high-end electronics and optoelectronics. While high performance s-SWCNT horizontal arrays have been synthesized with semiconducting purity higher than 99.9%, they are usually not directly grown on the functional target substrates. It is critical to transfer the as-grown SWCNTs from growth substrate to target substrate. However, the current transfer methods are far from satisfactory. Due to the use of either chemical etchants or metal support layers, the transfers are either CMOS-incompatible, substrate-nonreusable or low-yield. In this presentation, I will introduce an electrostatic repulsion enabled transfer method that is etching-free, CMOS-compatible, ultrafast, and cost-effective. The detachment of SWCNTs from quartz substrate happens instantly (with less than 5 seconds for 1×1 cm SWCNT arrays). The as-transferred SWCNTs remain aligned with greatly reduced metal/polymer contaminations and transfer-induced defects. In addition, this method is widely applicable to various van der Waals materials (e.g., SWCNTs, MoS₂, graphene, etc.) and substrates (e.g., oxide, nitride, metal, etc.), thus offering a facile and manufacturing-viable solution for the integration of SWCNTs as well as other van der Waals materials for atomically thin electronics.

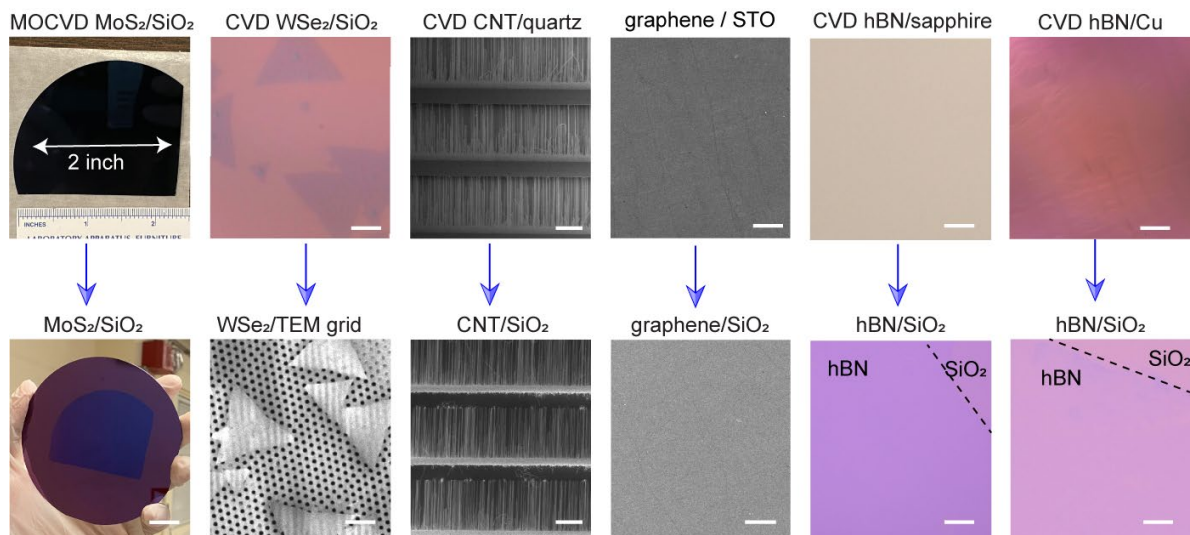


Figure 1: Optical and SEM images of typical vdW materials/substrates before and after the transfer. Scale bars from left to right, 1 mm, 10 μ m, 20 μ m, 5 μ m, 50 μ m, 50 μ m. The top and bottom images in the same column share the same scale bar.

Ultra-thick Carbon Nanotube Fiber and Copper Hybrid wires with a High Electrical Properties

Gwansik Kim¹, Chaeyoon Kim², Kyong Hwa Song¹, Seokmin Lee¹, Eunsoo Shim²,
Deok Woo Yun¹, Jae-Hong Lim²

¹*Electromagnetic Energy Materials Research Team, Hyundai Motor Company (Republic of Korea)*

²*Department of Materials Science and Engineering, Gachon University (Republic of Korea)*

The development of lightweight electronic devices/components are highly required for next generation conductor materials, which have not only a high electrical property but also a low weight load. Carbon nanotube (CNT) is a promising candidate for lightweight conductors due to their low density and excellent electrical and thermal conductivity, and high current carrying capacity. Especially, CNT fiber (CNTF), which is a collection of CNTs aligned along fiber axis, has attracted significant attention as a next generation conductor material for the future electro-thermal applications and advanced energy storage / harvesting devices. However, the electrical properties of macroscopic CNTFs deteriorate by several orders of magnitude due to the large contact resistance between the CNTs. As a result, the electrical conductivity of CNTFs is lower than that of copper (Cu, $5.8 \times 10^7 \text{ S m}^{-1}$), which limits their application in many fields. Therefore, the improvement of the electrical properties for the CNTFs is the great importance and challenging problem.

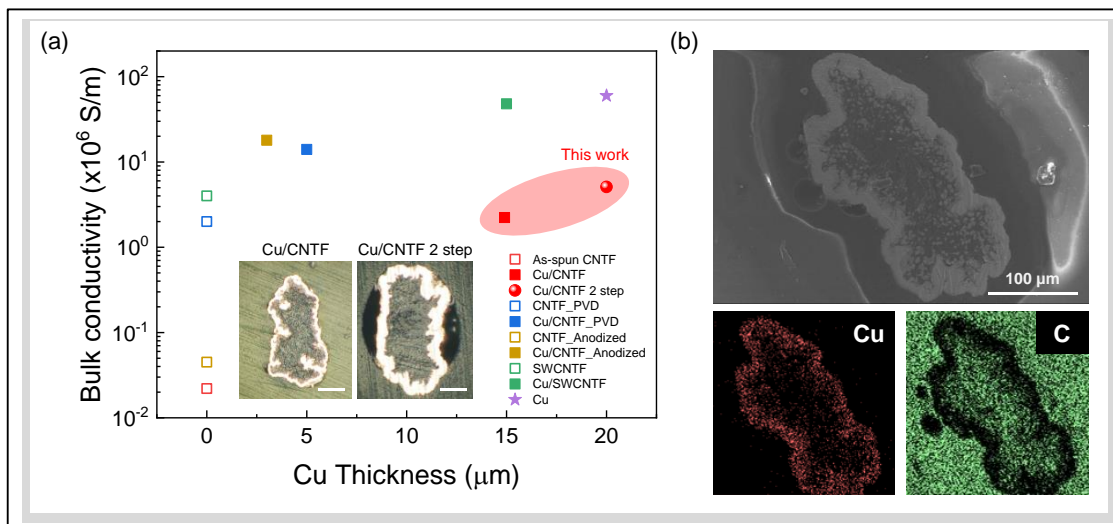
Hybridization of the metal and CNTFs have been considered a novel strategy for solving this problem. This hybrid strategy is the efficiently combination of the lightweight and high current carrying capacity of CNTs and the high conductivity of metals. According to previous reports, various methods including electrochemical deposition, electroless deposition, and physical/chemical vapor deposition have been developed to prepare CNT/Cu hybrid wires. Among the metals (Aluminum (Al), Cu, Silver (Ag), Platinum (Pt), and Gold (Au)) with high electrical conductivity, Cu has been considered suitable candidate for CNTF metallization due to its abundance, stability, and high electrical/thermal conductivity. Moreover, the interfacial modification between the core CNTFs and the shell metal layer was investigated to improve the interfacial interaction for the performance of the hybrid wire. The anodization and functionalization of the CNTFs were performed to improve the adhesion between the Cu layer and CNTs. Additionally, the introduction of the buffer/adhesion layer of Al, Titanium (Ti), Nickel (Ni), and Pt resulted in good affinity for both CNTs and Cu and improved the interfacial bonding.

However, the electrical properties and thickness of the reported metal/CNTF hybrid wires are not still satisfied for use as conductor. Therefore, there is a need to develop an advanced methods to fabricate ultra-thick metal/CNTF hybrid wires with excellent interfacial bonding and electrical properties.

In this study, we investigated an advanced electrochemical deposition to deposit uniform Cu on high-Tex direct-spun CNTF. We obtained ultra-thick CNTF ($\sim 200 \mu\text{m}$) with high-Tex (> 8) and crystallinity ($I_G/I_D \sim 5$) by controlling the reaction condition of the direct spinning, such as the precursor (carbon source, catalyst, promoter, and carrier gas), reaction temperature, furnace type, injection site, and production rate. Unlike wet-spun CNTF, high-Tex direct-spun CNTF had the rough surface, nano/micro size pores and the various functional group on the surface. Therefore, it is necessary to manipulate the additive agents (Suppressor, Accelerator, and leveler) for the modification of the interfacial interaction and morphology of the hybrid wires. By optimizing the electrochemical deposition conditions (additive agent, voltage, and coulomb), we were able to obtain a Cu/CNTF hybrid wires in which the internal pores were filled with Cu and the CNTF surface roughness was alleviated (Figure 1 (b)). The hybrid wires had a high electrical conductivity of $5.1 \times 10^6 \text{ S m}^{-1}$, which is 230 times higher than as-spun CNTF without considering pores area (Figure 1 (a)). Moreover, the current carrying capacity of the hybrid wire reached $1.17 \times 10^4 \text{ A cm}^{-2}$, which is 10 times of that of as-spun CNTF ($1.20 \times 10^3 \text{ A cm}^{-2}$). Although the electrical properties of the hybrid wire were lower than that of the commercial Cu wire ($5.8 \times 10^7 \text{ S m}^{-1}$ and $4.72 \times 10^4 \text{ A cm}^{-2}$), we expect to significantly improve the electrical properties of the ultra-thick hybrid wire by optimizing the materials design, interfacial bonding, and Cu shell properties (density, grain size, and crystal orientation).

This work is the first report for the ultra-thick ($\sim 200 \mu\text{m}$) Cu/CNTF hybrid wires by using

advanced electrochemical deposition process. The large diameter (high thickness) wires are advantageous for wire insulation or coating processes because they do not require a braiding process, which improve the stability of the wire because the air pores inside insulation are removed. Therefore, there is a significantly need to develop ultra-thick (>300 μm) Cu/CNTF hybrid wire with the good electrical properties.



References (if desired)

- [1] L. L. Xu *et al.*, *ACS Nano* **17**, 9245–9254 (2023).
- [2] G. J. Wang *et al.*, *Nano Lett.* **19**, 6255–6262 (2019).
- [3] A. P. Leggiero *et al.*, *Carbon* **168**, 290-301 (2020)
- [4] G. J. Wang *et al.*, *Carbon* **146**, 293-300 (2019).
- [5] C. Subramaniam *et al.*, *Nat. Commun.* **4**, 2202 (2013)
- [6] J. Zou *et al.*, *ACS Appl. Mater. Interfaces* **10**, 8197-8204 (2018)
- [7] A. P. Leggiero *et al.*, *ACS Appl. Nano Mater.* **2**, 118-126 (2019)
- [8] F. Daneshvar *et al.*, *Adv. Mater. Interfaces* **7**, 2000779 (2020)
- [9] M. B. Bazbouz *et al.*, *Adv. Electron. Mater.* **7**, 2001213 (2021)
- [10] D. J. McIntyre *et al.*, *J. Mater. Sci.* **55**, 6610-6622 (2020)

Unlocking the Potential of Phenanthroimidazole-based Bipolar Derivatives for High-performance Blue-Emitting OLEDs

A. Pidluzhna¹, A. Vembris¹, R. Grzibovskis¹

¹ *Institute of Solid State Physics, University of Latvia (Latvia)*

This study focuses on the photophysical and photoelectrical properties of carefully synthesized bipolar derivatives based on phenanthroimidazole, with the objective of their integration into OLEDs. By incorporating carbazolyl and diphenylamino substituents, these derivatives exhibit impressive blue-emitting characteristics in solid-state, with photoluminescence quantum yields ranging from 11% to 22%. When used in combination with CBP, these phenanthroimidazole-based derivatives facilitate the generation of deep blue exciplex emission within OLEDs. Additionally, the synthesized compounds demonstrate intriguing electroplex formation. These findings underscore the significant potential of the synthesized bipolar phenanthroimidazole-based derivatives in advancing efficient blue-emitting OLEDs. The combination of their efficient blue emission, favorable charge transport properties, and compatibility with CBP opens doors to exciting prospects in future OLED technologies. The utilization of these materials holds promise for advancements in display and lighting solutions, enabling captivating visual experiences, improved energy efficiency, and technological progress.

Key words: Blue-emission, OLEDs, Phenanthroimidazole derivatives.

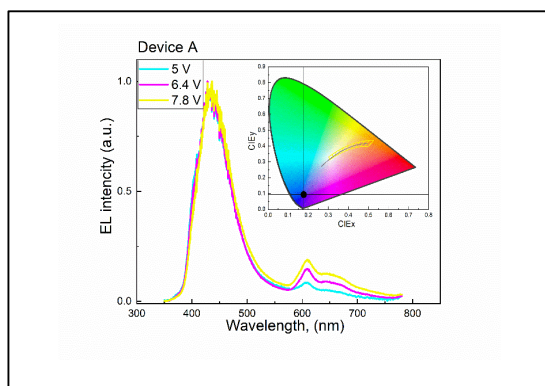


Figure. The EL spectra of the Device A at the different applied voltages and CIE1931 chromaticity diagram (inset)

Unlocking the Role of Sulfur in Carbon Nanotube Synthesis

Ghulam Yasin¹, Hirotaka Inoue^{1,2}, Anastasios Karakassides¹, Hua Jiang¹, Esko I. Kauppinen¹

¹ Aalto University (Finland), ² Sumitomo Electric Industries (Japan)

Since their discovery, carbon nanotubes (CNTs) possess a variety of promising structural characteristics and functional properties, enabling numerous applications in various fields, and have been shown potential currently in commercial uses [1]. Several synthesis strategies such as laser ablation, arc discharge, flame process, chemical vapor deposition (CVD), and so on, have been employed to prepare CNTs. Among them, the floating catalyst CVD (FCCVD) approach is considered the most potential candidate for the high-quality and large-scale production of CNTs [2]. To develop a scalable and controllable FCCVD approach, it is imperative to realize the mechanism of CNT growth and how the various synthesis conditions and parameters affect the overall production process [3,4].

Therefore, the addition of sulfur and/or sulfur-containing compounds is an important strategy to tune the growth and characteristics of CNTs, because sulfur-containing compounds can promote the growth of CNTs and thereby influence their structure and properties, such as, yield, length, diameter, and sheet resistance of the CNTs. We investigate the effect of sulfur content and different types of sulfur-containing compounds on the growth and corresponding characteristics of CNTs, typically in the FCCVD method. Sulfur could influence the interaction between catalyst particles and CNTs, enabling a favorable impact as a promoter role on the growth and conceded characteristics of CNTs. We believe that these findings will open a new avenue in the optimization and scalable synthesis of high-quality CNTs for impending functional applications and technologies.

References

- [1] A. Cao *et al.*, *ACS Nano* **15**, 7946–7974 (2021).
- [2] E. I. Kauppinen *et al.*, *Chem. Eng. J.* **378**, 122010 (2019).
- [3] A. G. Nasibulin *et al.*, *Carbon* **210**, 118051 (2023).
- [4] E. I. Kauppinen *et al.*, *J. Am. Chem. Soc.* **133**, 1224–1227 (2011).

Variable-amplitude fatigue testing of aerospace-grade composites reinforced with aligned carbon nanotube interlayers

V. Saseendran¹, C. X. Li², C.E. Bakis¹, N. Yamamoto¹, and B.L. Wardle²

¹Pennsylvania State University (USA), and ²Massachusetts Institute of Technology (USA)

The fatigue behavior of aerospace-grade carbon fiber reinforced polymer (CFRP) composite laminates with carbon nanotube (CNT) reinforced interlayers will be studied under variable-amplitude (VA) fatigue loading. Studying the fatigue behavior of CFRP composites is essential to predict and extend the lifespan of advanced aircraft. Traditionally, fatigue studies on composites have been conducted empirically, heavily relying on constant-amplitude (CA) fatigue data as has been the case with metals. However, the fatigue damage development process in CFRPs is more complex than in metals due to a wide range of damage modes such as matrix crack, delamination, and fiber fracture, and the complex interactions between these damage modes [1]. In addition, real-life structures experience not CA loading but VA loadings. Studies on VA fatigue testing of open-hole CFRP specimens exhibited loading sequence dependence; for example, less damage was observed when high-load was applied first [2]. Further investigation of CFRPs under VA fatigue loading can potentially overcome the currently over-conservative use of these materials and allow for the design of safe aircraft with improved performance metrics such as fuel burn, payload, and range.

Separately, the effectiveness of adding CNTs to CFRPs for improving fatigue behavior has been demonstrated experimentally [3-6]. For example, the number of cycles to failure was increased by 249% from integration of CNT forest (~1 vol%) between prepregs under a loading that was 60% of the static strength [3]. CNTs, or other stiff nanoparticles, in the presence of fibers, restrained formation and growth of inter-fiber fracture [5]. These promising data are so far obtained only under CA fatigue loading.

In this work, short-beam specimens of [45/0/-45/90]_{2s} AS4/8552 carbon/epoxy with vertically aligned CNTs at the interlayers, manufactured following the same process developed in the past [3] will be tested in VA flexural fatigue and compared to baseline specimens without CNTs. The specimen shape and loading configuration are adopted from the ASTM D2344 standard for quasi-static testing for interlaminar shear strength. VA loading will be a sequence of a low loading step (60% of the static SBS strength) followed by (or preceded by) a high loading (70% of the static short beam strength). The duration of each loading step will be set based on past CA loading tests. At various times during fatigue testing, specimens will be microCT scanned to characterize damage development. This work will provide the first VA fatigue test data on CNT-reinforced CFRPs, providing new insights on the effects of CNTs on the fatigue behavior of CFRPs.

References

1. Talreja, R.;Singh, C.V., *Damage and Failure of Composite Materials*. Cambridge University Press, 2012.
2. Found, M.;Quaresimin, M., *Fatigue Damage of Carbon Fibre Reinforced Laminates under Two-Stage Loading, in Experimental Techniques and Design in Composite Materials*. 2017, Routledge. p. 15-22.
3. Ni, X.;Furtado, C.;Kalfon-Cohen, E.;Zhou, Y.;Valdes, G.A.;Hank, T.J.;Camanho, P.P.;Wardle, B.L., "Static and Fatigue Interlaminar Shear Reinforcement in Aligned Carbon Nanotube-Reinforced Hierarchical Advanced Composites." *Composites Part A: Applied Science and Manufacturing*, Vol.120, No., 2019. pp. 106-115.
4. Davis, D.C.;Wilkerson, J.W.;Zhu, J.;Ayewah, D.O., "Improvements in Mechanical Properties of a Carbon Fiber Epoxy Composite Using Nanotube Science and Technology." *Composite Structures*, Vol.92, No.11, 2010. pp. 2653-2662.
5. Knoll, J.;Riecken, B.T.;Kosmann, N.;Chandrasekaran, S.;Schulte, K.;Fiedler, B., "The Effect of Carbon Nanoparticles on the Fatigue Performance of Carbon Fibre Reinforced Epoxy." *Composites Part A: Applied Science and Manufacturing*, Vol.67, No., 2014. pp. 233-240.
6. Boroujeni, A.Y.;Al-Haik, M., "Carbon Nanotube–Carbon Fiber Reinforced Polymer Composites with Extended Fatigue Life." *Composites Part B: Engineering*, Vol.164, No., 2019. pp. 537-545.

Vertically Aligned Carbon Nanotubes as Toughening Interleaves for Advanced Composite Manufacturing

Thomas GOISLARD de MONSABERT¹, Aurélien BOISSET¹, Blagoj KARAKASHOV¹, Kevin RETZ², Lingchuan LI³, Paul KLADITIS³

¹*NawaTechnologies, Rousset, France*

²*Nawa America, Dayton (OH), USA*

³*University of Dayton Research Institute, Dayton (OH), USA*

Vertically aligned carbon nanotubes (VACNT) have proven to be an efficient additive to reinforce carbon fiber reinforced polymers (CFRP) composite materials when inserted in the interply region of laminated parts [1, 2].

A classical way to integrate such reinforcing nanoengineered layer at the interface between plies is to mechanically transfer the VACNT film from its original support (used during the synthesis step by catalytic CVD [3]) onto the surface of a carbon fiber ply pre-impregnated with resin, the rest of the composite manufacturing process remaining unchanged. However, although simple and straightforward, this approach reveals to be limiting for a cost-effective spread of this technology to the industry.

Instead, a self-supported film being fully integrable to the final CFRP structure as an interleave would be a solution of choice allowing for easy supply and transparent insertion in the current manufacturing processes of advanced laminate composite parts.

Here, we report several strategies recently tested at NAWA to develop such a system, emphasizing the pros and cons of various support materials including thermoplastic and thermosetting polymers, their ability to host the VACNT layer, their compatibility with epoxy matrix, the transfer process they permit and their efficiency to reinforce the mechanical properties of laminated composites.

References

- [1] X. Ni et al, “Static and fatigue interlaminar shear reinforcement in aligned carbon nanotube-reinforced hierarchical advanced composites”, *Composites Part A* 120 (2019) 106–115
- [2] R. Li et al, “Strength and Life Enhancement of Vertically-Aligned Carbon Nanotube (VACNT)-Reinforced Composite Aerostructures”, presentation at ICCM 2023 conference, Belfast, UK
- [3] T. Goislard et al, “Large scale synthesis of Vertically Aligned Carbon Nanotubes on Metal Foils”, poster at NT’23 conference, Arcachon, France

Visualizing Living Cells and Nanoparticles via Total Internal Reflection Scattering Device

Cheng-An J. Lin^{1,2*}, Tzu-Yin Hou¹, You-Wei Li¹, Pin-Jun Liao¹, Yu-Wen Xu¹

¹Department of Biomedical Engineering, Chung Yuan Christian University (Taiwan, R.O.C),

²Center for Biomedical Engineering in Cancer, Chung Yuan Christian University (Taiwan, R.O.C)

*Email : chengan_lin@cycu.edu.tw

The design of a nanoscope is a unique specification in the field of optical microscopy, with only a few laboratories possessing the equipment to conduct nanomaterials analysis. With the flourishing development of the biomedical nanotechnology, the demand for on-site observation of nanomaterials and/or their dynamic interaction with cells through optical microscopy has become essential. Current techniques such as specified darkfield condenser from CytoViva or Nanoparticle Tracking Analysis from NanoSight, have provide the opportunity to meet this demand through the principle of dark-field microscopy. However, due to their specialized design, high prices, limited field of view, cumbersome sample preparation processes, and the need to use immersion oil etc., they fail to meet the most immediate observation and quantification needs of the scientific research. We have successfully developed a patented prototype of a nanoscopic optical module¹, which discards the framework of traditional dark-field condensers and instead uses the principle of total internal reflection scattering (TIRS) to make nanoscale samples visible and free of dead angles on conventional optical microscopes (Figure 1). Living cells and nanoparticles can simultaneously observed on a cell culture dish by using the adapted TIRS optical module. The tiny pseudopodia can be clearly identified and monitored on the traditional microscope. This innovative device was awarded the Platinum Award at the 2023 Taiwan Innotech Expo Competition². We continue to focus on addressing the needs of nanomaterials research and developing visualization techniques based on the Total Internal Reflection Scattering (TIRS) principle.

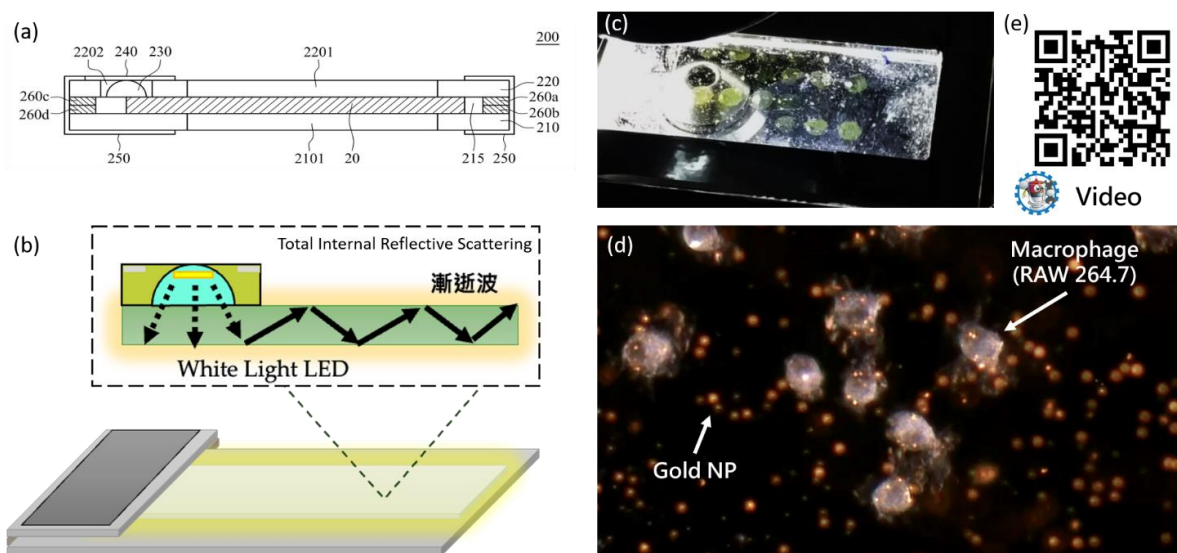


Figure 1: Total Internal Reflection Scattering Device. (a, b) illustration of TIRS illumination (c) illuminating the 50 nm gold nanoparticles array by TIRS device and (d) direct monitoring the interaction of living macrophage with 80 nm gold nanoparticles through TIRS illumination.

References

- [1] Lin, C.-A.; Hou, T.-Y.; Li, Y.-W.; Tsai, Y.-S.; Wang, M.-C. Device and Method for Performing Total Internal Reflection Scattering Measurement. US Patent Application No. 17/710,103, 2023. Taiwan Patent: I798041, 2023/04/01~2042/3/30
- [2] <https://www.inventaipei.com.tw/zh-tw/menu/379C8F72C52EC843D0636733C6861689/info.html>

Wafer-Scale Fabrication of Wearable All-Carbon Nanotube Photodetector Arrays

P. Liu^{1,*}, E.R. Ding¹, Q. Zhang¹, Z.P. Sun¹, E.I. Kauppinen¹

¹Aalto University - Espoo (Finland)

*Email: peng.l.liu@aalto.fi

The landscape of traditional electronics is evolving from bulky solid-state to portable, high-performance, multi-function, and flexible/wearable devices.^[1,2] Carbon nanotubes (CNTs) are ideal materials for flexible electronics due to their quasi-one-dimensional topology and unique properties, such as high intrinsic carrier mobility, electrical conductivity, mechanical flexibility, good chemical stability, and the potential for low-cost as well as wafer-scale production.^[3,4] However, the current research on CNTs in flexible electronics is still in the stage of partial component substitution. The research and fabrication on all-carbon nanotube (all-CNT) devices, constructed entirely from CNTs, remains relatively scarce, especially in-depth investigations and fabrication of flexible all-CNT devices.

Here, we introduce a scalable photolithography-free dry method to fabricate wearable all-CNT photodetector device arrays. Specifically, laser-assisted patterning and dry deposition techniques were used to assemble gas-phase CNTs into device arrays directly. Double-walled CNTs (DWCNTs)^[3] with high conductivity are used as flexible electrodes. Semiconductor-enriched SWCNTs^[4] showing high on/off current ratios in TFT-FET setting serve as the channel material. The wafer-scale all-CNT device arrays exhibit excellent uniformity, multifunctionality, good ohmic contact characteristics, wearability, transparency, and environmental stability. Furthermore, the wearable photodetector shows outstanding optoelectronic properties with a high responsivity of 44 A W^{-1} and an exceptional detectivity of 4.3×10^{11} Jones in the visible region. An exceptional responsivity of 2 A W^{-1} and an excellent detectivity of 1.6×10^{10} Jones at telecommunication wavelength has been achieved. This research provides an efficient, versatile, and scalable strategy for manufacturing wearable all-CNT device arrays, allowing a widespread adoption in wearable optoelectronics and multifunctional sensors.

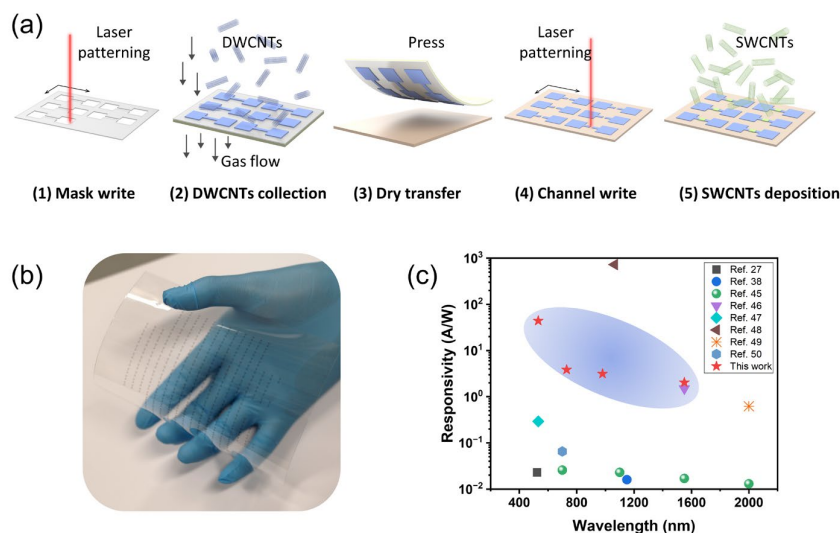


Figure 1. (a) Schematic of the preparation of all-CNT devices. The sizes of the components in the schematic are not actual proportions. (b) Optical images of wafer-scale all-CNT device arrays under bending states. (c) Comparison of the responsivity of all-CNT photodetectors with previously reported CNT-based photodetectors.

References

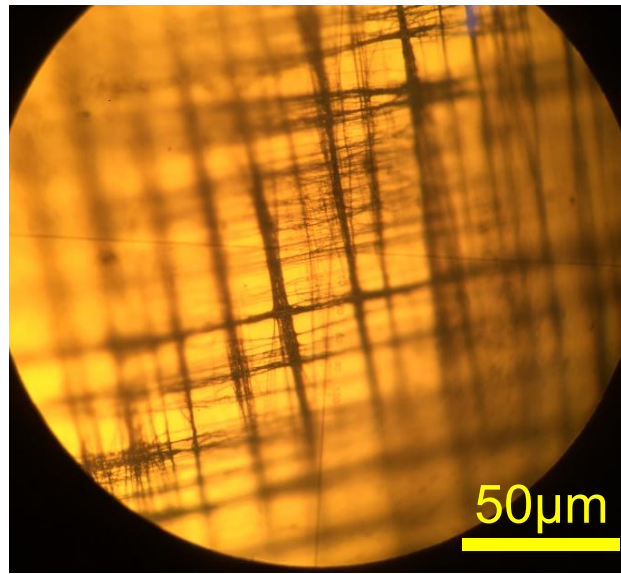
- [1] J. H. Koo *et al.*, *ACS Nano* **11**, 10032–10041 (2017).
- [2] H. C. Ates *et al.*, *Nat. Rev. Mater.* **7**, 887-907 (2022).
- [3] Q. Zhang *et al.*, *Adv. Funct. Mater.* **32**, 2103397 (2022).
- [4] P. Liu *et al.*, *Adv. Electron. Mater.* **9**, 2300196 (2023).

X-ray filter based on SACNT film

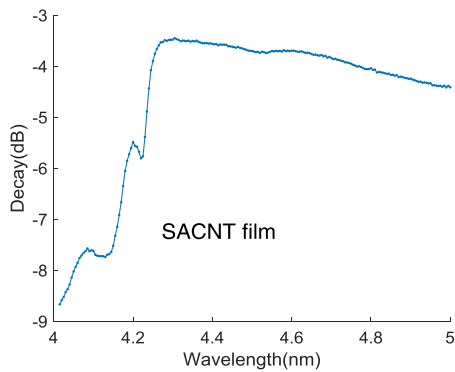
Zi Yuan¹, Kaili Jiang¹

¹Department of Physics, Tsinghua University (China)

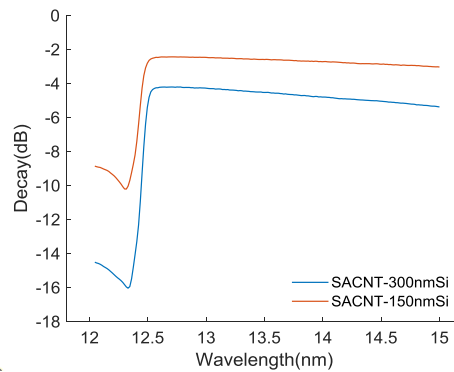
In this work, we prepared a series of X-ray filter based on SuperAligned Carbon Nanotube (SACNT) films. The filter is composed of SACNT films and elements that filter X-rays. Due to the high strength of SACNT film, the composite films can freestanding while having a nanoscale thickness. And diameter of the filter can reach several centimeters. Compared to existing X-ray filters based on nickel metal mesh, our filter has a higher transmittance area ratio and higher mechanical strength. The thickness of the filter can range from 10nm to several micrometers. The elements for filtering X-rays can be selected as carbon, silicon, gold, platinum, zirconium, molybdenum, etc.



(a)



(b)



(c)

a. 20nm gold film on SACNT film **b.** X-ray absorption edge of SACNT film **c.** X-ray absorption edge of 150nm and 300nm silicon film on SACNT film

Author Index

A

Abot, Jandro	105, 233
Acauan, Luiz	96, 104, 135, 142, 152, 188, 202, 237
AGUILAR, Alberto	117
Akada, Keishi.....	61
Akita, Seiji	208
Algan Simsek, Irem	229
Allam, Nageh	83
Alrai, Adel.....	214
Alvarez, Noe	54, 154
Alves da Silva, Leticia	149
Amjad, Zunaira	220
Ando, Yasunobu	156
Andrieux-Ledier, Amandine	80
Ang, Mervin.....	244
Ang, Mervin Chun-Yi.....	87
Antezza, Mauro.....	166
Ao, Geyou.....	276
Apaydin, Dogukan	109
Arenal, Raul	197
Arévalo, Luis.....	221
Arie, Takayuki	208
Arnold, Christophe.....	71, 80
Arnold, Michael	42, 213
Arnold, Michael S.....	195
Ashino, Makoto.....	189
Aso, Shuhei.....	211
Audebert, Pierre	171
Avouris, Phaedon.....	297

B

Badr, Hussein.....	203, 224, 229, 249
Bai, Jinbo	97
Bai, Lan.....	298
Bakis, Charles	305
Balaguera, Camilo.....	81
Banash, Mark	23
Barajas-Aguilar, Aaron	278
Barjon, Julien	71, 80, 107
Barsoum, Michel.....	22, 182, 203, 224, 229, 249
Baumgartner, Bodo	109
Baydin, Andrey	93, 200
Bayer, Bernhard	109, 206
Bediako, D. Kwabena	58
Beidaghi, Majid.....	69

Benavides Figueroa, Ana Victoria..	176, 179, 253
Berson, Arganthaël	42
Bets, Ksenia	39, 52, 271
Bianco, Alberto.....	114
Bichara, Christophe.....	12, 157
Bilotti, Emiliano.....	245
Bischoff, Darren.....	20
Blacha, Anna.....	171
Blankschtein, Daniel.....	19, 35, 185, 292
Blümel, Alexander	109
Bogani, Lapo.....	92
Boghossian, Ardemis	13
Boies, Adam.....	38, 108
BOISSET, Aurélien	306
BON, Pierre.....	117
Boncel, Slawomir.....	198, 220, 236
Boncel, Sławomir.....	168, 171, 209, 277, 282
Bondarev, Igor	166, 263
Borin Barin, Gabriela.....	119
Böttger, Simon	150, 186
Botura, Galdemir.....	32
Bracconi, Mauro	16
Brems, Steven	195
Brookes, Paul	20
Brooks, A. Merritt.....	132
Buchsbaum, Steven.....	18
Buffy, Jarrod	177
Bunkov, Alexey	261
Bystricky, Pavel	9

C

Cadranel, Alejandro	247
Cambré, Sofie	170, 230
Canaval, Johans.....	81
CANDELA, MARINA	296
Cao, Ethan.....	278
Cao, Jun.....	153
Cao, Ting.....	151
Card, Matthew.....	28
Carpena-Nuñez, Jennifer.....	36
Carré, Etienne	107
Carreno, Marcelo	233
casiraghi, cinzia.....	15
Castro Lopez, Natalia.....	212
Cebeci, Fevzi.....	214

Cebeci, Hulya.....	214
Cerruti, Marta.....	125
Chae, Jinwoong.....	183
Chaloin, Olivier.....	114
Champi, Ana.....	101
Chang, Ting-Wei.....	139
Chang, Wen Hsin.....	156
Chang, Young Jun.....	178
Chang, Yung.....	24
Chatterjee, Arka.....	65
Chen, Guo.....	145
Chen, Shaochuang.....	274
Chen, Yuan.....	53
Chen, YuFeng (Kevin).....	204
Cheng, Hui-Ming.....	46, 82, 234
Cheng, Ting.....	52, 271
Chiashi, Shohei.....	170, 196, 230
Cho, Sooyeon.....	25
Choi, In-Seung.....	191
Chua, Nam-Hai.....	244
Cohen, Assael.....	197
Cope, Jacob.....	182
Cruz Silva, Rodolfo.....	84
Cruz-Silva, Rodolfo.....	270
Cui, Jianqiao.....	244
Cunha, Carlos R.....	195

D

Dai, Jingyao.....	96, 104, 148, 152, 177, 188
Dai, Wanyu.....	43, 170, 286
Dale, Kathryn.....	253
Dantzler, Alex.....	146, 253
Davis, Virginia.....	69
Davletkhanov, Ayvaz.....	261
de Isidro-Gómez, Ana.....	280
de la Rosa, Cesar J. L.....	195
de Marneffe, Jean-Francois.....	195
Decams, Jean-Manuel.....	80
Dehm, Simone.....	7
Dei, Hillel.....	135
Deng, Fei.....	217
Desai, Darash.....	131
Dewey, Oliver.....	93, 111, 146, 253
Dey, Prasanjit.....	259
Ding, Erxiong.....	308
Ding, Er-Xiong.....	103

Ding, Feng.....	45
Doumani, Jacques.....	93, 139, 200
Dublak, Bruno.....	107
Ducastelle, François.....	71, 80
Duran Chaves, Michelle.....	253
Duran-Chaves, Michelle.....	111
Durso, Michael.....	254
Dzienia, Andrzej.....	70, 293
Dzombic, Nina.....	276

E

Eckstein, Klaus.....	120
Eder, Dominik.....	109, 206
El Abbassi, Maria.....	29
Eller, Benjamin.....	31
Elliott, James.....	75
Endo, Morinobu.....	84, 270
Endo, Tsuyoshi.....	196
Ernst, Martin.....	186

F

Fajardo Diaz, Juan.....	84, 84
Fajardo-Diaz, Juan.....	270
Fan, Jichao.....	93, 260
FANARRAGA, MONICA.....	296
Fang, Jen-Hung.....	202
Feng, Xinliang.....	92
Feng, Ya.....	170, 230
Feria Garnica, Deissy.....	233
Fickl, Bernhard.....	206
FIROUZEH, SEYEDAMIN.....	265
Foradori, Sean.....	42
Fornasiero, Francesco.....	18, 223
Fossard, Frédéric.....	80, 107
Franklin, Aaron.....	55
Fujimori, Toshihiko.....	61, 291
Fujita, Jun-icuh.....	61
Futaba, Don.....	258

G

Gailus, David.....	23
Gao, Hongze.....	153
Gao, Weilu.....	93, 200
Garcia Guerra, Iriana.....	233
GARCIA HEVIA, LORENA.....	296
García Hevia, Lorena.....	114

Gasimli, Ali.....	136
Gaufres, Etienne.....	107, 117
Gerein, Kevin.....	238
Ghiassi, Hossein.....	20
Ghosh, Aniruddha.....	202
Girao, Eduardo.....	76
Giudici, Clarissa.....	16, 219
Giwa, Ibraheem.....	201
Gladush, Yuriy.....	261
Glerum, Michael.....	108
Godwin, Anto.....	140
GOISLARD DE MONSABERT, Thomas	306
Goislard, Thomas.....	34
Gong, Mingrui.....	176, 179, 253
Gonzalez, Erick.....	152
GONZALEZ, JESUS.....	296
González, Jesús.....	114
Gorsse, Stephane.....	36
Goto, Sota.....	299
Goto, Takuma.....	30
Green, Micah.....	184, 221
Grigorieva, Irina.....	62
Grzibovskis, Raitis.....	303
Guevara-Vela, José M.....	289
Guldi, Dirk.....	247
Guo, Yunfan.....	151
Gupta, Amar.....	131
Gupta, Rajiv.....	131

H

Han, Bing.....	288
Hansen, Thomas.....	82
Harkin, Ethan.....	184
Hart, Anastasios.....	254
Hartmann, Martin.....	150, 186
Harutyunyan, Avetik.....	37, 255
Hayashi, Kosuke.....	281
Hayashi, Yasuhiko.....	211
He, Delong.....	97
He, Ziyang.....	264
Headrick, Robert.....	146
Hecla, Jake.....	131
Hedman, Daniel.....	26, 157
Heller, Daniel.....	11
Hennrich, Frank.....	7

Heo, So Jeong.....	242
Heppe, Brandon.....	276
Hermann, Sascha.....	149, 150, 186
Hernandez, Yenny.....	81
Hertel, Tobias.....	120
Hettler, Simon.....	197
Hibbard, Mark.....	23
Hioki, Yasunori.....	203
Hisama, Kaoru.....	129
Ho, Ching-Hwa.....	192
Hofer, Markus.....	109
Hong, Hyunsoo.....	188
Hong, Nina.....	93, 200
Horezan, Nicolas.....	107
Hossain, Md Anik.....	161
Hou, Tzu-Yin.....	307
Hrdá, Jana.....	252
Hu, Chechia.....	24
Hu, Guohua.....	163
Hu, Qingmei.....	170, 230
HUANG, Ben.....	256
Huang, Shengxi.....	65, 151
Hubert, Lauren.....	28
Hughes, Thomas.....	285
Hulman, Martin.....	252
Hussain, Aqeel.....	124
Hwang, Seongjoo.....	191

I

Ibrahim, Mohamed.....	203
Iervolino, Filippo.....	109
Iizumi, Yoko.....	258
Ikeda, Hiroya.....	294
Ikuhara, Yuichi.....	286
Inoue, Hirotaka.....	61, 290, 291, 304
Inoue, Hisashi.....	155
Inoue, Taiki.....	222
Inoue, Yoku.....	281, 294, 299
Irisawa, Toshifumi.....	156
Irvin, Glen.....	137, 146, 176, 179
Ishizeki, Keisuke.....	217
Ismach, Ariel.....	197
Iverson, Nicole.....	89, 133

J

Jagani, Shaan.....	96, 104, 135
--------------------	--------------

Jamieson, Amanda122
 Janas, Dawid70, 205, 207, 293
 Jaramillo, Rafael138
 Jarillo-Herrero, Pablo.....5
 Jędrysiak, Rafał.....168, 277
 Jeong, Jae-Moon188
 Jeong, Kwang Il188
 Jeong, Samuel61
 Jiang, Chaoran.....127
 Jiang, Hua158, 290, 291, 304
 Jiang, Kaili235
 Jiang, Kuiyang74
 Jinkins, Katherine R.....195
 Joo, Sang.....251
 Ju, Sang-Yong.....191, 241
 Ju, Yuchen.....269
 Jue, Melinda.....18
 Junnarkar, Jui137, 179
 Just, Dominik70, 207, 293

K

Kacica, Clay137
 Kaiser, Ashley.....128
 Kaiser, Ute2
 Kajale, Shivam98
 Kalfon Cohen, Estelle32, 237
 Kaneda, Ryotaro170, 196
 Kang, Byungha132
 Kang, Yoonbeen241
 Kappes, Manfred.....7
 Kar, Gouri S.195
 KARAKASHOV, Blagoj.....306
 Karakasidis, Anastasios290
 Karakassides, Anastasios158, 291, 304
 Karnik, Rohit.....57
 Kataura, Hiromichi99, 165
 Katsufuji, Takuro155
 Kauppinen, Esko86, 158, 181, 286, 290,
 291, 304, 308
 Kauppinen, Esko I.....103
 Kavokine, Nikita79
 Keil, Joseph.....276
 Kempainen, Josh.....8
 Kessler, Seth32, 173, 237
 Khabushev, Eldar67, 137, 176
 Khaliji, Kaveh.....297
 Khan, Abu181
 Khoury, Joe231
 Kidambi, Piran21
 Kilic, Ufuk133
 Kilin, Dmitri.....123, 246
 Kilina, Svetlana.....272
 Kim, Chae Won118
 Kim, Chaeyoon301
 Kim, Gunn.....183
 Kim, Gwansik301
 Kim, Hyuk Jin.....178
 Kim, Junghwan118, 242
 Kim, Ki Kang.....59
 Kim, Mijin.....187
 Kim, Seo Gyun.....118, 242
 Kim, Seong Su188
 Kim, Steven.....177
 Kim, Suhan204
 Kim, Youngwook.....115
 Kindopp, Aidan.....122
 Kitagawa, Hiroshi273
 Kizhakke Veetil, Abhindev.....187
 KLADITIS, Paul306
 Klein, Julian72
 Kloza, Philipp75
 Kobayashi, Yoshihiro222
 Kohata, Ikuma.....129
 Köken, Deniz214
 Kolanowska, Anna.....198
 Kollosche, Matthias20, 100
 Komatsu, Natsumi.....111
 Kong, Fanmiao.....92
 Kong, Jing.....151, 262, 300
 Kono, Junichiro.....93, 111, 139, 200
 Koo, Joseph.....177
 Korczeniewski, Emil.....209, 282
 Koshino, Mikito115
 Kou, Tongtong180
 Krull, Wolfgana131
 Krupke, Ralph.....7
 Kruss, Sebastian.....27, 257
 Ku, Bon-Cheol118, 242
 Kubo, Toshitaka156
 Kukowski, Tom.....9
 Kumamoto, Akihito286
 Kumar, S112

Kurian, Eldho140
Kurono, Haruto294
Kusada, Kohei.....273
Kuznetsov, Oleg.....255

L

L Fanarraga, Mónica.....114, 114
Lado, Jose49
Lamparski, Michael119
Lan, Yun-Xiang275
Lashmore, David.....9
Lee, Chang Young164, 226, 267
Lee, Cheongha164, 267
Lee, Dongju.....118
Lee, Seokmin301
Lee, Seongwoo.....164
Lei, Jincheng.....39
Lekawa-Raus, Agnieszka.....199, 287
Lepak-Kuc, Sandra287
Li, Carina148, 152, 305
Li, Han47
Li, Lingchuan.....306
Li, Mingda.....98
Li, Min-Ken7
Li, Shengman68
Li, Xiaochen.....104
Li, Xinyue284
Li, Xufan.....37
Li, Yan130, 159, 162, 174, 218, 274
Li, You-Wei307
Li, Yue85, 167, 190
Li, Zhikai.....61
Liang, Liangbo.....119
Liao, Pin-Jun.....307
Lim, Jae-Hong.....301
Lim, Seongyeop164
Lin, Cheng-An307
Lin, Ching-Wei88
Lin, Dennis.....195
Lin, Yen-Hsuan.....88
Lin, Yung-Chang156
Lin, Yuxuan Cosmi.....50
Lin, Yuying.....148, 152
Ling, Xi.....153
Lipsanen, Harri103
Liu, Bilu46, 234

Liu, Chang.....82
Liu, Huaping66, 160
Liu, Lijun195
Liu, Peng.....103, 308
Liu, Songwei.....163
Liu, Te-I88
Liu, Wei-Ren.....193
Liu, Xu162
Liu, Yang163
Liu, Zhenjing.....138
Loiseau, Annick71, 80, 107, 117
Lou, Minhan.....93
Lourenço, Leandro247
Low, Tony.....297

Łukawski, Damian199

Luo, Shuang35, 292
Lusson, Alain107
Lv, Zhou.....190
Lyles, Nyvia.....135
Lyons, Sarah122

M

Ma, Ji.....92, 92
Mack, Elena247
Madrona, Cristina289
MAE, Tomotaro256
Maestri, Matteo16, 219
Maggay, Irish24
Mafecka, Magdalena282
Mana, Luca195
MARCEAU, Jean-Baptiste.....117
Marek, Adam236, 282
MARTEL, Richard117
Marti, Angel.....231
Martinez-Iniesta, Armando.....84
Martin-Moreno, Luis.....297
Maruyama, Benji.....36
Maruyama, Mina.....286
Maruyama, Shigeo43, 129, 135, 170, 196,
230, 286
MARUYAMA, TAKAHIRO273
Masic, Admir228
Matsuda, Kazunari165
Matsumura, Tarojiro156

Matsuo, Yutaka	230
Matsuoka, Shu	273
Matuszewski, Michael	9
Mawire, Elton	201
McLean, Ben	268
Meidl, Rachel	51
Mekunye, Francis	69
Ménard-Moyon, Cécilia	114
Mérot, Jean-Sébastien	80
Meunier, Vincent	76, 119
Mikawa, Ryosuke	155
Mikhalchan, Anastasiia	221
Miller, Norah	177
Misra, Rahul	19, 292
Misra, Rahul Prasanna	35, 185
Miyauchi, Yuhei	165
Mkrtchyan, Aram	261
Mohapatra, Pranab	197
Molinari, Elisa	95
Moon, Pilkyung	115
Moon, Sook Young	102
Morelos-Gomez, Aaron	270
Mori, Kunio	170
Moulton, Tim	131
Moyer-Vanderburgh, Kathleen	18, 223
Murray, Karalyn	285
Mustonen, Kimmo	181
Muto, Dai	99

N

Nadeem, Aceer	122
Nakanishi, Takeshi	156
Nakano, Takayuki	281, 294, 299
Nallapureddy, Jyothi	251
Nallapureddy, Ramesh Reddy	251
Nannuri, Shivananad	140
Nasibulin, Albert	261
Nastran, Martin	109, 206
Naumov, Anton	40, 136, 212
Neto, Armando	142
Nguyen, Ai-Phuong	88
Nguyen, Thanh	98
Nicholas, Robin	92
Nie, Haoran	127
Nishibara, Kazuki	208
Nishida, Seiya	196

Nishihara, Taishi	165
Niu, Wenhui	92
Noda, Suguru	30, 256
Nonoguchi, Yoshiyuki	94
Nowicki, Lukasz	287

O

Odegard, Gregory	8
Oh, Sang-Hyun	297
Ohno, Yutaka	3, 99
Okada, Mitsuhiro	156
Okada, Naoya	156
Okada, Susumu	286
Okazaki, Toshiya	258
Okubo, Soichiro	291
Olaya, Daniel	81
Oliveira, Thaina	76
Onoki, Takamasa	61, 291
Osawa, Toshio	30
Ostuka, Keigo	170, 196
Otsuka, Keigo	43, 129, 230, 286

P

Pallavolu, Mohan Reddy	251
Parera, Aina	170, 230
Park, Cheol	194, 231
Park, Chiwoo	36
Park, Sanghwan	144, 164, 267
Park, Sei Jin	18, 223
Pasquali, Matteo	67, 93, 111, 137, 146, 176, 179, 231, 253
Patel, Palak	104, 177
Patil, Sagar	8
Patter, Paul	109
Peden, Jack	108
Pei, Jingfang	163
Pelucchi, Matteo	16, 219
Pendashteh, Afshin	221
Penev, Evgeni	194
Peng, zhisheng	266
Perebeinos, Vasili	200
Pereyra, Ines	233
Peschek, Paul	206
Piao, Yuanzhe	118
Piasecki, Adam	236
Pidluzhna, Anna	303

Pimenta, Marcos	91
Ping, Lu.....	153
Pioch, Thomas.....	169
Pitner, Gregory.....	262
Plange, Portia	89
Podlesny, Blazej.....	205
Porter, Thomas.....	172
Pramanik, Sandipan	161, 265
Pribusová Slušná, Lenka.....	252
Prussack, Brett	42
Pugh, Michael	166, 263

Q

Qian, Liu	85, 167, 190, 266
Qiao, Mabel.....	108
Qiu, Diana.....	41
Qiu, Xiyang.....	230
Quien, Michelle.....	175
Quintero, Ever.....	81
Quiroz, Carlos	88

R

Raabe, Marco	88
Rao, Rahul.....	36
Rath, Jakob.....	206
RECHER, Gaëlle	117
Rechnitz, Sharon.....	110
Reddy, Gadhadar.....	140
Reich, Stephanie	6
Reji, Treesa	203
Retz, Kevin	34, 306
Rhone, Trevor David	48
Ricci, Melissa.....	20, 100
Richter, Henning.....	20, 100
Riede, Moritz	92
Ritt, Cody.....	19, 239
Rodriguez-Lopez, Pablo.....	166
Rogers, Marianna.....	142, 148
Rontani, Massimo	95
Ross, Frances	138
Rotkin, Slava.....	230, 286
Roux, Sébastien.....	71, 80, 107
Roxbury, Daniel.....	28, 122
Ruczka, Szymon	168, 171, 277
Ryota, Jono	270

S

Sadak, Omer.....	133
Saida, Takahiro	273
Saito, Riichiro	93, 200
Salter, Luke	268
Sanchez, Fabian	201
Sanchez-Yamagishi, Javier	278
Sarkar, Deblina	98
Sarmah, Anubhav.....	184
Sarojam, Rajani.....	87, 121
Saseendran, Vishnu.....	305
Sasmal, Somesh	139
Scammell, Lyndsey.....	231
Schiel, Matthew	278
Schmidt, Jochen	206
Schneider, J.....	112
Schubert, Jasmin	206
Schubert, Mathias	133
Schwenk, Gregory.....	182, 203
Seikh, Firoz	263
Sénéor, Pierre.....	107
Sergiienko, Sergii.....	243
Sesti, Giacomo	95
Sharma, Himanshu	195
Sharma, Kamal.....	273
Sharma, Shweta.....	142
Sheremetyeva, Natalya	119
Shim, Eunsoo	301
Shimada, Yusaku	196
Shimizu, Makoto.....	222
Shin, Hyeon Suk	10
Shiozawa, Hidetsugu.....	232
SHIRAKI, TOMOHIRO.....	64
Shlafman, Michael	110
Shlafman, Shlomo.....	110
Shubert Kabban, Christine	173
Siddiqui, Shiraz Ahmed.....	232
Silva, Paloma	76
Silva-Quinones, Dhamelyz	283
Siqueira, Ivan	111
Siwy, Zuzanna.....	278
Skrzypek, Magdalena.....	168
Sloan, Arthur.....	137, 146, 176
Smet, Jurgen.....	115
Smiri, Adlen.....	156
Smith, Ailill.....	28

Sodergren, Lukas	285
Sojkova, Michaela.....	252
Soltani, Rym	114
Son, Minjung.....	77
Song, Kyong Hwa.....	301
Song, Yingru.....	111
Sponza, Lorenzo	107
Stallard, Joe.....	108
Stefaniuk, Damian.....	228
Stefanov, Ognyan.....	111
Stein, Yosef.....	32, 173, 237
Stein, Yosi.....	202
Stenger, Ingrid.....	107
Stevens, Molly	268
Strand, Steven	23
Strano, Michael ...	19, 87, 121, 126, 132, 172, 175, 239, 244
Sturdza, Bernd.....	92
Su, Cong.....	284
Sudhakar, Kaustubh	182
Suenaga, Kazu.....	156
Sugime, Hisashi	294, 299
Sun, Sida	130, 162, 218
Sun, Xue-Long.....	276
Sun, Zhipei.....	103, 308
Suzuki, Hiroo	211
Suzuki, Takehito	155
Swager, Timothy.....	169
Synnatschke, Kevin.....	247
Szabo, Gabriel.....	206

T

TA, Duc-Minh.....	117
Tabachnik, Tal	110
Tailpied, Laure.....	80
Takakura, Akira	165, 291
Takei, Haruki	155
Takeuchi, Kenji.....	84
Tan, Junyang.....	234
Tanaka, Koki.....	211
Tanaka, Takeshi	165
Tang, Dalue.....	235
Taniguchi, Takashi.....	115
Tanioka, Daisuke	291
Tarnowska, Monika	209
Tay, Fuyang	200

Tejima, Syogo.....	270
Terrones, Mauricio.....	147, 151, 153
Terzyk, Artur.....	171, 209, 282
Thapa, Dinesh	272
Thomas, Ned.....	210
Tilve Martinez, David.....	227
Timmermans, Marina Y.....	195
Tiprigan, Ovidiu.....	143, 248
Tivnan, Matt.....	131
Tjahjono, Nicholas.....	194
Topkiran, Ugur.....	136
Tseng, Yu-Ting	275
Tsuchie, Yoshitaka.....	94
Tsuzuki, Koichi.....	84
Tu, Yu-Ming	19

U

Uchiyama, Haruki.....	99
Ulm, Franz-Josef.....	228
Unzaga, James.....	213
Upama, Shegufta.....	221
Urano, Daisuke	244

V

VALIENTE, RAFAEL	296
Valimukhametova, Alina	212
van Veen, Frederik.....	295
Varsano, Daniele.....	95
Vazquez-Puffleau, Miguel	219
Vegso, Karol	252
Vembris, Aivars	303
Venault, Antoine.....	24
Vilatela, Juan.....	219, 221
Vilatela, Juan J.	289
Vilatela, Juan José.....	227
VOITURIEZ, Raphaël	117

W

Waelder, Robert	36
Wagner, Jakob.....	82
Walendzik, Izabela.....	206
Walter, Adam.....	182, 203
Wang, Haozhe.....	113, 283
Wang, Jiangtao.....	262, 300
Wang, Jingwei.....	234
Wang, Liang.....	180

Wang, Lucy.....	187
Wang, Luqing	39
Wang, Peng.....	185
Wang, Shurui	190
Wang, Song.....	121
Wang, YuHuang	1, 31, 185, 187, 230
Wang, Zifan	153
Wardle, Brian....	96, 104, 135, 142, 148, 152, 177, 188, 202, 237, 305
Wasiak, Tomasz.....	293
Watanabe, Kenji.....	115
Wavrunek, Trevor	8
Weaver, James	228
Wehbe, Evan.....	213
Wehmeyer, Geoff.....	111
Wei, Fei.....	134, 141, 215, 240, 264
Wei, Nan	181
Wei, Yuanqi	235
Wei, Zitang	126
Weisman, R. Bruce	4
Wen, Yingyi.....	163
Wenseleers, Wim	170, 230
Wheeldon, Alexander	109
Wilhelm, Richard.....	206
Williams, Ryan	90
Wojciechowski, Łukasz	168
Woods, Lilia.....	166
Woods, Mackenzie.....	69
Wormley, Floyd	212
Wu, Chien-Jung	24
Wu, Dufan.....	131
Wu, Hengkai	165
WU, Jingwei	240
Wu, Shuang.....	37
Wu, Wenjing.....	65
Wu, Xiangyu.....	195
Wu, Xiaojian.....	187
Wyndaele, Pieter-Jan	195

X

Xiang, Rong.....	43, 43, 135, 170, 230, 286
Xiao, Kailu.....	210
Xiao, Zhigang	201
Xie, Ying.....	85, 167, 266
Xu, Lei	127
Xu, Rui.....	200

Xu, Yu-Wen.....	307
Xu, Zhenyu	158
Xu, Zhiping.....	56
Xu, Zihan	159

Y

Yaish, Yuval	110
Yakobson, Boris.....	39, 52, 194, 271
Yamada, Takatoshi	156
Yamakov, Vesselin	194
Yamamoto, Namiko.....	305
Yan, Xiaodong	60
Yanagi, Kazuhiro	44, 93, 200
Yang, Chunxia	43
Yang, Guang	279
Yang, Kai	131
Yang, Mei	258
Yang, Sungyun.....	132
Yang, Yaodong	190
Yao, Xuelin.....	92
Yao, Yixi.....	174
Yarovsky, Irene.....	268
Yasin, Ghulam	86, 290, 291, 304
yeh, juiming	275
Yeh, Yin-Ting.....	147
Yildiz, Asya	214
Yildiz, Kaan	214
Yoho, Josh.....	36
Yomogida, Yohei.....	93, 200
Yoshikawa, Ryo.....	129, 170
Yu, Qiangmin.....	46
Yu, William.....	180
Yuan, Qunying.....	201
YUAN, ZI	309
Yue, Hongjie	215
Yun, Deok Woo	301
Yutaro, Senda.....	211

Z

Zahn, Keshav	93
Zakeri, Nima	125
Zatko, Victor	107
Zeng, Chongyang.....	245
Zerrouki, Nabila.....	97
Zhang, Bowen.....	230
Zhang, Chiyu.....	185

Zhang, Jin.....	85, 167, 190, 266
Zhang, Lili.....	82
Zhang, Minfang.....	258
Zhang, Qiang.....	17, 158, 308
Zhang, Rongjie.....	106
Zhang, Tianyi.....	151
Zhang, Xinjie	74
Zhang, Xinrui.....	162
Zhang, Xu	78
Zhang, Zeyao	159, 174, 274
Zhao, Shen	116
Zhao, Ziqiang.....	167, 190
Zheng, Xiaolin	14
Zheng, Xudong	262, 300
Zheng, Yongjia	43, 170, 230, 286
Zhexembekova, Anar.....	226
ZHONG, JING.....	63
Zhou, Chongwu.....	73
Zhou, Da	153
Zhu, Hanyu	200
Zhu, Zhenxing.....	134, 141